Dissertation zur Erlangung des Doktorgrades

der Fakultät für Chemie und Pharmazie

der Ludwig-Maximilians-Universität München

Kinetics and Mechanisms of the Reactions of

Nitrogen Ylides with Acceptor-Substituted Olefins

Dominik Sebastian Allgäuer

aus

Wolfratshausen

2013

Für Anja

Scientific progress goes 'Boink'

–Calvin and Hobbes–

By Bill Watterson

Danksagung

Zu allererst gilt mein Dank natürlich meinem Doktorvater Prof. Dr. Herbert Mayr für die Möglichkeit meine Doktorarbeit bei ihm durchzuführen, die freie Hand bei meiner Themenwahl, die langen, ergiebigen Diskussionen, seine Hilfsbereitschaft und vor allem für seine Geduld.

Vielen Dank auch an die Mitglieder des Prüfungsausschusses für ihre Teilnahmebereitschaft.

Mein Dank gilt Dr. Armin Ofial (Dr. O), zum einen für die schnelle Durchsicht meiner Publikationen und die Freude über die dabei endeckten Fehler, zum anderen für seine stete Diskussions- und Hilfsbereitschaft. Außerdem natürlich für die schöne Zeit bei der ESOC auf Kreta.

Für den Anstoß zu den Ylid-Projekten und die Hilfe bei den ersten Schritten, schon während der Master-Arbeit, sowie seine stete Diskussionsbereitschaft, Begeisterungsfähigkeit und Freundschaft möchte ich Dr. Sami Lakhdar danken.

Danke auch an Angel Puente, Alexander Wagner, Elija Wiedemann, Katharina Böck, Francisco Corral, und Johannes Ammer für die zügige Durchsicht dieser Arbeit.

Außerdem möchte ich natürlich unseren „Kindergärtnerinnen" Nathalie Hampel, Hildegard Lipfert und Brigitte Janker danken, die den Arbeitskreis am Laufen halten. Ein besonderes Dankeschön geht an Hildegard Lipfert für ihr Eintreten für mich. Nathalie Hampel möchte ich dafür danken, dass sie eine leiwand Laborkollegin ist mit der ich sehr viel Spaß hatte, und die nebenbei auch noch Zeit für die ein oder andere meiner Synthesen gefunden hat.

Ich möchte auch den von mir betreuten Auszubildenden Marie Kunze, Thomas Schmelmer und Sandra Konstantinou für ihr Engagement, ihre Lern- und Leistungsbereitschaft danken.

Natürlich möchte ich auch meinen Laborkollegen Alexander Wagner, Konstantin Troshin, Johannes Ammer, Jörg Bartl, Tobias Nigst, Katharina Böck, und den Stopped-Flow Geräten für das gute Miteinander und den Spaß danken. Besonderer Dank geht an Konstantin Troshin für die musikalische Untermalung meiner Arbeit.

Ich danke auch meinen übrigen Kollegen aus dem AK Mayr, allen voran Francisco Corral und Hans Laub, für die gute Zusammenarbeit. Ich möchte mich auch bei unseren ehemaligen AK-Mitgliedern, allen voran Nicolas Streidl, für die gute Zeit mit ihnen bedanken. Der Ball ist rund.

Ich danke unserer Kochgruppe Nathalie Hampel, Francisco Corral, Angel Puente und Hans Laub für die freitäglichen Schlemmereien.

Ich möchte meiner Familie herzlich danken! Sie hat mich immer unterstützt und ohne sie wäre ich nie so weit gekommen.

Zu guter Letzt möchte ich meiner Frau für ihre Unterstützung, den Rückhalt, die Aufbauarbeit und auch für alles andere danken, was sie für mich getan hat!

Publikationen

A Facile One-Pot Two-step Synthesis of 1-Ethoxycarbonyl-indolizines via Pyridinium Ylides

D. S. Allgäuer, H. Mayr, *Eur. J. Org. Chem.* **2013**, 6379−6388.

Nucleophilicity Parameters of Pyridinium Ylides and Their Use in Mechanistic Analyses

D. S. Allgäuer, P. Mayer, H. Mayr, *J. Am. Chem. Soc.* **2013**, *135*, 15216−15224.

Electrophilicities of 1,2-Disubstituted Ethylenes

D. S. Allgäuer, H. Mayr, *Eur. J. Org. Chem.* **2014**, in press.

Konferenzbeiträge

02/2013   Industrietag LMU München; Posterpräsentation: "Structure-Reactivity Relationships of Acrylates and Simple Michael-Acceptors"

07/2011   ESOC Chersonissos, Griechenland; Posterpräsentation: „Structure-Reactivity Relationships in Reactions via Nitrogen Ylides"

03/2011   SFB-Antrag LMU München; Posterpräsentation: „Nucleophilicity Parameters for Sulfur- and Nitrogen Ylides: Reference Compounds for Elucidating the Ambident Reactivities of α,β-Unsaturated Carbonyl Compounds"

07/2010   ISOμ Mühlheim; Posterpräsentation: „Structure-Reactivity Relationships in Reactions via Ammonium Ylides"

Table of Contents

0   Summary

0.1   General

The second-order rate constants $k_{20°C}$ ($M^{-1}s^{-1}$) of nucleophile-electrophile combinations can be described by eq 0.1, in which the nucleophile-specific slope parameter is s_N, N is the nucleophilicity parameter and E is the electrophilicity parameter.

$$\log k_{20°C} = s_N(N + E) \qquad (0.1)$$

Based on this correlation a broad range of nucleophiles, including various phosphorous and sulfonium ylides, have been studied, while characterizations of the electrophilicities E of electrophiles other than colored cations and Michael acceptors with absorption maxima in the visible or near UV-vis range have hardly been attempted. Only recently the electrophilicity parameters of some colorless aldehydes, imines, and chalcones were determined.

The purpose of this thesis is to investigate the kinetics and mechanisms of the reactions of nitrogen ylides with acceptor-substituted olefins. Therefore, the reactions of ammonium ylides and pyridinium ylides with reference electrophiles were studied in order to quantify their reactivity by using eq 0.1. The nucleophilicity parameters of pyridinium ylides derived in this way could then be used for the characterization of the electrophilicities of a large number of synthetically important colorless acceptor-substituted olefins, namely acceptor-substituted ethylenes, propylenes, and styrenes. The electrophilicity parameters of these compounds allowed us to test the applicability of eq 0.1 to reported second-order rate constants for the reactions of acceptor-substituted olefins with various nucleophiles, which were collected from the literature.

0.2 The Wide Mechanistic Spectrum of Ammonium Ylide Mediated Cyclopropanations

Kinetics and mechanisms of the reactions of stabilized ammonium ylides with diarylcarbenium ions and several Michael acceptors have been determined by UV–vis and NMR spectroscopy in DMSO at 20 °C (Scheme 0.1). The cyclopropanations of the Michael acceptors by ammonium ylides were found to proceed via intermediate betaines (Scheme 0.1), which could be observed and characterized in some cases.

The overall reaction, betaine formation and ring closure, was found to follow four different types of mechanisms depending on the nature of the Michael acceptor and the electron-withdrawing groups at the ylide.

The more basic, cyano, amido, and ester-substituted, ylides ($pK_{aH} \geq 20$ in DMSO) were found to form the intermediate betaines irreversibly with fast or slow subsequent ring closure depending on the Michael acceptor, while the less basic, acyl-substituted, ylides ($pK_{aH} = 15–16$) formed the intermediate betaines reversibly with rate determining ring closure.

The energy profiles of four different types of mechanisms for the cyclopropanations with ammonium ylides, i.e., irreversible betaine formation with fast (case 1a) and slow subsequent ring-closure (case 2a), and reversible formation of non-observable (case 1b) and observable betaines (case 2b) are constructed (Figure 0.2b).

Scheme 0.1. Reactions of ammonium ylides with diarylcarbenium ions and Michael acceptors.
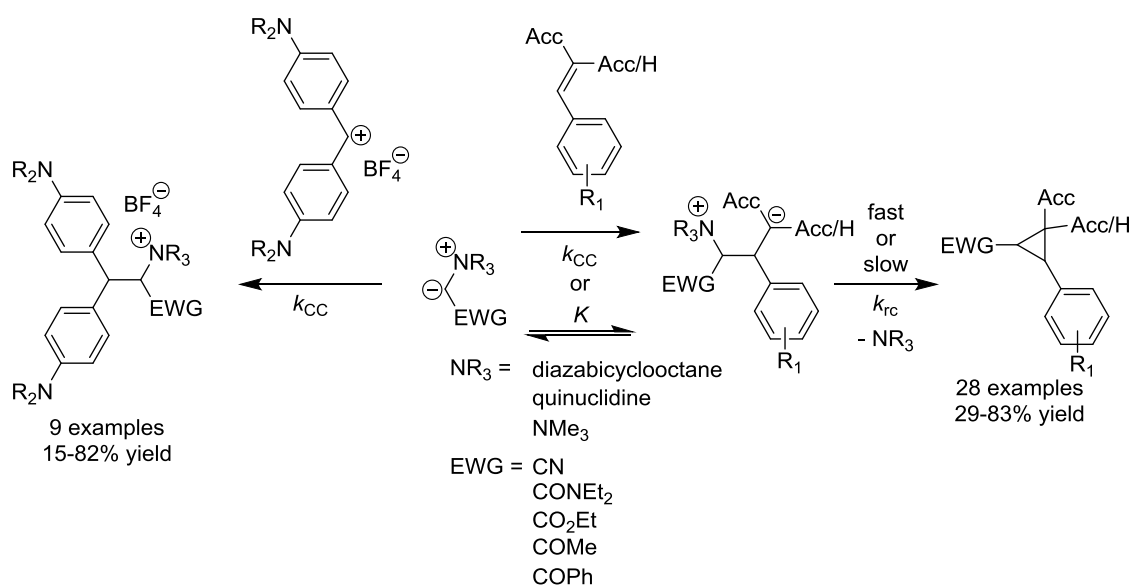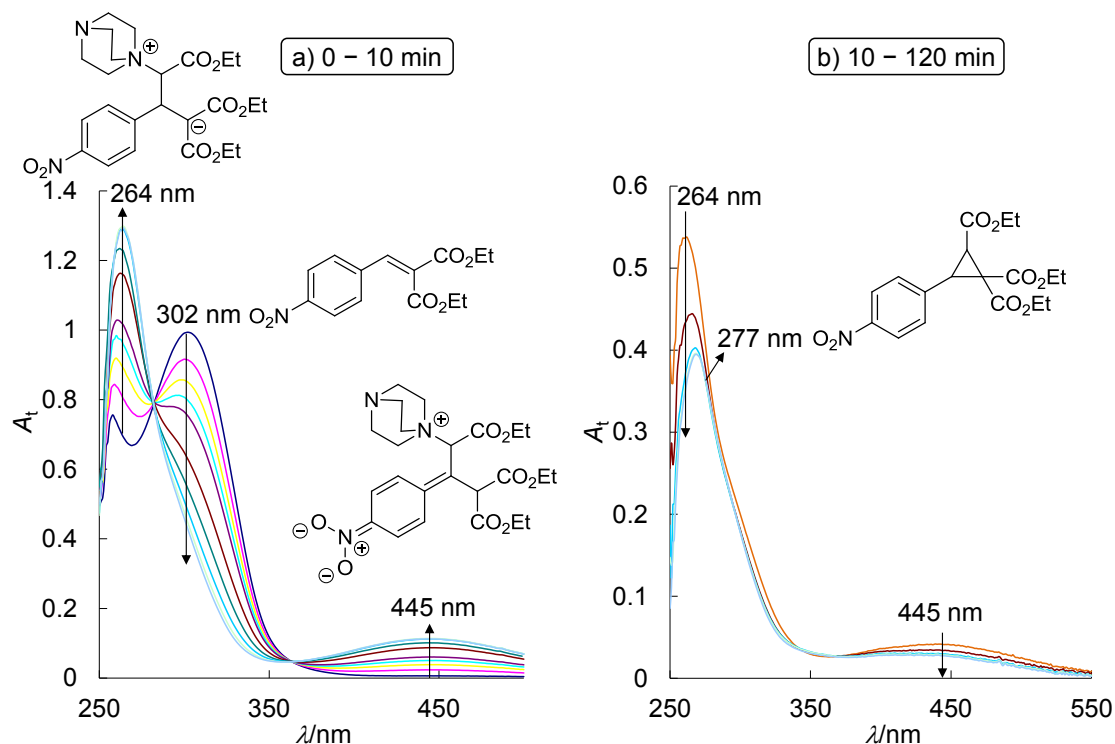
Figure 0.1. UV-vis spectra of the reaction of an ester-substituted ammonium ylide with a benzylidene malonate with formation of an intermediate betaine during the first 10 min of the reaction (a) and of the ring-closure of the betaine to the cyclopropane in the following 120 min (b).
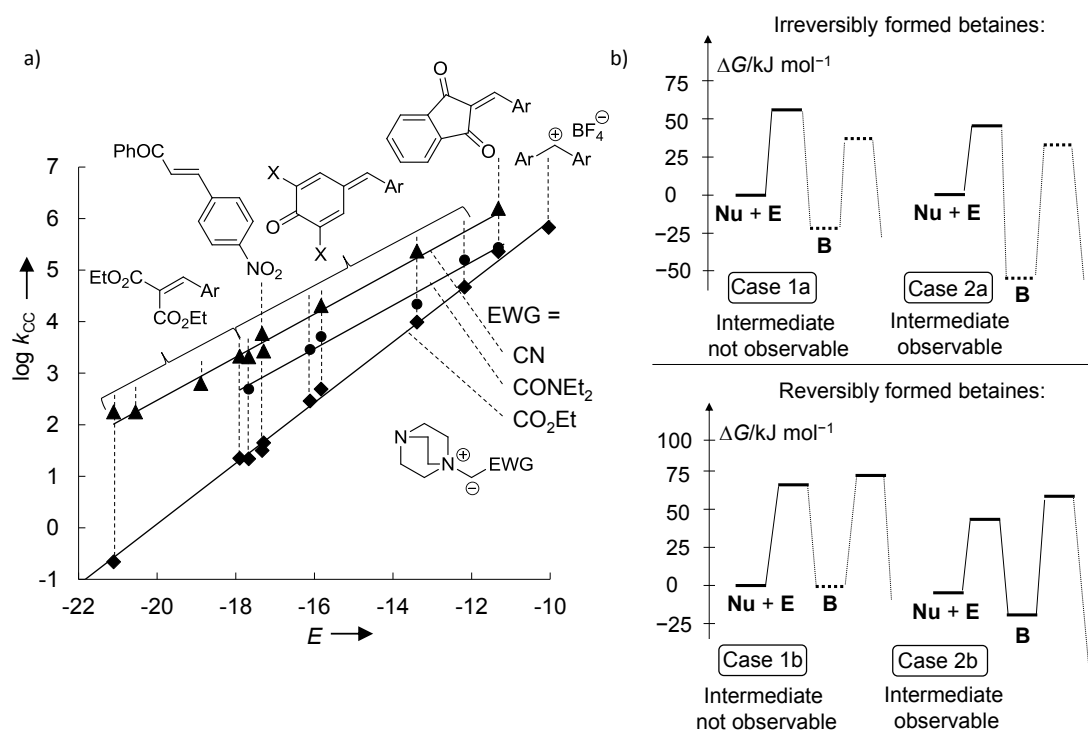
Figure 0.2. a) Plots of the observed second order rate constants k_{CC} of the reactions of different ammonium ylides with benzhydrylium ions and Michael acceptors versus the corresponding electrophilcity parameters E; b) Energy profiles for the four different mechanisms observed for the cyclopropanations of Michael acceptors (E) by ammonium ylides (Nu) via intermediate betaines (B).

3

The correlations of log k_2 for the reactions of the ammonium ylides with benzhydrylium ions and for the formation of betaines from ammonium ylides and Michael acceptors versus the electrophilicity parameters E were linear (Figure 0.2a) and allowed us to determine the nucleophile-specific parameters N and s_N for the ammonium ylides, as defined by the eq 0.1. By including them into our comprehensive nucleophilicity scale a direct comparison with other types of nucleophiles was achieved (Figure 0.3).
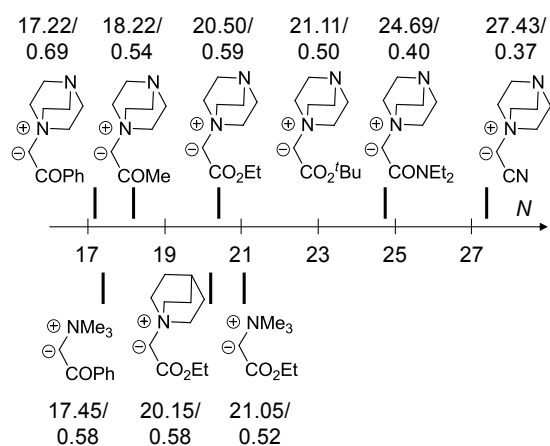
Figure 0.3. Reactivity parameters N/s_N of ammonium ylides investigated in this work.

0.3 One-Pot Two-step Synthesis of 1-Ethoxycarbonyl-indolizines via Pyridinium Ylides

The pyridinium salts Py^+-CH_2-EWG were found to react with substituted Michael acceptors of the type Ar-CH=C(CO$_2$Et)(Acc) at ambient temperature in the presence of base to give [3+2]-cycloadducts via stepwise [3+2]-cycloadditions of the intermediate pyridinium ylides (Scheme 0.2).

Oxidization of the intermediate [3+2]-cycloadduct in the crude reaction mixtures with 1 equivalent of chloranil in the presence of atmospheric oxygen and sodium hydroxide gave 1-ethoxycarbonyl-indolizines by dehydrogenation and elimination of the acceptor group (Acc). A mechanism for the formation of the 1-ethoxycarbonyl-indolizines was proposed as depicted in Scheme 0.3.

Scheme 0.2. Scope of the one-pot indolizine synthesis developed in this work.

EWG = CO$_2$Et, CONEt$_2$
CN, COMe,
COPh
R = 3-Cl, 4-NMe$_2$,
isoquinoline

Acc = CO$_2$Et, CONH$_2$
COMe, SO$_2$Me
Ar = p-NO$_2$, p-CN,
m-Cl, p-Br, H,
p-Me, p-OMe,
p-NMe$_2$, julolidyl

19-89%
22 examples
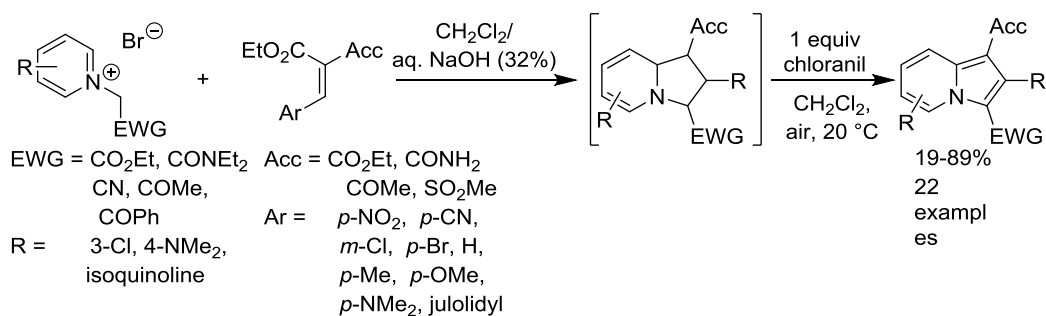
Scheme 0.3. Proposed mechanism for the formation of 1-ethoxycarbonyl-indolizines.
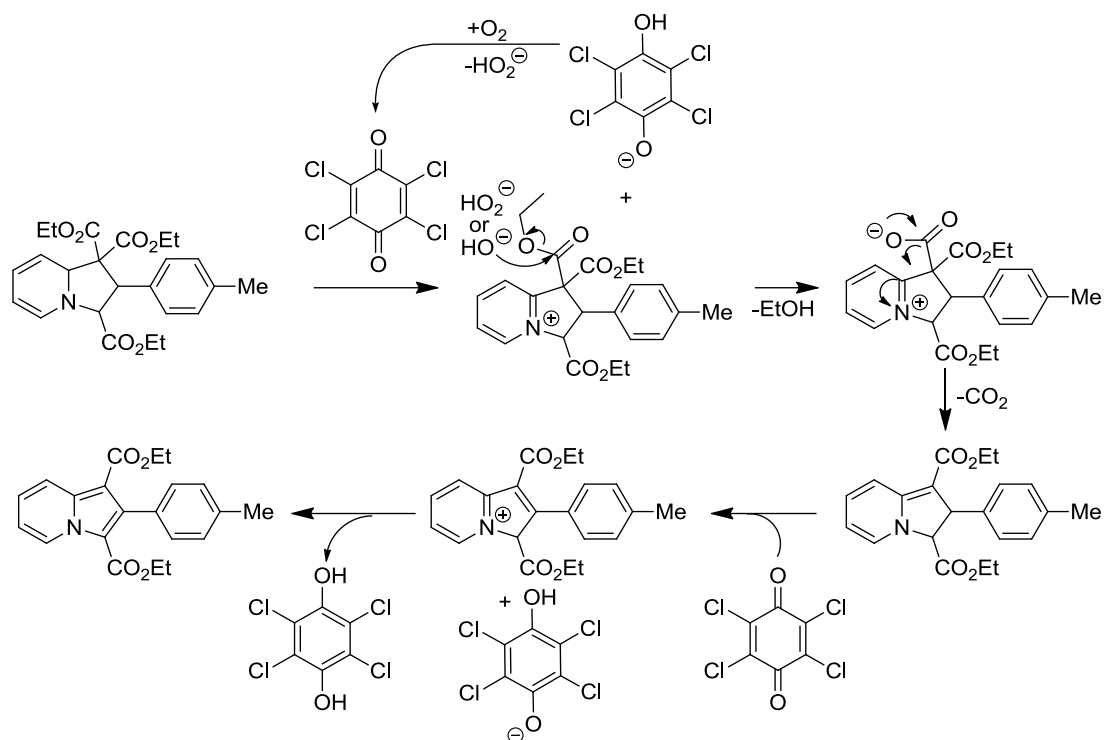
The developed synthetic procedure was found to tolerate a broad range of electron-withdrawing groups and substituents on the ylides and the Michael acceptors as shown in Scheme 0.2. Structurally related isoquinolinium salts react with Michael acceptors analogously to give pyrrolo[2,1-*a*]isoquinolines.

As also a 2-alkyl substituted indolizine was accessible from Py^+-CH_2CN and ^iPr-$CH=C(CO_2Et)_2$ by this method, this indicates that the protocol is not restricted to aromatic Michael acceptors.

0.4 Nucleophilicity Parameters of Pyridinium Ylides and Their Use in Mechanistic Analysis

The kinetics of the reactions of pyridinium, isoquinolinium, and quinolinium ylides with diarylcarbenium ions, quinone methides, and arylidene malonates (reference electrophiles) have been studied in DMSO solution by UV−Vis spectroscopy. The reactions of pyridinium ylides with benzhydrylium ions and quinone methides gave the simple alkylation products (Scheme 0.4).

Scheme 0.4. Reactions of pyrinium ylides with benzydrylium ions and quinone methides.
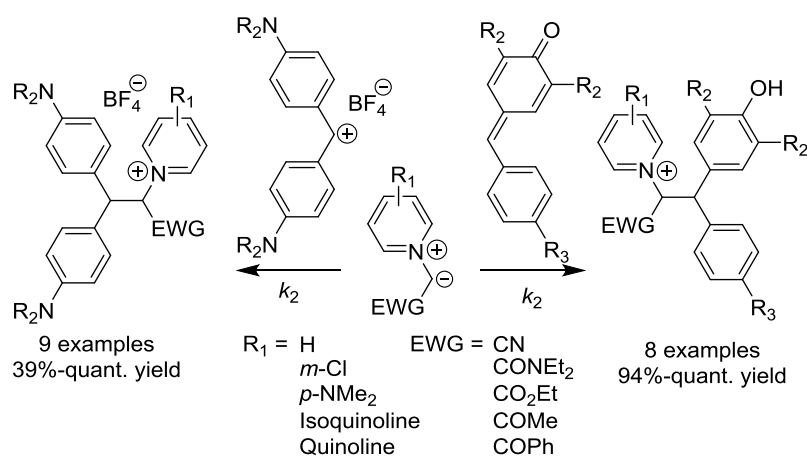
The measured second-order rate constants (log k_2) were found to correlate linearly with the electrophilicity parameters E of the reference electrophiles as required by eq 0.1, allowing us to derive the nucleophile-specific parameters N and s_N for the investigated pyridinium ylides (Figure 0.4).

The measured rate constants for the 1,3-dipolar cycloadditions of pyridinium, isoquinolinium, and quinolinium ylides with acceptor substituted dipolarophiles (arylidene malononitrile and substituted chalcone) were found to agree with those calculated from E, N, and s_N, showing that the above correlation is a suitable tool for the prediction of absolute rate constants of stepwise or highly unsymmetrical concerted cycloadditions (Scheme 0.5). Changes of the reaction mechanism were demonstrated by deviations between calculated and experimental rate constants by a factor of 10^6.

Pyridinium-substitution is found to have a similar effect on the reactivity of carbanionic reaction centers as alkoxycarbonyl substitution (Figure 0.5).
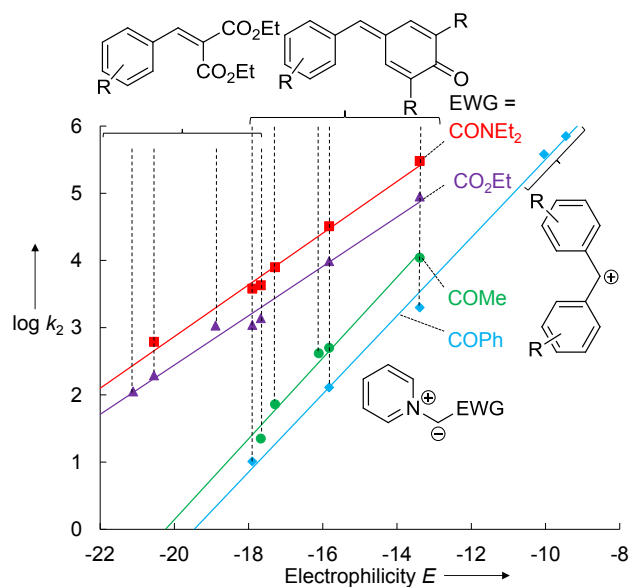
Figure 0.4. Plots of log k_2 for the reactions of pyridinium ylides with reference electrophiles in DMSO at 20 °C versus the corresponding electrophilicity parameters.

Scheme 0.5. Stepwise reactions of pyridinium ylides with benzylidene malononitriles (a) and chalcones (b).
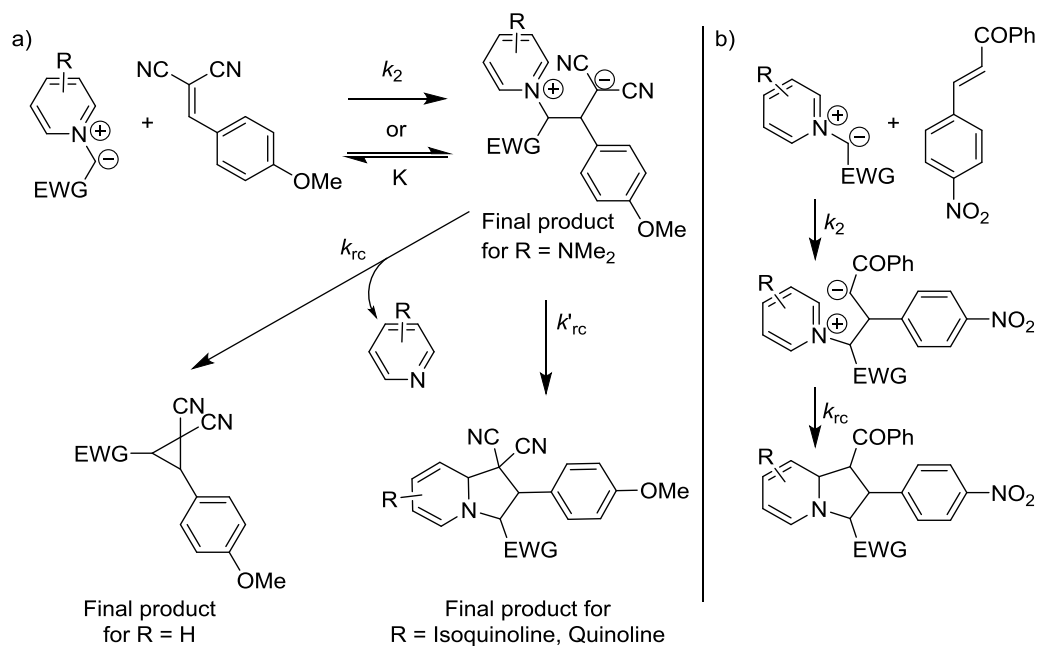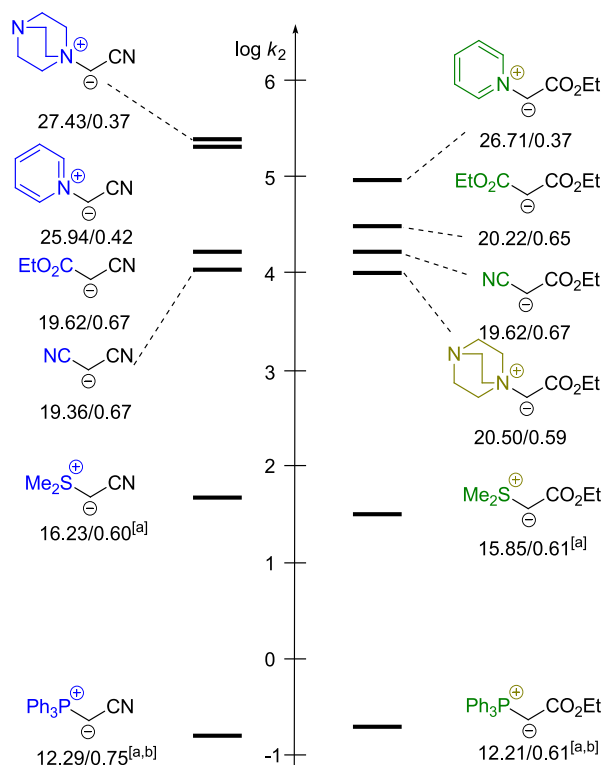
Figure 0.5. Comparison of k_2-values of the reactions of analogously substituted pyridinium, ammonium, sulfur, and phosphorous ylides and carbanions towards *p*-NMe$_2$-substituted diphenyl quinone methide. *N* and s_N-values are given below each nucleophile (reactivities refer to DMSO as solvent). [a] Calculated by eq 0.1 from s_N, *N*, and *E*; [b] In CH$_2$Cl$_2$.

0.5 Electrophilicities of 1,2-Disubstituted Ethylenes

The kinetics of the reactions of maleic anhydride, *N*-methyl maleimide, fumaro nitrile, diethyl fumarate, and diethyl maleate with pyridinium and sulfonium ylides were studied in DMSO at 20 °C (Chart 0.1).
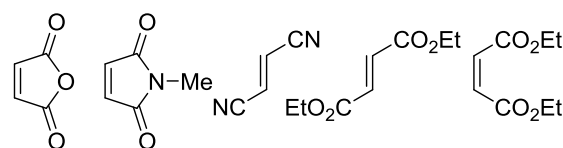
Chart 0.1. 1,2-Disubstituted ethylenes investigated in this work.

The reactions of pyridinium ylides with the 1,2-disubstituted ethylenes gave tetrahydroindolizines as initial products, which were isolated in case of the benzoyl-substituted isoquinolinium ylide (Scheme 0.6a), or oxidized to the corresponding indolizines in case of the benzoyl-substituted pyridinium ylide (Scheme 0.6b). The reactions of 1,2-disubstituted ethylenes with sulfonium ylides gave cyclopropanes (Scheme 0.6c).

Scheme 0.6. Reactions of 1,2-disubstituted etyhlenes with isoquinolinium, pyridinium, and sulfonium ylides.
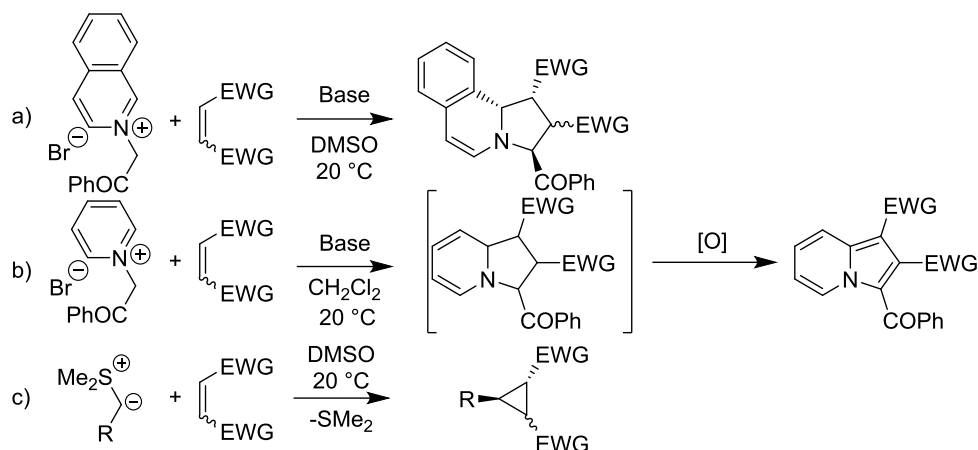
All reactions follow a second-order rate law and can be described by the linear free energy relationship $\log k_2 = s_N(N + E)$ (Figure 0.6). The electrophilicity parameters E of the investigated dipolarophiles were derived from the linear correlations of $(\log k_2)/s_N$ versus N and range from $-19.8 < E < -11.1$ (Figure 0.7).
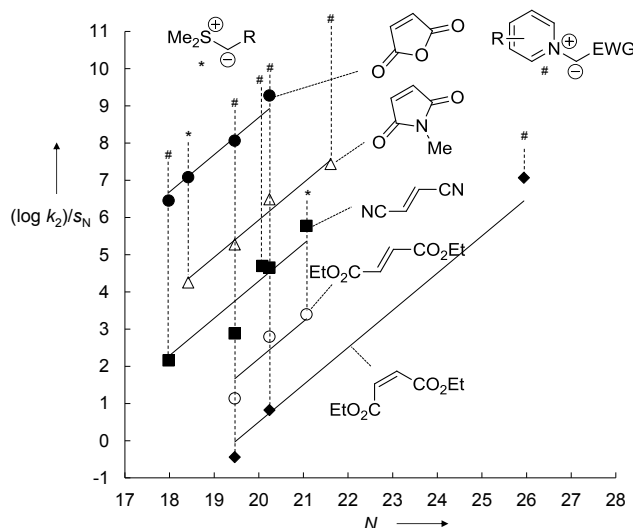
Figure 0.6. Correlation of $(\log k_2)/s_N$-values derived from the reactions of 1,2-disubstituted ethylenes with pyridnium and sulfonium ylide against the corresponding nucleophilicity parameters N of the ylides.
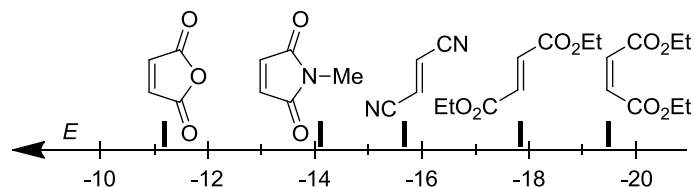
Figure 0.7. Reactivity ordering of the 1,2-disubstituted ethylenes investigated in this work.

0.6 Quantification of the Ambient Electrophilicities of α,β-Unsaturated Aldehydes

The ambient reactivity of the α,β-unsaturated aldehydes acrolein, crotonaldehyde, and cinnamaldehyde (Chart 0.2) was studied in their reactions with pyridinium and sulfonium ylides (Scheme 0.7).
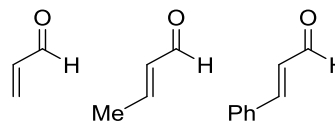
Chart 0.2. α,β-unsaturated aldehydes investigated in this work.

The rate constants of their stepwise [3+2]-cycloadditions with pyridinium ylides, and their cyclopropanations or epoxidations by sulfonium ylides have been determined photometrically in DMSO at 20°C.

Pyridinium ylides gave indolizines (after oxidation) which are the products of the conjugate attack at the enal. The reaction of benzoyl and acetyl substituted pyridinium ylides with 2 equiv. of acrolein gave the 3-(oxopropyl) indolizine-1-carbaldehyde after elimination of the acyl group from the intermediate. Stabilized sulfonium ylides exclusively gave cyclopropanes by conjugate attack, while the semi-stabilized ylides also formed epoxides by 1,2-addition to the aldehyde (Scheme 0.7).

Scheme 0.7. Reactions of pyridinium and sulfonium ylides with α,β-unsaturated aldehydes.
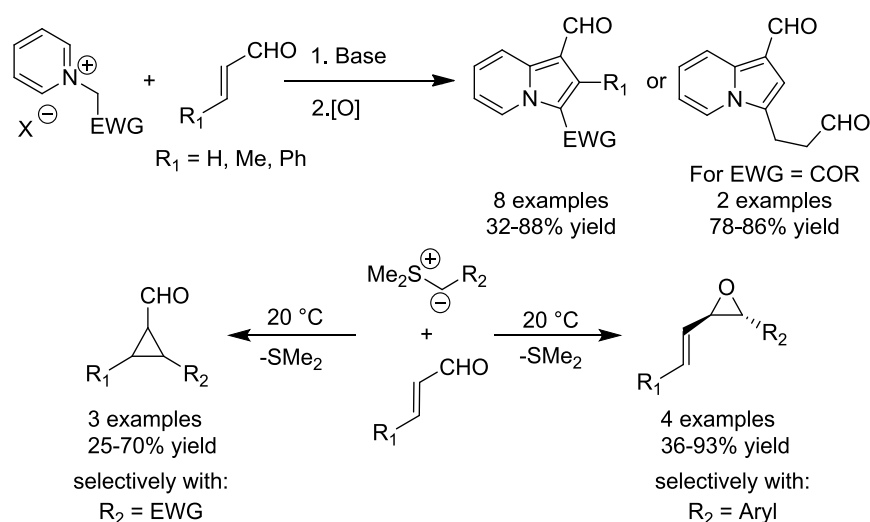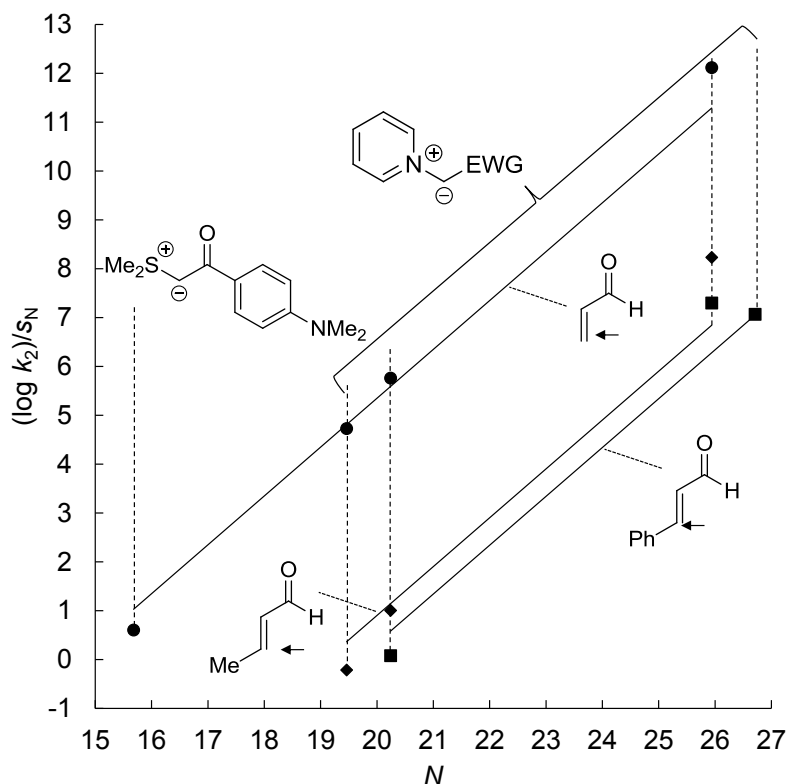
Figure 0.8. Plots of the (log k_2)/s_N values for the 1,4-attack of pyridinium and stabilized sulfonium ylides at the α,β-unsaturated aldehydes versus the corresponding N-parameters. The slopes of the correlations were set to 1.0 as required by eq 0.1.

All investigated reactions were found to follow a second-order rate law and the rate constants refer to the initial formations of the intermediate betaines. The obtained rate constants (log k_2) were combined with the known nucleophilicity parameters N and s_N of the pyridinium and sulfonium ylides to derive the electrophilicities E of the C=C and C=O-double bonds of the α,β-unsaturated aldehydes according to the linear free-energy relationship log $k_2 = s_N(N + E)$ (Figure 0.8).

Reported rate constants for the reactions of substituted pyridines, morpholine, and cysteine dianion with the α,β-unsaturated aldehydes were collected from the literature and compared with those calculated by eq 0.1 from the E parameters of the α,β-unsaturated aldehydes determined in this work and the previously published s_N and N-parameters of the nucleophiles.

The investigation provides a quantitative description of the ambient electrophilicities of α,β-unsaturated aldehydes and allows us to include them into our comprehensive nucleophilicity scale (Figure 0.9).
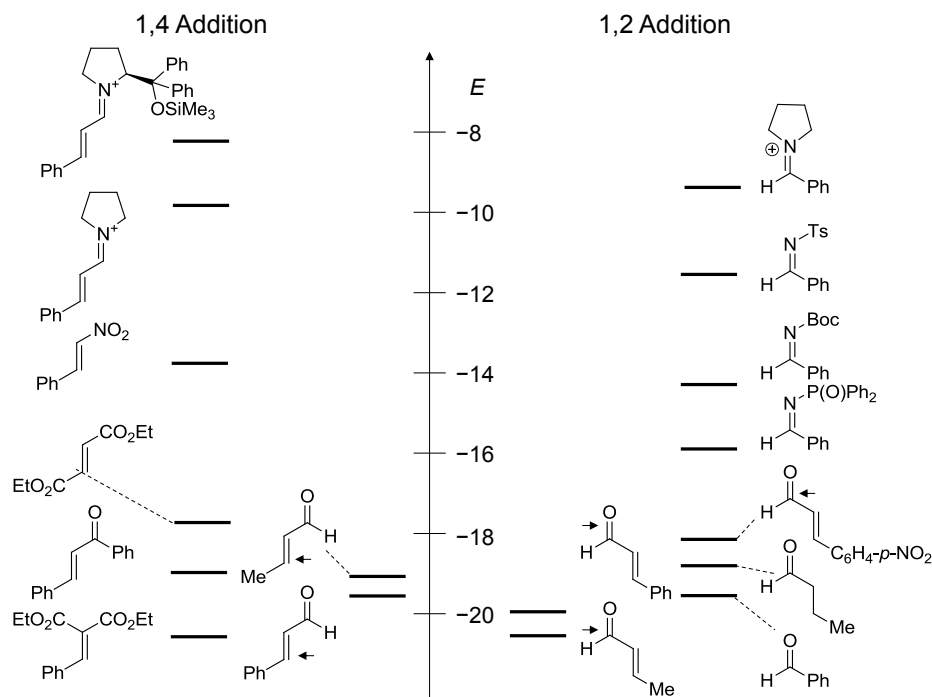
Figure 0.9. Comparison of the electrophilicity parameters E of α,β-unsaturated aldehydes with those of Michael acceptors, aldehydes, imines, and iminium ions.

0.7 Electrophilicities of Acceptor-Substituted Olefins

The rate constants of the reactions of acceptor substituted olefins, in particular ethylenes, propylenes, and styrenes (Chart 0.3), with pyridinium and sulfonium ylides have been determined photometrically in dimethyl sulfoxide.

The reactions of pyridinium ylides with the acceptor-substituted olefins from Chart 0.3 gave dihydroindolizines or indolizines after oxidation, while the reactions of activated ethylenes with a sulfonium ylide gave cyclopropanes (Scheme 0.8).

All of these reactions were shown to follow a second-order rate law. Plots of (log k_2)/s_N versus the nucleophilicity parameters N of the ylides were linear with a slope of approximately 1.0 as required by eq 0.1 (Figure 0.10).
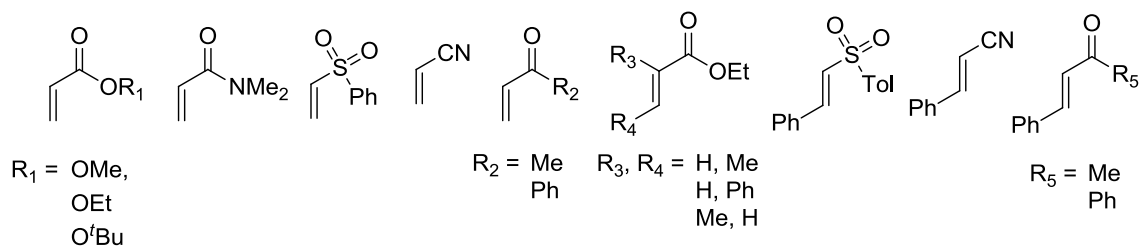
Chart 0.3. Acceptor-substituted olefins investigated in this work.

Scheme 0.8. Reactions of activated acceptor-substituted olefins with pyridnium and sulfonium ylides.
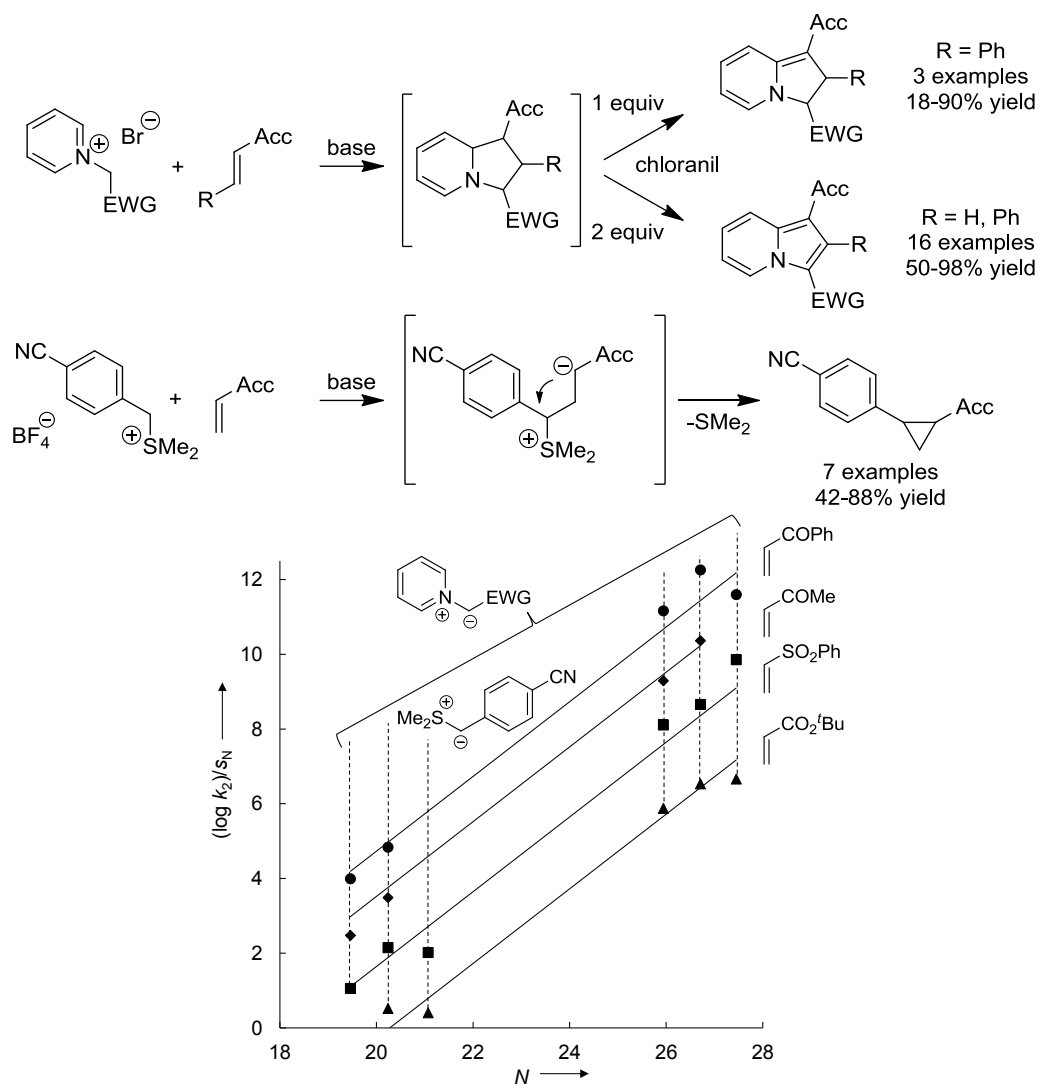
Figure 0.10. Correlation of (log k_2)/s_N with the nucleophilicity parameters N for the reactions of acceptor-substituted olefins with pyridinium and sulfonium ylides.

The linear correlations allowed us to derive the electrophilicity parameters E of the Michael acceptors in Chart 0.3 according to eq 0.1 (Figure 0.11), which range from $-24.7 < E < -15.2$. The derived electrophilicity parameters E of the acceptor-substituted olefins allow many comparisons with other Michael acceptors and can help to increase the understanding of the nucleophile independent ordering of electrophilic reactivities (Figure 0.11).
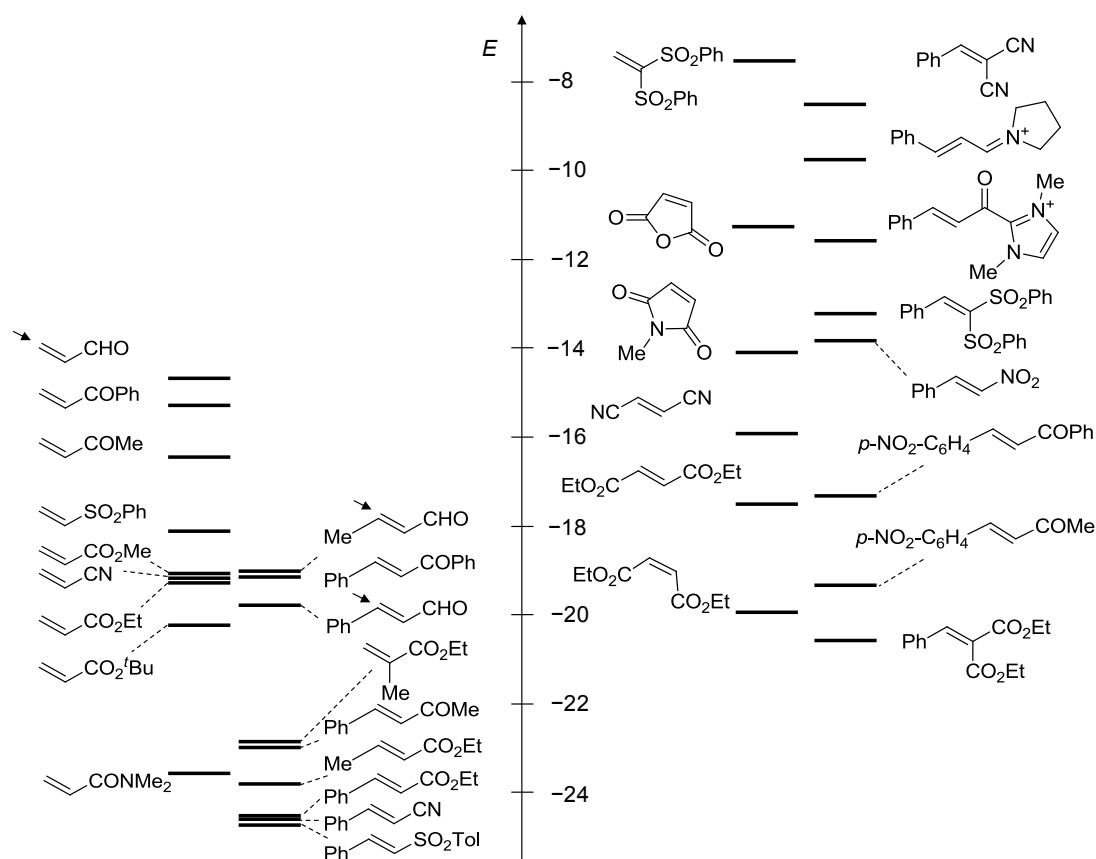
Figure 0.11. Comparison of the electrophilicities *E* activated ethylenes, propylenes, and styrenes with those of other Michael acceptors.

0.8   Applications of the Linear Free-Energy Relationship log $k_2 = s_N(N + E)$

We collected 110 rate constants for reactions of the acceptor-substituted olefins investigated in this work (Charts 0.1−0.3) with C, N, O, S, and P-nucleophiles from the literature. Subsequently we compared these experimental rate constants with those calculated by eq 0.1 using the known reactivity parameters of the reactants. In 96 cases we found that the rate constant could be predicted within the limit of confidence of eq 0.1 of two orders of magnitude. This agreement demonstrates the reliability of eq 0.1 for the prediction of rate constants of polar organic reactions.

The rate constants of the reactions of glutathione with Michael acceptors of known electrophilicity and the rate constants for the reactions of different activated ethylenes with amines, pyridines, and alkoxides, whose nucleophilicities are known, were collected from the literature to estimate the nucleophilicity parameters of glutathione and the electrophilicity parameters of the activated ethylenes. The comparison with the reactivity parameters of related compounds was used to analyze the reliability of these parameters.
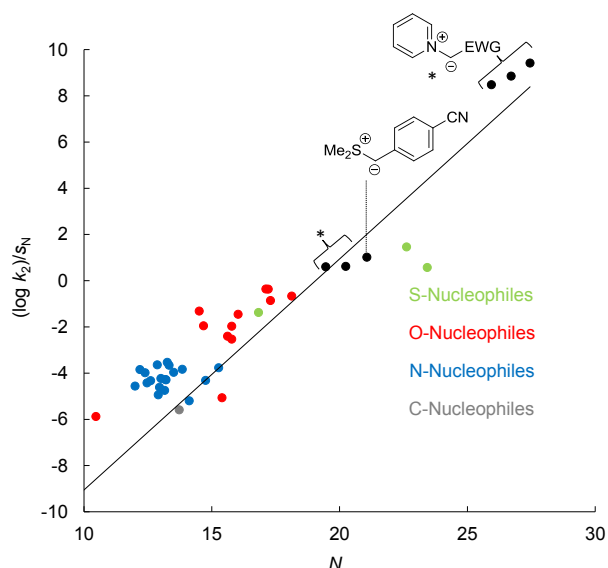
Figure 0.12. Correlation of rate constants for the reactions of acrylonitrile with pyridinium and sulfonium ylides (black dots) used to draw the correlation line (the slope is set to 1.0). Colored dots refer to rate constants for its reactions with nucleophiles collected from the literature.

Although eq 0.1 cannot be used to predict the rates of pericyclic reactions, we collected the rate constants of the reactions of diazomethanes and dienes with the acceptor-substituted olefins investigated in this work (Charts 0.1−0.3). The nucleophilicity parameters N and s_N of different diazomethanes and dienes were previously determined from their stepwise reactions with benzhydrylium ions. Plots of log k_2 versus the electrophilicity parameters E and of (log k_2)/s_N versus the nucleophilicity parameters N showed that the reactions of diazomethanes and dienes deviate from the correlation lines for the stepwise reactions because these reactions proceed by a concerted mechanism in agreement with previous interpretations of these reactions. Although these reactions do not follow eq 0.1, the rate constants still show a dependence on the reactivity parameters (Figure 0.13) as they increase with increasing reactivity of the reactants.

The concertedness of these reactions can be analyzed by calculating the "free enthalpies of concert" $\Delta G_{concert} = RT\ln k_2^{exp}/k_2^{calcd}$ from the ratio of the experimental (k_2^{exp}) and calculated (k_2^{calcd}, by eq 0.1) second-order rate constants for these pericyclic reactions.
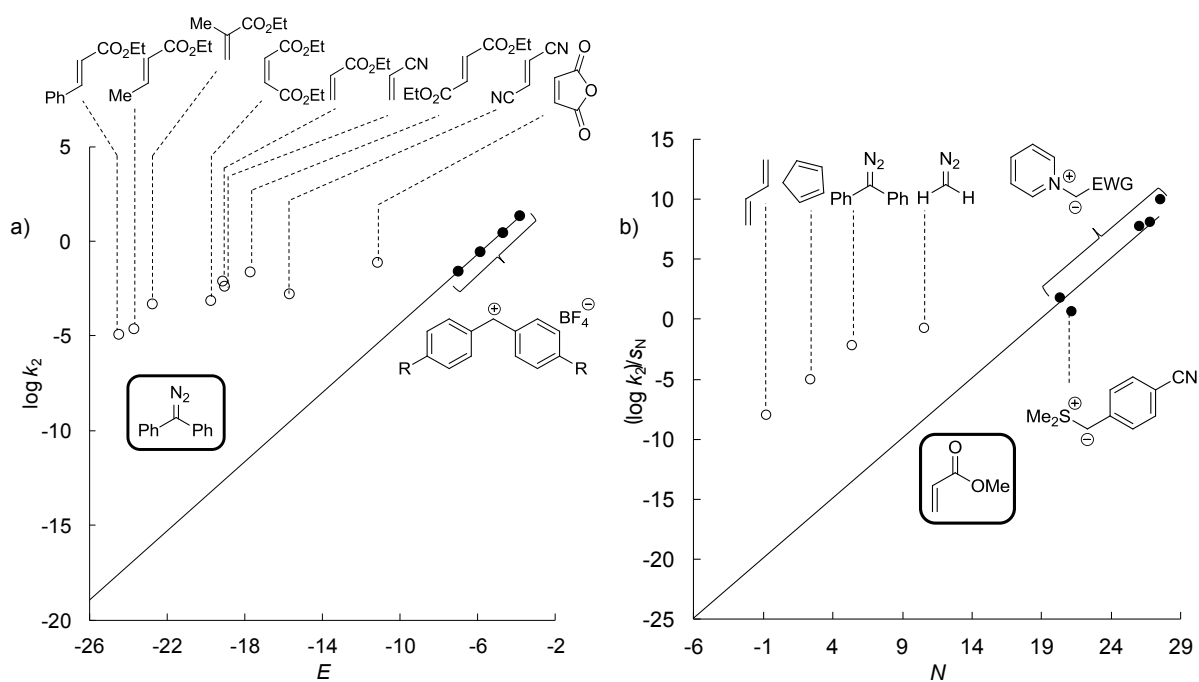
Figure 0.13. a) Plot of the log k_2 values of the reactions of diphenyl diazomethane with benzhydrylium tetrafluoroborates (filled dots, CH_2Cl_2, 20 °C) and Michael acceptors (open dots) versus the corresponding E parameters; b) Correlation of the (log k_2)/s_N values of the reactions of methyl acrylate with pyridinium ylides and sulfonium ylide (filled dots, DMSO, 20 °C), diazomethanes and dienes versus the corresponding N parameters.

1 Introduction and Objectives

1.1 Introduction

The numerous types of organic reactions described today facilitate a vast amount of possible nucleophile electrophile combinations. The sheer number of possible combinations leads to the need for simple and reliable tools to predict organic reactions. The development of such tools has been a great challenge to physical-organic chemists over the last decades.

A major progress to describe organic reactivity was made by Ingold in the 1930s as he found that organic reactions are in many case the combinations of electron-rich species, which he called "nucleophiles", with electron-poor species, which he named "electrophiles".[1] This classification was the basis for the first systematic attempts by Swain and Scott[2] to quantify organic reactivity by using kinetics. When they investigated the kinetics of S_N2 reactions they found that their rate constants followed a linear free-energy relation (eq 1.1), in which nucleophiles are characterized by one parameter (n) and electrophiles by two parameters (s and $\log k_0$).

$$\log (k/k_0) = s \cdot n \qquad (1.1)$$

In 1972 Ritchie showed, that the rates of the reactions of nucleophiles with carbocations and diazonium ions can be described by a simple equation (2), in which the reactivity of the electrophile ($\log k_0$) and the nucleophile (N_+) is described by one parameter.[3] However, the applicability of eq 1.2 was found to be limited and a separate treatment of the different classes of electrophiles gave better correlations.[4]

$$\log (k/k_0) = N_+ \qquad (1.2)$$

In 1994 Mayr and Patz developed a linear free-energy relationship (eq 1.3) based on the reaction rates of benzhydrylium ions, cationic metal-π-complexes, and diazonium ions with n, π, and σ-nucleophiles.[5] In the three parameter equation $k_{20\,°C}$ is the second-order rate constant ($M^{-1}s^{-1}$), s_N is the nucleophile specific slope parameter, N is the nucleophilicity parameter, and E is the electrophilicity parameter.

$$\log k_{20\,°C} = s_N(N + E) \tag{1.3}$$

The application of eq 1.3 was simplified by defining benzhydrylium ions and quinone methides as reference electrophiles, what allowed broad variations of the reactivity at a constant reaction center by changing the substituents of the aromatic rings. Subsequently, various highly substituted Michael acceptors have been added to the reactivity scale, allowing the construction of a comprehensive nucleophilicity and electrophilicity scale with currently 947 nucleophiles and 249 electrophiles characterized.[6]

1.2 Objectives

Nitrogen ylides are known to be highly reactive nucleophiles and are used for the preparation of a wide range of products, e.g. cyclopropanes (from ammonium ylides) or indolizines (from pyridinium ylides).[7]

By studying the kinetics and mechanisms of the reactions of ammonium ylides with carbocations and Michael acceptors, a better understanding of their reactivity should become possible (Scheme 1.1a).

Similar investigations with the related pyridinium ylides should show, if their [3+2]-cycloadditions to Michael acceptors proceed stepwise and follow eq 1.3 (Scheme 1.1b). The comparison of the reactivities of ammonium and pyridinium ylides with the reactivities of the recently characterized phosphonium[8] and sulfonium ylides[9] should show the effect of the onium moiety on the reactivities.

Scheme 1.1. Reactions of ammonium (a) and pyridinium ylides (b) with Michael Acceptors.
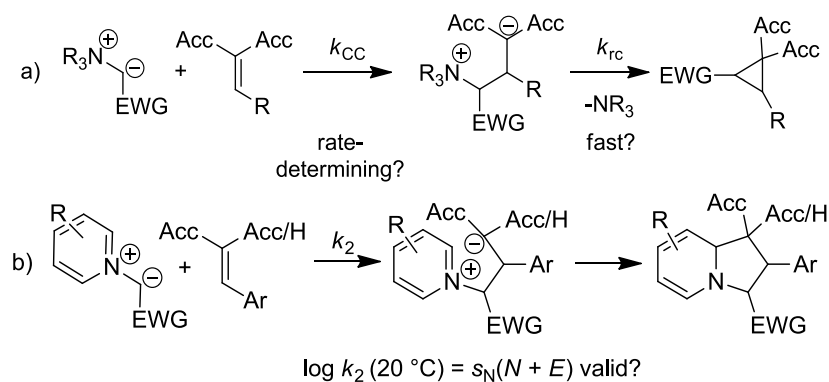
As mentioned, above four times more nucleophiles (947 examples) were characterized by means of eq 1.3 (N, s_N) than electrophiles (249 examples).[6f] Until now mainly the reactivity of colored carbocations (136 examples), including heteroatom substituted carbocations and cationic metal-π-complexes, have been quantified by eq 1.3. The quantification of Michael acceptors has been restricted to highly substituted systems, having absorption maxima in the visible or near UV-vis range. The reactivity of synthetically important colorless acceptor-substituted olefins has not been investigated by our methods, as suitable colored reference nucleophiles were not available.

Applying the colored pyridinium ylides as reference nucleophiles should allow us to study the electrophilicities of such acceptors-substituted olefins, as the internal electrophile of the pyridinium ylide, the pyridinium moiety, should be able to trap the carbanion formed in the intermediate (cf. Scheme 1.1).

1,2-Disubstituted ethylenes are common electrophiles in pericyclic reactions.[10] The kinetic investigation of their reactions with pyridinium ylides should allow us to analyze which substitution pattern of the ylide induces a concerted mechanism (Scheme 1.2).

It is known that semi-stabilized sulfonium ylides add to the formyl group of α,β-unsaturated aldehydes[9b] while pyridinium ylides add to the conjugate position (Scheme 1.3). Combining both reactivities should offer the possibility to quantify the electrophilicities of the formyl group and of the conjugate position of α,β-unsaturated aldehydes.

In further studies, the use of suitable pyridinium ylides as reference nucleophiles should allow us to quantify the electrophilic reactivities of other acceptor-substituted olefins (Scheme 1.4). Variations of their substituents should allow a systematic quantification of their electrophilicities.

Scheme 1.2. Stepwise and concerted reactions of pyridinium ylides with 1,2-disubstituted ethylenes.
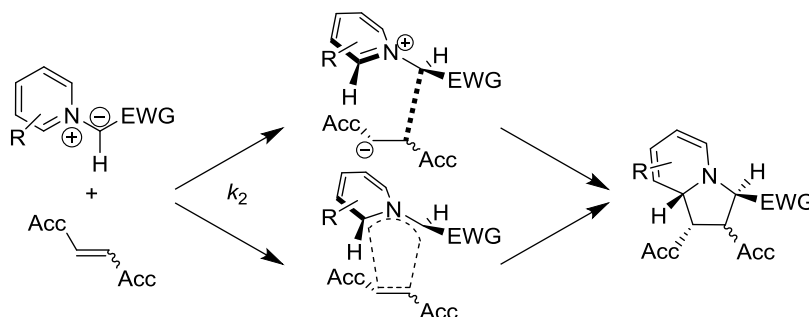
Scheme 1.3. Reaction of α,β-unsaturated aldehydes with pyridinium and sulfonium ylildes.
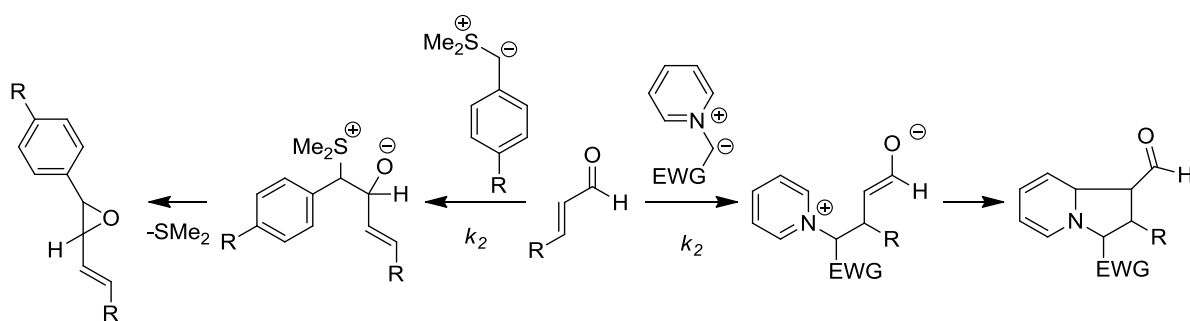
Scheme 1.4. Reactions of pyridinium ylides with acceptor-substituted olefins.

$R^1 = H, Me$
$R^2 = H, Me, Ph$
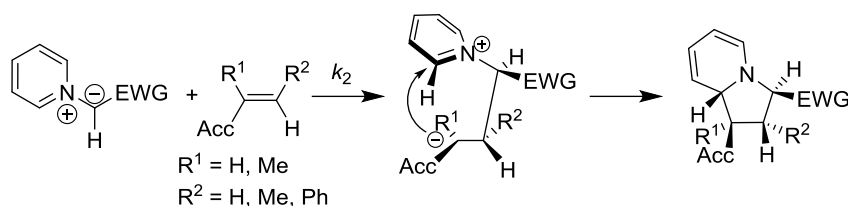
Many rate constants for the additions of nucleophiles to acceptor-substituted olefins have been determined over the last decades (Figure 1.1a).[11-15] The previous quantification of the electrophilicities of acceptor-substituted olefins should allow us to study the reliability of eq 1.3 by com-

a) $\log k_{20\,°C} = s_N(N + E)$ always vaild?

b) determination of $\Delta G_{concert}$

Figure 1.1. Applications of the electrophilicity parameters of acceptor-substitued olefins investigated in this work.

paring the reported experimental rate constants with those calculated by eq 1.3. Furthermore, many rate constants for the reactions of acceptor-substituted olefins with diazomethanes ([3+2]-cycloaddition)[16] and dienes (Diels-Alder reaction)[17] have previously been reported (Figure 1.1b). The comparison of the experimental rate constants with those calculated by eq 1.3 should allow us to analyze the degree of concertedness ($\Delta G_{concert}$) of these reactions.

As parts of this thesis have been published or submitted for publication, individual introductions will be given at the beginning of each chapter. Some of the presented kinetics have been performed during the master thesis of the author as indicated in the experimental sections.

1.3   References

[1]   (a) C. K. Ingold, *J. Chem. Soc.* **1933**, 1120−1127; (b) C. K. Ingold, *Chem. Rev.* **1934**, *15*, 225−274.

[2]   C. G. Swain, C. B. Scott, *J. Am. Chem. Soc.* **1953**, *75*, 141−147.

[3]   C. D. Ritchie, *Acc. Chem. Res.* **1972**, *5*, 348−354.

[4]   C. D. Ritchie, *Can. J. Chem.* **1986**, *64*, 2239−2250.

[5]   H. Mayr, M. Patz, *Angew. Chem. Int. Ed. Engl.* **1994**, *33*, 938−957.

[6]   (a) H. Mayr, T. Bug, M. F. Gotta, N. Hering, B. Irrgang, B. Janker, B. Kempf, R. Loos, A. R. Ofial, G. Remennikov, H. Schimmel, *J. Am. Chem. Soc.* **2001**, *123*, 9500−9512; (b) H. Mayr, B. Kempf, A. R. Ofial, *Acc. Chem. Res.* **2003**, *36*, 66−77; (c) H. Mayr, A. R. Ofial, *Pure Appl. Chem.* **2005**, 1807−1821; (d) H. Mayr, A. R. Ofial, *J. Phys. Org. Chem.* **2008**, *21*, 584−595; (e) H. Mayr, S. Lakhdar, B. Maji, A. R. Ofial, *Beilstein J. Org. Chem.* **2012**, *8*, 1458−1478; (f) For a comprehensive database of nucleophilicity parameters   *N*, s_N and   electrophilicity   parameters   *E*,   see http://www.cup.lmu.de/oc/mayr/.

[7]   (a) A. Kakehi, *Heterocycles* **2012**, *85*, 1529-1577; (b) M. J. Gaunt, C. C. C. Johanson, *Chem. Rev.* **2007**, *107*, 5596−5605.

[8]   R. Appel, R. Loos, H. Mayr, *J. Am. Chem. Soc.* **2009**, *131*, 704−714.

[9]   (a) S. Lakhdar, R. Appel, H. Mayr, *Angew. Chem. Int. Ed.* **2009**, *48*, 5034−5037; (b) R. Appel, N. Hartmann, H. Mayr, *J. Am. Chem. Soc.* **2010**, *132*, 17894−17900; (c) R. Appel, H. Mayr, *Chem. Eur. J.* **2010**, *16*, 8610−8614.

[10]   (a) J. Sauer, R. Sustmann, *Angew. Chem. Int. Ed. Engl.* **1980**, *19*, 779−807; (b) R. Huisgen, in *1,3-Dipolar Cycloaddition Chemistry* (Ed.: A. Padwa), Wiley, New York, **1984**, p. 1−176.

[11]   Reactions with C-Nucleophiles: K. T. Finley, D. R. Call, G. W. Sovocool, W. J. Hayles, *Can. J. Chem.* **1967**, *45*, 571-573.

[12]   Reactions with N-Nucleophiles: (a) Y. Ogata, M. Okano, Y. Furuya, I. Tabushi, *J. Am. Chem. Soc.* **1956**, *78*, 5426-5428; (b) N. Ogata, T. Asahara, *Bull. Chem. Soc. Jap.* **1966**, *39*, 1486-1490; (c) M. Friedman, J. S. Wall, *J. Org. Chem.* **1966**, *31*, 2888-2894; (d) I. Šestáková, V. Horák, P. Zuman, *Collect. Czech. Chem. Commun.* **1966**, *31*, 3889-3902; (e) Z. Grunbaum, S. Patai, Z. Rappoport, *J. Chem. Soc. B* **1966**, 1133−1137; (f) K. Sanui, N. Ogata, *Bull. Chem. Soc. Jap.* **1967**, *40*, 1727-1727; (g) H. Shenhav, Z. Rappoport, S. Patai, *J. Chem. Soc. B* **1970**, 469-476; (h) G. J. Dienys, L. J. J. Kunskaite,

A. K. Vaitkevicius, A. V. Klimavicius, *Org. Reactiv., Engl. Ed.* **1975**, *12*, 275-282; (i) J. Szczesna, M. Kostecki, S. Kinastowski, *Rocz. Akad. Roln. Poznaniu* **1988**, *192*, 99-104; (j) J. W. Bunting, A. Toth, C. K. M. Heo, R. G. Moors, *J. Am. Chem. Soc.* **1990**, *112*, 8878-8885; (k) C. K. M. Heo, J. W. Bunting, *J. Org. Chem.* **1992**, *57*, 3570-3578; (l) M. Kostecki, J. Szczesna, S. Kinastowski, *Rocz. Akad. Roln. Poznaniu* **1993**, *256*, 25-32; (m) K. L. Mallik, M. N. Das, *Z. Phys. Chem.* **1960**, *25*, 205-216; (n) M. Friedman, *J. Am. Chem. Soc.* **1967**, *89*, 4709-4713.

[13]　Reactions with O-Nucleophiles: (a) N. Ferry, F. J. McQuillin, *J. Chem. Soc.* **1962**, 103-113; (b) B.-A. Feit, A. Zilkha, *J. Org. Chem.* **1963**, *28*, 406-410; (c) P. Carsky, P. Zuman, V. Horvak, *Collect. Czech. Chem. Commun.* **1965**, *30*, 4316-4336; (d) R. N. Ring, G. C. Tesoro, D. R. Moore, *J. Org. Chem.* **1967**, *32*, 1091−1094; (e) W. G. Davies, E. W. Hardisty, T. P. Nevell, R. H. Peters, *J. Chem. Soc. B, Phys. Org.* **1970**, 998-1004; (f) J. P. Guthrie, *Can. J. Chem.* **1974**, *52*, 2037-2040; (g) B. A. Feit, R. Pazhenchevsky, B. Pazhenchevsky, *J. Org. Chem.* **1976**, *41*, 3246-3250; (h) O. Adomeniene, G. Dienys, Z. Stumbreviciute, *Org. Reactiv., Engl. Ed.* **1978**, *15*, 38-44; (i) J. P. Guthrie, K. J. Cooper, J. Cossar, B. A. Dawson, K. F. Taylor, *Can. J. Chem.* **1984**, *62*, 1441-1445; (j) J. P. Guthrie, J. Cossar, K. F. Taylor, *Can. J. Chem.* **1984**, *62*, 1958-1964.

[14]　Reactions with S-Nucleophiles: (a) M. Morton, H. Landfield, *J. Am. Chem. Soc.* **1952**, *74*, 3523-3526; (b) M. Friedman, J. F. Cavins, J. S. Wall, *J. Am. Chem. Soc.* **1965**, *87*, 3672-3682; (c) T.-R. Kim, S.-J. Yun, B.-B. Park, *Bull. Kor. Chem. Soc.* **1986**, *7*, 25-29.

[15]　Reactions with P-Nucleophiles: I. Petnehazy, G. Clementis, Z. M. Jaszay, L. Toke, C. D. Hall, *J. Chem. Soc., Perkin Trans. 2* **1996**, 2279-2284.

[16]　[3+2]-Cycloadditions: (a) R. Huisgen, H. Stangl, H. J. Sturm, H. Wagenhofer, *Angew. Chem.* **1961**, *73*, 170; (b) A. Ledwith, Y. Shih-Lin, *J. Chem. Soc. B* **1967**, 83−84; (c) L. Fisera, J. Geittner, R. Huisgen, H.-U. Reissig, *Heterocycles* **1978**, *10*, 153−158; (d) J. Geittner, R. Huisgen, H.-U. Reissig, *Heterocycles* **1978**, *11*, 109−112; (e) G. Swieton, J. Von Jouanne, H. Kelm, R. Huisgen, *J. Org. Chem.* **1983**, *48*, 1035−1040; (f) T. Oshima, T. Nagai, *Tetrahedron Letters* **1985**, *26*, 4785−4788; (g) R. Huisgen, E. Langhals, *Tetrahedron Lett.* **1989**, *30*, 5369−5372.

[17]　Diels-Alder reactions: (a) J. Sauer, D. Lang, A. Mielert, *Angew. Chem., Int. Ed. Engl.* **1962**, *1*, 268−269; (b) J. Sauer, H. Wiest, A. Mielert, *Chem. Ber.* **1964**, *97*, 3183−3207; (c) J. Sauer, D. Lang, H. Wiest, *Chem. Ber.* **1964**, *97*, 3208−3218; (d) B. Blankenburg, H. Fiedler, M. Hampel, H. G. Hauthal, G. Just, K. Kahlert, J. Korn, K. H. Müller, W. Pritzkow, Y. Reinhold, M. Röllig, E. Sauer, D. Schnurpfeil, G. Zimmermann, *J. Prakt.*

Chem. **1974**, *316*, 804−816; (e) M. W. Lee, W. C. Herndon, *J. Org. Chem.* **1978**, *43*, 518−518; (f) A. Meijer, S. Otto, J. B. F. N. Engberts, *J. Org. Chem.* **1998**, *63*, 8989−8994.

2 The Wide Mechanistic Spectrum of Ammonium Ylide Mediated Cyclopropanations

Dominik S. Allgäuer, Peter Mayer, Konstantin Troshin, and Herbert Mayr

2.1 Introduction

Ammonium ylides are important reagents in organic synthesis.[1-5] They are intermediates in various rearrangements e.g., Stevens- and Sommelet-rearrangements,[6] and are used for the syn-

Scheme 2.1. Reactions of ammonium yides with aldehydes.[2]

thesis of epoxides from carbonyl compounds[2] (Scheme 2.1). Catalytic enantioselective cyclopropanations of Michael acceptors by ammonium ylides have been described by Papageorgiou, Ley, and Gaunt[7] to provide a straightforward stereoselective access to cyclopropanes (Scheme 2.2). Due to the large number of readily available chiral tertiary amines, this application has significantly increased the interest in ammonium ylides in recent years.[3a, b, 4, 5, 7]

So far, relative reactivities of ylides have mostly been associated with the acidities of their precursor salts (Table 2.1),[8] though the correlation between acidities and reactivities of carbon centered nucleophiles[9] is known to be only moderate even when reactions at the same centers are compared.[10]

While the mechanisms of sulfonium ylide mediated epoxidations and cyclopropanations have intensely been studied,[11] most kinetic and theoretical studies on reactions of ammonium ylides focused on rearrangement reactions,[12] and only few studies dealt with the mechanisms of ammonium ylide mediated epoxidations[13] or cyclopropanations.[14] Quantitative data on the nucleophilic reactivities of ammonium ylides have so far not been reported. Aggarwal and others[15] demonstrated that the leaving group abilities of R_3N,[2b, 13-14, 15c] as well as those of R_2S,[14, 15c] and R_3P[14, 15c] have a big influence on the course of the reactions.

Scheme 2.2. Organocatalytic cyclopropanations of Michael acceptors by ammonium ylides.[7c]
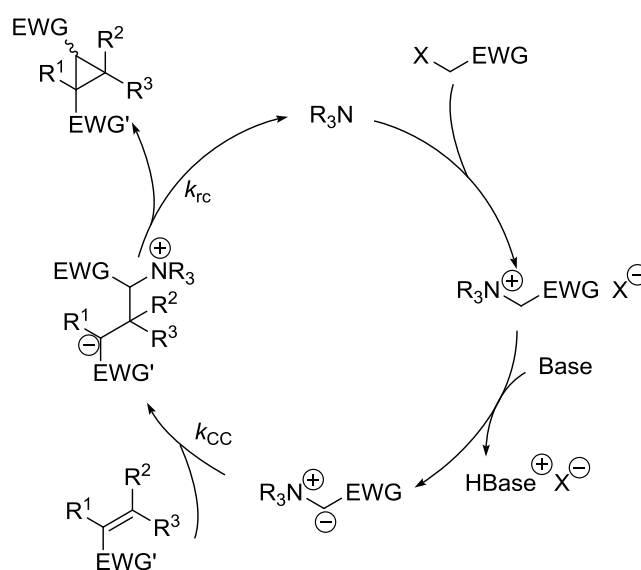
We recently studied the kinetics of the reactions of phosphonium,[16] sulfonium,[17] and pyridinium ylides.[18] with carbocations and Michael acceptors and showed that the rates of these reactions can be described by eq 2.1, where k_{CC} is the second-order rate constant in M^{-1} s^{-1} (at 20 °C), s_N is a nucleophile-specific sensitivity parameter, N is a nucleophilicity parameter, and E is an electrophilicity parameter.[16-18, 19]

$$\log k_{CC} = s_N (N + E) \tag{2.1}$$

In this way, ylides were included into the comprehensive nucleophilicity scale shown in ref. [19i] which provides a direct comparison of many different classes of nucleophiles.

We have now studied the kinetics and mechanisms of the reactions of the ammonium ylides **1a–i** (Table 2.1) with benzhydrylium ions **2a–d**, quinone methides **3a–f**, and benzylidene malonates **4a–d** which we generally employ as reference electrophiles, as well as with other common Michael acceptors, such as the benzylidene indandiones **5a–c** and the chalcone **6** (Chart 2.1). The results will be used to rationalize the changes of mechanism of ammonium ylide mediated cyclopropanations and to determine the nucleophilicity parameters of the ammonium ylides **1** as defined by eq 1.

Table 2.1. Synthesis[7a] and pK_a values of the ammonium salts 1H⁺X⁻ employed as precursors for the ammonium ylides 1 and UV absorption maxima of the ylides 1.

NR₃	X	EWG	Salt	Yield/%	pK_a(DMSO)[a]	Ylide	λ_{max}(DMSO)/nm
DABCO	Br	CN	**1aH⁺Br⁻**	quant.	(20.6)[c]	**1a**	<256
DABCO	Cl	CONEt₂	**1bH⁺Cl⁻**	91	(24.9)[c]	**1b**	<256
DABCO	Br	CO₂Et	**1cH⁺Br⁻**	quant.	(20.0)[c]	**1c**	<258
DABCO	Cl	COMe	**1dH⁺Cl⁻**	76	(16.3)[c]	**1d**	<260
			1dH⁺OTf⁻	83[b]	(16.3)[c]		
DABCO	Br	COPh	**1eH⁺Br⁻**	80	(14.6)[c]	**1e**	<257, 310
DABCO	Br	CO₂ᵗBu	**1fH⁺Br⁻**	95	(~21)[d]	**1f**	not determined
Quinuclidine	Br	CO₂Et	**1gH⁺Br⁻**	71	(20.0)[c]	**1g**	not determined
NMe₃	Br	CO₂Et	**1hH⁺Br⁻**	83	20.0[c]	**1h**	not determined
NMe₃	Br	COPh	**1iH⁺Br⁻**	quant.	14.6[c]	**1i**	<257, 307

[a] The pK_a-values of ⁺NMe₃-substituted salts were assumed to be good approximations for the structurally analogous DABCO⁺-compounds. Since benzoyl-substituted ammonium salts with quinuclidinium- and ⁺NMe₃-moiety have the same pK_a-values [8c, d]; [b] Synthesized by treatment of **1dH⁺Cl⁻** with TMS-OTf in MeCN under N₂ at 20 °C (for details see Experimental Section); [c] pK_a-value from ref. [8c]; [d] Estimated from the pK_a-value of **1cH⁺Br⁻** and ΔpK_a ≈ 1 of ethyl and *tert*-butyl phenylacetate.[20] .

2a E = -7.02

2b E = -8.76

2c E = -9.45 (n = 2)
2d E = -10.04 (n = 1)

3a E = -12.18 (R₁ = OMe)
3b E = -13.39 (R₁ = NMe₂)

3c E = -15.83 (R₂ = Me)
3d E = -16.11 (R₂ = OMe)
3e E = -17.29 (R₂ = NMe₂)

3f E = -17.90

4a E = -17.67 (R₃ = *p*-NO₂)
4b E = -18.98 (R₃ = *m*-Cl)
4c E = -20.55 (R₃ = H)
4d E = -21.11 (R₃ = *p*-Me)

5a E = -10.11 (R₄ = H)
5b E = -11.32 (R₄ = OMe)

5c E = -14.68

6 E = -17.33
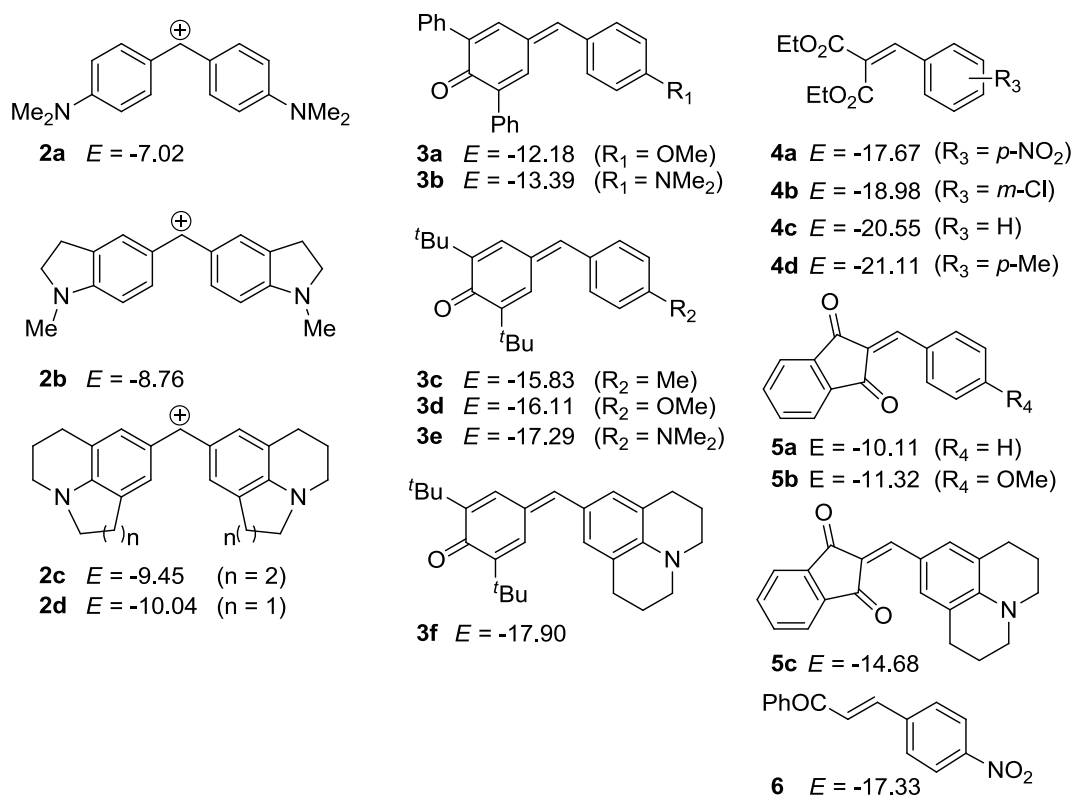
Chart 2.1. Electrophiles Employed in this Work.[11b, 19b, c, f, 21]

Because of their low stability at room temperature, the ylides **1a−i** were not isolated but generated in solution by treating their conjugate acids **1H⁺X⁻** with a base. The ammonium salts **1H⁺X⁻** listed in Table 2.1 were obtained by a Menschutkin reaction from the corresponding tertiary amines and alkyl halides in THF, according to a recently reported procedure.[7a]

2.2 General

2.2.1 Mechanistic Scenarios

The ylides **1** have been reported to react with Michael acceptors via zwitterionic intermediates (Scheme 2.3), [3a, b, 7, 14] which may be formed irreversibly or reversibly with the rate constant k_{CC} for the forward and the rate constant k_{-CC} for the backward reaction. The ring closure proceeds with the rate constant k_{rc} (Scheme 2.3; eqs 2.2–2.4).

Scheme 2.3. Mechanism of the reaction of ammonium ylides (Nu) with Michael acceptors (E) via intermediate betaines (I) to cyclopropanes (P).
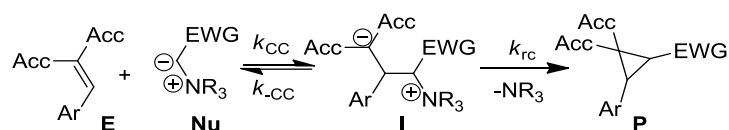
$$\frac{d[\mathbf{E}]}{dt} = -k_{CC}[\mathbf{E}][\mathbf{Nu}] + k_{-CC}[\mathbf{I}] \qquad (2.2)$$

$$\frac{d[\mathbf{I}]}{dt} = k_{CC}[\mathbf{Nu}][\mathbf{E}] - k_{-CC}[\mathbf{I}] - k_{rc}[\mathbf{I}] \qquad (2.3)$$

$$\frac{d[\mathbf{P}]}{dt} = k_{rc}[\mathbf{I}] \qquad (2.4)$$

One can now differentiate four extreme cases, depending on the relative rates of the various steps:

In the first two cases the intermediate betaine **I** is formed as a short-lived species and the steady state approximation holds (eq 2.5). In case 1a (eq 2.6), the backward reaction k_{-CC} is much slower than the ring closure k_{rc}, i.e., the intermediate betaine **I** is formed irreversibly, and the rate constants which are derived from the decays of the absorbances of the Michael acceptors (**E**) thus correspond to k_{CC}.

In case 1b (eq 2.7), the backward reaction k_{-CC} is much faster than the ring closure k_{rc}, i.e., the formation of the betaine is highly reversible, and the observed second-order rate constants k_{2obs}, which are derived from the mono-exponential decays of the absorbances of the Michael acceptors (**E**), equal $K \cdot k_{rc}$. These two cases (case 1a,b, eqs 2.6, 2.7) cannot simply be discriminated kinetically, as both cases follow a second-order rate law.

Case 1: $\dfrac{d[\mathbf{I}]}{dt} = 0$ $\Rightarrow$ $\dfrac{d[\mathbf{P}]}{dt} = -\dfrac{d[\mathbf{E}]}{dt} = \dfrac{k_{CC}k_{rc}[\mathbf{Nu}][\mathbf{E}]}{k_{-CC} + k_{rc}}$ (2.5)

Case 1a: $k_{-CC} \ll k_{rc}$ $\Rightarrow$ $\dfrac{d[\mathbf{P}]}{dt} = -\dfrac{d[\mathbf{E}]}{dt} = k_{CC}[\mathbf{Nu}][\mathbf{E}]$ (2.6)

Case 1b: $k_{-CC} \gg k_{rc}$ $\Rightarrow$ $\dfrac{d[\mathbf{P}]}{dt} = -\dfrac{d[\mathbf{E}]}{dt} = \dfrac{k_{CC}}{k_{-CC}} k_{rc}[\mathbf{Nu}][\mathbf{E}] = Kk_{rc}[\mathbf{Nu}][\mathbf{E}]$ (2.7)

with the equilibrium constant $K = \dfrac{k_{CC}}{k_{-CC}}$

In cases 2a and 2b the formation of the intermediate betaine **I** is much faster than its ring closure to cyclopropane **P** and the backward reaction ($v_{CC} \gg v_{-CC}$ and $v_{CC} \gg v_{rc}$; as reactions of different order are compared, we have to refer to rates, not to rate constants). In both cases the intermediate betaine **I** accumulates, and the rate constant which is derived from the consumption of the Michael acceptor (**E**) equals the rate of the formation of the intermediate betaine **I** (k_{CC}, eq 2.8). The backward reaction may be slower than the subsequent ring closure (case 2a, $k_{-CC} < k_{rc}$), or the backward reaction may be faster than the ring closure (case 2b, $k_{-CC} > k_{rc}$). The rate of the formation of the cyclopropane **P** (k_{rc}) by ring closure of the intermediate betaine **I** may be determined separately.

Case 2: $v_{CC} \gg v_{-CC}, v_{rc}$ $\qquad \dfrac{d[\mathbf{I}]}{dt} \neq 0$

Case 2a: $k_{-CC} < k_{rc}$

Case 2b: $k_{-CC} > k_{rc}$

First step (Cases 2a,b): $\dfrac{d[\mathbf{I}]}{dt} = -\dfrac{d[\mathbf{E}]}{dt} = k_{CC}[\mathbf{Nu}][\mathbf{E}]$ (8)

Second step (Cases 2a,b): $-\dfrac{d[\mathbf{I}]}{dt} = \dfrac{d[\mathbf{P}]}{dt} = k_{rc}[\mathbf{I}]$

2.2.2   Kinetic Methods

The kinetics of most reactions of the ammonium ylides **1** with the electrophiles **2–6** were monitored photometrically by following the disappearance of the colored electrophiles in the presence of more than 10 equiv. of the ylides **1** (pseudo-first-order conditions). Some kinetics were followed by ^{1}H NMR and GC as described in the Experimental Section.

Solutions of the ylides **1** were generated by combining freshly prepared solutions of the ammonium salts **1H$^+$X$^-$** and KO^{t}Bu (1.05 eq) in DMSO directly before the kinetic experiments. The formations of the ylides **1a–e,i** were verified by their UV–vis spectra (Table 2.1). To assure, that the ammonium salts **1H$^+$X$^-$** were quantitatively deprotonated under these conditions, the ammonium salt with the highest pK_a-value in the series (**1bH$^+$Cl$^-$**; pK_a = 24.9 in DMSO)[8d] was titrated with a solution of KO^{t}Bu in DMSO. Monitoring the absorbance of the ylide **1b** at 256 nm (for details see Experimental Section) showed that complete deprotonation of **1bH$^+$** was achieved with one equivalent of KO^{t}Bu, since further addition of KO^{t}Bu did not lead to an increase of the absorbance due to an increase of the concentration of the ylide **1b**. Combination of the electrophiles **2–6** with more than 10 equivalents of the ammonium ylides **1** usually resulted in monoexponential decays of the UV–vis absorbances of the electrophiles (Figure 2.1a), from which first-order rate constants k_{obs} were derived by least-squares fitting of the exponential function $A_t = A_0 \exp(-k_{obs}t)$ to the time-dependent absorbances A_t of the electrophiles **2–6**. Plots of k_{obs} (s^{-1}) versus the concentrations of the nucleophiles **1** were linear with negligible intercepts in most cases, and the slopes of these plots gave the second-order rate constants (Figure 2.1b).
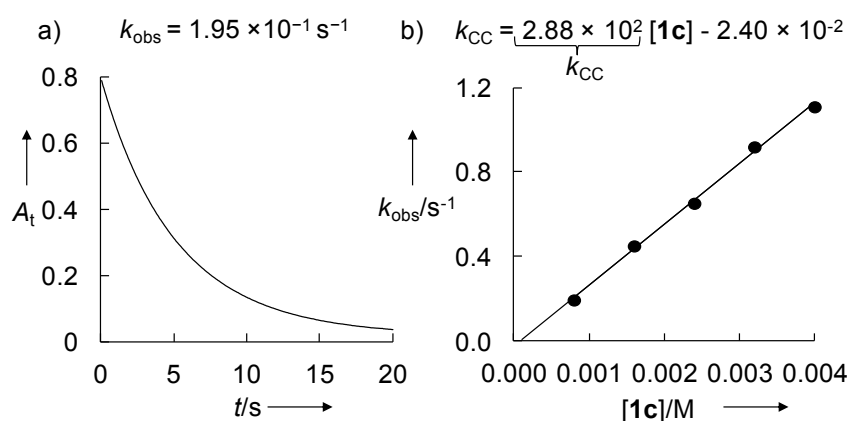
Figure 2.1. a) Decay of the absorbance of 3d ([3d]$_0$ = 4.00 × 10^{-5} M) at 393 nm during its reaction with 1c ([1c]$_0$ = 8.00 × 10^{-4} M) in DMSO at 20 °C. b) Linear correlation of k_{obs} with the concentration of 1c.

Several kinetic experiments have been repeated by using only 0.5 equivalents of KO^{t}Bu for the deprotonation of the salts **1H$^+$X$^-$**. In these experiments the concentrations of the ylides **1** correspond to the initial concentration of KO^{t}Bu, and the second-order rate constants agreed within 10% with those measured with 1.05 equivalents of KO^{t}Bu (for details see Experimental Section).

2.3 Results

2.3.1 Reactions with the Benzhydrylium Salts 2-BF$_4$

The bis(4-dimethylamino)benzhydrylium tetrafluoroborate **2a-BF$_4$** was chosen as representative electrophile to examine the course of the reactions of the stabilized benzhydrylium ions with **1a–i**. Slow addition of potassium *tert*-butoxide (KO^{t}Bu) to equimolar solutions of the benzhydrylium tetrafluoroborate **2a-BF$_4$** and the ammonium salts **1H$^+$X$^-$** in (MeCN:CH$_2$Cl$_2$)-mixtures at room temperature gave rise to the formation of the ammonium salts **7(a–i)-BF$_4$**, which were purified by recrystallization (Table 2.2). Most of the ammonium salts where obtained as tetrafluoroborates **7-BF$_4$**; only the ammonium salt **7d-OTf** was isolated as triflate (verified by fluorine coupling in the ^{13}C NMR and by HRMS).

Table 2.2. Reaction of the ylides 1 with the benzhydrylium tetrafluoroborate 2a-BF$_4$.
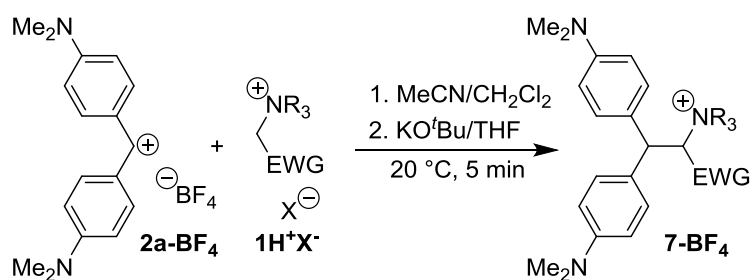
Salt	NR$_3$	EWG	Product	Yield/%[a]
1aH$^+$Br$^-$	DABCO	CN	**7a-BF$_4$**	21 (96)
1bH$^+$Cl$^-$	DABCO	CONEt$_2$	**7b-BF$_4^-$**	5 (91)
1cH$^+$Br$^-$	DABCO	CO$_2$Et	**7c-BF$_4$**	27
1dH$^+$OTf$^-$	DABCO	COMe	**7d-OTf**	73
1eH$^+$Br$^-$	DABCO	COPh	**7e-BF$_4$**	45 (94)
1fH$^+$Br$^-$	DABCO	CO$_2^t$Bu	**7f-BF$_4$**	78
1gH$^+$Br$^-$	Quinuclidine	CO$_2$Et	**7g-BF$_4$**	77
1hH$^+$Br$^-$	NMe$_3$	CO$_2$Et	**7h-BF$_4$**	51 (87)
1iH$^+$Br$^-$	NMe$_3$	COPh	**7i-BF$_4$**	76

[a] After recrystallization from MeCN or MeCN/Et$_2$O; Yields of the crude products in parentheses.

As mentioned above, the kinetics of these reactions were followed by monitoring the absorbances of the benzhydrylium ions **2** after adding >10 equiv. of the ylides **1**. All reactions led to complete consumption of the benzhydrylium ions **2** and followed a second-order rate law with the second-order rate constants k_{CC} listed in Table 2.3. The reactions of the ammonium ylides **1a**,**b** with the benzhydrylium ions **2** are too fast to be measured with our techniques.

Table 2.3. Rate constants for the reactions of the ammonium ylides 1 with the benzhydrylium ions 2 in DMSO at 20 °C.

$$\ominus\!\!\overset{\text{EWG}}{\underset{\oplus\text{NR}_3}{\big\langle}}$$

Ylide	NR$_3$	EWG	Ar$_2$CH$^+$ (**2**)	k_{CC}/M^{-1} s^{-1}
1c	DABCO	CO$_2$Et	**2d**	5.92×10^5
1d	DABCO	COMe	**2b**	1.41×10^5
			2c	3.69×10^4
1e	DABCO	COPh	**2c**	1.63×10^5
			2d	1.32×10^5
1f	DABCO	CO$_2{}^t$Bu	**2d**	2.52×10^5
1g	Quinuclidine	CO$_2$Et	**2d**	7.31×10^5
1h	NMe$_3$	CO$_2$Et	**2c**	6.88×10^5
			2d	6.77×10^5
1i	NMe$_3$	COPh	**2c**	4.08×10^4
			2d	3.24×10^4

2.3.2 Reactions with the Quinone Methides 3

In the reactions of the ylides **1** with the quinone methide **3c**, which was studied as a representative for **3a−f**, the spirocycles **9** were formed with variable stereoselectivity (Table 2.4), as derived from the NOESY correlations of the protons and the substituents of the cyclopropane rings. In addition, the structures of the spirocycles **9bc** and **9cc** were confirmed by the crystal structures of *cis*-**9bc** and *trans*-**9cc** as depicted in Figure 2.2.

While the reaction of the cyano-substituted ylide **1a** with **3c** gave **9ac** as a 33:67 mixture of *trans*:*cis* isomers, the amido-substituted ylide **1b** gave preferentially the *trans*-cyclopropane **9bc**, and the ester substituted ylides **1c**,**f–h** gave the *trans*-cyclopropanes **9cc** and **9fc** exclusively (Table 2.4). The reactions of the benzoyl-substituted ylides **1e**,**i** with **3c** yielded equal amounts of both diastereoisomers of **9ec**. In the reaction of **3c** with the acetyl substituted ylide **1d** no cyclopropanation product and only decomposition of the ylide was observed.

31

Table 2.4. Reactions of the ylides 1 with the quinone methide 3c. The first letter of the product number refers to the employed ylide 1, the second to the quinone methide 3.
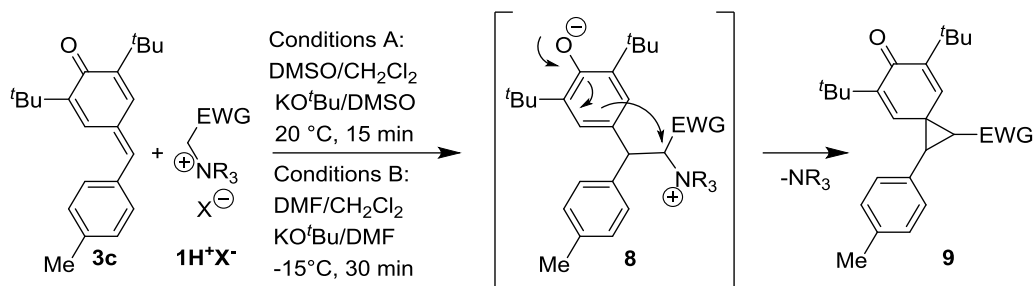
Salt	NR$_3$	EWG	Conditions	Betaine 8	Spirocycle	Yield 9/%[a]	(*trans*:*cis*)-9[b]
1aH$^+$Br$^-$	DABCO	CN	A	**8ac**	**9ac**	52	33:67
			B	**8ac**	**9ac**	(58)[d]	33:67
1bH$^+$Br$^-$	DABCO	CONEt$_2$	A	**8bc**	**9bc**	65	75:25
			B	**8bc**	**9bc**	87	83:17
1cH$^+$Br$^-$	DABCO	CO$_2$Et	A	**8cc**	**9cc**	83[c]	>95:5
			B[c]	**8cc**	**9cc**	(56)[c, d]	>95:5
1dH$^+$Cl$^-$	DABCO	COMe	A	**8dc**	**9dc**	0[c]	-
1eH$^+$Br$^-$	DABCO	COPh	A	**8ec**	**9ec**	64	50:50
			B	**8ec**	**9ec**	68	60:40
1fH$^+$Br$^-$	DABCO	CO$_2${\it t}Bu	A	**8fc**	**9fc·H$_2$O**	76[e]	>95:5
1gH$^+$Br$^-$	Quinuclidine	CO$_2$Et	A	**8gc**	**9gc (= 9cc)**	38	>95:5
1hH$^+$Br$^-$	NMe$_3$	CO$_2$Et	A	**8hc**	**9hc (= 9cc)**	33	>95:5
1iH$^+$Br$^-$	NMe$_3$	COPh	A	**8ic**	**9ic (= 9ec)**	57[c]	50:50

[a] After recrystallization from EtOH; [b] Determined by ^{1}H NMR of the crude product; [c] Reaction time 2 h; [d] Yield of the crude product; the product decomposed during the attempted purification by crystallization from MeOH; [e] Crystallization from CH$_2$Cl$_2$:*iso*-hexane.
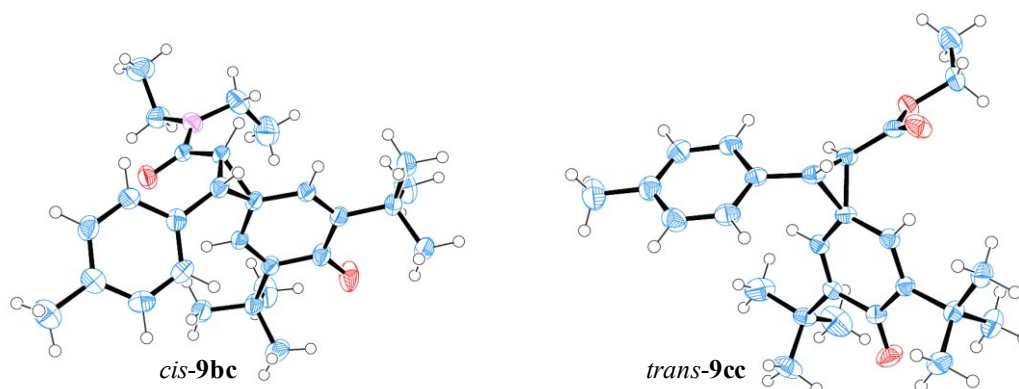
cis-**9bc**   *trans*-**9cc**

Figure 2.2. ORTEP-drawing of the crystal structure of *cis*-9bc and *trans*-9cc (thermal ellipsoids are shown at the 50% probability level).

Variation of the solvent (DMSO → DMF) and temperature (20 °C → − 15 °C) had little effect on the yields and stereoselectivities of the cyclopropanations (Table 2.4). Only for the reaction of **1b** with **3c**, and for the reaction of **1e** with **3c** a small change of stereoselectivity was observed, when the reactions were carried out in DMF at −15 °C instead of DMSO at 20 °C (Table 2.4, Conditions A→B).

As shown in Figure 2.1a, the absorbance of the quinone methide **3d** decayed mono-exponentially when combined with an excess of the ylide **1c** (pseudo-first order conditions) to give the first-order rate constant k_{obs} which increased linearly with the concentration of **1c** (Figure 2.1b). The same behavior, i.e., second-order kinetics with complete consumption of the quinone methides was observed for all reactions of the cyano-substituted ylide **1a**, of the amido-substituted ylide **1b**, and of the ester-substituted ylides **1c** and **1f–h**. The resulting second-order rate constants are listed in Table 2.5.

When the reactions of the ylides **1a–c** with equimolar amounts of the quinone methide **3c** were monitored by ^{1}H NMR in (DMSO-d_6 : CD$_2$Cl$_2$)-mixtures at 20 °C, the cyclopropanes **9ac–cc** were observed immediately after mixing the reactants, and neither ylides **1a–c** nor the intermediate betaines **8ac–cc** were observable. Monitoring the reaction of the ester-substituted trimethylammonium ylide **1h** with quinone methide **3f** by UV–vis spectroscopy showed a monoexponential decay of **3f** and gave no evidence for the formation of a long-lived intermediate betaine **8hf**, indicating that the reaction proceeds according to case 1. A mechanism according to case 1 can thus also be expected for the reactions of the other structurally related ester-substituted ammonium ylides **1c**,**f**,**g** with the quinone methide **3f**. Further evidence, which is presented below, indicates that case 1a, i.e., irreversible betaine formation with fast subsequent cyclization is also realized in the reactions of the cyano, amido, and ester-substituted ammonium ylides **1a–c**,**g–h** with the quinone methides **3**.

Table 2.5. Rate constants for the reactions of the ammonium ylides 1 with the quinone methides 3 in DMSO at 20 °C.

1	NR$_3$	EWG	3	k_{CC}/M^{-1} s^{-1}	$K \cdot k_{rc}$/M^{-1} s^{-1}	K/M^{-1}	k_{rc}/s^{-1}	Case[a]
1a	DABCO	CN	**3b**	2.47×10^5				1a
			3c	1.43×10^4				1a
			3d	1.04×10^4				1a
			3e	3.36×10^3				1a
			3f	1.32×10^3				1a
1b	DABCO	CONEt$_2$	**3a**	1.59×10^5 [b]				1a
			3a	1.57×10^5				1a
			3b	2.18×10^4 [b]				1a
			3c	5.07×10^3				1a
			3d	2.87×10^3				1a
1c	DABCO	CO$_2$Et	**3a**	4.68×10^4				1a
			3b	9.69×10^3				1a
			3c	4.85×10^2				1a
			3d	2.87×10^2				1a
			3e	4.50×10^1				1a
			3f	2.26×10^1				1a
1d	DABCO	COMe	**3a**	2.08×10^3 [b]	-	-	-	1b/2b
			3b	3.45×10^2 [b]	6.09	(1.6×10^2)	(3.8×10^{-2})[c]	1b/2b
1e	DABCO	COPh	**3a**	3.82×10^3	-	-	-	1b/2b
			3b	3.60×10^2	2.45	2.79×10^2	8.79×10^{-3}	1b/2b
			3c		(1.9×10^{-3})[d]			1b
1f	DABCO	CO$_2^t$Bu	**3b**	9.51×10^3				1a
			3c	6.49×10^2				1a
			3d	3.81×10^2				1a
			3e	6.80×10^1				1a
			3f	2.49×10^1				1a
1g	Quinuclidine	CO$_2$Et	**3a**	6.84×10^4				1a
			3b	6.33×10^3				1a
			3c	3.49×10^2				1a
1h	NMe$_3$	CO$_2$Et	**3a**	7.15×10^4				1a
			3b	1.12×10^4				1a
			3c	6.77×10^2				1a
			3d	4.67×10^2				1a
			3e	8.03×10^1				1a
			3f	4.37×10^1				1a
1i	NMe$_3$	COPh	**3b**	2.25×10^2	3.89[e]	(4×10^1)	(1×10^{-1})[c]	1b/2b

[a] Assignment of the individual reactions to the different cases see below; [b] Deprotonation of the conjugate CH-acids **1H$^+$X$^-$** with 0.5 equiv. of KO^{t}Bu; [c] Estimated from $K \cdot k_{rc}$; [d] $K \cdot k_{rc}$ estimated from ^{1}H NMR monitoring (see Figure 2.5); [e] Kinetics were reproduced on a diode array spectrophotometer and conventionally evaluated (cf. Figure 2.1; $K \cdot k_{rc} \sim 3.1$ M^{-1} s^{-1}).

In the reactions of the quinone methides **3a,b** with the less basic acetyl and benzoyl-substituted ylides **1d,e,i** ($pK_{aH} = 15$–16 in DMSO) we did not observe mono-exponential decays of the quinone methides **3a,b** when working under pseudo-first-order conditions. Instead, fast partial consumption of the absorbance of **3a,b** on the millisecond to second time scale was observed (Figure 2.3a, Inset), followed by complete consumption of the quinone methides **3a,b** on the minute to hour time scale (Figure 2.3a).

The initial fast and incomplete decays of the absorptions of the quinone methides **3a,b** were assigned to the reversible formations of the betaines **8**, while the slow subsequent decays were attributed to the formation of the cyclopropanes **9** (Table 2.4).

From the fast initial decays of the absorbances of the quinone methides **3a,b** (e.g. Figure 2.3a, Inset) first-order rate constants k_{obs} were derived as described above (see Figure 2.1). Plots of k_{obs} versus the concentration of the acyl-substituted ylides **1d,e,i** gave linear correlations from which the rate of the formation of the betaines **8** (k_{CC}) were derived.

The pseudo-first-order rate constants for the slow subsequent decays of the absorbances of the quinone methides **3a,b** depend on the equilibrium constant $K = k_{CC}/k_{-CC}$ (eq 2.7) and k_{rc}, as expressed by eq 2.9, which is derived in the General Section of the Experimental Section.
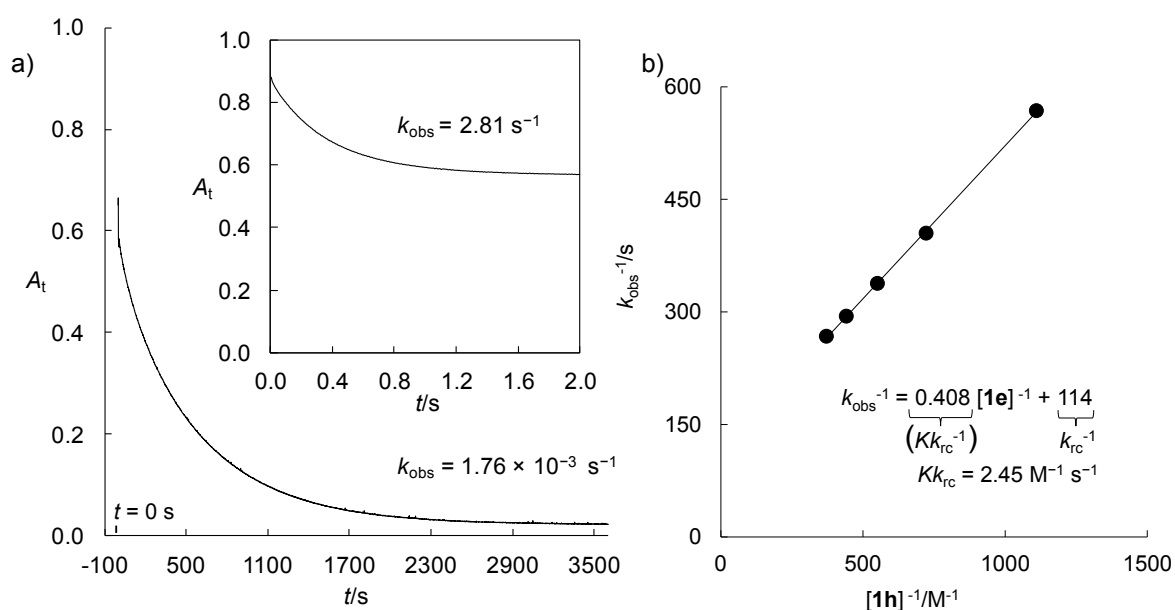
Figure 2.3. a) Slow decay of the absorbance of 3b ([3b]$_0$ = 1.80 × 10^{-5} M) at 533 nm during the reaction with 1e ([1e]$_0$ = 9.01 × 10^{-4} M) in DMSO at 20 °C (conventional photometry). Inset: Fast decay of the absorbance of 3b ([3b]$_0$ = 4.00 × 10^{-5} M) at 533 nm during the equilibrium reaction with 1e ([1e]$_0$ = 2.40 × 10^{-3} M) in DMSO at 20 °C (Stopped-flow photometry); b) Plot of k_{obs}^{-1} of the second decay versus [1e]$^{-1}$ for the determination of k_{rc} and K.

35

$$\frac{1}{k_{\text{obs}}} = \frac{1}{Kk_{\text{rc}}} \cdot \frac{1}{[\text{Nu}]} + \frac{1}{k_{\text{rc}}} \tag{2.9}$$

The plot of $1/k_{\text{obs}}$ versus $1/[\mathbf{1e}]$ for the reaction of the quinone methide **3b** with ylide **1e** was found to be linear (Figure 2.3b) with $1/k_{\text{rc}}$ as the intercept and $1/K \cdot k_{\text{rc}}$ as the slope, from which the rate of ring closure k_{rc} and the equilibrium constant K were derived as given in Table 2.5. The equilibrium constant K derived in this way agrees well with the equilibrium constant calculated from the ratio of the absorbances of **3b** at $t = 0$ and at the plateau of the A versus t correlation, which is reached when the initial equilibrium is established (for details see Experimental Section).

Plots of $1/k_{\text{obs}}$ versus $1/[\text{Nu}]$ for the second part of the reactions of the acyl-substituted ylides **1d,i** with the quinone methide **3b** are also linear, but the intercepts $1/k_{\text{rc}}$ are close to zero so that k_{rc} cannot reliably be derived from these plots. However, the slopes of these correlations, which correspond to $1/(K \cdot k_{\text{rc}})$, could be used to calculate $K \cdot k_{\text{rc}}$ and the separation into K and k_{rc} had to be achieved differently.

The equilibrium constants K of the reactions of the acyl-substituted ylides **1d,i** with the quinone methide **3b** could be determined from the initial absorbances (A_0) of the quinone methide **3b** and the plateaus of the absorbances (A_{eq}) observed when after the initial fast reaction on the millisecond to second timescale have reached equilibrium.

Figure 2.4 shows a linear correlation between $(A_0 - A_{\text{eq}})/A_{\text{eq}}$ and $[\mathbf{1d}]$, the slope of which corresponds to the equilibrium constant K as defined by eq 2.10. As the equilibrium constants K determined in this way are not very precise, the rate constants for ring-closure k_{rc} which are obtained by dividing $K \cdot k_{\text{rc}}$ by K are less accurate and are given in parentheses in Table 2.5.
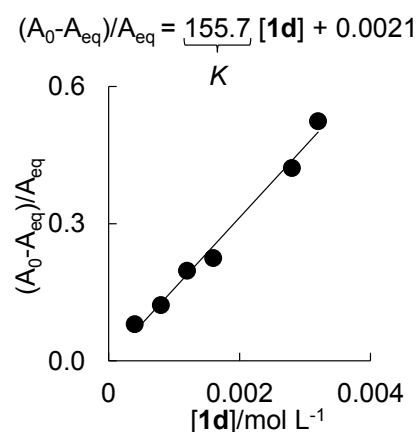
Figure 2.4. Determination of the equilibrium constant K for the reaction of 1e with 3b from plots of $(A_0 - A_{\text{eq}})/A_{\text{eq}}$ vs [1d].

$$K = \frac{[\text{I}]}{[\text{E}][\text{Nu}]} = \frac{A_0 - A_{\text{eq}}}{A_{\text{eq}}[\text{Nu}]} \qquad \Rightarrow \qquad K[\text{Nu}] = \frac{A_0 - A_{\text{eq}}}{A_{\text{eq}}} \tag{2.10}$$

For the reactions of the acyl-substituted ylides **1d**,**e** with the quinone methide **3a** only the first part, which corresponds to the reversible formations of the betaines **8da** and **8ea**, could be evaluated ($k_{CC;}$ Table 2.5), since the decay of the absorbance in the second part of the reaction was not mono-exponential. A determination of the equilibrium constants K was not possible.

The kinetics of the reactions of the less basic acyl-substituted ylides **1d**,**e**,**i** with the quinone methides **3a**,**b** indicate the partial conversion of the reactants into the betaines **8** in a fast reversible initial reaction, i.e., $k_{–CC} > k_{rc}$. According to eq 7, case 1b refers to reactions with infinitesimal concentrations of the intermediate betaine, while case 2b refers to reactions with complete reversible conversion of the reactants into the intermediates, we are now dealing with borderline cases between 1b and 2b.

^{1}H NMR spectroscopic monitoring of the reaction of equimolar amounts of the benzoyl-substituted ylide **1e** with the quinone methide **3c** in DMSO-d_6/CD$_2$Cl$_2$ showed the gradual decrease of the reactants **1e** and **3c** and the increasing amount of the cyclopropane **9ec** and DABCO during 3 h, while the intermediate betaine **8ec** was not detectable. The progress of the reaction was derived from the ^{1}H NMR signals of liberated DABCO (for details see Experimental Section). The second-order rate law for reactions with equal concentrations of the reactants is given by eq 2.11,[22] and plots of 1/[**3c**] versus time t gave a linear correlation for the first 20 min of the reaction with a slope of k_{2obs} and an intercept of 1/[**1h**]$_0$ (eq 2.11; Figure 2.5). For higher conversions the obtained data points deviate from the correlation line and were thus not included to determine k_{2obs}.

From the non-observance of an intermediate betaine in the reaction of ylide **1e** with quinone methide **3c** we conclude that the reaction follows case 1, and later we will show that it can be assigned to case 1b (Table 2.5) and the measured second-order rate constant k_{2obs} corresponds to $K{\cdot}k_{rc}$.

$$[\mathbf{1e}]^{-1} = 1.91 \times 10^{-3}\, t + 21.2$$
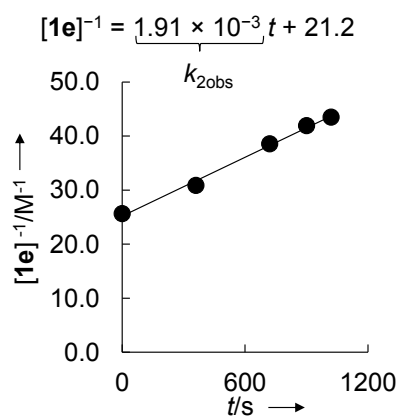
Figure 2.5. Determination of the second-order rate constant k_{2obs} (1.9×10^{-3} M^{-1} s^{-1}) for the reaction of 1e (5.00×10^{-2} M) with 3c (4.98×10^{-2} M) by ^{1}H NMR in DMSO-d_6 at 20 °C.

37

$$\frac{d[E]}{dt} = -k_{2obs}[E] \qquad \Rightarrow \qquad \frac{1}{[E]} - \frac{1}{[E]_0} = k_{2obs}t \qquad \Rightarrow \qquad \frac{1}{[E]} = k_{2obs}t + \frac{1}{[E]_0} \qquad (2.11)$$

when $[Nu]_0 \approx [E]_0$

$[Nu] = [Nu]_0 - [DABCO]$

$[E] = [E]_0 - [DABCO]$
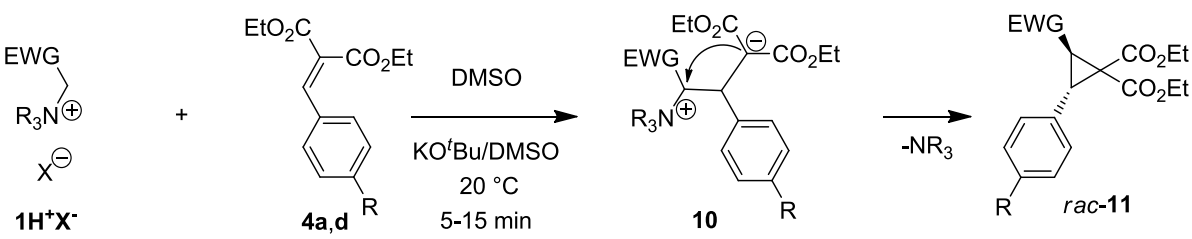
2.3.3 Reactions with Benzylidene Malonates 4

Addition of the benzylidene malonates **4a** and **4d** to solutions of the ylides **1** formed from **1H⁺X⁻** and KO^{t}Bu in DMSO generally led to the formation of the cyclopropanes **11** (Table 2.6). The preference for the formation of the *trans*-diastereomers of **11** was derived from the vicinal coupling constants $^3J = 7.4 - 7.9$ Hz (*cis*: $^3J \sim 10$ Hz) of the cyclopropane protons.[12a,c] These assignments were confirmed by NOESY correlations of the protons and the substituents of the cyclopropane ring of *trans*-**11ad**,**ba**,**cd** and the X-ray structure of *trans*-**11ca** (Figure 2.6). The acetyl-substituted ylide **1d** did not cyclopropanate the benzylidene malonate **4a**, but decomposed instead, in analogy to the attempted reaction of **1d** with the quinone methide **3c** described above (Table 2.4).

Table 2.7 shows that the reaction of the ammonium ylide **1c** with the benzylidene malonate **4a** gave better yields of the cyclopropane **11ca** when longer reaction times or elevated temperatures were used, although TLC analysis indicated complete consumption of the reactants within 10 min at room-temperature. The *trans*:*cis* ratio of the cyclopropane **11ca** was greater than 98:2 at short reaction times, but slow partial isomerization of *trans*-**11ca** into *cis*-**11ca** is observed when the product was kept in the presence of KO^{t}Bu for several hours.

UV–vis monitoring of the reaction of the ester-substituted ylide **1c** with the benzylidene malonate **4a** showed the complete consumption of **4a** ($\lambda_{max} = 302$ nm) within 10 min (Figure 2.7a). New bands at 264 nm and 445 nm were formed with the same rate constant as the 302 nm-absorption of **4a** disappeared.

The new absorption bands do not correspond to the UV–vis-spectrum of the cyclopropane **11ca** ($\lambda_{max} = 277$ nm; for details see Experimental Section). While the 264 nm-band can be assigned to the intermediate betaine **10ca**, the absorption band at 445 nm might correspond to a small concentration of zwitterionic *p*-nitro-benzyl anion **10ca'** as depicted in Figure 2.7a. As *p*-nitrotoluene was reported to be four orders of magnitude less acidic than diethyl malonate[23] one can rationalize the formation of a small concentration of **10ca'** by a proton shift from **10ca**.

Table 2.6. Reaction of the ylides 1 with the benzylidene malonates 4a,d. The first letter of the product number refers to the employed Ylide 1, the second to the employed benzylidene malonate 4.

Salt	NR$_3$	EWG	4	R	Betaine 10	Cyclopropane 11	Yield 11/%	(trans:cis)-11[a]
1aH⁺Br⁻	DABCO	CN	**4d**	Me	**10ad**	**11ad**	60	96:4
1bH⁺Cl⁻	DABCO	CONEt$_2$	**4a**	NO$_2$	**10ba**	**11ba**	50	87:13[b]
1cH⁺Br⁻	DABCO	CO$_2$Et	**4a**	NO$_2$	**10ca**	**11ca**	53[c]	97:3
1cH⁺Br⁻	DABCO	CO$_2$Et	**4d**	Me	**10cd**	**11cd**	64	96:4
1dH⁺Cl⁻	DABCO	COMe	**4a**	NO$_2$	**10da**	**11da**	0	-
1eH⁺Br⁻	DABCO	COPh	**4d**	NO$_2$	**10ed**	**11ed**	43[c]	>98:2[d]
1fH⁺Br⁻	DABCO	CO$_2$^{t}Bu	**4d**	Me	**10fd**	**11fd**	64	96:4
1gH⁺Br⁻	Quinuclidine	CO$_2$Et	**4d**	Me	**10gd**	**11gd** (= **11cd**)	63	96:4
1hH⁺Br⁻	NMe$_3$	CO$_2$Et	**4a**	NO$_2$	**10ha**	**11ha** (= **11ca**)	29	>98:2[d]
1hH⁺Br⁻	NMe$_3$	CO$_2$Et	**4d**	Me	**10hd**	**11hd** (= **11cd**)	63	96:4

[a] Determined by ^{1}H NMR of the crude product; [b] Determined by GC-MS of the crude product; [c] After stirring for 2 h at ambient temperature; [b] After purification.
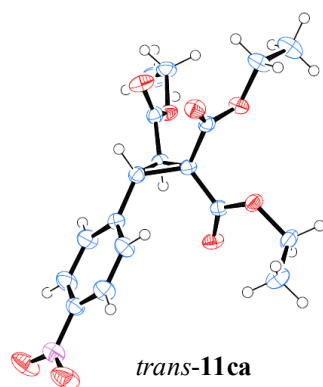
trans-**11ca**

Figure 2.6. ORTEP-drawing of the crystal structure of *trans*-11ca (thermal ellipsoids are shown at the 50% probability level).

Table 2.7. Time- and temperature dependence of the formation of cyclopropane 11ca by the reaction of the ylide 1c with the benzylidene malonate 4a.[a]

Entry	Time	T/°C	Yield/%^{c}	trans:cis[b]
1	10	20	32	>98:2
2	30	20	41	98:2
3	1 h	20	47	98:2
4	2 h	20	53	97:3
5	4 h	20	50	92:8
6	5 min	100	65	98:2
7	10	100	81	95:5

[a] Conditions: **4a** and **1cH⁺Br⁻** (1.7 eq) were suspended in DMSO and treated with KO^{t}Bu (1.7 eq); [b] Determined by ^{1}H NMR of the crude product.
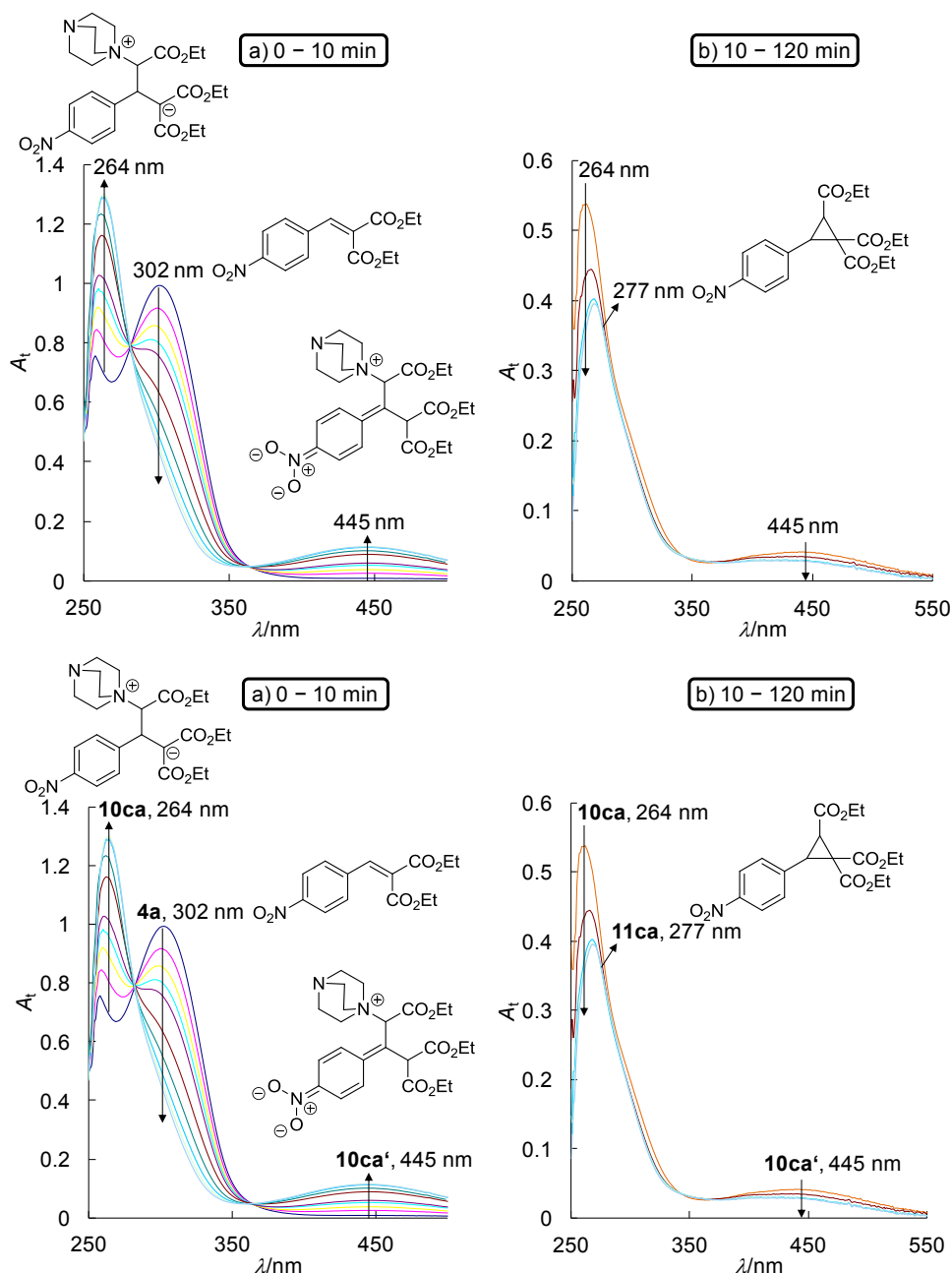
Figure 2.7. a) UV–vis-spectra of the first 10 min of the reaction of 1c ($[1c]_0 = 4.20 \times 10^{-4}$ M) with 4a ($[4a]_0 = 7.30 \times 10^{-5}$ M) following the decrease of the absorption of 4a at 302 nm ($k_{CC} = 2.21 \times 10^1$ M^{-1} s^{-1}) and increase of the absorption the of 10ca at 264 nm ($k_{CC} = 2.27 \times 10^1$ M^{-1} s^{-1}) and of 10ca' at 445 nm ($k_{CC} = 2.55 \times 10^1$ M^{-1} s^{-1}); **b)** UV–vis-spectra of the second part (10−120 min) of the reaction of 1c ($[1c]_0 = 5.71 \times 10^{-4}$ M) with 4a ($[4a]_0 = 7.30 \times 10^{-5}$ M) with the decrease of absorption of 10ca at 264 nm and of 10ca' at 445 nm ($k_{rc} = 6.28 \times 10^{-4}$ s^{-1}) and increase of the absorption of 11ca at 277 nm.

Similar proton-shifts have previously been observed in the reactions of phenylacetonitrile anions with benzylidene malonates **4**.[19h] A shift of the proton in **10ca** to form another ammonium ylide may occur. However, the proton next to the DABCO$^+$ group in **10ca** is approximately 5 pK_{aH}-units less acidic than the malonate moiety and the resulting ylide should not absorb above 400 nm (see Table 2.1).

The new bands at 264 nm and 445 nm, thus assigned to betaines **10ca** and **10ca'**, are subsequently consumed within 120 min with the rate constant k_{rc}, yielding the UV spectrum of the cyclopropane **11ca** (Figure 2.7b). From the decrease of the absorbance of betaine **10ca** evaluated at 270 nm, the rate constant of ring closure ($k_{rc} = 5.96 \times 10^{-4}$ s^{-1}) was derived. In line with this interpretation, the rate of ring closure k_{rc} was found to be independent of the concentration of the ylide **1c** (Figure 2.8a)

The cyclization of betaine **10ca** to cyclopropane **11ca** was also monitored by ^{1}H NMR, by generating betaine **10ca** from equimolar amounts of ylide **1c** and benzylidene malonate **4a** (Figure 2.8b). The spectra showed that the reactants were completely converted into the betaine **10ca** immediately after mixing, which subsequently underwent cyclization into cyclopropane **11ca** with expulsion of DABCO within 2 h (Figure 2.8b). Fitting of the concentrations of the evolved DABCO with an exponential function gave the rate constant of ring closure $k_{rc} = 6.29 \times 10^{-4}$ s^{-1} (for details see Experimental Section) which is in agreement with $k_{rc} = 5.96 \times 10^{-4}$ s^{-1} derived from the decrease of the UV−Vis absorbance of **10ca**.
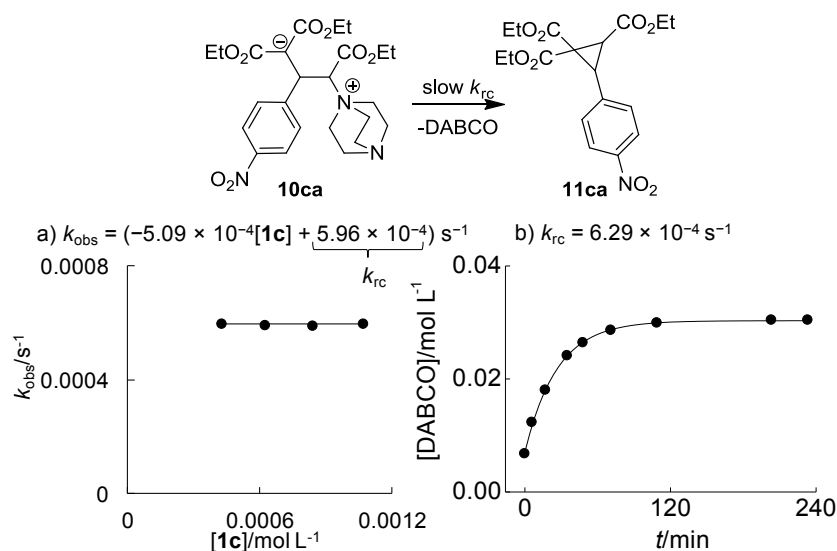
Figure 2.8. a) Plot of k_{obs}/s^{-1} obtained from the decays of the absorption of 10ca at 270 nm versus the concentration of 1c. b) ^{1}H NMR monitoring of the evolution of DABCO from 10ca in DMSO-d_6 at 20 °C.

The time-dependent absorbances at 264 nm and 302 nm due to the overlapping absorptions of benzylidene malonate **4a**, betaine **10ca**, and cyclopropane **11ca** were also simulated with MATLAB[24] by solving the system of linear differential eqs 2−4 (Figure 2.9; for details see Experimental Section).[25, 26] The simulation, which showed excellent agreement between calculated and observed absorbances, provided the rate constants $k_{CC}^{average}$ = 2.53 × 10^1 M^{-1} s^{-1} and $k_{rc}^{average}$ = 7.23 × 10^{-4} s^{-1} which are close to those derived from separate experients which were optimized for the determination of k_{CC} (high resolution of the first stage) and the determination of k_{rc} (Figure 2.9).

$k_{CC}^{average}$ = 2.53 × 10^1 mol L^{-1} s^{-1} [a]

$k_{rc}^{average}$ = 7.23 × 10^{-4} s^{-1} [a]

Figure 2.9. Simulation of the absorbance change at 264 and 302 nm during the reaction of 1c ([1c]$_0$ = 1.06 × 10^{-3} M) with 4a ([4a]$_0$ =4.25 × 10^{-5} M) by MATLAB (for details see Exerimental Section). [a] Average of two simulations at different concentrations (for details see Experimental Section).

The experimental observations reported so far are in accord with irreversible conversion of the reactants **1c** and **4a** into betaine **10ca** (case 2a) as well as with reversible formation of a high concentration of **10ca** (case 2b), in both cases followed by slow subsequent cyclization. In order differentiate these cases a DMSO solution of betaine **10ca**, generated from equimolar amounts of ylide **1c** and benzylidene malonate **4a**, was treated with a solution of quinone methide **3c** in CH_2Cl_2 and kept for 1 h at ambient temperature (Scheme 2.4).

Scheme 2.4. Crossover experiment to test the reversibility of the formation of betaine 10ca.

If the betaine **10ca** would undergo retroaddition (k_{-CC}) faster than cyclization (k_{rc}), the regenerated ylide **1c** should be trapped by the quinone methide **3c**, which reacts 22 times faster with **1c** than the benzylidene malonate **4a**. As the crossover product, the spirocycle **9cc**, was not observed and cyclopropane **11ca** was isolated in 46% yield, which is similar to the yield of **11ca** obtained from **1c** and **4a** after 1 h reaction time at ambient temperature (Table 2.7, entry 3), the reversible formation of betaine **10ac** can be ruled out. Thus the reaction of **1c** with **4a** can be assigned to case 2a (eq 2.8).

Monitoring of the reaction of the trimethylammonium-substituted ylide **1h** with benzylidene malonate **4a** by UV–vis spectrophotometry indicates the initial formation of the betaine **10ha**, which subsequently cyclizes to form the cyclopropane, similar to the reaction of ylide **1c** with **4a** described above. By analogy we assign the reaction of **1h** with **4a** to case 2a, but we have not performed crossing experiments as described in Scheme 2.4 to differentiate between cases 2a and 2b.

GC-MS-monitoring of the reaction of the ester-substituted ammonium ylide **1c** with benzylidene malonate **4d** showed that the consumption of the electrophile **4d** proceeds equally fast as the formation of the cyclopropane **11cd** (Figure 2.10), indicating that the intermediate betaine **10cd** is not accumulated. The reaction of ylide **1c** with benzylidene malonate **4d** can, therefore, be assigned to case 1 (eq 2.5). Further arguments which allow the assignment to case 1a (eq 2.6), i.e., rate-determining irreversible betaine formation with fast subsequent ring closure, will be presented below.

Analogous results were found for the reactions of the quinuclidinium-substituted ylide **1g** and the trimethylammonium-substituted ylide **1h** with benzylidene malonate **4d** (for details see Experimental Section) so that these reactions could also be assigned to case 1a.
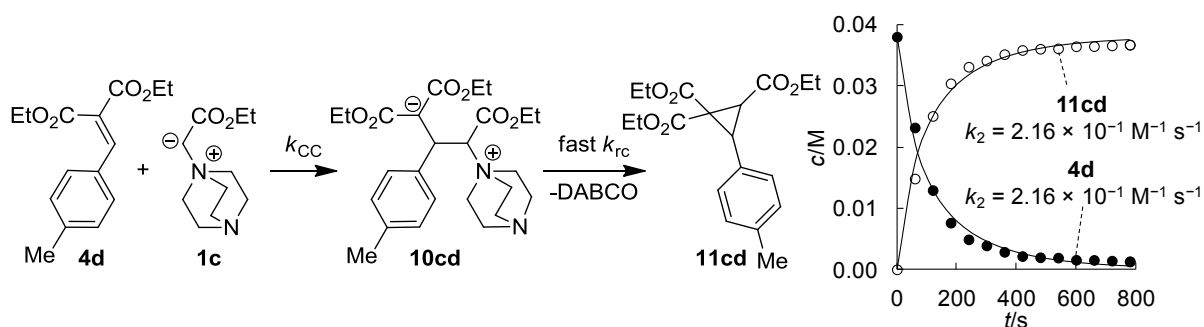
Figure 2.10. Decrease of the concentration of the electrophile 4d (filled dots; $[4d]_0 = 2.54 \times 10^{-2}$ M) during the reaction with the nucleophile 1c ($[1c]_0 = 5.72 \times 10^{-2}$ M) in DMSO at 20 °C and increase of the concentration of the product 11cd (open dots) monitored by GC-MS and GEPASI fit[27] of the obtained data (black curves).

The reactions of the cyano-substituted ammonium ylide **1a** with the most reactive *p*-nitro-substituted benzylidene malonate **4a** and the least reactive *p*-methyl-substituted **4d** were studied by ^{1}H NMR.
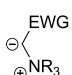
When equimolar amounts of ylide **1a** and benzylidene malonate **4a** were combined in DMSO-d_6, complete consumption of the reactants and formation of a 67:33 mixture of the intermediate betaine **10aa** and the cyclopropane **11aa** were observed in a ^{1}H NMR spectrum taken 1 min after combining the reactants at ambient temperature. In the corresponding reaction of the less reactive benzylidene malonate **4d**, the reactants were completely consumed after 1 min and a 37:63 mixture of betaine **10ad** and cyclopropane **11ad** was formed. The accumulation of the intermediate betaines **10aa** and **10ad** is similar as in the reactions of the ester-substituted ylide **1c** with benzylidene malonate **4a** described above and allows to assign the reactions of the cyano-substituted ylide **1a** with benzylidene malonates **4** to case 2 (eq 2.8).

The ^{1}H NMR spectrum taken immediately after mixing the amido-substituted ammonium ylide **1b** with benzylidene malonate **4a** showed complete conversion of the reactants to the cyclopropane **11ba**. The linear free-energy relationships discussed in the next section suggest that the reaction follows case 1a.

^{1}H NMR monitoring of the progress of the reaction of the less basic benzoyl-substituted ammonium ylide **1e** ($pK_{aH} = 15$ in DMSO) with benzylidene malonate **4a** for 3.5 h showed decreasing amounts of the reactants **1e** and **4a** and increasing amounts of the cyclopropane **11ea** and of DABCO, while the intermediate betaine **10ea** was not detectable. From the increasing concentration of DABCO k_{2obs} was derived, as described above for the reaction of ylide **1e** with quinone methide **3a** (see Figure 2.5; for details see Experimental Section). Since the intermediate betaine **10ea** did not accumulate, the reaction of the benzoyl-substituted ylide **1e** with benzylidene malonate **4a** must proceed according to case 1 (eq 2.5).

UV−vis monitoring of the reactions of the more basic cyano, amido, and ester-substituted ammonium ylides **1a−c,h** ($pK_{aH} \geq 20$ in DMSO) with the benzylidene malonates **4** showed the complete consumption of the absorbance of **4** by a mono-exponential decay from which the first-order rate constants k_{obs} for the formation of the betaines **10** were derived. The linear increase of the first-order rate constants k_{obs} with increasing concentration of the ylides **1** was used to derive the second-order rate constants k_{CC} listed in Table 2.8.

Table 2.8. Rate constants for the reactions of the ammonium ylides 1 with the benzylidene malonates 4 in DMSO at 20 °C.

$$\ominus\!\!<^{\text{EWG}}_{\oplus\text{NR}_3}$$

1	NR$_3$	EWG	4	k_{CC}/M^{-1} s^{-1}	$K \cdot k_{rc}$/M^{-1} s^{-1}	k_{rc}/s^{-1}	Case
1a	DABCO	CN	**4a**	5.65×10^3		[b]	2[c]
			4b	2.23×10^3		[b]	2[c]
			4c	4.08×10^2		[b]	2[c]
			4d	2.32×10^2		[b]	2[c]
1b	DABCO	CONEt$_2$	**4a**	5.64×10^2			1a
1c	DABCO	CO$_2$Et	**4a**	2.21×10^1		5.96×10^{-4} [d]	2a
			4d	2.16×10^{-1}[f]			1a
1e	DABCO	COPh	**4a**		(4.4×10^{-4})[e]		1b
1g	Quinuclidine	CO$_2$Et	**4d**	2.2×10^{-1} [f]			1a
1h	NMe$_3$	CO$_2$Et	**4a**	4.36×10^1		9.10×10^{-4}	2a
			4d	4.0×10^{-1} [f]			1a

[a] Assignment of the individual reactions to the different cases see below; [b] k_{rc} not determined; [c] Cross-over experiments to differentiate cases 2a and 2b were not made; [d] The rate constants were also derived from a simulation with MATLAB using the solution of the system of linear differential eqs 2−4 (k_{CC}^{average} = 2.53×10^1 M^{-1} s^{-1}; k_{rc}^{average} = 7.23×10^{-4} s^{-1}), and from following the evolution of DABCO by ^{1}H NMR (k_{rc} = 6.29×10^{-4} s^{-1}); for details see Figure 2.10; [e] Kinetics measured by ^{1}H NMR (for details Experimental Section); [f] Kinetics monitored by GC (for details see Figure 2.10 and Experimental Section).

2.3.4 Reactions with Benzylidene Indandiones 5

^{1}H NMR spectra taken immediately after mixing equimolar amounts of the more basic cyano, amido, and ester-substituted ylides **1a–c** (pK_{aH} ≥ 20 in DMSO) with benzylidene indandione **5b** in (DMSO-d_6/CDCl$_2$)-mixtures at ambient temperature showed complete conversion of the reactants into the intermediate betaines **12ab−12cb** which are formed as 1:1 mixtures of the two diastereoisomers with complete conversion of the reactants (Table 2.9). The lifetimes of the betaines **12ab–12cb** were sufficient to allow their characterization by NMR (^{1}H, ^{13}C, 2D NMR); a ^{13}C NMR signal at $\delta \sim 103$ ppm for the tertiary carbanionic center of the indandione fragment is in agreement with published ^{13}C NMR data for related tertiary carbanions derived from substituted indandiones.[28]

45

Table 2.9. Reaction of the ylides 1 with the benzylidene indandione 5b. The first letter of the product number refers to the employed ylide 1, the second to the employed benzylidene indandione 5.

dr 1:1 for **12ba-cb**
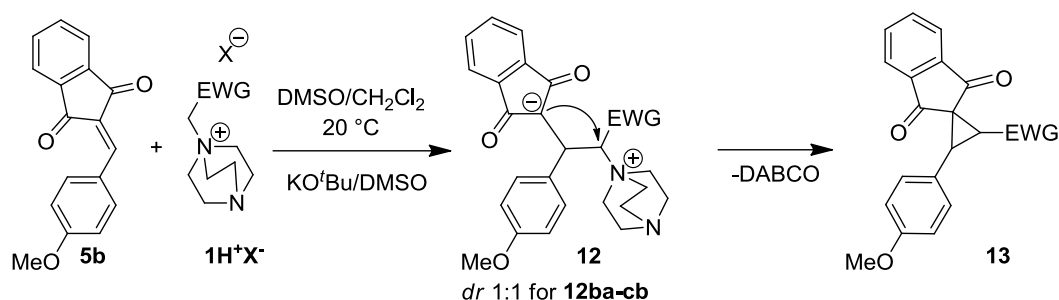
Salt	EWG	Conditions[a]	Betaine 12	Cyclopropane 13	Yield 12/%	(*trans*:*cis*)-13[b]
1aH⁺Br⁻	CN	A	**12ab**	**13ab**	19	25:75
		B	**12ab**	**13ab**	82	20:80
1bH⁺Cl⁻	CONEt$_2$	C	**12bb**	**13bb**	22	66:33
		B	**12bb**	**13bb**	66	66:33
1cH⁺Br⁻	CO$_2$Et	A	**12cb**	**13cb**	30	80:20
		B	**12cb**	**13cb**	50	89:11
1dH⁺Cl⁻	COMe	C	**12db**	**13db**	53	66:33
1eH⁺Br⁻	COPh	B	**12eb**	**13eb**	60	75:25

[a] Conditions A: A solution of **1H⁺X⁻** in DMSO was treated with KO^{t}Bu in DMSO for 30 s, then **5b** was added in CH$_2$Cl$_2$ and the solution was stirred for 5 min at 20 °C; B: A solution of **1H⁺X⁻** and **5b** in DMSO/CH$_2$Cl$_2$ was treated with KO^{t}Bu in DMSO and stirred for 0.5–1 h at 20 °C; C: Biphasic conditions CH$_2$Cl$_2$/aq. NaOH (32%) for 2 h at 20 °C; [b] Determined by ^{1}H NMR of the crude product.

In line with these observations, the cyclopropanes **13ab** and **13cb** were obtained only in low yields, when mixture of **1a** or **1c** with **5b** were quenched with sat. NH$_4$Cl solution after 5 minutes reaction time at 20 °C in DMSO (Table 2.9; Conditions A). The cyclopropanes **13ab−13cb** were isolated in 50% to 82% yield, however, when the reaction mixture was stirred for 1 h at 20 °C (Table 2.9; Conditions B).

The stereochemistry of the spirocycles **13ab−cb** was assigned on the basis of NOESY correlations of the protons and the substituents at the cyclopropane ring; the configuration of the spirocycle *cis*-**13ab** was furthermore confirmed by its X-ray structure (Figure 2.11).
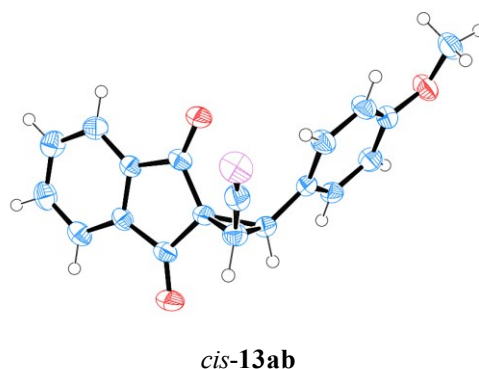
cis-**13ab**

Figure 2.11. ORTEP-drawing of the crystal structure of *cis*-13ab (thermal ellipsoids are shown at the 50% probability level).

Table 2.9 shows that the *trans:cis* ratios of the cyclopropanes **13ab−13cb** differed from the 1:1 diastereomeric ratios of the preceding betaines **12ab−12cb**. This change of configuration may either arise from retroaddition of **12ab−12cb** to the reactants or from epimerization of the DABCO$^+$-substituted carbon center of these betaines by deprotonation and reprotonation.

To test whether the betaines **12ab−12cb** undergo retroaddition ($-k_{CC}$) before cyclization (k_{rc}), the unsubstituted benzylidene indandione **5a** was added to a solution of betaine **12ab** in DMSO/CH$_2$Cl$_2$ (2.5:1) and kept for 1 h at ambient temperature (Scheme 2.5). After aqueous workup, the spirocycle **13ab** was isolated in 46% yield and 90% of the benzylidene indandione **5a** was recovered while the crossover product **13aa** was not observed. If the betaine **12ab** would undergo retroaddition parallel to the formation of **13ab**, the regenerated ylide **1a** would rather react with the unsubstituted benzylidene indandione **5a** to give the spirocycle **13aa** than to recombine with the 16-times less reactive *p*-methoxy-substituted benzylidene indandione **5b**.

For that reason we can to rule out the reversible formation of betaine **12ab**, and assign the reaction of the cyano-substituted ammonium ylide **1a** with benzylidene indandione **5b** to case 2a. As the reactions of the amido and ester-substituted ylides **1b**,**c** with benzylidene indandione **5b** behave similarly, their reactions were also assigned to case 2a.

Scheme 2.5. Crossover experiment to test the reversibility of the formation of betaine 12ab.
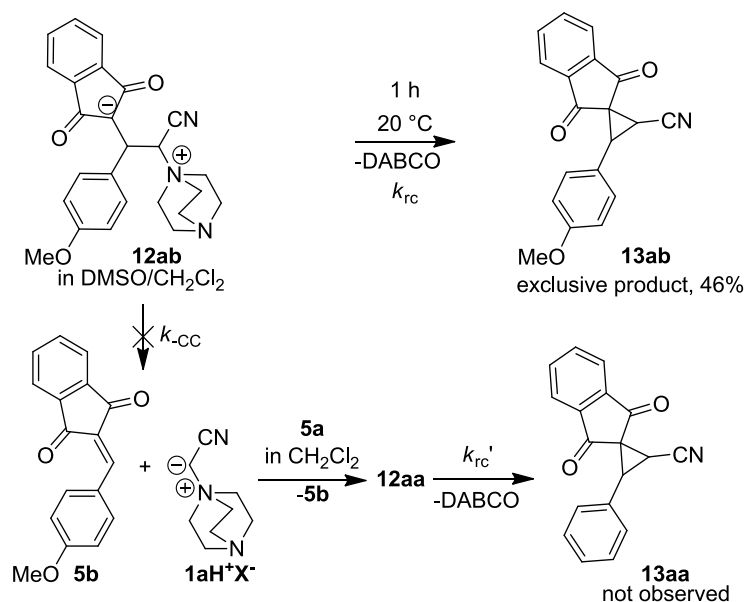
^{1}H NMR-monitoring of the reactions of the less basic acyl-substituted ammonium ylides **1d**,**e** (pK_{aH} = 15−16 in DMSO) with benzylidene indandione **5b** for 1 h in (DMSO-d_6/CDCl$_2$)-mixtures at room temperature showed complete conversion of the reactants into the cyclopropanes **13db** and **13eb** while the signals of the intermediate betaines **12db** and **12eb** were not observable.

The assignment of the stereochemistry of the spirocycle *trans*-**13eb** was based on the NOESY correlations of the protons and the substituents at the cyclopropane ring. The assignment of cyclopropane *trans*-**13db** was based on its coupling constant $^3J \sim 9$ Hz[29] for the cyclopropane protons, which is in the range of the coupling of the cyclopropanes *trans*-**13ab**−**cb**,**eb** assigned by NOESY.

The formation of the betaines **12ab**–**cb** from the more basic cyano, amido, and ester-substituted ammonium ylides **1a**–**c** and benzylidene indandione **5b** were monitored by UV–vis spectroscopy and the observed mono-exponential decays of the absorbance of **5b** were used to derive the second-order rate constants k_{CC} listed in Table 2.10.

The rates of ring-closure k_{rc} of the intermediate betaines **12ab**–**cb** to the cyclopropanes **13ab**–**cb** listed in Table 2.10 were determined by following the formation of DABCO by ^{1}H NMR spectroscopy (for details see Experimental Section).

In the reactions of the less basic acyl-substituted ylides **1d**,**e**,**i** with benzylidene indandione **5b** initial fast and incomplete decays of **5b** were observed on the millisecond to second time scale, followed by slow complete decays of the absorbance of **5b** on the minute time scale. An analogous behavior of the corresponding reactions of **1d**,**e**,**i** with the quinone methides **3a**,**b** was described in Table 2.5 (see illustration in Figure 2.3a).

Table 2.10. Rate constants for the reactions of the ammonium ylides 1 with the benzylidine indandiones 5 in DMSO at 20 °C.

Ylide	NR$_3$	EWG	5	k_{CC}/M^{-1} s^{-1}	$K \cdot k_{rc}$/M^{-1} s^{-1}	K/M^{-1}	k_{rc}/s^{-1}	Case[a]
1a	DABCO	CN	**5b**	1.60×10^6			6.8×10^{-4} [b]	2a
1b	DABCO	CONEt$_2$	**5b**	2.75×10^5			6.2×10^{-4} [b]	2a
1c	DABCO	CO$_2$Et	**5b**	2.22×10^5			6.5×10^{-4} [b]	2a
1d	DABCO	COMe	**5b**	8.80×10^3	9.52×10^1	(2×10^2)	(5×10^{-1})[c]	1b/2b
			5c		3.41			1b
1e	DABCO	COPh	**5b**	1.20×10^4	3.40×10^1	(2×10^2)	(2×10^{-1})[c]	1b/2b
			5c		2.75×10^{-1}			1b
1i	NMe$_3$	COPh	**5b**	3.07×10^3	4.55×10^1	(3×10^2)	(2×10^{-1})[c]	1b/2b

[a] Assignment of the individual reactions to the different cases see below; [b] Kinetics monitored by ^{1}H NMR.

[c] Estimated from $K \cdot k_{rc}$; K determined individually.

The initial fast and incomplete decays were assigned to the reversible formation of the intermediate betaines **12db**,**eb**,**ib**, with the rate constants k_{CC} and the subsequent complete decays of the absorbances of **5b** were assigned to the formation of the cyclopropanes **13db**,**eb**,**ib**. Because of the high reversibility of the formation of the betaines **12db**,**eb**,**ib**, these intermediates were not observable by the NMR experiments described above.

The first-order rate constants k_{obs} for the slow decays of the absorbances of benzylidene indandione **5b** in the second part of its reactions with **1d**,**e**,**i** depend on K and k_{rc} as described by eq 2.9. The slopes of the plots of $1/k_{obs}$ versus $1/[Nu]$ correspond to $1/K \cdot k_{rc}$, but the intercept, which equals $1/k_{rc}$, is almost zero, so that it cannot be used for the determination of k_{rc}. Therefore, the equilibrium constants K were derived from plots of $(A_0 - A_{eq})/A_{eq}$ versus $[Nu]$ according to eq 2.10 and combined with $K \cdot k_{rc}$ to determine the rate constants of ring closure k_{rc} which are given in Table 2.10. The reactions of the ylides **1d**,**e**,**i** with **5b** thus follow a mechanism between the cases 1b and 2b.

In the reactions of the acyl-substituted ylides **1d**,**e** with benzylidene indandione **5c** the intermediate betaines were not observable. Slow complete mono-exponential decays of the absorbances of **5c** were observed, from which the pseudo-first-order rate constants k_{obs} were derived. The observation of isosbestic points allows to assign these reactions to case 1 (eq 5) and since **5c** has a considerably lower Lewis acidity than **5b**, the equilibrium constant K for the formation of the betaines must be smaller than in the analogous reactions with **5b**, which allows us to assign the reactions of **1d** and **1e** with **5c** to case 1b. In line with these conclusions, the linear free-energy relationships discussed below also indicate that the observed second-order rate constants k_{2obs} correspond to $K \cdot k_{rc}$.

2.3.5 Reactions with Chalcone 6

Mixtures of the three diastereoisomers **A–C** of the cyclopropanes **15** were obtained from the reactions of the ylides **1** with chalcone **6** in 40–70% yield (Table 2.11).

The configurations of the diastereoisomers **15-(A−C)** were assigned on basis of the NOESY correlations of the protons and substituents of the cyclopropane moiety. The preferred formation of the cyclopropanes **15a-A** and **15a-B** from the cyano-substituted ylide **1a** and chalcone **6** was confirmed by the crystal structures of these diastereoisomers (Figure 2.12). The cyclopropanes **15c-(A−C)** were recently described by Taylor and co-workers, and our assignments of their configurations are in agreement with these data.[30] Cyclopropane **15e** is

preferentially formed as the *meso*-diastereoisomer **15e-B**, whose configuration was also verified by its crystal structure (Figure 2.12).

The diastereoisomer **15-C** may be formed by the rotation of the former CC-double bond in the intermediate betaines **14** (Table 2.11), but also through base mediated epimerization of the cyclopropanes **15**.

The ^{1}H NMR spectra taken immediately after combining the cyano, amido, and ester-substituted ylides **1a–c** with chalcone **6** showed complete consumption of the reactants and formation of the cyclopropanes **15a–c**, but no signals of the intermediate betaines **14a–c**.

In the kinetics of the reactions of the cyano and ester-substituted ylides **1a,c** with chalcone **6** mono-exponential decays of the absorbance of **6** were observed and evaluated as described above to derive the second-order rate constants listed in Table 2.12. For the reaction of ylide **1b** with chalcone **6** a bisexponential decay of the absorbance of chalcone **6** was observed, which could not be evaluated.

Table 2.11. Reaction of the ylides 1 with the chalcone 6.
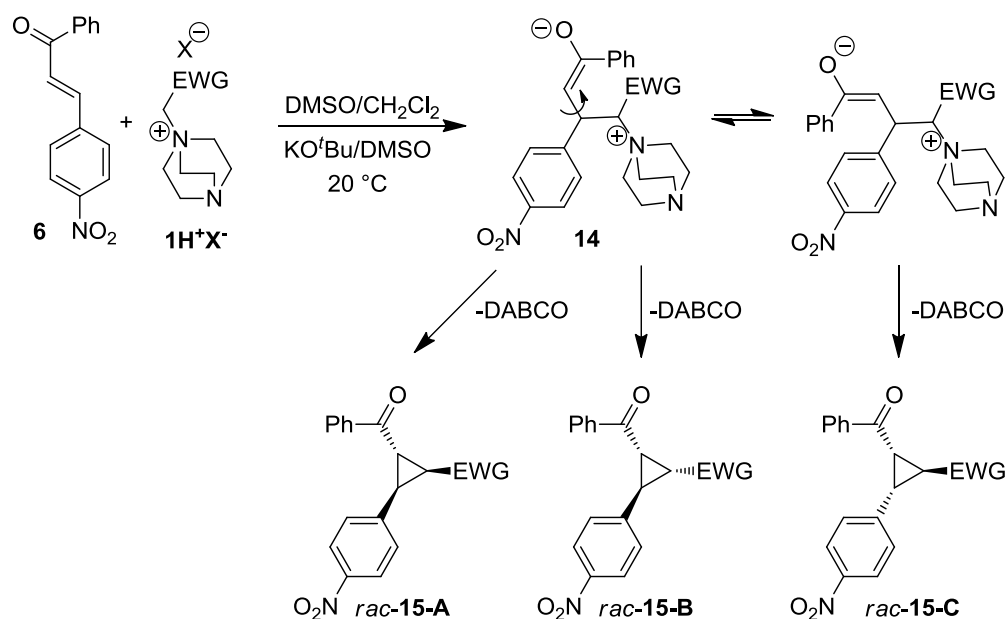
Salt	EWG	Betaine 14	Cyclopropane 15	Yield/%	*dr* 15-(A:B:C)[a]
1aH$^+$Br$^-$	CN	**14a**	**15a**	58	70:27:3
1bH$^+$Cl$^-$	CONEt$_2$	**14b**	**15b**	52[b]	50:50:0^c
1cH$^+$Br$^-$	CO$_2$Et	**14c**	**15c**	67[d]	40:40:20
1dH$^+$Cl$^-$	COMe	**14d**	**15d**	40[b]	78:20:2[c, e]
1eH$^+$Br$^-$	COPh	**14e**	**15e**	88[d]	8:92[f]

[a] Determined by ^{1}H NMR of the crude product; [b] Synthesized under biphasic conditions 50% NaOH/CH$_2$Cl$_2$ at 20 °C; [c] After column chromatography; [d] After 1 h stirring at 20 °C; [e] Tentative assignment based on ^3J coupling, as no NOESY spectrum was available; [f] Due to their symmetry **15e-A** and **15e-C** are enantiomers.
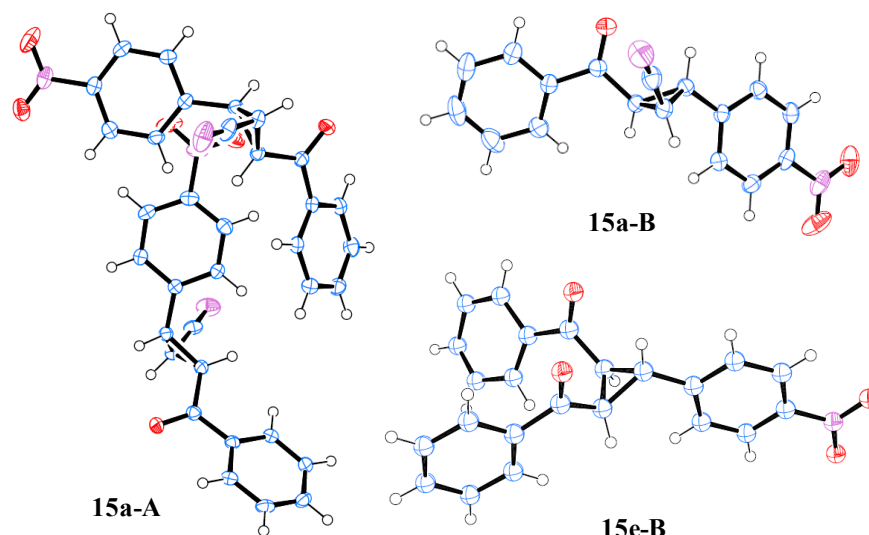
Figure 2.12. ORTEP-drawing of the crystal structures of 15a-A, 15a-B, and 15e-B (thermal ellipsoids are shown at the 50% probability level).

Table 2.12. Rate constants for the reactions of the ammonium ylides 1 with the chalcone 6 in DMSO at 20 °C.

Ylide	EWG	k_{CC}/M^{-1} s^{-1}	$K \cdot k_{rc}$/M^{-1} s^{-1}	Case[a]
1a	CN	4.47×10^3		1a
1c	CO$_2$Et	3.09×10^1		1a
1d	COMe		(9.6×10^{-5})[b]	1b
1e	COPh		(5.6×10^{-4})[b]	1b

[a] Assignment of the individual reactions to the different cases see below; [b] Kinetics monitored by ^{1}H NMR (for details see Experimental Section).

Monitoring the reactions of the less basic acyl-substituted ylides **1d**,**e** with chalcone **6** for 4 h in (DMSO-d_6:CD$_2$Cl$_2$)-mixtures by ^{1}H NMR showed a decrease of the concentrations of the reactants, and increasing concentrations of the cyclopropanes **15d**,**e** and DABCO, but no formation of the intermediate betaines **14d**,**e**. The absence of observable betaines in the ^{1}H NMR spectra indicates that these cyclopropanations follow case 1 (eq 2.5).

The considerably smaller second-order rate constants for the reaction of the acetyl (**1d**) and benzoyl-substituted ylide (**1e**) with chalcone **6** were derived by ^{1}H NMR spectroscopy from the increase of the ^{1}H NMR signals of DABCO as described above (Figure 2.5).

The linear free-energy relationships discussed in the next section allow us to assign the measured second-order rate constants k_{2obs} for the first two entries of Table 2.12 to k_{CC} and the lower two entries to $K \cdot k_{rc}$.

2.4 Discussion

2.4.1 Correlation Analysis

According to eq 1, plots of the second-order rate constants for the reactions of the ylides **1** with the benzhydrylium ions **2** and the Michael acceptors **3−6** versus the corresponding electrophilicity parameters E are expected to be linear, if the observed second-order rate constants k_{2obs} correspond to k_{CC}, the rate constant for the formation of the betaine.

Therefore, correlation analysis may allow to differentiate the cases 1a ($k_{2obs} = k_{CC}$) and 1b ($k_{2obs} = K \cdot k_{rc}$), which could not be discriminated by formal kinetics, as both mechanisms are characterized by a second-order rate law.

Figure 2.13 shows a linear correlation between the log k_{CC}-values of the reactions of the ylides **1a–c** and the Michael acceptors **3–6**. Rate constants which can unequivocally be assigned to k_{CC}, because the formation of **7** (from **2d**) or of the betaines was directly observable, are marked by filled symbols. As the observed second-order rate constants for the reactions of
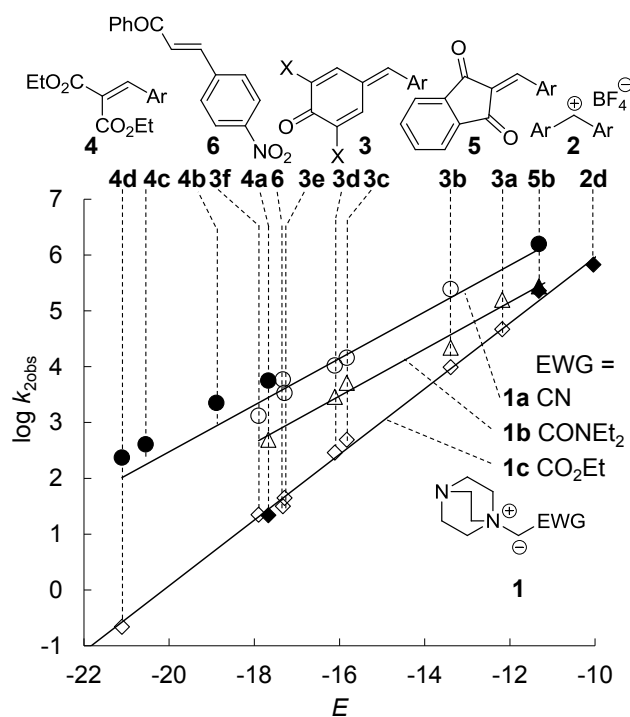
Figure 2.13. Correlation of log k_{2obs} (DMSO, 20°C) for the reactions of the cyano, amido, and ester-substituted ammonium ylides **1a–c** with the electrophiles **2–6** versus their electrophilicity parameters E. Filled symbols refer to case 2a reactions (including reaction with **2d**); open symbols refer to of case 1a reactions. Only the reactions of **1a−c** with the reference electrophiles **2−4** were used to draw the correlation lines. For the correlations of log k_{2obs} versus E of **1f–i** see Experimental Section.

1a–c with the other Michael acceptors included in Figure 2.13 (open symbols) are on the same correlation lines, we concluded that these rate constants also correspond to k_{CC} though the intermediate betaines were not observable. In these reactions, the rate-determining formation of the betaines is followed by fast subsequent cyclization, and the kinetics follow eq 6 (case 1a).

Analogous relationships were found between the rate constants of the reactions of the other ester-substituted ylides **1f−h** with the benzhydrylium ions **2** and the Michael acceptors **3** and **4** which are depicted in the Experimental Section. Thus, all measured second-order rate constants $k_{2\mathrm{obs}}$ for the reactions of the cyano (**1a**), amido (**1b**), and ester-substituted ylides (**1c,f,g,h**) with the electrophiles **2−6** correspond to the formation of one new CC bond, and therefore follow eq 1.

Figure 2.14 analyzes the observed second-order rate constants $k_{2\mathrm{obs}}$ of the reactions of the less basic acetyl-substituted ammonium ylide **1d** (pK_{aH} = 16 in DMSO; squares) and the benzoyl-substituted ammonium ylide **1e** (pK_{aH} = 15 in DMSO; circles) with the electrophiles **2–6**. One can see, that in the reactions of these ylides with the benzhydrylium ions **2b−d**, the quinone methides **3a,b**, and the benzylidene indandione **5b**, the second-order rate constants for the attack of ylides **1d** and **1e** at the electrophiles (i.e., $k_{2\mathrm{obs}} = k_{CC}$) lie on the same correlation lines log $k_{2\mathrm{obs}}$ versus E (filled symbols, Figure 2.14). This correlation confirms our interpretation of Figure 2.3a that in the reactions of the ylides **1d,e** with the quinone methides **3a,b** and the benzylidene indandione **5b**, small, but observable concentrations of the intermediate betaines are formed in a fast reversible process. Thus a situation between the cases 1b and 2b is encountered.

As the attack of the less basic acyl-substituted ylides **1d,e** at the quinone methides **3a,b** is reversible, one can expect that the degree of reversibility is even higher for the reactions of these ylides with the less electrophilic Michael acceptors **3c,4a,5c**, and **6**. The strong deviations of $k_{2\mathrm{obs}}$ for these combinations (open symbols) reactions of the ylides **1d,e** with these Michael acceptors from the correlation lines in Figure 2.14 are, therefore, not surprising. The betaine intermediates are formed in small steady state concentrations, and the measured second-order rate constants correspond to $k_{2\mathrm{obs}} = K \cdot k_{rc}$ (case 1b, eq 7), i.e., case 1b is realized.

Analogous correlations were found for the corresponding reactions of the trimethylammonium-substituted ylide **1i** with the benzhydrylium ions **2c,d** and the Michael acceptors **3a,b** and **5b**, which are described in the Experimental Section.
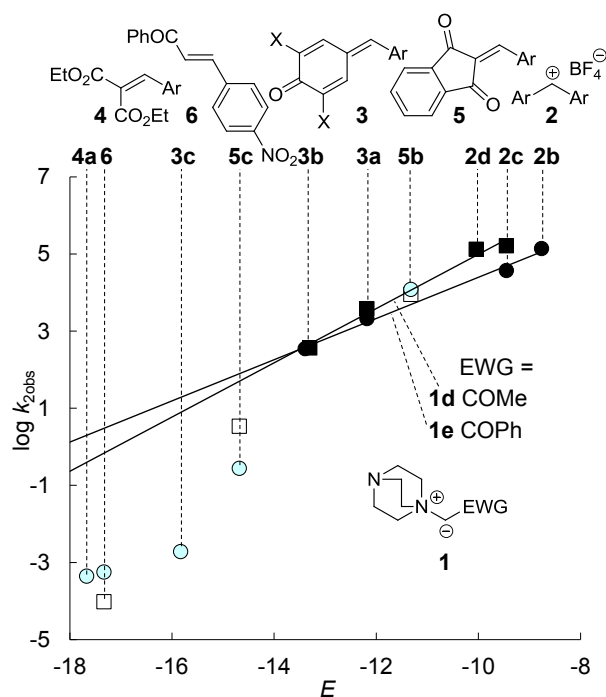
Figure 2.14. Correlation of log k_{2obs} (DMSO, 20°C) for the reactions of the acyl-substituted ammonium ylides 1d,e with the electrophiles 2−6 versus the electrophilicity parameters E. Filled symbols refer to rate constants of CC-bond formations; open symbols correspond to $K \cdot k_{rc}$. Only the reactions of 1d,e with the reference electrophiles 2b−d, and 3a,b were used to draw the correlation lines. For the analogous correlation of 1i see Experimental Section.

2.4.2 Energy Profiles

By combining the Gibbs free energies ΔG^0 and the activation free energies $\Delta G^{\neq}$ obtained from the different kinetic and mechanistic studies, energy profiles for the different types of reactions of ammonium ylides with Michael acceptors can be constructed. Figure 2.15 illustrates the different mechanistic scenarios for a representative highly basic ammonium ylide (**1c**) and a representative for a weakly basic ylide (**1e**).

As shown in the upper part of Figure 2.15 ylide **1c**, a representative for highly basic ylides, reacts irreversibly with **3b,c** and **5b**, i.e., cyclization is faster than retroaddition. Whereas in the two upper left cases, we only know that the transition state for cyclization is below that for retroaddition, in the upper right case (**1c** + **5b**), the barrier for cyclization of the quantitatively generated betaine was directly measured.

As shown in the lower part of Figure 2.15, ylide **1e**, a representative for less basic ylides, gives betaines with **3b,c** and **5b**, which cyclize more slowly than they undergo retroaddition. While the position of the first transition state for the reaction of **1e** + **3c** (bottom left) cannot be determined experimentally, but reliably calculated by eq 1, the position of the second transition

state can be derived from the measured value of $K \cdot k_{rc}$. Betaine **8ec** was set at the same level as the reactants, which implies that the intermediate is not observable at the low concentrations of the reactants.

The bisexponential decays observed for the reactions of **1e** with **3b** and **5b** allow us to construct the full energy profiles for the two reactions on the bottom right of Figure 2.15. The slightly exergonic formation of the betaines **8eb** and **12eb** implies that only small equilibrium concentrations of these intermediates are generated under the conditions of the kinetic experiments (high dilution).
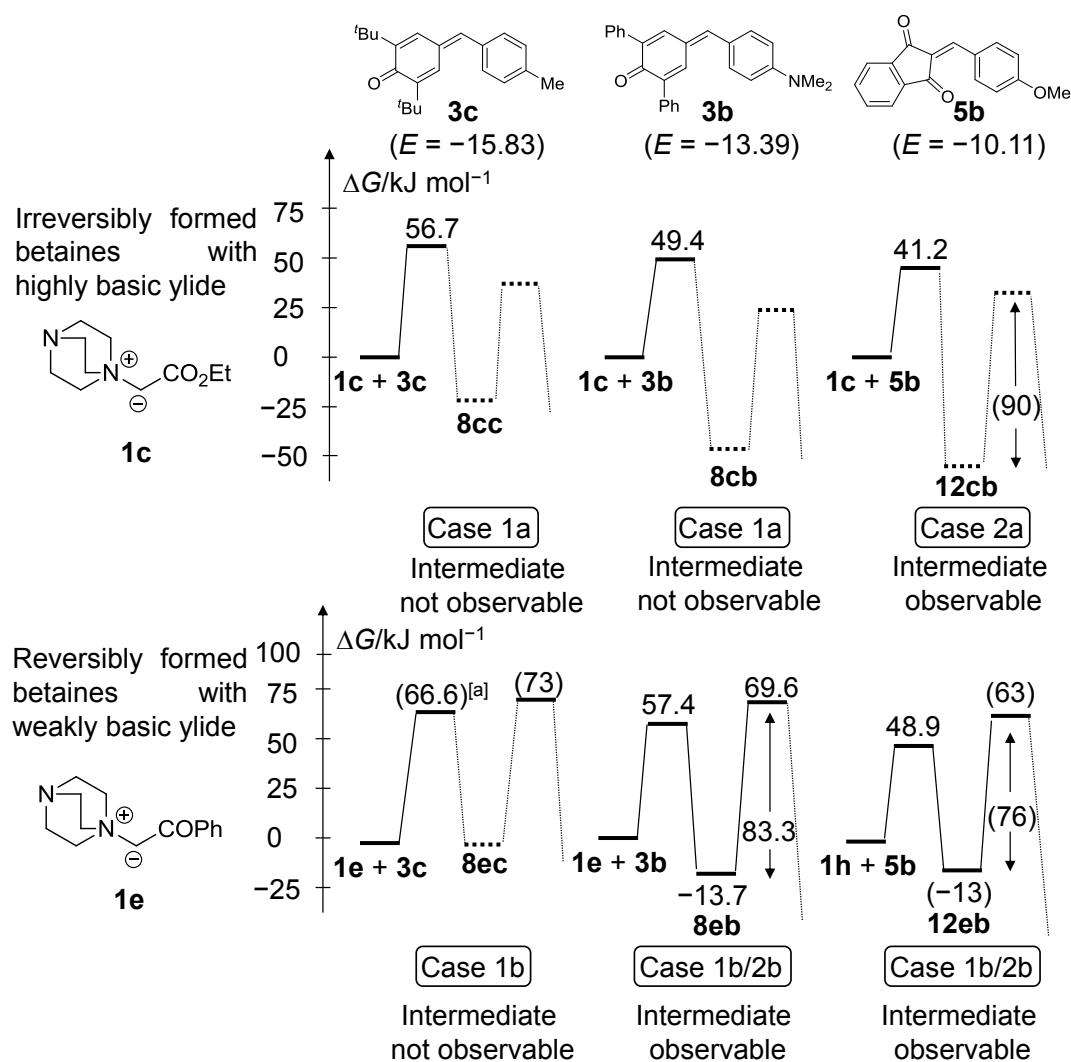
Figure 2.15. Energy Profiles for ammonium ylide mediated cyclopropanations with irreversible (1c) and reversible (1e) betaine formations. Dotted lines indicate qualitatively assigned relative energies of the intermediates. [a] The corresponding second-order rate constant was calculated by eq 1 using the N and s_N parameters of 1e in Table 2.14 and E from Chart 2.1.

2.4.3 Nucleophilicity Parameters and Reactivity Comparisons

From the correlations in Figures 2.13 and 2.14 the nucleophilicity parameters N and the sensitivities s_N for the ylides **1a–i** listed in Table 2.14 were derived which allows us to include **1a–i** into our comprehensive nucleophilicity scale.[19j]

The strongly varying s_N-parameters of the nucleophiles **1a–i** ($0.70 > s_N > 0.36$; Table 2.14) indicate a significant dependence of the relative reactivities of the ammonium ylides on the electrophilicities of their reaction partners. We therefore use the rate constants of the reactions of the ammonium ylides **1a–i** with the quinone methide **3b**, for which rate constants with all ylides **1a–i** have been determined, to compare the relative reactivities of the ammonium ylides **1a–i** (Table 2.13), realizing that their order will change for different electrophiles.

As shown in Table 2.13, the acetyl-substituted ammonium ylide **1d** has a similar reactivity towards **3b** as the benzoyl-substituted ylide **1e**. The ethoxycarbonyl substituted analogue **1c** is 28 times more reactive than **1d**. Exchanging the ethoxycarbonyl by the sterically more demanding *tert*-butoxycarbonyl (**1f**) has no effect on the reactivity. Replacement of the ester group by a carboxamido-group (**1b**) increases the reactivity by a factor of 2. Though the cyano- group is generally considered to be a better electron acceptor than acyl-, alkoxycarbonyl-, and aminocarbonyl-groups according to Hammett's substituent constants σ_p and σ_p^-,

Table 2.13. Relative reactivities of the DABCO-substituted ammonium ylides 1a–f towards the quinone methide 3b (DMSO, 20 °C).

Ylide	EWG	k_{CC}^{rel}(**3b**)
1d	COMe	1.0
1e	COPh	2.2
1c	CO$_2$Et	28
1f	CO$_2^t$Bu	28
1b	CONEt$_2$	63
1a	CN	748

Table 2.14. N- and s_N parameters of the ammonium ylides 1 in DMSO at 20 °C.

Ylide	NR$_3$	EWG	N	s_N
1a	DABCO	CN	27.43	0.37
1b	DABCO	CONEt$_2$	24.23	0.42
1c	DABCO	CO$_2$Et	20.15	0.58
1d	DABCO	COMe	18.21	0.54
1e	DABCO	COPh	17.22	0.69
1f	DABCO	CO$_2^t$Bu	21.05	0.50
1g	Quinuclidine	CO$_2$Et	20.14	0.59
1h	NMe$_3$	CO$_2$Et	21.06	0.52
1i	NMe$_3$	COPh	17.36	0.60

the cyano substituted ylide **1a** is by far the strongest nucleophile in this series. As it is even 10 times more reactive than the 10^4 times stronger base **1b**,[31] one can again conclude, that nucleophiles with cyano-substituted reaction centers react with relatively small reorganization energies (low intrinsic barriers), as previously demonstrated for the reactions of malononitrile with benzhydrylium ions.[19i]

Table 2.15 shows that the ester-substituted ammonium ylides **1c** ($k_{CC}^{rel} = 1.0$), **1g**, and **1h** have almost the same reactivities (k_{CC}) toward the electrophiles **2d**, **3b**, and **4d**, indicating that the nucleophilicities of the ylides are only slightly affected by the nature of the ammonium moiety.

Table 2.16 compares the relative rate constants of ring closure k_{rc}^{rel} of the betaines **12ab–eb,ib** with respect to the cyclization rate of betaine **12bb** which is set to 1.0. The cyclization rates of the cyano, amido, and ester-substituted betaines **12ab–cb** are almost the same, while the acyl-substituted betaines **12db,eb,ib** cyclize ~300–800 times faster than **12bb**. While changing the leaving group from DABCO (**12eb**) to NMe₃ (**12ib**) has no effect on the cyclization rate, the acetyl- substituted betaine **12db** cyclizes 2.5 times faster than its benzoyl-substituted analogue (**12eb**). The higher activating effect of vicinal acetyl and benzoyl groups compared to ethoxycarbonyl and cyano groups parallels that previously reported for intermolecular S_N2 reactions of alkyl chlorides with I⁻ in acetone. [32]

Table 2.15. Relative reactivities of the ester-substituted ammonium ylides 1c,g and 1f towards the benzhydrylium ion 2d, the quinone methide 3b and the benzylidene malonate 4d (DMSO, 20 °C).
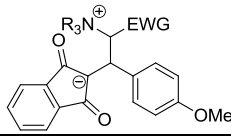
Ylide	NR₃	k_{CC}^{rel} (**2d**)	k_{CC}^{rel} (**3b**)	k_{CC}^{rel} (**4d**)
1c	DABCO	1.0	1.0	1.0
1g	Quinuclidine	1.2	0.7	1.0
1h	NMe₃	1.1	1.2	0.9

Scheme 2.6. Relative rates of ring closure of the betaines 10ca and 10ha in DMSO at 20 °C.
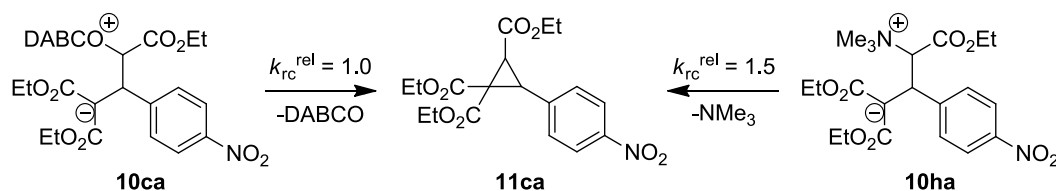
Scheme 2.6 shows that the relative cyclization rates if **10ca** and **10ha** depend only slightly on the nature of the nucleofuge. In accord with Aggarwal's conclusion,[13-14, 15c] the slightly better leaving group ability of NMe$_3$ (pK_{aH} = 8.5 in DMSO)[33] compared to DABCO (pK_{aH} = 8.9 in DMSO),[34] may be explained by the slightly smaller basicity of NMe$_3$.

Table 2.16. Relative rates of ring closure of the betaines 12ab–eb,ib in DMSO at 20 °C.

Betaine	NR$_3$	EWG	k_{rc}^{rel}
12bb	DABCO	CONEt$_2$	1.0
12cb	DABCO	CO$_2$Et	1.1
12ab	DABCO	CN	1.1
12ib	NMe$_3$	COPh	322
12eb	DABCO	COPh	322
12db	DABCO	COMe	806

2.5 Conclusion

Mechanistic investigations of the reactions of ammonium ylides with Michael acceptors have shown that the intermediate betaines are formed reversibly with ylides of low basicity and irreversibly with ylides of high basicity. Kinetic investigations have revealed the occurrence of four different mechanisms: The intermediate betaines are formed in low, but observable stationary concentrations by irreversible (case 1a) or reversible reactions (case 1b), or the intermediate betaines are formed in observable concentrations by irreversible (case 2a) or reversible reactions (case 2b).

The rates of the betaine formations in the reactions of ammonium ylides **1** with the Michael acceptors **3**−**6** can be described by eq 1, which enables us to include these synthetically important, highly nucleophilic ammonium ylides in our comprehensive nucleophilicity scale.[19j] Figure 2.16 compares the rates of attack of cyano (left) and ethoxycarbonyl-substituted (right) carbanions,[9a] phosphonium,[16] sulfonium,[17a] pyridinium,[18] and ammonium ylides at quinone methide **3b**. The cyano-substituted ammonium ylide **1a** reacts roughly six orders of magnitude faster with the quinone methide **3b** than the corresponding triphenylphosphonium ylide, and three orders of magnitude faster than the related dimethylsulfonium ylide. While the cyano substituted carbanions from malononitrile and cyanoacetate are significantly more nucleophilic than the structurally related phosphonium and sulfonium ylides, the reactivity of ammonium ylide **1a** and the corresponding pyridinium ylide exceed those of the corresponding carbanions by one order of magnitude. The ethoxycarbonyl-stabilized ammonium ylide **1c** behaves similarly, as it reacts almost five orders of magnitude

faster with **3b** than the corresponding phosphonium ylide, and three orders of magnitude faster than the related sulfonium ylide. In contrast to the reactivity order on the left side of Figure 2.16, the ammonium ylide **1c** reacts half an order of magnitude more slowly with **3b** than the ethoxycarbonyl-substituted carbanions diethyl malonate and ethyl cyanoacetate, and even one order of magnitude more slowly than the ethoxycarbonyl-substituted pyridinium ylide.

As reactions of ammonium ylides in vicarious nucleophilic aromatic substitution have already been described in the literature, ammonium ylides are now considered to be ideal candidates for the quantification of the electrophilic reactivities of electron-deficient arenes.[5, 35]
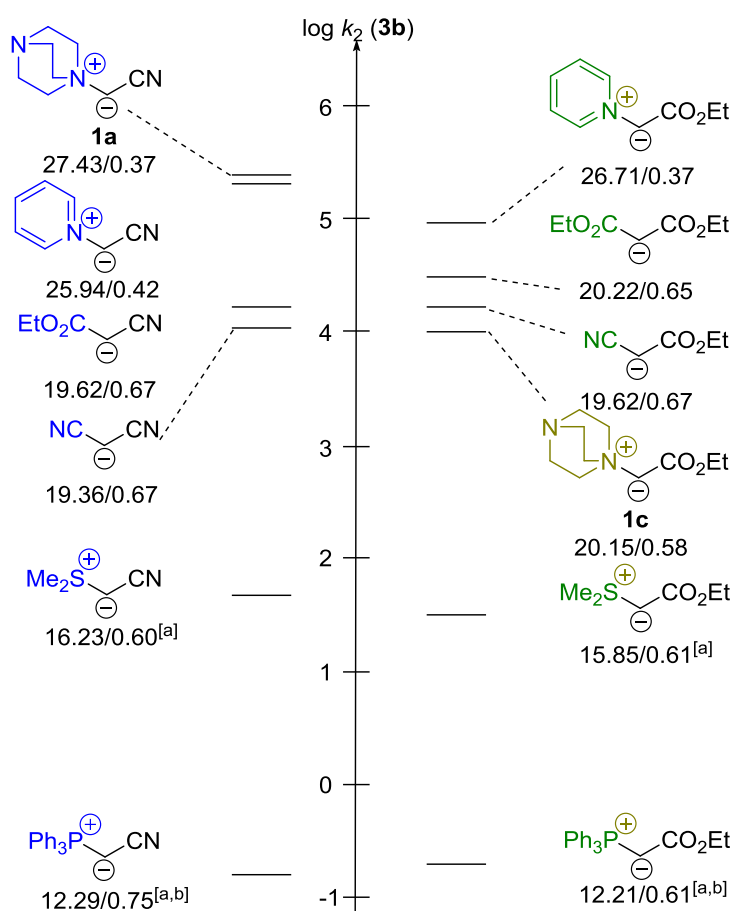
Figure 2.16. Comparison of the log k_{CC}-values of analogous substituted ylides[16-17, 18] and carbanions[19c] towards the quinone methide 3b in DMSO at 20 °C. N and s_N-Values are given below each Nucleophile. [a] Log k_2 (3b) calculated by eq 2.1 with E from Chart 2.1 and the given N and s_N values; [b] In CH₂Cl₂.

2.6 Addendum

2.6.1 Reactions of Ammonium Ylides with Activated Styrenes

The reactions of the ammonium ylides **1a**,**b** with the activated styrenes **16a–d** gave the cyclopropanes **18** via intermediate betaines **17a–d** (Table 2.17). While the cyclopropanes **18a–c** were formed in 34−57% yield at room temperature within 1 h, **18d** could only be obtained, when the ammonium salt **1aH⁺Br⁻** and 4-phenyl-buten-2-one **16d** were heated with K_2CO_3 in DMSO at 100 °C for 2 h.

The assignment of the diastereoisomers is preliminary as it is only based on the coupling constants of the protons in the cyclopropane ring and needs to be verified by 2D NMR (NOESY). The reactions selectively formed the diastereoisomers **18-A**, in which the *trans*-configuration of the substituents of the activated styrenes **16** was preserved (Table 2.17). In case of the cyclopropane **18c** the formation of the *meso*-diastereomer **18c-B** was observed, which could be unambiguously identified by the multiplicity (d, t) and coupling constant ($J^3 = 6.2$ Hz) of the protons of the cyclopropane ring.

Table 2.17. Reaction of the ylides 1a,b with the activated styrenes 16.
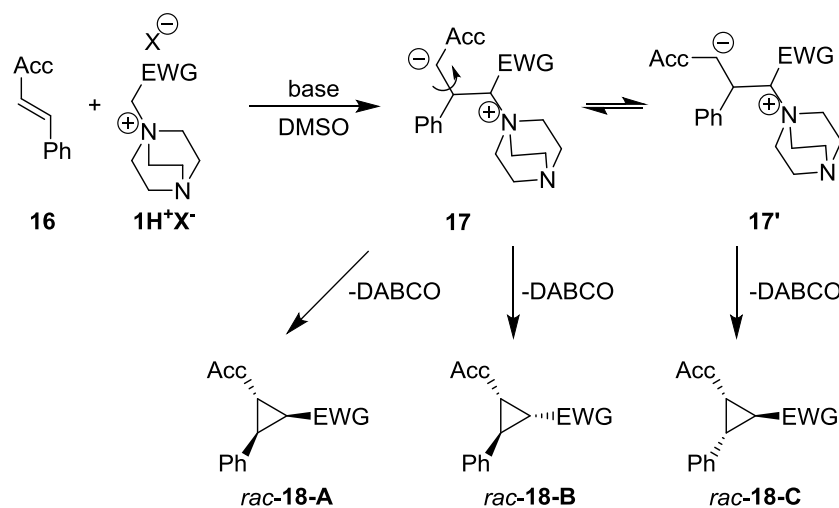
Salt 1H⁺X⁻	EWG	Styrene 16	Acc	Base	T/ °C	Betaine 17	Cyclo-propane 18	Yield 18/%	dr 18-A:B:C[a]
1aH⁺Br⁻	CN	**16a**	CO₂Et	KOᵗBu	20	**17a**	**18a**	57	66:33:0
1bH⁺Br⁻	CONEt₂	**16b**	Tos	KOᵗBu	20	**17b**	**18b**	49	92:8:0[b]
1aH⁺Br⁻	CN	**16c**	CN	KOᵗBu	20	**17c**	**18c**	34	50:50[c]
1aH⁺Br⁻	CN	**16d**	COMe	KOᵗBu	20	**17d**	**18d**	0	-
				K₂CO₃	100	**17d**	**18d**	77	66:33:0

[a] Determined by ¹H NMR of the crude product; [b] After purification, [c] Due to their symmetry **18c-A** and **18c-C** are enantiomers.

Rotation of the former CC-double bond in the intermediate betaines **17** seems not to take place as the diastereoisomers **18-C** were not observed (Table 2.17).
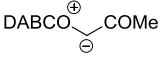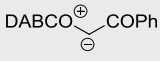
Attempts to study the kinetics of the reactions of the ylides **1a,b** with the activated styrenes **16a–d** by UV-vis spectrophotometry failed, due to an overlap of the UV-vis absorptions of the reactants. An assignment of the cyclopropanations of the activated styrenes **16** to one of the four mechanistic cases was thus not attempted.

2.6.2   Marcus Analysis

From the observed rate- and equilibrium constants, Marcus intrinsic barriers $\Delta G_0^{\neq}$ could be derived. The equilibrium constants K (Tables 2.5, 2.10) and rate constants k_{CC} (Tables 2.5, 2.10) for the CC-bond formation to the intermediate betaines were converted into ΔG^0 and $\Delta G^{\neq}$ and inserted into the Marcus equation (eq 2.12) to calculate $\Delta G_0^{\neq}$ (Table 2.18). Substituent effects on ΔG^0 and $\Delta G^{\neq}$ in the reactions of the less basic ylides **1d,e** with the Michael acceptors **3b** and **5b** are relatively small, as the acetyl-stabilized ylide **1d** has only ≈ 1 kJ mol^{-1} smaller intrinsic barriers than the benzoyl-substituted ylide **1e** (Table 2.18). The additions of the ylides **1d,e** to **3b** proceed with an intrinsic barrier which is 8–9 kJ mol^{-1} higher than that for the analogous reaction with **5b** (Table 2.18), which may be explained by the large reorganization energy when the resonance stabilization of the phenylogous amide **3b** is destroyed.

$$\Delta G^{\neq} = \Delta G_0^{\neq} + 0.5\Delta G^0 + \frac{(\Delta G^0)^2}{16\Delta G_0^{\neq}} \qquad (2.12)$$

Table 2.18: Reaction free energies (ΔG^0), activation free energies ($\Delta G^{\neq}$), and intrinsic barriers ($\Delta G_0^{\neq}$) for the reaction of the ylides 1d and 1e with the electrophiles 3b and 5b (DMSO, 20°C).

Nucleophile	Electrophile	ΔG^0/kJ mol^{-1} [a]	$\Delta G^{\neq}$/kJ mol^{-1} [b]	$\Delta G_0^{\neq}$/kJ mol^{-1} [c]
DABCO⊕ ⊖ COMe	**3b**	−12.4	57.5	63.5
	5b	(−13)	49.6	(56)
1d				
DABCO⊕ ⊖ COPh	**3b**	−13.7	57.4	64.1
	5b	(−13)	48.9	(55)
1e				

[a] $\Delta G^0 = RT\ln K$; [b] From k_{CC} in Tables 2.8, 2.10, using the Eyring equation; [c] From Marcus equation (eq 2.12).

2.6.3 pK_a-Correlation

The structurally related benzoyl-substituted quinuclidinium and trimethylammonium (**1iH$^+$Br$^-$**) salts have the same pK_a values (Table 2.1).[8c] Hence the pK_a values of trimethylammonium salts are assumed to be the same as these of the employed DABCO$^+$-substituted salts **1(a–e)H$^+$Br$^-$** (refs. [8c,d]) A plot of these pK_a values versus the log k_{CC}-values of the reactions of the ylides **1a–e** with the quinone methide **3b** shows only a poor correlation (Figure 2.17), as it was shown for many other nucleophiles before (ref. [10]). Therefore, the pK_a values of the ammonium ylides **1** cannot be used to predict their reactivity.
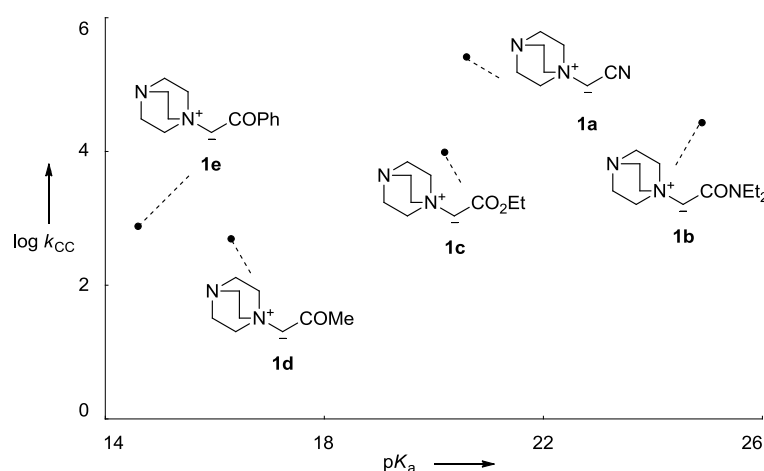
Figure 2.17. Plot of the pK_a values[8c,d] of the ammonium salts 1(a–e)H$^+$X$^-$ versus the log k_{CC} values of the reactions of the corresponding ylides 1a–e with quinone methide 3b.

2.6.4 Correlation of the log k_2-values of the Ylides 1 with Chalcone 6

The plots (log k_{2obs})/s_N versus the nucleophilicity parameters N for the reactions of the cyano and ester-substituted ammonium ylides **1a,c** and of the reactions with sulfonium and pyridinium ylides (Table 2.19) are linear (Figure 2.18). The rate constants of the reactions of the ammonium ylides **1a,c** with chalcone **6** follow this correlation line confirming our interpretation of a rate determining betaine formation according to case 1a (Table 2.19; filled dots). The (log k_{2obs})/s_N values for the reactions of **1d,e** with **6**, as well as the (log k_2)/s_N value of the reaction of Pyr$^+$CH$^-$COPh with **6**, deviate from this correlation, therefore, the observed rate constant can be assigned to $K \cdot k_{rc}$ (case 1b).
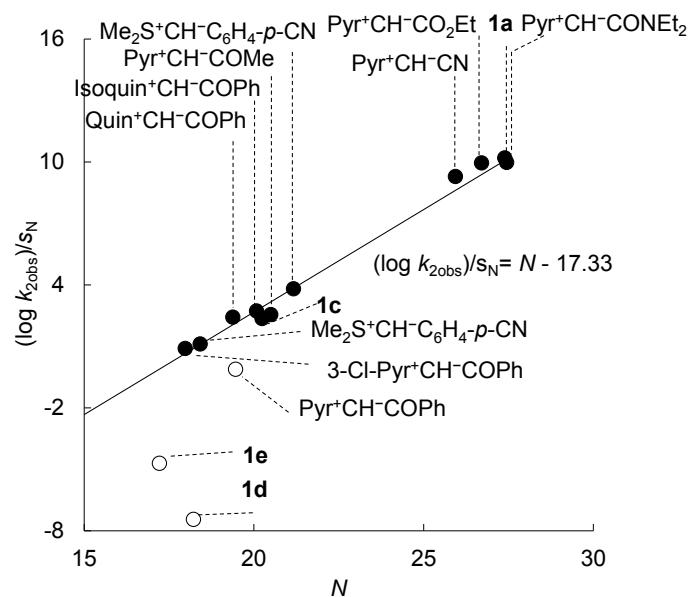
Figure 2.18. Plot of (log k_{2obs})/s_N versus N of the reactions of chalcone **6** ($E = -17.33$) with the ammonium ylides **1a,c,d,e**, pyridinium ylides, [18] and sulfonium ylides[11b] in DMSO at 20 °C. Filled dots refer to reactions where $k_{2obs} = k_{CC}$, open dots refer to reactions where $k_{2obs} = K \cdot k_{rc}$.

Table 2.19. Observed second-order rate constants of the reactions of ammonium, pyridinium,[18] and sulfonium[11b] Ylides with chalcone **6**.

Nucleophile	N	s_N	k_{2obs}
1a	27.39	0.37	4.47×10^3
1c	20.50	0.59	3.09×10^1
1d	18.47	0.52	(9.6×10^{-5})
1e	17.15	0.70	(5.3×10^{-4})
Pyr$^+$CH$^-$CO$_2$Et[18]	26.71	0.37	4.82×10^3
Pyr$^+$CH$^-$CONEt$_2$[18]	27.45	0.38	6.12×10^3
Pyr$^+$CH$^-$CN[18]	25.94	0.42	7.92×10^3
Pyr$^+$CH$^-$COMe[18]	20.24	0.60	2.55×10^1
Pyr$^+$CH$^-$COPh[18]	19.46	0.58	8.54×10^{-1}
3-Cl-Pyr$^+$CH$^-$COPh[18]	17.98	0.63	3.67
Isoquin$^+$CH$^-$COPh[18]	20.08	0.57	3.56×10^1
Quin$^+$CH$^-$COPh[18]	19.38	0.50	1.64×10^1
Me$_2$S$^+$CH$^-$-C$_6$H$_4$-p-NO$_2$[11b]	18.42	0.56	3.46×10^2
Me$_2$S$^+$CH$^-$-C$_6$H$_4$-p-CN[11b]	21.17	0.67	5.22

2.7 Experimental Section

2.7.1 General

Analytics. ^{1}H- and ^{13}C NMR spectra were recorded in CDCl$_3$ (δ_H 7.26, δ_c 77.16),[36a] CD$_2$Cl$_2$ (δ_H 5.32, δ_c 53.84),[36b] or DMSO-d_6 (δ_H 2.50, δ_c 39.52) [36a] on 200, 300, 400, or 600 MHz NMR spectrometers. The following abbreviations were used to designate chemical shift

multiplicities: s = singlet, d = doublet, t = triplet, q = quartet, m = multiplet, br = broad. For reasons of simplicity, the ^{1}H NMR signals of AA'BB'-spin systems of p-disubstituted aromatic rings were treated as doublets. The assignments of individual NMR signals were based on additional 2D-NMR experiments (COSY, NOESY, HSQC, HMBC). Diastereomeric ratios (dr) were determined by ^{1}H NMR of the crude products if not stated otherwise. Integrals for mixtures of diastereoisomers are set to 1.0 for one proton of the minor diastereoisomer. HRMS and MS were recorded on a Finnigan MAT 95 Q (EI) mass spectrometer or Thermo Finnigan LTQ FT Ultra (ESI). The melting points were recorded on a Büchi Melting Point B-540 device and are not corrected. The UV–vis spectra were recorded on a diode array-spectrophotometer system (J&M TIDAS DAD 2062) with 0.5 mm cuvette length in DMSO by generating the ylides **1** from their corresponding salts **1H$^+$X$^-$** by deprotonation with 1.05 equiv. KO^{t}Bu.

Chemicals. CH$_2$Cl$_2$ was dried over CaH$_2$ and freshly distilled prior to use; DMSO (99.7%, extra dry, over molecular sieves, AcroSeal), and MeCN (99.9%, extra dry, over molecular sieves, AcroSeal) were purchased and used without further purification.

Kinetics. Individual reaction rates were determined by UV-vis spectroscopy in DMSO at 20 °C by using stopped-flow spectrophotometer systems (Applied Photophysics SX.18MV-R and Hi-Tech SF-61DX2) as well as diode array-spectrophotometer systems (J&M TIDAS DAD 2062). The temperature of the solutions during the kinetic studies was maintained at 20 ± 0.2 °C by using circulating bath cryostats. The ylides were generated in DMSO at 20 °C immediately before each kinetic run by mixing DMSO solutions of the salts **1H$^+$X$^-$** and KO^{t}Bu (typically 1.00:1.05 equivalents). The kinetic runs were initiated by mixing DMSO solutions of the ylides and electrophiles with the ylide **1** in large excess over the electrophiles **2−6** (> 10 equivalents) to achieve first-order conditions. First-order rate constants k_{obs} (s^{-1}) were obtained by fitting the single exponential $A_t = A_0 \exp(-k_{obs}t) + C$ (mono-exponential decrease) to the observed time-dependent absorbances (average of at least three kinetic runs for each concentration for the stopped-flow method) of the electrophiles or ylides. Second-order rate constants k_2 (L mol^{-1} s^{-1}) were derived from the slopes of the linear correlations of the obtained k_{obs} values vs. the concentrations of the ylide **1**. Parts of the kinetic data have been determined during the master thesis of the author as indicated.[38]

For the kinetic studies on the ring-closure reactions of the intermediate betaines, the ylides **1c** and **1h** were generated from their corresponding salts **1(c,h)H$^+$X$^-$** with 1.05 eq. KO^{t}Bu (if not mentioned otherwise). The kinetics were monitored photometrically by following the disappearance of the benzylidene malonate **4a** at or close to the absorption maxima of the intermediate betaines **10ca,ha** under first-order conditions using at least 10 equiv. of the ylides

1 over **2–6**. From the exponential decays of the UV-Vis absorbances of the intermediate betaines **10ca,ha**, the first-order rate constants k_{rc} were obtained. The simulation of the absorption during the reaction of **1c** with **4a** was performed by Dr. K. Troshin using a MATLAB program code.[24, 39]

For evaluating the second slow decay of the absorbances of quinone methide **3b** and benzylidene indandione **5b** in the reactions with the acyl-substituted ylides **1d,e,i** a rate law was derived as follows:

$$K = \frac{[I]}{[E][Nu]} \qquad \Rightarrow \qquad [I] = K_\Psi[E] \qquad \Rightarrow \qquad \frac{d[I]}{dt} = K_\Psi \frac{d[E]}{dt}$$

with $K_\Psi = K[Nu]$ assuming a rapid pre-equilibrium.

$$[E]_0 = [E] + [I] + [P] \qquad \Rightarrow \qquad 0 = \frac{d[E]}{dt} + \frac{d[I]}{dt} + \frac{d[P]}{dt} \qquad \Rightarrow$$

$$0 = \frac{d[E]}{dt} + K_\Psi \frac{d[E]}{dt} + \frac{d[P]}{dt}$$

$$(1 + K_\Psi)\frac{d[E]}{dt} = -\frac{d[P]}{dt} \qquad \Rightarrow \qquad (1 + K_\Psi)\frac{d[E]}{dt} = -k_{rc}[I]$$

with $\dfrac{d[P]}{dt} = k_{rc}[I]$

$$-\frac{d[E]}{dt} = \frac{k_{rc}}{1 + K_\Psi}[I] = \frac{k_{rc}}{1 + K_\Psi}K_\Psi[E]$$

$$-\frac{d[E]}{[E]} == \frac{k_{rc}K_\Psi}{1 + K_\Psi}dt$$

$$k_{obs} = \frac{k_{rc}K_\Psi}{1 + K_\Psi} \qquad \text{or} \qquad k_{obs} = \frac{k_{rc}K[Nu]}{1 + K[Nu]}$$

for $K[Nu] \ll 1 \Rightarrow$ $k_{obs} = k_{rc}K[Nu]$ (case 1b)

for $K[Nu] \gg 1 \Rightarrow$ $k_{obs} = k_{rc}*$

$$\Rightarrow \qquad \frac{1}{k_{obs}} = \frac{1}{Kk_{rc}}\frac{1}{[Nu]} + \frac{1}{k_{rc}} \quad (1.10)$$

*This corresponds to the consumption of a small residual concentration of electrophile in the second step of case 2b, which can actually not be observed.

The equilibrium constants for the reactions of the ammonium ylides **1d,e,i** with the Michael acceptors **3b** and **5a** were determined by UV-Vis spectrophotometry in DMSO by using a stopped-flow spectrophotometer. The Michael acceptors **3b** and **5a** were treated with large excesses (> 10 equiv.) of the ammonium ylides **1** in variable concentrations. From the initial absorbances (A_0) and the absorbance plateaus in the ms or s time scale (A_{eq}), the equilibrium constants K were derived as defined in eq 2.10, as the slopes of the linear correlations of ($A_{eq} - A_0$)/A_{eq} with [**1**], assuming proportionality between the absorbances and the concentrations of the employed electrophiles. In most cases the CC-bond formations were the ring closure reactions of the intermediate betaines were too fast, to give clearly visible plateaus on the ms and s time scale. In these cases the equilibrium constants were determined from the initial absorbances A_0 and the constant C obtained by fitting the monoexponential function $A_t = A_0$ $\exp(-k_{obs}t) + C$ to the time-dependent absorbances.

The kinetics followed by NMR were performed on a 200 MHz NMR spectrometer. The experimental procedures for the ^{1}H NMR monitoring of the reactions of the ylides **1** with the Michael acceptors **3−6** are given below the analytical data of the corresponding reaction products in the Products Section; the corresponding kinetic measurements are given in the Kinetics Section. For the evaluation of the measurements, the HO^{t}Bu formed by the deprotonation of **1H$^+$X$^−$** was used as internal standard to derive the concentrations of the evolving DABCO, if not mentioned otherwise. For measuring the rates of ring-closure from the intermediate betaines the concentrations of DABCO were plotted versus time and fitted with OriginPro 6.0 by using the monoexponential function $y = y_0 + A_1e^{-x/t1}$ with t1 = $1/k_1$. For reactions following a second-order rate law the plots of the transient concentrations of the reactants [**1**] and [E] were calculated from the initial concentrations [**1**]$_0$ and [E]$_0$ and the concentration of the evolved DABCO. From the slopes of plots of [**1**]$^{-1}$ or [E]$^{-1}$ versus t, the second-order rate constant k_{2obs} was determined according to eq 2.11.

The kinetics followed by GC-MS were performed on an Agilent 5973 Network GC-MS. For performing these kinetics, the ylides **1** were generated by addition of solutions of KO^{t}Bu (128 mg, 1.14 mmol) in DMSO (4 mL) to solutions of **1H$^+$X$^−$** (1.14 mmol) in DMSO (10 mL). After 30 s the electrophile **4d** (200 mg, 0.762 mmol) dissolved in DMSO (6 mL) was added and the reaction mixture was stirred for 15 min at 20 °C. Every minute a sample of the reaction mixture (1 mL) was taken and quenched by addition of sat. aq. NH$_4$Cl (3 mL). The mixtures were extracted with Et$_2$O (4 mL) and filtrated through Na$_2$SO$_4$. A sample of each organic layer was subjected to GC-MS analysis. After 15 min the remaining solution was quenched with sat. aq. NH$_4$Cl (20 mL) and extracted with Et$_2$O (2×10 mL). The combined organic layers were

washed with water (10 mL) and dried over MgSO$_4$. The solvent was evaporated and the corresponding cyclopropanes were obtained. For evaluation of the kinetics, the reactant/product ratios were converted into concentrations and fitted by a second-order rate law using the GEPASI (v. 3.30) software. The reaction was described as [**Nu**]+[**E**]->[**I**]->[**P**], with k_{CC} as the rate constant for the rate-determining, irreversible first, and k_{rc} as the rate constant for the fast subsequent reaction.

2.7.2 Preparation of the Ammonium Salts 1H$^+$X$^-$

General Procedure A for the Preparation of the ammonium salts 1H+X−. The ammonium salts **1H+X–** were prepared from the corresponding α-alkylhalides and tertiary amines in THF. The amine was dissolved in THF and the α-alkylhalides was added dropwise at ambient temperature. After 30 min the resulting precipitate was removed, washed with Et$_2$O, and subsequently recrystallized from MeOH:C$_6$H$_5$CH$_3$.

1-(Cyanomethyl)-1,4-diazabicyclo[2.2.2]octan-1-ium bromide (1aH$^+$Br$^-$). From bromoacetonitrile (1.7 g, 1.0 mL, 14 mmol) and DABCO (1.6 g, 14 mmol) according to procedure **A**. **1aH$^+$Br$^-$** was obtained as colorless solid (3.2 g, 14 mmol, quant.). **Mp** (MeOH:C$_6$H$_5$CH$_3$) 195 °C (decomp.). **^{1}H NMR** (400 MHz, DMSO-d_6) δ = 4.98 (s, 2 H, CH$_2$), 3.53 − 3.42 (m, 6 H, 3×$^+$NCH$_2$), 3.16 − 3.06 (m, 6 H, 3×NCH$_2$). **^{13}C NMR** (100 MHz, DMSO-d_6) δ = 111.5 (s, CN), 52.6 (t, 3×$^+$NCH$_2$), 50.2 (t, CH$_2$), 44.5 (t, 3×NCH$_2$). **HRMS** (ESI+): m/z calcd. for [C$_8$H$_{14}$N$_3$]$^+$: 152.1182, found 152.1183. DA131

1-(2-(Diethylamino)-2-oxoethyl)-1,4-diazabicyclo[2.2.2]octan-1-ium chloride (1bH$^+$Cl$^-$). From 2-chloro-N,N-diethylacetamide (1.6 g, 11 mmol) and DABCO (1.2 g, 11 mmol) according to procedure **A**. **1bH$^+$Cl$^-$** was obtained as colorless solid (2.7 g, 10 mmol, 91%). **Mp** (MeOH:C$_6$H$_5$CH$_3$) 216 °C (decomp.). **^{1}H NMR** (400 MHz, DMSO-d_6) δ = 4.58 (s, 2 H, CH$_2$), 3.68 − 3.65 (br m, 6 H, 3×$^+$NCH$_2$), 3.31 − 3.25 (m, 4 H, 2×NCH$_2$, superimposed by H$_2$O signal), 3.06 − 3.02 (br, m, 6 H, 3×NCH$_2$), 1.12 (t, J = 7.1 Hz, 3 H, CH$_3$), 1.02 (t, J = 7.1 Hz, 3 H, CH$_3$). **^{13}C NMR** (100 MHz, DMSO-d_6) δ = 163.0 (s, CO), 60.4 (d, CH$_2$), 52.5 (t, 3×$^+$NCH$_2$), 45.0 (t, 3×NCH$_2$), 41.55 (t, NCH$_2$), 40.4 (t, NCH$_2$), 14.3 (q, CH$_3$), 13.2 (q, CH$_3$). **HRMS** (ESI+): m/z calcd. for [C$_{12}$H$_{24}$N$_3$O]$^+$: 226.1914, found 226.1912. DA181

1-(2-Ethoxy-2-oxoethyl)-1,4-diazabicyclo[2.2.2]octan-1-ium bromide (1cH$^+$Br$^-$). From ethylbromoacetate (2.0 g, 12 mmol) and DABCO (3.0 g, 27 mmol) according to procedure **A**. **1cH$^+$Br$^-$** was obtained as colorless solid (5.0 g, 18 mmol, quant.). **Mp** (MeOH:C$_6$H$_5$CH$_3$) 235 °C (decomp.). **^{1}H NMR** (400 MHz, DMSO-d_6) δ = 4.40
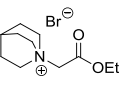
(br s, 2 H, CH$_2$), 4.23 (q, J = 7.1 Hz, 2 H, CH$_2$), 3.52 (br s, 6 H, 3×$^+$NCH$_2$), 3.13 – 3.03 (m, 6 H, 3×NCH$_2$), 1.25 (t, J = 7.1 Hz, 3 H, CH$_3$). ^{13}C NMR (100 MHz, DMSO-d_6) δ = 164.4 (s, CO$_2$), 61.9 (t, CH$_2$), 60.7 (t, CHH), 52.3 (t, 3×$^+$NCH$_2$), 44.4 (t, 3×NCH$_2$), 13.8 (q, CH$_3$). **HRMS** (ESI+): m/z calcd. for [C$_{10}$H$_{19}$N$_2$O$_2$]$^+$: 199.1441, found 199.1435. DA62

1-(2-Oxopropyl)-1,4-diazabicyclo[2.2.2]octan-1-ium chloride (1dH$^+$Cl$^-$). From chloroacetone (4.3 g, 5.0 mL, 47 mmol) and DABCO (5.2 g, 47 mmol) according to procedure **A**. **1dH$^+$Cl$^-$** was obtained as colorless solid (7.2 g, 35 mmol, 76%). **Mp** (MeOH: C$_6$H$_5$CH$_3$) 160 °C (decomp.). **^{1}H NMR** (400 MHz, DMSO-d_6) δ = 4.66 (s, 2 H, CH$_2$), 3.53 – 3.44 (m, 6 H, 3×$^+$NCH$_2$), 3.11 – 3.01 (m, 6 H, 3×NCH$_2$), 2.16 (s, 3 H, CH$_3$). **^{13}C NMR** (100 MHz, DMSO-d_6) δ = 200.37 (s, CO), 66.9 (s, CH$_2$), 52.0 (t, 3×$^+$NCH$_2$), 44.4 (t, 3×NCH$_2$), 28.7 (q, CH$_3$). **HRMS** (ESI+): m/z calcd. for [C$_9$H$_{17}$N$_2$O]$^+$: 169.1335, found 169.1335. DA168
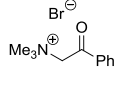
1-(2-Oxopropyl)-1,4-diazabicyclo[2.2.2]octan-1-ium triflate (1dH$^+$OTf$^-$). Trimethylsilyl triflate (0.82 g, 3.7 mmol) was added to a solution of **1dH$^+$Cl$^-$** (0.50 g, 2.4 mmol) in MeCN (5 mL) under N$_2$ at ambient temperature. After the evolution of HCl stopped, stirring was continued for 30 min. The solvent was evaporated and the crude product was recrystallized from MeCN:Et$_2$O . **1dH$^+$OTf$^-$** was obtained as colorless solid (0.62 g, 2.0 mmol, 83%). **Mp** (MeCN:Et$_2$O) 201 °C (decomp.). **^{1}H NMR** (400 MHz, DMSO-d_6) δ = 4.66 (s, 2 H, CH$_2$), 3.82 – 3.75 (br, m, 6 H, 3×$^+$NCH$_2$), 3.60 – 3.52 (br, m, 6 H, 3×NCH$_2$), 2.18 (s, 3 H, CH$_3$). **^{13}C NMR** (100 MHz, DMSO-d_6) δ = 200.3 (s, CO), 120.7 (q, J = 322 Hz, CF$_3$) , 67.7 (t, CH$_2$), 51.7 (t, 3×$^+$NCH$_2$), 43.7 (t, 3×NCH$_2$), 28.9 (q, CH$_3$). **HRMS** (ESI+): m/z calcd. for [C$_9$H$_{17}$N$_2$O]$^+$: 169.1335, found 169.1335; m/z calcd. for [C$_9$H$_{17}$N$_2$O(2×CF$_3$O$_3$S)]$^-$: 467.0387, found 467.0377. DA168

1-(2-Oxo-2-phenylethyl)-1,4-diazabicyclo[2.2.2]octan-1-ium bromide (1eH$^+$Br$^-$). From bromoacetophenone (0.50 g, 2.5 mmol) and DABCO (0.28 g, 2.5 mmol) according to procedure **A**. **1eH$^+$Br$^-$** was obtained as colorless solid (0.62 g, 2.0 mmol, 80%). **Mp** (MeOH:C$_6$H$_5$CH$_3$) 255 °C; lit: 252–255 °C.[37c] **^{1}H NMR** (400 MHz, DMSO-d_6) δ = 8.07 – 7.98 (m, 2 H, 2×C$_{Ar}$-H), 7.79 – 7.72 (m, 1 H, C$_{Ar}$-H), 7.65 – 7.57 (m, 2 H, 2×C$_{Ar}$-H), 5.35 (s, 2 H, CH$_2$), 3.70 – 3.59 (m, 6 H, 3×$^+$NCH$_2$), 3.18 – 3.06 (m, 6 H, 3×NCH$_2$). ^{13}C NMR (100 MHz, DMSO-d_6) δ = 191.2 (s, CO), 134.7 (d, C$_{Ar}$-H), 134.5 (s, C$_{Ar}$), 129.0 (d, 2×C$_{Ar}$-H), 128.1 (d, 2×C$_{Ar}$-H), 65.1 (t, CH$_2$), 52.4 (t, 3×$^+$NCH$_2$), 44.4 (t, 3×NCH$_2$). **HRMS** (ESI+): m/z calcd. for [C$_{14}$H$_{19}$N$_2$O]$^+$: 231.1492, found 231.1485. DA72
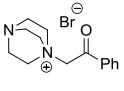
1-(2-(*tert*-Butoxy)-2-oxoethyl)-1,4-diazabicyclo[2.2.2]octan-1-ium bromide (1fH⁺Br⁻). From *tert*-butylbromoacetate (4.68 g, 24.0 mmol) and DABCO (2.70 g, 24.0 mmol) according to procedure **A**. **1fH⁺Br⁻** was obtained as colorless solid (7.01 g, 22.8 mmol, 95%). **Mp** (MeOH:C₆H₅CH₃) 250 °C. **¹H NMR** (400 MHz, DMSO-d_6) δ = 4.28 (s, 2 H, CH₂), 3.53 – 3.44 (m, 6 H, 3×⁺NCH₂), 3.11 – 3.03 (m, 6 H, 3×NCH₂), 1.48 (s, 9 H, 3×CH₃). **¹³C NMR** (100 MHz, DMSO-d_6) δ = 163.5 (s, CO), 84.0 (s, C_q), 61.2 (t, CH₂), 52.2 (t, 3×⁺NCH₂), 44.4 (t, 3×NCH₂), 27.6 (q, 3×CH₃). **HRMS** (ESI+): *m/z* calcd. for [C₁₂H₂₃N₂O₂]⁺: 227.1754, found 227.1747. DA54

1-(2-Ethoxy-2-oxoethyl)quinuclidin-1-ium bromide (1gH⁺Br⁻). From ethylbromoacetate (0.75 g, 4.5 mmol) and quinuclidine (0.50 g, 4.5 mmol) according to procedure **A**. **1gH⁺Br⁻** was obtained as colorless solid (0.89 g, 3.2 mmol, 71%). **Mp** (MeOH:C₆H₅CH₃) 162 °C; lit 162–163 °C.[37a] **¹H NMR** (400 MHz, DMSO-d_6) δ = 4.34 (s, 2 H, CH₂CO), 4.24 (q, *J* = 7.1 Hz, 2 H, OCH₂), 3.67 – 3.59 (br m, 6 H, 3×⁺NCH₂), 2.07–2.03 (br m, 1 H, CH), 1.92–1.85 (br m, 6 H, 3×CH₂), 1.21 (t, *J* = 7.1 Hz, 3 H, CH₃). **¹³C NMR** (100 MHz, DMSO-d_6) δ = 164.5 (s, CO₂), 61.9 (t, OCH₂), 60.8 (t, *C*H₂CO), 54.6 (q, 3×⁺NCH₂), 23.1 (t, 3×CH₂), 18.8 (t, CH), 13.8 (q, CH₃). **HRMS** (ESI+): *m/z* calcd. for [C₁₁H₂₀NO₂]⁺: 198.1489, found 198.1482. DA78

2-Ethoxy-*N,N,N*-trimethyl-2-oxoethan-1-aminium bromide (1hH⁺Br⁻). From ethylbromoacetate (1.0 g, 6.0 mmol) and NMe₃ (0.35 g, 5.9 mmol, 50 wt% in H₂O) according to procedure **A**. **1hH⁺Br⁻** was obtained as colorless solid (1.1 g, 4.9 mmol, 83%). **Mp** (MeOH:C₆H₅CH₃): 156°C. **¹H NMR** (400 MHz, DMSO-d_6) δ = 4.50 (s, 2 H, CH₂), 4.20 (q, *J* = 7.1 Hz, 2 H, OCH₂), 3.24 (s, 9 H, 3×⁺NCH₃, 1.21 (t, *J* = 7.1 Hz, 3 H, CH₃). **¹³C NMR** (100 MHz, DMSO-d_6) δ = 165.3 (s, CO), 62.9 (t, OCH₂), 62.4 (t, CH₂), 53.5 (q, 3×⁺NCH₃), 14.3 (q, CH₃). **HRMS** (ESI+): *m/z* calcd. for [C₇H₁₆NO₂]⁺: 146.1176 found 146.1171. DA96

***N,N,N*-Trimethyl-2-oxo-2-phenylethan-1-aminium bromide (1iH⁺Br⁻).** From bromoacetophenone (1.0 g, 5.0 mmol) and NMe₃ (0.31 g, 5.2 mmol, 50 w% in water) according to procedure **A**. The precipitate was additionally washed with CH₂Cl₂. **1iH⁺Br⁻** was obtained as colorless solid (1.29 g, 5.00 mmol, quant.). **Mp** (MeOH:C₆H₅CH₃) 220 °C; lit: 220 °C.[37b] **¹H NMR** (400 MHz, DMSO-d_6) δ = 8.05 – 7.96 (m, 2 H, 2×C_{Ar}-H), 7.79 – 7.70 (m, 1 H, C_{Ar}-H), 7.67 – 7.56 (m, 2 H, 2C_{Ar}-H), 5.47 (s, 2 H, CH₂), 3.36 (s, 9 H, NMe₃). **¹³C NMR** (100 MHz, DMSO-d_6) δ = 191.5 (s, CO), 134.7 (s, C_{Ar}), 134.4 (d, C_{Ar}-H), 129.0 (d, 2×C_{Ar}-H), 127.9 (d, 2×C_{Ar}-H), 67.2 (t, CH₂), 53.3 (q, NMe₃). **HRMS** (ESI+): *m/z* calcd. for [C₁₁H₁₆NO]⁺: 178.1226 found 178.1222. DA95

2.7.3 Products of the Reactions of the Ammonium Ylides 1 with the Electrophiles 2−6

2.7.3.1 Reactions with Benzhydrylium Ion 2a-BF₄

General procedure B for the synthesis of the products 7-BF₄. KO^tBu (1.1 Equiv) in THF (5 mL) was added to a suspension of **2a-BF₄** (147−294 μmol) and **1H⁺X⁻** (147−294 μmol) in CH₂Cl₂/MeCN (5 mL, 3:2) at ambient temperature until discoloration of **2a-BF₄** was observed. The solvent was evaporated and the resulting solid was taken up in MeCN (10 mL) and insoluble solids were removed. After removal of the solvent the crude product was obtained. The crude product was recrystallized from Et₂O:MeCN (10:1) or MeCN to give the ammonium salts **7-BF₄**. The ammonium salts **7-BF₄** are sensitive to moisture and acids and are decomposed easily.

1-(1-Cyano-2,2-bis(4-(dimethylamino)phenyl)ethyl)-1,4-diazabicyclo[2.2.2]octan-1-ium tetrafluoroborate (7a-BF₄). From **2a-BF₄** (100 mg, 294 μmol), **1aH⁺Br⁻** (68.2 mg, 294 μmol) and KO^tBu (35.0 mg, 312 μmol) according to procedure **B**. The crude product was obtained in 96% yield (139 mg, 283 μmol). After recrystallization from MeCN **7a-BF₄** was obtained as a yellow solid (30.1 mg, 61.3 μmol, 21%). **Mp** (MeCN) 133 °C. **¹H NMR** (400 MHz, DMSO-d_6) δ = 7.38 (d, J = 8.8 Hz, 2 H, 2×C$_{Ar}$-H), 7.30 (d, J = 8.9 Hz, 2 H, 2×C$_{Ar}$-H), 6.66 (d, J = 8.9 Hz, 4 H, 4×C$_{Ar}$-H), 6.18 (d, J = 8.2 Hz, 1 H, CH), 4.94 (d, J = 8.2 Hz, 1 H, CH), 3.51 − 3.42 (m, 6 H, 3×CH₂), 3.04 (t, J = 6.7 Hz, 6 H, 3×CH₂), 2.84 (s, 6 H, 2×CH₃), 2.83 (s, 6 H, 2×CH₃). **¹³C NMR** (100 MHz, DMSO-d_6) δ = 150.1 (s, C$_{Ar}$), 149.9 (s, C$_{Ar}$), 129.4 (d, 2×C$_{Ar}$-H), 128.7 (d, 2×C$_{Ar}$-H), 127.7 (s, C$_{Ar}$), 127.5 (s, C$_{Ar}$), 113.6 (s, CN), 113.0 (d, 2×C$_{Ar}$-H), 112.9 (d, 2×C$_{Ar}$-H), 68.34 (d, CH), 52.8 (t, 3×CH₂), 46.0 (d, CH) , 44.9 (t, 3×CH₂), 40.7 (q, 2×CH₃), 40.3 (q, 2×CH₃). **HRMS** (ESI+): m/z calcd. for [C₂₅H₃₄N₅]⁺: 404.2809, found 404.2807. DA164

1-(1-(Diethylamino)-3,3-bis(4-(dimethylamino)phenyl)-1-oxopropan-2-yl)-1,4-diazabi-cyclo[2.2.2]octan-1-ium tetrafluoroborate (7b-BF₄). From **2a-BF₄** (100 mg, 294 μmol), **1bH⁺Cl⁻** (77.0 mg, 294 μmol) and KO^tBu (35.0 mg, 312 μmol) according to procedure **B**. The crude product was obtained in 91% yield (151 mg, 267 μmol). After recrystallization from MeCN **7b-BF₄** was obtained as a yellow solid (8.8 mg, 16 μmol, 5%). **Mp** (MeCN) 181 °C (decomp.). **¹H NMR** (400 MHz, DMSO-d_6) δ = 7.54 (d, J = 8.8 Hz, 2 H, 2×C$_{Ar}$-H), 7.13 (d, J = 8.8 Hz, 2 H, 2×C$_{Ar}$-H), 6.69 (d, J = 8.8 Hz, 2 H, 2×C$_{Ar}$-H), 6.55 (d, J = 8.9 Hz, 2 H, 2×C$_{Ar}$ H), 5.44 (d, J = 10.7 Hz, 1 H, CH), 4.61 (d, J = 10.6 Hz, 1 H, CH), 3.90 − 3.78 (m, 1 H, CHH^b), 3.59 − 3.41 (m, 6 H, 3×CH₂),

3.33–3.28 (m, 1 H, CHH^b), 3.15–3.08 (m, 1 H, CHH^a), 3.01 − 2.91 (m, 6 H, 3×CH$_2$), 2.86 (s, 6 H, 2×CH$_3$), 2.77 (s, 6 H, 2×CH$_3$), 2.73 − 2.65 (m, 1 H, CHH^a), 1.09 (t, J = 7.0 Hz, 3 H, CH$_3$), 0.38 (t, J = 7.0 Hz, 3 H, CH$_3$). **^{13}C NMR** (100 MHz, DMSO-d_6) δ = 164.6 (s, CO), 150.0 (s, C$_{Ar}$), 149.7 (s, C$_{Ar}$), 129.6 (d, 2×C$_{Ar}$-H), 129.5 (d, 2×C$_{Ar}$-H), 128.4 (s, C$_{Ar}$), 128.3 (s, C$_{Ar}$), 113.0 (d, 2×C$_{Ar}$-H), 112.6 (d, 2×C$_{Ar}$-H), 71.1 (d, CH), 52.4 (t, 3×CH$_2$), 49.7 (d, CH), 45.1 (t, 3×CH$_2$), 45.0 (t, CHH), 42.1 (t, CHH), 40.7 (q, 2×CH$_3$), 40.4 (q, 2×CH$_3$), 13.9 (q, CH$_3$), 11.5 (q, CH$_3$). **HRMS** (ESI+): m/z calcd. for [C$_{29}$H$_{44}$N$_5$O]$^+$: 478.3540, found 478.3538. DA189-2

1-(1,1-Bis(4-(dimethylamino)phenyl)-3-ethoxy-3-oxopropan-2-yl)-1,4-diazabicyclo-[2.2.2]octan-1-ium tetrafluoroborate (7c-BF$_4$). From **2a-BF$_4$** (50.0 mg, 147 μmol), **1cH$^+$Br$^−$** (41.0 mg, 147 μmol) and KO^{t}Bu (25.0 mg, 223 μmol) according to procedure **B**. The crude product was recrystallized from MeCN to give **7c-BF$_4$** as a colorless solid (21.7 mg, 40.3 μmol, 27%). **Mp** (Et$_2$O:MeCN) 187 °C. **^{1}H NMR** (400 MHz, DMSO-d_6) δ = 7.44 (d, J = 8.8 Hz, 2 H, 2×C$_{Ar}$-H), 7.13 (d, J = 8.8 Hz, 2 H, 2×C$_{Ar}$-H), 6.65 (d, J = 8.9 Hz, 2 H, 2×C$_{Ar}$-H), 6.56 (d, J = 8.8 Hz, 2 H, 2×C$_{Ar}$-H), 5.37 (d, J = 10.2 Hz, 1 H, CH), 4.66 (d, J = 10.3 Hz, 1 H, CH), 3.87 − 3.70 (m, 2 H, CH$_2$), 3.50–3.33 (m, 6 H, 3×CH$_2$), 3.02–2.91 (m, 6 H, 3×CH$_2$), 2.83 (s, 6 H, 2×CH$_3$), 2.79 (s, 6 H, 2×CH$_3$), 0.86 (t, J = 7.1 Hz, 3 H, CH$_3$). **^{13}C NMR** (100 MHz, DMSO-d_6) δ = 166.4 (s, CO), 149.9 (s, C$_{Ar}$), 149.7 (s, C$_{Ar}$), 129.6 (s, 2×C$_{Ar}$-H), 129.0 (d, 2×C$_{Ar}$-H), 128.5 (s, C$_{Ar}$), 128.0 (s, C$_{Ar}$), 113.2 (d, 2×C$_{Ar}$-H), 112.5 (d, 2×C$_{Ar}$-H), 76.4 (d, CH), 62.3 (t, CH$_2$), 52.1 (t, 3×CH$_2$), 47.4 (d, CH), 45.0 (t, 3×CH$_2$), 40.5 (q, 2×CH$_3$), 40.4 (q, 2×CH$_3$), 13.6 (q, CH$_3$). **HRMS** (ESI+): m/z calcd. for [C$_{27}$H$_{39}$N$_4$O$_2$]$^+$: 451.3068, found 451.3067. DA157-2
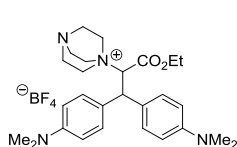
1-(1,1-Bis(4-(dimethylamino)phenyl)-3-oxobutan-2-yl)-1,4-diazabicyclo[2.2.2]octan-1-ium trifluoromethanesulfonate (7d-OTf). From **2a-BF$_4$** (100 mg, 294 μmol), **1dH$^+$OTf$^−$** (93.6 mg, 294 μmol) and KO^{t}Bu (84.0 mg, 749 μmol) according to procedure **B**. After recrystallization from Et$_2$O:MeCN **7d-OTf** was obtained as a colorless solid (123 mg, 216 μmol, 73%). **Mp** (Et$_2$O:MeCN) 176 °C. **^{1}H NMR** (400 MHz, DMSO-d_6) δ = 7.45 (d, J = 8.8 Hz, 2 H, 2×C$_{Ar}$-H), 7.14 (d, J = 8.8 Hz, 2 H, 2×C$_{Ar}$-H), 6.67 (d, J = 8.9 Hz, 2 H, 2×C$_{Ar}$-H), 6.57 (d, J = 8.9 Hz, 2 H, 2×C$_{Ar}$-H), 5.67 (d, J = 10.7 Hz, 1 H, CH), 4.55 (d, J = 10.7 Hz, 1 H, CH), 3.48 − 3.39 (m, 3 H, 3×CHH^b), 3.32–3.25 (m, 3 H, 3×CH^aH), 3.02 − 2.85 (m, 6 H, 3×CH$_2$), 2.83 (s, 6 H, 2×CH$_3$), 2.80 (s, 6 H, 2×CH$_3$), 1.97 (s, 3 H, CH$_3$). **^{13}C NMR** (100 MHz, DMSO-d_6) δ = 205.4 (s, CO), 149.73 (s, C$_{Ar}$), 149.7 (s, C$_{Ar}$), 130.0 (d, 2×C$_{Ar}$-H), 129.1 (d, 2×C$_{Ar}$-H), 128.4 (s, C$_{Ar}$), 127.0 (s, C$_{Ar}$), 121.1 (q, J = 322.3 Hz, CF$_3$), 113.2 (d, 2×C$_{Ar}$-H), 112.7 (d, 2×C$_{Ar}$-H), 77.0 (d, CH), 65.3

(d, CH), 52.1 (t, 3×CHH), 44.9 (t, 3×CH$_2$), 40.8 (q, 2×CH$_3$), 40.4 (q, 2×CH$_3$), 35.1 (q, CH$_3$). **HRMS** (ESI+): *m/z* calcd. for [C$_{26}$H$_{37}$N$_4$O]$^+$: 421.2962, found 421.2962. DA173

1-(1,1-Bis(4-(dimethylamino)phenyl)-3-oxo-3-phenylpropan-2-yl)-1,4-diazabicyclo-[2.2.2]octan-1-ium tetrafluoroborate (7e-BF$_4$). From **2a-BF$_4$** (100 mg, 294 μmol), **1eH$^+$Br$^−$** (91.6 mg, 294 μmol) and KO^{t}Bu (34.6 mg, 308 μmol) according to procedure **B** to yield 94% of the crude product (157 mg, 275 μmol). The crude product was recrystallized from MeCN to give **7e-BF$_4$** as a give solid (75.2 mg, 132 μmol, 45%). **Mp** (Et$_2$O:MeCN) 134 °C. **^{1}H NMR** (400 MHz, DMSO-d_6) δ = 8.05 (d, *J* = 7.4 Hz, 2 H, 2×C$_{Ar}$-H), 7.60–7.58 (m, 3 H, 3×C$_{Ar}$-H), 7.44 (t, *J* = 7.8 Hz, 2 H, 2×C$_{Ar}$-H), 6.96 (d, *J* = 8.9 Hz, 2 H, 2×C$_{Ar}$-H), 6.68 (d, *J* = 8.9 Hz, 2 H, 2×C$_{Ar}$-H), 6.38 (d, *J* = 10.8 Hz, 1 H, CH), 6.23 (d, *J* = 8.9 Hz, 2 H, 2× C$_{Ar}$-H), 4.76 (d, *J* = 10.7 Hz, 1 H, CH), 3.59–3.47 (m, 6 H, 3×CH$_2$), 2.98 – 2.88 (m, 6 H, 3×CH$_2$), 2.84 (s, 6 H, 2×CH$_3$), 2.62 (s, 6 H, 2×CH$_3$). **^{13}C NMR** (100 MHz, DMSO-d_6) δ = 196.3 (s, CO), 149.7 (s, C$_{Ar}$), 149.5 (s, C$_{Ar}$), 137.6 (s, C$_{Ar}$), 134.8 (d, C$_{Ar}$-H), 130.2 (d, 2×C$_{Ar}$-H), 129.4 (d, 2×C$_{Ar}$-H), 129.3 (d, 2×C$_{Ar}$-H), 129.1 (d, 2×C$_{Ar}$-H), 128.7 (s, C$_{Ar}$), 126.9 (s, C$_{Ar}$), 113.1 (d, 2×C$_{Ar}$-H), 112.4 (d, 2×C$_{Ar}$-H), 72.6 (d, CH), 52.6 (t, 3×CH$_2$), 49.3 (d, CH), 45.0 (t, 3×CH$_2$), 40.4 (q, 2×CH$_3$), 40.3 (q, 2×CH$_3$). **HRMS** (ESI+): *m/z* calcd. for [C$_{31}$H$_{39}$N$_4$O]$^+$: 483.3118, found 483.3116. DA158

1-(1-(*tert*-Butoxy)-3,3-bis(4-(dimethylamino)phenyl)-1-oxopropan-2-yl)-1,4-diaza-bicyclo[2.2.2]octan-1-ium tetrafluoroborate (7f-BF$_4$). From **2a-BF$_4$** (50 mg, 147 μmol), **1fH$^+$Br$^−$** (45.3 mg, 147 μmol), KO^{t}Bu (25.0 mg, 223 μmol) according to procedure **B**. After recrystallization from MeCN **7f-BF$_4$** was obtained as a yellow solid (64.6 mg, 114 μmol, 78%). **Mp** 166 °C (decomp.). **^{1}H NMR** (400 MHz, DMSO-d_6) δ = 7.41 (d, *J* = 8.7 Hz, 2 H, 2×C$_{Ar}$-H), 7.15 (d, *J* = 8.8 Hz, 2 H, 2×C$_{Ar}$-H), 6.64 (d, *J* = 8.8 Hz, 2 H, 2×C$_{Ar}$-H), 6.58 (d, *J* = 8.9 Hz, 2 H, 2×C$_{Ar}$-H), 5.19 (d, *J* = 10.9 Hz, 1 H, CH), 4.54 (d, *J* = 11.0 Hz, 1 H, CH), 3.51 – 3.45 (m, 3 H, 3×CHH^b), 3.38 – 3.30 (m, 3 H, 3×CH^aH), 3.00–2.94 (m, 6 H, 3×CH$_2$), 2.82 (s, 6 H, 2×CH$_3$), 2.77 (s, 6 H, 2×CH$_3$), 1.07 (s, 9 H, 3×CH$_3$). **^{13}C NMR** (100 MHz, DMSO-d_6) δ = 165.4 (s, CO), 150.1 (s, C$_{Ar}$), 149.7 (s, C$_{Ar}$), 129.7 (d, 2×C$_{Ar}$-H), 129.0 (d, 2×C$_{Ar}$-H), 128.6 (s, C$_{Ar}$), 128.4 (s, C$_{Ar}$), 113.2 (d, 2×C$_{Ar}$-H), 112.7 (d, 2×C$_{Ar}$-H), 84.3 (s, C$_q$), 76.8 (d, CH), 52.1 (t, 3×CH$_2$), 47.9 (d, CH), 45.0 (t, 3×CH$_2$), 40.6 (q, 2×CH$_3$), 40.4 (q, 2×CH$_3$), 27.2 (q, 3×CH$_3$). HRMS (ESI+): *m/z* calcd. for [C$_{29}$H$_{43}$N$_4$O$_2$]$^+$: 479.3381, found 479.33878. DA159
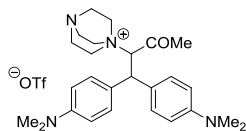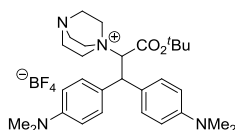
1-(1,1-Bis(4-(dimethylamino)phenyl)-3-ethoxy-3-oxopropan-2-yl)quinuclidin-1-ium tetrafluoroborate (7g-BF$_4$). From **2a-BF$_4$** (100 mg, 294 µmol), **1gH$^+$Br$^-$** (81.8 mg, 294 µmol), and KO^{t}Bu (35.0 mg, 312 µmol) according to procedure **B**. After recrystallization from Et$_2$O:MeCN **7g-BF$_4$** was obtained as a yellow solid (121 mg, 225 µmol, 77%). **Mp** (Et$_2$O:MeCN) 213 °C. **^{1}H NMR** (400 MHz, DMSO-d_6) δ = 7.43 (d, J = 8.8 Hz, 2 H, 2×C$_{Ar}$-H), 7.12 (d, J = 8.8 Hz, 2 H, 2×C$_{Ar}$-H), 6.65 (d, J = 8.8 Hz, 2 H, 2×C$_{Ar}$-H), 6.56 (d, J = 8.9 Hz, 2 H, 2×C$_{Ar}$-H), 5.26 (d, J = 10.1 Hz, 1 H, CH), 4.62 (d, J = 10.1 Hz, 1 H, CH), 3.86 – 3.67 (m, 2 H, CH$_2$), 3.62 – 3.56 (m, 3 H, 3×CHH^b), 3.51 – 3.40 (m, 3 H, 3×CH^{a}H), 2.83 (s, 6 H, 2×CH$_3$), 2.77 (s, 6 H, 2×CH$_3$), 1.99 – 1.93 (m, 1 H, CH), 1.84 – 1.69 (br s, 6 H, 3×CH$_2$), 0.85 (t, J = 7.1 Hz, 3 H, CH$_3$). **^{13}C NMR** (100 MHz, DMSO-d_6) δ = 166.6 (s, CO), 149.8 (s, C$_{Ar}$), 149.7 (s, C$_{Ar}$), 129.6 (d, 2×C$_{Ar}$-H), 129.0 (d, 2×C$_{Ar}$-H), 128.7 (s, C$_{Ar}$), 128.1 (s, C$_{Ar}$), 113.1 (d, 2×C$_{Ar}$-H), 112.5 (d, 2×C$_{Ar}$-H), 76.1 (d, CH), 62.3 (t, CH$_2$), 54.2 (t, 3×CHH), 47.6 (d, CH), 40.5 (q, 2×CH$_3$), 40.4 (q, 2×CH$_3$), 23.7 (t, 3×CH$_2$), 19.1 (d, CH), 13.6 (q, CH$_3$). **HRMS** (ESI+): m/z calcd. for [C$_{28}$H$_{40}$N$_3$O$_2$]$^+$: 450.3115, found 450.3115. DA169
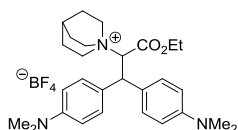
1,1-Bis(4-(dimethylamino)phenyl)-3-ethoxy-*N*,*N*,*N*-trimethyl-3-oxopropan-2-aminium tetrafluoroborate (7h-BF$_4$). From **2a-BF$_4$** (100 mg, 294 µmol), **1hH$^+$Br$^-$** (90.6 mg, 401 µmol), and KO^{t}Bu (35.0 mg, 312 µmol) according to procedure **B**. After recrystallization from MeCN:Et$_2$O **7h-BF$_4$** was obtained as a colorless solid (61.5 mg, 150 µmol, 51%). **Mp** (Et$_2$O:MeCN) 148 °C. **^{1}H NMR** (400 MHz, DMSO-d_6) δ = 7.45 (d, J = 8.9 Hz, 2 H, 2×C$_{Ar}$-H), 7.16 (d, J = 8.9 Hz, 2 H, 2×C$_{Ar}$-H), 6.66 (d, J = 8.9 Hz, 2 H, 2×C$_{Ar}$-H), 6.58 (d, J = 8.9 Hz, 2 H, 2×C$_{Ar}$-H), 5.46 (d, J = 10.9 Hz, 1 H, CH), 4.55 (d, J = 10.9 Hz, 1 H, CH), 3.94 – 3.69 (m, 2 H, CH$_2$), 3.06 (s, 9 H, 3×CH$_3$), 2.82 (s, 6 H, 2×CH$_3$), 2.78 (s, 6 H, 2×CH$_3$), 0.83 (t, J = 7.1 Hz, 3 H, CH$_3$). **^{13}C NMR** (100 MHz, DMSO-d_6) δ = 166.9 (s, CO), 150.0 (s, C$_{Ar}$), 149.9 (s, C$_{Ar}$), 129.4 (d, 2×C$_{Ar}$-H), 129.1 (d, 2×C$_{Ar}$-H), 128.0 (s, C$_{Ar}$), 127.9 (s, C$_{Ar}$), 113.2 (d, 2×C$_{Ar}$-H), 112.6 (d, 2×C$_{Ar}$-H), 76.4 (d, CH), 62.3 (t, CH$_2$), 53.4 (q, 3×CH$_3$), 48.6 (d, CH), 40.5 (q, 2×CH$_3$), 40.4 (q, 2×CH$_3$), 13.6 (q, CH$_3$). **HRMS** (ESI+): m/z calcd. for [C$_{24}$H$_{36}$N$_3$O$_2$]$^+$: 398.2802, found 398.2801. DA161
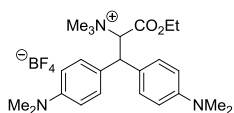
1,1-Bis(4-(dimethylamino)phenyl)-*N,N,N*-trimethyl-3-oxo-3-phenylpropan-2-aminium tetrafluoroborate (7i-BF$_4$). was synthesized from **2a-BF$_4$** (100 mg, 294 µmol), **1iH$^+$Br$^-$** (76 mg, 294 µmol) and KO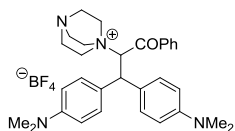^{t}Bu (35.0 mg, 312 µmol) according to procedure **B**. The crude product was recrystallized from MeCN:Et$_2$O to yield **7i-BF$_4$** as a yellow solid (116 mg, 224 µmol, 76%). **Mp.** (Et$_2$O:MeCN) 159 °C. **^{1}H NMR** (400 MHz, DMSO-d_6) δ = 8.13 − 8.05 (m, 2 H, 2×C$_{Ar}$-H), 7.66 − 7.58 (m, 3 H, 3×C$_{Ar}$-H), 7.46 (t, *J* = 7.8 Hz, 2 H, 2×C$_{Ar}$-H), 7.06 − 7.00 (m, 2 H, 2×C$_{Ar}$-H), 6.75 − 6.68 (m, 2 H, 2×C$_{Ar}$-H), 6.40 (d, *J* = 10.9 Hz, 1 H, CH), 6.32 − 6.23 (m, 2 H, 2×C$_{Ar}$-H), 4.68 (d, *J* = 10.9 Hz, 1 H, CH), 3.14 (s, 9 H, 3×CH$_3$), 2.87 (s, 6 H, 2×CH$_3$), 2.64 (s, 6 H, 2×CH$_3$). **^{13}C NMR** (100 MHz, DMSO-d_6) δ = 195.8 (s, CO), 149.5 (s, C$_{Ar}$), 149.1 (s, C$_{Ar}$), 136.8 (s, C$_{Ar}$), 134.3 (d, C$_{Ar}$-H), 129.6 (d, 2×C$_{Ar}$-H), 129.0 (d, 2×C$_{Ar}$-H), 128.8 (d, 2×C$_{Ar}$-H), 128.5 (d, 2×C$_{Ar}$-H), 127.7 (s, C$_{Ar}$), 126.1 (s, C$_{Ar}$), 112.6 (d, 2×C$_{Ar}$-H), 112.0 (d, 2×C$_{Ar}$-H), 72.2 (d, CH), 53.4 (q, 3×CH$_3$), 49.9 (d, CH), 39.8 (q, 2×CH$_3$), 39.7 (q, 2×CH$_3$). **HRMS** (ESI+): *m/z* calcd. for [C$_{28}$H$_{36}$N$_3$O]$^+$: 430.2853, found 430.2851. DA495-2
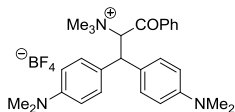
2.7.3.2 Reactions with Quinone Methide 3c

General procedure C for the synthesis of the products 9. KO^{t}Bu (0.39−1.0 mmol) in DMSO (2 mL) was added to **1H$^+$X$^-$** (0.4−1.0 mmol) in DMSO (5 mL) at ambient temperature. After stirring for 1 min **3c** (0.2−0.5 mmol) dissolved CH$_2$Cl$_2$ (2 mL) was added. After 5 minutes reaction time aq. sat. NH$_4$Cl (25 mL) was added and the mixture was extracted with Et$_2$O or CH$_2$Cl$_2$ (3×20 mL). The combined organic layers were washed with water (2×20 mL) and brine (2×20 mL) dried over MgSO$_4$. The solvent was removed and the crude product was recrystallized from ethanol or purified by column chromatography (silica). The diastereomeric excess of **9** was determined from the crude product after aqueous work-up.

General procedure D for the low temperature synthesis of the products 9. KO^{t}Bu (0.55−0.57 mmol) in DMF (3 mL) was added to suspensions of **1H$^+$X$^-$** (0.55−0.57 mmol) in DMF (5 mL) at −15 °C. The solution was stirred for 1 min, then **3c** (0.37−0.38 mmol) in CH$_2$Cl$_2$ (2 mL) was added dropwise and stirring was continued for 30 min. The reaction mixture was quenched with water (5 mL) at −15 °C and allowed to warm to ambient temperature. The mixture was extracted with CH$_2$Cl$_2$ (3×10 mL), and the combined organic layers were washed with water (3×20 mL). The solvent was evaporated and the crude was subjected to an NMR analysis. If possible, **9** was crystallized from EtOH or MeOH.

5,7-Di-*tert*-butyl-6-oxo-2-(*p*-tolyl)spiro[2.5]octa-4,7-diene-1-carbonitrile (*rac*-**9ac**)
From **1aH⁺Br⁻** (90.3 mg, 389 µmol), KO*t*Bu (44 mg, 0. 39 mmol), and **3c** (100 mg, 324 µmol) according to procedure **C**. After purification by column chromatography (SiO$_2$, *n*-pentane:EtOAc 25:1) *rac*-**9ac** was obtained in 2 fractions as colorless oils (59 mg, 170 µmol, 52%, *trans*:*cis* 33:67). *rac*-*cis*-**9ac** solidified slowly on treatment with EtOH. **Fraction 1**: *rac*-*trans*-**9ac** (obtained as mixture with **3c**). **¹H NMR** (300 MHz, CDCl$_3$) δ = 7.08 (d, *J* = 7.8 Hz, 2 H, 2×C$_{Ar}$-H), 7.00 (d, *J* = 8.0 Hz, 2 H, 2×C$_{Ar}$-H), 6.41 (d, *J* = 2.8 Hz, 1 H, C=CH), 5.61 (d, *J* = 2.8 Hz, 1 H, C=CH), 3.35 (d, *J* = 6.9 Hz, 1 H, CH), 2.61 (d, *J* = 7.1 Hz, 1 H, CH), 2.27 (s, 3 H, CH$_3$), 1.24 (s, 9 H, C(CH$_3$)$_3$), 1.00 (s, 9 H, C(CH$_3$)$_3$). **¹³C NMR** (75 MHz, CDCl$_3$) δ = 185.3 (s, CO), 151.1 (s, *C*=CH), 150.9 (s, *C*=CH), 138.4 (s, C$_{Ar}$), 138.0 (d, C=*C*H), 136.4 (d, C=*C*H), 130.0 (s, C$_{Ar}$) 129.7 (d, 2×C$_{Ar}$-H) 128.7 (d, 2×C$_{Ar}$-H), 111.5 (s, CN), 39.7 (d, CH), 35.5 (s, *C*(CH$_3$)$_3$), 35.4 (s, *C*(CH$_3$)$_3$), 35.1 (s, C$_q$), 29.4 (q, C(*C*H$_3$)$_3$), 29.2 (q, C(*C*H$_3$)$_3$), 21.3 (q, CH$_3$), 20.1 (d, CH). **Fraction 2**: *rac*-*cis*-**9ac**. **Mp** 101−102 °C. **¹H NMR** (300 MHz, CDCl$_3$) δ = 7.22 – 7.15 (m, 4 H, 4×C$_{Ar}$-H), 6.18 (d, *J* = 2.9 Hz, 1 H, C=CH), 6.02 (d, *J* = 2.8 Hz, 1 H, C=CH), 3.23 (d, *J* = 9.0 Hz, 1 H, CH), 2.62 (d, *J* = 9.0 Hz, 1 H, CH), 2.35 (s, 3 H, CH$_3$), 1.27 (s, 9 H, C(CH$_3$)$_3$), 1.17 (s, 9 H, C(CH$_3$)$_3$). **¹³C NMR** (75 MHz, CDCl$_3$) δ = 185.4 (s, CO), 151.2 (s, *C*=CH), 150.4 (s, *C*=CH), 139.8 (d, C=*C*H), 138.5 (s, C$_{Ar}$), 135.8 (d, C=*C*H), 130.0 (d, 2×C$_{Ar}$-H), 129.7 (d, 2×C$_{Ar}$-H), 128.5 (s, C$_{Ar}$), 116.4 (s, CN), 36.9 (d, CH), 35.7 (s, *C*(CH$_3$)$_3$), 35.2 (s, *C*(CH$_3$)$_3$), 33.9 (s, C$_q$), 29.4 (q, C(*C*H$_3$)$_3$), 29.3 (q, C(*C*H$_3$)$_3$), 21.3 (q, CH$_3$), 20.9 (d, CH). **HRMS** (EI): *m/z* calcd. for [C$_{24}$H$_{29}$NO]⁺: 347.2244, found 347.2241. **MS** (EI) *m/z* = 348 (13), 347 (44), 320 (100), 305 (21), 276 (13), 189 (17). DA256-3
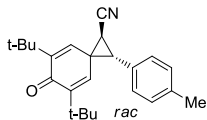
5,7-Di-*tert*-butyl-6-oxo-2-(*p*-tolyl)spiro[2.5]octa-4,7-diene-1-carbonitrile (*rac*-**9ac**).
From **1aH⁺Br⁻** (132 mg, 568 µmol), KO*t*Bu (64 mg, 0.57 mmol), and **3c** (117 mg, 379 µmol) according to procedure **D**. *rac*-**9a** was obtained only as crude product (76.4 mg, 219 µmol, 58%, *trans*:*cis* 33:67), and decomposed during the attempted recrystallization from MeOH. (Analytical data see above) DA504

¹H NMR Monitoring of the reaction of 1a with 3c. KO^{t}Bu (28.1 mg, 250 µmol) in DMSO-d_6 (1 mL) was added dropwise to a stirred solution of **1aH⁺Br⁻** (58.0 mg, 250 µmol) and quinone methide **3c** (77.1 mg 250 µmol) in DMSO-d_6: CD$_2$Cl$_2$ (2 mL, 1:1) at ambient temperature over 1 min. After stirring for 1 min the solution was quenched by freezing at − 20 °C. For NMR-analysis the solution was brought back to 20 °C. The reaction mixture showed only signals of the product **9ac**, but no signals of the intermediate betaine **8ac** or ylide **1a**. DA807

5,7-Di-*tert*-butyl-*N,N*-diethyl-6-oxo-2-(*p*-tolyl)spiro[2.5]octa-4,7-diene-1-carboxamide (*rac*-**9bc**). From **1bH⁺Cl⁻** (262 mg, 1.00 mmol), KO^{t}Bu (112 mg, 998 µmol) and **3c** (154 mg, 499 µmol) according to procedure **C**. After column chromatography (SiO$_2$; *n*-Pentane: CH$_2$Cl$_2$ 1:1) *rac*-**9bc** was obtained as light yellow oil (137 mg, 325 µmol, 65%, *trans:cis* 75:25), from which *cis*-*rac*-**9bc** solidified on treatment with EtOH. *trans*-*rac*-**9bc**. **¹H NMR** (300 MHz, CDCl$_3$) δ = 7.11 (s, 4 H, 4×C$_{Ar}$-H), 6.52 (d, J = 2.7 Hz, 1 H, C=CH), 5.94 (d, J = 2.7 Hz, 1 H, C=CH), 3.91 (d, J = 7.4 Hz, 1 H, CH), 3.71 − 3.58 (m, 1 H, C*H*H), 3.26 – 3.16 (m, 3 H, C*H*H, 2×CH*H*), 3.07 (d, J = 7.3 Hz, 1 H, CH), 2.33 (s, 3 H, CH$_3$), 1.23 (s, 9 H, C(CH$_3$)$_3$), 1.15 – 1.01 (m, 15 H, 2×CH$_3$, C(CH$_3$)$_3$, signal superimposed by *cis*-isomer).**¹³C NMR** (75 MHz, CDCl$_3$) δ = 185.8 (s, CO), 166.8 (s, CON), 149.8 (s, *C*=CH), 149.7 (s, *C*=CH), 139.5 (s, C=*C*H), 139.3 (s, C=*C*H), 137.2 (s, C$_{Ar}$), 132.7 (s, C$_{Ar}$), 129.3 (d, 2×C$_{Ar}$-H), 129.1 (d, 2×C$_{Ar}$-H), 42.2 (t, CHH), 41.2 (t, CHH), 39.3 (d, CH), 37.5 (d, CH), 37.0 (s, C$_q$), 35.3 (s, *C*(CH$_3$)$_3$), 35.2 (s, *C*(CH$_3$)$_3$), 29.5 (q, C(*C*H$_3$)$_3$), 29.4 (q, C(*C*H$_3$)$_3$), 21.3 (q, C$_{Ar}$-*C*H$_3$), 14.5 (q, CH$_3$), 13.3 (q, CH$_3$). **HRMS** (EI): *m/z* calcd. for [C$_{28}$H$_{39}$NO$_2$]$^{+}$: 421.2975, found 421.2967. **MS** (EI) *m/z* = 421 (13), 176 (11), 100 (100).
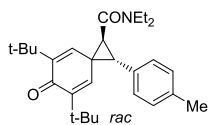
cis-*rac*-**9bc**. **Mp** (EtOH) 130−132 °C. **¹H NMR** (300 MHz, CDCl$_3$) δ = 7.06 (s, 4 H, 4×C$_{Ar}$-H), 6.86 (d, J = 2.7 Hz, 1 H, C=CH), 6.12 (d, J = 2.8 Hz, 1 H, C=CH), 3.53 – 3.14 (m, 5 H, 2×CH$_2$, CH, signal superimposed by *trans*-isomer), 2.79 (d, J = 9.7, 1 H, CH), 2.29 (s, 3 H, CH$_3$), 1.27 (s, 9 H, C(CH$_3$)$_3$, signal superimposed by *cis*-isomer), 1.15 (s, 9 H, C(CH$_3$)$_3$, signal superimposed by *trans*-isomer), 1.14 – 1.02 (m, 6 H, 2×CH$_3$, signal superimposed by *trans*-isomer). **¹³C NMR** (75 MHz, CDCl$_3$) δ = 186.1 (s, CO), 166.0 (s, CON), 148.9 (s, *C*=CH), 148.4 (s, *C*=CH), 143.4 (d, C=*C*H), 138.6 (d, C=*C*H), 136.9 (s, C$_{Ar}$), 130.8 (s, C$_{Ar}$), 129.8 (d, 2×C$_{Ar}$-H), 128.7 (d, 2×C$_{Ar}$-H), 42.1 (t, CH$_2$), 40.5 (t, CH$_2$), 39.7 (d, CH), 36.4 (d, CH), 35.5 (s, C$_q$), 34.9 (s, *C*(CH$_3$)$_3$), 34.7 (s, *C*(CH$_3$)$_3$), 29.5 (q, C(*C*H$_3$)$_3$), 29.4 (q, C(*C*H$_3$)$_3$), 21.2 (q, C$_{Ar}$-*C*H$_3$), 14.4 (q, CH$_3$), 13.1 (q, CH$_3$). **HRMS** (APCI): *m/z* calcd. for [C$_{28}$H$_{40}$NO$_2$]$^+$: 422.3054, found 422.3052. DA324

Table 2.20. Crystallographic data *rac-cis*-9bc.

net formula	$C_{28}H_{39}NO_2$
M_r/g mol^{-1}	421.615
crystal size/mm	$0.30 \times 0.10 \times 0.05$
T/K	173(2)
radiation	MoKα
diffractometer	'KappaCCD'
crystal system	monoclinic
space group	$P2_1/c$
a/Å	12.0043(5)
b/Å	20.5212(9)
c/Å	11.2053(4)
α/°	90
β/°	112.369(2)
γ/°	90
V/Å^3	2552.63(18)
Z	4
calcd. density/g cm^{-3}	1.09709(8)
μ/mm^{-1}	0.068
absorption correction	none
refls. measured	16349
R_{int}	0.0660
mean $\sigma(I)/I$	0.0572
θ range	3.31–25.39
observed refls.	3084
x, y (weighting scheme)	0.0692, 0.7088
hydrogen refinement	constr
refls in refinement	4669
parameters	289
restraints	0
$R(F_{obs})$	0.0546
$R_w(F^2)$	0.1480
S	1.021
shift/error$_{max}$	0.001
max electron density/e Å^{-3}	0.222
min electron density/e Å^{-3}	−0.225
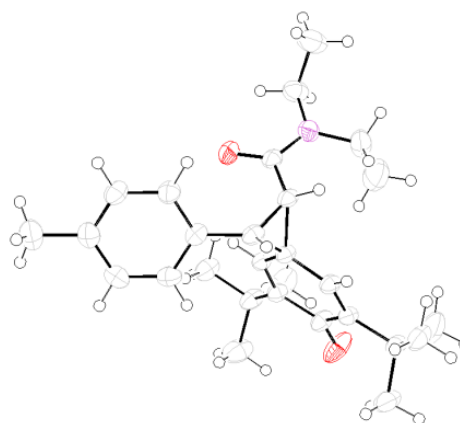
5,7-Di-*tert*-butyl-*N*,*N*-diethyl-6-oxo-2-(*p*-tolyl)spiro[2.5]octa-4,7-diene-1-carboxamide (*rac*-**9bc**). From **1bH⁺Cl⁻** (146 mg, 558 μmol), KO*t*Bu (63 mg, 0.56 μmol), and **3c** (114 mg, 370 μmol) according to procedure **D**. After recrystallization from MeOH *rac*-**9bc** was obtained as colorless solid (135 mg, 320 μmol, 87%, *trans*:*cis* 83:17 in crude product; *trans*:*cis* 1:6 after recrystallization from MeOH). (Analytical data see above). DA501

NMR-Monitoring of the reactions of 1b and 3c. **1bH⁺Cl⁻** (32.3 mg, 123 μmol) and **3c** (38.2 mg, 124 μmol) were dissolved in DMSO-*d₆*:CD₂Cl₂ (2 mL, 1.5:1) and KO*t*Bu dissolved in DMSO-*d₆* (900 μl, 2.57×10^{-1} M) was added at ambient temperature. After 30 s stirring the

solution was subjected to ^{1}H NMR. The spectra show only the product **9bc** and no formation of the intermediate betaine **8bc** or ylide **1b**. DA893
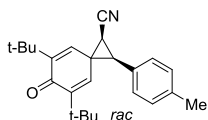
Ethyl 5,7-di-*tert*-butyl-6-oxo-2-(*p*-tolyl)spiro[2.5]octa-4,7-diene-1-carboxylate (*rac*-**9cc**). From **1cH⁺Br⁻** (136 mg, 487 μmol), KO^{t}Bu (55 mg, 0.49 mmol), and **3c** (100 mg, 324 μmol) according to procedure **C**. After crystallization from EtOH *rac*-**9cc** was obtained as colorless needles (106 mg, 269 μmol, 83%, *trans*:*cis* >95:5). **Mp** (EtOH) 141 °C. **^{1}H NMR** (300 MHz, CDCl$_3$) δ = 7.15 – 7.06 (m, 4 H, 4×C$_{Ar}$-H), 6.87 (d, *J* = 2.7 Hz, 1 H, C=CH), 5.81
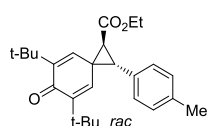
(d, *J* = 2.8 Hz, 1 H, C=CH), 4.31 – 4.18 (m, 2 H, CH$_2$), 3.66 (d, *J* = 7.4 Hz, 1 H, CH), 3.02 (d, *J* = 7.4 Hz, 1 H, CH), 2.33 (s, 3 H, C$_{Ar}$-CH$_3$), 1.32 (t, *J* = 7.1 Hz, 3 H, CH$_3$), 1.27 (s, 9 H, C(CH$_3$)), 1.07 (s, 9 H, C(CH$_3$)). **^{13}C NMR** (75 MHz, CDCl$_3$) δ = 185.9 (s, CO), 169.8 (s, CO$_2$), 149.4 (s, *C*=CH), 149.4 (s, *C*=CH), 139.2 (d, C=*C*H), 138.0 (d, C=*C*H), 137.5 (s, C$_{Ar}$), 131.8 (s, C$_{Ar}$), 129.3 (d, 2×C$_{Ar}$-H), 128.8 (d, 2×C$_{Ar}$-H), 61.7 (t, CH$_2$), 40.1 (s, C$_q$), 38.2 (d, CH), 36.7 (d, CH), 35.4 (s, *C*(CH$_3$)$_3$), 35.2 (s, *C*(CH$_3$)$_3$), 29.5 (q, C(*C*H$_3$)$_3$), 29.3 (q, C(*C*H$_3$)$_3$), 21.3 (q, CH$_3$), 14.4 (q, CH$_3$). **HRMS** (EI): *m/z* calcd. for [C$_{26}$H$_{34}$O$_3$]$^{+}$: 394.2502, found 394.2508. DA356

Ethyl 5,7-di-*tert*-butyl-6-oxo-2-(*p*-tolyl)spiro[2.5]octa-4,7-diene-1-carboxylate (*rac*-**9cc**). From **1cH⁺Br⁻** (148 mg, 530 μmol), KO^{t}Bu (60 mg, 0.53 mmol) and **3c** (109 mg, 353 μmol) according to procedure **D**. *rac*-**9cc** was obtained only as crude product (78 mg, 198 μmol, 56%, *trans*:*cis* >95:5), and decomposed during attempted recrystallization from MeOH. (Analytical data see above) DA515
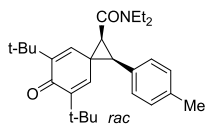
NMR-Monitoring of the reaction of 1c with 3c. KO^{t}Bu dissolved in DMSO-d_6 (900 μl, 1.38 × 10^{-1} M) was added to a solution of **1cH⁺Br⁻** (35.7 mg, 128 μmol) and **3c** (36.8 mg, 119 μmol) in DMSO-d_6:CD$_2$Cl$_2$ (2 mL, 1.5:1) at ambient temperature. After 30 s stirring the solution was subjected to ^{1}H NMR. The spectra show only the product **9cc** and no formation of an intermediate betaine **8cc** or of ylide **1c**. DA892

Table 2.21. Crystallographic data *rac-trans*-9cc.

net formula	$C_{26}H_{34}O_3$
M_r/g mol^{-1}	394.546
crystal size/mm	$0.25 \times 0.20 \times 0.11$
T/K	173(2)
radiation	MoKα
diffractometer	'Oxford XCalibur'
crystal system	monoclinic
space group	$P2_1/n$
a/Å	10.3896(4)
b/Å	15.3439(7)
c/Å	14.6025(8)
α/°	90
β/°	91.264(4)
γ/°	90
V/Å^3	2327.32(19)
Z	4
calcd. density/g cm^{-3}	1.12605(9)
μ/mm^{-1}	0.072
absorption correction	'multi-scan'
transmission factor range	0.95108–1.00000
refls. measured	8184
R_{int}	0.0296
mean $\sigma(I)/I$	0.0489
θ range	4.22–26.37
observed refls.	3390
x, y (weighting scheme)	0.0497, 0.6860
hydrogen refinement	constr
refls in refinement	4709
parameters	270
restraints	0
$R(F_{obs})$	0.0503
$R_w(F^2)$	0.1289
S	1.014
shift/error$_{max}$	0.001
max electron density/e Å^{-3}	0.198
min electron density/e Å^{-3}	−0.182
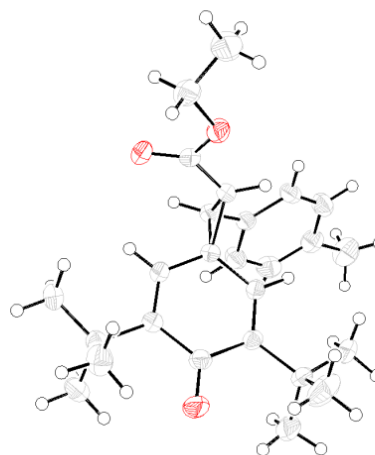
1-Benzoyl-5,7-di-*tert*-butyl-2-(*p*-tolyl)spiro[2.5]octa-4,7-dien-6-one (*rac*-**9ec**). From **1eH⁺Br⁻** (151 mg, 485 µmol), KO^{t}Bu (55 mg, 0.49 mmol) and **3c** (100 mg, 324 µmol) according to procedure **C**. The reaction mixture was stirred for 2 h in this case. After recrystallization from EtOH *rac*-**9ec** was obtained as colorless solid (89 mg, 209 µmol, 64%, *trans*:*cis* 50:50). **Mp** (EtOH) 147−150 °C. The integral of one signal of one of the diastereoisomers of *rac*-**9ec** was set to 1.0. **¹H NMR** (300 MHz, CDCl₃) δ = 7.93 (dd, *J* = 5.3, 3.3 Hz, 2 H, 2×C$_{Ar}$-H), 7.85 (dd, *J* = 5.3, 3.3 Hz, 2 H, 2×C$_{Ar}$-H), 7.63 − 7.54 (m, 2 H, 2×C$_{Ar}$-H), 7.53 − 7.43 (m, 4 H, 4×C$_{Ar}$-H), 7.14 (s,
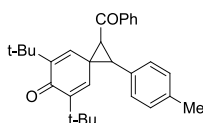
4 H, 4×C$_{Ar}$-H), 7.08 (d, J = 7.9 Hz, 2 H, 2×C$_{Ar}$-H), 7.03 (d, J = 2.7 Hz, 1 H, C=CH), 6.98 (d, J = 8.0 Hz, 2 H, 2×C$_{Ar}$-H), 6.61 (d, J = 2.8 Hz , 1 H, C=CH), 6.24 (d, J = 2.7 Hz, 1 H, C=CH), 6.06 (d, J = 2.8 Hz, 1 H, C=CH), 4.04 (d, J = 7.5 Hz, 1 H, CH), 3.91 (d, J = 7.5 Hz, 1 H, CH), 3.76 (d, J = 9.5 Hz, 1 H, CH), 3.57 (d, J = 9.6 Hz, 1 H, CH), 2.35 (s, 3 H, CH$_3$), 2.32 (s, 3 H, CH$_3$), 1.32 (s, 9 H, C(CH$_3$)$_3$), 1.18 – 1.14 (m, 27 H, 3×C(CH$_3$)$_3$). **^{13}C NMR** (75 MHz, CDCl$_3$) δ = 194.8 (s, CO), 194.0 (s, CO), 186.1 (s, CO), 185.8 (s, CO), 150.1 (s, C=CH), 149.8 (s, C=CH), 149.0 (s, C=CH), 148.8 (s, C=CH), 142.7 (d, C=CH), 138.9 (s, C$_{Ar}$), 138.7 (d, C=CH), 137.9 (s, C$_{Ar}$), 137.7 (d, C=CH), 137.5 (s, C$_{Ar}$), 137.2 (s, C$_{Ar}$), 137.1 (d, C=CH), 133.6 (d, C$_{Ar}$-H), 133.3 (d, C$_{Ar}$-H), 132.2 (s, C$_{Ar}$), 130.3 (d, 2× C$_{Ar}$-H), 129.9 (d, 2×C$_{Ar}$-H), 129.4 (s, C$_{Ar}$), 129.1 (d, 2×C$_{Ar}$-H), 129.0 (d, 2× C$_{Ar}$-H), 128.9 (d, 2× C$_{Ar}$-H), 128.9 (d, 2× C$_{Ar}$-H), 128.3 (d, 2× C$_{Ar}$-H), 128.2 (d, 2× C$_{Ar}$-H), 42.0 (d, CH), 41.2 (d, CH), 40.7 (s, C$_q$), 40.0 (d, CH), 39.5 (d, CH), 37.6 (s, C$_q$), 35.6 (s, C(CH$_3$)$_3$), 35.3 (s, C(CH$_3$)$_3$), 35.3 (s, C(CH$_3$)$_3$), 35.1 (s, C(CH$_3$)$_3$), 29.5 (q, C(CH$_3$)$_3$), 29.4 (q, 2×C(CH$_3$)$_3$), 29.4 (q, C(CH$_3$)$_3$), 21.3 (q, CH$_3$), 21.3 (q, CH$_3$). **HRMS** (APCI): m/z calcd. for [C$_{30}$H$_{35}$O$_2$]$^+$: 427.2632, found 427.2629. **MS** (EI) m/z = 426 (25), 309 (10), 105 (100). DA329

1-Benzoyl-5,7-di-*tert*-butyl-2-(*p*-tolyl)spiro[2.5]octa-4,7-dien-6-one (*rac*-**9ec**). From **1eH$^+$Br$^−$** (165 mg, 530 µmol), KO^{t}Bu (59 mg, 0.53 mmol), and **3c** (109 mg, 353 µmol) according to procedure **D**. The reaction mixture was stirred for 2 h in this case. After recrystallization from MeOH *rac*-**9ec** was obtained as colorless solid (103 mg, 241 µmol, 68%, *trans*:*cis* 60:40). (Analytical data see above) DA505

NMR-Monitoring of the reaction of 1e with 3c. KO^{t}Bu in DMSO-d_6 (500 µL, 2.61 × 10$^{−1}$ M) was added to a solution of **1eH$^+$Br$^−$** (40.4 mg, 130 µmol) and **3c** (36.6 mg, 119 µmol) in DMSO-d_6:CD$_2$Cl$_2$ (2.00 mL; 1:1) at ambient temperature. After stirring for 30 s the solution was subjected to ^{1}H NMR. The spectra show decreasing signals of the reactants **1e** and **3c**, and increasing signals of the product **9ec**, but now formation of an intermediate betaine **8ec**. (Evaluation of the kinetics see Kinetics Section) DA894

***tert*-Butyl 5,7-di-*tert*-butyl-6-oxo-2-(*p*-tolyl)spiro[2.5]octa-4,7-diene-1-carboxylate hydrate** (*rac*-**9fc·H₂O**). From **1fH$^+$Br$^−$** (149 mg, 485 µmol), KO^{t}Bu (55 mg, 0.49 mmol) and **3c** (100 mg, 324 µmol) according to procedure **C**. After column chromatography (*n*-pentane:EtOAc 25:1) and recrystallization from *i*-hexane:CH$_2$Cl$_2$ *rac*-**9fc** was obtained as
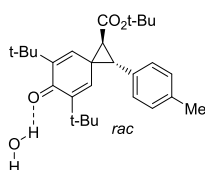
colorless solid (109 mg, 247 µmol, 76%, *trans*:*cis* >95:5). **Mp** (*i*-hexane : CH$_2$Cl$_2$): 123−124 °C. **^{1}H NMR** (300 MHz, CDCl$_3$) δ = 6.99 (d, J = 8.0 Hz, 2 H, 2×C$_{Ar}$-H), 6.92 (d, J = 8.1 Hz, 2 H, 2×C$_{Ar}$-H), 6.72 (s, 2 H, 2×C=CH), 5.03 (s, 1 H, HOH--OC), 4.91 (d, J = 8.6 Hz, 1 H, CH), 3.64 (d, J = 8.6 Hz,

1 H, CH), 3.20 (br s, 1 H, *H*OH), 2.27 (s, 3 H, CH$_3$), 1.46 (s, 9 H, C(CH$_3$)$_3$), 1.31 (s, 18 H, 2×C(CH$_3$)$_3$). **^{13}C NMR** (75 MHz, CDCl$_3$) δ = 173.3 (s, CO$_2$), 152.9 (s, CO), 138.7 (s, C$_{Ar}$), 137.1 (s, C$_{Ar}$), 135.5 (s, *C*=CH), 128.6 (d, 2×C$_{Ar}$-H), 126.7 (d, 2×C$_{Ar}$-H), 126.5 (s, *C*=CH), 125.2 (d, 2×C=*C*H), 81.5 (s, O*C*(CH$_3$)$_3$), 77.2 (d, CH, superimposed by solvent), 60.7 (d, CH), 34.3 (s, 2×*C*(CH$_3$)$_3$), 30.3 (q, 2×C(*C*H$_3$)$_3$), 29.9 (s, C$_q$), 28.2 (q, C(*C*H$_3$)$_3$), 21.2 (q, CH$_3$). **HRMS** (EI): *m/z* calcd. for [C$_{28}$H$_{38}$O$_3$]$^{+}$: 422.2815, found 422.2812. **MS** (EI) *m/z* = 441 (40), 425 (30), 422 (18), 367 (100). DA720

Ethyl 5,7-di-*tert*-butyl-6-oxo-2-(*p*-tolyl)spiro[2.5]octa-4,7-diene-1-carboxylate (*rac*-**9gc** (= *rac*-**9cc**)). From **1gH$^+$Br$^-$** (57 mg, 0.20 mmol), KO*^{t}*Bu (26 mg, 0.23 mmol), and **3c** (51 mg, 0.17 mmol) according to procedure **C**. After recrystallization from EtOH *rac*-**9gc** (=*rac*-**9cc**) was obtained as colorless solid (25 mg, 63 µmol, 38%, *trans*:*cis* >95:5). (Analytical data see above). DA911

Ethyl 5,7-di-*tert*-butyl-6-oxo-2-(*p*-tolyl)spiro[2.5]octa-4,7-diene-1-carboxylate (*rac*-**9hc** (= *rac*-**9cc**)). From **1hH$^+$Br$^-$** (52.4 mg, 232 µmol), KO*^{t}*Bu (55 mg, 0.49 mmol), and **3c** (100 mg, 324 µmol) according to procedure **C**. *rac*-**9hc** (= *rac*-**9cc**) was obtained as colorless needles (30.0 mg, 76.0 µmol, 33%, *trans*:*cis* >95:5). (Analytical data see above). DA250

1-Benzoyl-5,7-di-*tert*-butyl-2-(*p*-tolyl)spiro[2.5]octa-4,7-dien-6-one (*rac*-**9ic** (=*rac*-**9dc**)). From **1iH$^+$Br$^-$** (142 mg, 550 µmol), KO*^{t}*Bu (62 mg, 0.55 mmol) and **3c** (113 mg, 367 µmol) according to procedure **C**. The reaction mixture was stirred for 2 h in this case. After recrystallization from EtOH *rac*-**9ic** (=*rac*-**9dc**) was obtained as colorless solid (88.8 mg, 208 µmol, 57%, *trans:cis* 50:50). (Analytical data see above). DA496

2.7.3.3 Reactions with Benzylidene Malonates 4

General procedure E for the synthesis of the Products 11. KO*^{t}*Bu (0.6−1.2 mmol) dissolved in DMSO (5 mL) was added to a solution of **1H$^+$X$^-$** (0.6−1.2 mmol) in DMSO (5 mL) at ambient temperature. After 30 s **4** (0.3−0.6 mmol) was added and the solution was stirred for 5−15 min. The reaction mixture was quenched with aq. sat. NH$_4$Cl solution (25 mL) and the mixture was extracted with CH$_2$Cl$_2$ or Et$_2$O (3 × 20 mL). The combined organic layers were washed with water (2 × 20 mL) and brine (2 × 20 mL), and dried over MgSO$_4$. The solvent was evaporated and if necessary the products where purified by flash column chromatography (*n*-pentane:EtOAc, 20:1; oils and solids) and/or recrystallized from ethanol (solids).

Diethyl 2-cyano-3-(4-methylphenyl)cyclopropane-1,1-dicarboxylate (*rac*-**11ad**). A solution of KO^{t}Bu (124 mg, 1.11 mmol) in THF (10 mL) was added dropwise to a suspension of **1aH$^+$Br$^-$** (244 mg, 1.05 mmol) and **4d** (250 mg, 953 µmol) in MeCN (25 mL) and the solution was stirred for 5 min at ambient temperature. The reaction mixture was quenched with aq. sat. NH$_4$Cl (50 mL) and extracted with Et$_2$O (3 × 10 mL). The combined organic layers were washed with water (20 mL) and dried over MgSO$_4$. The solvent was removed and the crude product was purified by chromatography (silica, *n*-pentane: Et$_2$O = 20:1) to give *rac*-
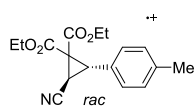
11ad as yellow oil (130 mg, 0.430 µmol, 45%, 93:7 *trans*:*cis* after work-up). **^{1}H NMR** (400 MHz, CDCl$_3$) δ = 7.11 (d, *J* = 8.1 Hz, 2 H, 2×C$_{Ar}$-H), 7.06 (d, *J* = 8.2 Hz, 2 H, 2×C$_{Ar}$-H), 4.45 − 4.32 (m, 2 H, CH$_2$), 4.02 − 3.89 (m, 2 H, CH$_2$), 3.68 (d, *J* = 7.6 Hz, 1 H, CH), 3.02 (d, *J* = 7.6 Hz, 1 H, CH), 2.31 (s, 3 H, CH$_3$), 1.36 (t, *J* = 7.1 Hz, 3 H, CH$_3$), 0.97 (t, *J* = 7.1 Hz, 3 H, CH$_3$). **^{13}C NMR** (100 MHz, CDCl$_3$) δ = 165.3 (s, CO$_2$), 164.0 (s, CO$_2$), 138.5 (s, C$_{Ar}$), 129.4 (d, 2×C$_{Ar}$-H), 128.2 (d, 2×C$_{Ar}$-H), 128.0 (s, C$_{Ar}$), 116.2 (s, CN), 63.2 (t, CH$_2$), 62.5 (t, CH$_2$), 42.8 (s, C$_q$), 35.6 (d, CH), 21.3 (q, CH$_3$), 15.6 (d, CH) 14.3 (q, CH$_3$), 13.9 (q, CH$_3$). **HRMS** (EI): *m/z* calcd. for [C$_{17}$H$_{19}$NO$_4$]$^+$: 301.1309, found 301.1306. DA198

Diethyl 2-cyano-3-(4-methylphenyl)cyclopropane-1,1-dicarboxylate (*rac*-**11ad**). From **1aH$^+$Br$^-$** (332 mg, 1.43 mmol), **4d** (250 mg, 953 µmol), and KO^{t}Bu (160 mg, 1.43 mmol) according to general procedure **E**. *rac*-**11ad** was obtained as yellow oil (173 mg, 574 µmol, 60%, *trans*:*cis* 96:4). (Analytical data see above). DA388

^{1}H NMR Monitoring of the Reaction of 1a with 4a. A solution of KO^{t}Bu (28.1 mg, 250 µmol) in DMSO-d_6 (1 mL) was added dropwise to a stirred solution of **1aH$^+$Br$^-$** (58.0 mg, 250 µmol) and **4a** (73.3 mg 250 µmol) in DMSO-d_6 (1 mL) over 1 min at ambient temperature. After stirring for 1 min the solution was quenched by freezing at −20 °C. For NMR-analysis the solution was brought back to 20 °C. The reaction mixture showed signals of the intermediate betaine **10aa** and the product *rac*-**11aa**, but no signals of ylide **1a**. The ratio between **10aa** and *rac*-**11aa** was 66:33. DA795

^{1}H NMR Monitoring of the Reaction of 1a with 4d. A solution of KO^{t}Bu (28.1 mg, 250 µmol) in DMSO-d_6 (1 mL) was added dropwise to a stirred solution of **1aH$^+$Br$^-$** (58.0 mg, 250 µmol) and **4d** (65.6 mg 250 µmol) in DMSO-d_6 (1 mL) at ambient temperature over 1 min. After stirring at for 1 min the solution was quenched by freezing at −20 °C. For NMR-analysis the solution was brought back to 20 °C. The spectrum showed signals of the reactants **1aH$^+$Br$^-$** and **4d**, the intermediate betaine **11ad** and the product **12ad**. The ratio between **11ad** and DABCO (corresponds to **12ad**) is 37:63. DA806

Diethyl 2-(diethylcarbamoyl)-3-(4-nitrophenyl)cyclopropane-1,1-dicarboxylate (*rac*-**11ba**). From **1bH$^+$Cl$^-$** (618 mg, 2.36 mmol), KO^{t}Bu (265 mg, 2.36 mmol), and **4a** (250 mg, 0.85 mmol) according to procedure **E**. After purification chromatography (silica, *i*-hexane:EtOAc = 20:1) *rac*-**11ba** was obtained as colorless oil (172 mg, 423 μmol, 50%, *trans*:*cis* 87:13 by GC-MS). **^{1}H NMR** (400 MHz, CDCl$_3$) δ = 8.09 (d, *J* = 8.7 Hz, 2 H, 2×C$_{Ar}$-H), 7.37 (d, *J* = 8.5 Hz, 2 H, 2×C$_{Ar}$-H), 4.22 – 4.13 (m, 2 H, CH$_2$), 3.97 – 3.88 (m, 2 H, CH$_2$), 3.80 (d, *J* = 7.6 Hz, 1 H, CH), 3.63 – 3.35 (m, 4 H, 2 × CH$_2$), 3.26 (d, *J* = 7.6 Hz, 1 H, CH), 1.30 – 1.21 (m, 6 H, 2 × CH$_3$), 1.05 (t, *J* = 7.1 Hz, 3 H, CH$_3$), 0.97 (t, *J* = 7.1 Hz, 3 H, CH$_3$). **^{13}C NMR** (100 MHz, CDCl$_3$) δ = 165.8 (s, CO), 165.6 (s, CO), 165.2 (s, CO), 147.4 (s, C$_{Ar}$),

141.7 (s, C$_{Ar}$), 129.8 (d, 2×C$_{Ar}$-H), 123.6 (d, 2×C$_{Ar}$-H), 62.4 (t, CH$_2$), 62.2 (t, CH$_2$), 44.6 (s, C$_q$), 42.4 (t, CH$_2$), 41.0 (t, CH$_2$), 34.4 (d, CH), 31.2 (d, CH), 14.8 (q, CH$_3$), 14.2 (q, CH$_3$), 14.0 (q, CH$_3$), 13.1 (q, CH$_3$). **HRMS** (EI): *m/z* calcd. for [C$_{20}$H$_{26}$N$_2$O$_7$]$^{+}$: 406.1735, found 406.1732. **MS** (EI): *m/z* 406, 361, 333, 306, 260, 232, 100, 72. DA238-2

NMR-Monitoring of the reaction of 1b and 4a. KO^{t}Bu dissolved in DMSO-d_6 (900 μl, 2.61 × 10^{-1} M) was added to a solution of **1bH$^+$Cl$^-$** (35.5 mg, 136 μmol) and **4a** (36.1 mg, 123 μmol) in DMSO-d_6 (1.5 mL) at ambient temperature. After 30 s stirring the solution was subjected to ^{1}H NMR. The spectra show constant ratios of HO^{t}Bu and DABCO and no signals of the reactants **1bH$^+$Cl$^-$** and **4a** or an intermediate betaine **10ba** over 30 min. The product **11ba** could not be unambiguously identified in the reaction mixture and may be decomposed by the excess of KO^{t}Bu present in the reaction mixture. DA895

Triethyl 3-(4-nitrophenyl)cyclopropane-1,1,2-tricarboxylate. (*rac*-**11ga** (= *rac*-**11ca**)). From **1gH$^+$Br$^-$** (533 mg, 1.92 mmol), KO^{t}Bu (265 mg, 2.36 mmol), and **4a** (250 mg, 852 μmol) according to procedure **E**. After purification by flash column chromatography (*i*-hexane:EtOAc, 20:1) and recrystallization from ethanol *rac*-**11ga** (= *rac*-**11ca**) was obtained as colorless solid (95.4 mg, 0.25 mmol, 29%, *trans*:*cis* >98:2 after purification). **Mp** (EtOH) 100−101 °C. **^{1}H NMR** (300 MHz, CDCl$_3$) δ = 8.20 – 8.12 (m, 2 H, 2×C$_{Ar}$-H), 7.50 – 7.42 (m, 2 H, 2×C$_{Ar}$-H), 4.21 (m, 4 H, 2×CH$_2$), 4.09 – 3.89 (m, 2 H, CH$_2$), 3.67 (d, *J* = 7.6 Hz, 1 H, CH), 3.26 (d, *J* = 7.6 Hz, 1 H, CH), 1.31 (t, *J* = 7.1 Hz, 1.3, 3 H), 1.06 (t, *J* = 7.1 Hz, 1 H, CH$_3$), 1.01 (t, *J* = 7.1 Hz, 3 H, CH$_3$). **^{13}C NMR** (75 MHz, CDCl$_3$) δ = 168.4 (s, CO$_2$), 165.4 (s, CO$_2$), 165.0

(s, CO$_2$), 147.6 (s, C$_{Ar}$), 140.8 (s, C$_{Ar}$), 129.9 (d, 2×C$_{Ar}$-H), 123.6 (d, 2×C$_{Ar}$-H), 62.5 (t, CH$_2$), 62.4 (t, CH$_2$), 62.0 (t, CH$_2$), 44.5 (s, C$_q$), 35.2 (d, CH), 31.4 (d, CH), 14.3 (q, CH$_3$), 14.1 (q, CH$_3$), 14.0 (q, CH$_3$). **HRMS** (EI): *m/z* calcd. for [C$_{18}$H$_{21}$NO$_8$]$^{+}$:

379.1262, found 379.1264. **MS** (EI): m/z 334, 306, 278, 261, 250, 232, 204, 180, 150, 114. λ_{max} (DMSO) = 276 nm. DA236

Table 2.22. Crystallographic data *rac-trans*-11ca.

net formula	$C_{18}H_{21}NO_8$
M_r/g mol^{-1}	379.361
crystal size/mm	$0.28 \times 0.12 \times 0.03$
T/K	173(2)
radiation	MoKα
diffractometer	'Oxford XCalibur'
crystal system	monoclinic
space group	$P2_1/c$
a/Å	12.5464(7)
b/Å	17.1786(8)
c/Å	8.6949(5)
α/°	90
β/°	94.423(5)
γ/°	90
V/Å^3	1868.43(17)
Z	4
calcd. density/g cm^{-3}	1.34863(12)
μ/mm^{-1}	0.107
absorption correction	'multi-scan'
transmission factor range	0.85439–1.00000
refls. measured	6865
R_{int}	0.0344
mean $\sigma(I)/I$	0.0593
θ range	4.27–28.74
observed refls.	2945
x, y (weighting scheme)	0.0453, 0.1805
hydrogen refinement	constr
refls in refinement	4140
parameters	247
restraints	0
$R(F_{obs})$	0.0488
$R_w(F^2)$	0.1189
S	1.020
shift/error$_{max}$	0.001
max electron density/e Å^{-3}	0.261
min electron density/e Å^{-3}	−0.218
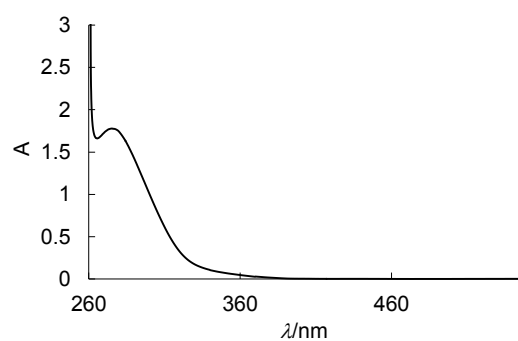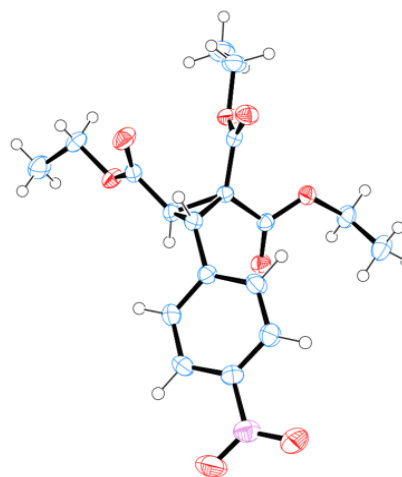
Figure 2.19. UV–vis spectrum of *rac*-11ca (c = 6.00×10^{-5} M).

General procedure F for the Time- and Temperature Dependence of the Formation of 11ca. KO^{t}Bu (64 mg, 570 μmol, 1.7 equiv) in DMSO (2 mL) was added dropwise to a solution

of **1cH⁺Br⁻** (160 mg, 573 µmol, 1.7 equiv) and **4a** (100 mg, 341 µmol, 1.0 equiv) in DMSO (5 mL) at the temperature given in Table 2.23. For reactions performed at elevated temperature, the suspension of **1cH⁺Br⁻** and **4a** was heated to 100 °C prior to the addition of KO^{t}Bu. After the time indicated in Table 2.23, HCl (2 M, 15 mL) was added to quench the reaction. The mixture was extracted with CH_2Cl_2 (3×10mL). The combined organic layers were washed with brine (2×20 mL) and dried over Na_2SO_4. If the crude product was solid after evaporation of the solvent, it was recrystallized from EtOH (Table 2.23). Otherwise it was subjected to a column chromatography (silica; *n*-pentane:EtOAc = 10:1; Table 2.23). (Analytical data see above). DA713-1–7

Table 2.23. Time- and Temperature Dependence of the Formation of 11ca.

t	*T*/°C	*m*/mg	*n*/mmol	Purification method	Yield/%	*trans*:*cis*[a]
10 min	20	40	0.11	column	32	>98:2
30 min	20	52	0.14	recryst.	41	98:2
1 h	20	59	0.16	column	47	98:2
2 h	20	68	0.18	column	53	97:3
4 h	20	64	0.17	recryst.	50	92:8
5 min	100	83	0.22	recryst.	65	98:2
10 min	100	105	0.277	column	81	95:5

[a] Determined from crude reaction mixture by ¹H NMR.

NMR-Monitoring of the reaction of 1c with 4a. A solution of KO^{t}Bu in DMSO-d_6 (500 µL, 2.61 × 10⁻¹ M) was added to a solution of **1cH⁺Br⁻** (41.9 mg, 150 µmol) and **4a** (35.8 mg, 122 µmol) in DMSO-d_6 (2.00 mL) at ambient temperature. After stirring for 30 s the solution was subjected to ¹H NMR. The spectra show constant decreasing signals of the intermediate betaine **10ca** and increasing signals of the products *rac*-**11ca** and DABCO. The formation of ylide **1c** was not observed. For details on the kinetic evaluation of the NMR data see Kinetics Section.

Crossover experiment to test the reversibility of the formation of 10ca. A solution of KO^{t}Bu (59 mg, 0.53 mmol) in DMSO (2 mL) was added dropwise to a solution of **1cH⁺Br⁻** (147 mg, 527 µmol) and **4a** (147 mg, 501 µmol) in DMSO (5 mL) over 1 min at ambient temperature. After 3 min reaction time a solution of **3c** (154 mg, 499 µmol) in CH_2Cl_2 (2 mL) was added and the reaction mixture was stirred for 1 h at ambient temperature. The reaction was quenched with 2 M HCl (20 mL) and extracted with CH_2Cl_2 (3 × 10 mL). The combined organic layers were washed with brine (2 × 20 mL) and dried over Na_2SO_4. The crude product was subjected to column chromatography (silica, *n*-pentane:EtOAc 10:1). **11ca** was obtained

as colorless solid (88 mg, 232 μmol, 46%); 73 mg (0.25 mmol, 50%) of **4a** and 116 mg (376 μmol, 75%) of **3c** were reisolated. DA813

Triethyl 3-(4-Methylphenyl)cyclopropane-1,1,2-tricarboxylate (*rac*-**11cd**). From **1cH⁺Br⁻** (319 mg, 1.14 mmol), KO*t*Bu (128 mg, 1.14 mmol), and **4d** (200 mg, 762 μmol) according to procedure **E**. *rac*-**11cd** was obtained as colorless oil (169 mg, 485 μmol, 64%; *trans:cis* 96:4). **¹H NMR** (400 MHz, CDCl₃) δ = 7.14 (d, *J* = 7.9 Hz, 2 H, 2×C$_{Ar}$-H), 7.07 (d, *J* = 8.0 Hz, 2 H, 2×C$_{Ar}$-H), 4.27 – 4.13 (m, 4 H, 2×CH₂), 4.00 – 3.88 (m, 2 H, CH₂), 3.58 (d, *J* = 7.5 Hz, 1 H, CH), 3.19 (d, *J* = 7.5 Hz, 1 H, CH), 2.29 (s, 3 H, CH₃), 1.30 – 1.26 (m, 6 H, 2×CH₃), 0.96 (t, *J* = 7.1 Hz, 3 H, CH₃). **¹³C NMR** (100 MHz, CDCl₃) δ = 169.2 (s, CO₂), 166.1 (s, CO₂), 165.5 (s, CO₂), 137.4 (s, C$_{Ar}$), 130.0 (s, C$_{Ar}$), 129.0 (d, 2×C$_{Ar}$-H), 128.6 (d, 2×C$_{Ar}$-H), 62.1 (t, CH₂), 62.0 (t, CH₂), 61.6 (t, CH₂), 44.4 (s, C$_q$), 35.6 (d, CH), 31.1 (d, CH), 21.2 (q, CH₃), 14.3 (q, CH₃), 14.1 (q, CH₃), 13.9 (q, CH₃). **HRMS** (ESI): *m/z* calcd. for [C₁₉H₂₄NaO₆]⁺: 371.1465, found 371.1464. **MS** (EI): *m/z* 348, 302, 275, 228, 201, 184, 173, 149, 129, 115, 91. DA332

Triethyl 3-(4-Methylphenyl)cyclopropane-1,1,2-tricarboxylate (*rac*-**11gd** (= *rac*-**11cd**)). From **1gH⁺Br⁻** (160 mg, 575 μmol), KO*t*Bu (64 mg, 0.57 mmol), and **4d** (100 mg, 381 μmol) according to procedure **E**. *rac*-**11gd** (= *rac*-**11cd**) was obtained as colorless oil (85 mg, 0.24 mmol, 63%, *trans:cis* 96:4). (Analytical data see above). DA334

Triethyl 3-(4-Methylphenyl)cyclopropane-1,1,2-tricarboxylate (*rac*-**11hd** (= *rac*-**11cd**)). From **1hH⁺Br⁻** (129 mg, 571 μmol), KO*t*Bu (64.2 mg, 572 μmol), and **4d** (100 mg, 381 μmol) according to procedure **E**. *rac*-**11hd** (= *rac*-**11cd**) was obtained as colorless oil (84 mg, 0.24 mmol, 63%, *trans:cis* 96:4). (Analytical data see above). DA333

Diethyl 2-benzoyl-3-(4-nitrophenyl)cyclopropane-1,1-dicarboxylate (*rac*-**11ea**). From **1eH⁺Br⁻** (318 mg, 1.02 mmol), KO*t*Bu (115 mg, 1.02 μmol), and **4a** (200 mg, 682 μmol) according to procedure **E**. After purification by chromatography (silica; *n*-pentane:EtOAc = 10:1) *rac*-**11ea** was obtained as colorless oil (120 mg, 292 μmol, 43%, *trans:cis* >98:2 after purification). **¹H NMR** (300 MHz, CDCl₃) δ = 8.18 (d, *J* = 8.8 Hz, 2 H, 2×C$_{Ar}$-H), 8.14 – 8.06 (m, 2 H, 2×C$_{Ar}$-H), 7.71–7.43 (m, 5 H, 5× C$_{Ar}$-H), 4.21 – 3.99 (m, 5 H, 2×CH₂, CH), 3.95 (d, *J* = 7.9 Hz, 1 H, CH), 1.13 – 1.03 (m, 6 H, 2×CH₃). **¹³C NMR** (75 MHz, CDCl₃) δ = 192.9 (s, CO), 165.4 (s, CO₂), 165.4 (s, CO₂), 147.6 (s, C$_{Ar}$), 141.3 (s, C$_{Ar}$), 136.6 (s, C$_{Ar}$), 134.1 (d, 2×C$_{Ar}$-H), 129.9 (d, 2×C$_{Ar}$-H), 129.0 (d, C$_{Ar}$-H), 128.8 (d, 2×C$_{Ar}$-H), 123.7 (d, 2×C$_{Ar}$-H), 62.6 (t, CH₂), 62.4 (t, CH₂), 46.5 (s, C$_q$), 35.2 (d, CH), 35.1 (d, CH), 14.1 (q, CH₃), 14.0 (q, CH₃). **HRMS** (ESI): *m/z* calcd. for [C₂₂H₂₁NO₇Cl]⁻: 446.1012, found 446.1011. DA350

NMR-Monitoring of the reaction of 1e with 4a. KO^{t}Bu in DMSO-d_6 (500 µL, 2.61×10^{-1} M) was added to a solution of **1eH$^+$Br$^-$** (40.4 mg, 130 µmol) and **4a** (36.6 mg, 125 µmol) in DMSO-d_6 (2.00 mL) at ambient temperature. After stirring for 30 s the solution was subjected to ^{1}H NMR. The spectra show decreasing signals of the reactants **1e** and **4a**, and increasing signals of the product *rac*-**11ea**, but no signals of the intermediate betaine **10ea**. (Evaluation of the kinetics see Kinetics Section)

2-*tert*-Butyl 1,1-diethyl 3-(*p*-tolyl)cyclopropane-1,1,2-tricarboxylate (*rac*-**11fd**). From **1fH$^+$Br$^-$** (172 mg, 560 µmol), KO^{t}Bu (64.2 mg, 572 µmol), and **4d** (100 mg, 381 µmol) according to procedure **E**. *rac*-**11fd** was obtained as colorless oil (91.5 mg, 243 µmol, 64%, *trans:cis* 96:4). **^{1}H NMR** (600 MHz, CDCl$_3$) δ = 7.15 (d, *J* = 8.0 Hz, 2 H, 2×C$_{Ar}$-H), 7.07 (d, *J* = 7.8 Hz, 2 H, 2×C$_{Ar}$-H), 4.36 – 4.15 (m, 2 H, CH$_2$), 4.01 – 3.87 (m, 2 H, CH$_2$), 3.53 (d, *J* = 7.6 Hz, 1 H, CH), 3.14 – 3.08 (m, 1 H, CH), 2.30 (s, 3 H, CH$_3$), 1.48 – 1.44 (m, 9 H, C(CH$_3$)$_3$), 1.32 – 1.27 (m, 3 H, CH$_3$), 1.02 – 0.94 (m, 3 H, CH$_3$). **^{13}C NMR** (150 MHz, CDCl$_3$) δ = 168.3 (s, CO$_2$), 166.2 (s, CO$_2$), 165.7 (s, CO$_2$), 137.3 (s, C$_{Ar}$), 130.3 (s, C$_{Ar}$), 129.0 (d, 2×C$_{Ar}$-H), 128.7 (d, 2×C$_{Ar}$-H), 82.2 (s, *C*(CH$_3$)$_3$), 62.0 (t, CH$_2$), 61.9 (t, CH$_2$), 44.5 (s, C$_q$), 35.4 (d, CH), 32.2 (d, CH), 28.1 (q, C(*C*H$_3$)$_3$), 21.3 (q, CH$_3$), 14.2 (q, CH$_3$), 14.0 (q, CH$_3$). **HRMS** (ESI): *m/z* calcd. for [C$_{21}$H$_{28}$O$_6$ Na]$^+$: 399.1778, found 399.1779. **MS** (EI): *m/z* 303, 275, 247, 230, 201, 129, 119, 105, 91, 57, 41. DA335

2.7.3.4 Reactions with Benzylidene Indandione 5b

General procedure G for the synthesis of the products 13. KO^{t}Bu (0.7 mmol) in DMSO (2 mL) was added dropwise to a solution of **1H$^+$X$^-$** (0.7 mmol) and benzylidene indandione **5b** (0.4 mmol) in DMSO/CH$_2$Cl$_2$ (3:2, 5 mL) at ambient temperature. After 30 min reaction time additional **1H$^+$X$^-$** (0.4 mmol) and KO^{t}Bu (0.4 mmol) were added and stirring was continued for 30 min. Water (20 mL) was added and the mixture was extracted with CH$_2$Cl$_2$ (3×10 mL). The combined organic layers were washed with water (2×20 mL) and dried over Na$_2$SO$_4$. The solvent was evaporated, and if necessary the products **13** were purified by filtration (EtOAc over silica). The diastereomeric excesses were determined from the crude products after aqueous work-up. General note: Benzylidene indandione **5b** is labile under the employed basic reaction conditions and decomposes. One decomposition product is anisaldehyde, whose separation from the cyclopropanes **13** was not always successful.

2-(2-(1,4-Diazabicyclo[2.2.2]octan-1-ium-1-yl)-2-cyano-1-(4-methoxyphenyl)ethyl)-1,3-dioxo-2,3-dihydro-1*H*-inden-2-ide (12ab). KO^{t}Bu (28.1 mg, 250 µmol) in DMSO-d_6 (1 mL) was added dropwise over 1 min to a solution of **1aH$^+$Br$^-$** (58.0 mg, 250 µmol) and **5b** (66.1 mg, 250 µmol) in DMSO-d_6/CD$_2$Cl$_2$ (1:1, 2 mL) at ambient temperature. During the addition of the base the solution turned deep red. After stirring at 20 °C for approximately 5 min the solution was quenched by freezing at –20 °C. For NMR-analysis the solution was brought back to 20 °C. The spectra showed a mixture of ratio **12ab**:**13ab** (10:1) with full conversion of the reactants to **12ab** (*dr* 1:1). The amount of **13ab** increased during the acquisition of the spectra. **^{1}H NMR** (400 MHz, DMSO-d_6) δ = 7.66 (d, *J* = 8.8 Hz, 2 H, 2×C$_{Ar}$-H), 7.51 (d, *J* = 8.8 Hz, 2 H, 2×C$_{Ar}$-H), 7.22–7.17 (m, 4 H, 4×C$_{Ar}$-H), 7.09 – 7.03 (m, 4 H, 4×C$_{Ar}$-H), 6.85 – 6.78 (m, 4 H, 4×C$_{Ar}$-H), 6.32 (d, *J* = 8.4 Hz, 1 H, CHCN), 5.99 (d, *J* = 8.9 Hz, 1 H, CHCN), 4.58 (d, *J* = 8.9 Hz, 1 H, CH-C$_{Ar}$), 4.46 (d, *J* = 8.3 Hz, 1 H, CH-C$_{Ar}$), 3.70 (s, 3 H, CH$_3$), 3.69 (s, 3 H, CH$_3$), 3.61 (t, *J* = 6.3, 6 H, $^+$N(CH$_2$)$_3$), 3.53 – 3.47 (m, 6 H, $^+$N(CH$_2$)$_3$), 3.14 – 3.02 (m, 12 H, 2×N(CH$_2$)$_3$). **^{13}C NMR** (100 MHz, DMSO-d_6) δ= 187.8 (s, 2×CO), 187.4 (s, 2×CO), 158.2 (s, C$_{Ar}$), 157.8 (s, C$_{Ar}$), 140.0 (s, 2×C$_{Ar}$), 139.8 (s, 2×C$_{Ar}$), 134.6 (s, C$_{Ar}$), 133.6 (s, C$_{Ar}$), 129.9 (d, 2×C$_{Ar}$-H), 129.5 (d, 2×C$_{Ar}$-H), 129.3 (d, 2×C$_{Ar}$-H), 129.1 (d, 2×C$_{Ar}$-H), 117.0 (d, 2×C$_{Ar}$-H), 116.9 (d, 2×C$_{Ar}$-H), 113.7 (s, CN), 113.6 (d, 2×C$_{Ar}$-H), 113.5 (d, 2×C$_{Ar}$-H), 113.3 (s, CN), 103.5 (s, C$^-$), 102.8 (s, C$^-$), 67.8 (d, *C*HCN), 65.9 (d, *C*HCN), 55.0 (q, CH$_3$), 55.0 (q, CH$_3$), 51.7 (t, $^+$N(CH$_2$)$_3$), 51.5 (t, $^+$N(CH$_2$)$_3$), 44.7 (t, N(CH$_2$)$_3$), 44.7 (t, N(CH$_2$)$_3$), 38.0 (d, *C*H-C$_{Ar}$), 37.7 (d, *C*H-C$_{Ar}$). DA792
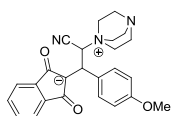
3-(4-Methoxyphenyl)-1',3'-dioxo-1',3'-dihydrospiro[cyclopropane-1,2'-indene]-2-carbonitrile (*rac*-13ab). was synthesized according to procedure **C** (stirring for 5 min at 20 °C) from **1aH$^+$Br$^-$** (158 mg, 681 µmol), KO^{t}Bu (76.5 mg, 682 µmol) and **5b** (150 mg, 568 µmol). After chromatography (silica; *n*-pentane:EtOAc = 5:1) and recrystallization from ethanol *rac*-**13ab** was obtained as a colorless solid (35 mg, 0.11 mmol, 19%, *trans:cis* 25:75). (Analytical data see below). DA447

3-(4-Methoxyphenyl)-1',3'-dioxo-1',3'-dihydrospiro[cyclopropane-1,2'-indene]-2-carbonitrile (*rac*-13ab). From **1aH$^+$Br$^-$** (155 mg, 668 µmol), **5b** (100 mg, 378 µmol) and KO^{t}Bu (76 mg, 0.68 mmol) according to procedure **G** (stirring for 60 min at 20 °C). After column filtration *rac*-**13ab** was obtained as colorless solid (93 mg, 0.31 mmol, 82%, *trans:cis* 20:80). **Mp** 212−213 °C. *rac*-*cis*-**13ab**. **^{1}H NMR** (300 MHz, CDCl$_3$) δ = 8.07 – 7.94 (m, 2 H, 2×C$_{Ar}$-H), 7.89 – 7.85 (m, 2 H, 2×C$_{Ar}$-H), 7.35 (d, *J* = 8.4 Hz, 2 H, 2×C$_{Ar}$-H), 6.89 (d, *J* = 8.8 Hz, 2 H, 2×C$_{Ar}$-H), 3.80 (s, 3 H, CH$_3$), 3.52 (d, *J* = 9.1 Hz, 1H, CH), 3.04 (d, *J* = 9.2 Hz, 1 H, CH). **^{13}C NMR** (75 MHz, CDCl$_3$) δ = 194.7 (s,
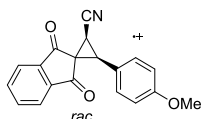
CO), 191.0 (s, CO), 159.9 (s, C_{Ar}), 143.2 (s, C_{Ar}), 140.8 (s, C_{Ar}), 136.1 (d, C_{Ar}-H), 135.7 (d, C_{Ar}-H), 131.0 (d, 2×C_{Ar}-H), 123.5 (d, C_{Ar}-H), 123.4 (d, C_{Ar}-H), 121.4 (s, C_{Ar}), 114.3 (d, 2×C_{Ar}-H), 114.2 (s, CN), 55.4 (q, CH_3), 42.1 (s, C_q), 38.2 (d, CH), 19.8 (d, CH). **HRMS** (EI): *m/z* calcd. for $[C_{19}H_{13}NO_3]^{+}$: 303.0890, found 303.0874. **MS** (EI) *m/z* = 304 (10), 303 (53), 272 (63), 203 (10), 133 (40), 104 (21), 58 (40), 43 (100). *rac-trans-***13ab.** **^{1}H NMR** (600 MHz, $CDCl_3$) δ = 8.08–8.05 (m, 1 H, C_{Ar}-H), 7.87–7.80 (m, 3 H, 3×C_{Ar}-H, superimposed by *cis*-product), 7.17 (d, *J* = 8.5 Hz, 2 H, 2× C_{Ar}-H), 6.85 (d, *J* = 8.8 Hz, 2 H, 2× C_{Ar}-H), 3.78 (s, 3 H, CH_3, superimposed by *rac-cis-***13ab** diastereoisomer), 3.75 (d, *J* = 8.1 Hz, 1 H, CH), 3.20 (d, *J* = 8.1 Hz, 1 H, CH). **^{13}C NMR** (150 MHz, $CDCl_3$) δ = 192.7 (s, CO), 192.3 (s, CO), 160.0 (s, C_{Ar}), 142.1 (s, C_{Ar}), 142.0 (s, C_{Ar}), 135.9 (d, C_{Ar}-H), 135.9 (d, 3×C_{Ar}-H), 130.1 (d, 2×C_{Ar}-H), 122.1 (d, 2×C_{Ar}-H), 115.2 (s, C_{Ar}), 114.2 (s, CN), 58.6 (t, CH_3), 43.6 (s, C_q), 41.6 (d, CH), 19.1 (d, CH). DA447-3

NMR-Monitoring of the reaction of 1a with 5b. KO^{t}Bu dissolved in DMSO-d_6 (500 µl, 0.520 M) was added to a solution of **1aH$^-$Br$^+$** (53.3 mg, 230 µmol) and **5b** (49.8 mg, 188 µmol) in DMSO-d_6: CD_2Cl_2 (2.1 mL, 5:2) at ambient temperature. After 30 s stirring the solution was subjected to ^{1}H NMR. The spectra show quantitative formation of the intermediate betaine **12ab**, the signals of which decrease with time, while the signals of the product *rac-***13ab** increase. The formation of ylide **1a** was not observed. For a detailed kinetic analysis of the NMR data see kinetic section. DA876

Crossover experiment to test the reversibility of the formation of betaine 12ab. A solution of KO^{t}Bu (59 mg, 0.53 mmol) in DMSO (2 mL) was added dropwise to a solution of **1aH$^+$Br$^-$** (122 mg, 526 µmol) and **5b** (132 mg, 499 µmol) in DMSO/CH_2Cl_2 (5 mL, 3:2) over 1 min at ambient temperature. After 3 min reaction time a solution of **5a** (117 mg, 499 µmol) in CH_2Cl_2 (2 mL) was added and the reaction mixture was stirred for 1 h at ambient temperature. The reaction was quenched with 2 M HCl (20 mL) and extracted with CH_2Cl_2 (3 × 10 mL). The combined organic layers were washed with brine (2 × 20 mL) and dried over Na_2SO_4. The crude product was subjected to column chromatography (silica, *n*-pentane:EtOAc 10:1). **13ab** was obtained as colorless solid (70 mg, 231 µmol, 46%); 105 mg (448 mmol, 90%) of **5a** and 12 mg (45 µmol, 9%) of **5b** were reisolated. DA815

Table 2.24. Crystallographic data for *rac-cis*-13ab.

net formula	$C_{19}H_{13}NO_3$
M_r/g mol^{-1}	303.311
crystal size/mm	$0.28 \times 0.04 \times 0.02$
T/K	200(2)
radiation	MoKα
diffractometer	'KappaCCD'
crystal system	monoclinic
space group	$P2_1/c$
a/Å	5.8676(2)
b/Å	30.1350(12)
c/Å	8.1744(3)
α/°	90
β/°	92.707(2)
γ/°	90
V/Å^3	1443.79(9)
Z	4
calcd. density/g cm^{-3}	1.39540(9)
μ/mm^{-1}	0.095
absorption correction	none
refls. measured	9074
R_{int}	0.0593
mean $\sigma(I)/I$	0.0547
θ range	3.22–25.35
observed refls.	1671
x, y (weighting scheme)	0.0418, 0.3886
hydrogen refinement	constr
refls in refinement	2615
parameters	209
restraints	0
$R(F_{obs})$	0.0448
$R_w(F^2)$	0.1106
S	1.054
shift/error$_{max}$	0.001
max electron density/e Å^{-3}	0.159
min electron density/e Å^{-3}	−0.214

NMR-Monitoring of the reaction of 1a with 5b. KO^{t}Bu dissolved in DMSO-d_6 (500 µl, 0.520 M) was added to a solution of **1aH⁻Br⁺** (53.3 mg, 230 µmol) and **5b** (49.8 mg, 188 µmol) in DMSO-d_6: CD_2Cl_2 (2.1 mL, 5:2) at ambient temperature. After 30 s stirring the solution was subjected to ^{1}H NMR. The spectra show quantitative formation of the intermediate betaine **12ab**, the signals of which decrease with time, while the signals of the product *rac*-**13ab** increase. The formation of ylide **1a** was not observed. For a detailed kinetic analysis of the NMR data see kinetic section. DA876

2-(2-(1,4-Diazabicyclo[2.2.2]octan-1-ium-1-yl)-3-(diethylamino)-1-(4-methoxyphenyl)-3-oxopropyl)-1,3-dioxo-2,3-dihydro-1H-inden-2-ide (12bb). A solution of KO^{t}Bu in DMSO-d_6 (500µl, 415 mM) was added dropwise over 1 min to a solution of **1bH$^+$Cl$^-$** (49.4 mg, 189 µmol) and **5b** (50 mg 189 µmol) in DMSO-d_6/CH$_2$Cl$_2$ (2.5:1; 2.1 mL) at ambient temperature. During the addition of base the solution turned deep red. After stirring for approximately 5 min at 20 °C the solution was quenched by freezing at –20 °C. For NMR-analysis the solution was brought back to 20 °C. The spectrum immediately taken after thawing showed a ratio of **12bb**:**13bb** ~10:1 and two diastereoisomers of **12bb** (*dr* 1:1) with complete conversion of **5b.** The ratio of **12bb**:**13bb** changed to 4:5 during the time needed to perform a complete NMR analysis (^{1}H, ^{13}C NMR, COSY, HMBC, HSQC). One isomer of **12bb** obviously forms **13bb** faster than the other, so that after the complete the NMR analysis it becomes the minor diastereoisomer (*dr* 1:18). *major diastereoisomer after thawing, [#]minor diastereoisomer after thawing; in the ^{13}C NMR "*" corresponds to the signals with lower intensity, as the initial major diastereoisomer is the minor diastereoisomer after the complete NMR measurements. For the ^{1}H NMR the integrals of the signals are not given. **^{1}H NMR** (400 MHz, DMSO-d_6) δ = 7.82 (d, *J* = 8.5 Hz, 2×C$_{Ar}$-H),* 7.46 – 7.37 (m, 2×C$_{Ar}$-H),[#] 7.20 – 7.16 (m, 2×C$_{Ar}$-H),[#] 7.12 – 7.03 (m, 4×C$_{Ar}$-H),*,[#] 6.99 – 6.92 (m, 2×C$_{Ar}$-H),* 6.82 (d, *J* = 8.3 Hz, 2×C$_{Ar}$-H),* 6.67 (d, *J* = 8.3 Hz, 2×C$_{Ar}$-H),[#] 5.67 (d, *J* = 9.0 Hz, CH, superimposed by solvent),* 5.60 (d, *J* = 10.8 Hz, CH),[#] 4.59 (d, *J* = 7.5 Hz, CH),* 4.46 (d, *J* = 7.7 Hz, CH),[#] 3.97 – 3.75 (m, $^+$N(C*H*H)$_3$, 2×C*H*H^a),[#] 3.71 (s, CH$_3$),* 3.64 (s, CH$_3$),[#] 3.53 – 3.32 (m, $^+$N(C*H*H)$_3$, 2×$^+$N(CH*H*)$_3$),*,[#] 3.32 – 3.03 (m, CH*H*^{a}, C*H*H^b, superimposed by **13bb**),*,[#] 3.03 – 2.82 (m, 2×N(CH$_2$)$_3$),*,[#] 2.82 – 2.65 (m, CH*H*^{b}, superimposed by **13bb**),[#] 1.11 – 1.00 (m, 2×CH$_3$, superimposed by **13bb**),*,[#] 0.54 (s, CH$_3$),* 0.45 (s, CH$_3$).[#] **^{13}C NMR** (100 MHz, DMSO-d_6) δ = 188.4 (br s, 2×CO),[#] 187.3 (br s, 2×CO),* 165.2 (br s, CON),[#] 164.7 (br s, CON),* 157.9 (s, C$_{Ar}$),[#] 157.5 (s, C$_{Ar}$),* 140.6 (s, 2×C$_{Ar}$),* 140.0 (s, 2×C$_{Ar}$),[#] 136.7 (s, C$_{Ar}$),* 134.0 (s, C$_{Ar}$),[#] 130.7 (d, 2×C$_{Ar}$-H),[#] 129.0 (d, 2×C$_{Ar}$-H),[#] 128.5 (d, 2×C$_{Ar}$-H),* 128.2 (d, 2×C$_{Ar}$-H),* 116.7 (d, 2×C$_{Ar}$-H),[#] 116.2 (d, 2×C$_{Ar}$-H),* 112.7 (d, 2×C$_{Ar}$-H),[#] 112.3 (d, 2×C$_{Ar}$-H),* 103.8 (s, C$_q^-$),[#] 103.5 (s, C$_q^-$),* 71.1 (d, CH),* 68.7 (d, CH),[#] 54.7 (q, CH$_3$) 52.2 (q, CH$_3$), 51.3 (br t, $^+$N(CHH)$_3$),[#] 50.5 (t, $^+$N(CHH)$_3$),* 44.8 (t, N(CH$_2$)$_3$),* 44.4 (t, N(CH$_2$)$_3$),[#] 42.1 (t, CHH),* 41.8 (t, CHH),[#] 38.7 (br t, CHH),[#] 38.6 (t, CHH),* 38.4 (d, CH),[#] 37.7 (d, CH),* 13.5 (q, CH$_3$),* 13.4 (q, CH$_3$),[#] 11.2 (q, CH$_3$),[#] 11.1 (q, CH$_3$).* DA875
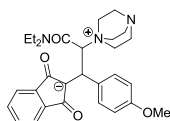
N,N-Diethyl-3-(4-methoxyphenyl)-1',3'-dioxo-1',3'-dihydrospiro[cyclopropane-1,2'-indene]-2-carboxamide (*rac-trans*-**13bb**). **1bH⁺Cl⁻** (179 mg, 684 μmol) and **5b** (101 mg, 382 μmol) were suspended in CH_2Cl_2 (10 mL) and aq. NaOH (1 mL, 32%) was added at ambient temperature. After 30 min stirring another portion of **1bH⁺Cl⁻** (50 mg, 191 μmol) was added and stirring was continued for 30 min. The reaction mixture was diluted with water (20 mL) and extracted with EtOAc (3×25 mL). The combined organic layers were washed with brine and dried over Na_2SO_4. The solvent was removed and the crude product was subjected to a gradient column chromatography (silica, *n*-Pentane:EtOAc 5:1→1:1). *rac-trans*-**13bb** was obtained as yellow oil (32 mg, 85 μmol, 22%, *trans:cis* 66:33). (Analytical data see below). DA498

N,N-Diethyl-3-(4-methoxyphenyl)-1',3'-dioxo-1',3'-dihydrospiro[cyclopropane-1,2'-indene]-2-carboxamide (*rac-trans*-**13bb**). From **1bH⁺Cl⁻** (179 mg, 684 μmol), **5b** (100 mg, 378 μmol), and KO^{t}Bu (77 mg, 0.69 mmol) according to procedure **G**. *rac-trans*-**13bb** was obtained as yellow oil (95 mg, 0.25 mmol, 66%, *trans:cis* 66:33). **¹H NMR** (300 MHz, CDCl₃) δ = 7.96 (dd, *J* = 6.1, 1.6 Hz, 1 H, C$_{Ar}$-H), 7.85 – 7.71 (m, 3 H, 3×C$_{Ar}$-H), 7.21 (d, *J* = 8.6 Hz, 2 H, 2×C$_{Ar}$-H), 6.81 (d, *J* = 8.7 Hz, 2 H, 2×C$_{Ar}$-H), 4.03 (d, *J* = 8.8 Hz, 1 H, CH), 3.76 (s, 3 H, CH₃), 3.57 (d, *J* = 8.8 Hz, 1 H, CH), 3.53 – 3.11 (m, 4 H, 2×CH₂), 1.13 (t, *J* = 7.1 Hz, 3 H, CH₃), 1.02 (t, *J* = 7.1 Hz, 3 H, CH₃). **¹³C NMR** (75 MHz, CDCl₃) δ = 194.8 (s, CO), 194.6 (s, CO), 164.1 (s, CON), 159.4 (s, C$_{Ar}$), 142.3 (s, C$_{Ar}$), 141.8 (s, C$_{Ar}$), 135.2 (d, C$_{Ar}$-H), 135.0 (d, C$_{Ar}$-H), 130.3 (d, 2×C$_{Ar}$-H), 124.6 (s, C$_{Ar}$), 122.9 (d, C$_{Ar}$-H), 122.8 (d, C$_{Ar}$-H), 113.7 (d, 2×C$_{Ar}$-H), 55.3 (q, CH₃), 47.1 (s, C$_q$), 43.9 (d, CH), 41.9 (t, CH₂), 40.3 (t, CH₂), 38.2 (d, CH), 14.1 (q, CH₃), 13.0 (q, CH₃). **HRMS** (EI): *m/z* calcd. for [C₂₃H₂₃NO₄] $^+$: 377.1622, found 377.1624. **MS** (EI) *m/z* = 377 (15), 276 (10), 100 (100), 72 (33). DA450-2
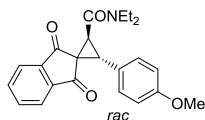
¹H NMR Monitoring of the reaction of 1b with 5b. KO^{t}Bu in DMSO-d_6 (1.00 mL, 2.54 × 10⁻¹ M) was added to a solution of **1bH⁺Cl⁺** (32.7 mg, 125 μmol) and **5b** (31.5 mg, 119 μmol) in DMSO-d_6:CH₂Cl₂ (1:1, 2.00 mL) at ambient temperature. After 30 s stirring the solution was subjected to ¹H NMR. The spectra show decreasing signals of the intermediate betaine **12bb** and increasing signals of the product **13bb**. The formation of ylide **1b** was not observed. For a detailed kinetic analysis of the NMR data see kinetic section.

2-(2-(1,4-Diazabicyclo[2.2.2]octan-1-ium-1-yl)-3-ethoxy-1-(4-methoxyphenyl)-3-oxo-propyl)-1,3-dioxo-2,3-dihydro-1*H*-inden-2-ide (12cb). KO*t*Bu (77 mg, 0.69 mmol) dissolved in DMSO (2 mL) was added to a solution of **1cH⁺Br⁻** (191 mg, 684 μmol) and **5b** (150 mg, 568 μmol) in DMSO:CH$_2$Cl$_2$ (3 mL, 2:1) at ambient temperature. The reaction was stirred for 5 min, then water (30 mL) was added and the mixture was extracted with CH$_2$Cl$_2$ (3×10 mL). The solvent was removed and the crude product was subjected to NMR. The spectrum after work-up showed a ~16:1 ratio of **12cb**:**13cb** with two diastereoisomers of **12cb** (*dr* 1:1), and complete conversion of **5b**. After performing the complete NMR-analysis (¹H-, ¹³C NMR, COSY, HMBC, HSQC) the ratio of **12cb**:**13cb** changed to 2:1 with only one diastereoisomer of **12cb** remaining. **¹H NMR** (300 MHz, CDCl$_3$) δ = 7.49 (d, *J* = 8.6 Hz, 2 H, 2×C$_{Ar}$-H), 7.20 − 7.14 (m, 4 H, 4×C$_{Ar}$-H), 6.62 (d, *J* = 8.9 Hz, 2 H, 2×C$_{Ar}$-H), 5.29 (d, *J* = 11.3 Hz, 1 H, CH), 4.49 (d, *J* = 11.3 Hz, 1 H, CH), 3.98 − 3.88 (m, 3 H, ⁺N(C*H*H)$_3$), 3.77 − 3.67 (m, 2 H, CH$_2$, superimposed by **13cb**), 3.62 (s, 3 H, CH$_3$), 3.45 − 3.34 (m, 3 H, ⁺N(CH*H*)$_3$), 3.02 − 2.92 (m, 6 H, N(CH$_2$)$_3$), 0.78 (t, *J* = 7.1 Hz, 3 H, CH$_3$). **¹³C NMR** (75 MHz, CDCl$_3$) δ = 189.8 (s, 2×CO), 166.2 (s, CO$_2$), 158.2 (s, C$_{Ar}$), 139.5 (s, 2×C$_{Ar}$), 132.6 (s, C$_{Ar}$), 130.4 (d, 2× C$_{Ar}$-H), 129.4 (d, 2× C$_{Ar}$-H), 117.4 (d, 2× C$_{Ar}$-H), 113.2 (d, 2×C$_{Ar}$-H), 102.8 (s, C$_q^-$), 74.6 (d, CH), 62.0 (t, CH$_2$), 54.9 (q, CH$_3$), 51.6 (t, ⁺N(CHH)$_3$), 45.2 (t, N(CH$_2$)$_3$), 39.0 (d, CH), 13.1 (q, CH$_3$). DA439-2
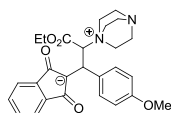
Ethyl 3-(4-methoxyphenyl)-1',3'-dioxo-1',3'-dihydrospiro[cyclopropane-1,2'-indene]-2-carboxylate (*rac-trans*-13cb). **1cH⁺Br⁻** (191 mg, 682 μmol), **5b** (150 mg, 568 μmol), and KO*t*Bu (77 mg, 0.68 mmol) according to procedure **C** (5 min stirring at 20 °C). After purification by chromatography (silica; *n*-Pentane:EtOAc, 5:1→2:1) *rac-trans*-**13cb** was obtained as yellow oil (58 mg, 0.17 mmol, 30%, *trans:cis* 80:20). (Analytical data see below). DA439

Ethyl 3-(4-methoxyphenyl)-1',3'-dioxo-1',3'-dihydrospiro[cyclopropane-1,2'-indene]-2-carboxylate (*rac-trans*-13cb) was synthesized according to procedure **G** from **1cH⁺Br⁻** (191 mg, 684 μmol), **5b** (100 mg, 378 μmol) and KO*t*Bu (77 mg, 0.68 mmol). *rac-trans*-**13cb** is obtained as yellow oil (66 mg, 0.19 mmol, 50%, *trans:cis* 89:11). **¹H NMR** (300 MHz, CDCl$_3$) δ = 7.97 − 7.91 (m, 1 H, C$_{Ar}$-H), 7.83 − 7.71 (m, 3 H, 3×C$_{Ar}$-H), 7.18 (d, *J* = 8.9 Hz, 2 H, 2×C$_{Ar}$-H), 6.83 − 6.75 (m, 2 H, 2×C$_{Ar}$-H), 4.30 − 4.16 (m, 2 H, CH$_2$), 3.93 (d, *J* = 8.8 Hz, 1 H, CH), 3.75 (s, 3 H, CH$_3$), 3.54 (d, *J* = 8.8 Hz, 1 H, CH), 1.27 (q, *J* = 7.0, 3 H, CH$_3$). **¹³C NMR** (75 MHz, CDCl$_3$) δ = 194.9 (s, CO), 193.7 (s, CO), 166.6 (s, CO$_2$), 159.4 (s, C$_{Ar}$), 142.1 (s, C$_{Ar}$), 142.0 (s, C$_{Ar}$), 135.2 (d, C$_{Ar}$-H), 135.1 (d, C$_{Ar}$-H), 130.3 (d, 2×C$_{Ar}$-H), 123.9 (s, C$_{Ar}$), 122.9 (d, C$_{Ar}$-H), 122.8 (d, C$_{Ar}$-H), 113.8 (d, 2×C$_{Ar}$-H), 61.8
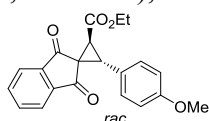
(t, CH_2), 55.3 (q, CH_3), 46.1 (s, C_q), 42.3 (d, CH), 36.9 (d, CH), 14.2 (q, CH_3). **HRMS** (EI): *m/z* calcd. for $[C_{21}H_{18}O_5]^+$: 350.1149, found 350.11476. **MS** (EI) *m/z* = 350 (29), 305 (19), 304 (32), 277 (100), 276 (67), 262 (16), 234 (11), 178 (10), 58 (17), 43 (38). DA439-3

NMR-Monitoring of the reaction of 1c with 5b. KO^tBu (26 mg, 0.23 µmol) dissolved in DMSO-d_6 (0.50 mL) was added to a solution of **1cH⁻Br⁺** (64 mg, 0.23 mmol) and **5b** (50 mg, 0.19 mmol) in DMSO-d_6:CH_2Cl_2 (1.6 mL, 1.6:1) at ambient temperature. After 30 s stirring the solution was subjected to ¹H NMR. The spectra show decreasing amounts of the intermediate betaine **12cb** and increasing amounts of the product **13cb**. The formation of ylide **1c** was not observed. For a kinetic analysis of the NMR data see kinetic section. DA653

2-Acetyl-3-(4-methoxyphenyl)spiro[cyclopropane-1,2'-indene]-1',3'-dione (*rac-trans-***13db**). Aq. NaOH (5 mL, 32%) was added to suspension of **1dH⁺Cl⁻** (116 mg, 567 µmol) and **5b** (100 mg, 378 µmol) in CH_2Cl_2 (10 mL) and at ambient temperature. After 30 min stirring another portion of **1dH⁺Cl⁻** (50 mg, 0.24 mmol) was added and stirring was continued for 30 min. The reaction mixture was diluted with 20 mL water and extracted with EtOAc (3×25 mL). The combined organic layers were washed with brine (2×30 mL) and dried over Na_2SO_4. The solvent was removed and the crude was subjected to chromatography (silica; *n*-Pentane:EtOAc 5:1→1:1). *rac-trans-***13db** was obtained as brown oil (64 mg, 200 µmol, 53%, *trans:cis* 66:33) contaminated by **5b**. **¹H NMR** (400 MHz, CDCl₃) δ = 8.00 − 7.96 (m, 2 H, 2×C_{Ar}-H), 7.83 −
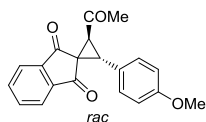
7.80 (m, 2 H, 2×C_{Ar}-H), 7.55 (d, *J* = 8.7 Hz, 2 H, 2×C_{Ar}-H), 6.93 (d, *J* = 8.8 Hz, 2 H, 2×C_{Ar}-H), 3.99 (d, *J* = 9.1 Hz, 1 H, CH), 3.82 (s, 3H, CH_3), 3.66 (d, *J* = 9.1 Hz, 1 H, CH), 2.40 (s, 3 H, CH_3). **¹³C NMR** (100 MHz, CDCl₃) δ = 198.7 (s, 2×CO), 198.1 (s, CO), 161.2 (s, C_{Ar}), 142.0 (s, 2×C_{Ar}), 135.3 (d, 2×C_{Ar}-H) 130.8 (d, 2×C_{Ar}-H), 127.1 (s, C_{Ar}), 123.4 (d, 2×C_{Ar}-H), 114.5 (d, 2×C_{Ar}-H), 55.5 (q, CH_3), 47.6 (s, C_q), 44.2 (d, CH), 42.8 (d, CH), 24.9 (q, CH_3). **HRMS** (EI): *m/z* calcd. for $[C_{20}H_{16}O_4]^+$: 320.1043, found 320.1044. DA500

NMR-Monitoring of the reaction of 1d with 5b. KO^tBu in DMSO-d_6 (500 µL, 2.61 × 10⁻¹ M) was added to a solution of **1dH⁻Cl⁺** (26.7 mg, 130 µmol) and **5b** (31.5 mg, 119 µmol) in DMSO-d_6:CH_2Cl_2 (2.00 mL, 1:1) at ambient temperature. After 30 s stirring the solution was subjected to ¹H NMR. The spectra show constant signals of the product **13db**, but no betaine **12db**. For a kinetic evaluation of the NMR data see Kinetic Section.

2-Benzoyl-3-(4-methoxyphenyl)spiro[cyclopropane-1,2'-indene]-1',3'-dione (*rac-trans-*
13eb). From **1eH⁺Br⁻** (265 mg, 851 μmol), KO*t*Bu (96 mg, 0.85 mmol) and **5b** (150 mg,
568 μmol) according to procedure **C**. After purification by chromatography (*n*-Pentane:EtOAc,
5:1→2:1) *rac-trans-***13eb** was obtained as brown oil (131 mg, 343 μmol, 60%, *trans:cis* 75:25).
¹H NMR (300 MHz, CDCl₃) δ = 7.97 – 7.91 (m, 2 H, 2×C_{Ar}-H), 7.88 – 7.81 (m, 2 H, 2×C_{Ar}-
H), 7.78 – 7.72 (m, 2 H, 2×C_{Ar}-H), 7.51 (t, *J* = 7.4 Hz, 1 H, C_{Ar}-H), 7.38 (t, *J* = 7.6 Hz, 2 H,
2×C_{Ar}-H), 7.29 (d, *J* = 8.8 Hz, 2 H, 2×C_{Ar}-H), 6.85 (d, *J* = 8.7 Hz, 2 H, 2×C_{Ar}-H), 4.26 (d, *J* =
8.9 Hz, 1 H, CH), 4.17 (d, *J* = 8.9 Hz, 1 H, CH), 3.17 (s, 3 H, CH₃). **¹³C NMR** (75 MHz, CDCl₃)

δ = 194.4 (s, CO), 194.2 (s, CO), 190.7 (s, CO), 159.5 (s, C_{Ar}), 142.1 (s,
C_{Ar}), 142.0 (s, C_{Ar}), 136.2 (s, C_{Ar}), 135.2 (d, C_{Ar}-H), 135.1 (d, C_{Ar}-H),
133.8 (d, C_{Ar}-H), 130.4 (d, 2×C_{Ar}-H), 128.9 (d, 2×C_{Ar}-H), 128.4 (d, 2×C_{Ar}-

H), 124.2 (s, C_{Ar}), 123.0 (d, C_{Ar}-H), 122.8 (d, C_{Ar}-H), 113.8 (d, 2×C_{Ar}-H), 55.2 (q, CH₃), 47.8
(s, C_q), 42.6 (d, CH), 41.0 (d, CH). **HRMS** (EI): *m/z* calcd. for [$C_{25}H_{18}O_4$]⁺⁺: 382.1200, found
382.1199. DA435
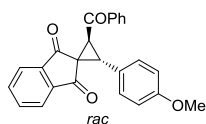
NMR-Monitoring of the reaction of 1e with 5b. KO*t*Bu in DMSO-d_6 (500 μL, 2.61 × 10⁻¹
M) was added to a solution of **1eH⁻Br⁺** (39.3 mg, 126 μmol) and **5b** (30.2 mg, 114 μmol) in
DMSO-d_6:CH₂Cl₂ (2.00 mL, 1:1) at ambient temperature. After 30 s stirring the solution was
subjected to ¹H NMR. The spectra show constant signals of the product **13eb**, but no formation
of the intermediate betaine **12eb**. For a kinetic evaluation of the NMR data see Kinetic Section.
DA898

2-(3-Ethoxy-1-(4-methoxyphenyl)-3-oxo-2-(trimethylammonio)propyl)-1,3-dioxo-2,3-
dihydro-1*H*-inden-2-ide (12hb). KO*t*Bu (21 mg, 0.19 mmol) in DMSO-d_6 (1 mL) was added
to a solution of **1hH⁺Br⁻** (50 mg, 0.16 mmol) and **5b** (43 mg, 0.16 mmol) in DMSO-d_6:CD₂Cl₂
(1.5 mL, 2:1) at ambient temperature. After 10 min CH₂Cl₂ was evaporated under reduced
pressure and the remaining solution was subjected to NMR analysis. The spectrum after
evaporation of CH₂Cl₂ shows a >20:1 ratio of **12hb**:**13hb** (= **13cb**) and two diastereoisomers
of **12hb** (*dr* 1:1). After performing the complete NMR analysis (¹H, ¹³C NMR, COSY, HMBC,
HSQC) the ratio of **12hb**:**13hb** changed to 1:1 with only one diastereoisomer of **12f** remaining.
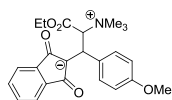
The spectrum is contaminated by **1hH⁺Br⁻**. **¹H NMR** (400 MHz, DMSO-d_6)
δ = 7.48 (d, *J* = 8.7 Hz, 2 H, 2×C_{Ar}-H), 7.20 − 7.19 (m, 2 H, 2×C_{Ar}-H), 7.06
− 7.04 (m, 2 H, 2×C_{Ar}-H), 6.74 (d, *J* = 8.9 Hz, 2 H, 2×C_{Ar}-H), 5.13 (d, *J* =

11.5 Hz, 1 H, CH), 4.29 (d, *J* = 11.5 Hz, 1 H, CH), 4.13 (q, *J* = 7.1 Hz, 2 H, CH₂), 3.72 (s, 3 H,
CH₃), 3.27 (s, 9 H, ⁺N(CH₃)₃), 1.18 (t, *J* = 7.1 Hz, 3 H, CH₃). **¹³C NMR** (100 MHz, DMSO-d_6)
δ = 188.0 (s, 2×CO), 167.3 (s, CO_2), 158.8 (s, C_{Ar}), 139.9 (s, 2×C_{Ar}), 133.3 (s, C_{Ar}) 130.5 (d,

2×C$_{Ar}$-H), 129.2 (d, 2×C$_{Ar}$-H), 116.9 (d, 2×C$_{Ar}$-H), 113.3 (d, 2×C$_{Ar}$-H), 102.0 (s, C$_q^-$), 74.3 (d, CH), 61.9 (t, CH$_2$), 55.0 (q, CH$_3$), 53.0 (q, $^+$N(CH$_3$)$_3$) 40.2 (d, CH), 13.9 (q, CH$_3$). DA479

2.7.3.5 Reactions with Chalcone 6

If not mentioned otherwise the reactions of the ylides **1** with the chalcone **6** were performed according to general procedure **C**. All products **15** where purified by flash-column chromatography (silica; *n*-Pentane:EtOAc, 10:1). The diastereomeric excesses were determined from the crude products after aqueous work-up.

2-Benzoyl-3-(4-nitrophenyl)cyclopropanecarbonitrile (*rac*-**15a**). From **1aH$^+$Br$^-$** (200 mg, 0.86 mmol), **6** (200 mg, 790 μmol), and KO^{t}Bu (134 mg, 1.19 mmol) according to procedure **C**. After column chromatography *rac*-**15a** (overall: 134 mg, 458 μmol, 58%; *dr* **A**:**B**:**C** 70:27:3) was obtained in two fractions as yellow solid (fraction 1: *rac*-**15a-A**, 67.0 mg, 229 μmol, 29%) and red solid (fraction 2: *rac*-**15a-B**, *rac*-**15a-C**, 67.0 mg, 229 μmol, 29%, *dr*

15a-B:**15a-C** 5:1). **Fraction 1**: *rac*-**15a-A**. **Mp** (acetone) 134 − 135 °C. **^{1}H NMR** (300 MHz, CDCl$_3$) δ = 8.31 − 8.22 (m, 2 H, 2×C$_{Ar}$-H), 8.09 − 8.03 (m, 2 H, 2×C$_{Ar}$-H), 7.73 − 7.66 (m, 1 H, C$_{Ar}$-H), 7.59 − 7.52 (m, 4 H, 4×C$_{Ar}$-H), 3.71 (dd, *J* = 5.9, 5.1 Hz, 1 H, CH), 3.17 (dd, *J* = 9.0, 5.9 Hz, 1 H, CH),
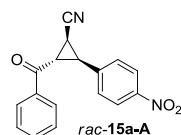
2.78 (dd, *J* = 9.0, 5.1 Hz, 1 H, CH). **^{13}C NMR** (75 MHz, CDCl$_3$) δ = 193.4 (s, CO), 147.9 (s, C$_{Ar}$), 140.9 (s, C$_{Ar}$), 135.9 (s, C$_{Ar}$), 134.6 (d, C$_{Ar}$-H), 129.2 (d, 2×C$_{Ar}$-H), 129.0 (d, 2×C$_{Ar}$-H), 128.6 (d, 2×C$_{Ar}$-H), 124.2 (d, 2×C$_{Ar}$-H), 116.8 (s, CN), 32.0 (d, CH), 30.8 (d, CH), 15.9 (d, CH). **HRMS** (ESI): *m/z* calcd. for [C$_{17}$H$_{12}$ClN$_2$O$_3$]$^-$: 327.0542, found 327.0555. **Fraction 2**: *rac*-**15a-B**. Signals of minor diastereoisomer *rac*-**15a-C** not given, due to overlap with the major diastereoisomer *rac*-**15a-B**. **^{1}H NMR** (300 MHz, CDCl$_3$) δ = 8.23 − 8.16 (m, 2 H, 2×C$_{Ar}$-H), 8.09 − 8.02 (m, 2 H, 2×C$_{Ar}$-H), 7.69 − 7.61 (m, 1 H, C$_{Ar}$-H), 7.56 − 7.50 (m, 2 H, 2×C$_{Ar}$-H), 7.42 − 7.34 (m, 2 H, C$_{Ar}$-H), 3.55 − 3.46 (m, 2 H, 2×CH), 2.49 (dd,
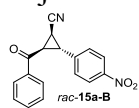
J = 8.3, 6.4 Hz, 1 H, CH). **^{13}C NMR** (75 MHz, CDCl$_3$) δ = 191.9 (s, CO), 147.6 (s, C$_{Ar}$), 143.2 (s, C$_{Ar}$), 136.3 (s, C$_{Ar}$), 134.4 (d, C$_{Ar}$-H), 129.1 (d, 2×C$_{Ar}$-H), 128.6 (d, 2×C$_{Ar}$-H), 127.7 (d, 2×C$_{Ar}$-H), 124.3 (d, 2×C$_{Ar}$-H), 116.2 (s, CN), 31.4 (d, CH), 31.3 (d, CH), 16.3 (d, CH). **HRMS** (EI): *m/z* calcd. for [C$_{17}$H$_{12}$N$_2$O$_3$]$^+$: 292.0842, found 292.0851. **MS** (EI) *m/z* = 293 (10), 292 (40), 291 (19), 265 (32), 245 (18), 189 (17), 141 (86), 140 (100). DA424

Table 2.25. Crystallographic data for *rac*-15a-A.

net formula	$C_{17}H_{12}N_2O_3$
M_r/g mol^{-1}	292.289
crystal size/mm	$0.119 \times 0.103 \times 0.059$
T/K	173(2)
radiation	'MoKα
diffractometer	'Bruker D8Venture'
crystal system	monoclinic
space group	$P2_1$
a/Å	5.6718(4)
b/Å	17.3942(14)
c/Å	13.8976(12)
α/°	90
β/°	94.576(2)
γ/°	90
V/Å^3	1366.72(19)
Z	4
calcd. density/g cm^{-3}	1.42052(20)
μ/mm^{-1}	0.099
absorption correction	multi-scan
transmission factor range	0.9401–0.9590
refls. measured	25447
R_{int}	0.0354
mean σ(I)/I	0.0402
θ range	3.17–27.61
observed refls.	5097
x, y (weighting scheme)	0.0359, 0.1801
hydrogen refinement	constr
Flack parameter	1.1(8)
refls in refinement	6224
parameters	397
restraints	1
$R(F_{obs})$	0.0385
$R_w(F^2)$	0.0833
S	1.067
shift/error$_{max}$	0.001
max electron density/e Å^{-3}	0.185
min electron density/e Å^{-3}	−0.193
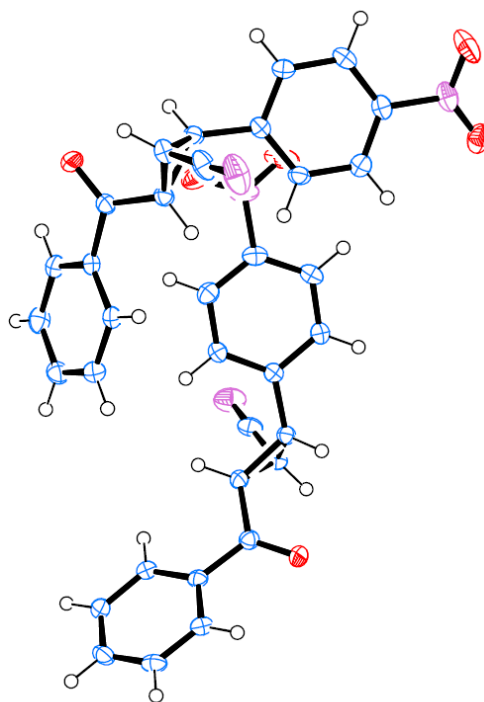
NMR-Monitoring of the reaction of 1a with 6. KO^{t}Bu in DMSO-d_6 (1.00 mL, 2.54×10^{-1} M) was added to a solution of **1aH$^+$Br$^-$** (58.0 mg, 250 µmol) and **6** (63.3 mg, 250 µmol) in DMSO-d_6:CH$_2$Cl$_2$ (2.00 mL, 1:1) at ambient temperature. After 1 min stirring the solution the solution was quenched by freezing at –20 °C. The solution was brought back to ambient temperature and subjected to ^{1}H NMR. The spectrum shows only signals of the product **15a**. The formation of an intermediate betaine **14a** or ylide **1a** was not observed. DA900

Table 2.26. Crystallographic data for *rac*-15a-B.

net formula	$C_{17}H_{12}N_2O_3$
M_r/g mol^{-1}	292.289
crystal size/mm	0.144 × 0.143 × 0.083
T/K	173(2)
radiation	'MoKα
diffractometer	'Bruker D8Venture'
crystal system	monoclinic
space group	$P2_1/n$
a/Å	10.6057(6)
b/Å	9.0729(6)
c/Å	14.7093(9)
$α$/°	90
$β$/°	99.0411(17)
$γ$/°	90
V/Å^3	1397.81(15)
Z	4
calcd. density/g cm^{-3}	1.38893(15)
$μ$/mm^{-1}	0.097
absorption correction	multi-scan
transmission factor range	0.9206–0.9585
refls. measured	28066
R_{int}	0.0384
mean σ(I)/I	0.0194
θ range	3.15–26.43
observed refls.	2315
x, y (weighting scheme)	0.0460, 0.6158
hydrogen refinement	constr
refls in refinement	2867
parameters	199
restraints	0
$R(F_{obs})$	0.0397
$R_w(F^2)$	0.1072
S	1.039
shift/error$_{max}$	0.001
max electron density/e Å^{-3}	0.259
min electron density/e Å^{-3}	−0.180
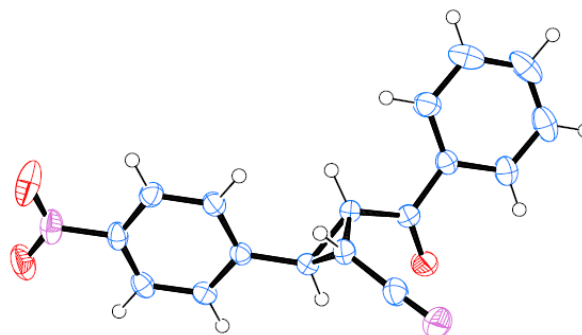
2-Benzoyl-*N,N*-diethyl-3-(4-nitrophenyl)cyclopropane-1-carboxamide (*rac*-**15b**). **1bH⁺Cl⁻** (312 mg, 1.19 mmol) and **6** (200 mg, 790 μmol) were dissolved in CH_2Cl_2 (10 mL) and aq. NaOH (1 mL, 32%) was added at ambient temperature. After 30 min the reaction mixture was diluted with water (20 mL) and extracted with EtOAc (3×25 mL). The organic layer was washed with brine (2×20 mL) and dried over Na_2SO_4. The solvent was removed and the crude product was subjected to chromatography (silica, *n*-pentane:EtOAc 5:1). After column chromatography *rac*-**15b** (overall: 151 mg, 0.41, 52% *dr* **A**:**B**:**C** ~50:50:0) was obtained in two fractions as yellow oils (fraction 1: *rac*-**15b-A**: 69 mg, 0.19 mmol, 24%; fraction 2: *rac*-**15b-**

B: 82 mg, 0.22 mmol, 28%). **Fraction 1. *rac*-15b-A. ^{1}H NMR** (300 MHz, CDCl$_3$) δ = 8.19 − 8.07 (m, 4 H, 4×C$_{Ar}$-H), 7.65 − 7.58 (m, 1 H, C$_{Ar}$-H), 7.56 − 7.48 (m, 2 H, 2×C$_{Ar}$-H), 7.47 − 7.40 (m, 2 H, 2×C$_{Ar}$-H), 4.10 (dd, *J* = 5.7, 5.1 Hz, 1 H, CH), 3.65 − 3.36 (m, 2 H, 2×CH^{a}H), 3.32 − 3.14 (m, 2 H, CH, CHH^b), 3.12 − 2.99(m, 1 H, CHH^b), 2.94 (dd, *J* = 9.9, 5.0 Hz, 1 H, CH), 1.13 (t, *J* = 7.2 Hz, 3 H, CH$_3$), 0.84 (t, *J* = 7.1 Hz, 3 H, CH$_3$). **^{13}C NMR** (75 MHz, CDCl$_3$) δ = 197.2 (s, CO), 165.1 (s, CON), 147.0 (s, C$_{Ar}$), 143.5 (s, C$_{Ar}$), 137.0 (s, C$_{Ar}$), 133.8 (d, C$_{Ar}$-H), 129.1 (d, 2×C$_{Ar}$-H), 128.9 (d, 2×C$_{Ar}$-H), 128.6 (d, 2×C$_{Ar}$-H), 123.5 (d, 2×C$_{Ar}$-H), 41.9 (t, CH$_2$), 40.6 (t, CH$_2$), 34.4 (d, CH), 33.8 (d, CH), 30.4 (d, CH), 14.5 (q, CH$_3$), 12.9 (q, CH$_3$). **HRMS** (ESI): *m/z* calcd. for [C$_{21}$H$_{22}$N$_2$O$_4$]$^+$: 366.1574, found 366.1580. **Fraction 2. *rac*-15b-B. ^{1}H NMR** (300 MHz, CDCl$_3$) δ = 8.11 − 8.00 (m, 2 H, 2×C$_{Ar}$-H), 7.97 − 7.89 (m, 2 H, 2×C$_{Ar}$-H), 7.58 − 7.51 (m, 1 H, C$_{Ar}$-H), 7.46 − 7.40 (m, 2 H, 2×C$_{Ar}$-H), 7.35 (d, *J* = 8.8 Hz, 2 H, 2×C$_{Ar}$-H), 3.69 − 3.51 (m, 3 H, CH$_2$, CH), 3.51 − 3.36 (m, 4 H, CH$_2$, 2×CH), 1.32 (t, *J* = 7.2 Hz, 3 H, CH$_3$), 1.16 (t, *J* = 7.1 Hz, 3 H, CH$_3$). **^{13}C NMR** (75 MHz, CDCl$_3$) δ = 193.9 (s, CO), 168.8 (s, CON), 147.0 (s, C$_{Ar}$), 142.7 (s, C$_{Ar}$), 137.3 (s, C$_{Ar}$), 133.7 (d, C$_{Ar}$-H), 129.7 (d, 2×C$_{Ar}$-H), 128.8 (d, 2×C$_{Ar}$-H), 128.4 (d, 2×C$_{Ar}$-H), 123.5 (d, 2×C$_{Ar}$-H), 42.7 (t, CH$_2$), 41.4 (t, CH$_2$), 35.4 (d, CH), 34.9 (d, CH), 25.3 (d, CH), 15.2 (q, CH$_3$), 13.3 (q, CH$_3$). **HRMS** (ESI): *m/z* calcd. for [C$_{21}$H$_{22}$N$_2$O$_4$]$^+$: 366.1574, found 366.1577. DA494
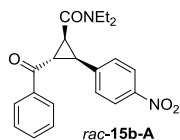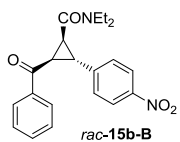
^{1}H NMR Monitoring of the reaction of 1b with 6. KO^{t}Bu in DMSO-d_6 (1.00 mL, 2.54 × 10^{-1} M) was added to a solution of **1bH$^+$Cl$^-$** (32.7 mg, 125 μmol) and **6** (31.5 mg, 124 μmol) in DMSO-d_6:CH$_2$Cl$_2$ (2.00 mL, 1:1) at ambient temperature. After 30 s stirring the solution was subjected to ^{1}H NMR. The spectra show only signals of the product **15b**. The formation of an intermediate betaine **14b** or ylide **1b** was not observed. DA900

Ethyl 2-benzoyl-3-(4-nitrophenyl)cyclopropane-1-carboxylate (*rac*-15c). From **1cH$^+$Br$^-$** (322 mg, 1.15 mmol), **6** (190 mg, 750 μmol), and KO^{t}Bu (134 mg, 1.19 mmol) according to procedure **C** by stirring for 1 h at ambient temperature. After 30 min stirring another portion of **1cH$^+$Br$^-$** (322 mg, 1.15 mmol) and KO^{t}Bu (134 mg, 1.19 mmol) was added. After chromatography *rac*-15c (overall: 171 mg, 504 μmol, 67%, *dr* **A**:**B**:**C** 40:40:20) was obtained in two fractions as yellow oils (fraction 1: *rac*-15c-A: 65 mg, 0.19 mmol, 25%; fraction 2: *rac*-15c-B and *rac*-15c-C: 106 mg, 312 μmol, 42%, *dr* **15c-B**:**15c-C** 2.5:1). **Fraction 1.** Spectrum also contains small amounts of the minor diastereoisomers. **^{1}H NMR** (300 MHz, CDCl$_3$) δ = 8.21 − 8.14 (m, 2 H, 2×C$_{Ar}$-H), 8.13 − 8.07 (m, 2 H, 2×C$_{Ar}$-H), 7.67 − 7.62 (m, 3 H, 3×C$_{Ar}$-H), 7.53 − 7.48 (m, 2 H, 2×C$_{Ar}$-H, superimposed by minor diastereoisomer), 4.07 − 3.98 (m, 2 H, CH$_2$), 3.88 (dd, *J* = 6.2, 5.0 Hz, 1 H, CH,
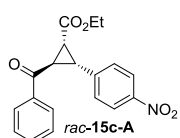
superimposed by minor diastereoisomer), 3.33 (dd, J = 9.9, 6.3 Hz, 1 H, CH), 2.88 (dd, J = 9.9, 4.8 Hz, 1 H, CH), 1.12 (t, J = 7.1 Hz, 3 H, CH$_3$). **^{13}C NMR** (75 MHz, CDCl$_3$) δ = 195.9 (s, CO), 168.5 (s, CO$_2$), 147.0 (s, C$_{Ar}$), 142.6 (s, C$_{Ar}$), 136.8 (s, C$_{Ar}$), 134.0 (d, C$_{Ar}$-H), 130.1 (d, 2×C$_{Ar}$-H), 129.1 (d, 2×C$_{Ar}$-H), 128.5 (d, 2×C$_{Ar}$-H), 123.6 (d, 2×C$_{Ar}$-H), 61.5 (t, CH$_2$), 34.0 (d, CH), 32.5 (d, CH), 29.9 (d, CH), 14.3 (q, CH$_3$). **Fraction 2** *rac*-**15c-B** and *rac*-**15c-C**. *-signals of major diastereoisomer *rac*-**15c-B**; #-signals of minor diastereoisomer *rac*-**15c-C**. For the analysis of the ^{1}H NMR spectrum no integral are given due to the odd ratio of **15c-C**:**15c-B**, which results in confusing dimensions of the integrals. **^{1}H NMR** (300 MHz, CDCl$_3$) δ = 8.22 – 8.15 (m, 2×C$_{Ar}$-H),* 8.09 – 7.99 (m, 4×C$_{Ar}$-H),*,# 7.95 – 7.89 (m, 2×C$_{Ar}$-H),# 7.63 – 7.53 (m, 2×C$_{Ar}$-H),*,# 7.52 – 7.43 (m, 4×C$_{Ar}$-H),*,# 7.41 – 7.34 (m, 4×C$_{Ar}$-H),*,# 4.25 (q, J = 7.1 Hz, CH$_2$),# 4.13 – 4.01 (m, CH$_2$)*, 3.66 (dd, J = 10.1, 4.9 Hz, CH),# 3.46 (t, J = 6.2 Hz, CH),* 3.38 (dd, J = 10.1, 6.3 Hz, CH),# 3.25 (dd, J = 6.3, 4.9 Hz, CH),# 3.17 (dd, J = 9.7, 6.4 Hz, CH),* 2.73 (dd, J = 9.7, 6.0 Hz, CH),* 1.34 (t, J = 7.1 Hz, CH$_3$),# 1.11 (t, J = 7.1 Hz, CH$_3$).* **^{13}C NMR** (75 MHz, CDCl$_3$) δ = 192.8 (s, CO),# 192.7 (s, CO),* 171.5 (s, CO$_2$),# 168.4 (s, CO$_2$),* 147.2 (s, C$_{Ar}$),# 147.1 (s, C$_{Ar}$),* 146.0 (s, C$_{Ar}$),* 141.6 (s, C$_{Ar}$),# 137.2 (s, C$_{Ar}$),# 136.7 (s, C$_{Ar}$),* 133.8 (d, C$_{Ar}$-H),# 133.7 (d, C$_{Ar}$-H),* 129.9 (d, 2× C$_{Ar}$-H),# 128.9 (d, 2×C$_{Ar}$-H),* 128.5 (d, 2×C$_{Ar}$-H),# 128.9 (d, 2×C$_{Ar}$-H),* 128.3 (d, 2×C$_{Ar}$-H),# 127.5 (d, 2× C$_{Ar}$-H),* 124.1 (d, 2×C$_{Ar}$-H),* 123.5 (d, 2×C$_{Ar}$-H),# 61.8 (t, CH$_2$),# 61.6 (t, CH$_2$),* 35.6 (d, CH),* 34.9 (d, CH),# 34.8 (d, CH),# 32.3 (d, CH),* 28.9 (d, CH),* 26.7 (d, CH),# 14.3 (q, CH$_3$),# 14.1 (q, CH$_3$).* **HRMS** (EI): m/z calcd. for [C$_{19}$H$_{17}$NO$_5$]$^{+\cdot}$: 339.1101, found 339.1119. **MS** (EI) m/z: 267 (17), 266 (100), 105 (52), 77 (25). λ_{max} (*rac*-**15c**, DMSO) = 285 nm. DA426
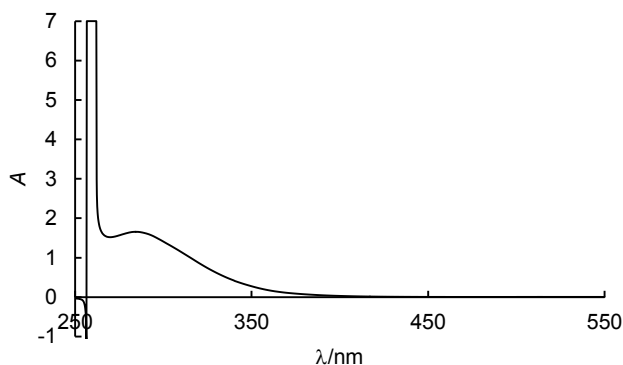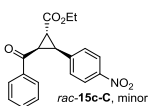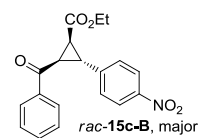
Figure 2.20. UV-Vis spectrum of *rac*-15c (c ~ 1×10^{-4} M).

NMR-Monitoring of the reaction of 1c and 6. A solution of KO^{t}Bu in DMSO-d_6 (500 µL, 2.54×10^{-1} M) was added to **1cH$^+$Br$^-$** (27 mg, 98 µmol) and **6** (30.2 mg, 119 µmol) in DMSO-d_6:CH$_2$Cl$_2$ (1:1, 2.00 mL) at ambient temperature. After 30 s stirring the reaction mixture was subjected to ^{1}H NMR. The spectra show only constant signals of the product **15c**. The formation of the intermediate betaine **14c** or ylide **1c** was not observed. DA901

1-(2-Benzoyl-3-(4-nitrophenyl)cyclopropyl)ethan-1-one (*rac*-**15d**). Aq. NaOH (1 mL, 32%) was added to solutions of **1dH$^+$OTf$^-$** (379 mg, 1.19 mmol) and **6** (200 mg, 790 µmol) in CH$_2$Cl$_2$ (10 mL) at ambient temperature. After 30 min stirring another portion of **1bH$^+$OTf$^-$** (50 mg, 0.16 mmol) was added and stirring was continued till TLC-analysis showed a complete conversion (~ 2 h). The reaction mixture was diluted with water (20 mL) and extracted with EtOAc (3×25 mL). The organic layer was washed with brine (2×20 mL) and dried over Na$_2$SO$_4$. The solvent was removed and the crude product was subjected to chromatography (silica; *n*-pentane:EtOAc 5:1→1:1). *rac*-**15d** (over all: 97 mg, 314 µmol, 40%, *dr* **A**:**B**:**C** 78:28:2 after work-up) was obtained in two fractions as brown oils (fraction 1: *rac*-**15d-B** 31 mg, 100 µmol, 13%; fraction 2: *rac*-**15d-A,** 66 mg, 214 µmol, 27%,). **Fraction 1**: *rac*-**15d-A.** ^{1}H NMR
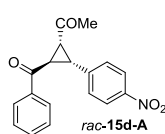
(300 MHz, CDCl$_3$) δ = 8.20 – 8.14 (m, 2 H, 2×C$_{Ar}$-H), 8.11 – 8.06 (m, 2 H, 2×C$_{Ar}$-H), 7.68 – 7.61 (m, 1 H, C$_{Ar}$-H), 7.59 – 7.52 (m, 2 H, 2×C$_{Ar}$-H), 7.46 – 7.42 (m, 2 H, 2×C$_{Ar}$-H), 4.02 (dd, J = 6.3, 4.9 Hz, 1 H, CH), 3.42 (dd, J = 9.8, 6.3 Hz, 1 H, CH), 3.19 (dd, J = 9.8, 4.8 Hz, 1 H, CH), 2.21 (s, 3 H, CH$_3$). ^{13}C NMR (75 MHz, CDCl$_3$) δ = 201.5 (s, CO), 196.1 (s, CO), 147.3 (s, C$_{Ar}$), 142.0 (s, C$_{Ar}$), 136.7 (s, C$_{Ar}$), 134.1 (d, C$_{Ar}$-H), 129.9 (d, 2×C$_{Ar}$-H), 129.1 (d, 2×C$_{Ar}$-H), 128.6 (d, 2×C$_{Ar}$-H), 123.7 (d, 2×C$_{Ar}$-H), 40.2 (d, CH), 36.2 (d, CH), 31.8 (q, CH$_3$), 30.4 (d, CH). **HRMS** (EI): *m/z* calcd. for [C$_{18}$H$_{13}$NO$_3$]$^+$ (M–H$_2$O): 291.0895, found 291.0882. **MS** (EI) *m/z* = 291 (17), 266 (15), 254 (13), 204 (63), 158 (10), 105 (100), 77 (42), 58 (10), 43 (44). **Fraction 2** *rac*-**15d-B.** ^{1}H NMR (400 MHz,
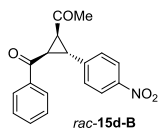
CDCl$_3$) δ = 8.09 – 8.04 (m, 2 H, 2×C$_{Ar}$-H), 7.94 – 7.88 (m, 2 H, 2×C$_{Ar}$-H), 7.60 – 7.53 (m, 1 H, C$_{Ar}$-H), 7.47 – 7.42 (m, 2 H, 2×C$_{Ar}$-H), 7.37 – 7.32 (m, 2 H, 2×C$_{Ar}$-H), 3.66 (dd, J = 10.0 Hz, 4.9, 1 H, CH), 3.54 (dd, J = 6.1, 4.9 Hz, 1 H, CH), 3.37 (dd, J = 10.0, 6.2 Hz, 1 H, CH), 2.49 (s, 3 H, CH$_3$). ^{13}C NMR (150 MHz, CDCl$_3$) δ = 204.9 (s, CO), 193.1 (s, CO), 147.2 (s, C$_{Ar}$), 141.9 (s, C$_{Ar}$), 137.1 (s, C$_{Ar}$), 133.9 (d, C$_{Ar}$-H), 129.8 (d, 2×C$_{Ar}$-H), 129.0 (d, 2×C$_{Ar}$-H), 128.4 (d, 2×C$_{Ar}$-H), 123.6 (d, 2×C$_{Ar}$-H), 37.1 (d, CH), 36.7 (d, CH), 33.6 (d, CH), 31.7 (q, CH$_3$).**MS** (EI): *m/z* = 309, 291, 266, 220, 204, 192, 105, 77. DA497-2

NMR-Monitoring of the reaction of 1d with 6. KO^{t}Bu in DMSO-d_6 (500 µL, 2.54×10^{-1} M) was added to a solution of **1dH$^+$Cl$^-$** (27.4 mg, 134 µmol) and **6** (31.5 mg, 124 µmol) in DMSO-d_6:CH$_2$Cl$_2$ (2.00 mL, 1:1) at ambient temperature. After 30 s stirring the solution was subjected to ^{1}H NMR. The spectra show decreasing amounts of the reactants **1dH$^+$Cl$^-$**, **6**, and ylide **1d**, and increasing amounts of the product **15d**. No formation of an intermediate betaine **14d** was observed. For a kinetic analysis of the NMR data see kinetic section. DA903

(3-(4-Nitrophenyl)cyclopropane-1,2-diyl)bis(phenylmethanone) (*rac*-**15e**). From **1eH$^+$Br$^-$** (370 mg, 1.19 mmol), **6** (200 mg, 790 µmol), and KO^{t}Bu (134 mg, 1.19 mmol) according to procedure **C**. *rac*-**15e** was obtained as pale yellow needles (258 mg, 695 µmol, 88%, *dr* **A**:**B**:**C** 8:92:0). **15e-B**. **Mp.** (EtOH) 169 − 170 °C. **^{1}H NMR** (300 MHz, CDCl$_3$) δ = 8.27 − 8.21 (m, 2 H, 2×C$_{Ar}$-H), 8.01 − 7.95 (m, 4 H, 4×C$_{Ar}$-H), 7.59 − 7.52 (m, 2 H, 2×C$_{Ar}$-H), 7.49 − 7.39 (m, 6 H, 6×C$_{Ar}$-H), 3.65 (t, *J* = 6.1 Hz, 1 H, CH), 3.48 (d, *J* = 6.1 Hz, 2 H, 2×CH). **^{13}C NMR** (75 MHz, CDCl$_3$) δ = 193.3 (s, 2×CO), 147.2 (s, C$_{Ar}$), 146.4 (s, C$_{Ar}$), 136.9 (s, 2×C$_{Ar}$), 133.6 (d, 2×C$_{Ar}$-H), 128.9 (d, 4×C$_{Ar}$-H), 128.5 (d, 4×C$_{Ar}$-H), 127.5 (d, 2×C$_{Ar}$-H), 124.3 (d, 2×C$_{Ar}$-H), 37.4 (d, 2×CH), 30.3 (d, CH) **HRMS** (EI): *m/z* calcd. for (M–2 H) [C$_{23}$H$_{15}$NO$_4$$^{.+}$: 369.0996, found 369.1009. **MS** (EI) *m/z* = 369 (3), 339 (10), 266 (61), 220 (12), 105 (100), 77 (49). DA418-2
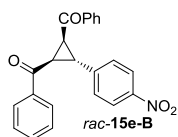
NMR-Monitoring of the reaction of 1e with 6. KO^{t}Bu in DMSO-d_6 (500 µL, 2.54×10^{-1} M) was added to a solution of **1eH$^+$Br$^-$** (40.4 mg, 130 µmol) and **6** (30.7 mg, 121 µmol) in DMSO-d_6:CH$_2$Cl$_2$ (2.00 mL, 1:1) at ambient temperature. After 30 s stirring the solution was subjected to ^{1}H NMR. The spectra show decreasing signals of the ylide **1e** and **6**, and increasing signals of the product **15e**, but no formation of the intermediate betaine **14e** was observed. DA902

Table 2.27. Crystallographic Data of *rac*-15e-B.

net formula	$C_{23}H_{17}NO_4$
M_r/g mol^{-1}	371.385
crystal size/mm	0.156 × 0.096 × 0.056
T/K	200(2)
radiation	'MoKα
diffractometer	'Bruker D8Quest'
crystal system	monoclinic
space group	$P2_1/n$
a/Å	13.8242(17)
b/Å	6.0419(7)
c/Å	22.426(3)
α/°	90
β/°	100.387(4)
γ/°	90
V/Å^3	1842.4(4)
Z	4
calcd. density/g cm^{-3}	1.3389(3)
μ/mm^{-1}	0.092
absorption correction	multi-scan
transmission factor range	0.8778–0.9280
refls. measured	10224
R_{int}	0.0652
mean $\sigma(I)/I$	0.0690
θ range	2.90–25.07
observed refls.	1875
x, y (weighting scheme)	0.0462, 0.0250
hydrogen refinement	constr
refls in refinement	3231
parameters	299
restraints	0
$R(F_{obs})$	0.0508
$R_w(F^2)$	0.1131
S	1.024
shift/error$_{max}$	0.001
max electron density/e Å^{-3}	0.181
min electron density/e Å^{-3}	−0.179

One phenyl ring disordered, split model applied, sof ratio 0.56/0.44. The figure shows the main component.
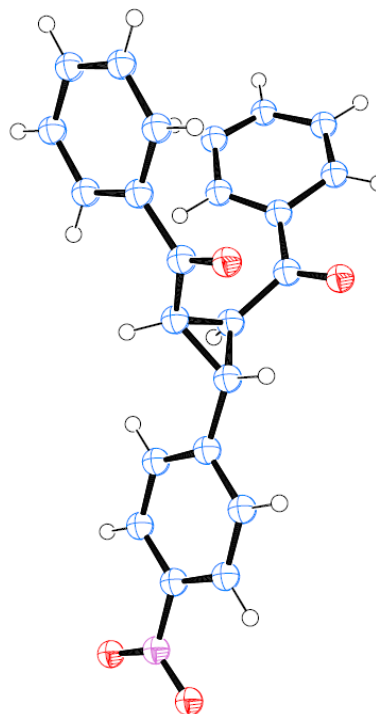
2.7.3.6 Reactions with the Activated Styrenes 16

General Procedure H for the Synthesis of Cyclopropanes *rac*-18. KO^{t}Bu (1.1 eq) in DMSO (3 mL) was added dropwise to solutions of **1H$^+$X$^-$** (0.6 mmol) and **16** (0.5 mmol) in DMSO (5 mL) at room temperature over 1–2 min. The reaction mixture was stirred for 1 h and quenched with aq. sat. NH$_4$Cl (25 mL). The aqueous layer was extracted with CH$_2$Cl$_2$

(3×15 mL), the combined organic layers were washed with brine (2×20 mL) and dried over Na$_2$SO$_4$. The solvent was evaporated and the residue was purified by column chromatography (silica, *n*-pentane:EtOAc 20:1–10:1).

Ethyl 2-cyano-3-phenylcyclopropanecarboxylate (*rac*-**18a**). From **1aH$^+$Br$^-$**(140 mg, 603 μmol), **16a** (88 mg, 0.50 mmol), and KO^{t}Bu (67 mg, 0.60 mmol) according to procedure B. *rac*-**18a** was obtained as colorless oil (61 mg, 283 μmol, 57%, *dr* **A**:**B**:**C** 66:33:0). *major *rac*-**18a-A**, $^\#$minor diastereoisomer *rac*-**18a-B**; one integral of a signal of the minor diastereoisomer was set to 1.0. **^{1}H NMR** (300 MHz, CDCl$_3$) δ 1.19 – 1.32 (m, 9 H, 2×CH$_3$),*$^,\#$ 2.02 (dd, *J* = 8.5, 6.3, 1 H, CH),$^\#$ 2.32 – 2.41 (m, 3 H, CH),*$^,\#$ 2.53 – 2.62 (m, 2 H, CH),* 2.89 (dd, *J* = 9.1, 6.0 Hz, 2 H, CH),* 3.08 (t, *J* = 6.2 Hz, 1 H, CH),$^\#$ 4.10 – 4.28 (m, 6 H, 2×CH$_2$),*$^,\#$ 7.01 – 7.08 (m, 2 H, 2×C$_{Ar}$-H),$^\#$ 7.17 – 7.36 (m, 13 H, 8×C$_{Ar}$-H, superimposed by solvent).*$^,\#$ **^{13}C NMR** (75 MHz, CDCl$_3$) δ 14.0 (t, CH$_2$),* 14.2 (q, CH$_3$),* 14.3 (q, CH$_3$),$^\#$ 14.3 (t, CH$_2$),$^\#$ 27.2 (d, CH),* 28.0 (d, CH),$^\#$ 30.7 (d, CH),* 31.1 (d, CH),$^\#$ 62.1 (t, CH$_2$),$^\#$ 62.2 (t, CH$_2$),* 116.8 (s, CN),$^\#$ 117.0 (s, CN)*, 126.7 (d, 2×C$_{Ar}$-H),$^\#$ 128.1 (d, 2×C$_{Ar}$-H),* 128.2 (d, C$_{Ar}$-H),$^\#$ 128.4 (d, 2×C$_{Ar}$-H),$^\#$ 128.9 (d, 2×C$_{Ar}$-H),* 129.1 (d, C$_{Ar}$-H),* 133.0 (s, C$_{Ar}$),* 135.3 (s, C$_{Ar}$),$^\#$ 168.2 (s, CO$_2$),$^\#$ 169.9 (s, CO$_2$).* **HRMS** (EI): calcd. for [C$_{13}$H$_{13}$NO$_2$]$^+$ 215.0941, found 215.0936. **MS** (EI) *m/z*: 215 (14), 170 (15), 156 (17), 143 (100), 142 (68), 115 (73). DA678
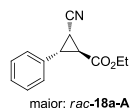
***N,N*-Diethyl-2-phenyl-3-tosylcyclopropanecarboxamide** (*rac*-**18b**). From **1bH$^+$Cl$^-$** (157 mg, 600 μmol), **16b** (129 mg, 470 μmol), and KO^{t}Bu (67 mg, 0.60 mmol) according to procedure B. *rac*-**18b** was obtained as colorless oil (over all 90 mg, 0.23 mmol, 49%, *dr* **A**:**B**:**C** 92:8:0 after work-up). The NMR-signals of the minor diastereoisomer could not be assigned unambiguously due to overlap with the major diastereoisomer. **^{1}H NMR** (300 MHz, CDCl$_3$) δ 0.74 (t, *J* = 7.1 Hz, 3 H, CH$_3$), 1.14 (t, *J* = 7.1 Hz, 3 H, CH$_3$), 2.43 (s, 3 H, CH$_3$), 2.79 – 2.97 (m, 2 H, CH, C*H*H^a), 3.09 – 3.26 (m, 1 H, C*H*H^B), 3.32 (dd, *J* = 10.5, 6.1 Hz, 1H), 3.37 – 3.51 (m, 1 H, CH*H*^{a}, superimposed by minor diastereoisomer), 3.51 – 3.68 (m, 1 H, CH*H*^{b}), 3.81 (dd, *J* = 6.1, 4.9 Hz, 1 H), 7.02 – 7.08 (m, 2 H, 2×C$_{Ar}$-H), 7.16 – 7.23 (m, 3 H, 3×C$_{Ar}$-H), 7.35 (m, 2 H, 2×C$_{Ar}$-H, superimposed by minor diastereoisomer), 7.80 – 7.87 (m, 2 H, 2×C$_{Ar}$-H). **^{13}C NMR** (75 MHz, CDCl$_3$) δ = 12.5 (t, CH$_3$), 14.5 (t, CH$_3$), 21.8 (t, CH$_3$), 28.9 (d, CH), 30.1 (d, CH), 40.3 (t, CH$_2$), 41.7 (t, CH$_2$), 43.5 (d, CH), 127.6 (d, C$_{Ar}$-H), 127.7 (d, 2×C$_{Ar}$-H), 128.2 (d, 2×C$_{Ar}$-H), 128.4 (d, 2×C$_{Ar}$-H), 130.2 (d, 2×C$_{Ar}$-H), 133.0 (s, C$_{Ar}$), 137.2 (s, C$_{Ar}$), 144.8 (s, C$_{Ar}$), 163.7 (s, CON). **HRMS** (EI): calcd. for [C$_{21}$H$_{25}$NO$_3$S]$^+$ 371.1550, found 371.1543. **MS** (EI) *m/z*: 371 (<1), 217 (12), 216 (100), 115 (12). DA684
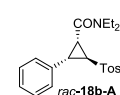
3-Phenylcyclopropane-1,2-dicarbonitrile (*rac*-**18c**). From **1aH⁺Br⁻** (140 mg, 603 µmol), **16c** (65 mg, 0.50 mmol), and KO*t*Bu (67 mg, 600 µmol) according to procedure B. *rac*-**18c** was obtained as colorless solid (29 mg, 0.17 mmol, 34%, *dr* **A**:**B**:**C** 50:50:0; **A** and **C** are enantiomers). **Mp** 134−135 °C. *rac*-**18c-A**#, *rac*-**18c-B***. **¹H NMR** (300 MHz, CDCl₃) δ 2.25 (d, *J* = 6.2 Hz, 2 H, 2×CH),* 2.43 (dd, *J* = 6.4, 5.2 Hz, 1 H, CH),# 2.52 (dd, *J* = 9.1, 5.1 Hz, 1 H, CH),# 3.12 (dd, *J* = 9.1, 5.2 Hz, 2H, CH),# 3.16 (t, *J* = 6.2 Hz, 1H, CH),* 7.09 – 7.16 (m, 2 H, 2×C$_{Ar}$-H),* 7.26 – 7.31 (m, 2 H, 2×C$_{Ar}$-H),# 7.33 – 7.46 (m, 6 H, 6×C$_{Ar}$-H).*,# **¹³C NMR** (75 MHz, CDCl₃) δ = 11.5 (d, CH),# 13.2 (d, 2×CH),* 13.9 (d, CH),# 30.0 (d, CH),* 31.6 (d, CH),# 115.2 (s, CN), 116.0 (s, 2×CN), 117.1 (s, CN), 126.7 (d, 2×C$_{Ar}$-H),# 128.0 (d, 2×C$_{Ar}$-H),* 129.2 (d, C$_{Ar}$-H),* ^{or}# 129.3 (d, C$_{Ar}$-H),* ^{or}# 129.3 (d, 2×C$_{Ar}$-H),* 129.4 (d, 2×C$_{Ar}$-H),# 131.0 (s, C$_{Ar}$),* ^{or}# 133.0 (s, C$_{Ar}$).* ^{or}# **HRMS** (EI): calcd. for [C₁₁H₈N₂]⁺ 168.0682, found 168.0672. **MS** (EI) *m/z*: 169 (13), 168 (100), 141 (95), 140 (53), 91 (18). DA680

2-Acetyl-3-phenylcyclopropane-1-carbonitrile (*rac*-**18d**): **1aH⁺Br⁻** (140 mg, 603 µmol), **16d** (73 mg, 500 µmol), and K₂CO₃ (207 mg, 1.50 mmol) were dissolved in DMSO (5 mL) and heated at 100 °C for 2 h. The reaction mixture was cooled to room temperature and quenched with sat. NH₄Cl (25 mL, aq.). The aqueous layer was extracted with CH₂Cl₂ (3×15 mL). The combined organic layers were washed with brine (2×25 mL) and dried over Na₂SO₄. The solvent was removed and the residue was subjected to a column chromatography (silica, *n*-pentane:EtOAc 15:1). *rac*-**18d** was obtained as colorless oil (71 mg, 383 µmol, 77%, *dr* **A**:**B**:**C** 33:66:0, 13:87:0 after work-up). *major *rac*-**18d-B**, #minor diastereoisomer *rac*-**18d-A**; the integral of one signal of the minor diastereoisomer was set to 1.0. **¹H NMR** (300 MHz, CDCl₃) δ 2.15 (s, 3 H, CH₃),# 2.43 (s, 24 H, CH₃),*,# 2.46 (dd, *J* = 8.9, 5.0 Hz, 8 H, CH),* 2.74 (dd, *J* = 6.6, 5.2 Hz, 1 H, CH),# 2.84 – 2.94 (m, 16 H, 2×CH),* 2.98 (dd, *J* = 10.1, 5.2 Hz, 1 H, CH),# 3.19 (dd, *J* = 10.0, 6.5 Hz, 1H, CH),# 7.09 – 7.15 (m, 2 H, 2×C$_{Ar}$-H),# 7.26 – 7.32 (m, 19 H, 3×C$_{Ar}$-H),*,# 7.33 – 7.43 (m, 24 H, 3×C$_{Ar}$-H).* **¹³C NMR** (75 MHz, CDCl₃) δ 9.0 (d, CH),# 15.4 (d, CH),* 31.2 (q, 2×CH₃),*,# 32.6 (d, CH),* 33.8 (d, CH),* 33.9 (s, CH), 35.8 (s, CH), 117.1 (s, CN),* 119.2 (s, CN),# 127.8 (d, 2×C$_{Ar}$-H),* 128.0 (d, C$_{Ar}$-H),# 128.3 (d, C$_{Ar}$-H),* 128.5 (d, 2×C$_{Ar}$-H),# 128.5 (d, 2×C$_{Ar}$-H),# 128.8 (d, 2×C$_{Ar}$-H),* 131.6 (s, C$_{Ar}$),# 133.2 (s, C$_{Ar}$),* 199.1 (s, CO),# 202.5 (s, CO).* **HRMS** (EI): calcd. for [C₁₂H₁₀NO]⁺ 184.0757, found 184.0752. **MS** (EI) *m/z*: 184 (4), 143 (92), 115. (84), 89 (16), 43 (100). DA690-2

2.7.4 Kinetics of the Reactions of the Ylides 1 with the Electrophiles 2−6

2.7.4.1 Kinetics of the Reactions of Ylide 1a
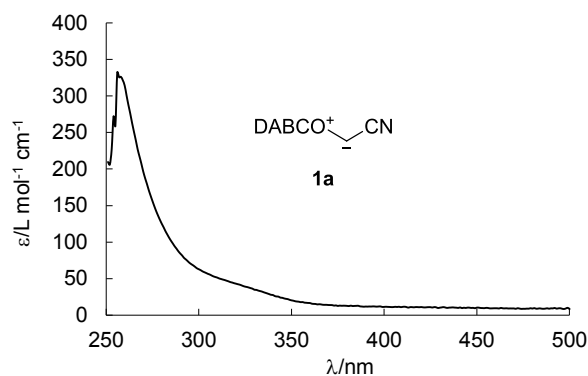
Figure 2.21. Absorption spectrum of 1a (λ_{max}= 256 nm, DMSO, 20 °C).

Table 2.28. Determination of the nucleophilicity parameters N and s_N for 1a with the electrophiles 3,4 (filled dots). Open dots refer to the reactions with 5b,6 and were not used for the determination of N and s_N.

Electrophile	E	$\log k_2$
3b	-13.39	5.39
3c	-15.83	4.15
3d	-16.11	4.02
3e	-17.29	3.53
3f	-17.90	3.12
4a	-17.67	3.75
4b	-18.89	3.35
4c	-20.55	2.61
4d	-21.11	2.37
5b	-11.32	6.20
6	-17.32	3.65

$\log k_2 = 0.3665\, E + 10.052$
$R^2 = 0.9463$
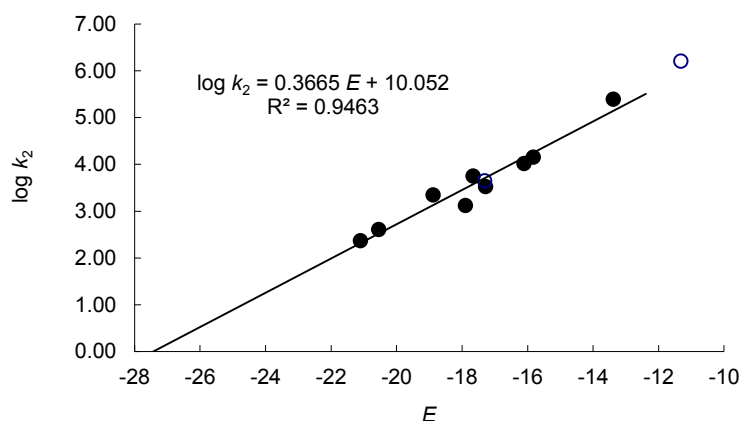
Nucleophilicity parameters for **1a** in DMSO: $N = 27.43$, $s_N = 0.37$.

Table 2.29. Kinetics of the reaction of 1a with 3b (DMSO, 20 °C, Stopped-flow method, detection at 533 nm).

No.	[**3b**]/mol L^{-1}	[**1a**]/mol L^{-1}	k_{obs}/s^{-1}
da131s6-1	4.00×10^{-5}	4.00×10^{-4}	6.19×10^{1}
da131s6-4	4.00×10^{-5}	5.00×10^{-4}	8.63×10^{1}
da131s6-2	4.00×10^{-5}	6.00×10^{-4}	1.13×10^{2}
da131s6-5	4.00×10^{-5}	7.00×10^{-4}	1.31×10^{2}
da131s6-3	4.00×10^{-5}	8.00×10^{-4}	1.63×10^{2}
k_2(20 °C) = 2.47×10^{5} L mol^{-1} s^{-1}			

$y = 246900x - 37.1$
$R^2 = 0.9946$

Table 2.30. Kinetics of the reaction of 1a with 3c (DMSO, 20 °C, Stopped-flow method, detection at 371 nm).

No.	$[3c]$/mol L^{-1}	$[1a]$/mol L^{-1}	k_{obs}/s^{-1}
da131s1-2	2.00×10^{-5}	3.00×10^{-4}	2.31
da131s1-3	2.00×10^{-5}	4.00×10^{-4}	3.93
da131s1-4	2.00×10^{-5}	5.00×10^{-4}	5.34
da131s1-5	2.00×10^{-5}	6.00×10^{-4}	6.60
k_2(20 °C) = 1.43×10^4 L mol^{-1} s^{-1}			

y = 14280x - 1.881
R² = 0.9968
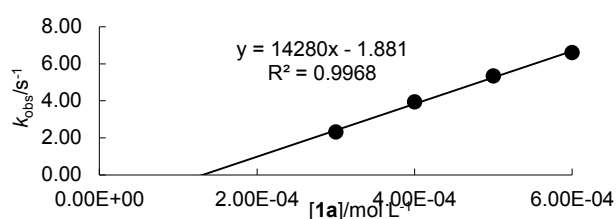
Table 2.31. **Kinetics of the reaction of 1a with 3d (DMSO, 20 °C, Stopped-flow method, detection at 393 nm).**

No.	$[3d]$/mol L^{-1}	$[1a]$/mol L^{-1}	k_{obs}/s^{-1}
da131s4-1	2.00×10^{-5}	5.00×10^{-4}	3.47
da131s4-2	2.00×10^{-5}	6.00×10^{-4}	4.68
da131s4-3	2.00×10^{-5}	7.00×10^{-4}	5.25
da131s4-4	2.00×10^{-5}	8.00×10^{-4}	6.47
da131s4-5	2.00×10^{-5}	9.00×10^{-4}	7.76
k_2(20 °C) = 1.04×10^4 L mol^{-1} s^{-1}			

y = 10370x - 1.733
R² = 0.9865
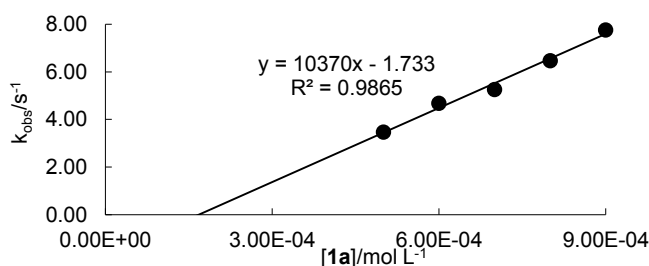
Table 2.32. Kinetics of the reaction of 1a with 3e (DMSO, 20 °C, Stopped-flow method, detection at 486 nm).

No.	$[3e]$/mol L^{-1}	$[1a]$/mol L^{-1}	k_{obs}/s^{-1}
da131s3-1	2.00×10^{-5}	5.00×10^{-4}	1.07
da131s3-2	2.00×10^{-5}	6.00×10^{-4}	1.26
da131s3-4	2.00×10^{-5}	8.00×10^{-4}	2.08
da131s3-5	2.00×10^{-5}	9.00×10^{-4}	2.34
k_2(20 °C) = 3.36×10^3 L mol^{-1} s^{-1}			

y = 3360x - 0.6645
R² = 0.987
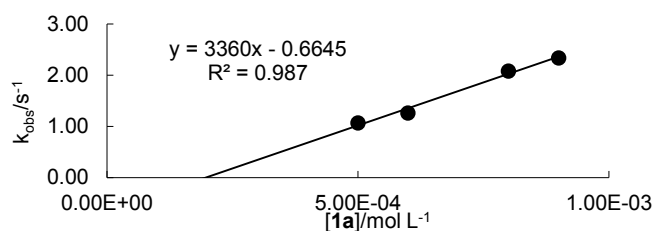
Table 2.33. Kinetics of the reaction of 1a with 3f (DMSO, 20 °C, Stopped-flow method, detection at 521 nm).

No.	$[3f]$/mol L^{-1}	$[1a]$/mol L^{-1}	k_{obs}/s^{-1}
da131s2-1	4.00×10^{-5}	5.00×10^{-4}	4.90×10^{-1}
da131s2-2	4.00×10^{-5}	6.00×10^{-4}	5.90×10^{-1}
da131s2-3	4.00×10^{-5}	8.00×10^{-4}	8.50×10^{-1}
da131s2-4	4.00×10^{-5}	9.00×10^{-4}	1.02
k_2(20 °C) = 1.32×10^3 L mol^{-1} s^{-1}			

y = 1320x - 0.1865
R² = 0.993
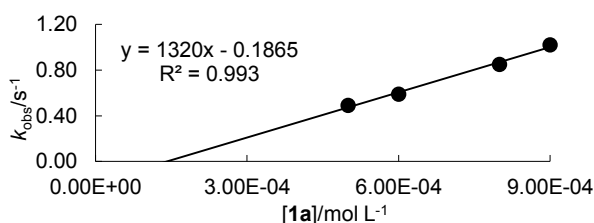
Table 2.34. Kinetics of the reaction of 1a with 4a (DMSO, 20 °C, Stopped-flow method, detection at 302 nm).

No.	$[4a]$/mol L^{-1}	$[1a]$/mol L^{-1}	k_{obs}/s^{-1}
da131s5-1	4.00×10^{-5}	1.00×10^{-3}	5.06
da131s5-2	4.00×10^{-5}	1.20×10^{-3}	6.16
da131s5-3	4.00×10^{-5}	1.40×10^{-3}	7.35
da131s5-4	4.00×10^{-5}	1.60×10^{-3}	8.43
k_2(20 °C) = 5.65×10^3 L mol^{-1} s^{-1}			

y = 5650x - 0.595
R² = 0.9997
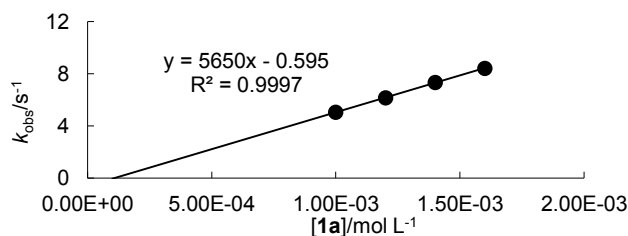
Table 2.35. Kinetics of the reaction of 1a with 4b (DMSO, 20 °C, Stopped-flow method, detection at 277 nm).

No.	$[4b]$/mol L^{-1}	$[1a]$/mol L^{-1}	k_{obs}/s^{-1}
da131s7-1	8.00×10^{-5}	8.00×10^{-4}	1.23
da131s7-2	8.00×10^{-5}	1.00×10^{-3}	2.17
da131s7-3	8.00×10^{-5}	1.20×10^{-3}	2.99
da131s7-4	8.00×10^{-5}	1.40×10^{-3}	1.61
da131s7-5	8.00×10^{-5}	1.60×10^{-3}	2.54
$k_2(20\ °C) = 2.23 \times 10^3$ L mol^{-1} s^{-1}			
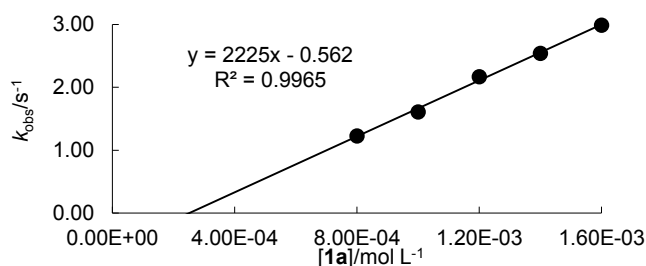
Table 2.36. Kinetics of the reaction of 1a with 4c (DMSO, 20 °C, Stopped-flow method, detection at 283 nm).

No.	$[4c]$/mol L^{-1}	$[1a]$/mol L^{-1}	k_{obs}/s^{-1}
da131s8-1	8.00×10^{-5}	8.00×10^{-4}	2.07×10^{-1}
da131s8-2	8.00×10^{-5}	1.00×10^{-3}	2.66×10^{-1}
da131s8-3	8.00×10^{-5}	1.20×10^{-3}	3.66×10^{-1}
da131s8-4	8.00×10^{-5}	1.40×10^{-3}	4.59×10^{-1}
da131s8-5	8.00×10^{-5}	1.60×10^{-3}	5.18×10^{-1}
$k_2(20\ °C) = 4.08 \times 10^2$ L mol^{-1} s^{-1}			
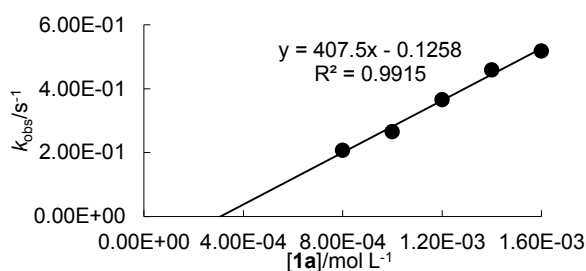
Table 2.37. Kinetics of the reaction of 1a with 4d (DMSO, 20 °C, Stopped-flow method, detection at 295 nm).

No.	$[4d]$/mol L^{-1}	$[1a]$/mol L^{-1}	k_{obs}/s^{-1}
da131s9-1	6.00×10^{-5}	6.00×10^{-4}	6.92×10^{-2}
da131s9-2	6.00×10^{-5}	7.50×10^{-4}	1.08×10^{-1}
da131s9-3	6.00×10^{-5}	9.00×10^{-4}	1.48×10^{-1}
da131s9-4	6.00×10^{-5}	1.05×10^{-3}	1.73×10^{-1}
da131s9-5	6.00×10^{-5}	1.20×10^{-3}	2.11×10^{-1}
$k_2(20\ °C) = 2.32 \times 10^2$ L mol^{-1} s^{-1}			
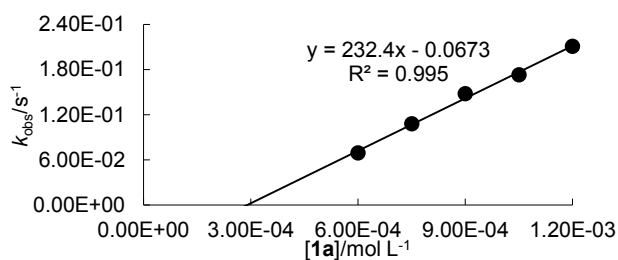
Table 2.38. Kinetics of the reaction of 1a with 5b (DMSO, 20 °C, Stopped-flow method, detection at 388 nm).

No.	$[5b]$/mol L^{-1}	$[1a]$/mol L^{-}	k_{obs}/s^{-1}
da131s11-1	1.00×10^{-5}	2.00×10^{-4}	1.17×10^2
da131s11-2	1.00×10^{-5}	2.50×10^{-4}	2.09×10^2
da131s11-3	1.00×10^{-5}	3.00×10^{-4}	3.09×10^2
da131s11-4	1.00×10^{-5}	3.50×10^{-4}	3.71×10^2
da131s11-5	1.00×10^{-5}	4.00×10^{-4}	4.36×10^2
$k_2(20\ °C) = 1.60 \times 10^6$ L mol^{-1} s^{-1}			

108

Table 2.39. ^{1}H NMR monitoring of the kinetics of the formation of 13aa (DMSO-d_6:CD$_2$Cl$_2$; 20 °C; evolution of DABCO followed; Experimental procedure see Products section).

[HO^{t}Bu] = 8.84 × 10^{-2} mol L^{-1}	
t/s	[DABCO]/mol L^{-1}
0	7.15 × 10^{-3}
2.40 × 10^2	7.96 × 10^{-3}
7.80 × 10^2	8.77 × 10^{-3}
9.00 × 10^2	8.99 × 10^{-3}
1.08 × 10^3	8.91 × 10^{-3}
1.26 × 10^3	8.99 × 10^{-3}
1.38 × 10^3	9.13 × 10^{-3}
3.66 × 10^3	9.95 × 10^{-3}
4.32 × 10^3	1.01 × 10^{-2}
5.46 × 10^3	1.02 × 10^{-2}
8.46 × 10^3	1.04 × 10^{-2}
1.16 × 10^4	1.05 × 10^{-2}
1.34 × 10^4	1.06 × 10^{-2}
k_{rc}(20 °C) = 6.77 × 10^{-4} s^{-1}	

Data: Data1_B
Model: ExpDec1

Chi^2 = 2.9198E-8
R^2 = 0.97795

y0   0.01039   ±0.00008
A1   -0.00302   ±0.00015
1/k1   1477.9178   ±167.61394

The time at which the first spectrum was taken equals $t = 0$ s. Therefore [DABCO] $\neq$ 0 M at $t = 0$ s.

Table 2.40. **Kinetics of the reaction of 1a with 6 (DMSO, 20 °C, Stopped-flow method, detection at 325 nm).**

No.	[6]/mol L^{-1}	[1a]/mol L^{-1}	k_{obs}/s^{-1}
da131s10-2	1.00 × 10^{-5}	2.50 × 10^{-4}	4.63 × 10^{-1}
da131s10-4	1.00 × 10^{-5}	3.50 × 10^{-4}	9.69 × 10^{-1}
da131s10-5	1.00 × 10^{-5}	4.00 × 10^{-4}	1.42
k_2(20 °C) = 4.47 × 10^3 L mol^{-1} s^{-1}			

y = 4467.1x - 0.6647
R² = 0.9927

2.7.4.2   Kinetics of the Reactions of Ylide 1b

UV-Vis monitoring of the titration of 1bH$^+$Cl$^-$ with KO^{t}Bu. The formation of the ylide **1b** from its conjugate CH-acid **1bH$^+$Cl$^-$** was recorded by using a diode array UV-Vis spectrometer. The temperature during the experiment was kept constant by using a circulating bath (20.0 ± 0.02 °C). The CH acid **1bH$^+$Cl$^-$** ($c = 3.39 × 10^{-4}$ M) was dissolved in DMSO and subsequently treated with 160 µl portions of KO^{t}Bu dissolved in DMSO (5.25 × 10^{-2} M).
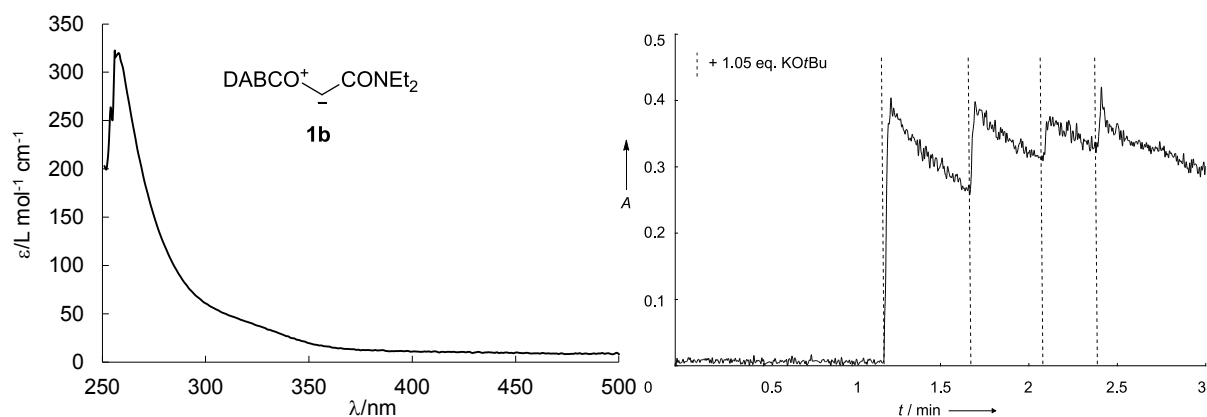
Figure 2.22. UV–Vis spectrum of 1b in DMSO at 20 °C (λ_{max}= 256 nm, DMSO, 20 °C; left); Monitoring of the UV–Vis absorption band (256 nm) of 1b during its generation from 1bH$^+$Br$^-$ by addition of KO^{t}Bu (right). The experiment was performed by adding 160 µl portions of a solution of KO^{t}Bu in DMSO (dashed lines; [KO^{t}Bu] = 5.25 × 10^{-2} M) to an c = 3.39 × 10^{-4} mol L^{-1} solution of 1bH$^+$Br$^-$ in DMSO (23.8 mL).

Table 2.41. Determination of the nucleophilicity parameters N and s_N for 1b with the electrophiles 3,4 (filled dots). Open dot refers to the reaction with 5b and was not used for the determination of N and s_N.

Electrophile	E	log k_2
3a	-12.18	5.20
3b	-13.39	4.34
3c	-15.83	3.71
3d	-16.11	3.46
3e	-17.29	2.85
4a	-17.67	2.75
5b	-11.32	5.44

log k_2 = 0.4217 E + 10.216
R² = 0.9765
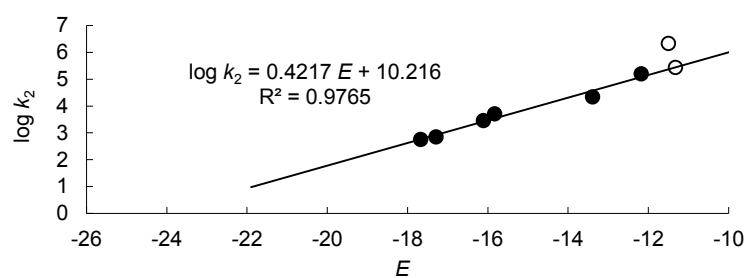
Nucleophilicity parameters for **1b** in DMSO: N = 24.23, s_N = 0.42.
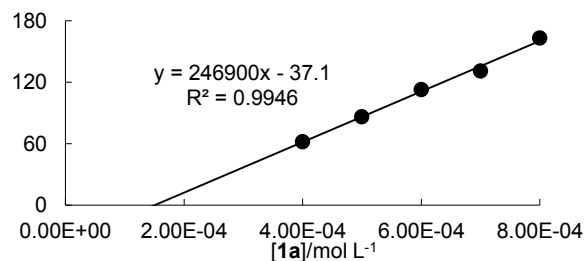
Table 2.42. Kinetics of the reaction of 1b with 3a (DMSO, 20 °C, Stopped-flow method, detection at 422 nm).

No.	[3a]/mol L^{-1}	[KO^{t}Bu]/mol L^{-1}	[1bH$^+$Cl$^-$]/mol L^{-1}	k_{obs}/s^{-1}
da181s6r-1	4.00 × 10^{-5}	4.20 × 10^{-4}	8.00 × 10^{-4}	1.42 × 10^1
da181s6r-2	4.00 × 10^{-5}	5.25 × 10^{-4}	1.00 × 10^{-3}	2.63 × 10^1
da181s6r-3	4.00 × 10^{-5}	6.30 × 10^{-4}	1.20 × 10^{-3}	4.59 × 10^1
da181s6r-4	4.00 × 10^{-5}	7.35 × 10^{-4}	1.40 × 10^{-3}	5.83 × 10^1
da181s6r-5	4.00 × 10^{-5}	8.40 × 10^{-4}	1.60 × 10^{-3}	8.16 × 10^1
k_2(20 °C) = 1.59 × 10^5 L mol^{-1} s^{-1}				

y = 158857x - 54.82
R² = 0.9883
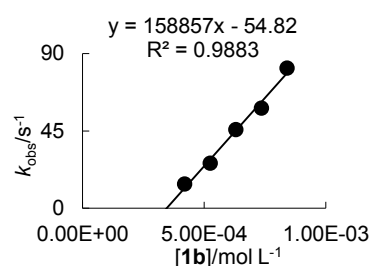
Table 2.43. Kinetics of the reaction of 1b with 3a (DMSO, 20 °C, Stopped-flow method, detection at 422 nm).

No.	[3a]/mol L^{-1}	[1b]/mol L^{-1}	k_{obs}/s^{-1}
da181s6r-1	4.00 × 10^{-5}	4.00 × 10^{-4}	2.10 × 10^1
da181s6r-3	4.00 × 10^{-5}	6.00 × 10^{-4}	5.14 × 10^1
da181s6r-4	4.00 × 10^{-5}	7.00 × 10^{-4}	6.30 × 10^1
da181s6r-5	4.00 × 10^{-5}	8.00 × 10^{-4}	8.60 × 10^1
k_{2r}(20 °C) = 1.57 × 10^5 L mol^{-1} s^{-1}			
k_{2repro}/k_2 = 0.99			

y = 157314x - 42.971
R² = 0.9872

Table 2.44. **Kinetics of the reaction of 1b with 3b (DMSO, 20 °C, Stopped-flow method, detection at 533 nm).**

| No.	$[3b]$/mol L^{-1}	$[KO^tBu]$/mol L^{-1}	$[1bH^+Cl^-]$/mol L^{-1}	k_{obs}/s^{-1}
da181s2-1	4.00×10^{-5}	4.20×10^{-4}	8.00×10^{-4}	5.43 ± 0.02
da181s2-2	4.00×10^{-5}	6.30×10^{-4}	1.20×10^{-3}	1.00×10^1
da181s2-3	4.00×10^{-5}	8.40×10^{-4}	1.60×10^{-3}	1.32×10^1
da181s2-5	4.00×10^{-5}	1.26×10^{-3}	2.40×10^{-3}	2.39×10^1
$k_2(20\ °C) = 2.18 \times 10^4$ L mol^{-1} s^{-1}				

y = 21808x - 4
R² = 1
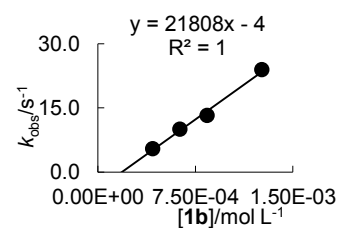
Table 2.45. Kinetics of the reaction of 1b with 3c (DMSO, 20 °C, Stopped-flow method, detection at 371 nm).

No.	$[3c]$/mol L^{-1}	$[1b]$/mol L^{-1}	k_{obs}/s^{-1}
da181s3-1	4.00×10^{-5}	4.00×10^{-4}	4.65×10^{-1}
da181s3-2	4.00×10^{-5}	6.00×10^{-4}	1.42
da181s3-3	4.00×10^{-5}	8.00×10^{-4}	2.34
da181s3-4	4.00×10^{-5}	1.00×10^{-3}	3.29
da181s3-5	4.00×10^{-5}	1.20×10^{-3}	4.60
$k_2(20\ °C) = 5.07 \times 10^3$ L mol^{-1} s^{-1}			

y = 5070x - 1.633
R² = 0.9946
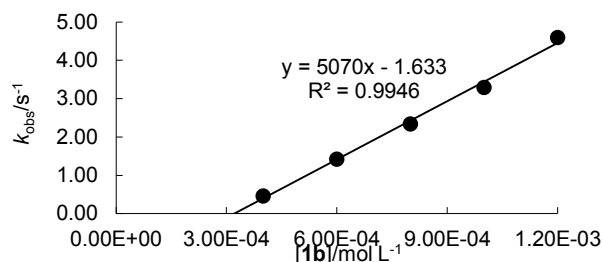
Table 2.46. Kinetics of the reaction of 1b with 3d (DMSO, 20 °C, Stopped-flow method, detection at 393 nm).

No.	$[3d]$/mol L^{-1}	$[1b]$/mol L^{-1}	k_{obs}/s^{-1}
da181s4-1	4.00×10^{-5}	6.00×10^{-4}	6.18×10^{-1}
da181s4-2	4.00×10^{-5}	8.00×10^{-4}	1.37
da181s4-3	4.00×10^{-5}	1.00×10^{-3}	1.95
da181s4-5	4.00×10^{-5}	1.40×10^{-3}	2.95
$k_2(20\ °C) = 2.87 \times 10^3$ L mol^{-1} s^{-1}			

y = 2866.3x - 1.001
R² = 0.9906
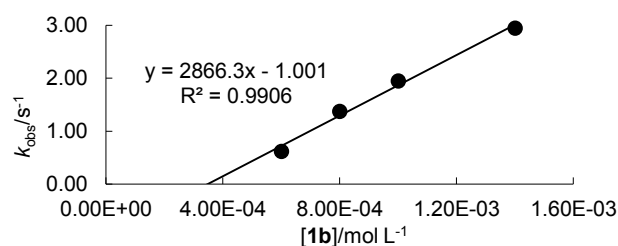
Table 2.47. **Kinetics of the reaction of 1b with 4a (DMSO, 20 °C, Stopped-flow method, detection at 302 nm).**

No.	$[4a]$/mol L^{-1}	$[1b]$/mol L^{-1}	k_{obs}/s^{-1}
da181s1-1	8.00×10^{-5}	8.00×10^{-4}	2.70×10^{-1}
da181s1-2	8.00×10^{-5}	1.20×10^{-3}	4.10×10^{-1}
da181s1-3	8.00×10^{-5}	1.60×10^{-3}	6.81×10^{-1}
da181s1-4	8.00×10^{-5}	2.00×10^{-3}	9.24×10^{-1}
da181s1-5	8.00×10^{-5}	2.40×10^{-3}	1.14
$k_2(20\ °C) = 5.64 \times 10^2$ L mol^{-1} s^{-1}			

y = 563.5x - 0.2166
R² = 0.9923
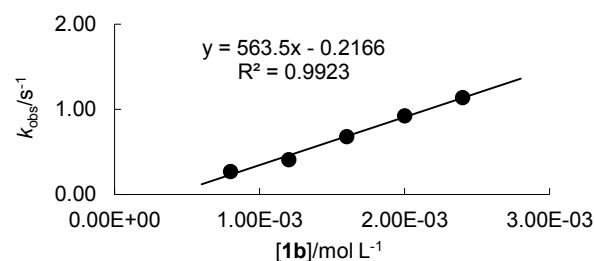
Table 2.48. **Kinetics of the reaction of 1b with 5b (DMSO, 20 °C, Stopped-flow method, detection at 388 nm).**

No.	$[5b]$/mol L^{-1}	$[1b]$/mol L^{-1}	k_{obs}/s^{-1}
da181s10-1	1.00×10^{-5}	2.50×10^{-4}	5.75×10^1
da181s10-2	1.00×10^{-5}	3.00×10^{-4}	7.15×10^1
da181s10-3	1.00×10^{-5}	3.50×10^{-4}	8.16×10^1
da181s10-4	1.00×10^{-5}	4.00×10^{-4}	1.00×10^2
$k_2(20\ °C) = 2.75 \times 10^5$ L mol^{-1} s^{-1}			

y = 275240x - 11.808
R² = 0.9872
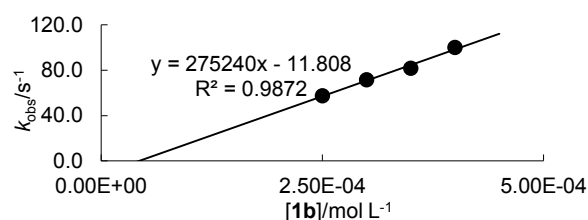
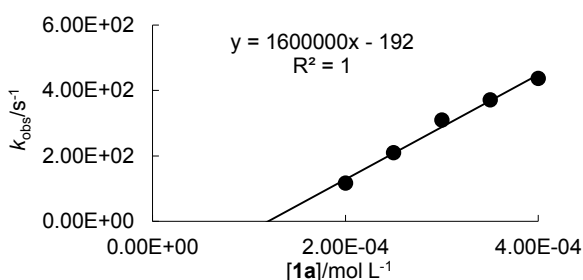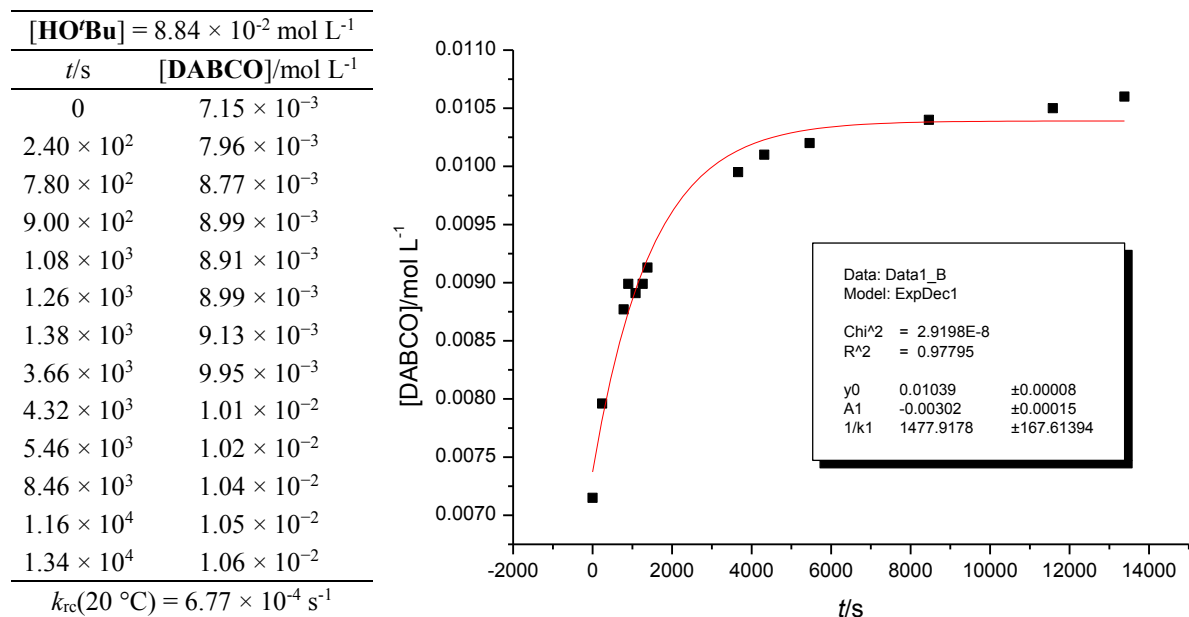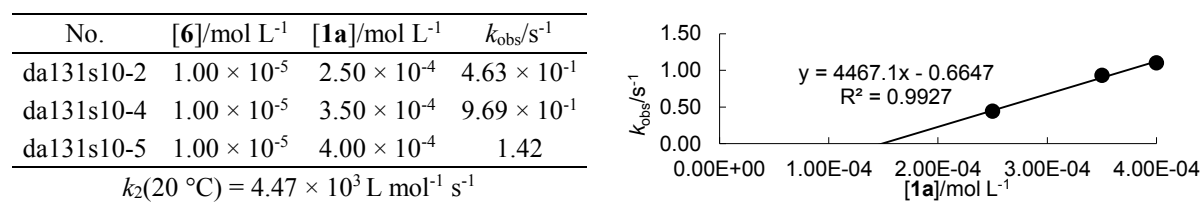**Table 2.49**. ^{1}H NMR monitoring of the formation of **13ba** (DMSO-d_6:CH$_2$Cl$_2$; 20 °C; evolution of DABCO followed, Experimental procedure see Products section)

t/s	[**DABCO**]/mol L^{-1}
\multicolumn{2}{c}{[**HO^{t}Bu**] = 8.82 × 10^{-2} mol L^{-1}}	
0	8.60 × 10^{-3}
6.60 × 10^2	1.36 × 10^{-2}
9.60 × 10^2	1.71 × 10^{-2}
1.68 × 10^3	2.23 × 10^{-2}
2.04 × 10^3	2.48 × 10^{-2}
4.74 × 10^3	2.97 × 10^{-2}
7.86 × 10^3	3.03 × 10^{-2}
9.66 × 10^3	3.04 × 10^{-2}
\multicolumn{2}{c}{k_{rc}(20 °C) = 5.76 × 10^{-4} s^{-1}}	

Data: Data1_B
Model: ExpDec1

Chi^2 = 9.2468E-7
R^2 = 0.99038

y0   0.03082   ±0.00067
A1   -0.02304   ±0.00102
1/k1 1735.08286   ±177.80467
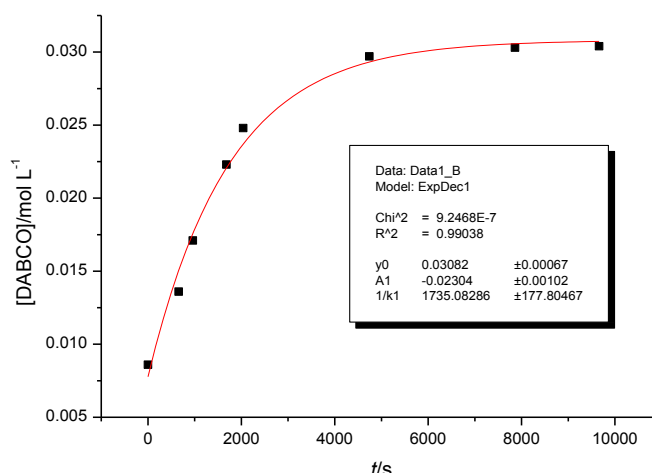
The time at which the first spectrum was taken equals t = 0 s. Therefore [DABCO] ≠ 0 M at t = 0 s.

2.7.4.3 Kinetics of the Reactions of Ylide 1c

DABCO$^+$ CO$_2$Et

1c
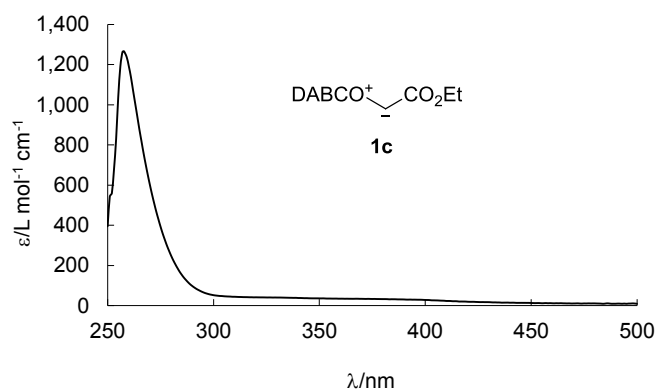
Figure 2.23. Absorption spectrum of 1c (λ_{max} = 258 nm).

Table 2.50. Determination of the nucleophilicity parameters N and s_N for 1c with the electrophiles 2−4 (filled dots). Open dots refer to the reactions with 5b,6 and were not used for the determination of N and s_N.

Electrophile	E	log k_2
2d-BF$_4$	-10.04	5.77
3a	-12.18	4.67
3b	-13.39	3.99
3c	-15.83	2.69
3d	-16.11	2.46
3e	-17.29	1.65
3f	-17.90	1.35
4a	-17.67	1.34
4d	-21.11	-0.67
5b	-11.32	5.35
6	-17.32	1.50

log k_2 = 0.5845 E + 11.775
R² = 0.9974
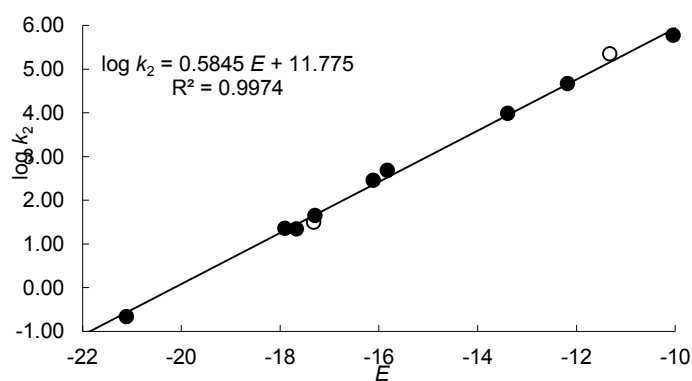
Nucleophilicity parameters for **1c** in DMSO: N = 20.15, s_N = 0.58.

Table 2.51. Kinetics of the reaction of 1c with 2d-BF₄ (DMSO, 20 °C, Stopped-flow method, detection at 630 nm).

| No.	[2d-BF$_4$]/mol L^{-1}	[1c]/mol L^{-1}	k_{obs}/s^{-1}
da62s7-1	1.00×10^{-5}	1.00×10^{-4}	4.16×10^1
da62s7-2	1.00×10^{-5}	1.10×10^{-4}	4.74×10^1
da62s7-3	1.00×10^{-5}	1.20×10^{-4}	5.44×10^1
da62s7-4	1.00×10^{-5}	1.30×10^{-4}	5.94×10^1
da62s7-5	1.00×10^{-5}	1.40×10^{-4}	6.52×10^1
k_2(20 °C) = 5.92 × 10^5 L mol^{-1} s^{-1}			

y = 592000x - 17.44
R² = 0.9977
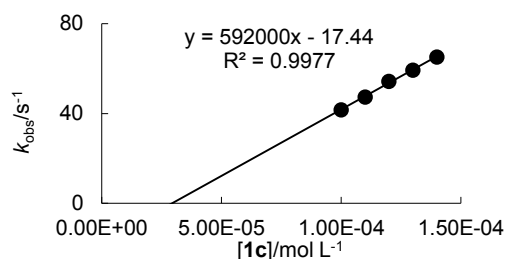
Table 2.52. Kinetics of the reaction of 1c with 3a (DMSO, 20 °C, Stopped-flow method, detection at 422 nm).

No.	[3a]/mol L^{-1}	[1c]/mol L^{-1}	k_{obs}/s^{-1}
da62s6-1	2.00×10^{-5}	4.00×10^{-4}	1.97×10^1
da62s6-2	2.00×10^{-5}	6.00×10^{-4}	3.17×10^1
da62s6-3	2.00×10^{-5}	8.00×10^{-4}	3.87×10^1
da62s6-4	2.00×10^{-5}	1.00×10^{-3}	4.75×10^1
da62s6-5	2.00×10^{-5}	1.20×10^{-3}	5.86×10^1
k_2(20 °C) = 4.68 × 10^4 L mol^{-1} s^{-1}			

y = 46800x + 1.8
R² = 0.9933
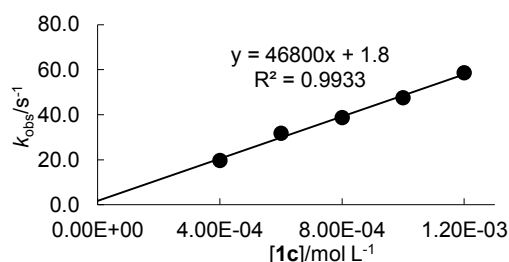
Table 2.53. Kinetics of the reaction of 1c with 3b (DMSO, 20 °C, Stopped-flow method, detection at 533 nm; from ref. [38]).

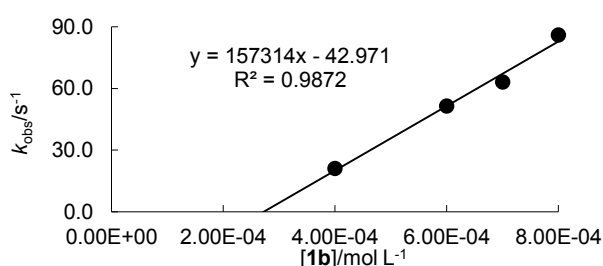| No.	[3b]/mol L^{-1}	[1c]/mol L^{-1}	k_{obs}/s^{-1}
da62s5-1	2.00×10^{-5}	2.00×10^{-4}	1.50
da62s5-2	2.00×10^{-5}	3.00×10^{-4}	2.41
da62s5-3	2.00×10^{-5}	4.00×10^{-4}	3.27
da62s5-4	2.00×10^{-5}	5.00×10^{-4}	4.26
da62s5-5	2.00×10^{-5}	6.00×10^{-4}	5.42
k_2(20 °C) = 9.69 × 10^3 L mol^{-1} s^{-1}			

y = 9690x - 0.504
R² = 0.9964
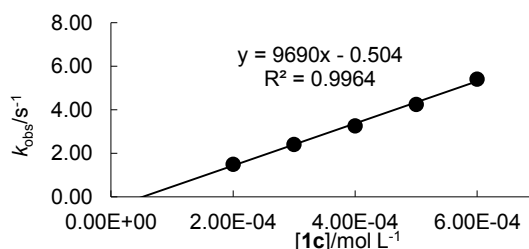
Table 2.54. Kinetics of the reaction of 1c with 3c (DMSO, 20 °C, Stopped-flow method, detection at 371 nm; from ref. [38]).

No.	[3c]/mol L^{-1}	[1c]/mol L^{-1}	k_{obs}/s^{-1}
da62s1-1	4.00×10^{-5}	8.00×10^{-4}	3.04×10^{-1}
da62s1-2	4.00×10^{-5}	1.60×10^{-3}	8.01×10^{-1}
da62s1-3	4.00×10^{-5}	2.40×10^{-3}	1.14
da62s1-4	4.00×10^{-5}	3.20×10^{-3}	1.51
da62s1-5	4.00×10^{-5}	4.00×10^{-3}	1.89
k_2(20 °C) = 4.85 × 10^2 L mol^{-1} s^{-1}			

y = 485.12x - 0.0353
R² = 0.9958
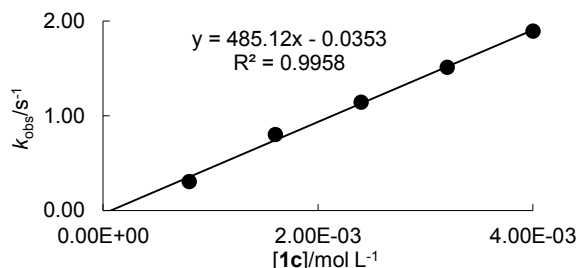
Table 2.55. Kinetics of the reaction of 1c with 3d (DMSO, 20 °C, Stopped-flow method, detection at 393 nm; from ref. 38).

No.	$[3d]$/mol L^{-1}	$[1c]$/mol L^{-1}	k_{obs}/s^{-1}
da62s2-1	4.00×10^{-5}	8.00×10^{-4}	1.95×10^{-1}
da62s2-2	4.00×10^{-5}	1.60×10^{-3}	4.51×10^{-1}
da62s2-3	4.00×10^{-5}	2.40×10^{-3}	6.53×10^{-1}
da62s2-4	4.00×10^{-5}	3.20×10^{-3}	9.20×10^{-1}
da62s2-5	4.00×10^{-5}	4.00×10^{-3}	1.11
$k_2(20\ °C) = 2.87 \times 10^2$ L mol^{-1} s^{-1}			

$y = 287.37x - 0.0239$
$R^2 = 0.9975$
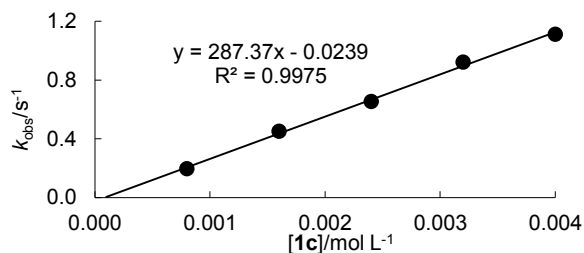
Table 2.56. Kinetics of the reaction of 1c with 3e (DMSO, 20 °C, Stopped-flow method, detection at 486 nm; from ref. [38]).

No.	$[3e]$/mol L^{-1}	$[1c]$/mol L^{-1}	k_{obs}/s^{-1}
da62s3-1	4.00×10^{-5}	8.00×10^{-4}	2.72×10^{-2}
da62s3-2	4.00×10^{-5}	1.60×10^{-3}	6.83×10^{-2}
da62s3-3	4.00×10^{-5}	2.40×10^{-3}	1.03×10^{-1}
da62s3-4	4.00×10^{-5}	3.20×10^{-3}	1.33×10^{-1}
da62s3-5	4.00×10^{-5}	4.00×10^{-3}	1.75×10^{-1}
$k_2(20\ °C) = 4.50 \times 10^1$ L mol^{-1} s^{-1}			

$y = 45.037x - 0.0068$
$R^2 = 0.9971$
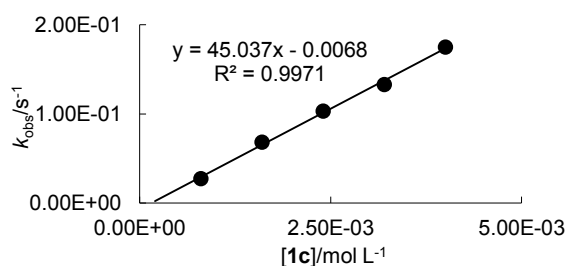
Table 2.57. Kinetics of the reaction of 1c with 3f (DMSO, 20 °C, Stopped-flow method, detection at 521 nm; from ref. [38]).

$[3f]$/mol L^{-1}	$[1c]$/mol L^{-1}	k_{obs}/s^{-1}
4.00×10^{-5}	2.00×10^{-3}	3.96×10^{-2}
4.00×10^{-5}	4.00×10^{-3}	9.37×10^{-2}
4.00×10^{-5}	6.00×10^{-3}	1.37×10^{-1}
4.00×10^{-5}	8.00×10^{-3}	1.76×10^{-1}
$k_2(20\ °C) = 2.26 \times 10^1$ L mol^{-1} s^{-1}		
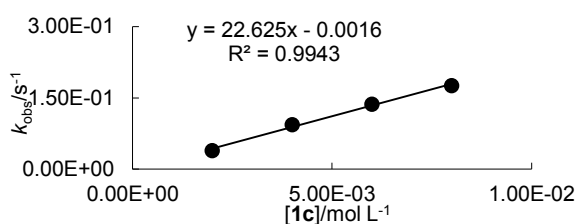
$y = 22.625x - 0.0016$
$R^2 = 0.9943$

For the determination of the pseudo first-order rate constants of the reaction of **1c** with **4a** the decrease of the absorption of **4a** at 302 nm and the increases of the absorption of **11ca** at 263 and 446 nm were monitored by UV-Vis spectroscopy.

Table 2.58. Kinetics of the reaction of 1c with 4a (DMSO, 20 °C, J&M method, detection at 302 nm).

$[4a]$/mol L^{-1}	$[1c]$/mol L^{-1}	k_{obs}/s^{-1}
4.20×10^{-5}	4.20×10^{-4}	9.63×10^{-3}
3.99×10^{-5}	5.99×10^{-4}	1.43×10^{-2}
4.04×10^{-5}	8.08×10^{-4}	1.84×10^{-2}
1.69×10^{-5}	1.06×10^{-3}	2.51×10^{-2}
1.66×10^{-5}	1.24×10^{-3}	2.74×10^{-2}
$k_2(20\ °C) = 2.21 \times 10^1$ L mol^{-1} s^{-1}		

$y = 22.1x + 0.0007$
$R^2 = 0.9921$
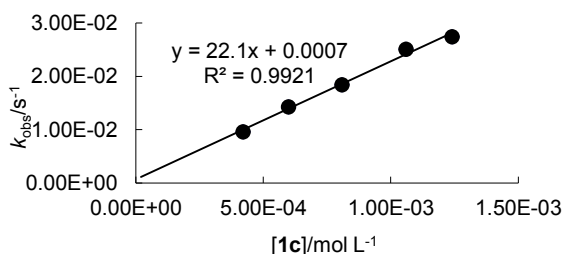
Table 2.59. Kinetics of the reaction of 1c with 4a (DMSO, 20 °C, J&M method, detection at 263 nm).

[4a]/mol L^{-1}	[1c]/mol L^{-1}	k_{obs}/s^{-1}
4.20×10^{-5}	4.20×10^{-4}	1.21×10^{-2}
3.99×10^{-5}	5.99×10^{-4}	1.77×10^{-2}
4.04×10^{-5}	8.08×10^{-4}	2.24×10^{-2}
1.69×10^{-5}	1.06×10^{-3}	2.81×10^{-2}
1.66×10^{-5}	1.24×10^{-3}	3.08×10^{-2}
k_2(20 °C) = 2.27×10^{1} L mol^{-1} s^{-1}		

$y = 22.716x + 0.0035$
$R^2 = 0.9889$
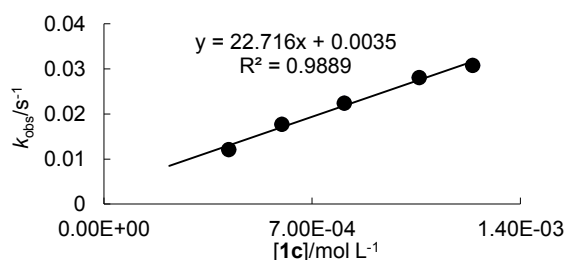
Table 2.60. Kinetics of the reaction of 1c with 4a (DMSO, 20 °C, J&M method, detection at 446 nm).

[4a]/mol L^{-1}	[1c]/mol L^{-1}	k_{obs}/s^{-1}
4.20×10^{-5}	4.20×10^{-4}	1.12×10^{-2}
3.99×10^{-5}	5.99×10^{-4}	1.66×10^{-2}
4.04×10^{-5}	8.08×10^{-4}	1.99×10^{-2}
1.69×10^{-5}	1.06×10^{-3}	2.73×10^{-2}
1.66×10^{-5}	1.24×10^{-3}	3.26×10^{-2}
k_2(20 °C) = 2.55×10^{1} L mol^{-1} s^{-1}		

$y = 25.46x + 0.0005$
$R^2 = 0.9918$
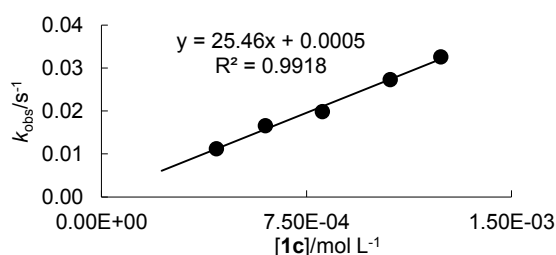
For the determination of the first-order rate constants of the formation of **11ca** the decrease of the absorption of **10ca** at 270 and 440 nm was monitored by UV-Vis spectroscopy. k_{rc} was determined from the intercept.

Table 2.61. Kinetics of the formation of 11ca (DMSO, 20 °C, J&M method, detection at 270 nm).

[4a]/mol L^{-1}	[1c]/mol L^{-1}	k_{obs}/s^{-1}
4.21×10^{-5}	4.21×10^{-4}	5.99×10^{-4}
4.12×10^{-5}	6.17×10^{-4}	5.94×10^{-4}
4.17×10^{-5}	8.34×10^{-4}	5.92×10^{-4}
4.25×10^{-5}	1.06×10^{-3}	5.99×10^{-4}
k_{rc}(20 °C) = 5.96×10^{-4} s^{-1}		

$y = -5.09\text{E-}04x + 5.96\text{E-}04$
$R^2 = 1.57\text{E-}03$
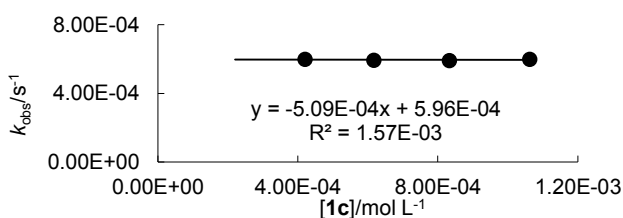
Table 2.62. Kinetics of the formation of 11ca (DMSO, 20 °C, J&M method, detection at 445 nm).

[4a]/mol L^{-1}	[1c]/mol L^{-1}	k_{obs}/s^{-1}
4.21×10^{-5}	4.21×10^{-4}	6.99×10^{-4}
4.12×10^{-5}	6.17×10^{-4}	9.15×10^{-4}
4.17×10^{-5}	8.34×10^{-4}	9.81×10^{-4}
4.25×10^{-5}	1.06×10^{-3}	9.31×10^{-4}
k_{rc}(20 °C) = 6.28×10^{-4} s^{-1}		

$y = 3.45\text{E-}01x + 6.28\text{E-}04$
$R^2 = 5.87\text{E-}01$
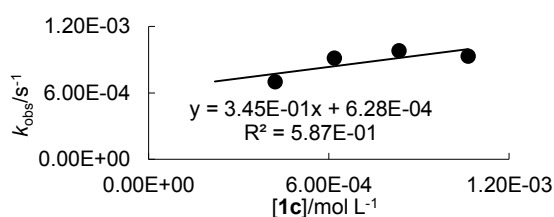
Table 2.63. MATLAB fit of the UV-Vis absorptions of the reaction of 1c with 4a (DMSO, 20 °C, J&M method, detection at 264 and 302 nm; from ref [39]).

No.	da62j3-1	da62j3-4
$[\mathbf{1c}]$/ mol L^{-1}	4.21×10^{-4}	1.06×10^{-3}
$[\mathbf{4a}]$/mol L^{-1}	4.21×10^{-5}	4.25×10^{-5}
k_{CC}/ mol L^{-1} s^{-1}	1.35×10^{1}	3.71×10^{1}
k_{-CC}/ mol L^{-1} s^{-1}	2.51×10^{-36}	2.19×10^{-36}
k_{rc}/ s^{-1}	8.35×10^{-4}	6.11×10^{-4}
f_1	7.72×10^{-1}	7.72×10^{-1}
f_2	2.34×10^{-1}	1.67×10^{-1}
f_3	5.54×10^{-1}	4.05×10^{-1}
f_4	2.67×10^{-1}	1.71×10^{-1}
c_0	7.09×10^{-1}	9.75×10^{-1}
t_0/s	1.68×10^{2}	8.43×10^{2}
k_{CC}/mol L^{-1} s^{-1}	1.35×10^{1}	3.71×10^{1}
$k_{CC}^{average}$/mol L^{-1} s^{-1}	2.53×10^{1}	
k_{-CC}/s^{-1}	2.51×10^{-36}	2.19×10^{-36}
$k_{-CC}^{average}$/s^{-1}	2.35×10^{-36}	
k_{rc}/s^{-1}	8.35×10^{-4}	6.11×10^{-4}
$k_{rc}^{average}$/s^{-1}	7.23×10^{-4}	
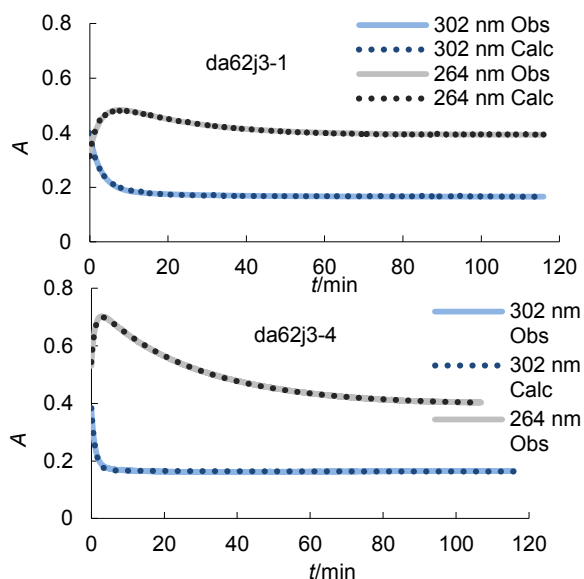
f_1 proportionality between extinctions of intermediate **10ca** and substrate **4a**.

f_2 proportionality between extinctions of final product **11ca** and substrate **4a**.

f_3 proportionality between extinctions of intermediate **10ca** and final product **11ca**.

f_4 proportionality between extinctions of the intermediate **10ca** and substrate **4a**.

c_0 dead-time correction factor for the concentration.

t_0 dead-time.

The symbolic form of the kinetic equations **Symsol** was derived from eqs (2) and (4) according to ref. [26].

```
Function [AC, ACB]=symsol(kcc, kmcc, krc, c0, t);
AC=1/2*c0*(exp(1/2*(-kmcc-krc-
kcc+(kmcc^2+2*kmcc*krc+2*kmcc*kcc+krc^2-
2*kcc*krc+kcc^2)^(1/2))*t)*kmcc+exp(1/2*(-kmcc-krc-
kcc+(kmcc^2+2*kmcc*krc+2*kmcc*kcc+krc^2-
2*kcc*krc+kcc^2)^(1/2))*t)*krc-exp(1/2*(-kmcc-krc-
kcc+(kmcc^2+2*kmcc*krc+2*kmcc*kcc+krc^2-
2*kcc*krc+kcc^2)^(1/2))*t)*kcc+exp(1/2*(-kmcc-krc-
kcc+(kmcc^2+2*kmcc*krc+2*kmcc*kcc+krc^2-
2*kcc*krc+kcc^2)^(1/2))*t)*(kmcc^2+2*kmcc*krc+2*kmcc*kcc+krc^2-
2*kcc*krc+kcc^2)^(1/2)-exp(-
1/2*(kmcc+krc+kcc+(kmcc^2+2*kmcc*krc+2*kmcc*kcc+krc^2-
2*kcc*krc+kcc^2)^(1/2))*t)*kmcc-exp(-
1/2*(kmcc+krc+kcc+(kmcc^2+2*kmcc*krc+2*kmcc*kcc+krc^2-
2*kcc*krc+kcc^2)^(1/2))*t)*krc+exp(-
1/2*(kmcc+krc+kcc+(kmcc^2+2*kmcc*krc+2*kmcc*kcc+krc^2-
2*kcc*krc+kcc^2)^(1/2))*t)*kcc+exp(-
```

```
1/2*(kmcc+krc+kcc+(kmcc^2+2*kmcc*krc+2*kmcc*kcc+krc^2-
2*kcc*krc+kcc^2)^(1/2))*t)*(kmcc^2+2*kmcc*krc+2*kmcc*kcc+krc^2-
2*kcc*krc+kcc^2)^(1/2))/(kmcc^2+2*kmcc*krc+2*kmcc*kcc+krc^2-
2*kcc*krc+kcc^2)^(1/2);
ACB=-c0*kcc*(-exp(1/2*(-kmcc-krc-
kcc+(kmcc^2+2*kmcc*krc+2*kmcc*kcc+krc^2-
2*kcc*krc+kcc^2)^(1/2))*t)+exp(-
1/2*(kmcc+krc+kcc+(kmcc^2+2*kmcc*krc+2*kmcc*kcc+krc^2-
2*kcc*krc+kcc^2)^(1/2))*t))/(kmcc^2+2*kmcc*krc+2*kmcc*kcc+krc^2-
2*kcc*krc+kcc^2)^(1/2);
```

The program code[39] below was used to calculate the fit for both wavelengths:

```
function ssd=ssddom(k,inp,inps,nu,tr);
[r,c]=size(inp);
[r2,c2]=size(inps);
j=1;
ssd=0;
for i=[1:1:length(k)]
    if k(i)<0
    ssd=100500;
end
end
if ssd<100500
for i=[1:2:c-1]
    kcc=nu(j)*k(1);
    kmcc=k(2);
    krc=k(3);
    c0=k(8+i-1);
    t0=k(9+i-1);
    f1=k(4);
        %proportionality between extinctions of intermediate and
substrate
    f2=k(5);
    %proportionality between extinctions of final product and
substrate
    f3=k(6);
    %proportionality between extinctions of intermediate and final
product
    f4=k(7);
    %proportionality between extinctions of the intermediate and
substrate
    %at the wavelength of the substrate
    for b=[1:tr:r]
        t=inp(b,i)+t0;
        [A I] = symsol(kcc,kmcc,krc,c0,t);
        Acalc= A+(c0-A-I)*f2+I*f4;
    ssd=ssd+(Acalc-inp(b,i+1))^2;
    end
    for b=[1:tr:r2]
        t=inps(b,i)+t0;
```

```
      [A I] = symsol(kcc,kmcc,krc,c0,t);
      Icalc= f1*I+(c0-A-I)*f3;
   ssd=ssd+(Icalc-inps(b,i+1))^2;
   end
 j=j+1;
end
end
```

Table 2.64.^{1}H NMR monitoring of the formation of 11ca (DMSO-d_6, 20 °C, evolution of DABCO followed; experimental procedure see Products section).

[HO^{t}Bu] = 6.53×10^{-2} mol L^{-1}	
t/s	[DABCO]/mol L^{-1}
0	6.75×10^{-3}
3.60×10^2	1.23×10^{-2}
1.02×10^3	1.80×10^{-2}
2.10×10^3	2.41×10^{-2}
2.88×10^3	2.64×10^{-2}
4.26×10^3	2.86×10^{-2}
6.54×10^3	2.99×10^{-2}
1.22×10^4	3.04×10^{-2}
1.40×10^4	3.04×10^{-2}
k_{rc}(20 °C) = 6.29×10^{-4} s^{-1}	

Data: Data1_B
Model: ExpDec1

Chi^2 = 7.0798E-8
R^2 = 0.9993

y0   0.03031   ±0.00015
A1   -0.02323   ±0.00025
1/k1 1589.35282 ±43.99264
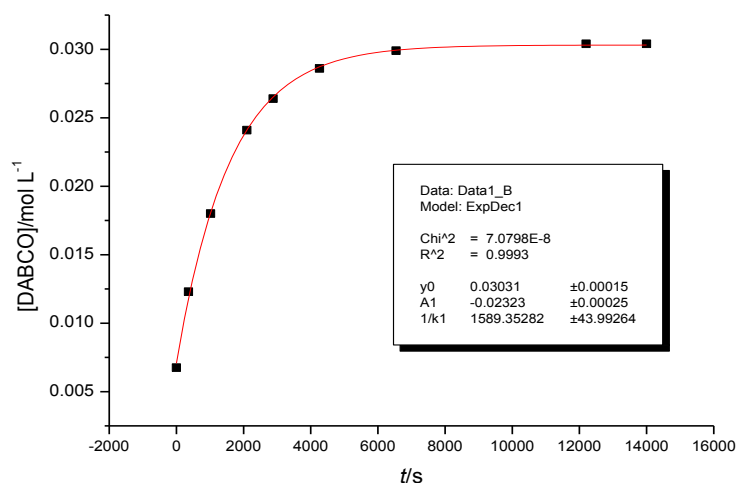
The time at which the first spectrum was taken equals $t = 0$ s. Therefore [DABCO] $\neq$ 0 M at t = 0 s.

The kinetics of the reaction of **1c** with **4d** were monitored by GC as outlined in the General Section with concentrations of [**1c**]$_0$ = 5.72×10^{-2} mol L^{-1} and [**4d**]$_0$ = 3.81×10^{-2} mol L^{-1}.

Table 2.65. Experimental ([4d]^{exp}) and calculated ([4d]^{calcd}) decrease of the time-dependent concentrations of 4d during the reaction of 1c with 4d (DMSO, 20 °C, GC-MS-methods).

t/s	[**4d**]^{exp}/mol L^{-1}	[**4d**]^{calcd}/mol L^{-1}	Δ[**4d**]$^{exp\text{-}calcd}$
0	3.81×10^{-2}	3.81×10^{-2}	0
60	2.32×10^{-2}	2.07×10^{-2}	2.49×10^{-3}
120	1.29×10^{-2}	1.31×10^{-2}	-1.23×10^{-4}
180	7.62×10^{-3}	8.88×10^{-3}	-1.26×10^{-3}
240	4.91×10^{-3}	6.30×10^{-3}	-1.39×10^{-3}
300	3.90×10^{-3}	4.59×10^{-3}	-6.92×10^{-4}
360	2.86×10^{-3}	3.41×10^{-3}	-5.53×10^{-4}
420	2.17×10^{-3}	2.57×10^{-3}	-3.99×10^{-4}
480	1.97×10^{-3}	1.95×10^{-3}	2.01×10^{-5}
540	1.91×10^{-3}	1.49×10^{-3}	4.23×10^{-4}
600	1.56×10^{-3}	1.15×10^{-3}	4.16×10^{-4}
660	1.54×10^{-3}	8.84×10^{-4}	6.55×10^{-4}
720	1.42×10^{-3}	6.84×10^{-4}	7.37×10^{-4}
780	1.31×10^{-3}	5.31×10^{-4}	7.78×10^{-4}
840	1.29×10^{-3}	5.31×10^{-4}	7.61×10^{-4}
k_2(20 °C) = 2.16×10^{-1} L mol^{-1} s^{-1}			

118
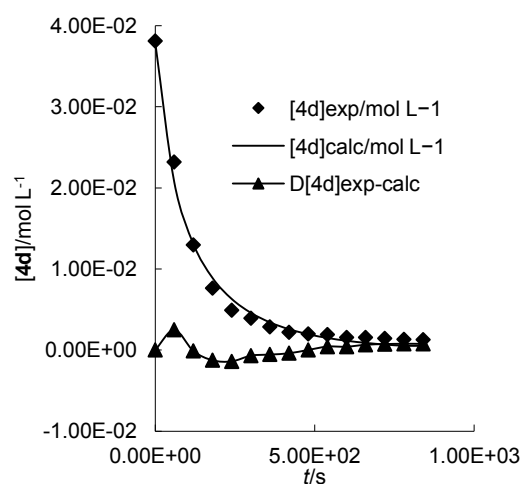
Table 2.66. Experimental ($[11ca]^{exp}$) and calculated ($[11ca]^{calc}$) increase of the time-dependent concentrations of 11ca during the reaction of 1c with 4d (DMSO, 20 °C, GC-MS-method).

t/s	$[11ca]^{exp}/mol\ L^{-1}$	$[11ca]^{calcd}/mol\ L^{-1}$	$\Delta[11ca]^{exp-calcd}$
0	0	0	0
60	1.48×10^{-2}	1.73×10^{-2}	-2.48×10^{-3}
120	2.51×10^{-2}	2.49×10^{-2}	1.24×10^{-4}
180	3.04×10^{-2}	2.91×10^{-2}	1.26×10^{-3}
240	3.31×10^{-2}	3.17×10^{-2}	1.40×10^{-3}
300	3.41×10^{-2}	3.34×10^{-2}	6.93×10^{-4}
360	3.51×10^{-2}	3.46×10^{-2}	5.54×10^{-4}
420	3.58×10^{-2}	3.54×10^{-2}	4.00×10^{-4}
480	3.60×10^{-2}	3.61×10^{-2}	-1.95×10^{-5}
540	3.61×10^{-2}	3.65×10^{-2}	-4.22×10^{-4}
600	3.64×10^{-2}	3.69×10^{-2}	-4.15×10^{-4}
660	3.65×10^{-2}	3.71×10^{-2}	-6.55×10^{-4}
720	3.66×10^{-2}	3.73×10^{-2}	-7.37×10^{-4}
780	3.67×10^{-2}	3.75×10^{-2}	-7.77×10^{-4}
840	3.67×10^{-2}	3.75×10^{-2}	-7.61×10^{-4}
$k_2(20\ °C) = 2.16 \times 10^{-1}\ L\ mol^{-1}\ s^{-1}$			
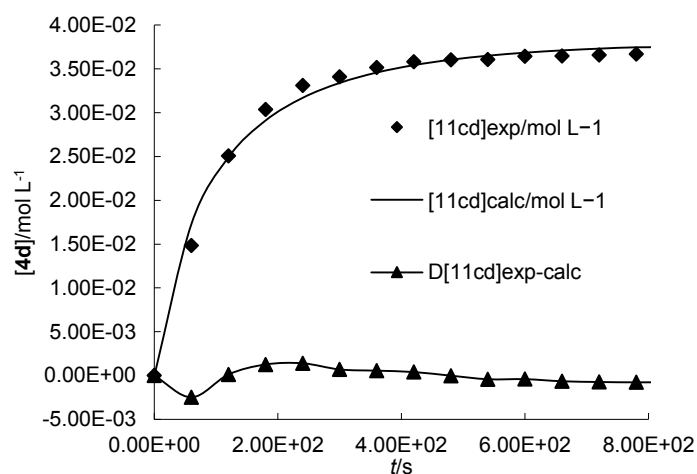
Table 2.67. Kinetics of the reaction of 1c with 5b (DMSO, 20 °C, Stopped-flow method, detection at 388 nm).

No.	$[5b]/mol\ L^{-1}$	$[1c]/mol\ L^{-1}$	k_{obs}/s^{-1}
da62s9-1	1.00×10^{-5}	2.00×10^{-4}	2.63×10^{1}
da62s9-2	1.00×10^{-5}	3.00×10^{-4}	5.59×10^{1}
da62s9-3	1.00×10^{-5}	4.00×10^{-4}	7.09×10^{1}
da62s9-4	1.00×10^{-5}	5.00×10^{-4}	1.00×10^{2}
da62s9-5	1.00×10^{-5}	6.00×10^{-4}	1.15×10^{2}
$k_2(20\ °C) = 2.22 \times 10^{5}\ L\ mol^{-1}\ s^{-1}$			
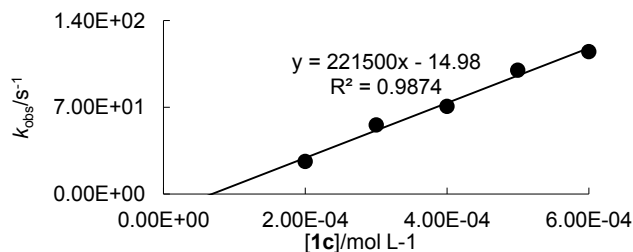
Table 2.68. ^{1}H NMR monitoring of kinetics of the formation of 12ca (DMSO-d_6, 20 °C, evolution of DABCO followed; experimental procedure see Products Section.

[HO^{t}Bu] = 1.09×10^{-1} mol L^{-1}	
t/s	[DABCO]/mol L^{-1}
0	1.19×10^{-3}
3.00×10^2	3.03×10^{-3}
7.20×10^2	4.86×10^{-3}
1.92×10^3	9.17×10^{-3}
3.42×10^3	1.16×10^{-2}
5.58×10^3	1.24×10^{-2}
8.76×10^3	1.24×10^{-2}
k_1(20 °C) = 6.52×10^{-4} s^{-1}	

Data: Data1_B
Model: ExpDec1

Chi^2 = 9.2813E-8
R^2 = 0.99663

y0   0.01263   ±0.00025
A1   -0.01193   ±0.00043
1/k1   1534.63413   ±149.72743
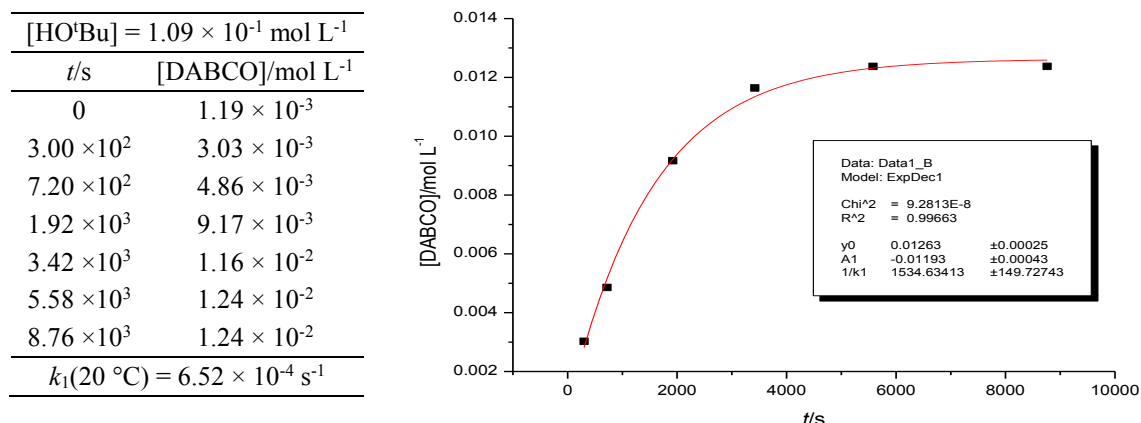
The time at which the first spectrum was taken equals $t = 0$ s. Therefore [DABCO] $\neq$ 0 M at $t = 0$ s.

Table 2.69. Kinetics of the reaction of 1c with 6 (DMSO, 20 °C, J&M method, detection at 325 nm).

No.	[6]/mol L^{-1}	[1c]/mol L^{-1}	k_{obs}/s^{-1}
da62j2-1	3.60×10^{-5}	3.75×10^{-4}	7.30×10^{-3}
da62j2-2	3.71×10^{-5}	5.64×10^{-4}	1.18×10^{-2}
da62j2-3	3.64×10^{-5}	7.29×10^{-4}	1.77×10^{-2}
da62j2-5	3.67×10^{-5}	1.12×10^{-4}	3.03×10^{-2}
k_2(20 °C) = 3.09×10^1 L mol^{-1} s^{-1}			

y = 30.912x - 0.0044
R² = 0.999
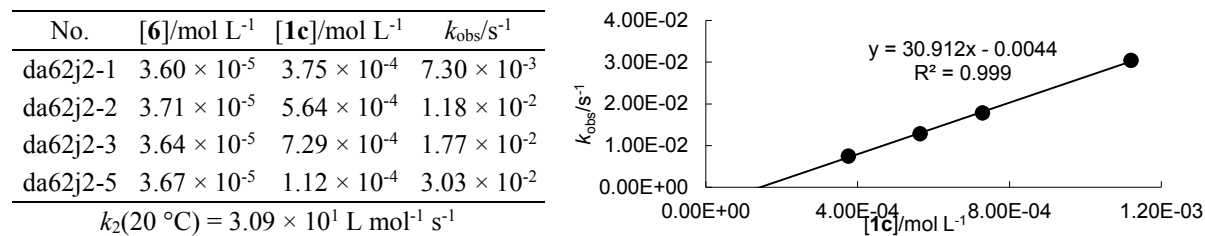
2.7.4.4 Kinetics of the Reactions of Ylide 1d

General note: If not mentioned otherwise **1dH$^+$OTf$^-$** was used as precursor salt.

DABCO$^+$ COMe

1d
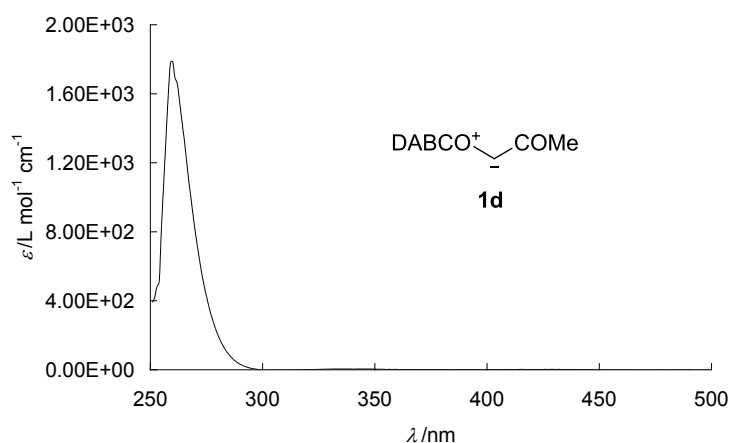
Figure 2.24. Absorption spectrum of 1d (λ_{max} = 260 nm).

Table 2.70. Determination of the nucleophilicity parameters N and s_N for 1d with the electrophiles 2,3 (filled dots). Open dots refer to the reactions with 5,6 and were not used for the determination of N and s_N.

Electrophile	E	$\log k_2$
2b-BF$_4$	-8.76	5.15
2c-BF$_4$	-9.45	4.57
3a	-12.18	3.32
3b	-13.39	2.54
5b	-11.32	3.95
5c	-14.68	0.53
6	-17.32	-0.77

$\log k_2 = 0.5356\,E + 9.7552$
$R^2 = 0.9921$
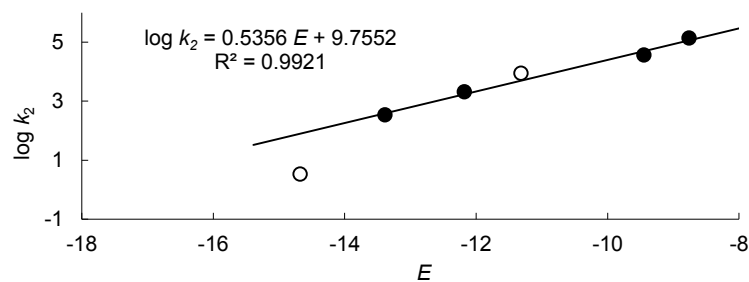
Nucleophilicity parameters for **1d** in DMSO: $N = 18.21$, $s_N = 0.54$.

Table 2.71. Kinetics of the reaction of 1d with 2b-BF$_4$ (DMSO, 20 °C, Stopped-flow method, detection at 627 nm).

No.	[2b-BF$_4$]/mol L^{-1}	[1d]/mol L^{-1}	k_{obs}/s^{-1}
da168s4-1	4.00×10^{-5}	4.00×10^{-4}	7.19×10^1
da168s4-6	4.00×10^{-5}	5.00×10^{-4}	8.75×10^1
da168s4-3	4.00×10^{-5}	8.00×10^{-4}	1.21×10^2
da168s4-4	4.00×10^{-5}	1.00×10^{-3}	1.60×10^2
$k_2(20\ °C) = 1.41 \times 10^5$ L mol^{-1} s^{-1}			

$y = 140835x + 15.04$
$R^2 = 0.9855$
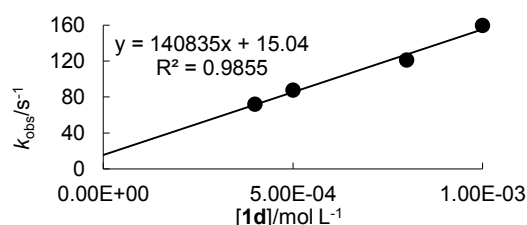
Table 2.72. Kinetics of the reaction of 1d with 2c-BF$_4$ (DMSO, 20 °C, Stopped-flow method, detection at 635 nm).

No.	[2c-BF$_4$]/mol L^{-1}	[1d]/mol L^{-1}	k_{obs}/s^{-1}
da168s4-7	4.00×10^{-5}	6.00×10^{-4}	3.45×10^1
da168s4-1	4.00×10^{-5}	8.00×10^{-4}	4.52×10^1
da168s4-3	4.00×10^{-5}	1.20×10^{-3}	5.77×10^1
da168s4-4	4.00×10^{-5}	1.40×10^{-3}	6.51×10^1
$k_2(20\ °C) = 3.69 \times 10^4$ L mol^{-1} s^{-1}			

$y = 36850x + 13.775$
$R^2 = 0.9893$
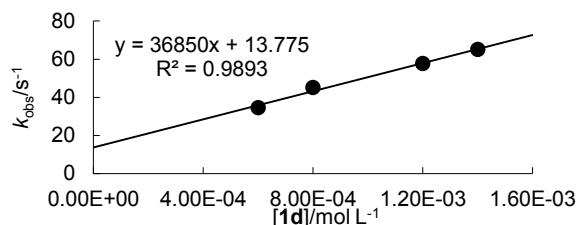
Table 2.73. Kinetics of the reaction of 1d with 3a (DMSO, 20 °C, Stopped-flow method, detection at 422 nm).

No.	[3a]/mol L^{-1}	[KO^{t}Bu]/mol L^{-1}	[1dH$^+$OTf$^-$]/mol L^{-1}	k_{obs}/s^{-1}
da168s2r2-1	4.00×10^{-5}	4.20×10^{-4}	8.00×10^{-4}	6.23
da168s2r2-2	4.00×10^{-5}	8.40×10^{-4}	1.60×10^{-3}	6.68
da168s2r2-3	4.00×10^{-5}	1.26×10^{-3}	2.40×10^{-3}	7.92
da168s2r2-5	4.00×10^{-5}	2.10×10^{-3}	4.00×10^{-3}	9.59
$k_2(20\ °C) = 2.08 \times 10^3$ L mol^{-1} s^{-1}				

$y = 2080.3x + 5.2023$
$R^2 = 0.9844$
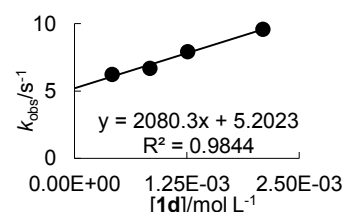
Table 2.74. Kinetics of the reaction of 1d with 3b (DMSO, 20 °C, Stopped-flow method, detection at 533 nm).

No.	[3b]/mol L^{-1}	[KO^{t}Bu]/mol L^{-1}	[1dH$^+$Cl$^-$]/mol L^{-1}	k_{obs}/s^{-1}
da168s1r-1	4.00×10^{-5}	4.20×10^{-4}	8.00×10^{-4}	1.67
da168s1r-2	4.00×10^{-5}	8.40×10^{-4}	1.60×10^{-3}	1.78
da168s1r-3	4.00×10^{-5}	1.26×10^{-3}	2.40×10^{-3}	1.97
da168s1r-4	4.00×10^{-5}	1.68×10^{-3}	3.20×10^{-3}	2.09
$k_2(20\ °C) = 3.45 \times 10^2$ L mol^{-1} s^{-1}				
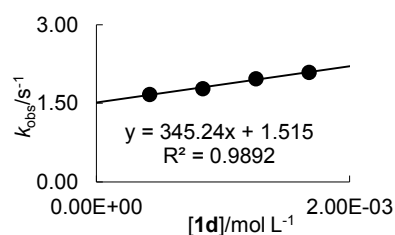
Table 2.75. Kinetics of the formation of 9db (DMSO, 20 °C, J&M method, detection at 533 nm).

No.	[3b]/M	[1d]/M	k_{obs}/s^{-1}	[1d]$^{-1}$/M^{-1}	k_{obs}^{-1}/s
da168j4-1	1.80×10^{-5}	3.60×10^{-4}	2.17×10^{-3}	2.78×10^3	4.61×10^2
da168j4-2	3.53×10^{-5}	7.06×10^{-4}	3.89×10^{-3}	1.42×10^3	2.57×10^2
da168j4-3	3.98×10^{-5}	1.19×10^{-3}	6.68×10^{-3}	8.40×10^2	1.50×10^2
da168j4-4	3.78×10^{-5}	1.51×10^{-3}	8.80×10^{-3}	6.61×10^2	1.14×10^2
da168j4-5	3.82×10^{-5}	1.91×10^{-3}	1.09×10^{-2}	5.24×10^2	9.17×10^1
$1/K \cdot k_{rc} = 1.64 \times 10^{-1}$ M s $=> K \cdot k_{rc}(20\ °C) = 6.09$ L mol^{-1} s^{-1}					
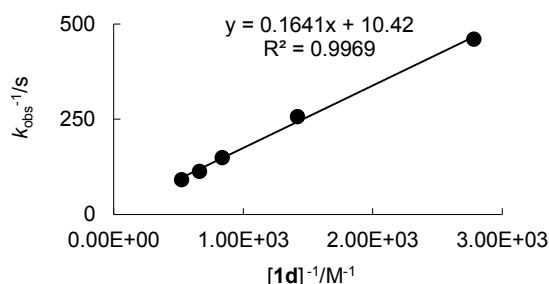
Table 2.76. Determination of the equilibrium constant of the reaction of 1d with 3b (DMSO, 20 °C, Stopped-flow method, detection at 533 nm).

No.	[3b]/mol L^{-1}	[1d]/mol L^{-1}	A_0	A_{eq}[a]	$(A_0-A_{eq})/A_{eq}$
da168s1-1	4.00×10^{-5}	4.00×10^{-4}	0.998	0.924	0.080
da168s1-2	4.00×10^{-5}	8.00×10^{-4}	1.004	0.895	0.122
da168s1-3	4.00×10^{-5}	1.20×10^{-3}	1.003	0.838	0.197
da168s1-4	4.00×10^{-5}	1.60×10^{-3}	1.002	0.818	0.225
da168s1-7	4.00×10^{-5}	2.80×10^{-3}	0.998	0.702	0.422
da168s1-8	4.00×10^{-5}	3.20×10^{-3}	0.992	0.651	0.524
$K(20\ °C) = 1.6 \times 10^2$ M^{-1}					
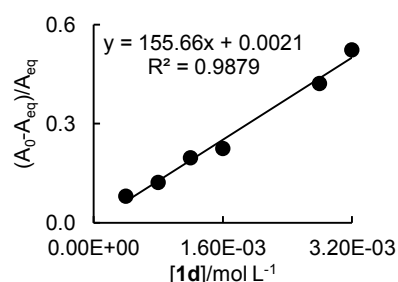
[a] The equilibrium absorbances have been determined from the constant C obtained by fitting the monoexponential function $A = A_0 e^{-k_{obs} t} + C$ to the time-dependent absorbances.

Table 2.77. Kinetics of the reaction of 1d with 5b (DMSO, 20 °C, Stopped-flow method, detection at 388 nm).

No.	[5b]/mol L^{-1}	[1d]/mol L^{-1}	k_{obs}/s^{-1}
da168s5-2	2.00×10^{-5}	3.00×10^{-4}	1.76×10^1
da168s5-3	2.00×10^{-5}	4.00×10^{-4}	1.84×10^1
da168s5-4	2.00×10^{-5}	5.00×10^{-4}	1.91×10^1
da168s5-5	2.00×10^{-5}	6.00×10^{-4}	2.03×10^1
$k_2(20\ °C) = 8.80 \times 10^3$ L mol^{-1} s^{-1}			
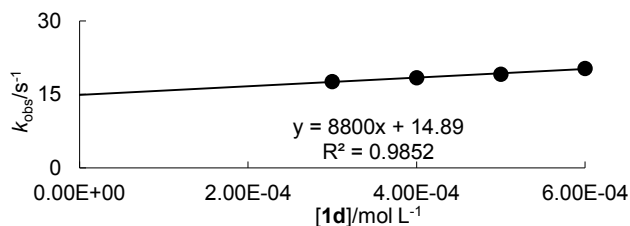
Table 2.78. Kinetics of the formation of 13da (DMSO, 20 °C, Stopped-flow method, detection at 388 nm).

No.	[5b]/M	[1d]/M	k_{obs}/s^{-1}	[1d]$^{-1}$/M^{-1}	k_{obs}^{-1}/s
da168s5-22	2.00×10^{-5}	3.00×10^{-4}	2.55×10^{-2}	3.33×10^3	3.92×10^1
da168s5-32	2.00×10^{-5}	4.00×10^{-4}	3.15×10^{-2}	2.50×10^3	3.17×10^1
da168s5-42	2.00×10^{-5}	5.00×10^{-4}	3.89×10^{-2}	2.00×10^3	2.57×10^1
da168s5-52	2.00×10^{-5}	6.00×10^{-4}	4.63×10^{-2}	1.67×10^3	2.16×10^1
$1/K \cdot k_{rc} = 1.05 \times 10^{-2}$ M s $=> K \cdot k_{rc}(20\ °C) = 9.52 \times 10^1$ L mol^{-1} s^{-1}					
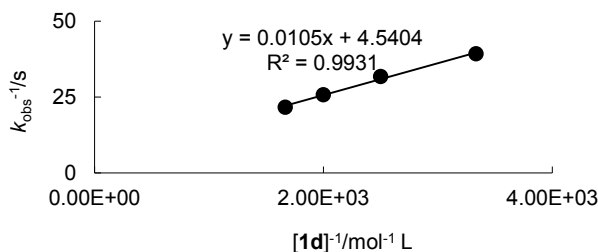
**Table 2.79. Determination of the equilibrium constant of the reaction of 1d with 5b (DMSO, 20 °C, Stopped-flow method, detection at 388 nm).**

No.	[5b]/mol L^{-1}	[1d]/mol L^{-1}	A_0	A_{eq}[a]	$(A_0-A_{eq})/A_{eq}$
da168s5-1	2.00×10^{-5}	2.00×10^{-3}	1.18	0.828	0.425
da168s5-3	2.00×10^{-5}	4.00×10^{-4}	1.15	0.773	0.488
da168s5-4	2.00×10^{-5}	5.00×10^{-4}	1.13	0.776	0.456
da168s5100	2.00×10^{-5}	2.00×10^{-3}	1.03	0.596	0.728
da168s5110	2.00×10^{-5}	2.20×10^{-3}	1.04	0.578	0.799
da168s5140	2.00×10^{-5}	2.80×10^{-3}	1.04	0.548	0.898
$K(20\ °C) = 2 \times 10^2$ L mol^{-1}					

[a] The equilibrium absorbances have been determined from the constant C obtained by fitting the monoexponential function $A = A_0 e^{-k_{obs} t} + C$ to the time-dependent absorbances.
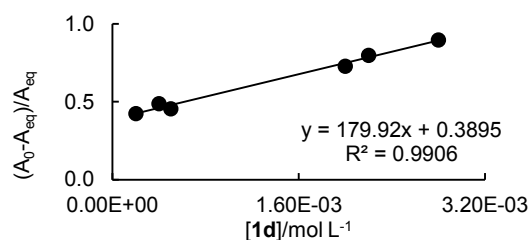
The large positive intercept shows the uncertainty of the method. If the values $(A_0 - A_{eq})/A_{eq}$ obtained with the highest concentration of **1e** is divided by [**1e**], one obtains an equilibrium constant of $K = 3 \times 10^2$.

Table 2.80. Kinetics of the reaction of 1d with 5c (DMSO, 20 °C, J&M method, detection at 523 nm).

No.	[5c]/mol L^{-1}	[1d]/mol L^{-1}	k_{obs}/s^{-1}
da168j2-12	3.61×10^{-5}	7.23×10^{-4}	5.28×10^{-3}
da168j2-1	3.72×10^{-5}	9.30×10^{-4}	5.89×10^{-3}
da168j2-22	3.71×10^{-5}	1.11×10^{-3}	6.67×10^{-3}
da168j2-42	3.44×10^{-5}	1.38×10^{-3}	7.38×10^{-3}
da168j2-5	3.72×10^{-5}	1.67×10^{-3}	8.54×10^{-3}
$K \cdot k_{rc}(20\ °C) = 3.41$ L mol^{-1} s^{-1}			
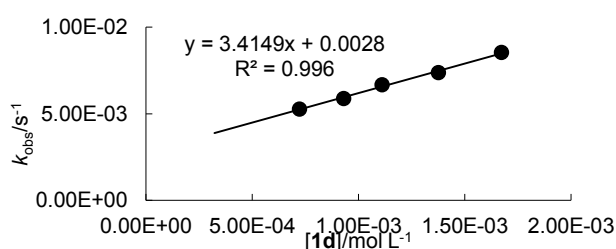
Table 2.81. Kinetics of the reaction of 1e and 3c (DMSO, 20 °C, ^{1}H NMR method, evolution of DABCO and consumption of 3c followed). For the experimental procedure Products Section.

t/s	$[KO^tBu] = 5.08 \times 10^{-2}$ M	$[\mathbf{1d}]^0 = 5.36 \times 10^{-2}$ M	$[\mathbf{6}]^0 = 4.96 \times 10^{-2}$ M	
t/s	[DABCO]/M	[**1d**]/M	[**6**]/M	$[\mathbf{6}]^{-1}$/M^{-1}
0	3.05×10^{-3}	5.06×10^{-2}	4.66×10^{-2}	2.15×10^1
6.60×10^2	3.18×10^{-3}	5.04×10^{-2}	4.64×10^{-2}	2.15×10^1
1.20×10^3	3.30×10^{-3}	5.03×10^{-2}	4.63×10^{-2}	2.16×10^1
3.96×10^3	3.85×10^{-3}	4.97×10^{-2}	4.57×10^{-2}	2.19×10^1
$K \cdot k_{rc} = 9.6 \times 10^{-5}$ M^{-1} s^{-1}				
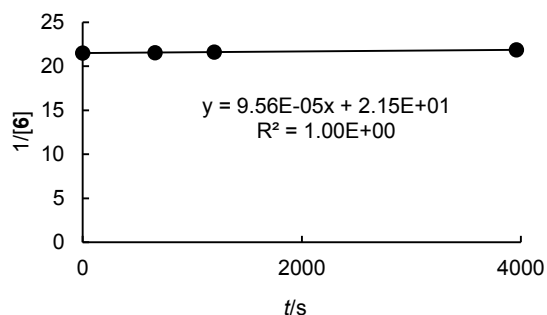
The time at which the first spectrum was taken equals $t = 0$ s. Therefore [DABCO] $\neq 0$ M at $t = 0$ s.

2.7.4.5 Kinetics of the Reactions of Ylide 1e
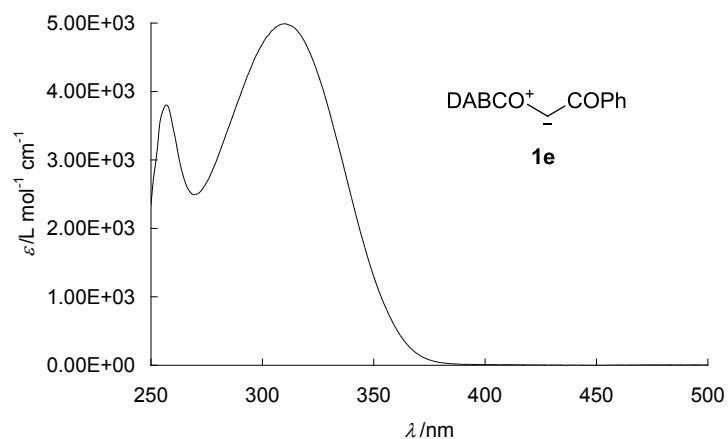
Figure 2.25. Absorption spectrum of 1e ($\lambda_{max} = 257, 310$ nm).

124

Table 2.82. Determination of the nucleophilicity parameters N and s_N for 1e with the electrophiles 2,3 (filled dots). Open dots refer to the reactions with 4−6 and were not used for the determination of N and s_N.

Electrophile	E	$\log k_2$
2c-BF$_4$	-9.45	5.21
2d-BF$_4$	-10.04	5.12
3a	-12.18	3.58
3b	-13.39	2.56
3c	-15.83	-2.72
4a	-17.67	-3.36
5b	-11.32	4.08
5c	-14.68	-0.56
6	-17.33	-3.25

$$\log k_2 = 0.6917\,E + 11.909$$
$$R^2 = 0.9862$$
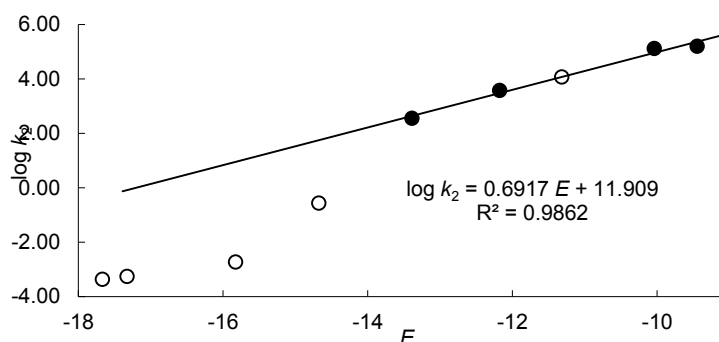
Nucleophilicity parameters for **1e** in DMSO: $N = 17.22$, $s_N = 0.69$.

Table 2.83. Kinetics of the reaction of 1e with 2c-BF$_4$ (DMSO, 20 °C, Stopped-flow method, detection at 635 nm; from ref. [38]).

No.	[2c-BF$_4$]/mol L^{-1}	[1e]/mol L^{-1}	k_{obs}/s^{-1}
da72s1-1	4.00×10^{-5}	4.00×10^{-4}	6.70×10^{1}
da72s1-2	4.00×10^{-5}	6.00×10^{-4}	8.80×10^{1}
da72s1-3	4.00×10^{-5}	8.00×10^{-4}	1.31×10^{2}
da72s1-4	4.00×10^{-5}	1.00×10^{-3}	1.61×10^{2}
k_2(20 °C) = 1.63×10^{5} L mol^{-1} s^{-1}			

$$y = 162500x - 2$$
$$R^2 = 0.9848$$
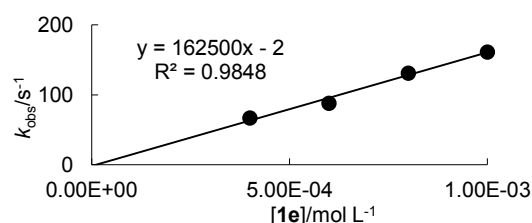
Table 2.84. Kinetics of the reaction of 1e with 2d-BF$_4$ (DMSO, 20 °C, Stopped-flow method, detection at 630 nm; from ref. [38]).

No.	[2d-BF$_4$]/mol L^{-1}	[1e]/mol L^{-1}	k_{obs}/s^{-1}
da72s2-1	8.00×10^{-6}	4.00×10^{-4}	4.10×10^{1}
da72s2-2	8.00×10^{-6}	6.00×10^{-4}	6.98×10^{1}
da72s2-3	8.00×10^{-6}	8.00×10^{-4}	9.38×10^{1}
da72s2-4	8.00×10^{-6}	1.00×10^{-3}	1.23×10^{2}
da72s2-5	8.00×10^{-6}	1.20×10^{-3}	1.46×10^{2}
k_2(20 °C) = 1.32×10^{5} L mol^{-1} s^{-1}			

$$y = 131600x - 10.56$$
$$R^2 = 0.9986$$
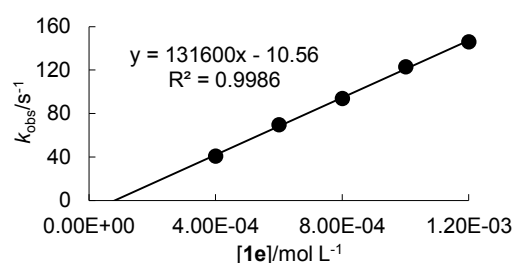
Table 2.85. Kinetics of the reaction of 1e with 3a (DMSO, 20 °C, Stopped-flow method, detection at 422 nm; from ref. [38]).

No.	[3a]/mol L^{-1}	[1e]/mol L^{-1}	k_{obs}/s^{-1}
da72s4-1	2.00×10^{-5}	8.00×10^{-4}	3.96
da72s4-3	2.00×10^{-5}	2.40×10^{-3}	1.04×10^{1}
da72s4-4	2.00×10^{-5}	3.20×10^{-3}	1.25×10^{1}
da72s4-5	2.00×10^{-5}	4.00×10^{-3}	1.65×10^{1}
k_2(20 °C) = 3.82×10^{3} L mol^{-1} s^{-1}			

$$y = 3820x + 0.908$$
$$R^2 = 0.9927$$
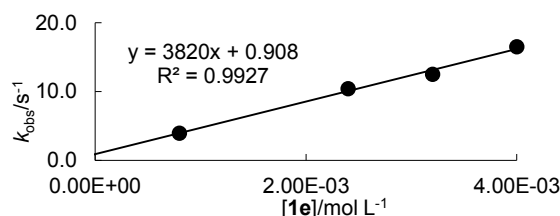
Table 2.86. Kinetics of the reaction of 1e with 3b (DMSO, 20 °C, Stopped-flow method, detection at 533 nm).

No.	$[3b]$/mol L^{-1}	$[1e]$/mol L^{-1}	k_{obs}/s^{-1}
da72s3r-1	2.00×10^{-5}	4.00×10^{-4}	2.13
da72s3r-2	2.00×10^{-5}	8.00×10^{-4}	2.24
da72s3r-3	2.00×10^{-5}	1.20×10^{-3}	2.40
da72s3r-4	2.00×10^{-5}	1.60×10^{-3}	2.59
da72s3r-5	2.00×10^{-5}	2.00×10^{-3}	2.64
da72s3r-6	2.00×10^{-5}	2.40×10^{-3}	2.81
da72s3r-7	2.00×10^{-5}	2.80×10^{-3}	3.03
da72s3r-8	2.00×10^{-5}	3.20×10^{-3}	3.11
$k_2(20\ °C) = 3.60 \times 10^2$ L mol^{-1} s^{-1}			

$y = 359.82x + 1.9711$
$R^2 = 0.9904$
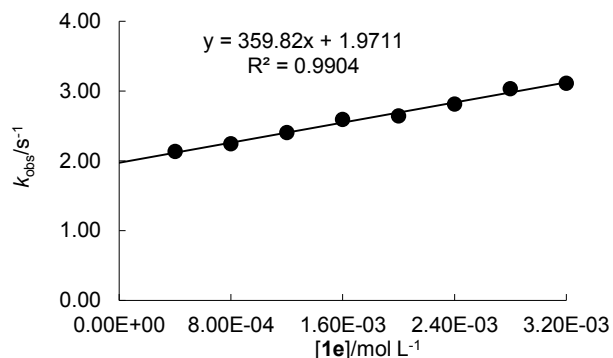
Table 2.87. Kinetics of the formation of 9eb (DMSO, 20 °C, J&M method, detection at 533 nm).

No	$[3b]$/M	$[1e]$/M	k_{obs}/s^{-1}	$[1e]^{-1}$/M^{-1}	k_{obs}^{-1}/s
da72j6-1	1.80×10^{-5}	9.01×10^{-4}	1.76×10^{-3}	1.11×10^{3}	5.68×10^{2}
da72j6-2	1.82×10^{-5}	1.38×10^{-3}	2.47×10^{-3}	7.25×10^{2}	4.05×10^{2}
da72j6-3	1.81×10^{-5}	1.81×10^{-3}	2.96×10^{-3}	5.52×10^{2}	3.38×10^{2}
da72j6-4	1.80×10^{-5}	2.26×10^{-3}	3.40×10^{-3}	4.42×10^{2}	2.94×10^{2}
da72j6-5	1.79×10^{-5}	2.69×10^{-3}	3.74×10^{-3}	3.71×10^{2}	2.67×10^{2}
$1/K \cdot k_{rc} = 4.08 \times 10^{-1}$ M s => $K \cdot k_{rc}(20\ °C) = 2.45$ L mol^{-1} s^{-1}					
$1/k_{rc} = 1.14 \times 10^{1}$ M s => $k_{rc}(20\ °C) = 8.79 \times 10^{-3}$ s^{-1}					
$K(20\ °C) = 2.79 \times 10^2$ L mol^{-1}					

$y = 0.4077x + 113.78$
$R^2 = 0.9997$
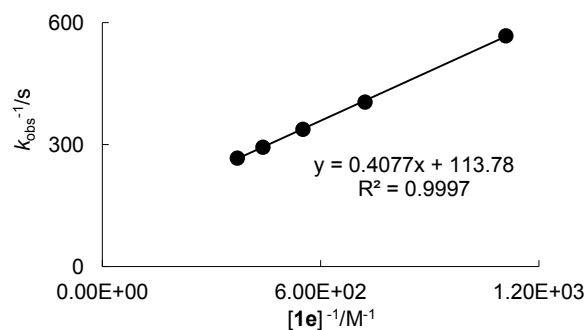
Table 2.88. Determination of the equilibrium constant of the reaction of 1e with 3b (DMSO, 20 °C, Stopped-flow method, detection at 533 nm).

No.	$[3b]$/mol L^{-1}	$[1e]_0$/mol L^{-1}	A_0	A_{eq}	$(A_0 - A_{eq})/A_{eq}$
da72s3r-4	2.00×10^{-5}	1.60×10^{-3}	0.885	0.693	0.277
da72s3r-5	2.00×10^{-5}	2.00×10^{-3}	0.874	0.622	0.405
da72s3r-6	2.00×10^{-5}	2.40×10^{-3}	0.866	0.571	0.517
da72s3r-7	2.00×10^{-5}	2.80×10^{-3}	0.861	0.514	0.673
da72s3r-8	2.00×10^{-5}	3.20×10^{-3}	0.861	0.496	0.736
$K(20\ °C) = 3.0 \times 10^2$ M^{-1}					
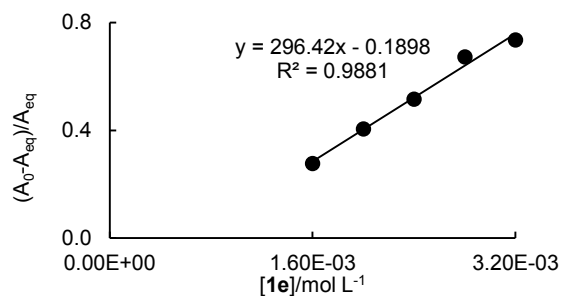
The negative intercept of the correlation shows the uncertainty of the method.

Table 2.89. Kinetics of the reaction of 1e and 3c (DMSO, 20 °C, ^{1}H NMR method, evolution of DABCO and consumption of 3c followed). For the experimental procedure Products Section.

t/s	equiv. DABCO	$[1e]_0 = 5.00 \times 10^{-2}$ M	$[3c]_0 = 4.98 \times 10^{-2}$ M	
		$[1e]$/M	$[3c]$/M	$[3c]^{-1}$/M^{-1}
0	0.217	3.92×10^{-2}	3.90×10^{-2}	2.56×10^1
3.60×10^2	0.349	3.25×10^{-2}	3.24×10^{-2}	3.09×10^1
7.20×10^2	0.479	2.60×10^{-2}	2.59×10^{-2}	3.86×10^1
9.00×10^2	0.52	2.40×10^{-2}	2.39×10^{-2}	4.19×10^1
1.02×10^3	0.538	2.31×10^{-2}	2.30×10^{-2}	4.35×10^1
$K \cdot k_{rc} = 1.9 \times 10^{-3}$ M^{-1} s^{-1}				
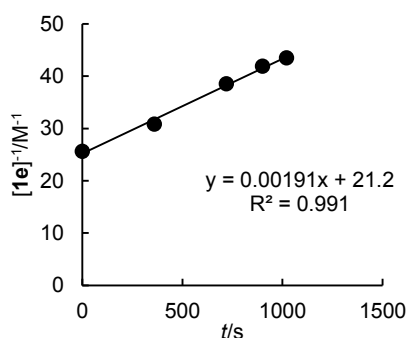
The ratio of the signals of CDHCl$_2$ (residual in CD$_2$Cl$_2$) and of DABCO was used to determine the decrease of the concentration of the reactants by $[1e/3c] = [1e/3c]_0 - [1e/3c] \times (equiv.\ DABCO)$. The time at which the first spectrum was taken equals $t = 0$ s. Therefore $[DABCO] \neq 0$ M at $t = 0$ s.

Table 2.90. Kinetics of the reaction of 1e and 4a (DMSO, 20 °C, ^{1}H NMR method, evolution of DABCO followed; experimental procedure see Products Section).

[HO^{t}Bu] = 5.05×10^{-2} M	[**1e**]$_0$ = 6.49×10^{-2} M		[**4a**]$_0$ = 6.24×10^{-2} M	
t/s	[DABCO]/M	[**1e**]/M	[**4a**]/M	[**4a**]$^{-1}$/M^{-1}
0	6.73×10^{-4}	6.42×10^{-2}	6.17×10^{-2}	1.62×10^1
3.60×10^2	1.56×10^{-3}	6.33×10^{-2}	6.08×10^{-2}	1.64×10^1
7.80×10^2	2.57×10^{-3}	6.23×10^{-2}	5.98×10^{-2}	1.67×10^1
1.14×10^3	3.07×10^{-3}	6.18×10^{-2}	5.93×10^{-2}	1.69×10^1
2.16×10^3	4.71×10^{-3}	6.02×10^{-2}	5.77×10^{-2}	1.73×10^1
4.74×10^3	8.42×10^{-3}	5.65×10^{-2}	5.40×10^{-2}	1.85×10^1
1.01×10^4	1.41×10^{-2}	5.08×10^{-2}	4.83×10^{-2}	2.07×10^1
1.26×10^4	1.65×10^{-2}	4.84×10^{-2}	4.59×10^{-2}	2.18×10^1
$K \cdot k_{rc} = 4.4 \times 10^{-4}$ M^{-1} s^{-1}				

$y = 4.37\text{E-}04x + 1.63\text{E+}01$
$R^2 = 9.99\text{E-}01$
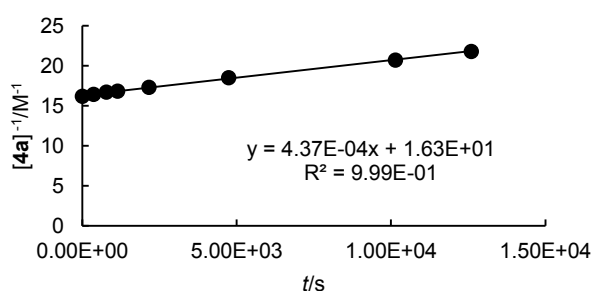
The time at which the first spectrum was taken equals $t = 0$ s. Therefore [DABCO] $\neq 0$ M at $t = 0$ s.

Table 2.91. Kinetics of the reaction of 1e with 5b (DMSO, 20 °C, Stopped-flow method, detection at 388 nm).

No.	[**5b**]/mol L^{-1}	[**1e**]/mol L^{-1}	k_{obs}/s^{-1}
da72s5-2	2.00×10^{-5}	3.00×10^{-4}	1.79×10^1
da72s5-3	2.00×10^{-5}	4.00×10^{-4}	1.90×10^1
da72s5-4	2.00×10^{-5}	5.00×10^{-4}	2.05×10^1
da72s5-5	2.00×10^{-5}	6.00×10^{-4}	2.14×10^1
$k_2(20 °C) = 1.20 \times 10^4$ L mol^{-1} s^{-1}			

$y = 12000x + 14.3$
$R^2 = 0.9917$
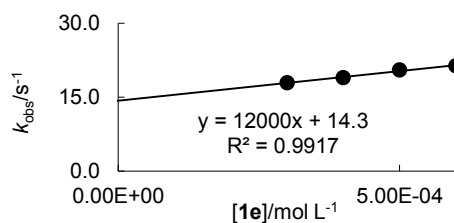
Table 2.92. Kinetics of the formation of 13ea (DMSO, 20 °C, Stopped-flow method, detection at 388 nm).

No	[5b]/M	[1e]/M	k_{obs}/s^{-1}	[1e]$^{-1}$/M^{-1}	k_{obs}^{-1}/s
da72s5-22	2.00×10^{-5}	3.00×10^{-4}	1.02×10^{-2}	3.33×10^{3}	9.80×10^{1}
da72s5-32	2.00×10^{-5}	4.00×10^{-4}	1.33×10^{-2}	2.50×10^{3}	7.52×10^{1}
da72s5-42	2.00×10^{-5}	5.00×10^{-4}	1.57×10^{-2}	2.00×10^{3}	6.37×10^{1}
da72s5-52	2.00×10^{-5}	6.00×10^{-4}	1.91×10^{-2}	1.67×10^{3}	5.24×10^{1}
da72s5-1002	2.00×10^{-5}	2.00×10^{-3}	6.94×10^{-2}	5.00×10^{2}	1.44×10^{1}
$1/K \cdot k_{rc} = 2.94 \times 10^{-1}$ M s => $K \cdot k_{rc}$(20 °C) = 3.40×10^{1} L mol^{-1} s^{-1}					
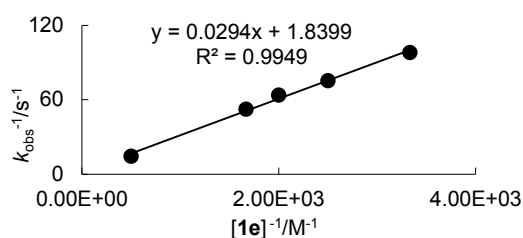
Table 2.93. Determination of the equilibrium constant of the reaction of 1e with 5b (DMSO, 20 °C, Stopped-flow method, detection at 388 nm).

No.	[5b]/M	[1e]$_0$/M	A_0	A_{eq}[a]	$(A_0 - A_{eq})/A_{eq}$
da72s5-1	2.00×10^{-5}	2.00×10^{-4}	1.11	0.866	0.305
da72s5-2	2.00×10^{-5}	3.00×10^{-4}	1.11	0.848	0.309
da72s5-3	2.00×10^{-5}	4.00×10^{-4}	1.11	0.798	0.391
da72s5-100	2.00×10^{-5}	2.00×10^{-3}	1.11	0.653	0.700
da72s5-110	2.00×10^{-5}	2.20×10^{-3}	1.11	0.634	0.751
da72s5-120	2.00×10^{-5}	2.40×10^{-3}	1.11	0.624	0.779
da72s5-130	2.00×10^{-5}	2.60×10^{-3}	1.11	0.592	0.875
K(20 °C) = 2×10^{2} M^{-1}					

[a] The equilibrium absorbances have been determined from the constant C obtained by fitting the monoexponential function $A = A_0 e^{-k_{obs} t} + C$ to the time-dependent absorbances.
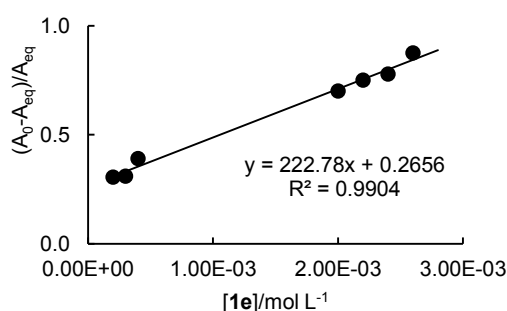
If the values $(A_0 - A_{eq})/A_{eq}$ obtained with the highest concentration of **1e** is divided by [**1e**], one obtains an equilibrium constant of $K = 3 \times 10^2$. The time at which the first spectrum was taken equals $t = 0$ s. Therefore [DABCO] $\neq 0$ M at $t = 0$ s.

Table 2.94. Kinetics of the reaction of 1e with 5c (DMSO, 20 °C, J&M method, detection at 523 nm).

No.	$[5c]$/mol L^{-1}	$[1e]$/mol L^{-1}	k_{obs}/s^{-1}
da72j5-1	1.88×10^{-5}	1.88×10^{-4}	1.65×10^{-4}
da72j5-2	1.85×10^{-5}	3.71×10^{-4}	2.13×10^{-4}
da72j5-3	1.85×10^{-5}	5.55×10^{-4}	2.51×10^{-4}
da72j5-4	1.84×10^{-5}	7.37×10^{-4}	3.25×10^{-4}
da72j5-5	1.83×10^{-5}	9.15×10^{-4}	3.59×10^{-4}
$K \cdot k_{rc}(20\ °C) = 2.75 \times 10^{-1}$ L mol^{-1} s^{-1}			

y = 0.2746x + 0.0001
R² = 0.988

Table 2.95. Kinetics of the reaction of 1e and 6 (DMSO, 20 °C, ^{1}H NMR method, evolution of DABCO followed; experimental procedure see Products Section).

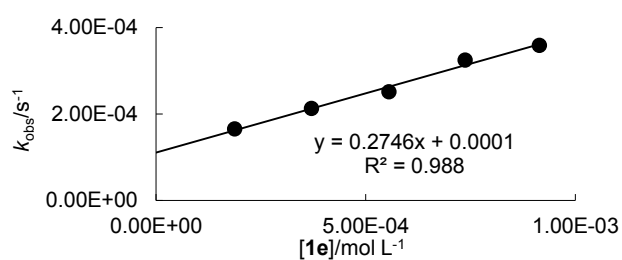| t/s	$[HO^tBu] = 5.08 \times 10^{-2}$ M	$[1e]_0 = 5.08 \times 10^{-2}$ M	$[6]_0 = 4.84 \times 10^{-2}$ M	
	$[DABCO]$/M	$[1e]$/M	$[6]$/M	$[1e]^{-1}$/M^{-1}
0	3.43×10^{-3}	4.74×10^{-2}	4.50×10^{-2}	2.22×10^{1}
6.60×10^{2}	4.28×10^{-3}	4.65×10^{-2}	4.41×10^{-2}	2.27×10^{1}
1.26×10^{3}	4.91×10^{-3}	4.59×10^{-2}	4.35×10^{-2}	2.30×10^{1}
4.56×10^{3}	8.13×10^{-3}	4.27×10^{-2}	4.03×10^{-2}	2.48×10^{1}
$K \cdot k_{rc}$ (20 °C) = 5.64×10^{-4} M^{-1} s^{-1}				

The time at which the first spectrum was taken equals $t = 0$ s. Therefore $[DABCO] \neq 0$ M at $t = 0$ s.

y = 5.64E-04x + 2.23E+01
R² = 1.00E+00
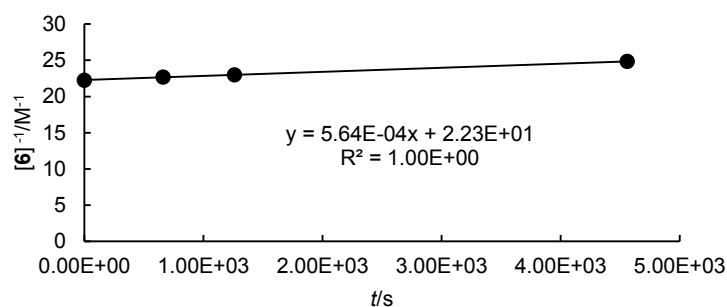
2.7.4.6 Kinetics of the Reactions of Ylide 1f

Table 2.96. Determination of the nucleophilicity parameters N and s_N for 1f with the electrophiles 2,3.

Electrophile	E	log k_2
2d-BF$_4$	-10.04	5.40
3b	-13.39	3.98
3c	-15.83	2.81
3d	-16.11	2.55
3e	-17.29	1.83
3f	-17.90	1.40

log k_2 = 0.5025 E + 10.579
R² = 0.9854

DABCO$^+$⌣CO$_2t$Bu

1f
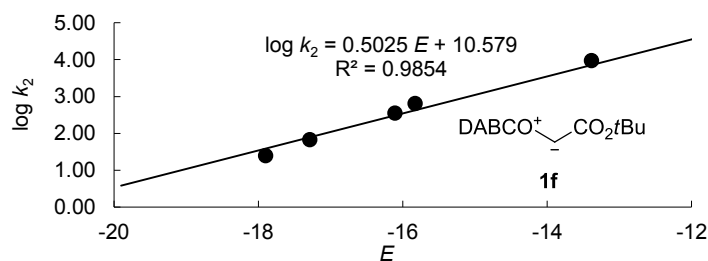
Nucleophilicity parameters for **1f** in DMSO: $N = 21.05$, $s_N = 0.50$.

Table 2.97. Kinetics of the reaction of 1f with 2d-BF$_4$ (DMSO, 20 °C, Stopped-flow method, detection at 630 nm).

No.	[2d-BF$_4$]/mol L^{-1}	[1f]/mol L^{-1}	k_{obs}/s^{-1}
da54s6-1	1.00×10^{-5}	1.00×10^{-4}	3.79×10^1
da54s6-2	1.00×10^{-5}	1.10×10^{-4}	3.96×10^1
da54s6-3	1.00×10^{-5}	1.20×10^{-4}	4.26×10^1
da54s6-4	1.00×10^{-5}	1.30×10^{-4}	4.53×10^1
k_2(20 °C) = 2.52×10^5 L mol^{-1} s^{-1}			

y = 252000x + 12.37
R² = 0.9882
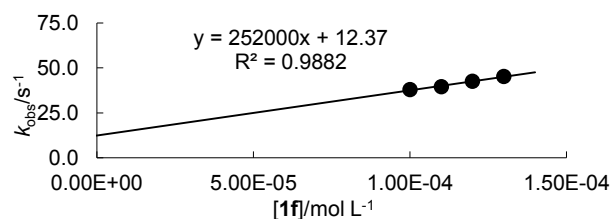
Table 2.98. Kinetics of the reaction of 1f with 3b (DMSO, 20 °C, Stopped-flow method, detection at 533 nm; from ref. [38]).

No.	[3b]/mol L^{-1}	[1f]/mol L^{-1}	k_{obs}/s^{-1}
da54s5-1	2.00×10^{-5}	2.00×10^{-4}	1.46
da54s5-2	2.00×10^{-5}	3.00×10^{-4}	2.07
da54s5-3	2.00×10^{-5}	4.00×10^{-4}	3.05
da54s5-4	2.00×10^{-5}	5.00×10^{-4}	4.06
da54s5-5	2.00×10^{-5}	6.00×10^{-4}	5.22
k_2(20 °C) = 9.51×10^3 L mol^{-1} s^{-1}			

y = 9510x - 0.632
R² = 0.9892

Table 2.99. Kinetics of the reaction of 1f with 3c (DMSO, 20 °C, Stopped-flow method, detection at 371 nm; from ref. [38]).

No.	[3c]/mol L^{-1}	[1f]/mol L^{-1}	k_{obs}/s^{-1}
da54s1-1	4.00×10^{-5}	8.00×10^{-4}	1.91×10^{-1}
da54s1-2	4.00×10^{-5}	1.20×10^{-3}	5.35×10^{-1}
da54s1-3	4.00×10^{-5}	1.60×10^{-3}	7.82×10^{-1}
da54s1-5	4.00×10^{-5}	2.40×10^{-3}	1.25
k_2(20 °C) = 6.49×10^2 L mol^{-1} s^{-1}			

y = 649.29x - 0.2844
R² = 0.9918
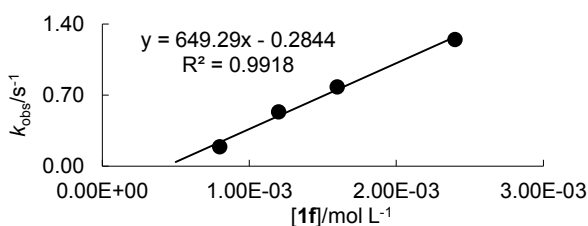
Table 2.100. Kinetics of the reaction of 1f with 3d (DMSO, 20 °C, Stopped-flow method, detection at 393 nm; from ref. [38]).

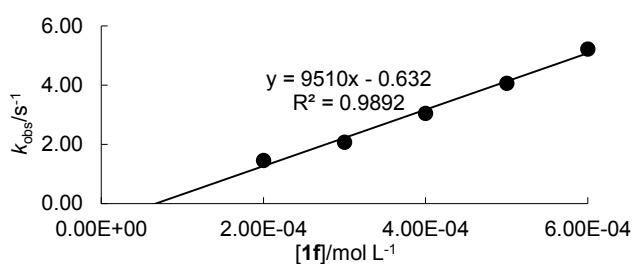| No.	[3d]/mol L^{-1}	[1f]/mol L^{-1}	k_{obs}/s^{-1}
da54s2-1	4.00×10^{-5}	8.00×10^{-4}	2.39×10^{-1}
da54s2-2	4.00×10^{-5}	1.20×10^{-3}	3.83×10^{-1}
da54s2-3	4.00×10^{-5}	1.60×10^{-3}	5.40×10^{-1}
da54s2-4	4.00×10^{-5}	2.00×10^{-3}	6.68×10^{-1}
da54s2-5	4.00×10^{-5}	2.40×10^{-3}	8.58×10^{-1}
k_2(20 °C) = 3.81×10^2 L mol^{-1} s^{-1}			

y = 380.75x - 0.0716
R² = 0.9967
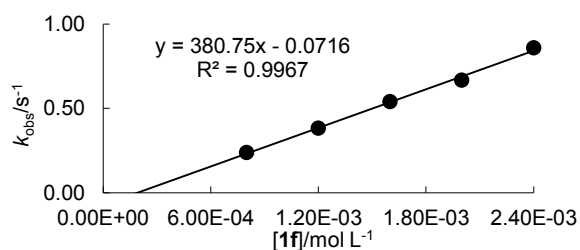
Table 2.101. Kinetics of the reaction of 1f with 3e (DMSO, 20 °C, Stopped-flow method, detection at 486 nm; from ref. [38]).

No.	[3e]/mol L^{-1}	[1f]/mol L^{-1}	k_{obs}/s^{-1}
da54s3-1	4.00×10^{-5}	1.20×10^{-3}	6.68×10^{-2}
da54s3-2	4.00×10^{-5}	1.60×10^{-3}	9.65×10^{-2}
da54s3-3	4.00×10^{-5}	2.00×10^{-3}	1.24×10^{-1}
da54s3-4	4.00×10^{-5}	2.40×10^{-3}	1.54×10^{-1}
da54s3-5	4.00×10^{-5}	2.80×10^{-3}	1.74×10^{-1}
$k_2(20\,°C) = 6.80 \times 10^1$ L mol^{-1} s^{-1}			

$y = 67.975x - 0.0129$
$R^2 = 0.9959$
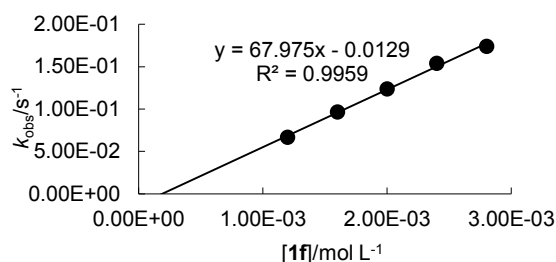
Table 2.102. Kinetics of the reaction of 1f with 3f (DMSO, 20 °C, Stopped-flow method, detection at 521 nm; from ref. [38]).

No.	[3f]/mol L^{-1}	[1f]/mol L^{-1}	k_{obs}/s^{-1}
da54s4-1	2.00×10^{-5}	1.60×10^{-3}	4.40×10^{-2}
da54s4-2	2.00×10^{-5}	2.40×10^{-3}	7.32×10^{-2}
da54s4-3	2.00×10^{-5}	3.20×10^{-3}	8.55×10^{-2}
da54s4-4	2.00×10^{-5}	4.00×10^{-3}	1.08×10^{-2}
da54s4-5	2.00×10^{-5}	4.80×10^{-3}	1.26×10^{-2}
$k_2(20\,°C) = 2.49 \times 10^1$ L mol^{-1} s^{-1}			

$y = 24.85x + 0.0078$
$R^2 = 0.9873$
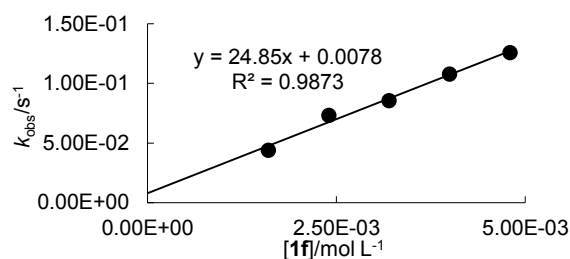
2.7.4.7 Kinetics of the Reactions of Ylide 1g

Table 2.103. Determination of the nucleophilicity parameters N and s_N for 1g with the electrophiles 2,3 (filled dots). Open dot refers to the reaction with 4d and was not used for the determination of N and s_N.

Electrophile	E	$\log k_2$
2d-BF$_4$	-10.04	5.86
3a	-12.18	4.83
3b	-13.39	3.80
3c	-15.83	2.54
4d	-21.11	-0.66

Nucleophilicity parameters for **1g**
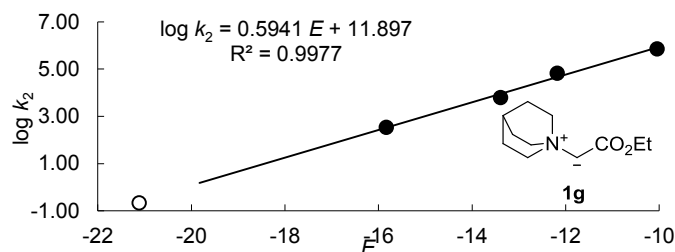
in DMSO $N = 20.14$, $s_N = 0.59$.

$\log k_2 = 0.5941\,E + 11.897$
$R^2 = 0.9977$

Table 2.104. Kinetics of the reaction of 1g with 2d-BF$_4$ (DMSO, 20 °C, Stopped-flow method, detection at 630 nm).

| No.	[2d-BF$_4$]/mol L^{-1}	[1g]/mol L^{-1}	k_{obs}/s^{-1}
da78s4-1	5.00×10^{-6}	1.00×10^{-4}	3.37×10^1
da78s4-2	5.00×10^{-6}	1.10×10^{-4}	3.95×10^1
da78s4-3	5.00×10^{-6}	1.20×10^{-4}	4.69×10^1
da78s4-4	5.00×10^{-6}	1.30×10^{-4}	5.46×10^1
da78s4-5	5.00×10^{-6}	1.40×10^{-4}	6.27×10^1
$k_2(20\,°C) = 7.31 \times 10^5$ L mol^{-1} s^{-1}			

$y = 731000x - 40.24$
$R^2 = 0.9965$

Table 2.105. Kinetics of the reaction of 1g with 3a (DMSO, 20 °C, Stopped-flow method, detection at 422 nm; from ref. [38]).

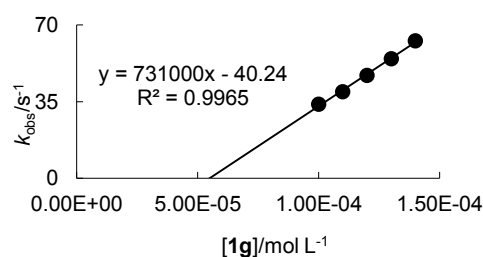| No.	[3a]/mol L^{-1}	[1g]/mol L^{-1}	k_{obs}/s^{-1}
da78s1-1	4.00×10^{-5}	4.00×10^{-4}	2.52×10^1
da78s1-2	4.00×10^{-5}	8.00×10^{-4}	5.51×10^1
da78s1-3	4.00×10^{-5}	1.20×10^{-3}	8.33×10^1
da78s1-4	4.00×10^{-5}	1.60×10^{-3}	1.11×10^2
da78s1-5	4.00×10^{-5}	2.00×10^{-3}	1.34×10^2
$k_2(20 °C) = 6.84 \times 10^4$ L mol^{-1} s^{-1}			

y = 68375x - 0.33
R² = 0.9979

Table 2.106. Kinetics of the reaction of 1g with 3b (DMSO, 20 °C, Stopped-flow method, detection at 533 nm; from ref. [38]).

No.	[3b]/mol L^{-1}	[1g]/mol L^{-1}	k_{obs}/s^{-1}
da78s2-1	4.00×10^{-5}	4.00×10^{-4}	2.07
da78s2-2	4.00×10^{-5}	8.00×10^{-4}	4.34
da78s2-3	4.00×10^{-5}	1.20×10^{-3}	6.77
da78s2-4	4.00×10^{-5}	1.60×10^{-3}	9.41
da78s2-5	4.00×10^{-5}	2.00×10^{-3}	1.22×10^1
$k_2(20 °C) = 6.33 \times 10^3$ L mol^{-1} s^{-1}			

y = 6332.5x - 0.641
R² = 0.9983

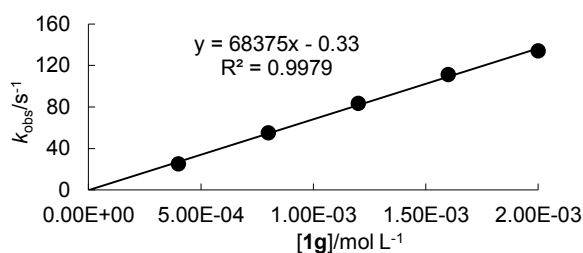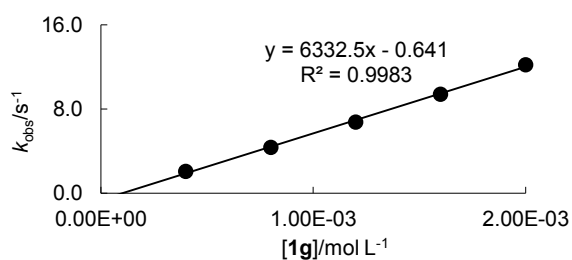**Table 2.107. Kinetics of the reaction of 1g with 3c (DMSO, 20 °C, Stopped-flow method, detection at 371 nm; from ref. [38]).**

No.	[3c]/mol L^{-1}	[1g]/mol L^{-1}	k_{obs}/s^{-1}
da78s3-1	8.00×10^{-5}	8.00×10^{-4}	1.69×10^{-1}
da78s3-2	8.00×10^{-5}	1.60×10^{-3}	4.95×10^{-1}
da78s3-3	8.00×10^{-5}	2.40×10^{-3}	7.74×10^{-1}
da78s3-4	8.00×10^{-5}	3.20×10^{-3}	9.84×10^{-1}
da78s3-5	8.00×10^{-5}	3.50×10^{-3}	1.15
$k_2(20 °C) = 3.49 \times 10^2$ L mol^{-1} s^{-1}			

y = 348.6x - 0.0874
R² = 0.9935
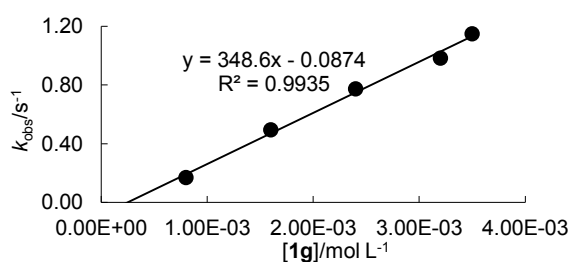
The kinetics of the reaction of **1g** with **4d** were monitored by GC as outlined on in the General Section with concentrations of $[\mathbf{1g}]_0 = 5.72 \times 10^{-2}$ mol L^{-1} and $[\mathbf{4d}]_0 = 3.81 \times 10^{-2}$ mol L^{-1}. The deviations between the experimental and calculated concentrations are a result of the uncertainty of the method.

Table 2.108. Experimental ($[\mathbf{4d}]^{exp}$) and calculated ($[\mathbf{4d}]^{calcd}$) decrease of the time-dependent concentrations of 4d during the reaction of 1g with 4d (DMSO, 20 °C, GC-method).

t/s	$[\mathbf{4d}]^{exp}$/mol L^{-1}	$[\mathbf{4d}]^{calc}$/ mol L^{-1}	$\Delta[\mathbf{4d}]^{exp\text{-}calcd}$
0	3.80×10^{-2}	3.80×10^{-2}	0
60	3.04×10^{-2}	2.06×10^{-2}	9.74×10^{-3}
120	1.40×10^{-2}	1.30×10^{-2}	1.01×10^{-3}
180	4.20×10^{-3}	8.84×10^{-3}	-4.64×10^{-3}
240	1.05×10^{-3}	6.27×10^{-3}	-5.22×10^{-3}
300	1.07×10^{-3}	4.56×10^{-3}	-3.50×10^{-3}
360	6.29×10^{-4}	3.39×10^{-3}	-2.76×10^{-3}
$k_2(20\ °C) = 2.2 \times 10^{-1}$ L mol^{-1} s^{-1}			
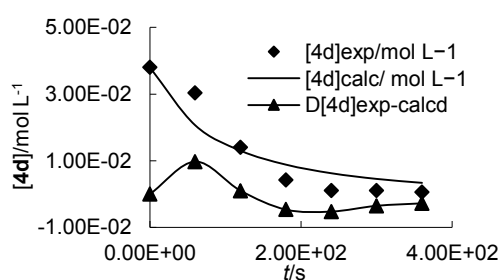
Table 2.109. Experimental ($[\mathbf{11gd}]^{exp}$) and calculated ($[\mathbf{11gd}]^{calcd}$) increase of the time-dependent concentrations of 11gd during the reaction of 1h with 4d (DMSO, 20 °C, GC-method).

t/s	$[\mathbf{11gd}]^{exp}$/mol L^{-1}	$[\mathbf{11gd}]^{calc}$/ mol L^{-1}	$\Delta[\mathbf{11gd}]^{exp\text{-}calcd}$
0	0	0	0
60	7.62×10^{-3}	1.76×10^{-2}	-1.00×10^{-2}
120	2.40×10^{-2}	2.52×10^{-2}	-1.27×10^{-3}
180	3.38×10^{-2}	2.94×10^{-2}	4.41×10^{-3}
240	3.70×10^{-2}	3.19×10^{-2}	5.02×10^{-3}
300	3.69×10^{-2}	3.36×10^{-2}	3.33×10^{-3}
360	3.74×10^{-2}	3.48×10^{-2}	2.62×10^{-3}
$k_2(20\ °C) = 2.2 \times 10^{-1}$ L mol^{-1} s^{-1}			
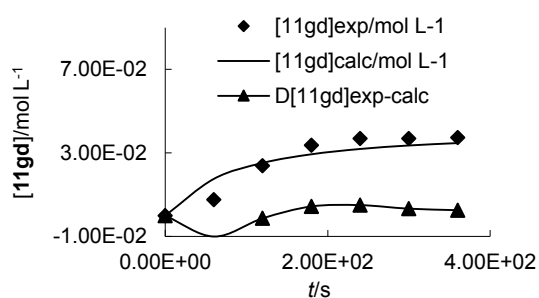
2.7.4.8 Kinetics of the Reactions of Ylide 1h

Table 2.110. Determination of the nucleophilicity parameters N and s_N for 1h with the electrophiles 2−4 (filled dots). Open dot refers to the reaction with 4d and was not used for the determination of N and s_N.

Electrophile	E	$\log k_2$
2c-BF$_4$	-9.45	5.84
2d-BF$_4$	-10.04	5.83
3a	-12.18	4.85
3b	-13.39	4.05
3c	-15.83	2.83
3d	-16.11	2.67
3e	-17.29	1.90
3f	-17.90	1.64
4a	-17.67	1.64
4d	-21.11	-0.70

$\log k_2 = 0.5234\,E + 11.025$
$R^2 = 0.9939$

$Me_3N^+\!\!-\!\!CO_2Et$

1h
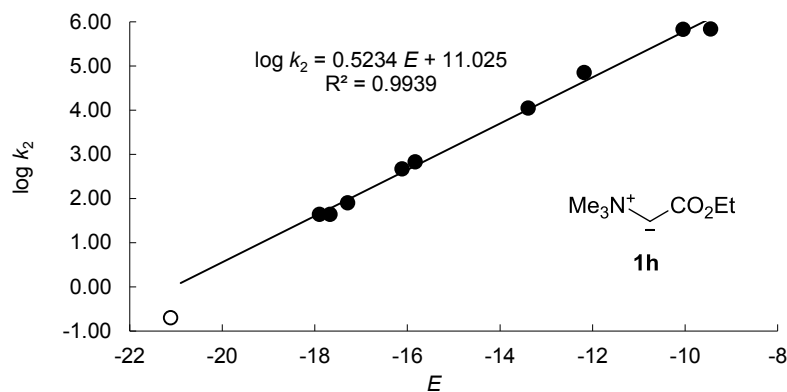
Nucleophilicity parameters for **1h** in DMSO: $N = 21.06$, $s_N = 0.52$.

Table 2.111. Kinetics of the reaction of 1h with 2c-BF$_4$ (DMSO, 20 °C, Stopped-flow method, detection at 635 nm).
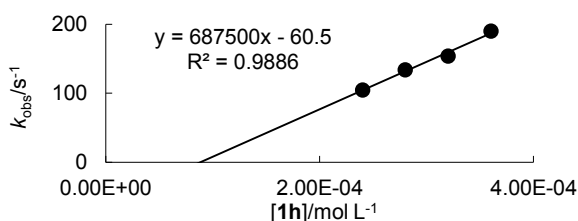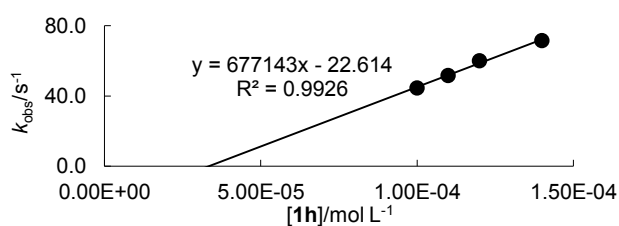
No.	[2c-BF$_4$]/mol L^{-1}	[1h]/mol L^{-1}	k_{obs}/s^{-1}
da96s2-2	2.00×10^{-5}	2.40×10^{-4}	1.05×10^2
da96s2-3	2.00×10^{-5}	2.80×10^{-4}	1.34×10^2
da96s2-4	2.00×10^{-5}	3.20×10^{-4}	1.54×10^2
da96s2-5	2.00×10^{-5}	3.60×10^{-4}	1.90×10^2
k_2(20 °C) = 6.88×10^5 L mol^{-1} s^{-1}			

$y = 687500x - 60.5$
$R^2 = 0.9886$

Table 2.112. Kinetics of the reaction of 1h with 2d-BF$_4$ (DMSO, 20 °C, Stopped-flow method, detection at 630 nm).

No.	[2d-BF$_4$]/mol L^{-1}	[1h]/mol L^{-1}	k_{obs}/s^{-1}
da96s7-1	5.00×10^{-6}	1.00×10^{-4}	4.45×10^1
da96s7-2	5.00×10^{-6}	1.10×10^{-4}	5.17×10^1
da96s7-3	5.00×10^{-6}	1.20×10^{-4}	6.01×10^1
da96s7-5	5.00×10^{-6}	1.40×10^{-4}	7.15×10^1
k_2(20 °C) = 6.77×10^5 L mol^{-1} s^{-1}			

$y = 677143x - 22.614$
$R^2 = 0.9926$

Table 2.113. Kinetics of the reaction of 1h with 3a (DMSO, 20 °C, Stopped-flow method, detection at 422 nm).

No.	[3a]/mol L^{-1}	[1h]/mol L^{-1}	k_{obs}/s^{-1}
da96s6-1	2.00×10^{-5}	2.00×10^{-4}	1.28×10^1
da96s6-2	2.00×10^{-5}	3.00×10^{-4}	2.02×10^1
da96s6-3	2.00×10^{-5}	4.00×10^{-4}	2.74×10^1
da96s6-4	2.00×10^{-5}	5.00×10^{-4}	3.47×10^1
da96s6-5	2.00×10^{-5}	6.00×10^{-4}	4.13×10^1
k_2(20 °C) = 7.15×10^4 L mol^{-1} s^{-1}			

$y = 71500x - 1.32$
$R^2 = 0.9996$

Table 2.114. Kinetics of the reaction of 1h with 3b (DMSO, 20 °C, Stopped-flow method, detection at 533 nm).

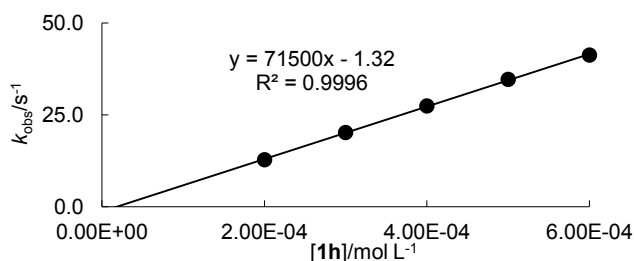| No.	$[3b]/mol\ L^{-1}$	$[1h]/mol\ L^{-1}$	k_{obs}/s^{-1}
da96s1-1	2.00×10^{-5}	2.00×10^{-4}	1.21
da96s1-2	2.00×10^{-5}	4.00×10^{-4}	4.27
da96s1-3	2.00×10^{-5}	6.00×10^{-4}	5.40
da96s1-4	2.00×10^{-5}	8.00×10^{-4}	8.29
da96s1-5	2.00×10^{-5}	1.00×10^{-3}	1.04×10^{1}
$k_2(20\ °C) = 1.12 \times 10^4\ L\ mol^{-1}\ s^{-1}$			

y = 11200x - 0.806
R² = 0.9865

Table 2.115. Kinetics of the reaction of 1h with 3c (DMSO, 20 °C, Stopped-flow method, detection at 371 nm).

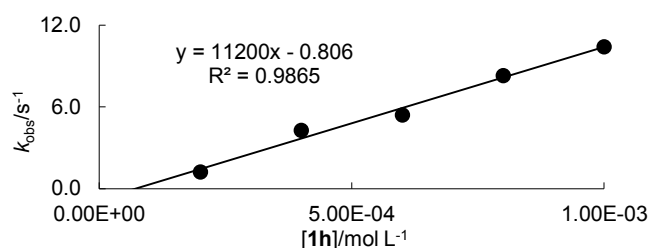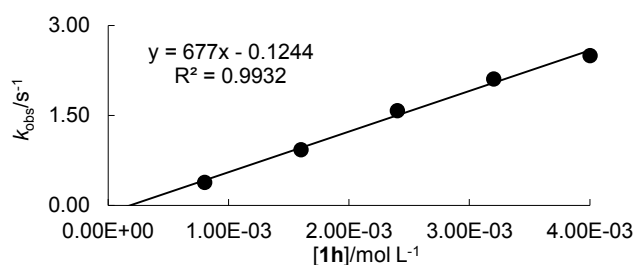| No.	$[3c]/mol\ L^{-1}$	$[1h]/mol\ L^{-1}$	k_{obs}/s^{-1}
da96s3-1	4.00×10^{-5}	8.00×10^{-4}	3.82×10^{-1}
da96s3-2	4.00×10^{-5}	1.60×10^{-3}	$9.30 \times 10^{-}$
da96s3-3	4.00×10^{-5}	2.40×10^{-3}	1.58
da96s3-4	4.00×10^{-5}	3.20×10^{-3}	2.11
da96s3-5	4.00×10^{-5}	4.00×10^{-3}	2.50
$k_2(20\ °C) = 6.77 \times 10^2\ L\ mol^{-1}\ s^{-1}$			

y = 677x - 0.1244
R² = 0.9932

Table 2.116. Kinetics of the reaction of 1h with 3d (DMSO, 20 °C, Stopped-flow method, detection at 393 nm).

No.	$[3d]/mol\ L^{-1}$	$[1h]/mol\ L^{-1}$	k_{obs}/s^{-1}
da96s4-1	2.00×10^{-5}	4.00×10^{-4}	1.17×10^{-1}
da96s4-3	2.00×10^{-5}	8.00×10^{-4}	3.53×10^{-1}
da96s4-4	2.00×10^{-5}	1.00×10^{-3}	4.23×10^{-1}
da96s4-5	2.00×10^{-5}	1.20×10^{-3}	4.87×10^{-1}
$k_2(20\ °C) = 4.67 \times 10^2\ L\ mol^{-1}\ s^{-1}$			

y = 467.43x - 0.0523
R² = 0.9767
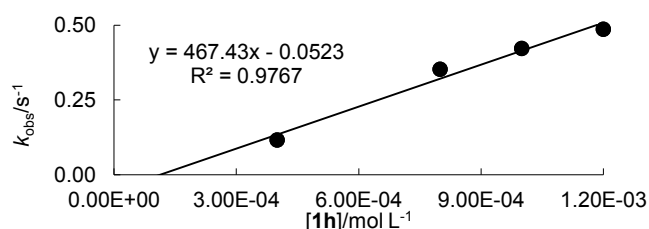
Table 2.117. Kinetics of the reaction of 1h with 3e (DMSO, 20 °C, Stopped-flow method, detection at 486 nm).

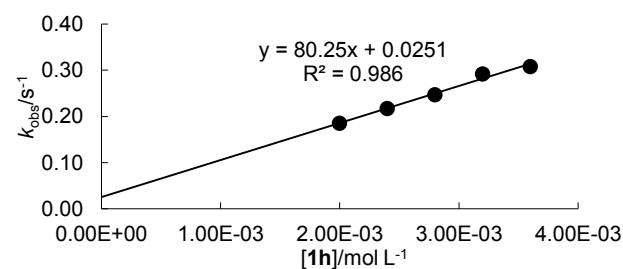| No.	$[3e]/mol\ L^{-1}$	$[1h]/mol\ L^{-1}$	k_{obs}/s^{-1}
da96s5r-1	2.00×10^{-5}	2.00×10^{-3}	1.85×10^{-1}
da96s5r-2	2.00×10^{-5}	2.40×10^{-3}	2.17×10^{-1}
da96s5r-3	2.00×10^{-5}	2.80×10^{-3}	2.47×10^{-1}
da96s5r-4	2.00×10^{-5}	3.20×10^{-3}	2.92×10^{-1}
da96s5r-5	2.00×10^{-5}	3.60×10^{-3}	3.08×10^{-1}
$k_2(20\ °C) = 8.03 \times 10^1\ L\ mol^{-1}\ s^{-1}$			

y = 80.25x + 0.0251
R² = 0.986

Table 2.118. Kinetics of the reaction of 1h with 3f (DMSO, 20 °C, Stopped-flow method, detection at 521 nm).

| No.	$[3f]$/mol L^{-1}	$[1h]$/mol L^{-1}	k_{obs}/s^{-1}
da96j1-3	3.95×10^{-5}	3.95×10^{-4}	1.23×10^{-2}
da96j1-1	4.24×10^{-5}	4.24×10^{-4}	1.42×10^{-2}
da96j1-4	4.06×10^{-5}	6.09×10^{-4}	2.40×10^{-2}
da96j1-5	4.06×10^{-5}	1.02×10^{-3}	4.00×10^{-2}
da96j1-2	4.16×10^{-5}	1.25×10^{-3}	5.04×10^{-2}
$k_2(20\ °C) = 4.37 \times 10^1$ L mol^{-1} s^{-1}			
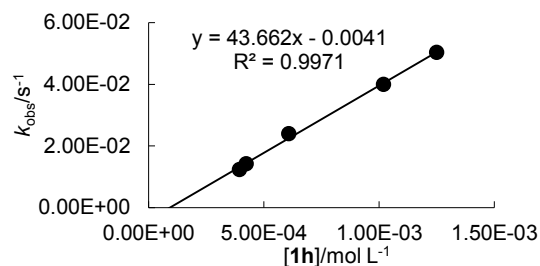
The for the determination of the pseudo first-order rate constants of the reaction of **1h** with **4a** the decrease of the absorption of **4a** at 302 nm and the increases of the absorption of **10ha** at 263 and 446 nm were monitored by UV-Vis spectroscopy.

Table 2.119. Kinetics of the reaction of 1h with 4a (DMSO, 20 °C, J&M method, detection at 302 nm).

No.	$[4a]$/mol L^{-1}	$[1h]$/mol L^{-1}	k_{obs}/s^{-1}
da96j2-1	4.12×10^{-5}	4.24×10^{-4}	1.75×10^{-2}
da96j2-2	4.09×10^{-5}	6.13×10^{-4}	2.80×10^{-2}
da96j2-3	3.90×10^{-5}	7.80×10^{-4}	3.65×10^{-2}
da96j2-4	4.05×10^{-5}	1.01×10^{-3}	4.44×10^{-2}
da96j2-5	4.10×10^{-5}	1.23×10^{-3}	5.38×10^{-2}
$k_2(20\ °C) = 4.36 \times 10^1$ L mol^{-1} s^{-1}			
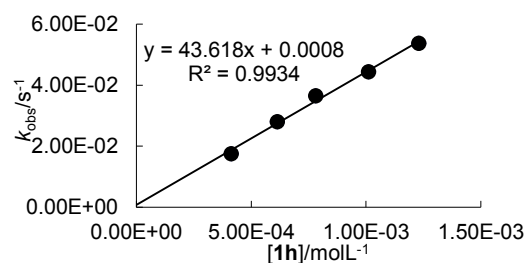
Table 2.120. Kinetics of the reaction of 1h with 4a (DMSO, 20 °C, J&M method, detection at 263 nm).

No.	$[4a]$/mol L^{-1}	$[1h]$/mol L^{-1}	k_{obs}/s^{-1}
da96j2-1	4.12×10^{-5}	4.24×10^{-4}	2.12×10^{-2}
da96j2-2	4.09×10^{-5}	6.13×10^{-4}	3.45×10^{-2}
da96j2-3	3.90×10^{-5}	7.80×10^{-4}	4.53×10^{-2}
da96j2-4	4.05×10^{-5}	1.01×10^{-3}	5.88×10^{-2}
da96j2-5	4.10×10^{-5}	1.23×10^{-3}	7.40×10^{-2}
$k_2(20\ °C) = 6.38 \times 10^1$ L mol^{-1} s^{-1}			
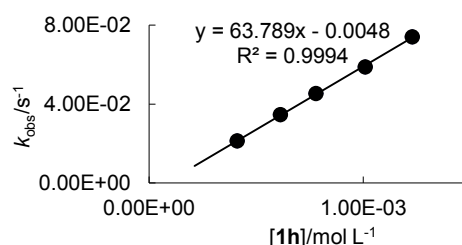
The deviation between the rate constant of the consumption of **4a** (302 nm, see above) and the formation of **10ha** (263 nm) may be caused by an absorption overlap.

Table 2.121. Kinetics of the reaction of 1h with 4a (DMSO, 20 °C, J&M method, detection at 446 nm).

No.	$[4a]$/mol L^{-1}	$[1h]$/mol L^{-1}	k_{obs}/s^{-1}
da96j2-1	4.12×10^{-5}	4.24×10^{-4}	1.95×10^{-2}
da96j2-2	4.09×10^{-5}	6.13×10^{-4}	3.05×10^{-2}
da96j2-3	3.90×10^{-5}	7.80×10^{-4}	3.99×10^{-2}
da96j2-4	4.05×10^{-5}	1.01×10^{-3}	4.81×10^{-2}
da96j2-5	4.10×10^{-5}	1.23×10^{-3}	5.57×10^{-2}
$k_2(20\ °C) = 4.40 \times 10^1$ L mol^{-1} s^{-1}			

137
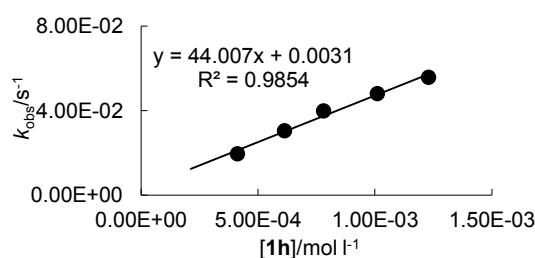
Table 2.122. Kinetics of the formation of 11ha (DMSO, 20 °C, J&M method, detection at 270 nm).

| No.	$[\textbf{4a}]$/mol L^{-1}	$[\textbf{1h}]$/mol L^{-1}	k_{obs}/s^{-1}
da96j3-2	4.22×10^{-5}	6.33×10^{-4}	9.10×10^{-4}
da96j3-3	4.02×10^{-5}	8.03×10^{-4}	9.07×10^{-4}
da96j3-4	4.18×10^{-5}	1.05×10^{-3}	9.10×10^{-4}
$k_{rc}(20\ °C) = 9.10 \times 10^{-4}$ s^{-1}			
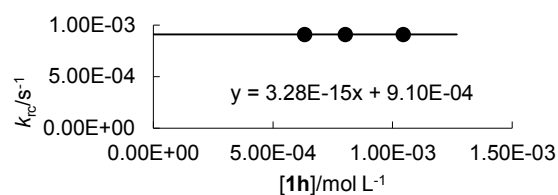
The kinetics of the reaction of **1h** with **4d** were monitored by GC as outlined on in the General Section with concentrations of $[\textbf{1h}]_0 = 5.72 \times 10^{-2}$ mol L^{-1} and $[\textbf{4d}]_0 = 3.81 \times 10^{-2}$ mol L^{-1}. The deviations between the experimental and calculated concentrations are a result of the uncertainty of the method.

**Table 2.123. Experimental ($[\textbf{4d}]^{exp}$) and calculated ($[\textbf{4d}]^{calcd}$) decrease of the time-dependent concentrations of 4d during the reaction of 1h with 4d (DMSO, 20 °C, GC-method).**

| t/s	$[\textbf{4d}]^{exp}$/mol L^{-1}	$[\textbf{4d}]^{calc}$/ mol L^{-1}	$\Delta[\textbf{4d}]^{exp-calcd}$
0	3.80×10^{-2}	3.80×10^{-2}	0
60	1.84×10^{-2}	2.13×10^{-2}	-2.90×10^{-3}
120	4.64×10^{-3}	1.37×10^{-2}	-9.09×10^{-3}
180	1.25×10^{-3}	9.47×10^{-3}	-8.22×10^{-3}
240	8.60×10^{-4}	6.81×10^{-3}	-5.95×10^{-3}
300	4.92×10^{-4}	5.03×10^{-3}	-4.54×10^{-3}
360	4.23×10^{-4}	3.78×10^{-3}	-3.36×10^{-3}
420	2.35×10^{-4}	2.88×10^{-3}	-2.65×10^{-3}
$k_2(20\ °C) = 2.0 \times 10^{-1}$ L mol^{-1} s^{-1}			
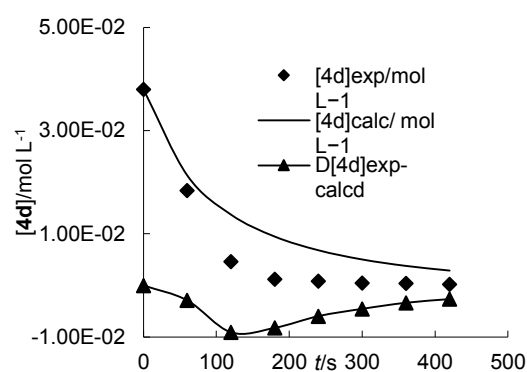
Table 2.124. Experimental ($[\textbf{11hd}]^{exp}$) and calculated ($[\textbf{11hd}]^{calcd}$) increase of the time-dependent concentrations of 11hd during the reaction of 1h with 4d (DMSO, 20 °C, GC-method).

| t/s	$[\textbf{11hd}]^{exp}$/mol L^{-1}	$[\textbf{11hd}]^{calc}$/ mol L^{-1}	$\Delta[\textbf{11hd}]^{exp-calcd}$
0	0	0	0
60	1.96×10^{-2}	2.41×10^{-2}	-4.47×10^{-3}
120	3.34×10^{-2}	3.10×10^{-2}	2.35×10^{-3}
180	3.68×10^{-2}	3.41×10^{-2}	2.66×10^{-3}
240	3.71×10^{-2}	3.57×10^{-2}	1.45×10^{-3}
300	3.75×10^{-2}	3.66×10^{-2}	9.12×10^{-4}
360	3.76×10^{-2}	3.71×10^{-2}	4.45×10^{-4}
420	3.78×10^{-2}	3.75×10^{-2}	3.08×10^{-4}
$k_2(20\ °C) = 4.0 \times 10^{-1}$ L mol^{-1} s^{-1}			
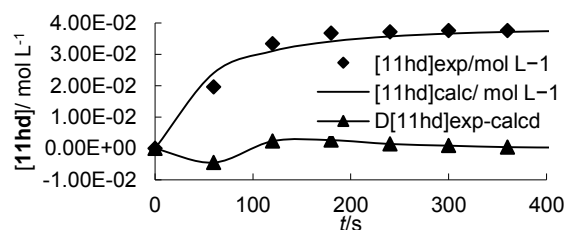
2.7.4.9 Kinetics of the Reactions of Ylide 1i
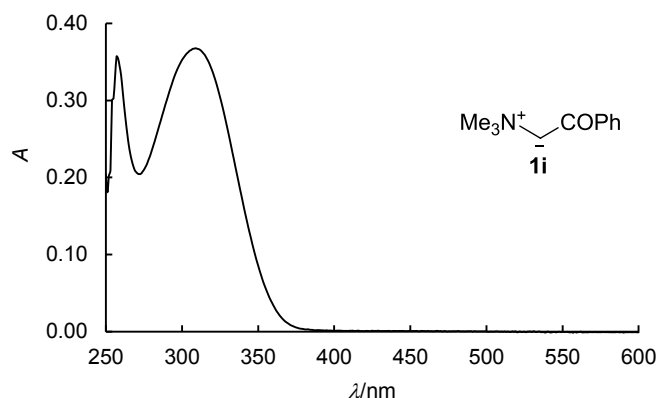
Figure 2.26. Absorption spectrum of 1i (λ_{max} = 257, 307 nm).

Table 2.125. Determination of the nucleophilicity parameters N and s_N for 1i with the electrophiles 2,3 (filled dots). Open dot refers to the reaction with 5b and was not used for the determination of N and s_N.

Electrophile	E	$\log k_2$
2c-BF$_4$	−9.45	4.61
2d-BF$_4$	−10.04	4.51
3b	−13.39	2.35
5b	−11.32	3.49

Nucleophilicity parameters for **1i**

in DMSO: N = 17.36; s_N = 0.60.
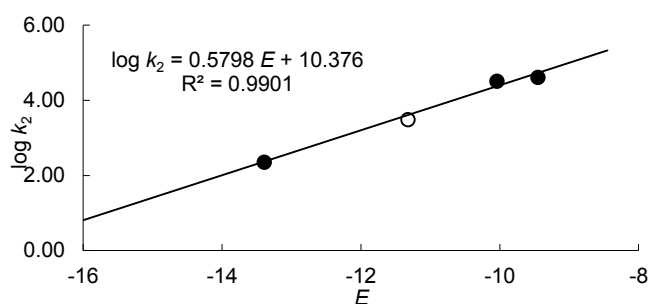
Table 2.126. Kinetics of the reaction of 1i with 2c-BF$_4$ (DMSO, 20 °C, Stopped-flow method, detection at 635 nm).

No.	[2c-BF$_4$]/mol L^{-1}	[1i]/mol L^{-1}	k_{obs}/s^{-1}
da95s1-1	2.00×10^{-5}	3.00×10^{-4}	4.00×10^{1}
da95s1-2	2.00×10^{-5}	4.00×10^{-4}	4.33×10^{1}
da95s1-4	2.00×10^{-5}	6.00×10^{-4}	5.30×10^{1}
da95s1-5	2.00×10^{-5}	7.00×10^{-4}	5.56×10^{1}
da95s1-3	2.00×10^{-5}	8.00×10^{-4}	6.02×10^{1}
	k_2(20 °C) = 4.08×10^4 L mol^{-1} s^{-1}		
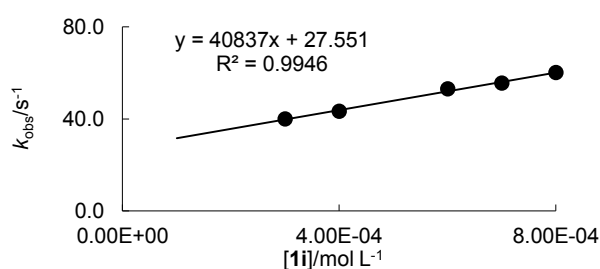
Table 2.127. Kinetics of the reaction of 1i with 2d-BF$_4$ (DMSO, 20 °C, Stopped-flow method, detection at 630 nm).

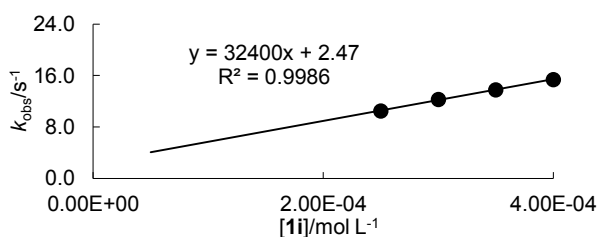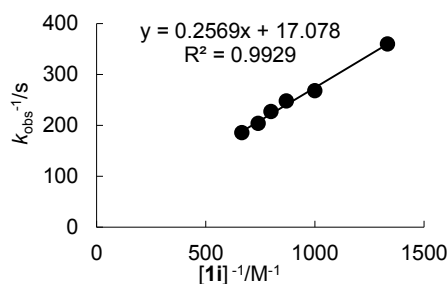| No.	[2d-BF$_4$]/mol L^{-1}	[1i]/mol L^{-1}	k_{obs}/s^{-1}
da95s2-1	1.00×10^{-5}	2.50×10^{-4}	1.05×10^{1}
da95s2-2	1.00×10^{-5}	3.00×10^{-4}	1.23×10^{1}
da95s2-3	1.00×10^{-5}	3.50×10^{-4}	1.38×10^{1}
da95s2-4	1.00×10^{-5}	4.00×10^{-4}	1.54×10^{1}
	k_2(20 °C) = 3.24×10^4 L mol^{-1} s^{-1}		

139

Table 2.128. Kinetics of the reaction of 1i with 3b (DMSO, 20 °C, Stopped-flow method, detection at 533 nm).

No.	[3b]/mol L^{-1}	[1i]/mol L^{-1}	k_{obs}/s^{-1}
da95s4-1	1.00×10^{-5}	2.50×10^{-4}	1.70
da95s4-3	1.00×10^{-5}	7.50×10^{-4}	1.78
da95s4-4	1.00×10^{-5}	1.00×10^{-3}	1.87
da95s4-6	1.00×10^{-5}	1.25×10^{-3}	1.92
da95s4-7	1.00×10^{-5}	1.35×10^{-3}	1.94
da95s4-8	1.00×10^{-5}	1.50×10^{-3}	1.97
k_2(20 °C) = 2.25×10^3 L mol^{-1} s^{-1}			

y = 224.57x + 1.635
R² = 0.9859
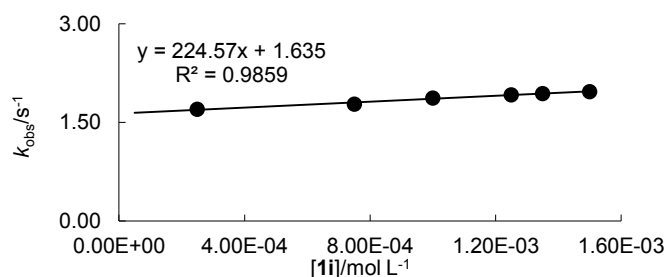
Table 2.129.Kinetics of the formation of 9ib (DMSO, 20 °C, Stopped flow method, detection at 533 nm).

No.	[3b]/M	[1i]/M	k_{obs}/s^{-1}	[1i]$^{-1}$/M^{-1}	$k_{obs}$$^{-1}$/s
da95s4-3	1.00×10^{-5}	7.50×10^{-4}	2.78×10^{-3}	1.33×10^3	3.60×10^2
da95s4-4	1.00×10^{-5}	1.00×10^{-3}	3.81×10^{-3}	1.00×10^3	2.68×10^2
da95s4-5	1.00×10^{-5}	1.15×10^{-3}	4.03×10^{-3}	8.70×10^2	2.48×10^2
da95s4-6	1.00×10^{-5}	1.25×10^{-3}	4.40×10^{-3}	8.00×10^2	2.27×10^2
da95s4-7	1.00×10^{-5}	1.35×10^{-3}	4.91×10^{-3}	7.41×10^2	2.04×10^2
da95s4-8	1.00×10^{-5}	1.50×10^{-3}	5.39×10^{-3}	6.67×10^2	1.86×10^2
$1/K \cdot k_{rc}$ = 2.57×10^{-1} => $K \cdot k_{rc}$(20 °C) = 3.89 L mol^{-1} s^{-1}					

y = 0.2569x + 17.078
R² = 0.9929

Table 2.130. Reproduction of the kinetics of the formation of 9ib (DMSO, 20 °C, J&M method, detection at 533 nm).

No.	[3b]/mol L^{-1}	[1i]/mol L^{-1}	k_{obs}/s^{-1}
da95j1-2	1.79×10^{-5}	3.58×10^{-4}	1.16×10^{-3}
da95j1-3	1.83×10^{-5}	5.49×10^{-4}	1.92×10^{-3}
da95j1-4	1.81×10^{-5}	7.25×10^{-4}	2.44×10^{-3}
da95j1-5	1.83×10^{-5}	9.15×10^{-4}	2.90×10^{-3}
$K \cdot k_{rc}$(20 °C) ≈ (3.1×10^{-1} L mol^{-1} s^{-1})			

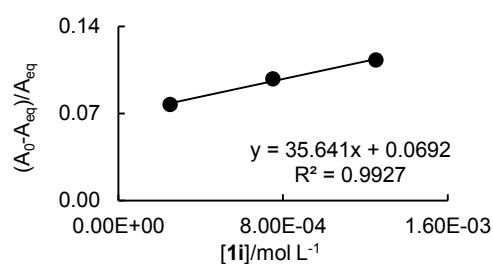

y = 3.1144x + 0.0001
R² = 0.9868

Evaluated by plotting k_{obs} versus as the evaluation according to eq 9 gave a poor fit.

Table 2.131. Determination of the equilibrium constant of the reaction of 1i with 3b (DMSO, 20 °C, Stopped-flow method, detection at 533 nm).

No.	[3b]/mol L^{-1}	[1e]/mol L^{-1}	A_0	A_{eq}[a]	$(A_0 - A_{eq})/A_{eq}$
da95s4-1	1.00×10^{-5}	2.50×10^{-4}	0.489	0.453	0.077
da95s4-3	1.00×10^{-5}	7.50×10^{-4}	0.487	0.440	0.098
da95s4-6	1.00×10^{-5}	1.25×10^{-3}	0.483	0.434	0.113
		$K(20 °C) = 4 \times 10^1$ L mol^{-1}			

[a] The equilibrium absorbances have been determined from the constant C obtained by fitting the monoexponential function $A = A_0 e^{-k_{obs} t} + C$ to the time-dependent absorbances.
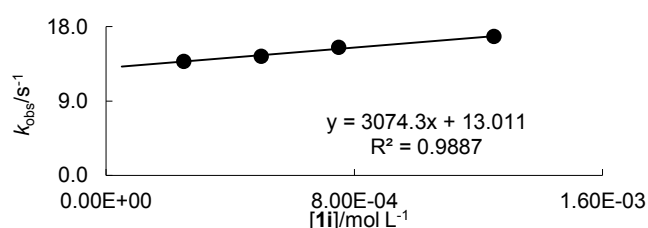

If the values $(A_0 - A_{eq})/A_{eq}$ obtained with the highest concentration of **1e** is divided by [**1e**], one obtains an equilibrium constant of $K = 9 \times 10^1$.

Table 2.132. Kinetics of the reaction of 1i with 5b (DMSO, 20 °C, Stopped-flow method, detection at 388 nm).

No.	[5b]/mol L^{-1}	[1i]/mol L^{-1}	k_{obs}/s^{-1}
da95s3-1	2.00×10^{-5}	2.50×10^{-4}	1.38×10^1
da95s3-2	2.00×10^{-5}	5.00×10^{-4}	1.44×10^1
da95s3-3	2.00×10^{-5}	7.50×10^{-4}	1.55×10^1
da95s3-5	2.00×10^{-5}	1.25×10^{-3}	1.68×10^1
$k_2(20 °C) = 3.07 \times 10^3$ L mol^{-1} s^{-1}			

Table 2.133. Kinetics of the formation of 13ia (DMSO, 20 °C, Stopped-flow method, detection at 388 nm).

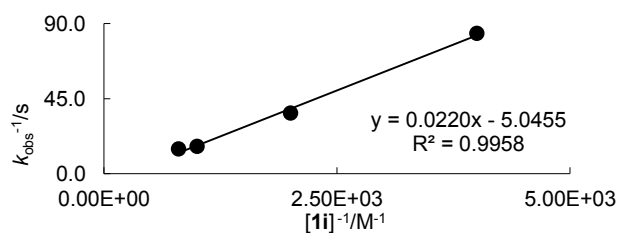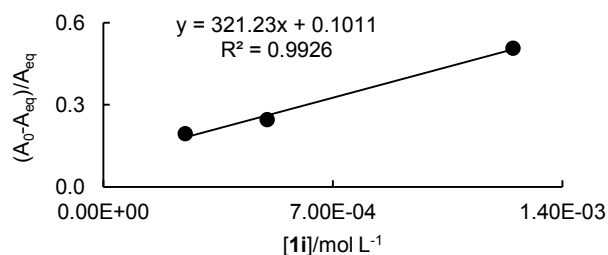| No.	[5b]/M	[1i]/M	k_{obs}/s^{-1}	[1i]$^{-1}$/M^{-1}	k_{obs}^{-1}/s
da95s3-11	2.00×10^{-5}	2.50×10^{-4}	1.19×10^{-2}	4.00×10^3	8.40×10^1
da95s3-21	2.00×10^{-5}	5.00×10^{-4}	2.75×10^{-2}	2.00×10^3	3.64×10^1
da95s3-31	2.00×10^{-5}	1.00×10^{-3}	6.52×10^{-2}	1.00×10^3	1.53×10^1
da95s3-51	2.00×10^{-5}	1.25×10^{-3}	6.76×10^{-2}	8.00×10^2	1.48×10^1
$1/K \cdot k_{rc} = 2.20 \times 10^{-2} => K \cdot k_{rc} (20 °C) = 4.55 \times 10^1$ L mol^{-1} s^{-1}					

Table 2.134. Determination of the equilibrium constant of the reaction of 1i with 5b (DMSO, 20 °C, Stopped-flow method, detection at 388 nm).

No.	[**5b**]/mol L^{-1}	[**1i**]/mol L^{-1}	A_0	A_{eq}[a]	$(A_0 - A_{eq})/A_{eq}$
da95s3-1	2.00×10^{-5}	2.50×10^{-4}	0.792	0.662	0.193
da95s3-2	2.00×10^{-5}	5.00×10^{-4}	0.797	0.639	0.246
da95s3-5	2.00×10^{-5}	1.25×10^{-3}	0.803	0.531	0.507
$K(20\ °C) = 3 \times 10^2$ L mol^{-1}					

[a] The equilibrium absorbances have been determined from the constant C obtained by fitting the monoexponential function $A = A_0 e^{-k_{obs} t} + C$ to the time-dependent absorbances.

The large intercept shows the uncertainty of the method. If the values $(A_0 - A_{eq})/A_{eq}$ obtained with the highest concentration of **1e** is divided by [**1e**], one obtains an equilibrium constant of $K = 4 \times 10^2$.

2.8 References

[1] I. Zugravescu, M. Petrovanu, *N-Ylid Chemistry*, McGraw-Hill, New York, **1976**.

[2] (a) M. Waser, R. Herchl, N. Müller, *Chem. Comm.* **2011**, *47*, 2170-2172; (b) M. Waser, R. Herchl, N. Müller, *Org. Biomol. Chem.* **2011**, 7023-7027; (c) S. Aichhorn, G. N. Gururaja, M. Reisinger, M. Waser, *RSC Advances* **2013**, *3*, 4552-4557; (d) T. Kimachi, H. Kinoshita, K. Kusaka, Y. Takeuchi, M. Aoe, M. Ju-Ichi, *Synlett* **2005**, *5*, 842-844; (e) A. Alex, B. Larmanjat, J. Marrot, F. Couty, O. David, *Chemical Communications* **2007**, 2500-2502.

[3] (a) A. Jonczyk, A. Konarska, *Synlett* **1999**, 1085-1087; (b) S. S. Bhattacharjee, H. Ila, H. Junjappa, *Synthesis* **1982**, 301-303; (c) A. Kowalkowska, D. Suchołbiak, A. Jończyk, *Eur. J. Org. Chem.* **2005**, *5*, 925-933.

[4] (a) X. L. L. Guo, W. Liu, Y Liang, *Synthesis* **2005**, 391-396; (b) Z. Yang, M. Fan, R. Mu, W. Liua, Y. Liang, *Tetrahedron Lett.* **2005**, *61*, 9140–9146.

[5] A. Kowalkowska, A. Jończyk, *Synthesis* **2002**, *5*, 674-680.

[6] (a) M. Sommelet, *Compt. rend.* **1913**, *157*, 852–854; (b) T. S. Stevens, E. M. Creighton, A. B. Gordon, K. MacNicol, *J. Chem. Soc.* **1928**, *50*, 3193-3197; (c) J. Clayden, M.

Donnard, J. Lefranc, D. J. Tetlow, *Chem. Commun.* **2011**, *47*, 4624–4639; (d) A. Kowalkowska, A. Jonczyk, *Syn. Comm.* **2011**, *41*, 3308-3317.

[7]   (a) C. D. Papageorgiou, S. V. Ley, M. J. Gaunt, *Angew. Chem. Int. Ed.* **2003**, *43*, 2681−2684; (b) C. D. Papageorgiou, M. A. Cubillo de Dios, S. V. Ley, M. J. Gaunt, *Angew. Chem.* **2004**, 4741−4744; (c) M. J. Gaunt, C. C. C. Johanson, *Chem. Rev.* **2007**, *107*, 5596–5605.

[8]   (a) W. G. Phillips, K. W. Ratts, *J. Org. Chem.* **1970**, *35*, 3144-3147; (b) K. W. Ratts, *J. Org. Chem.* **1972**, *37*, 848-851; (c) F. G. Bordwell, X. Zhang, *J. Org. Chem.* **1990**, *55*, 6078-6079; (d) X.-M. Zhang, F. G. Bordwell, M. Van Der Puy, H. E. Fried, *J. Org. Chem.* **1993**, *58*, 3060−3066; (e) X. M. Zhang, F. G. Bordwell, M. Van Der Puy, H. E. Fried, *J. Am. Chem. Soc.* **1994**, *116*, 968-972; (f) J.-P. Cheng, B. Liu, X.-M. Zhang, *J. Org. Chem.* **1998**, *63*, 7574-7575; (g) B. L. J.-P. Cheng, Y. Zhao, Y. Sun, X.-M. Zhang, Y. Lu, *J. Org. Chem.* **1999**, *64*, 604-610; (h) Y. Fu, H.-J. Wang, S.-S. Chong, Q.-X. Guo, L. Liu, *J. Org. Chem.* **2009**, *74*, 810−819; (i) For a comprehensive database of pK_a-values in DMSO see http://www.chem.wisc.edu/areas/reich/pkatable/

[9]   (a) F. G. Bordwell, A. Cripe, D. L. Hughes, in *Nucleophilicity* (Eds.: J. M. Harris, S. P. McManus), American Chemical Society, Washington, DC, **1987**, p. 137−154; (b) W. P. Jencks, in *Nucleophilicity* (Eds.: J. M. Harris, S. P. McManus), American Chemical Society, Washington, DC, **1987**, p. 155−168.

[10]   (a) S. T. A. Berger, A. R. Ofial, H. Mayr, *J. Am. Chem. Soc.* **2007**, *129*, 9753–9761; (b) T. A. Nigst, A. Antipova, H. Mayr, *J. Org. Chem* **2012**, *77*, 8142−8155.

[11]   (a) A. Solladié-Cavallo, L. Bouérat, M. Roje, *Tetrahedron Lett.* **2000**, *41*, 7309-7312; (b) R. Appel, H. Mayr, *J. Am. Chem. Soc.* **2011**, *113*, 8240−8251; (c) O. Illa, M. Arshad, A. Ros, E. M. McGarrigle, V. K. Aggarwal, *J. Am. Chem. Soc.* **2010**, *132*, 1828−1830; (d) V. K. Aggarwal, I. Bae, H.-Y. Lee, J. Richardson, D. T. Williams, *Angew. Chem., Int. Ed.* **2003**, *42*, 3274−3278; (e) D. J. Phillips, A. E. Graham, *Synlett* **2010**, *2010*, 769-773; (f) D. Janardanan, R. B. Sunoj, *Org. Biomol. Chem.* **2011**, *9*, 1642-1652; (g) Y. L. Stanc, M. L. Corre, *Can. J. Chem.* **1985**, *63*, 2958-2960; (h) A. Solladié-Cavallo, A. Diep-Vohuule, T. Isarno, *Angew. Chem. Int. Ed.* **1998**, *37*, 1689-1691; (i) V. K. Aggarwal, S. Calamai, J. Gair Ford, *J. Chem. Soc., Perkin Trans. 1* **1997**, 593−600; (j) D. R. Edwards, P. Montoya-Peleaz, C. M. Crudden, *Org.Lett.* **2007**, *9*, 5481-5484.

[12]   (a) R. Bonneau, I. Reuter, M. T. H. Liu, *J. Am. Chem. Soc.* **1994**, *116*, 3145-3146; (b) G. L. Heard, B. F. Yates, *J. Org. Chem.* **1996**, *61*, 7276-7284; (c) E. M. Arnett, P. C. Wernett, *J. Org. Chem.* **1993**, *58*, 301-303.

[13]   R. Robiette, M. Conza, V. K. Aggarwal, *Org. Biomol. Chem.* **2006**, *4*, 621−623.

[14]   S. L. Riches, C. Saha, N. F. Filgueira, E. Grange, E. M. McGarrigle, V. K. Aggarwal, *J. Am. Chem. Soc.* **2010**, *132*, 7626−7630.

[15]   (a) F. Volatron O. Eisenstein, *J. Am. Chem. Soc.* **1987**, *109*, 1-14; (b) T. Naito, S. Nagase, H. Yamataka, *J. Am. Chem. Soc.* **1994**, *116*, 10080-10088; (c) V. K. Aggarwal, J. N. Harvey, R. Robiette, *Angew. Chem., Int. Ed.* **2005**, *44*, 5468−5471.

[16]   R. Appel, R. Loos, H. Mayr, *J. Am. Chem. Soc.* **2009**, *131*, 704−714.

[17]   (a) R. Appel, H. Mayr, *Chem. Eur. J.* **2010**, *16*, 8610−8614; (b) R. Appel, N. Hartmann, H. Mayr, *J. Am. Chem. Soc.* **2010**, *132*, 17894−17900; (c) S. Lakhdar, R. Appel, H. Mayr, *Angew. Chem., Int. Ed.* **2009**, *48*, 5034−5037.

[18]   D. S. Allgäuer, P. Mayer, H. Mayr, *J. Am. Chem. Soc.* **2013**, *135*, 15216–15224.

[19]   (a) H. Mayr, M. Patz, *Angew. Chem. Int. Ed. Engl.* **1994**, *33*, 938−957; (b) H. Mayr, T. Bug, M. F. Gotta, N. Hering, B. Irrgang, B. Janker, B. Kempf, R. Loos, A. R. Ofial, G. Remennikov, H. Schimmel, *J. Am. Chem. Soc.* **2001**, *123*, 9500−9512; (c) R. Lucius, R. Loos, H. Mayr, *Angew. Chem. Int. Ed.* **2002**, *41*, 91−95; (d) H. Mayr, B. Kempf, A. R. Ofial, *Acc. Chem. Res.* **2003**, *36*, 66−77; (e) H. Mayr, A. R. Ofial, *Pure Appl. Chem.* **2005**, 1807−1821; (f) S. T. A. Berger, F. H. Seeliger, F. Hofbauer, H. Mayr, *Org. Biomol. Chem.* **2007**, *5*, 3020−3026; (g) H. Mayr, A. R. Ofial, *J. Phys. Org. Chem.* **2008**, *21*, 584−595; (h) O. Kaumanns, R. Appel, T. Lemek, F. Seeliger, H. Mayr, *J. Org. Chem.* **2009**, 75−81; (i) Bug, T.; Mayr, H. *J. Am. Chem. Soc.* **2003**, *125*, 12980−12986; (j) For a comprehensive database of nucleophilicity parameters N, s_N and electrophilicity parameters E, see http://www.cup.lmu.de/oc/mayr/.

[20]   F. G. Bordwell, H. E. Fried, *J. Org. Chem.* **1981**, *46*, 4327-4331.

[21]   O. Kaumanns, R. Lucius, H. Mayr, *Chem. Eur. J.* **2008**, *14*, 9675−9682.

[22]   R. Schmid, V. N. Sapunov, *Non-Formal Kinetics*, Verlag Chemie GmbH, Weinheim, **1982**.

[23]   (a) F. G. Bordwell, D. Algrim, N. R. Vanier, *J. Org. Chem.* **1977**, *42*, 1817-1819; (b) W. N. Olmstead, F. G. Bordwell, *J. Org. Chem.* **1980**, *45*, 3299-3305.

[24]   MATLAB v 7.10 The Mathwork Inc.

[25]   K. Troshin, H. Mayr, *J. Am. Chem. Soc.* **2013**, *135*, 252-265.

[26]   R. A. Alberty, W. G. Miller, *J. Chem. Phys.* **1957**, *26*, 1231-1237.

[27]   Gepasi v 3.30 Copyright P. Mendes 1989, 1992, 1993, 1996-1999, 2002.

[28]   M. V. Petrova, E. Liepins, J. Paulins, E. Gudriniece, *Magn. Reson. Chem.* **1992**, *30*, 216-220.

[29]   The cyclopropanes *cis*-**13** have a coupling constant of $^3J \sim 10$ Hz.

[30]   M. F. Oswald, S. A. Raw, R. J. K. Taylor, *Org. Lett.* **2004**, *6*, 3997-4000.

[31]   For a plot of pK_{aH} versus log k_{CC} (**3b**) see Experimental Section.

[32]   D. J. McLennan, A. Pross, *J. Chem. Soc., Perkin Trans. 2* **1984**, 981-984.

[33]   I. A. Koppel, J. B. Koppel, L. T. Muuga, V. O. Pihl, *Org. Reactiv., Engl. Ed.* **1988**, *25*, 131−146.

[34]   M. R. Crampton, I. A. Robotham, *J. Chem. Res., Synop.* **1997**, 22-23.

[35]   F. Seeliger, S. Błażej, S. Bernhardt, M. Mąkosza, H. Mayr, *Chem. Eur. J.* **2008**, *14*, 6108−6118.

[36]   a) H. E. Gottlieb, V. Kotlyar, A. Nudelman, *J. Org. Chem.* **1997**, *62*, 7512−7515; b) G. F. Fulmer, A. J. M. Miller, N. H. Sherden, H. E. Gottlieb, A. Nudelman, B. M. Stoltz, J. E. Bercaw, K. I. Goldberg, *Organometallics* **2010**, *29*, 2176−2179..

[37]   a) W. E. von Doering, L. H.Knox, *J. Am. Chem. Soc.* **1961**, *83*, 1989–1992; b) J. R. Boissier, E. Renier *Chimica Therapeutica*, **1969** , *4*, 224–227; a) V. I. Vysochin, G. V. Shishkin, *Chem. Heterocyc. Compd.* **1985** , *21*, 559–563.

[38]   D. S. Allgäuer, Master Thesis, Ludwig-Maximilian-Universität, München (Germany) **2009**.

[39]   K. Troshin, *unpublished results* **2013**.

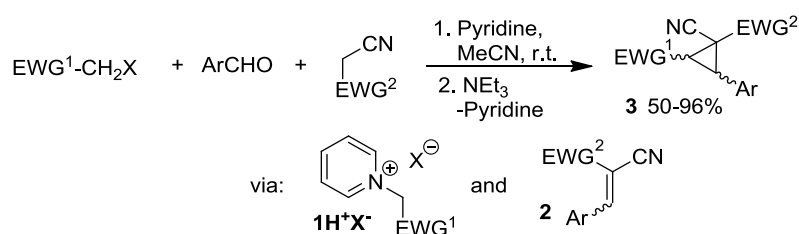# 3 One-Pot Two-Step Synthesis of 1-Ethoxycarbonyl-Indolizines via Pyridinium Ylides
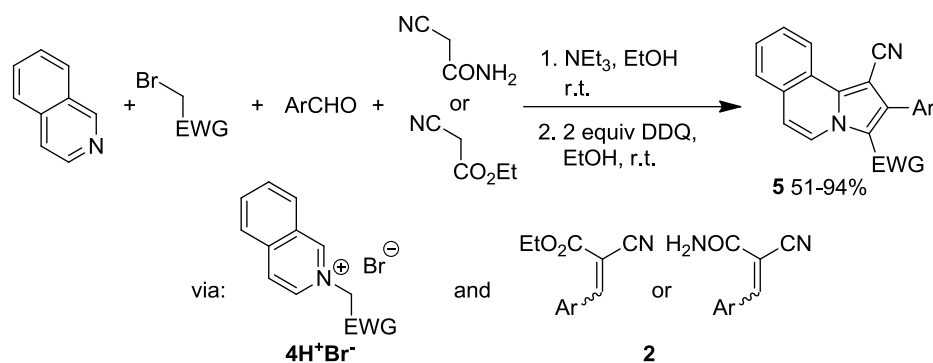
Dominik S. Allgäuer, Peter Mayer, and Herbert Mayr

3.1 Introduction

Since their discovery by Kröhnke in 1935,[1] the properties and reactions of pyridinium ylides have been intensively studied.[2,3] In recent years, pyridinium ylides have attracted a lot of attention, as they react with various electrophiles to form a great variety of products,[4] including indolizines.[5] The indolizine scaffold has a broad pharmacological profile, as it can act as calcium-channel blocker[6] or aromatase inhibitor,[7] and it is found in agents with antibiotic,[8] antitumor,[9] anti-inflammatory,[10] and antiviral activities.[11] Moreover, several indolizines are potent, inexpensive, and easily modifiable fluorescent probes.[12] Reactions of pyridinium ylides with benzylidenemalononitriles and other unsaturated nitriles have already been reported.[4b–4f,4o] Cyclopropanes **3** have been obtained from the reactions of pyridinium salts **1H⁺X⁻** with benzylidenemalononitriles **2** and related compounds under basic conditions (Scheme 3.1).[4f] At least one of the two acceptor groups of the Michael acceptor has to be a cyano group, however.[4b,4d–4f] The corresponding reactions of isoquinolinium salts **4H⁺Br⁻** with Michael acceptors **2** under basic conditions produced pyrrolo[2,1-*a*]isoquinolines **5** after oxidative work-up (Scheme 3.2).[4o]

Scheme 3.1. Cyclopropanations of benzylidene malononitriles and related compounds 2 via pyridinium ylides.[4f]

Scheme 3.2. Reaction of isoquinolinium ylide 4 with benzylidene cyanoactetates and cyanoacetamides 2.[4o]

The same pyrrolo[2,1-*a*]isoquinolines (i.e., **5**) were obtained from the reaction of isoquinolinium salt **4H⁺Br⁻** with either of the two electrophiles **2** shown in Scheme 3.2

The nitrile group was preserved in these products, while the amide or the ester group was eliminated during the oxidative aromatization. The different reaction course for pyridinium and isoquinolinium ylides has been explained by the *ab initio* MO calculations of Matsumura and co-workers.[3i] They showed that the addition of pyridinium and isoquinolinium ylides to alkylidenemalononitriles proceeds stepwise, and not in a concerted manner. As cyclization of the intermediate betaine to give the [3+2]-cycloadduct leads to a greater loss of aromaticity for the pyridinium ylides than for the isoquinolinium ylides, only the latter ylides undergo [3+2]-cycloadditions with Michael acceptors **2**. In contrast, the betaines formed from pyridinium ylides undergo intramolecular S_N2 reactions that result in the formation of cyclopropanes and the elimination of pyridine. We now report that in contrast to cyano-substituted Michael acceptors **2**, benzylidene-malonates **6** undergo [3+2]-cycloaddition with pyridinium ylides. Subsequent oxidation provides a simple and straightforward access to indolizines.

This investigation is part of our program to determine the nucleophile-specific parameters N and s_N by studying the rates of reactions with benzylidene-malonates **6**, which have been introduced as reference electrophiles ($-24 < E < -17$ for *p*-NMe₂ to *p*-NO₂)[13] for the characterization of strong nucleophiles by the linear-free-energy relationship given in eq 3.1.[14]

$$\log k_{20\,°C} = s_N(N + E) \tag{3.1}$$

3.2 Results and Discussion

As most pyridinium (**1**) and isoquinolinium ylides (**4**) are unstable compounds, we made no attempts to isolate them. Instead we used their conjugate acids **1H⁺X⁻** or **4H⁺Br⁻**, which were obtained by nucleophilic substitution from the corresponding pyridines or from isoquinoline in THF in moderate to high yields (Table 3.1).[3c,15]

Treatment of **1H⁺X⁻** or **4H⁺Br⁻** with a base in the presence of arylidene-malonates **6a–i** or alkylidenemalonate **6j** (Scheme 3.3) gave ylides **1** and **4**, which subsequently reacted with Michael acceptors **6**. As shown by Table 3.3, entries 1–5 Michael adduct **M-1a** was formed exclusively when an equimolar mixture of **1aH⁺Br⁻** and **6f** was treated with an excess of HNMe₂, NEt₃, or KO'Bu in various solvents at ambient temperature. Analogous reactions with NEt₃ (2 equiv.) in CH₂Cl₂ or Et₂O/MeCN (2:1) at ambient temperature gave mixtures of Michael adduct **M-1a** and [3+2]-cycloadduct **C-1a** within 15 min (Table 3.1), entries 6 and 7). [3+2]-Cycloadduct **C-1a**, contaminated by traces of **7a**, was observed exclusively, when the mixture of **1aH⁺Br⁻** and **6f** was combined with KO'Bu (1.1 equiv.) in THF (Table 2, entry 8) or with NaOH (32% aq.) under biphasic conditions (Table 3.3, entry 9).

Table 3.1. Synthesis of the pyridinium 1H⁺X⁻ and isoquinolinium salts 4H⁺Br⁻ employed as precursors for the pyridinium ylides 1.

R	X	EWG	Product	Yield/%
H	Br	CO₂Et	**1aH⁺Br⁻**	82
H	Br	CONEt₂	**1bH⁺Br⁻**	83
H	Br	CN	**1cH⁺Br⁻**	quant.
H	Cl	COMe	**1dH⁺Cl⁻**	45[a]
H	Br	COPh	**1eH⁺Br⁻**	94
3-Cl	Br	CN	**1fH⁺Br⁻**	31
4-NMe₂	Br	CN	**1gH⁺Br⁻**	97
Isoquinoline	Br	CN	**4aH⁺Br⁻**	49
Isoquinoline	Br	COPh	**4bH⁺Br⁻**	93

[a] After refluxing in THF for 4 h.

Although [3+2]-cycloadduct **C-1a** was a labile compound that could not be purified, [3+2]-cycloadduct **C-4a**, from the reaction of **4a** and **6f**, was purified and characterized by 2D NMR spectroscopy and HRMS (Scheme 3.4). The ratio of the diastereoisomers was determined from the ^{1}H NMR spectrum of the crude product, and the stereochemistry was assigned on basis of NOESY-correlation of the protons at the 2-, 3-, and 10b-positions of the adduct. From the configuration of the stereocenters, one can conclude that the major diastereoisomer of **C-4a** shown is preferentially formed by an *anti*-2-*endo* approach of ylide **4a** and benzylidene-malonate **6f**. The stereochemistry of the minor diastereoisomers could not be assigned unambiguously.

Table 3.2. Electrophilicity parameters E of the arylidene (6a−i) and alkylidene malonate (6j).[a]

No.	R	E[b]
6a	C_6H_4-*p*-NO_2	−17.67
6b	C_6H_4-*p*-CN	−18.06
6c	C_6H_4-*p*-Br	-
6d	C_6H_4-*m*-Cl	−18.98
6e	C_6H_5	−20.55
6f	C_6H_4-*p*-Me	−21.11
6g	C_6H_4-*p*-OMe	−21.47
6h	C_6H_4-*p*-NMe_2	−23.10
6i		−23.80
6j	$CH(CH_3)_2$	-

[a] Generated by Knoevenagel condensation according to refs. [13, 16]; [b] E parameters taken from ref. [13].

To find the best conditions for the conversion of [3+2]- cycloadduct **C-1a** into indolizine **7a** in CH_2Cl_2 at ambient temperature, we tested different oxidants. Catalytic amounts of Pd-C under an O_2 atmosphere, di-*tert*-butyl hydroperoxide (4 equiv.), or *N*-chlorosuccinimide (4 equiv.) did not promote the oxidation of **C-1a** into indolizine **7a** within 18 h at 20 °C (Table 3.4, entries 1–3). The formation of indolizine **7a** was observed when DDQ was used as an oxidant (Table 3.4, entry 4). Chloranil gave a significantly higher conversion into indolizine **7a**

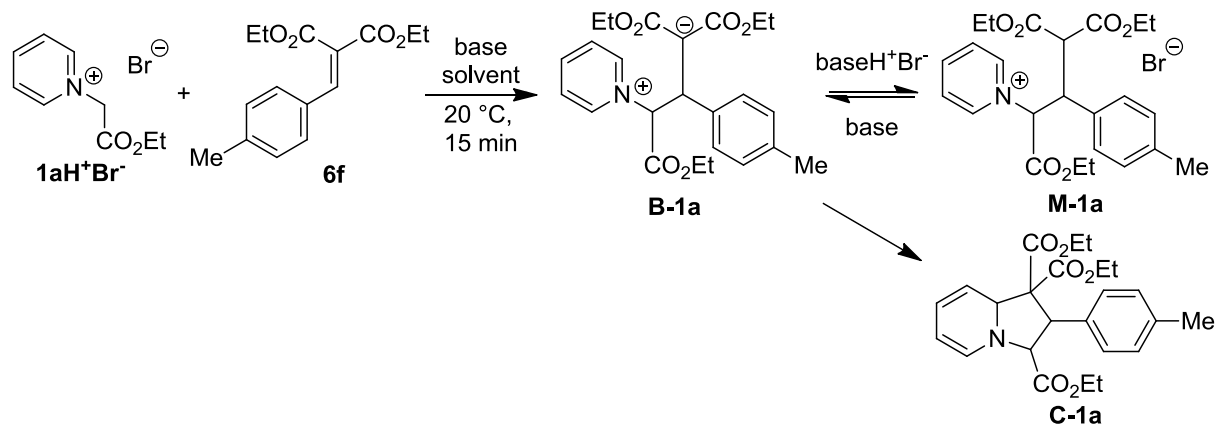**Scheme 3.3. Base induced reactions of the pyridinium salt 1aH⁺Br⁻ with the arylidene malonate 6f.**

Table 3.3. Base induced reactions of the pyridinium salt 1aH⁺Br⁻ with the arylidene malonate 6f at ambient temperature (B = betaine; M = Michael adduct, C = [3+2]-cycloadduct).

Entry	Base	Equiv. base	Solvent	Conv. of 6f/%[a]	Ratio M-1a/C-1a[b]
1	aq. HNMe₂ (30%)	36	DMSO	75[c]	>98/2
2	NEt₃	2.0	DMSO	40[c]	>98/2
3	KOtBu	1.2	DMSO	93[c]	>98/2
4	NEt₃	1.4	MeOH	78	>98/2
5	NEt₃	2.0	MeCN	88	>98/2
6	NEt₃	1.5	CH₂Cl₂	92	72/28
7	NEt₃	1.5	Et₂O/MeCN[d]	86	34/66
8	KOtBu	1.1	THF	99	>2/98[e]
9	aq. NaOH (32%)	32	CH₂Cl₂	97[f]	>2/98

[a] By ¹H NMR as ratio of (M-1a+C-1a)/(6f+M-1a+C-1a); [b] By ¹H NMR; [c] After aqueous work-up; [d] Et₂O:MeCN = 2:1; [e] Contaminated by traces of indolizine 7a; [f] After filtration through silica (*n*-pentane:EtOAc:NEt₃ 5:1:1).

(Table 3.4, entry 5). When the amount of chloranil was reduced and the reaction time was decreased from 18 to 3 h, a further increase in the conversion to indolizine 7a was observed (Table 3.4, entry 6). After a reaction time of 1 h, the conversion to 7a was the same as after 3 h, but decreasing the reaction time further led to a decrease in the conversion (Table 3.4, entries 7 and 8). Under all the conditions examined, the oxidation of C-1a to 7a was accompanied by regeneration of 6f, which indicates that the formation of C-1a by cyclization of betaine B-1a must be a reversible process (Table 3.3). The existence of the base-mediated equilibrium between Michael adduct M-1a and [3+2]-cycloadduct C-1a was proved by the formation of indolizine 7a when the solution obtained under the conditions of Table 3.3, entry 2 was heated with MnO₂ at 100 °C for 3 h in DMSO (for details, see Experimental Section).
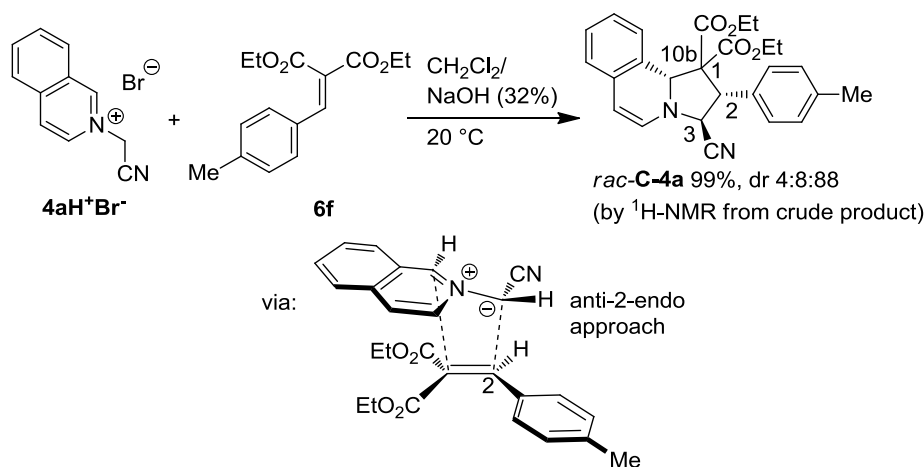
**Scheme 3.4. Formation of the [3+2]-cycloadduct C-4a.**

rac-C-4a 99%, dr 4:8:88
(by ¹H-NMR from crude product)

Table 3.4. Oxidant-screening for the formation of indolizine 7a.

Entry	Oxidant	Equiv.	t/h	Conversion/%
1	Pd-C/O$_2$	[a]	18	0[b]
2	DTBPO/air[c]	4.0	18	0[b]
3	NCS/air[d]	4.0	18	0[b]
4	DDQ/air[e]	1.4	18	54[f, g]
5	Chloranil/air	2.0	18	69[f, g]
6	Chloranil/air	1.0	3	74[f]
7	Chloranil/air	1.0	1	74[f]
8	Chloranil/air	1.0	0.5	65[f]

[a] Under O$_2$-atmosphere; [b] By TLC; [c] TBPO = Di-*tert*-butyl-peroxide; [d] NCS = *N*-Chlorosuccinimide; [e] DDQ = 2,3-Dichloro-5,6-dicyano-1,4-benzoquinone; [f] By ^{1}H NMR as ratio of **7a**/(**6f**+**7a**); [g] After filtration through silica with CH$_2$Cl$_2$.

To clarify why 1 equiv. of chloranil is sufficient to promote the full oxidation of [3+2]-cycloadduct **C-1a** into indolizine **7a** (Table 3.4, entries 6–8), isolated [3+2]-cycloadduct **C-4a** (Table 3.5) was treated with 1 equiv. of chloranil under different conditions. When the reaction with chloranil was performed under a nitrogen atmosphere, only 21% of **C-4a** was converted into indolizine **8a** (Table 3.5, entry 1), whereas in an open flask, the oxidation of **C-4a** with 1 equiv. of chloranil gave a 58% conversion of **C-4a** into **8a** (Table 3.5, entry 2). Addition of a small amount of NaOH (32% aq.) to the reaction mixture significantly lowered the conversion of **C-4a** into indolizine **8a** (Table 4, entry 3). When CH$_2$Cl$_2$ was stirred with NaOH (32% aq.) for 1 h, the aqueous layer was subsequently removed, and the CH$_2$Cl$_2$ was dried over Na$_2$SO$_4$ before dissolving **C-4a** and chloranil, complete conversion of **C-4a** into **8a** was achieved (Table 3.5, entry 4). These experiments show that air and traces of anhydrous hydroxide are favorable to promote the oxidation of the [3+2]-cycloadduct into the indolizine.

A mechanism for the conversion of [3+2]-cycloadduct **C-1a** into indolizine **7a** that requires only 1 equiv. of chloranil is proposed Scheme 3.5. Chloranil abstracts a hydride from the 8a-position of **C-1a** to give pyridinium ion **9**. One ester group of **9** is subsequently hydrolyzed by traces of hydroxide to give intermediate **10**, which decarboxylates in a Grob-type fragmentation[17] to give 2,3-dihydroindolizine **11**. Oxidation of the initially generated hydrochloranil anion (redox potential of hydrochloranil –0.71 V in CH$_2$Cl$_2$ at 25 °C)[18] with oxygen (redox potential +0.65 V)[19] regenerates chloranil and produces a hydroperoxide anion

Table 3.5. Direct oxidation of the [3+2]-cycloadduct C-4a with chloranil to indolizine 8a under various conditions.
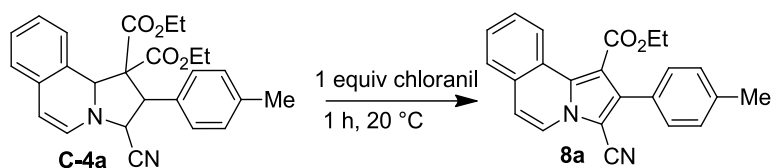
Entry	Atmosphere	Additive	Conversion/%[a]
1	N₂	-	21
2	air	-	58
3	air	aq. NaOH (32%)	17
4	air	NaOH[b]	quant.

[a] Determined by ¹H NMR; [b] CH₂Cl₂ was stirred with aq. NaOH (32%) for 1 h; the aqueous layer was removed and CH₂Cl₂ was dried over Na₂SO₄ before **C-4a** and chloranil were dissolved.

that might also attack the ethyl ester. Hydride abstraction from dihydroindolizine **11** by chloranil forms pyridinium ion **12**, which loses a proton to form indolizine **7a** and dihydrochloranil (whose formation was verified by GC–MS). Direct oxidation of dihydroindolizine **11** into indolizine **7a** by air seems unlikely, as the closely related dihydroindolizines derived from cyanoacetamides **2** and isoquinolinium ylides **4** are air-stable.[4o]
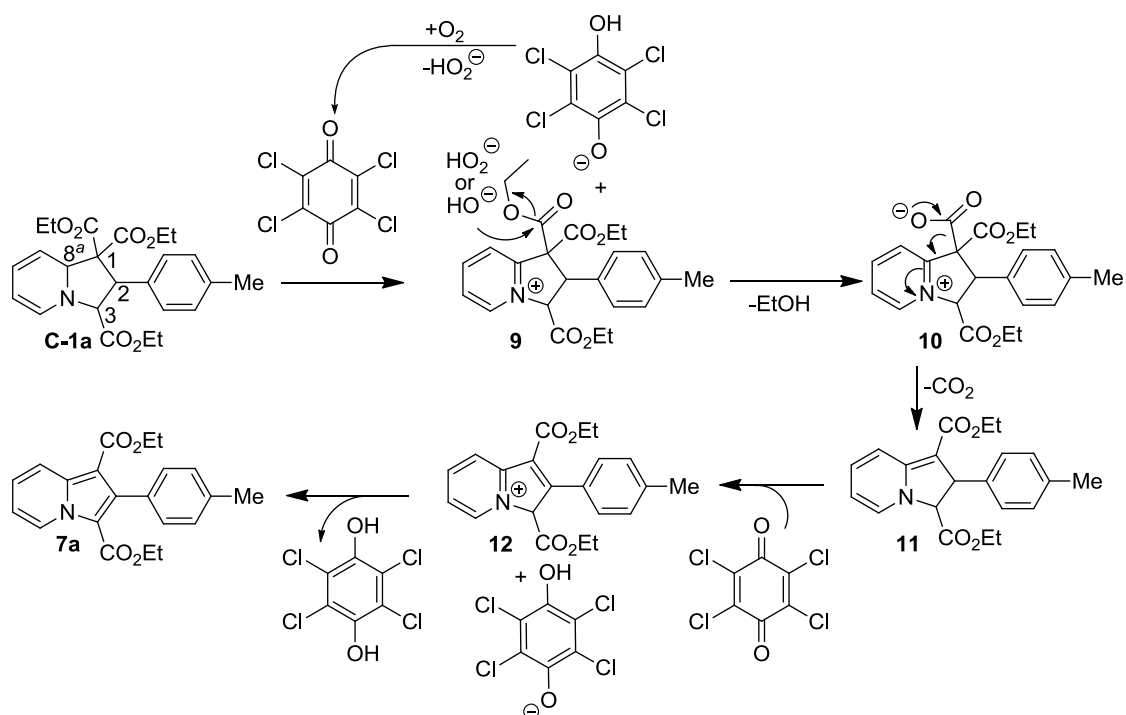
Scheme 3.5. Proposed mechanism for the formation of indolizine 7a.

Table 3.6. Dependency of indolizine formation on the stabilization of ylides 1 and 2.

Entry	Salt	R[1]	EWG	Electrophile	R[2]	Product	Yield/%
1	**1aH⁺Br⁻**	H	CO₂Et	**6f**	Me	**7a**	65
2	**1bH⁺Br⁻**	H	CONEt₂	**6f**	Me	**7b**	52
3	**1cH⁺Br⁻**	H	CN	**6f**	Me	**7c**	74
4	**1dH⁺Cl⁻**	H	COMe	**6f**	Me	**7d**	52
5	**1eH⁺Br⁻**	H	COPh	**6a**	NO₂	**7e**	(21)[a]
6	**1fH⁺Br⁻**	3-Cl	CN	**6f**	Me	**7f**	54
7	**1gH⁺Br⁻**	4-NMe₂	CN	**6f**	Me	**7g**	19
8	**4aH⁺Br⁻**	-	CN	**6f**	Me	**8a**	89

[a] Purification not successful.

As shown in Table 3.6, indolizines can be analogously synthesized from other pyridinium and isoquinolinium ylides. Exchanging the ester group in **1a** for an *N,N*-diethylamido group (in **1b**) or an acetyl group (in **1d**) led to slightly decreased yields of the corresponding indolizines (i.e., **7b** and **7d**), while a cyano substituent led to indolizine **7c** in a higher isolated yield (Table 3.6, entries 1–4). With benzoyl-substituted ylide **1e**, indolizine formation was only observed when *p*-nitro-substituted benzylidene-malonate **6a** was used as the electrophile, and even then, indolizine **7e** was only observed in low conversion (Table 3.6, entry 5). The reason for this behavior will be discussed below.

As cyano-substituted ylide **1c** gave the best results, cyano-substituted ylides were used to investigate substituent effects in the pyridine ring (Scheme 6, entries 6–8). A 3-chloro substituent (in **1f**) was tolerated and led regioselectively to indolizine **7f** with chlorine in the 6-position, as shown by the dd (^3J = 1.8 and 0.9 Hz) of 5-H in the ^{1}H NMR spectrum (Table 3.6, entry 6). In contrast, a strong electron donor such as the 4-NMe₂ substituent in ylide **1g** resulted in a reduced yield of indolizine **7g** (Table 3.6, entry 7). Probably, the decreased electrophilicity of the pyridinium ring retarded the cyclization of betaine **B-1g** to give [3+2]-cycloadduct **C-1g** (see Table 3.3). The reaction of isoquinolinium ylide **4h** with benzylidene malonate **6f** resulted in an almost quantitative formation of indolizine **8a** (Table 3.6, entry 8), which can be explained by the smaller loss of aromaticity in the cyclization step.

Scheme 3.6. Reaction of salt 1eH⁺Br⁻ with benzylidene malonates 6 in ethanol and proposed mechanism for the formation of the salts 13.
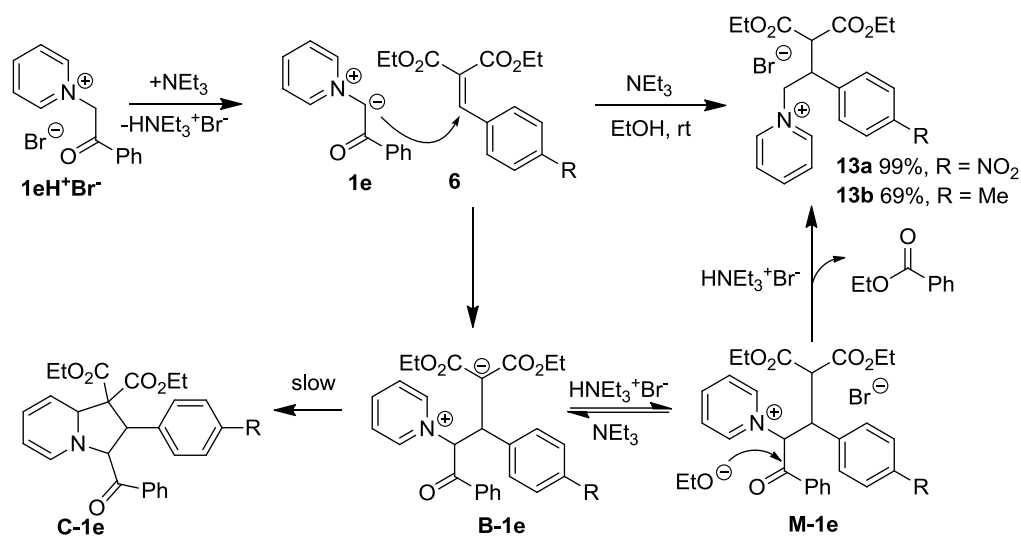
To rationalize the low yield of indolizine **7e**, we examined the reactions of benzoyl-substituted ylide **1e** more closely. When **1eH⁺Br⁻** was combined with benzylidene-malonate **6a** in EtOH at 20 °C in the presence of NEt₃, debenzoylated pyridinium salt **13a** was formed in 99% yield (Scheme 3.6). This product was unambiguously identified by NMR spectroscopy, high-resolution mass spectrometry, and elemental analysis (see Experimental Section). Its formation may be explained by the mechanism shown in Scheme 3.6. The initially generated ylide (i.e., **1e**) undergoes a 1,4-addition to Michael acceptor **6a** to form betaine **B-1e**. This intermediate is protonated by HNEt₃⁺Br⁻ to give Michael adduct **M-1e**. Obviously, nucleophilic attack by ethoxide and elimination of the benzoyl group (the formation of ethyl benzoate was detected by GC–MS) is faster than the generation of [3+2]-cycloadduct **C-1e** by cyclization of betaine **B-1e**. This process seems to be general, as debenzoylated pyridinium salt **13b** was obtained under the same conditions from the reaction of ylide **1e** with *p*-methylbenzylidenemalonate **6f**.

An easier cyclization step, as had previously been observed in the isoquinolinium series, was now also found with benzoyl-substituted ylides, and a good yield of [3+2]- cycloadduct **C-4b** was obtained when isoquinolinium salt **4bH⁺Br⁻** was combined with benzylidene-malonate **6a** in DMSO under basic conditions (Scheme 3.7). The diastereomeric ratio was determined from the ¹H NMR spectrum of the crude product. Recrystallization of **C-4b** from EtOH resulted in the formation of needle-shaped and prismatic crystals, which were separated for analysis (see Experimental Section). The needle-shaped crystals were composed of all three diastereoisomers, whereas the prismatic crystals were composed of a single diastereoisomer (by

Scheme 3.7. Reaction of 4bH⁺Br⁻ with benzylidene malonate 6a in DMSO at 20 °C.

4bH⁺Br⁻   **6a**   **C-4b** 75%, *dr* 6:38:56
(by ¹H-NMR from crude product)
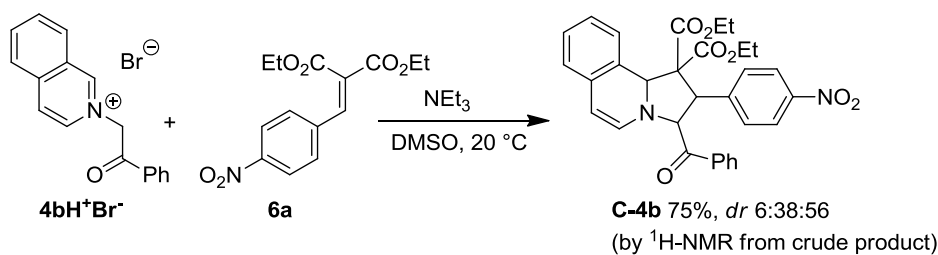
¹H NMR spectroscopy). Solutions of this single diastereoisomer in CDCl₃ slowly isomerized to give a mixture of three diastereoisomers, which prevented an unambiguous assignment of the stereochemistry. The isomerization may be due to a deprotonation of the proton α to the benzoyl group or reversible opening of the pyrrolidine ring of **C-4b**.

As shown in Table 3.7, the indolizine synthesis presented in this work tolerates strongly electron-withdrawing and electron-donating groups on the phenyl ring of the electrophile. The most electrophilic and the least electrophilic arylidene-malonates tested (i.e., **6a** and **6i**, respectively) gave the corresponding indolizines (i.e., **7h** and **7o**) in lower yields (Table 3.7, entries 1 and 9). It was even possible to replace the aryl ring in the arylidene-malonates by an isopropyl group (in **6j**) and obtain 83% of the corresponding indolizine (i.e., **7p**; Table 3.7, entry 10). Product **7p** has an isopropyl group in the 2-position, as does the calcium-channel blocker fantofarone.[6]

Indolizine **7l** was not only obtained as described in Table 3.7, but also when pyridinium bromide **1cH⁺Br⁻** was combined with Michael acceptors **14a** or **14b** under the conditions described above, followed by oxidation with chloranil (1 equiv.) in air (Scheme 9). The yield of **7l** decreased from 34 to 22% when 2 equiv. of chloranil was used for the oxidation of [3+2]-cycloadduct **15b**. Indolizine **7q** was obtained from pyridinium bromide **1cH⁺Br⁻** and **14c** under the same conditions.

While the selective formation of **7l** from **15a**, i.e., the preferential elimination of the acetyl group over the ethoxycarbonyl group, can be explained by the mechanism described in Scheme 3.5 (nucleophilic attack at COCH₃ is easier than that at CO₂Et), the preferential cleavage of the SO₂Me group can be explained by the high nucleofugality of this group, which has recently been quantified (Scheme 3.9).[20]

The preferential cleavage of the formamido group over the ethoxycarbonyl group, which has previously been observed in the isoquinolinium series,[4o] may be explained by the elimination of isocyanic acid, as shown in Scheme 3.10.[21]

In agreement with literature reports,[4o] the leaving-group abilities of different electron-with-

drawing substituents in the oxidative aromatizations of the [3+2]-cycloadducts to give indolizines can roughly be ordered: $CN^{[4o]} < CO_2Me \approx CO_2Et < COMe, SO_2Me, CONH_2$.

The preliminary results shown in Scheme 3.11 illustrate that less activated Michael acceptors like ethyl methacrylate could also be used for this reaction sequence, although the isolated yields of indolizine **18** were low.

Table 3.7. Indolizines 7c,h−p from pyridinium salt 1cH+Br− and the Michael acceptors 6a−j.
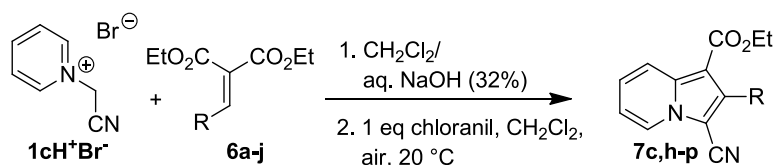
Entry	Reactant	R	Product	Yield/%
1	**6a**	C_6H_4-p-NO_2	**7h**	48
2	**6b**	C_6H_4-p-CN	**7i**	82
3	**6c**	C_6H_4-p-Br	**7j**	81
4	**6d**	C_6H_4-m-Cl	**7k**	77
5	**6e**	C_6H_5	**7l**	69
6	**6f**	C_6H_4-p-Me	**7c**	74
7	**6g**	C_6H_4-p-OMe	**7m**	78
8	**6h**	C_6H_4-p-NMe_2	**7n**	80
9	**6i**	julolidyl	**7o**	53
10	**6j**	$CH(CH_3)_2$	**7p**	83

Scheme 3.8. Reaction of 1cH+Br− with 14a−c to indolizine 7l and 7q.
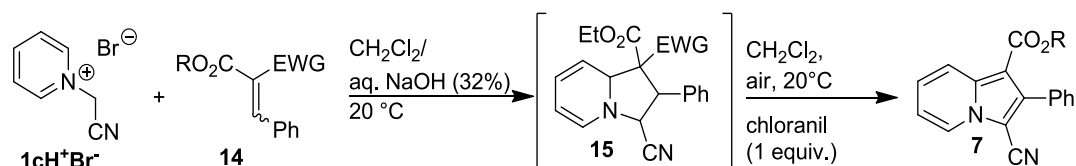
Electrophile	R	EWG	[3+2]-Cycloadduct	Product	Yield/%
14a	Et	COMe	**15a**	**7l**	56
14b	Et	SO_2Me	**15b**	**7l**	34[a]
14c	Me	$CONH_2$	**15c**	**7q**	56

[a] 2 equiv. chloranil: 22 % yield.

Scheme 3.9. Elimination of the −SO2Me group during the formation of indolizine 7l.
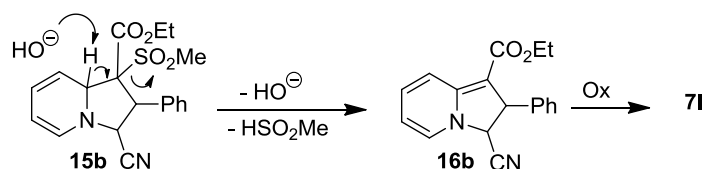
Scheme 3.10. Cleavage of the formamido group in the formation of indolizine 7q.
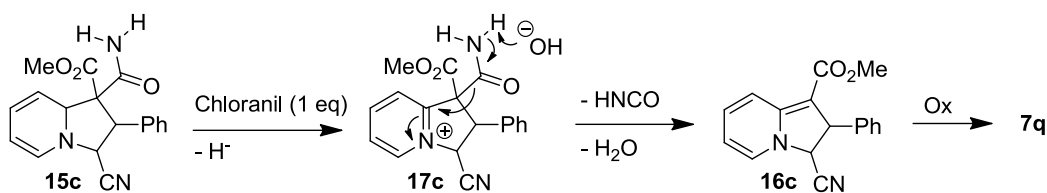
Scheme 3.11. Reaction of 1eH⁺Br⁻ and ethyl methacrylate to indolizine 18.
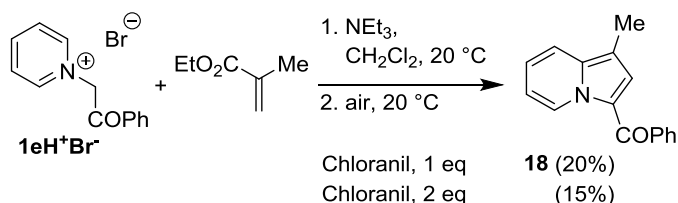
3.3 Conclusion

In contrast to arylidene malononitriles and other cyano-substituted Michael acceptors, which are cyclopropanated by pyridinium ylides **1**, arylidene-malonates **6** undergo stepwise [3+2]-cycloaddition with pyridinium ylides **1** to give [3+2]-cycloadducts **C-1**. Under certain conditions, intermediate Michael adducts **M-1** can be observed. In the presence of air and sodium hydroxide, only 1 equiv. of chloranil is needed to convert [3+2]-cycloadducts **C-1** into indolizines **7** by hydride abstraction and degradation of the ethoxycarbonyl group. Michael acceptors **14a–c**, in which one ester group of the benzylidene-malonates (i.e., **6**) is replaced by an acetyl, methylsulfonyl, or amidocarbonyl group, behave similarly, and yield the same indolizines (i.e., **7**), because the latter groups are eliminated faster than are alkoxycarbonyl groups. As isoquinolinium ylides react analogously, the sequence of [3+2]-cycloaddition and oxidation provides a simple one-pot synthesis of indolizines **7** and benzindolizines **5** from readily accessible pyridinium salts Py⁺-CH₂-EWG or isoquinolinium salts IQ⁺-CH₂-EWG and a variety of Michael acceptors.

3.4 Experimental Section

3.4.1 General

Chemicals. Solvents and chemicals were used as purchased without further purification. The diethyl benzylidene and alkylidenemalonates were synthesized according to ref. [12, 15].

Analytics. ^{1}H- and ^{13}C NMR spectra were recorded in CDCl$_3$ (δ_H 7.26, δ_c 77.16),[22a] CD$_2$Cl$_2$ (δ_H 7.26, δ_c 77.16),[22b] or DMSO-d_6 (δ_H 2.50, δ_c 39.52)[22a] on 200, 300, 400, or 600 MHz NMR spectrometers and are given in ppm. The following abbreviations were used to designate chemical shift multiplicities: s = singlet, d = doublet, t = triplet, q = quartet, m = multiplet, br = broad. For reasons of simplicity, the ^{1}H NMR signals of AA'BB'-spin systems of *p*-disubstituted aromatic rings were treated as doublets. The assignments of individual NMR signals were based on additional 2D-NMR experiments (COSY, NOESY, HSQC, HMBC). Diastereomeric ratios (*dr*) were determined by ^{1}H NMR of the crude reaction products if not stated otherwise. HRMS and MS were recorded on a Finnigan MAT 95 Q (EI) mass spectrometer or Thermo Finnigan LTQ FT Ultra (ESI). An Elementar Vario Micro Cube or an Elementar Vario EL device was used for elemental analysis. The melting points were recorded on a Büchi Melting Point B-540 device and are not corrected. IR-spectra were recorded on a PerkinElmer FT-IR-BX spectrometer with ATR probe.

3.4.2 Synthesis of the Pyridinium Salts 1H$^+$X$^-$

Procedure A for the Synthesis of the Pyridinium Salts 1H$^+$X$^-$. An equimolar amount of the halo compound was added to a solution of the corresponding pyridine in THF. The solution was stirred at room temperature over night. The solvent was evaporated and the residue was washed with ether. Recrystallization from EtOH/Et$_2$O or MeOH/toluene afforded the salts **1H$^+$X$^-$**.

1-(2-Ethoxy-2-oxoethyl)pyridin-1-ium bromide (1aH$^+$Br$^-$). The title compound was synthesized by procedure **A** from ethyl bromoacetate (15.5 g, 90.0 mmol) and pyridine (7.12 g, 90.0 mmol). **1aH$^+$Br$^-$** was obtained as colorless solid (18.1 g, 73.6 mmol, 82%). **Mp** 135–136 °C; lit.: 135–136 °C.[15a] ^{1}**H NMR** (400 MHz, DMSO-d_6) δ = 1.22 (t, *J* = 7.1 Hz, 3 H, CH$_3$), 4.20 (q, *J* = 7.1 Hz, 2 H, CH$_2$), 5.74 (s, 2 H, CH$_2$), 8.24 (dd, *J* = 7.7, 6.8 Hz, 2 H, 2×C$_{Ar}$-H), 8.71 (t, *J* = 7.8 Hz, 1 H, C$_{Ar}$-H), 9.08 − 9.16 (m, 2 H, 2×C$_{Ar}$-H). ^{13}**C NMR** (100 MHz, DMSO-d_6) δ = 14.4 (q, CH$_3$), 60.7 (t, CH$_2$), 62.8 (t, CH$_2$), 128.3 (d,

$2 \times$C$_{Ar}$-H), 146.7 (d, $2 \times$C$_{Ar}$-H), 147.3 (d, C$_{Ar}$-H), 166.9 (s, CO). **HRMS** (ESI+): *m/z* [C$_9$H$_{12}$NO$_2$]$^+$: calcd.: 166.0863, found: 166.0857. DA79

1-(2-(Diethylamino)-2-oxoethyl)pyridin-1-ium bromide (1bH$^+$Br$^-$). The title compound was synthesized by procedure **A** from 2-bromo-*N,N*-diethylacetamide[24] (2.00 g, 10.3 mmol) and pyridine (8.14 g, 10.3 mmol). **1bH$^+$Br$^-$** was obtained as colorless wax (2.33 g, 8.53 mmol, 83%, *dr* (amide) 1:12) which solidified slowly at −18 °C in Et$_2$O. **Mp** < 20 °C. **^{1}H NMR** (400 MHz, DMSO-*d$_6$*) δ = 1.04 (t, *J* = 7.1 Hz, 3 H, CH$_3$), 1.24 (t, *J* = 7.1 Hz, 3 H, CH$_3$), 3.31 (q, *J* = 7.1 Hz, 2 H, CH$_2$), 3.37 (q, *J* = 7.1 Hz, 2 H, CH$_2$), 5.81 (s, 2 H, CH$_2$), 8.16–8.22 (m, 2 H, $2 \times$C$_{Ar}$-H), 8.66 (tt, *J* = 7.9, 1.4 Hz, 1 H, C$_{Ar}$-H), 8.97–9.01 (m, 2 H, $2 \times$C$_{Ar}$-H). **^{13}C NMR** (100 MHz, DMSO-*d$_6$*) δ = 13.2 (q, CH$_3$) 14.2 (q, CH$_3$), 40.7 (t, CH$_2$), 41.2 (t, CH$_2$), 61.4 (t, CH$_2$), 127.9 (d, $2 \times$C$_{Ar}$-H), 146.6 (d, $2 \times$C$_{Ar}$-H), 146.9 (d, C$_{Ar}$-H), 163.9 (s, CO). **HRMS** (ESI+): *m/z* [C$_{11}$H$_{17}$N$_2$O]$^+$: calcd.: 193.1335, found: 193.1335. DA191

1-(Cyanomethyl)pyridin-1-ium bromide (1cH$^+$Br$^-$). The title compound was synthesized by procedure **A** from bromoacetonitrile (1.71 g, 14.3 mmol) and pyridine (1.47 g, 18.6 mmol). **1aH$^+$Br$^-$** was obtained as colorless solid (2.85 g, 14.3 mmol, 100%). **Mp** 164–165°C; lit.: 166–167 °C.[3b] **^{1}H NMR** (400 MHz, DMSO-*d$_6$*) δ = 6.07 (s, 2 H, CH$_2$) 8.18–8.43 (m, 2 H, $2 \times$C$_{Ar}$-H), 8.75 (tt, *J* = 7.9 Hz, 1.3, 1 H, C$_{Ar}$-H), 9.24 (dd, *J* = 6.8, 1.3 Hz, 2 H, $2 \times$C$_{Ar}$-H). **^{13}C NMR** (100 MHz, DMSO-*d$_6$*) δ = 47.7 (t, CH$_2$), 114.3 (s, CN), 128.6 (d, $2 \times$C$_{Ar}$-H), 145.5 (d, $2 \times$C$_{Ar}$-H), 147.6 (d, C$_{Ar}$-H). **HRMS** (ESI+): *m/z* [C$_7$H$_7$N$_2$]$^+$: calcd.: 119.0604, found: 119.0604. DA130

1-(2-Oxopropyl)pyridinium chloride (1dH$^+$Cl$^-$). The title compound was synthesized by procedure **A** from chloroacetone (4.3 g, 46 mmol) and pyridine (3.7 g, 47 mmol) under reflux in THF for 4 h. **1dH$^+$Cl$^-$** was obtained as colorless solid (3.6 g, 21 mmol, 45%). **Mp** 208–209 °C; lit.: 201 °C. (decomp.).[15a] **^{1}H NMR** (400 MHz, DMSO-*d$_6$*) δ = 2.29 (s, 3 H, CH$_3$), 6.03 (s, 2 H, CH$_2$), 8.18–8.25 (m, 2 H, $2 \times$C$_{Ar}$-H), 8.66 (tt, *J* = 7.9, 1.4 Hz, 1 H, C$_{Ar}$-H), 9.06 (dd, *J* = 6.6, 1.2 Hz, 2 H, $2 \times$C$_{Ar}$-H). **^{13}C NMR** (100 MHz, DMSO-*d$_6$*) δ = 27.6 (q, CH$_3$), 68.6 (t, CH$_2$), 128.1 (d, $2 \times$C$_{Ar}$-H), 146.4 (d, $2 \times$C$_{Ar}$-H), 146.6 (d, C$_{Ar}$-H), 200.0 (s, CO). **HRMS** (ESI+): *m/z* [C$_8$H$_{10}$NO]$^+$: calcd.: 136.0757, found: 136.0757. DA167
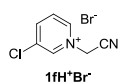
1-(2-Oxo-2-phenylethyl)pyridin-1-ium bromide (1eH$^+$Br$^-$). The title compound was synthesized by procedure **A** from bromoacetophenone (500 mg, 2.51 mmol) and pyridine (289 mg, 3.65 mmol). **1eH$^+$Br$^-$** was obtained as needle-shaped crystals (657 g, 2.36 mmol, 94%). **Mp** 201 °C; lit.: 204–206 °C.[15a] **^{1}H NMR** (400 MHz, DMSO-*d$_6$*) δ = 6.57 (s, 2 H, CH$_2$), 7.63 (dd, *J* = 10.6, 4.8 Hz, 2 H, $2 \times$ C$_{Ar}$-H), 7.72–7.81 (m, 1
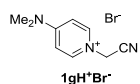
H, C_{Ar}-H), 8.01–8.08 (m, 2 H, 2× C_{Ar}-H), 8.22–8.31 (m, 2 H, 2× C_{Ar}-H), 8.68–8.77 (m, 1 H, C_{Ar}-H), 9.05 (dd, J = 6.7, 1.3 Hz, 2 H, 2×C_{Ar}-H). **^{13}C NMR** (100 MHz, DMSO-d_6) δ = 66.7 (t, CH_2), 128.3 (d, 2×C_{Ar}-H), 128.7 (d, 2×C_{Ar}-H), 129.6 (d, 2×C_{Ar}-H), 134.0 (s, C_{Ar}), 135.2 (d, C_{Ar}-H), 146.7 (d, 2×C_{Ar}-H), 146.8 (d, C_{Ar}-H), 191.2 (s, CO). **HRMS** (ESI+): m/z [$C_{13}H_{12}NO$]$^+$: calcd.: 198.0913, found: 198.0908. DA71

3-Chloro-1-(cyanomethyl)pyridin-1-ium bromide (1fH$^+$Br$^-$). The title compound was synthesized by procedure **A** from 3-chloropyridine (815 mg, 7.18 mmol) and bromoacetonitrile (861 mg, 7.18 mmol). **1fH$^+$Br$^-$** was obtained as beige solid (525 mg, 2.25 mmol, 31%). **Mp** 201–202 °C. **^{1}H NMR** (400 MHz, DMSO-d_6) δ = 6.02 (s, 2 H, CH_2), 8.31 (dd, J = 8.5, 6.2 Hz, 1 H, C_{Ar}-H), 8.92 (ddd, J = 8.5, 2.1, 1.0 Hz, 1 H, C_{Ar}-H), 9.25 (dt, J = 6.2, 1.2 Hz, 1 H, C_{Ar}-H), 9.63 (t, J = 1.6 Hz, 1 H, C_{Ar}-H). **^{13}C NMR** (100 MHz, DMSO-d_6) δ = 47.7 (t, CH_2), 113.8 (s, CN), 129.1 (d, C_{Ar}-H), 134.2 (s, C_{Ar}), 144.3 (d, C_{Ar}-H), 145.1 (d, C_{Ar}-H), 147.1 (d, C_{Ar}-H). **HRMS** (ESI+): [$C_7H_6ClN_2$]$^+$ calcd.: 153.0214; found: 153.0213; **HRMS** (ESI−): [$C_7H_6Br_2ClN_2$]$^-$ calcd.: 310.8592; found: 310.8594. Da727

1-(Cyanomethyl)-4-(dimethylamino)pyridin-1-ium bromide (1gH$^+$Br$^-$). The title compound was synthesized by procedure **A** from 4-(dimethylamino)pyridine (DMAP) (877 mg, 7.18 mmol) and bromoacetonitrile (861 mg, 7.18 mmol). **1gH$^+$Br$^-$** was obtained as colorless solid (1.68g, 6.94 mmol, 97%). **Mp** 241–242 °C. **^{1}H NMR** (400 MHz, DMSO-d_6) δ = 3.23 (s, 6 H, N(CH$_3$)$_2$), 5.57 (s, 2 H, CH_2), 7.11 – 7.17 (m, 2 H, 2×C_{Ar}-H), 8.36 – 8.42 (m, 2 H, 2×C_{Ar}-H). **^{13}C NMR** (100 MHz, DMSO-d_6) δ = 40.0 (q, N(CH$_3$)$_2$), 43.7 (t, CH_2), 108.2 (d, 2×C_{Ar}-H), 115.4 (s, CN), 141.9 (d, 2×C_{Ar}-H), 156.2 (s, C_{Ar}). **HRMS** (ESI+): [$C_9H_{12}N_3$]$^+$ calcd.: 162.1026; found: 162.1025. Da730

2-(Cyanomethyl)isoquinolin-2-ium bromide (4aH$^+$Br$^-$). The title compound was synthesized by procedure **A** from isoquinoline (927 mg, 7.18 mmol) and bromoacetonitrile (861 mg, 7.18 mmol). **4aH$^+$Br$^-$** was obtained as beige solid (881 mg, 3.54 mmol, 49%). **Mp** 208–209 °C; lit.: 207–209.[23] **^{1}H NMR** (400 MHz, DMSO-d_6) δ = 6.19 (s, 2 H, CH_2), 8.13 (t, J = 7.2 Hz, 1 H, C_{Ar}-H), 8.34 (t, J = 7.1 Hz, 1 H, C_{Ar}-H), 8.41 (d, J = 8.2 Hz, 1 H, C_{Ar}-H), 8.60 (d, J = 8.3 Hz, 1 H, C_{Ar}-H), 8.70 (d, J = 6.8 Hz, 1 H, C_{Ar}-H), 8.90 (dd, J = 6.8, 1.4 Hz, 1 H, C_{Ar}-H), 10.27 (s, 1 H, C_{Ar}-H). **^{13}C NMR** (100 MHz, DMSO-d_6) δ = 47.5 (t, CH_2), 114.3 (s, CN), 126.3 (d, C_{Ar}-H), 127.0 (s, C_{Ar}), 127.4 (d, C_{Ar}-H), 131.0 (d, C_{Ar}-H), 131.6 (d, C_{Ar}-H), 134.6 (s, C_{Ar}), 137.5 (d, C_{Ar}-H), 138.0 (d, C_{Ar}-H), 151.5 (d, C_{Ar}-H). **HRMS** (ESI+): $C_{11}H_9N_2$$^+$ calcd.: 169.0760; found: 169.0759. Da729

2-(2-Oxo-2-phenylethyl)isoquinolin-2-ium bromide (4bH⁺Br⁻). The title compound was synthesized by procedure **A** from bromoacetophenone (4.00 g, 20.1 mmol) and isoquinoline (2.60 g, 20.1 mmol). **4bHBr⁻** was obtained as colorless solid (6.15 g, 18.5 mmol, 93%).

Mp 207–208 °C; lit.: 209–210.[3b] **¹H NMR** (400 MHz, DMSO-d_6) δ = 6.68 (s, 2 H, CH$_2$), 7.61 − 7.74 (m, 2 H, 2×C$_{Ar}$-H), 7.75 − 7.92 (m, 1 H, C$_{Ar}$-H), 8.09 − 8.16 (m, 3 H, 3×C$_{Ar}$-H), 8.34 (ddd, J = 8.3, 7.0, 1.2 Hz, 1 H, C$_{Ar}$-H), 8.43 (d, J = 7.6 Hz, 1 H, C$_{Ar}$-H), 8.53 − 8.59 (m, 1 H, C$_{Ar}$-H), 8.70 (d, J = 6.9 Hz, 1 H, C$_{Ar}$-H), 8.77 (dd, J = 6.8, 1.4 Hz, 1 H, C$_{Ar}$-H), 10.07 (s, 1 H, C$_{Ar}$-H). **¹³C NMR** (100 MHz, DMSO-d_6) δ = 66.1 (t, CH$_2$), 125.5 (d, C$_{Ar}$-H), 126.8 (s, C$_{Ar}$), 127.4 (d, C$_{Ar}$-H), 128.3 (d, 2×C$_{Ar}$-H), 129.2 (d, 2×C$_{Ar}$-H), 130.6 (d, C$_{Ar}$-H), 131.4 (d, C$_{Ar}$-H), 133.6 (s, C$_{Ar}$), 134.8 (d, C$_{Ar}$-H), 136.3 (s, C$_{Ar}$), 137.2 (d, C$_{Ar}$-H), 137.5 (d, C$_{Ar}$-H), 151.7 (d, C$_{Ar}$-H), 190.9 (s, CO). **HRMS** (ESI+): m/z [C$_{17}$H$_{14}$NO]⁺: calcd.: 248.1070, found: 248.1071. Da448
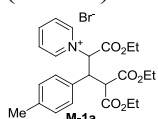
3.4.3 System Development

3.4.3.1 Base and Solvent Dependence

Synthesis of Michael Adduct M-1a in DMSO with HNMe₂ (30% aq.). 1aH⁺Br⁻ (62 mg, 0.25 mmol) and **6f** (66 mg, 0.25 mmol) were dissolved in DMSO (2 mL) and HNMe$_2$ (2 mL, 30% aq.) was added at 20 °C in one portion. The solution turned immediately red and was stirred for 15 min at 20 °C. Brine was added (20 mL) and the solution was extracted with CH$_2$Cl$_2$ (3×20 mL). The combined organic layers were washed with water (20 mL) and brine (20 mL) and dried over Na$_2$SO$_4$. The solvent was evaporated and the crude material was subjected to ¹H NMR: 75:25 mixture of **M-1a** (*dr* 2:1) and **6f**. Da629-1

Synthesis of Michael Adduct M-1a in DMSO with NEt₃. 1aH⁺Br⁻ (123 mg, 500 μmol) and **6f** (131 mg, 500 μmol) were dissolved in DMSO (2 mL) and NEt$_3$ (140 μL, 102 mg, 1.01 mmol) was added at 20 °C in one portion. The solution turned immediately red and was stirred for 15 min at 20 °C. Then TFA (80 μl, 54 mg, 0.47 mmol) was added to quench the reaction. Brine was added (20 mL) and the solution was extracted with CH$_2$Cl$_2$ (3×20 mL). The combined organic layers were washed with water (20 mL) and brine (20 mL) and dried over Na$_2$SO$_4$. The solvent was evaporated and the crude material was subjected to ¹H NMR: 40:60 mixture of **M-1a** (*dr* ~1:1) and **6f**. Da626-1

Synthesis of Michael Adduct M-1a in DMSO with KO^{t}Bu. 1-(1,5-Diethoxy-4-(ethoxycarbonyl)-1,5-dioxo-3-(*p*-tolyl)pentan-2-yl)pyridin-1-ium bromide (M-1a). **1aH$^+$Br$^-$** (123 mg, 500 μmol) and **6f** (131 mg, 500 μmol) were dissolved in DMSO (2 mL) and KO^{t}Bu (67 mg, 0.60 mmol) in 2 mL DMSO was added at 20 °C in one portion. The solution turned immediately red and was stirred for 15 min at 20 °C. Then TFA (80 μl, 54 mg, 0.47 mmol) was added to quench the reaction. Brine was added (20 mL) and the solution was extracted with CH$_2$Cl$_2$ (3×20 mL). The combined organic layers were washed with water (20 mL) and brine (20 mL) and dried over Na$_2$SO$_4$. The solvent was evaporated and the crude material was subjected to ^{1}H NMR: 93:7 mixture of **M-1a** (*dr* ~1:1.2) and **6f**. Tentative assignment of the ^{1}H NMR-signals in the mixture of diastereoisomers. **^{1}H NMR** (200 MHz, CDCl$_3$) δ = 0.64−0.77 (m, 2×CH$_3$), 0.83 (t, J = 7.1 Hz, CH$_3$), 0.98 (t, J = 7.1 Hz, CH$_3$), 1.18 − 1.10 (m, 2×CH$_3$, superimposed by **6f**), 2.00 (s, CH$_3$), 2.15 (s, CH$_3$), 3.53 − 3.68 (m, 2×CH$_2$), 3.76 − 3.91 (m, 2×CH, 2×CH$_2$), 4.01 − 4.19 (m, 3×CH, 2×CH$_2$), 4.50 (d, J = 10.6 Hz, CH), 6.77 (d, J = 8.0 Hz, 2×C$_{Ar}$-H), 6.94 − 7.00 (m, 4×C$_{Ar}$-H), 7.06 − 7.11 (m, 2×C$_{Ar}$-H), 7.82 (t, J = 6.9 Hz, 2×C$_{Ar}$-H), 8.01 (t, J = 6.9 Hz, 2×C$_{Ar}$-H), 8.38 (t, J = 7.7 Hz, C$_{Ar}$-H), 8.62 (t, J = 7.7 Hz, C$_{Ar}$-H), 9.21 (d, J = 5.8 Hz, 2×C$_{Ar}$-H), 9.36 (d, J = 6.0 Hz, 2×C$_{Ar}$-H). Da626-2

Synthesis of Michael Adduct M-1a in Methanol with NEt$_3$. **1aH$^+$Br$^-$** (62 mg, 0.25 mmol) and **6f** (66 mg, 0.25 mmol) were dissolved in methanol (2 mL) and NEt$_3$ (37 mg, 0.37 mmol) was added at 20 °C in one portion. The solution turned immediately red and was stirred for 15 min at 20 °C. The solvent was evaporated and the crude material was subjected to ^{1}H NMR: 78:22 mixture of **M-1a** (*dr* 1:1) and **6f**. Da629-2

Synthesis of Michael Adduct M-1a in MeCN with NEt$_3$. **1aH$^+$Br$^-$** (123 mg, 500 μmol) and **6f** (131 mg, 500 μmol) were dissolved in MeCN (2 mL) and NEt$_3$ (102 mg, 1.01 mmol) was added at 20 °C in one portion. The solution turned immediately red and was stirred for 15 min at 20 °C. Then the solvent was evaporated and the crude material was subjected to ^{1}H NMR: 88:12 mixture of **M-1a** (*dr* 2:1) and **6f**. Da626-3

Synthesis of Michael Adduct M-1a in CH$_2$Cl$_2$ with NEt$_3$. **1aH$^+$Br$^-$** (59 mg, 0.24 mmol) and **6f** (62 mg, 0.24 mmol) were suspended in CH$_2$Cl$_2$ (2 mL) and NEt$_3$ (37 mg, 0.37 mmol) was added at 20 °C in one portion. The solution turned immediately red and was stirred for 15 min at 20 °C. Then the solvent was evaporated and the crude material was subjected to ^{1}H NMR: 8:92 mixture of **6f** and **M-1a** (*dr* 3:1)/**C-1a** (*dr* not determined) in a 72/28 ratio. Da649-roh

Synthesis of [3+2]-Cycloadduct C-1a in Et₂O/MeCN with NEt₃. $1aH^+Br^-$ (59 mg, 0.24 mmol) and **6f** (62 mg, 0.24 mmol) were suspended in Et₂O/MeCN (3 mL, 2:1) and NEt₃ (50 μL, 37 mg, 0.36 mmol) was added at 20 °C in one portion. The solution turned immediately red and was stirred for 15 min at 20 °C. Then the solvent was evaporated and the crude material was subjected to ¹H NMR: 14:86 mixture of **6f** and **M-1a** (*dr* 1:1)/**C-1a** (*dr* 3:2) in a 342/66 ratio. Da649-2

Synthesis of [3+2]-Cycloadduct C-1a in THF with KOᵗBu. $1aH^+Br^-$ (59 mg, 0.24 mmol) and **6f** (62 mg, 0.24 mmol) were suspended in THF (2 mL) and KOᵗBu (28 mg, 0.25 mmol) in 1 mL THF was added. The solution turned immediately red and was stirred for 5 min at 20 °C. The solvent was evaporated and the crude material was subjected to ¹H NMR: 99:1 mixture of **C-1a** (*dr* 1:1) and **6f**. Da649-4

Synthesis of [3+2]-Cycloadduct C-1a in CH₂Cl₂ with NaOH (32%). $1aH^+Br^-$ (59 mg, 0.24 mmol) and **6f** (62 mg, 0.24 mmol) were suspended in CH₂Cl₂ (5 mL) and NaOH (1 mL, 32%) was added at 20 °C in one portion. The solution turned immediately red and was stirred

for 15 min at 20 °C. Water was added (20 mL) and the solution was extracted with CH₂Cl₂ (3×20 mL). The combined organic layers were washed with water (20 mL) and brine (20 mL) and dried over Na₂SO₄. The solvent was evaporated , the crude material was filtrated over SiO₂ (*n*-pentane:EtOAc:NEt₃ 5:1:1) and subjected to ¹H NMR: 97:3 mixture of **C-1a** (*dr* 1.7:1) and **6f**. Tentative assignment of the ¹H NMR-signals in the mixture of diastereoisomers; *-major, #-minor diastereoisomer. **¹H NMR** (200 MHz, CDCl₃) δ = 0.68 (t, *J* = 7.1 Hz, CH₃),# 0.83 – 0.97 (m, 2×CH₃),# 1.11 – 1.24 (m, 3×CH₃),* 2.18 (s, CH₃),# 2.23 (s, CH₃),* 3.45 – 3.97 (m, 3×CH₂),*,# 4.00 – 4.34 (m, 3×CH₂, 2×2-H, 3-H, 8ᵃ-H),*,# 4.52 – 4.65 (m, 8ᵃ-H),# 4.88 (d, *J* = 8.1 Hz, 3-H),# 4.91 – 5.18 (m, 5-H, 8-H),*,# 5.66 (t, *J* = 2.2 Hz, 7-H),# 5.69 – 5.76 (m, 8-H),# 5.80 (d, *J* = 7.7 Hz, 5-H, 7-H),*,# 5.85 (d, *J* = 5.7 Hz, 6-H),# 5.92 (d, *J* = 7.3 Hz, 6-H),* 6.92 (s, 4×Cₐᵣ-H),# 6.98−7.04 (m, 2×Cₐᵣ-H),* 7.07 − 7.18 (m, 2×Cₐᵣ-H).* Da649-6

Oxidation by MnO₂. $1aH^+Br^-$ (59 mg, 0.24 mmol) and **6f** (62 mg, 0.24 mmol) were dissolved in DMSO (2 mL) and NEt₃ (76 mg, 0.75 mmol) were added at 20 °C in one portion under stirring, After 5 min MnO₂ (55 mg, 0.63 mmol, 2.6 eq) was added and the solution was stirred for 3 h at 100 °C. Then 2N HCl (20 mL) was added and the mixture was extracted against EtOAc (3×20 mL). The combined organic layers were washed with water (20 mL) and brine (20 mL) and dried over Na₂SO₄. The solvent was evaporated and the crude material was

subjected to ^{1}H NMR. **7a** was obtained with 50% conversion (by NMR) with ethyl (4-methyl) cinnamate (50%) formed from **6f** by degradation to EtOH and CO_2 as byproduct. Da645-2

Synthesis of [3+2]-Cycloadduct *rac*-C-4a in CH₂Cl₂ with NaOH (32%). Diethyl 3-cyano-2-(*p*-tolyl)-2,3-dihydropyrrolo[2,1-*a*]isoquinoline-1,1(10*b*H)-dicarboxylate (*rac*-C-4a): **4aH⁺Br⁻** (159 mg, 6382 μmol) and **6f** (132 mg, 503 μmol) were suspended in CH_2Cl_2 (5 mL) and NaOH (1 mL, 32%) was added at 20 °C in one portion. The solution turned immediately orange and was stirred for 15 min at 20 °C. Water was added (20 mL) and the solution was extracted with CH_2Cl_2 (3×20 mL). The combined organic layers were washed with water (20 mL) and dried over Na_2SO_4. The solvent was evaporated and the crude material was recrystallized from Et_2O. *rac*-C-4a was obtained as orange solid (213 mg; 495 μmol; 98%; *dr* 4:9:100 for anti-exo approach). **Mp** (anti-exo-**C-4a**): 132−135 °C. **^{1}H NMR** (anti-exo-**C-4a**, 400 MHz, CDCl₃) δ = 0.69 (t, *J* = 7.2 Hz, 3 H, CH₃), 0.74 (t, *J* = 7.2 Hz, 3 H, CH₃), 2.33 (s, 3 H, CH₃), 3.34 − 3.47 (m, 2 H, CH₂), 3.71 − 3.86 (m, 2 H, CH₂), 4.37 (d, *J* = 10.2 Hz, 1 H, 2-H), 4.53 (d, *J* = 10.2 Hz, 1 H, 1-H), 5.53 (d, *J* = 7.7 Hz, 1 H, 6-H), 5.68 (s, 1 H, 10^b-H), 6.53 (d, *J* = 7.8 Hz, 1 H, 5-H), 6.98 (dd, *J* = 7.7, 1.4 Hz, 1 H, 7-H), 7.06 − 7.17 (m, 5 H, 4×C$_{Ar}$-H, 8- or 9-H), 7.21 (td, *J* = 7.5, 1.3 Hz, 1 H, 8- or 9-H), 7.32 (dd, *J* = 7.6, 1.4, 1 H, 10-H). **^{13}C NMR**

(anti-exo-**C-4a**,100 MHz, CDCl₃) δ = 13.3 (q, CH₃), 13.3 (q, CH₃), 21.2 (q, CH₃), 54.7 (d, C-1), 59.2 (d, C-2), 61.7 (t, CH₂), 62.0 (t, CH₂), 67.0 (d, C-10^b), 70.9 (s, C-3), 103.7 (d, C-6), 115.7 (s, CN), 124.5 (d, C-7), 125.9 (d, C-8), 126.9 (s, C-10^a), 128.6 (d, C-10), 128.8 (d, C-9), 129.5 (d, 4×C$_{Ar}$-H), 131.3 (d, C-5), 131.5 (s, C-6^a), 132.1 (s, C$_{Ar}$), 138.4 (s, C$_{Ar}$), 168.5 (s, CO₂), 169.3 (s, CO₂). **HRMS** (EI): $C_{26}H_{26}N_2O_4$ calcd.: 430.1893; found: 430.1894. **MS** (EI) *m/z* = 430.13 (2), 262.03 (8), 217.00 (9), 169.00 (10), 167.99 (100), 144.00 (10), 116.01 (18), 115.00 (11). Da884-4
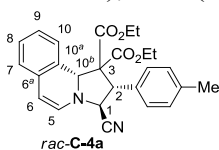
3.4.3.2 Oxidant-Screening

Pd/C/O₂. **1aH⁺Br⁻** (62 mg, 0.25 mmol) and **6f** (66 mg, 0.25 mmol) were dissolved in CH_2Cl_2 (5 mL) and aq. NaOH (1 mL, 30%) was added at 20 °C in one portion. The solution turned immediately red and was stirred till all of **6f** was consumed (by TLC). Then 20 mL water was added, the organic layer was separated and the aqueous layer was extracted by CH_2Cl_2 (2×10 mL). The combined organic layers were dried over Na_2SO_4. The dried solution was transferred to a Schlenk-flask and Pd/C (20 mg Pd/C $\cong$ 2 mg Pd (10%)) was added. The flask was set under O_2 and stirred for 18 h at 20 °C. No conversion of **6f** to **7a** was observed by TLC. Da654-3

DTBPO. A solution of DTBPO (146 mg, 1.00 mmol, 4.0 eq) was added to a dried solution of **C-1a** generated as described for Pd/C/O$_2$ (see above) at 20 °C and stirred for 18 h. Only **6f** and not a trace of **7a** was observed by TLC. Da654-5

NCS. NCS (133 mg, 1.00 mmol, 4 eq) was added to a dried solution of **C-1a** generated as described in 0 at 20 °C and stirred for 18 h. Only **6f** and not a trace of **7a** was observed by TLC. Da654-5

DDQ. DDQ (80 mg, 352 μmol, 1.4 eq) was added to a dried solution of **C-1a** generated as described for Pd/C/O$_2$ (see above) at 20 °C and stirred for 18 h. The solvent was evaporated and the crude material was filtrated over SiO$_2$ with CH$_2$Cl$_2$ as eluent. The solvent was evaporated and the product was subjected to ^{1}H NMR. **7a** was obtained with 54% conversion (by NMR; as ratio of **7a**/(**6f**+**7a**)). Da654-1

2.0 equiv. Chloranil for 18 h. Chloranil (122 mg, 0.50 mmol, 2.0 eq) was added was added to a dried solution of **C-1a** generated as described for Pd/C/O$_2$ (see above; double amount of reactants) at 20 °C and stirred for 18 h. The solvent was evaporated, the crude material was filtrated over SiO$_2$ with CH$_2$Cl$_2$ as eluent. The solvent was evaporated and the product was subjected to ^{1}H NMR. **7a** was obtained with 69% conversion (by NMR, as ratio of **7a**/(**6f**+**7a**)). Da654-2

Oxidation by 1.0 equiv. Chloranil for 3 h. Chloranil (62 mg, 0.25 mmol, 1.0 eq) was added to a dried solution of **C-1a** generated as described for Pd/C/O$_2$ (see above) at 20 °C and stirred for 3 h. The solvent was evaporated and subjected to ^{1}H NMR. **7a** was obtained with 74% conversion (by NMR, as ratio of **7a**/(**6f**+**7a**)). Da654-8

Oxidation by 1.0 equiv. Chloranil for 1 h. Chloranil (62 mg, 0.25 mmol, 1.0 eq) was added to a dried solution of **C-1a** generated as described for Pd/C/O$_2$ (see above) at 20 °C and stirred for 1 h. The solvent was evaporated and the crude material was subjected to ^{1}H NMR. **7a** was obtained with 74% conversion (by NMR; as ratio of **7a**/(**6f**+**7a**)). Da654-6

Oxidation by 1.0 equiv. Chloranil for 0.5 h. Chloranil (62 mg, 0.25 mmol, 1.0 eq) was added to a dried solution of **C-1a** generated as described for Pd/C/O$_2$ (see above) at 20 °C and stirred for 0.5 h. The solvent was evaporated and the crude material was subjected to ^{1}H NMR. **7a** was obtained with 65% conversion (by NMR; as ratio of **7a**/(**6f**+**7a**)). Da654-7

3.4.3.3 Mechanistic Studies

Oxidation of C-4a under inert atmosphere. **C-4a** (80 mg, 0.19 mmol) was dissolved in CD_2Cl_2 under N_2-atmosphere. Under N_2 at 20 °C chloranil (45.7 mg, 0.19 mmol) was added and the solution was stirred for 1 h. After 1 h the reaction mixture was subjected to ^{1}H NMR-analysis. 21% of **C-4a** were converted to indolizine **5a**.

Oxidation of C-4a under air. **C-4a** (80 mg, 0.19 mmol) was dissolved at 20 °C in CD_2Cl_2 under air and chloranil (45.7 mg, 0.19 mmol) was added and the solution was stirred for 1 h. After 1 h the reaction mixture was subjected to ^{1}H NMR-analysis. 58% of **C-4a** were converted to indolizine **5a**.

Oxidation of C-4a under air with aq. NaOH (32%). **C-4a** (166 mg, 0.39 mmol) was dissolved at 20 °C in CD_2Cl_2 under air, chloranil (93 mg, 0.38 mmol) and 20 μl aq. NaOH (32%) were added and the solution was stirred for 1 h. After 1 h the reaction mixture was subjected to ^{1}H NMR-analysis. 17% of **C-4a** were converted to indolizine **5a**.

Oxidation of C-4a under air with NaOH saturated CH_2Cl_2. 5 mL CH_2Cl_2 and 1 mL aq. NaOH (32%) were stirred for 1 h at 20 °C, then water was added and the CH_2Cl_2 was separated and dried over Na_2SO_4. Then **C-4a** (47 mg, 0.11 mmol) was dissolved in the NaOH sat. CH_2Cl_2 at 20 °C under air, chloranil (27 mg, 0.11 mmol) was added and the solution was stirred for 1 h. After 1 h the solvent was evaporated and the crude reaction mixture was subjected to ^{1}H NMR-analysis. 100% of **C-4a** were converted to indolizine **5a**.

3.4.4 Synthesis of the Products 5, 7, 12, C-4b, and 18

Procedure B for the Synthesis of the Indolizines 5, 7. The Michael acceptor **6a−j** or **13a−c** (0.25−0.50 mmol) and the salt **1a−hH⁺X⁻** or **4aH⁺Br⁻** (0.25−1.00 mmol) were suspended in dichloromethane (CH_2Cl_2, 0.1 M), and 1 mL of NaOH (aq. 30%, 1 mL) was added at room temperature. The suspension was stirred till the Michael acceptor was completely consumed (monitored by TLC; 15 min – 1 h). Water (30 mL) was added and the reaction mixture was extracted with CH_2Cl_2 (3×5 mL). The combined organic layers were dried over Na_2SO_4. Chloranil (1 eq.) was added and the solution was stirred at room temperature for 30 min to 3 h. The solvent was evaporated and the residue was subjected to column chromatography (*n*-pentane : EtOAc 15:1 – 3:1, depending on R_f). The resulting solids were dissolved in $CHCl_3$, and insoluble precipitates were removed by filtration. After evaporation the products were further purified by recrystallization from Et_2O.

3.4.4.1 Variation of the Ylides 1

Diethyl 2-(*p*-tolyl)indolizine-1,3-dicarboxylate (7a). According to procedure **B** from **1aH$^+$Br$^-$** (62 mg, 0.25 mmol), **6f** (60 mg, 0.23 mmol) and chloranil (56 mg, 0.23 mmol). **7a** was obtained as colorless crystalline solid (53 mg, 0.15 mmol, 65%).

R_f = 0.51 (*i*-Hexane:EtOAc 5:1). **Mp** 116–117 °C. **IR** (neat) $\widetilde{\nu}$ = 3329, 3148, 2981, 1727, 1664, 1628, 1499, 1401, 1384, 1334, 1257, 1200, 1187, 1175, 1118, 1092, 1054, 1037 cm^{-1}. **^{1}H NMR** (300 MHz, CDCl$_3$) δ = 0.88 (t, J = 7.1 Hz, 3 H, CH$_3$), 1.06 (t, J = 7.1 Hz, 3 H, CH$_3$), 2.41 (s, 3 H, CH$_3$), 4.05 (q, J = 7.1 Hz, 2 H, CH$_2$), 4.13 (q, J = 7.1 Hz, 2 H, CH$_2$), 6.98 (td, J = 6.9, 1.5 Hz, 1 H, 6-H), 7.09 – 7.21 (m, 4 H, 4×C$_{Ar}$-H), 7.32 (ddd, J = 9.0, 6.8, 1.2 Hz, 1 H, 7-H), 8.33 – 8.44 (m, 1 H, 8-H), 9.60 (dt, J = 7.2, 1.1 Hz, 1 H, 5-H). **^{13}C NMR** (75 MHz, CDCl$_3$) δ = 13.6 (q, CH$_3$), 14.1 (q, CH$_3$), 21.5(q, CH$_3$), 59.6 (t, CH$_2$), 60.0 (t, CH$_2$), 105.3 (s, C-1), 113.9 (s, C-3), 114.4 (d, C-6), 119.8 (d, C-8), 125.9 (d, C-7), 127.7 (d, 2×C$_{Ar}$-H), 128.1 (d, C-5), 129.2 (d, 2×C$_{Ar}$-H), 133.1 (s, C$_{Ar}$), 136.4 (s, C$_{Ar}$), 138.7 (s, C-8^a), 140.4 (s, C-2), 162.0 (s, CO$_2$), 164.5 (s, CO$_2$). **HRMS** (EI): C$_{21}$H$_{21}$NO$_4$ calcd.: 351.1471; found: 351.1463. **MS** (EI) m/z = 351 (100), 323 (5), 306 (10), 279 (22), 207 (12). Da659

Ethyl 3-(diethylcarbamoyl)-2-(*p*-tolyl)indolizine-1-carboxylate (7b). According to procedure **B** from **1bH$^+$Br$^-$** (163 mg, 597 μmol), **6f** (131 mg, 500 μmol) and chloranil (123 mg, 500 μmol). **7b** was obtained as colorless solid (98 mg, 0.26 mmol, 52%). R_f = 0.21 (*i*-Hexane:EtOAc 5:1). **Mp** 100–101 °C. **IR** (neat) $\widetilde{\nu}$ = 2975, 2931, 1695, 1617, 1542, 1502, 1439, 1382, 1266, 1230, 1218, 1171, 1148, 1133, 1048 cm^{-1}. **^{1}H NMR** (400 MHz, CDCl$_3$) δ = 0.61 (br s, 3 H, CH$_3$), 1.05 (br s, 3 H, CH$_3$), 1.24 (t, J = 7.1 Hz, 3 H, CH$_3$), 2.38 (s, 3 H, CH$_3$), 2.62 (br s, 1 H, CHH^a), 3.04 – 3.24 (m, 2 H, CHH^a, CHH^b), 3.74 (br s, 1 H, CHH^b), 4.13 – 4.35 (m, 2 H, CH$_2$), 6.75 – 6.81 (m, 1 H, 6-H), 7.11 – 7.17 (m, 3 H, 7-H, 2×C$_{Ar}$-H), 7.30 – 7.36 (m, 2 H, 2×C$_{Ar}$-H), 8.20 (dt, J = 7.0, 1.1 Hz, 1 H, 5-H), 8.27 (dt, J = 9.1, 1.3 Hz, 1 H, 8-H). **^{13}C NMR** (100 MHz, CDCl$_3$) δ = 12.5 (br q, CH$_3$), 14.1 (br q, CH$_3$), 14.5 (q, CH$_3$), 21.5 (q, CH$_3$), 38.9 (t br, CHH), 42.8 (t br, CHH), 59.6 (t, CH$_2$), 101.6 (s, C-1), 113.3 (d, C-6), 118.6 (s, C-3), 120.3 (d, C-8), 123.6 (d, C-7), 125.3 (d, C-5), 128.4 (d, 2×C$_{Ar}$-H), 130.6 (s, C$_{Ar}$), 130.6 (d, 2×C$_{Ar}$-H), 130.9 (s, C-2), 137.1 (s, C-8^a), 137.4 (s, C$_{ar}$), 163.1 (s, CO), 165.0 (s, CO). **HRMS** (EI): C$_{23}$H$_{26}$N$_2$O$_3$ calcd.: 378.1943; found: 378.1939. **MS** (EI) m/z = 378 (56), 279 (100), 234 (28), 204 (12). Da726-5

Ethyl 3-cyano-2-(*p*-tolyl)indolizine-1-carboxylate (7c). According to procedure **B** from **1cH$^+$Br$^-$** (149 mg, 750 μmol), **6f** (131 mg, 500 μmol) and chloranil (123 mg, 500 μmol). **7c** was obtained as colorless solid (112 mg, 370 μmol, 74%). R_f = 0.36 (*i*-Hexane:EtOAc 5:1). **Mp** 128–129 °C. **IR** (neat) $\widetilde{\nu}$ = 3402, 2920, 2201, 1747, 1680, 1502, 1446, 1401, 1264, 1243, 1153, 1055, 1012, 991 cm^{-1}. **^{1}H NMR** (300 MHz, CDCl$_3$) δ = 1.22 (t, *J* = 7.1 Hz, 3 H, CH$_3$), 2.42 (s, 3 H, CH$_3$), 4.26 (q, *J* = 7.1 Hz, 2 H, CH$_2$), 7.03 (td, *J* = 6.8, 1.4 Hz, 1 H, 6-H), 7.22 – 7.29 (m, 2 H, 2×C$_{Ar}$-H, superimposed by solvent), 7.34 (ddd, *J* = 9.1, 6.9, 1.3 Hz, 1 H, 7-H), 7.39 – 7.47 (m, 2 H, 2×C$_{Ar}$-H), 8.31 – 8.41 (m, 2 H, 5-H, 8-H). **^{13}C NMR** (75 MHz, CDCl$_3$) δ = 14.3 (q, CH$_3$), 21.5 (q, CH$_3$), 60.1 (t, CH$_2$), 97.4 (s, CN), 103.8 (s, C-1), 113.2 (s, C-3), 115.0 (d, C-6), 120.9 (d, C-5 or C-8), 125.6 (d, C-5 or C-8), 126.3 (d, C-7), 128.6 (s, C$_{Ar}$), 128.8 (d, 2×C$_{Ar}$-H), 130.0 (d, 2×C$_{Ar}$-H), 138.7 (s, C$_{Ar}$), 138.7 (s, C-8^a), 141.6 (s, C-2), 163.7 (s, CO$_2$). **HRMS** (EI): C$_{19}$H$_{16}$N$_2$O$_2$ calcd.: 304.1212; found: 304.1205. **MS** (EI) *m/z* = 304 (100), 276 (16), 259 (55), 232. (41). Da665
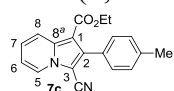
Diethyl 3-acetyl-2-(*p*-tolyl)indolizine-1-carboxylate (7d). According to procedure **B** from **1dH$^+$Cl$^-$** (162 mg, 944 μmol), **6f** (131 mg, 500 μmol) and chloranil (123 mg, 500 μmol). **7d** was obtained as colorless solid (82 mg, 0.26 mmol, 52%). R_f = 0.50 (*i*-Hexane:EtOAc 5:1). **Mp** 145 °C. **IR** (neat) $\widetilde{\nu}$ = 3405, 2921, 2852, 1747, 1553, 1445, 1400, 1372, 1256, 1196, 1172, 1012, 991 cm^{-1}. **^{1}H NMR** (600 MHz, CDCl$_3$) δ = 1.03 (t, *J* = 7.1 Hz, 3 H, CH$_3$), 1.91 (s, 3 H, CH$_3$), 2.42 (s, 3 H, CH$_3$), 4.10 (q, *J* = 7.1 Hz, 2 H, CH$_2$), 7.02 (td, *J* = 7.0, 1.5 Hz, 1 H, 6-H), 7.19 (d, *J* = 8.1 Hz, 2 H, 2×C$_{Ar}$-H), 7.23 (d, *J* = 7.9 Hz, 2 H, 2×C$_{Ar}$-H), 7.40 (ddd, *J* = 8.9, 6.8, 1.2 Hz, 1 H, 7-H), 8.41 (dt, *J* = 9.0, 1.2 Hz, 1H, 8-H), 10.04 (dt, *J* = 7.2, 1.1 Hz, 1H, 5-H). **^{13}C NMR** (150 MHz, CDCl$_3$) δ = 14.0 (q, CH$_3$), 21.5 (q, CH$_3$), 30.9 (q, CH$_3$), 59.7 (t, CH$_2$), 106.0 (s, C-1), 115.3 (d, C-6), 119.6 (d, C-8), 122.7 (s, C-3), 127.5 (d, C-7), 128.8 (d, 2×C$_{Ar}$-H), 129.2 (d, C-5), 129.3 (d, 2×C$_{Ar}$-H), 133.2 (s, C$_{Ar}$), 137.6 (s, C$_{Ar}$), 138.7 (s, C-8^a), 141.5 (s, C-2), 164.4 (s, CO$_2$), 190.2 (s, CO). **HRMS** (EI): C$_{20}$H$_{19}$NO$_3$ calcd.: 321.1365; found: 321.1363. **MS** (EI) *m/z* = 322 (18), 321 (100), 278 (16), 276 (23), 249 (18), 234 (27), 204 (11). Da743
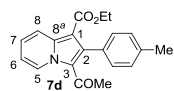
Ethyl 3-benzoyl-2-(4-nitrophenyl)indolizine-1-carboxylate (7e). According to procedure **B** from **1eH$^+$Br$^-$** (105 mg, 378 μmol), **6a** (73 mg, 249 μmol) and chloranil (123 mg, 500 μmol). **7e** was obtained as impure yellow solid (22 mg, 53 μmol, 21%). R_f = 0.26 (*i*-Hexane:EtOAc 5:1). **^{1}H NMR** (600 MHz, CDCl$_3$) δ = 1.11 (t, *J* = 7.1 Hz, 3 H, CH$_3$), 4.17 (q, *J* = 7.1 Hz, 2 H, CH$_2$), 7.03 (t, *J* = 7.8 Hz, 2 H, 2×C$_{Ar}$-H), 7.11 (t, *J* = 7.0 Hz, 1 H, 6-H), 7.18 (t, *J* = 7.5 Hz, 1 H, C$_{Ar}$-H), 7.22 – 7.28 (m, 2 H, 2×C$_{Ar}$-H, superimposed by
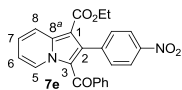
solvent), 7.30 − 7.33 (m, 2 H, 2×C_{Ar}-H), 7.45 – 7.52 (m, 1 H, 7-H), 7.86 (d, J = 8.8 Hz, 2 H, 2×C_{Ar}-H), 8.49 (d, J = 9.0 Hz, 1 H, 8-H), 9.64 (d, J = 7.1 Hz, 1 H, 5-H). ^{13}C NMR (150 MHz, CDCl$_3$) δ = 14.2 (q, CH$_3$), 60.2 (t, CH$_2$), 104.9 (s, C-1), 115.7 (d, C-6), 120.1 (d, C-8), 122.0 (d, 2×C_{Ar}-H), 122.4 (s, C-3), 127.9 (d, 2×C_{Ar}-H), 128.0 (d, C-7), 128.4 (d, C-5), 129.2 (d, 2×C_{Ar}-H), 131.6 (d, C_{Ar}-H), 132.2 (d, 2×C_{Ar}-H), 137.8 (s, C_{Ar}), 139.3 (s, C-8^a), 139.4 (s, C-2), 141.7 (s, C_{Ar}), 146.8 (s, C_{Ar}), 164.0 (s, CO$_2$), 187.9 (s, CO). **HRMS** (EI): C$_{24}$H$_{18}$N$_2$O$_5$ calcd.: 414.1216; found: 414.1214. **MS** (EI) m/z = 414 (100), 369 (12), 342 (10). Da688

Ethyl 6-chloro-3-cyano-2-(*p*-tolyl)indolizine-1-carboxylate (7f). According to procedure **B** from **1fH$^+$Br$^-$** (175 mg, 750 μmol), **6f** (132 mg, 503 μmol) and chloranil (123 mg, 500 μmol).

7f was obtained as colorless solid (92 mg, 0.27 mmol, 54%). R_f = 0.47 (*i*-Hexane:EtOAc 5:1). **Mp** 126–127 °C. **IR** (neat) $\widetilde{\nu}$ = 3364, 2916, 2208, 1771, 1685, 1501, 1433, 1423, 1379, 1324, 1264, 1241, 1180, 1098, 1060, 1031 cm^{-1}. ^{1}H NMR (400 MHz, CDCl$_3$) δ = 1.19 (t, J = 7.1 Hz, 3 H, CH$_3$), 2.40 (s, 3 H, CH$_3$), 4.23 (q, J = 7.1 Hz, 2 H, CH$_2$), 7.21 – 7.30 (m, 3 H, 7-H, 2×C_{Ar}-H, superimposed by solvent), 7.34 – 7.44 (m, 2 H, 2×C_{Ar}-H), 8.31 (dd, J = 9.6, 0.9 Hz, 1 H, 8-H), 8.37 (dd, J = 1.8, 0.9 Hz, 1 H, 5-H). ^{13}C NMR (100 MHz, CDCl$_3$) δ = 14.2 (q, CH$_3$), 21.5 (q, CH$_3$), 60.4 (t, CH$_2$), 97.7 (s, CN), 104.6 (s, C-1), 112.6 (s, C-3), 121.3 (d, C-8), 123.5 (d, C-5), 123.6 (s, C-6), 127.6 (d, C-7), 128.1 (s, C_{Ar}), 128.9 (d, 2×C_{Ar}-H), 130.0 (d, 2×C_{Ar}-H), 136.7 (s, C-8^a), 139.0 (s, C_{Ar}), 141.7 (s, C-2), 163.3 (s, CO$_2$). **HRMS** (EI): C$_{19}$H$_{15}$ClN$_2$O$_2$ calcd.: 338.0822; found: 338.0813. **MS** (EI) m/z = 340 (31), 338 (100), 295 (24), 293 (75), 266 (63), 229 (15). Da733

Ethyl 3-cyano-7-(dimethylamino)-2-(*p*-tolyl)indolizine-1-carboxylate (7g). According to procedure **B** from **1gH$^+$Br$^-$** (151 mg, 624 μmol), **6f** (132 mg, 503 μmol) and chloranil (123 mg, 500 μmol). **7g** was obtained as colorless solid (34 mg, 98 μmol, 19%). R_f = 0.19 (*i*-Hexane:EtOAc 5:1). **Mp** 190–191 °C. **IR** (neat) $\widetilde{\nu}$ = 3485, 2980, 2194, 1692, 1647, 1513, 1492, 1433, 1301, 1226, 1179, 1143, 1066, 1034 cm^{-1}. ^{1}H NMR (300 MHz, CDCl$_3$) δ = 1.17 (t, J = 7.1 Hz, 3 H, CH$_3$), 2.41 (s, 3 H, CH$_3$), 3.12 (s, 6 H, N(CH$_3$)$_2$), 4.19 (q, J = 7.1 Hz, 2 H, CH$_2$), 6.72 (dd, J = 7.6, 2.6 Hz, 1 H, 6-H), 7.23 (d, J = 7.9 Hz, 2 H, 2×C_{Ar}-H), 7.41 (d, J = 8.0 Hz, 2 H, 2×C_{Ar}-H), 7.48 (d, J = 2.6 Hz, 1 H, 8-H), 8.10 (d, J = 7.6 Hz, 1 H, 5-H). ^{13}C NMR (75 MHz, CDCl$_3$) δ = 14.3 (q, CH$_3$), 21.5 (q, CH$_3$), 40.6 (q, N(CH$_3$)$_2$), 59.6 (CH$_2$), 94.7 (s, C-1), 97.8 (br d, C-8), 99.7 (s, CN), 105.4 (d, C-6), 114.4 (s, C-3), 126.2 (d, C-5), 128.6 (d, 2×C_{Ar}-H), 129.3 (s, C_{Ar}), 129.9 (d, 2×C_{Ar}-H), 138.3 (s, C_{Ar}), 141.7 (br s, C-8^a), 142.6 (s, C-2), 148.1 (s, C-7), 164.4 (s, CO$_2$).

HRMS (EI): C$_{21}$H$_{21}$N$_3$O$_2$ calcd.: 347.1634; found: 347.1626. **MS** (EI) m/z = 347 (100), 319 (35), 302 (25), 275 (35). Da732

Ethyl 3-cyano-2-(*p*-tolyl)pyrrolo[2,1-*a*]isoquinoline-1-carboxylate hydrate (8a·H₂O). According to procedure **B** from **4aH⁺Br⁻** (175 mg, 703 µmol), **6f** (132 mg, 503 µmol) and chloranil (123 mg, 500 µmol). **8a·**H₂O was obtained as light yellow solid (165 mg, 443 µmol, 89%). R_f = 0.53 (*i*-Hexane:EtOAc 5:1). **Mp** 143–144 °C. **IR** (neat) $\tilde{v}$ = 3403, 2931, 2924, 2208, 1748, 1701, 1508, 1401, 1369, 1265, 1209, 1190, 1113, 1095, 1027 cm⁻¹. **¹H NMR** (600 MHz, CDCl₃) δ = 1.08 (t, *J* = 7.2 Hz, 3 H, CH₃), 1.56 (s, 2 H, H₂O), 2.43 (s, 3 H, CH₃), 4.26 (q, *J* = 7.1 Hz, 2 H, CH₂), 7.20 (d, *J* = 7.2 Hz, 1 H, 6-H), 7.28 (d, *J* = 7.8 Hz, 2 H, 2×C_Ar-H), 7.41 (d, *J* = 8.0 Hz, 2 H, 2×C_Ar-H), 7.57 – 7.64 (m, 2 H, 8-H, 9-H), 7.69 – 7.78 (m, 1 H, 7-H), 8.11 (d, *J* = 7.2 Hz, 1 H, 5-H), 8.74 – 8.82 (m, 1 H, 10-H).**¹³C NMR** (150 MHz, CDCl₃) δ = 13.8 (q, CH₃), 21.5 (q, CH₃), 61.5 (t, CH₂), 97.7 (s, CN), 110.0 (s, C-1), 113.3 (s, C-3), 115.4 (d, C-6), 122.3 (d, C-5), 124.6 (s, C-6ᵃ), 125.5 (d, C-7), 127.7 (d, C-10), 128.7 (d, C-8 or C-9), 129.0 (s, C_Ar), 129.0 (d, C-8 or C-9), 129.1 (d, 2×C_Ar-H), 129.3 (d, 2×C_Ar-H), 129.5 (s, C-10ᵃ), 132.9 (s, C-10ᵇ), 138.6 (s, C-2), 138.7 (s, C_Ar), 166.4 (s, CO₂). **HRMS** (EI): C₂₃H₁₈N₂O₂ calcd.: 354.1368; found: 354.1368. **MS** (EI) *m/z* = 354 (100), 326 (12), 309 (73), 282 (83), 266 (25). Da731-2
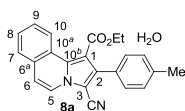
3.4.5 Reactions of Benzoyl Substituted Ylides with Benzylidene Malonates 6

**1-(4-Ethoxy-3-(ethoxycarbonyl)-2-(4-nitrophenyl)-4-oxobutyl)pyridin-1-ium bromide (13a).** **1eH⁺Br⁻** (73 mg, 0.26 mmol) and **6a** (70 mg, 0.24 mmol) were dissolved in ethanol (10 mL) and triethylamine (73 mg, 721 µmol) was added at room temperature. The mixture was stirred for 1 h and the solvent was evaporated. The crude product was recrystallized from ethanol to yield **13a** as colorless needles (112 mg, 240 µmol, 100%). **Mp** 206–207 °C. **¹H NMR** (300 MHz, CDCl₃) δ = 0.95 (t, *J* = 7.1 Hz, 3 H, CH₃), 1.25 (t, *J* = 7.1 Hz, 3 H, CH₃), 3.81 – 3.96 (m, 2 H, CH₂), 4.13 – 4.31 (m, 4 H, 2×CH, CH₂), 5.49 (dd, *J* = 13.1, 4.9 Hz, 1 H, C*H*H), 6.01 (dd, *J* = 13.0, 9.7 Hz, 1 H, CH*H*), 7.75 (d, *J* = 8.7 Hz, 2 H, 2×C_Ar-H), 7.90 − 8.02 (m, 2 H, 2×C_Ar-H), 8.08 (d, *J* = 8.8 Hz, 2 H, 2×C_Ar-H), 8.45 (t, *J* = 7.8 Hz, 1 H, C_Ar-H), 9.39 (d, *J* = 5.7 Hz, 2 H, 2×C_Ar-H). **¹³C NMR** (75 MHz, CDCl₃) δ = 13.8 (q, CH₃), 14.1 (q, CH₃), 47.3 (d, CH), 54.7 (d, CH), 62.2 (t, CH₂), 62.4 (br t, CHH), 62.9 (t, CH₂), 124.2 (d, 2×C_Ar-H), 128.4 (d, 2×C_Ar-H), 130.7 (d, 2×C_Ar-H), 142.4 (s, C_Ar), 145.5 (d, 2×C_Ar-H), 145.9 (d, C_Ar-H), 148.0 (s, C_Ar-H), 166.7 (s, CO₂), 167.5 (s, CO₂). **HRMS** (ESI): C₂₀H₂₃N₂O₆⁺ calcd.: 387.1551; found: 387.1548. **Elemental analysis**: calcd.: N 5.99, C 51.40, H 4.96; found: N 5.91, C 51.23, H 4.93. DA630-4
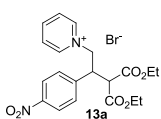
1-(4-Ethoxy-3-(ethoxycarbonyl)-4-oxo-2-(*p*-tolyl)butyl)pyridin-1-ium bromide (12b). **1eH⁺Br⁻** (146 mg, 525 µmol) and **6f** (131 mg, 500 µmol) were dissolved in ethanol (10 mL) and triethylamine (146 mg, 1.44 mmol) was added at room temperature. The mixture was then stirred for 1 h and the solvent was evaporated. The reaction crude was recrystallized from EtOH and from acetone to yield **13b** as colorless solid (151 mg, 346 µmol, 69%). The product is contaminated by **1eH⁺Br⁻**. **Mp** 183 °C (decomp.). **¹H NMR** (300 MHz, CDCl₃) δ = 0.91 (t, *J* = 7.1 Hz, 3 H, CH₃), 1.27 (t, *J* = 7.1 Hz, 3 H, CH₃), 2.22 (s, 3 H, CH₃), 3.76 (td, *J* = 10.7, 4.3 Hz, 1 H, CH), 3.87 (q, *J* = 7.1 Hz, 2 H, CH₂), 4.03 (d, *J* = 10.5 Hz, 1 H, CH), 4.16 – 4.33 (m, 2 H, CH₂), 5.25 (dd, *J* = 13.0, 4.3 Hz, 1 H, C*H*H), 5.62 (dd, *J* = 12.9, 11.0 Hz, 1 H, CH*H*), 6.97 – 7.04 (m, 2 H, 2×C$_{Ar}$-H), 7.04 – 7.12 (m, 2 H, 2×C$_{Ar}$-H), 7.86 – 7.95 (m, 2 H, 2×C$_{Ar}$-H), 8.45 (tt, *J* = 7.8, 1.4 Hz, 1 H, C$_{Ar}$-H), 8.91 – 9.00 (m, 2 H, 2×C$_{Ar}$-H). **¹³C NMR** (75 MHz, CDCl₃) δ = 13.7 (q, CH₃), 14.1 (q, CH₃), 21.1 (q, CH₃), 47.8 (d, CH), 55.0 (d, CH), 61.9 (t, CH₂), 62.6 (t, CH₂), 64.1 (t, CHH), 128.0 (d, 2×C$_{Ar}$-H), 128.6 (d, 2×C$_{Ar}$-H), 130.0 (d, 2×C$_{Ar}$-H), 131.2 (s, C$_{Ar}$), 138.7 (s, C$_{Ar}$), 145.1 (d, 2×C$_{Ar}$-H), 145.8 (d, C$_{Ar}$-H), 166.9 (s, CO₂), 168.0 (s, CO₂). **HRMS** (ESI): C₂₁H₂₆NO₄⁺ calcd.: 356.1856; found: 356.1856. DA881

Diethyl 3-benzoyl-2-(4-nitrophenyl)-2,3-dihydropyrrolo[2,1-*a*]isoquinoline-1,1(10b*H*)-dicarboxylate (C-4b). **4bH⁺Br⁻** (164 mg, 500 µmol) and **6a** (147 mg, 500 µmol) were dissolved in 5 mL of DMSO and NEt₃ (73 mg, 0.72 mmol) was added. The reaction mixture was stirred for 5 min at room temperature, then CH₂Cl₂ (15 mL) was added and the solution was poured onto brine (25 mL). The organic layer was separated and the aqueous layer was washed twice with CH₂Cl₂ (15 mL). The combined organic layers were washed with brine (2×25 mL), dried over Na₂SO₄ and the solvent was evaporated at room temperature. The resulting solid was recrystallized from ethanol to give **C-4b** (202 mg, 374 µmol, 75%, *dr* 1:6:9) as a mixture of orange needles (*dr* 1:4:6) and red prisms (single diastereoisomer), which isomerize slowly in solution. **Mp** (EtOH).: 148–149 °C. (mixture). **Mixture C-4b** (*dr* ~1:4:6). Tentative assignment of the ¹H NMR-signals in the mixture of diastereoisomers; *-major, #-first minor diastereoisomer, +-second minor diastereoisomer. **¹H NMR** (300 MHz, CDCl₃) δ = 0.65 – 0.76 (m, 2×CH₃),* 0.82 – 0.95 (m, 2×CH₃),# 1.19 – 1.30 (m, 2×CH₃),+ 3.27 −3.45 (m, CH₂),* 3.47 − 4.07 (m, 4×CH₂),*,#,+ 4.20 − 4.41 (m, CH₂),+ 4.49 (d, *J* = 7.3 Hz, 3-H),+ 4.62 (d, *J* = 8.6 Hz, 3-H),# 5.00 (d, *J* = 10.4 Hz, 3-H),* 5.10 (d, *J* = 10.4 Hz, 2-H),* 5.23 (d, *J* = 7.5 Hz, 2-H),+ 5.30 (d, *J* = 7.5 Hz, 2-H),# 5.38 (d, *J* = 7.7 Hz, 6-H),* 5.58 (d, *J* = 7.3 Hz, 6-H),+ 5.81 (d, *J* = 7.7 Hz, 5-H),* 5.87 (s, 10*b*-
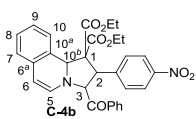
H), 5.91 (d, J = 8.6 Hz, 6-H),[#] 5.98 (s, 6 H, 10^b-H),* 6.03 (d, J = 7.5 Hz, 5-H),[#] 6.20 (d, J = 7.5 Hz, 5-H),[+] 6.24 (s, 10^b-H), 6.81 – 6.88 (m, 2×8-H or 9-H),*,+ 6.90 – 7.02 (m, 3×8-H or 9-H),*, #,+ 7.05 – 7.71 (m, 3×7-H, 8-H or 9-H, 3×10-H, 16×C$_{ar}$-H, superimposed by solvent),*, #,+ 7.82 – 7.94 (m, 4×C$_{ar}$-H),[#,+] 8.05 – 8.21 (m, 6×C$_{ar}$-H).*, #,+ ^{13}C NMR-Signals of the minor diastereoisomers [#,+] are partially superimposed by the major diastereoisomer *. The multiplicicity assignment of the aromatic carbon-atoms C$_{ar}$ was not unambiguous. **^{13}C NMR** (75 MHz, CDCl$_3$) δ = 13.3 (q), 13.4 (q), 13.7 (q), 14.1 (q), 51.5 (d), 51.6 (d), 51.9 (d), 61.6 (t), 61.7 (t), 61.9 (t), 62.2 (t), 62.3 (t), 64.7 (d), 68.4 (d), 70.3 (d), 70.5 (d), 71.1 (d), 71.2 (d), 73.1 (d), 73.4 (d), 99.2 (d), 100.1 (d), 104.4 (d), 123.0 (C$_{ar}$), 123.2 (C$_{ar}$), 123.5 (C$_{ar}$), 124.1 (C$_{ar}$), 124.2 (C$_{ar}$), 124.4 (C$_{ar}$), 125.2 (C$_{ar}$), 125.4 (C$_{ar}$), 125.5 (C$_{ar}$), 125.8 (C$_{ar}$), 126.4 (C$_{ar}$), 126.6 (C$_{ar}$), 127.3 (C$_{ar}$), 127.7 (C$_{ar}$), 128.2 (C$_{ar}$), 128.3 (C$_{ar}$), 128.4 (C$_{ar}$) 128.6 (C$_{ar}$), 128.7 (C$_{ar}$), 128.8 (C$_{ar}$), 128.8 (C$_{ar}$), 129.1 (C$_{ar}$), 129.4 (C$_{ar}$), 130.0 (br, C$_{ar}$), 131.1 (C$_{ar}$), 131.4 (C$_{ar}$), 131.5 (C$_{ar}$), 132.0 (C$_{ar}$), 132.6 (C$_{ar}$), 132.7 (C$_{ar}$), 133.5 (C$_{ar}$), 134.0 (C$_{ar}$), 134.6 (C$_{ar}$), 134.6 (C$_{ar}$), 135.2 (C$_{ar}$), 135.5 (C$_{ar}$), 135.8 (C$_{ar}$), 136.3 (s), 143.2 (s), 144.2 (s), 146.5 (s), 147.2 (s), 147.4 (s), 167.4 (s), 168.1 (s), 169.2 (s), 169.3 (s), 169.6 (s), 169.9 (s), 193.3 (s), 196.5 (s), 196.9 (s). **HRMS** (EI): C$_{31}$H$_{28}$N$_2$O$_7$ calcd.: 540.1897; found: 540.1887. **MS** (EI) m/z =540 (1), 465 (1), 435 (1), 293 (10), 248 (37), 247.12 (61), 246 (100), 203 (22), 147 (12), 129 (17), 115 (16). **Prisms C-4b** (1 diastereoisomer). **^{1}H NMR** (200 MHz, CDCl$_3$) δ = 0.79 – 0.99 (m, 6 H, 2×CH$_3$), 3.42–4.09 (m, 4 H, 2×CH$_2$), 4.61 (d, J = 8.6 Hz, 1 H, CH), 5.30 (d, J = 7.5 Hz, 1 H, CH), 5.91 (d, J = 8.6 Hz, 1 H, CH), 6.03 (d, J = 7.5 Hz, 1 H, CH), 6.23 (s, 1 H, CH), 6.86 (dd, J = 7.5, 1.4 Hz, 1 H, C$_{Ar}$-H), 6.92 – 7.02 (m, 1 H, C$_{Ar}$-H), 7.05 – 7.20 (m, 3 H, 3×C$_{Ar}$-H), 7.21 – 7.33 (m, 2 H, 2×C$_{Ar}$-H, superimposed by solvent), 7.36–7.50 (m, 2 H, 2×C$_{Ar}$-H), 7.59 (dd, J = 5.3, 3.3 Hz, 2 H, 2×C$_{Ar}$-H), 7.74–8.00 (m, 2 H, 2×C$_{Ar}$-H). **HRMS** (EI): C$_{31}$H$_{28}$N$_2$O$_7$ calcd.: 540.1897; found: 540.1895. **MS** (EI) m/z =540 (2), 464 (2), 435 (2), 293 (12), 248 (45), 247 (65), 246 (100), 203 (30), 147 (15), 129 (32), 115 (20). Da622
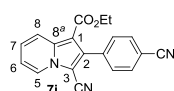
3.4.6 Variation of the Methylidene Malonates 6

Ethyl 3-cyano-2-(4-nitrophenyl)indolizine-1-carboxylate (7h). According to procedure **B** from **1cH$^+$Br$^-$** (149 mg, 749 µmol), **6a** (147 mg, 500 µmol) and chloranil (123 mg, 500 µmol). **7h** was obtained as colorless solid (80 mg, 0.24 mmol, 48%). R_f = 0.25 (i-Hexane:EtOAc 5:1). **Mp** 162–163 °C. **IR** (neat) $\tilde{v}$ = 3107, 2982, 2206, 1692, 1633, 1602, 1516, 1507, 1436, 1381, 1348, 1323, 1268, 1244, 1192, 1183, 1153, 1133, 1109, 1061, 1033, 1017 cm^{-1}. **^{1}H NMR** (300 MHz, CDCl$_3$) δ = 1.21 (t, J = 7.1 Hz, 3 H, CH$_3$), 4.26
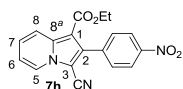
(q, J = 7.1 Hz, 2 H, CH$_2$), 7.12 (td, J = 6.8, 1.1 Hz, 1 H, C-6), 7.42 (dd, J = 9.1, 6.9 Hz, 1 H, C-7), 7.67 – 7.78 (m, 2 H, 2×C$_{Ar}$-H), 8.28 – 8.36 (m, 2 H, 2×C$_{Ar}$-H), 8.36 – 8.47 (m, 2 H, C-5, C-8). **^{13}C NMR** (75 MHz, CDCl$_3$) δ = 14.3 (q, CH$_3$), 60.5 (t, CH$_2$), 97.5 (s, CN), 104.0 (s, C-1), 112.3 (s, C-3), 115.8 (d, C-6), 121.1 (d, C-5 or C-8), 123.3 (d, 2×C$_{Ar}$-H), 125.7 (d, C-5 or C-8), 127.1 (d, C-7), 131.3 (d, 2×C$_{Ar}$-H), 138.6 (s, C-2 and C$_{Ar}$), 138.6 (s, C-8^a), 148.1 (s, C$_{Ar}$), 163.1 (s, CO$_2$). **HRMS** (EI): C$_{18}$H$_{13}$N$_3$O$_4$ calcd.: 335.0906; found: 335.0907. **MS** (EI) m/z = 335 (100), 307 (33), 290 (53), 263 (42), 244 (35), 215 (50), 188 (20). Da735

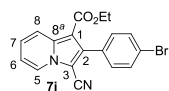**Ethyl 3-cyano-2-(4-cyanophenyl)indolizine-1-carboxylate (7i).** According to procedure **B** from **1cH$^+$Br$^-$** (125 mg, 628 µmol), **6b** (137 mg, 500 µmol) and chloranil (123 mg, 500 µmol). **7i** was obtained as colorless solid (130 mg, 412 µmol, 82%). R_f = 0.14 (*i*-Hexane:EtOAc 5:1). **Mp** 226–227 °C. **IR** (neat) $\widetilde{\nu}$ = 2952, 2921, 2849, 2219, 2206, 1680, 1631, 1607, 1499, 1432, 1381, 1241, 1194, 1176, 1115, 1059, 1034, 1017 cm^{-1}. **^{1}H NMR** (400 MHz, CD$_3$CN:CDCl$_3$ 20:1) δ = 1.16 (t, J = 7.1 Hz, 3 H, CH$_3$), 4.19 (q, J = 7.1 Hz, 2 H, CH$_2$), 7.17 (td, J = 6.9, 1.3 Hz, 1 H, C-6), 7.48 (ddd, J = 9.1, 6.9, 1.1 Hz, 1 H, C-7), 7.67 – 7.72 (m, 2 H, 2×C$_{Ar}$-H), 7.80 – 7.85 (m, 2 H, 2×C$_{Ar}$-H), 8.36 (dt, J = 9.1, 1.2 Hz, 1 H, 8-H), 8.44 (dt, J = 6.9, 1.1 Hz, 1 H, 5-H). **^{13}C NMR** (100 MHz, CD$_3$CN:CDCl$_3$ 20:1) δ = 14.3 (q, CH$_3$), 61.0 (t, CH$_2$), 104.3 (s, C-1), 112.9 (s, C$_{Ar}$), 113.2 (s, CN), 116.6 (d, C-6), 118.1 (s, CN, superimposed by solvent), 119.5 (s, C-3), 121.1 (d, C-5), 127.3 (d, C-8), 128.3 (d, C-7), 131.9 (d, 2×C$_{Ar}$-H), 132.7 (d, 2×C$_{Ar}$-H), 137.9 (s, C$_{Ar}$), 139.2 (s, C-8^a), 139.4 (s, C-2), 163.8 (s, CO$_2$). **HRMS** (EI): C$_{19}$H$_{13}$N$_3$O$_2$ calcd.: 315.1008; found: 315.1006. **MS** (EI) m/z =315.12 (91), 287.10 (33), 270.10(100), 243.11 (51), 215.08 (20). DA723

Ethyl 2-(4-bromophenyl)-3-cyanoindolizine-1-carboxylate (7j). According to procedure **B** from **1cH$^+$Br$^-$** (125 mg, 625 µmol), **6c** (164 mg, 500 µmol) and chloranil (123 mg, 500 µmol). **7j** was obtained as colorless solid (150 mg, 406 µmol, 81%). R_f = 0.40 (*i*-Hexane:EtOAc 5:1). **Mp** 122–123 °C. **IR** (neat) $\widetilde{\nu}$ = 3088, 2981, 2206, 1992, 1494, 1434, 1377, 1324, 1271, 1236, 1188, 1150, 1074, 1060, 1031, 1011 cm^{-1}. **^{1}H NMR** (300 MHz, CDCl$_3$) δ = 1.22 (t, J = 7.1 Hz, 3 H, CH$_3$), 4.25 (q, J = 7.1 Hz, 2 H, CH$_2$), 7.07 (td, J = 6.9, 1.3 Hz, 1 H, 6-H), 7.30 – 7.48 (m, 3 H, 7-H, 2×C$_{Ar}$-H), 7.53 – 7.66 (m, 2 H, 2×C$_{Ar}$-H), 8.29 – 8.45 (m, 2 H, 5-H, 8-H). **^{13}C NMR** (75 MHz, CDCl$_3$) δ = 14.3 (q, CH$_3$), 60.3 (t, CH$_2$), 97.3 (s, CN), 103.8 (s, C-1), 112.8 (s, C-3), 115.4 (d, C-6), 121.0 (d, C-5 or C-8), 123.3 (s, C$_{Ar}$), 125.6 (d, C-5 or C-8), 126.7 (d, C-7), 130.6 (s, C$_{Ar}$), 131.3 (d, 2×C$_{Ar}$-H), 131.8 (d, 2×C$_{Ar}$-H), 138.7 (s, C-8^a), 140.0 (s, C-2), 163.4 (s, CO$_2$). **HRMS** (EI): C$_{18}$H$_{13}$^{79}BrN$_2$O$_2$ calcd.: 368.0160; found: 368.0154. **HRMS** (EI): C$_{18}$H$_{13}$^{81}BrN$_2$O$_2$ calcd.: 370.0140; found: 370.0129. **MS** (EI) m/z =

370.15 (98), 368.15 (100), 340.11(25), 323.10 (33), 296.11 (45), 244.16 (100), 216.15 (42). Da756
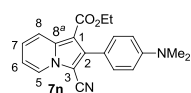
Ethyl 2-(3-chlorophenyl)-3-cyanoindolizine-1-carboxylate (7k). According to procedure **B** from **1cH⁺Br⁻** (125 mg, 625 μmol), **6d** (141 mg, 500 μmol) and chloranil (123 mg, 500 μmol). **7k** was obtained as colorless solid (125 mg, 385 μmol, 77%). R_f = 0.16 (*i*-Hexane:EtOAc 5:1). **Mp** 141–142 °C. **IR** (neat) $\widetilde{\nu}$ = 2212, 1698, 1596, 1564, 1499, 1440, 1388, 1323, 1271, 1235, 1178, 1147, 1130, 1080, 1030 cm⁻¹. **¹H NMR** (300 MHz, CDCl₃) δ = 1.19 (t, J = 7.1 Hz, 3 H, CH₃), 4.24 (q, J = 7.1 Hz, 2 H, CH₂), 7.08 (td, J = 6.9, 1.3 Hz, 1 H, C-6), 7.35 – 7.45 (m, 4 H, C-7, 3×C$_{Ar}$-H), 7.49 – 7.55 (m, 1 H, C$_{Ar}$-H), 8.36 (dt, J = 6.9, 1.1 Hz, 1 H, C-5), 8.42 (dt, J = 9.1, 1.2 Hz, 1 H, C-8). **¹³C NMR** (75 MHz, CDCl₃) δ = 14.1 (q, CH₃), 60.3 (d, CH₂), 97.4 (s, CN), 104.0 (s, C-1), 112.7 (s, C-3), 115.5 (d, C-6), 121.0 (d, C-8), 125.6 (d, C-5), 126.7 (d, C-7), 128.2 (d, C$_{Ar}$-H), 128.9 (d, C$_{Ar}$-H), 129.4 (d, C$_{Ar}$-H), 130.5 (d, C$_{Ar}$-H), 133.5 (s, C$_{Ar}$), 133.9 (s, C$_{Ar}$), 138.7 (s, C-8^a), 139.5 (s, C-2), 163.4 (s, CO₂). **HRMS** (EI): C₁₈H₁₃ClN₂O₂ calcd.: 324.0666; found: 324.0660. **MS** (EI) m/z = 326.09 (35), 324.09 (100), 279.07 (91), 252.09 (58), 216.09 (48). Da719

Ethyl 3-cyano-2-phenylindolizine-1-carboxylate (7l). According to procedure **B** from **1cH⁺Br⁻** (125 mg, 628 μmol), **6e** (124 mg, 500 μmol) and chloranil (123 mg, 500 μmol). **7l** was obtained as colorless solid (100 mg, 344 μmol, 69%). R_f = 0.45 (*i*-Hexane:EtOAc 5:1). **Mp** 122–123 °C. **IR** (neat) $\widetilde{\nu}$ = 2204, 1683, 1630, 1501, 1429, 1395, 1380, 1319, 1268, 1242, 1188, 1155, 1129, 1096, 1060, 1031 cm⁻¹. **¹H NMR** (300 MHz, CDCl₃) δ = 1.18 (t, J = 7.1 Hz, 3 H, CH₃), 4.23 (q, J = 7.1 Hz, 2 H, CH₂), 7.05 (td, J = 6.9, 1.3 Hz, 1 H, 6-H), 7.36 (ddd, J = 9.1, 6.9, 1.2 Hz, 1 H, 7-H), 7.41 – 7.55 (m, 5 H, 5×C$_{Ar}$-H), 8.36 (dt, J = 6.8, 1.1 Hz, 1 H, 5-H), 8.39 (dt, J = 9.1, 1.2 Hz, 1 H, 8-H). **¹³C NMR** (75 MHz, CDCl₃) δ = 14.2 (q, CH₃), 60.2 (t, CH₂), 97.4 (s, CN), 103.9 (s, C-1), 113.1 (s, C-3), 115.2 (d, C-6), 120.9 (d, C-8), 125.6 (d, C-5), 126.4 (d, C-7), 128.0 (d, 2×C$_{Ar}$-H), 128.8 (d, C$_{Ar}$-H), 130.1 (d, 2×C$_{Ar}$-H), 131.7 (s, C$_{Ar}$), 138.7 (s, C-8^a), 141.4 (s, C-2), 163.7 (s, CO₂). **HRMS** (EI): C₁₈H₁₄N₂O₂ calcd.: 290.1055; found: 290.1051. **MS** (EI) m/z = 290.15 (100), 262.12 (18), 245.12 (100), 218.11 (47), 216.09 (29). Da718

Ethyl 3-cyano-2-(4-methoxyphenyl)indolizine-1-carboxylate (7m). According to procedure **B** from **1cH⁺Br⁻** (128 mg, 625 μmol), **6g** (139 mg, 500 μmol) and chloranil (123 mg, 500 μmol). **7m** was obtained as colorless solid (125 mg, 390 μmol, 78%). R_f = 0.36 (*i*-Hexane:EtOAc 5:1). **Mp** 122–123 °C. IR (neat) $\widetilde{\nu}$ = 3105, 2976, 2202, 1690, 1614, 1538, 1503, 1465, 1432, 1393, 1378, 1295, 1239, 1187, 1172, 1126,

1112, 1058, 1025 cm^{-1}. **^{1}H NMR** (300 MHz, CDCl$_3$) δ = 1.23 (t, J = 7.1 Hz, 3 H, CH$_3$), 3.87 (s, 3 H, CH$_3$), 4.26 (q, J = 7.1 Hz, 2 H, CH$_2$), 6.67 − 7.07 (m, 3 H, 6-H, 2×C$_{Ar}$-H), 7.34 (ddd, J = 9.1, 6.9, 1.2 Hz, 1 H, C-7), 7.45 − 7.53 (m, 2 H, 2×C$_{Ar}$-H), 8.31 − 8.40 (m, 2 H, 5-H, 8-H). **^{13}C NMR** (75 MHz, CDCl$_3$) δ = 14.3 (q, CH$_3$), 55.5 (q, CH$_3$), 60.2 (t, CH$_2$), 97.3 (s, CN), 103.7 (s, C-1), 113.3 (s, C-3), 113.6 (d, 2×C$_{Ar}$-H), 115.0 (d, C-6), 120.9 (d, C-5 or C-8), 123.7 (s, C$_{Ar}$), 125.6 (d, C-5 or C-8), 126.4 (d, C-7), 131.5 (d, 2×C$_{Ar}$-H), 138.8 (s, C-8^a), 141.3 (s, C-2), 160.2 (s, C$_{Ar}$), 163.8 (s, CO$_2$). **HRMS** (EI): C$_{19}$H$_{16}$N$_2$O$_3$ calcd.: 320.1161; found: 320.1156. **MS** (EI) m/z = 320.14 (100), 292.12 (20), 275.12 (71), 248.13 (50), 232.10 (18), 191.18 (8). DA716
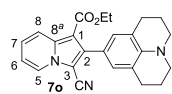
Ethyl 3-cyano-2-(4-(dimethylamino)phenyl)indolizine-1-carboxylate (7n). According to procedure **B** from **1cH$^+$Br$^−$** (125 mg, 625 µmol), **6h** (146 mg, 500 µmol) and chloranil (123 mg, 500 µmol). **7n** was obtained as light yellow solid (133 mg, 399 µmol, 80%). R_f = 0.35 (i-Hexane:EtOAc 5:1). **Mp** 150–151 °C. **IR** (neat) $\tilde{\nu}$ = 2915, 2210, 1693, 1611, 1541, 1490, 1437, 1390, 1356, 1320, 1268, 1229, 1203, 1166, 1146, 1060, 1030 cm^{-1}. **^{1}H NMR** (300 MHz, CDCl$_3$) δ = 1.28 (t, J = 7.1 Hz, 3 H, CH$_3$), 3.02 (s, 6 H, N(CH$_3$)$_2$), 4.29 (q, J = 7.1 Hz, 2 H, CH$_2$), 6.73 − 6.83 (m, 2 H, 2×C$_{Ar}$-H), 7.00 (td, J = 6.9, 1.2 Hz, 1 H, 6-H), 7.31 (ddd, J = 9.0, 6.9, 1.1 Hz, 1 H, 7-H), 7.43 − 7.51 (m, 2 H, 2×C$_{Ar}$-H), 8.29 − 8.38 (m, 2 H, 5-H, 8-H). **^{13}C NMR** (75 MHz, CDCl$_3$) δ = 14.5 (q, CH$_3$), 40.5 (q, N(CH$_3$)$_2$), 60.1 (t, CH$_2$), 97.0 (s, CN), 103.3 (s, C-1), 111.7 (d, 2×C$_{Ar}$-H), 113.8 (s, C-3), 114.7 (d, C-6), 118.7 (s, C$_{Ar}$), 120.8 (d, C-5 or C-8), 125.5 (d, C-5 or C-8), 126.1 (d, C-7), 131.2 (d, 2×C$_{Ar}$-H), 138.9 (s, C-8^a), 142.2 (s, C-2), 150.9 (s, C$_{Ar}$), 164.0 (s, CO$_2$). **HRMS** (EI): C$_{20}$H$_{19}$N$_3$O$_2$ calcd.: 333.1477; found: 333.1471. **MS** (EI) m/z = 333.18 (100), 304.14 (21), 288.15 (12), 216.09 (10). Da722

Ethyl 3-cyano-2-(julolidyl)indolizine-1-carboxylate (7o). According to procedure **B** from **1cH$^+$Br$^−$** (149 mg, 749 µmol), **6i** (172 mg, 500 µmol) and chloranil (123 mg, 500 µmol). **7o** was obtained as yellow solid (102 mg, 265 µmol, 53%). R_f = 0.30 (i-Hexane:EtOAc 5:1). **Mp** 188–189 °C. **IR** (neat) $\tilde{\nu}$ = 2939, 2913, 2831, 2203, 1679, 1630, 1608, 1504, 1466, 1443, 1384, 1309, 1233, 1210, 1174, 1127, 1095, 1057, 1033 cm^{-1}. **^{1}H NMR** (300 MHz, CDCl$_3$) δ = 1.28 (t, J = 7.1 Hz, 3 H, CH$_3$), 1.95 − 2.05 (m, 4 H, 2×CH$_2$), 2.80 (t, J = 6.4 Hz, 4 H, 2×CH$_2$), 3.16 − 3.23 (m, 4 H, 2×CH$_2$), 4.29 (q, J = 7.0 Hz, 2 H, CH$_2$), 6.97 (t, J = 6.8 Hz, 1 H, C-6), 7.02 (s, 2 H, 2×C$_{Ar}$-H), 7.24 − 7.31 (m, 1 H, C-7, superimposed by solvent), 8.31 − 8.36 (m, 2 H, C-5, C-8). **^{13}C NMR** (75 MHz, CDCl$_3$) δ = 14.5 (q, CH$_3$), 22.2 (t, 2×CH$_2$), 27.9 (t, 2×CH$_2$), 50.2 (t, 2×CH$_2$), 60.1 (t, CH$_2$), 96.8 (s, CN), 103.2 (s, C-1), 114.1 (s, C-3), 114.7 (d, C-6), 117.6 (s, C$_{Ar}$), 120.7 (d, C-5 or C-8), 120.7 (s, 2×C$_{Ar}$),

125.6 (d, C-5 or C-8), 126.1 (d, C-7), 129.1 (d, 2×C_{Ar}-H), 139.2 (s, C-8^a), 142.3 (s, C-2), 143.6 (s, C_{Ar}), 164.2 (s, CO_2). **HRMS** (EI): $C_{24}H_{23}N_3O_2$ calcd.: 385.1790; found: 385.1781. **MS** (EI) m/z = 385.26 (100). Da724

Ethyl 3-cyano-2-*iso*-propylindolizine-1-carboxylate (7p). According to procedure **B** from **1cH$^+$Br$^-$** (149 mg, 749 μmol), **6j** (107 mg, 500 μmol) and chloranil (123 mg, 500 μmol). **7p** was obtained as colorless solid (107 mg, 417 μmol, 83%). R_f = 0.63 (*i*-Hexane:EtOAc 5:1). **Mp** 79–80 °C. **IR** (neat) $\widetilde{v}$ = 1965, 2204, 1687, 1508, 1498, 1467, 1436, 1391, 1378, 1326, 1217, 1178, 1125, 1069, 1026 cm^{-1}. **^{1}H NMR** (300 MHz, CDCl$_3$) δ = 1.41 – 1.50 (m, 9 H, 3×CH$_3$), 4.06 (hept, J = 7.0 Hz, 1 H, CH), 4.40 (q, J = 7.2 Hz, 2 H, CH$_2$), 6.97 (td, J = 6.9, 1.5 Hz, 1 H, C-6), 7.21 – 7.35 (m, 1 H, C-7), 8.21 – 8.36 (m, 2 H, C-5, C-8). **^{13}C NMR** (75 MHz, CDCl$_3$) δ 14.6 (q, CH$_3$), 22.7 (q, 2×CH$_3$), 26.2 (d, CH), 60.2 (t, CH$_2$), 95.5 (s, CN), 103.2 (s, C-1), 114.0 (s, C-3), 114.6 (d, C-6), 120.7 (d, C-5 or C-8), 125.4 (d, C-5 or C-8), 126.1 (d, C-7), 138.4 (s, C-8^a), 149.7 (s, C-2), 164.1 (s, CO_2). **HRMS** (EI): $C_{15}H_{16}N_2O_2$ calcd.: 256.1212; found: 256.1192. **MS** (EI) m/z = 256.20 (93), 211.16 (44), 209.14 (69), 195.12 (35), 184.17 (12). Da742
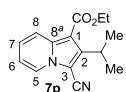
3.4.7 Leaving Group Studies

Ethyl 2-benzylidene-3-oxobutanoate (14a). Ethyl acetoacetate (4.66 g, 35.8 mmol) and benzaldehyde (3.80 g, 35.8 mmol) were dissolved in ethanol (50 mL) and piperidine (300 μl) and benzoic acid (100 mg) were added as catalysts. The solution was stirred at 20 °C for 18 h, then the solvent was removed and the crude material was subjected to distillation. **14a** was obtained as slightly yellow liquid (4.25 g, 19.5 mmol, 54%, *dr* 3:1). **Bp** 130°C, 9.2 × 10^{-1} mbar; lit: 129°C, 0.7 Torr.[25] *-major diastereoisomer, #-minor diastereoisomer; integrals of the minor diastereoisomer are set to 1.0 for the integral of one proton. **^{1}H NMR** (200 MHz, CDCl$_3$) δ = 1.41 – 1.18 (m, 12 H, CH$_3$),*,# 2.34 (s, 3 H, CH$_3$),# 2.42 (s, 9 H, CH$_3$),* 4.15 – 4.42 (m, 8 H, 2×CH$_2$),*,# 7.31 – 7.51 (m, 20 H, 10×C_{Ar}-H),*,# 7.56 (s, 3 H, CH),* 7.66 (s, 1 H, CH).# DA744
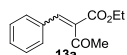
Ethyl 3-cyano-2-phenylindolizine-1-carboxylate (7l). According to procedure **B** from **1cH$^+$Br$^-$** (125 mg, 628 μmol), **14a** (109 mg, 500 μmol) and chloranil (123 mg, 500 μmol). **7l** was obtained as colorless solid (81 mg, 0.28 mmol, 56%). **Mp** 121–122 °C. (Analytical data see 3.4.6). Da750

(*E*)-Ethyl 2-(methylsulfonyl)-3-phenylacrylate (14b). To a solution of ethyl methylsulfonylacetate (590 mg, 3.55 mmol) and benzaldehyde (360 µl, 376 mg, 3.547 mmol) in toluene piperidine (43 mg, 505 µmol) and trifluoroacetic acid (50 µl, 74 mg, 649 µmol) was added. The reaction was heated under reflux for 2 h and the water formed was collected in a Dean-Stark trap. The reaction was quenched with 100 mL HCl (2 N) and extracted with CH_2Cl_2 (3×50mL). The combined organic layers were washed with aq. $NaHCO_3$ (sat.; 100 mL), water (100 mL) and dried over $MgSO_4$. The solvent was removed and the crude product was recrystallized from *n*-pentane:Et_2O to give **14b** as colorless solid (682 mg, 2.68 mmol, 76%). **Mp** 57 °C; lit 53−55 °C.[26] **^{1}H NMR** (200 MHz, $CDCl_3$) δ = 1.27 (t, *J* = 7.1, 0.4 Hz, 3 H, CH_3), 3.25 (s, 3 H, CH_3), 4.35 (q, *J* = 7.1 Hz, 2 H, CH_2), 7.35 − 7.53 (m, 5 H, 5×C_{Ar}-H), 7.83 (s, 1 H, CH). DA755
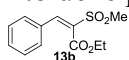
Ethyl 3-cyano-2-phenylindolizine-1-carboxylate (7l). According to procedure **B** from **1cH$^+$Br$^−$** (125 mg, 628 µmol), **14b** (127 mg, 500 µmol) and chloranil (123 mg, 500 µmol). **7l** was obtained as colorless solid (50 mg, 0.17 mmol, 34%). **Mp** 121–122 °C. (Analytical data see 3.4.6). Da759
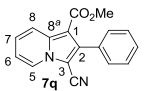
Ethyl 3-cyano-2-phenylindolizine-1-carboxylate (7l). According to procedure **B** from **1cH$^+$Br$^−$** (125 mg, 625 µmol), **13b** (127 mg, 500 µmol) and chloranil (246 mg, 1.00 mmol). **7l** was obtained as colorless solid (32 mg, 0.11 mmol, 22%). Da759-2

Methyl 2-carbamoyl-3-phenylacrylate (14c). Methylmalonate monoamide (3.00 g, 25.6 mmol) was dissolved in 20 mL of ethanol. To the solution benzaldehyde (1.81 g, 17.1 mmol), piperidine (600 µL) and TFA (200 µL) were added. The reaction mixture was stirred for 18 h at room temperature. The reaction was quenched with 100 mL HCL (2 N) and extracted with CH_2Cl_2 (3×50mL). The combined organic layers were washed with sat. aq. $NaHCO_3$ (100 mL), water (100 mL) and dried over $MgSO_4$. The solvent was evaporated and the residue was subjected to a vacuum distillation with a Büchi distillation apparatus. **14c** was obtained as viscous, yellow oil (1.66 g, 8.09 mmol, 47%, *dr* 3:1; 1:1 after distillation.). **Bp** 260 °C, 1.2^{-2} mbar. **IR** (neat) $\widetilde{\nu}$ = 3330, 3183, 2952, 1708, 1655, 1626, 1496, 1434, 1320, 1199, 1105, 1083, 1062, 1028, 1001 cm$^{−1}$. ^{1}H NMR (400 MHz, $CDCl_3$) δ = 3.69 (s, 3 H, CH_3), 3.85 (s, 3 H, CH_3), 5.81 − 5.97 (m, 2 H, N*H*H^a, N*H*H^b), 6.04 (br s, 1 H, NH*H^a*), 7.19 (br s, 1 H, NH*H^b*), 7.29 − 7.43 (m, 8 H, 8×C_{Ar}-H), 7.61 (dd, *J* = 4.7, 2.5 Hz, 2 H, 2×C_{Ar}-H), 7.75 (s, 1 H, CH), 8.14 (s, 1 H, CH). **^{13}C NMR** (100 MHz, $CDCl_3$) δ = 52.5 (q, CH_3), 52.9 (q, CH_3), 125.8 (s, *C*=CH), 127.6 (s, *C*=CH), 128.6 (d, 2×C_{Ar}-H), 129.0 (d, 2×C_{Ar}-H), 129.3 (d, 2×C_{Ar}-H), 130.1 (d, 2×C_{Ar}-H), 130.2 (d, C_{Ar}-H), 130.8 (d, C_{Ar}-H), 132.8 (s, C_{Ar}),
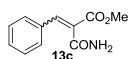
134.1 (s, C$_{Ar}$), 142.9 (d, CH), 146.7 (d, CH), 164.6 (s, CO), 165.4 (s, CO), 168.4 (s, CO), 169.3 (s, CO). **HRMS** (EI): C$_{11}$H$_{11}$NO$_3$ calcd.: 205.0739; found: 205.0714; [C$_{11}$H$_{10}$NO$_3$]$^-$ calcd.: 204.0661; found: 204.0655. **MS** (EI) m/z =205.17 (35), 204.16 (100), 172.12 (22), 129.10 (37), 102.10 (25), 77.08 (18). DA818

Methyl 3-cyano-2-phenylindolizine-1-carboxylate (7q). According to procedure **B** from **1cH⁺Br⁻** (125 mg, 628 µmol), **14c** (127 mg, 619 µmol) and chloranil (123 mg, 500 µmol). **7q** was obtained as colorless solid (96 mg, 0.35 mmol, 56%). R_f = 0.25 (*i*-Hexane:EtOAc 5:1). **Mp** 143–144 °C. **IR** (neat) $\tilde{\nu}$ = 3340, 2207, 1695, 1535, 1493, 1457, 1438, 1418, 1405, 1374, 1327, 1288, 1234, 1172, 1149, 1134, 1066, 1018 cm^{-1}. **¹H NMR** (400 MHz, CDCl$_3$) δ = 3.76 (s, 3 H, CH$_3$), 7.06 (td, J = 6.8, 1.4 Hz, 1 H, 6-H), 7.37 (ddd, J = 9.1, 6.9, 1.3 Hz, 1 H, 7-H), 7.41 – 7.50 (m, 3 H, 3×C$_{Ar}$-H), 7.51 – 7.56 (m, 2 H, 2×C$_{Ar}$-H), 8.34 – 8.41 (m, 2 H, 5-H, 8-H). **¹³C NMR** (100 MHz, CDCl$_3$) δ = 51.2 (q, CH$_3$), 97.6 (br s, CN), 103.5 (s, C-1), 113.1 (s, C-3), 115.2 (d, C-6), 121.0 (d, C-5 or C-8), 125.6 (d, C-5 or C-8), 126.6 (d, C-7), 128.2 (d, 2×C$_{Ar}$-H), 128.9 (d, C$_{Ar}$-H), 130.1 (d, 2×C$_{Ar}$-H), 131.5 (s, C$_{Ar}$), 138.7 (s, C-8^a), 141.4 (s, C-2), 164.1 (s, CO$_2$). **HRMS** (EI): C$_{17}$H$_{12}$N$_2$O$_2$ calcd.: 276.0899; found: 276.0892. **MS** (EI) m/z =277.27 (16), 276.27 (82), 245,23 (100), 216.20 (25), 190.17 (10). DA822

(1-Methylindolizin-3-yl)(phenyl)methanone (18). 1eH⁺Br⁻ (140 mg, 500 µmol) and ethyl methacrylate (**17**) (228 mg, 2.00 mmol) were suspended in CH$_2$Cl$_2$, then NEt$_3$ (146 mg, 1.44 mmol) was added. The suspension was stirred at room temperature till it cleared off (~1 h). Then chloranil (123 mg, 500 µmol) was added and stirring was continued for 1 h. **18** was obtained after column chromatography (SiO$_2$, *n*-pentane:EtOAc 10:1) as yellow oil (40 mg, 0.17 mmol, 34%). R_f = 0.58 (*i*-Hexane:EtOAc 5:1). **IR** (neat) $\tilde{\nu}$ = 3056, 2915, 1593, 1569, 1465, 1418, 1359, 1298, 1232, 1155, 1092, 1055, 1016 cm^{-1}. **¹H NMR** (300 MHz, CDCl$_3$) δ = 2.33 (s, 3 H, CH$_3$), 6.92 (td, J = 6.9, 1.3 Hz, 1 H, 6-H), 7.09 – 7.23 (m, 2 H, 2-H, 7-H), 7.40 – 7.59 (m, 4 H, 8-H, 3×C$_{Ar}$-H), 7.72 – 7.86 (m, 2 H, 2×C$_{Ar}$-H), 9.97 (dd, J = 7.1, 1.0 Hz, 1 H, 5-H). **¹³C NMR** (75 MHz, CDCl$_3$) δ = 10.6 (q, CH$_3$), 111.8 (s, C-1), 113.8 (d, C-6), 116.9 (d, C-8), 121.3 (s, C-3), 123.7 (d, C-7), 126.7 (d, C-2), 128.2 (d, 2×C$_{Ar}$-H), 129.0 (d, C-5), 129.0 (d, 2×C$_{Ar}$-H), 130.7 (d, C$_{Ar}$-H), 138.1 (s, C-8^a), 141.3 (s, C$_{Ar}$), 183.9 (s, CO). **HRMS** (EI): C$_{16}$H$_{13}$NO calcd.: 235.0997; found: 235.0987. **MS** (EI) m/z = 236.21 (13), 235.22 (100), 234.22 (41), 206.21 (21), 158.15 (22), 130.14 (25), 77.09 (20). Da741

(1-Methylindolizin-3-yl)(phenyl)methanone (18). 1eH⁺Br⁻ (140 mg, 500 µmol) and ethyl methacrylate (**17**) (228 mg, 2.00 mmol) were suspended in CH$_2$Cl$_2$, then NEt$_3$ (146 mg, 1.44 mmol) was added. The suspension was stirred at room temperature till it cleared off (~1 h).

Then chloranil (246 mg, 1.00 mmol) was added and stirring was continued for 1 h. **18** was obtained after column chromatography (SiO$_2$, *n*-pentane:EtOAc 10:1) as yellow oil (18 mg, 76.5 μmol, 15%). Da741-2

3.5 References

[1]   F. Kröhnke, *Ber. Dtsch. Chem. Ges.* **1935**, *68*, 1177–1195.

[2]   For reviews, see: a) A. G. Mikhailovskii, V. S. Shklyaev, *Chem. Heterocylc. Compd.* **1997**, *33*, 243–265; b) J. Jacobs, E. Van Hende, S. Claessens, N. De Kimpe, *Curr. Org. Chem.* **2011**, *15*, 1340–1362; c) A. Kakehi, *Heterocyles* **2012**, *85*, 1529–1577.

[3]   For selected publications, see: a) W. G. Phillips, K. W. Ratts, *J. Org. Chem.* **1970**, *35*, 3144–3147; b) O. Tsuge, S. Kanemasa, S. Takenaka, *Bull. Chem. Soc. Jpn.* **1985**, *58*, 3137–3157; c) O. Tsuge, S. Kanemasa, S. Takenaka, *Bull. Chem. Soc. Jpn.* **1985**, *58*, 3320–3336; d) A. R. E. Carey, S. Al-Quatami, R. A. More O'Ferrall, B. A. Murray, *J. Chem. Soc., Chem. Commun.* **1988**, 1097–1098; e) A. R. E. Carey, R. A. More O'Ferrall, B. A. Murray, *J. Chem. Soc. Perkin Trans. 2* **1993**, 2297–2302; f) X.-M. Zhang, F. G. Bordwell, M. Van Der Puy, H. E. Fried, *J. Org. Chem.* **1993**, *58*, 3060–3066; g) P. Karafiloglou, G. Surpateanu, *Int. J. Quantum Chem.* **2004**, *98*, 456–464; h) Y. Fu, H.-J. Wang, S.-S. Chong, Q.-X. Guo, L. Liu, *J. Org. Chem.* **2009**, *74*, 810–819; i) S. Matsumura, R. Takagi, S. Kojima, K. Ohkata, M. Abe, *Heterocycles* **2010**, *81*, 2479–2495.

[4]   For selected publications, see: a) O. Tsuge, S. Kanemasa, S. Takenaka, *Bull. Chem. Soc. Jpn.* **1987**, *60*, 1489–1495; b) A. M. Shestopalov, V. P. Litvinov, L. A. Rodinovskaya, Y. A. Sharanin, *Bull. Acad. Sci. USSR Chem.* **1991**, *40*, 129–138; c) A. M. Shestopalov, Y. A. Sharanin, V. N. Nesterov, L. A. Rodinovskaya, V. E. Shklover, Y. T. Struchkov, V. P. Litvinov, *Chem. Heterocycl. Compd.* **1991**, *27*, 1006–1011; d) S. Kojima, K. Fujitomo, Y. Shinohara, M. Shimizu, K. Ohkata, *Tetrahedron Lett.* **2000**, *41*, 9847–9851; e) S. Yamada, J. Yamamoto, E. Ohta, *Tetrahedron Lett.* **2007**, *48*, 855–858; f) Q.-F. Wang, X.-K. Song, J. Chen, C.-G. Yan, *J. Comb. Chem.* **2009**, *11*, 1007–1010; g) K.-P. Chen, Y.-J. Chen, C.-P. Chuang, *Eur. J. Org. Chem.* **2010**, 5292–5300; h) Y. Han, J. Chen, L. Hui, C.-G. Yan, *Tetrahedron* **2010**, *66*, 7743–7748; i) N. Kanomata, R. Sakaguchi, K. Sekine, S. Yamashita, H. Tanaka, *Adv. Synth. Catal.* **2010**, *352*, 2966–2978; j) S. Muthusaravanan, S. Perumal, P. Yogeeswari, D. Sriram, *Tetrahedron Lett.*

2010, *51*, 6439–6443; k) Q.-F. Wang, L. Hui, H. Hou, C.-G. Yan, *J. Comb. Chem.* **2010**, *12*, 260–265; l) N. Fernández, L. Carrillo, J. L. Vicario, D. Badía, E. Reyes, *Chem. Commun.* **2011**, *47*, 12313–12315; m) J. L. García Ruano, A. Fraile, M. R. Martín, G. González, C. Fajardo, A. M. Martín-Castro, *J. Org. Chem.* **2011**, *76*, 3296–3305; n) M. Ghandi, A. H. Jameà, *Tetrahedron Lett.* **2011**, *52*, 4005–4007; o) Y. Han, H. Hou, Q. Fu, C.-G. Yan, *Tetrahedron* **2011**, *67*, 2313–2322; p) A. Kumar, G. Gupta, S. Srivastava, *Org. Lett.* **2011**, *13*, 6366–6369; q) D. Belei, C. Abuhaie, E. Bicu, P. G. Jones, H. Hopf, L. M. Birsa, *Synlett* **2012**, *23*, 545–548; r) C.-P. Chuang, K.-P. Chen, *Tetrahedron* **2012**, *68*, 1401–1406; s) P. Gunasekaran, K. Balamurugan, S. Sivakumar, S. Perumal, J. C. Menéndez, A. I. Almansour, *Green Chem.* **2012**, *14*, 750–757; t) S. M. Rajesh, S. Perumal, J. C. Menendez, S. Pandian, R. Murugesan, *Tetrahedron* **2012**, *68*, 5631–5636; u) I. Yavari, G. Khalili, F. Sadeghizadeh, *Synlett* **2012**, *23*, 557–558; v) J. H. Lee, I. Kim, *J. Org. Chem.* **2013**, *78*, 1283–1288.

[5]   For selected publications, see: a) A. R. Katritzky, G. Qiu, B. Yang, H.-Y. He, *J. Org. Chem.* **1999**, *64*, 7618–7621; b) F. Dumitraşcu, M. Vasilescu, C. Drăghici, M. T. Căproiu, L. Barbu, D. G. Dumitreşcu, *ARKIVOC* **2011**, *10*, 346–358; c) A. Hazra, S. Mondal, A. Maity, S. Naskar, P. Saha, R. Paira, K. B. P. Sahu, P. S. Ghosh, C. Sinha, A. Samanta, S. Banerjee, N. B. Mondal, *Eur. J. Med. Chem.* **2011**, *46*, 2132–2140; d) E. Kim, M. Koh, B. J. Lim, S. B. Park, *J. Am. Chem. Soc.* **2011**, *133*, 6642–6649; e) F. Proença, M. Costa, *Tetrahedron* **2011**, *67*, 1071–1075; f) I. Dorange, R. Forsblom, I. Macsari, M. M. Svensson, J. Bylund, Y. Besidski, J. Blid, D. Sohn, Y. Gravenfors, *Bioorg. Med. Chem. Lett.* **2012**, *22*, 6888–6895; g) H. Hu, J. Feng, Y. Zhu, N. Gu, Y. Kan, *RSC Adv.* **2012**, *2*, 8637–8644; h) M. Kucukdisli, T. Opatz, *Eur. J. Org. Chem.* **2012**, 4555–4564; i) Z. Mao, X. Li, X. Lin, P. Lu, Y. Wang, *Tetrahedron* **2012**, *68*, 85–91; j) Y. Shang, L. Wang, X. He, M. Zhang, *RSC Adv.* **2012**, *2*, 7681–7688; k) Q. Cai, Y.-P. Zhu, Y. Gao, J.-J. Sun, A.-X. Wu, *Can. J. Chem.* **2013**, *91*, 414–419.

[6]   J. Gubin, J. Lucchetti, J. Mahaux, D. Nisato, G. Rosseels, M. Clinet, P. Polster, P. Chatelain, *J. Med. Chem.* **1992**, *35*, 981–988.

[7]   P. Sonnet, P. Dallemagne, J. Guillon, C. Enguehard, S. Stiebing, J. Tanguy, R. Bureau, S. Rault, P. Auvray, S. Moslemi, P. Sourdaine, G.-E. Séralini, *Bioorg. Med. Chem.* **2000**, *8*, 945–955.

[8]   L.-L. Gundersen, C. Charnock, A. H. Negussie, F. Rise, S. Teklu, *Eur. J. Pharm. Sci.* **2007**, *30*, 26–35.

[9]   Y.-M. Shen, P.-C. Lva, W. Chen, P.-G. Liua, M.-Z. Zhang, H.-L. Zhu, *Eur. J. Med. Chem.* **2010**, *45*, 3184–3190.

[10]   K. Kitadokoro, S. Hagishita, T. Sato, M. Ohtani, K. Miki, *J.Biochem.* **1998**, *123*, 619–623.

[11]   L. De Bolle, G. Andrei, R. Snoeck, Y. Zhang, A. Van Lommel, M. Otto, A. Bousseau, C. Roy, E. De Clercq, L. Naesens, *Biochem. Pharmacol.* **2004**, *67*, 325–336.

[12]   a) W. Rettig, B. Strehmel, S. Schrader, H. Seifert, *Applied Fluorescence in Chemistry, Biology, and Medicine*, Springer, New York, **1999**; b) J. R. Lakowicz, *Principles of Fluorescence Spectroscopy*, 3rd ed., Springer, New York, **2006**.

[13]   O. Kaumanns, R. Lucius, H. Mayr, *Chem. Eur. J.* **2008**, *14*, 9675–9682.

[14]   a) For a comprehensive database of nucleophilicity parameters N and sN, and electrophilicity parameters E, see: http://www.cup.lmu.de/oc/mayr/; b) H. Mayr, M. Patz, *Angew. Chem.* **1994**, *106*, 990–1010; *Angew. Chem. Int. Ed. Engl.* **1994**, *33*, 938–957; c) H. Mayr, T. Bug, M. F. Gotta, N. Hering, B. Irrgang, B. Janker, B. Kempf, R. Loos, A. R. Ofial, G. Remennikov, H. Schimmel, *J. Am. Chem. Soc.* **2001**, *123*, 9500–9512.

[15]   a) F. Kröhnke, *Ber. Dtsch. Chem. Ges.* **1933**, *66*, 604–610; b) F. Kröhnke, *Ber. Dtsch. Chem. Ges.* **1937**, *70*, 543–547.

[16]   W. Fraser, C. J. Suckling, H. C. S. Wood, *J. Chem. Soc. Perkin Trans. 1* **1990**, 3137–3144.

[17]   a) A. Eschenmoser, A. Frey, *Helv. Chim. Acta* **1952**, *35*, 1660–1666; b) C. A. Grob, J. Csapilla, G. Cseh, *Helv. Chim. Acta* **1964**, *47*, 1590–1602; c) G. Köbrich, H. Fröhlich, *Chem. Ber.* **1965**, *98*, 3637–3651; d) G. W. Fischer, *Chem. Ber.* **1969**, *102*, 2609–2620; e) C. A. Grob, *Angew. Chem.* **1969**, *81*, 543–554; *Angew. Chem. Int. Ed. Engl.* **1969**, *8*, 535–546; f) T. Damiano, D. Morton, A. Nelson, *Org. Biomol. Chem.* **2007**, *5*, 2735–2752; g) A. Krief, S. Jeanmart, A. Kremer, *Bioorg. Med. Chem.* **2009**, *17*, 2555–2575.

[18]   A. Aumüller, S. Hünig, *Liebigs Ann. Chem.* **1986**, *119*, 165–176.

[19]   W. Peter, *J. Phys. Chem. Ref. Data* **1989**, *18*, 1637–1755.

[20]   M. Baidya, S. Kobayashi, H. Mayr, *J. Am. Chem. Soc.* **2010**, *132*, 4796–4805.

[21]   a) W. E. McEwen, I. C. Mineo, Y. H. Shen, *J. Am. Chem. Soc.* **1971**, *93*, 4479–4484; b) T. Nishio, K. Katahira, Y. Omote, *Tetrahedron Lett.* **1980**, *21*, 2825–2826.

[22]   (a) H. E. Gottlieb, V. Kotlyar, A. Nudelman, *J. Org. Chem.* **1997**, *62*, 7512−7515; (b) G. F. Fulmer, A. J. M. Miller, N. H. Sherden, H. E. Gottlieb, A. Nudelman, B. M. Stoltz, J. E. Bercaw, K. I. Goldberg *Organometallics* **2012**, *29*, 2176−2179.

[23]   B. Wang, X. Zhang, J. Li, X. Jiang, Y. Hu, H. Hu *J. Chem. Soc., Perkin Trans. 1* **1999**, 1571–1575.

[24]   Synthezised according to: J. Pospísil, M. Potácek *Tetrahedron* **2007**, *63*, 337–346.

[25]   S. S. Al-Hassan, R. J. Kulick, D. B. Livingstone, C. J. Suckling, H. C. S. Wood, R. Wrigglesworth, R. Ferone, *J. Chem. Soc., Perkin Trans.I* **1980**, 2645–2656.

[26]   D. A. R. Happer, B. E. Steenson, *Synthesis* **1980**, 806−807.

4 Nucleophilicity Parameters of Pyridinium Ylides and Their Use in Mechanistic Analyses

Dominik S. Allgäuer, Peter Mayer, Herbert Mayr

4.1 Introduction

Pyridinium ylides are readily accessible nucleophiles and their chemistry has been studied intensively.[1−6] They undergo various reactions, e. g., 1,3-dipolar cycloadditions,[7−9] Michael additions,[10] or cyclopropanations[11] depending on the nature of the employed electrophile. The nucleophilic reactivities of pyridinium ylides have mostly been rationalized by the pK_a values of the corresponding pyridinium ions,[2a,c] although it is known that pK_a values are not a reliable gauge of relative reactivities of nucleophiles,[12] even when the reaction center is kept constant.[13] While some kinetic studies on the formation[3] and reactions[4] of pyridinium ylides have been performed, their reactivities have, to our knowledge, not been analyzed in relationship with other nucleophiles, such as carbanions. In previous work we have shown that the rates of the reactions of carbocations and Michael acceptors with n-, π-, and σ-nucleophiles, including various ylides,[14] can be described by eq 4.1, where $k_{20°C}$ is the second-order rate constant in M^{-1} s^{-1}, s_N is a nucleophile-specific sensitivity parameter, N is a nucleophilicity parameter, and E is an electrophilicity parameter.[15, 16] The reactivity parameters N and E were used to develop comprehensive reactivity scales, which provide direct comparisons of many different classes of nucleophiles and electrophiles.

We recently reported that the [3+2]-cycloaddition reactions of pyridinium ylides with benzylidene malonates proceed stepwise.[9] This observation encouraged us to analyze the kinetics of reactions of pyridinium ylides with various electrophiles, including electron-deficient ethylenes, by eq 4.1, in order to include the ylides 1 (Table 4.1) into our comprehensive nucleophilicity scale. We now report on the kinetics of the reactions of the pyridinium ylides **1a−g**, the isoquinolinium ylide **1h**, and the quinolinium ylide **1i** with the benzhydrylium ions **2**, the quinone methides **3**, and the benzylidene malonates **4**, which were
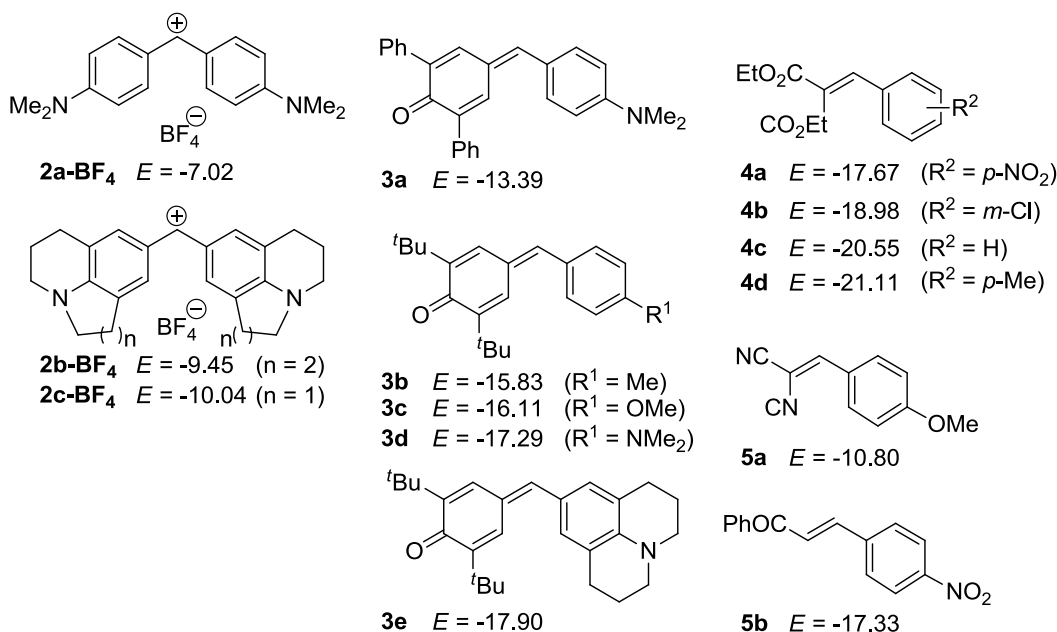
$$\log k_{20°C} = s_N(N + E) \tag{4.1}$$

Table 4.1. Synthesis and pK_a values of the pyridinium salts 1H$^+$X$^-$ employed as precursors for the pyridinium ylides 1 and visible absorption maxima of the ylides 1.

Pyr	EWG	X	Salt	Yield/%	pK_a(DMSO)	Ylide	λ_{max}(DMSO)[a]/nm
Pyridine	CO$_2$Et	Br	1aH$^+$Br$^-$	82[b]	14.1[c]	1a	425
Pyridine	CONEt$_2$	Br	1bH$^+$Br$^-$	83[b]	~20[d]	1b	425
Pyridine	CN	Br	1cH$^+$Br$^-$	quant.[b]	16.5[c]	1c	433
Pyridine	COMe	Cl	1dH$^+$Cl$^-$	45[b]	11.8[c]	1d	425
Pyridine	COPh	Br	1eH$^+$Br$^-$	94[b]	10.7[c]	1e	443
4-Me$_2$N-Pyridine	COPh	Br	1fH$^+$Br$^-$	98	13.2[e]	1f	425
3-Cl-Pyridine	COPh	Br	1gH$^+$Br$^-$	88	-	1g	453
Isoquinoline	COPh	Br	1hH$^+$Br$^-$	93[b]	~10[f]	1h	479
Quinoline	COPh	Br	1iH$^+$Br$^-$	85	-	1i	516

[a] Absorption maximum in the visible range; full UV–Vis spectra are given in the Experimental Section. [b] From ref. [9]. [c] From ref. [2c]. [d] Estimated from the average difference of ΔpK_a ~ 4.5 between pyridinium and analogously substituted trimethylammonium salts.[2c] [e] In H$_2$O; from ref. [2d]; [f] Estimated from the difference of ΔpK_a ~ 3 between the pK_a (1eH$^+$Br$^-$) and pK_a (1aH$^+$Br$^-$), and pK_a of the analogously substituted isoquinolinium salt Isoquin$^+$CH$_2$CO$_2$Et Br$^-$ (pK_a = 13.5 in DMSO).[2c]

commonly used as reference electrophiles (Chart 4.1).[14–16] Subsequently we investigated the kinetics of the reactions of pyridinium ylides with benzylidene malononitrile **5a** and chalcone **5b** to examine whether the N and s_N parameters for pyridinium ylides derived from the reactions of **1a–i** with reference electrophiles can also be employed for predicting the rates of the reactions of pyridinium ylides with other types of Michael acceptors, which undergo diverse subsequent reactions after a common initial rate-determining C−C bond-forming step.

2a-BF$_4$ E = -7.02

2b-BF$_4$ E = -9.45 (n = 2)
2c-BF$_4$ E = -10.04 (n = 1)

3a E = -13.39

3b E = -15.83 (R^1 = Me)
3c E = -16.11 (R^1 = OMe)
3d E = -17.29 (R^1 = NMe$_2$)

3e E = -17.90

4a E = -17.67 (R^2 = p-NO$_2$)
4b E = -18.98 (R^2 = m-Cl)
4c E = -20.55 (R^2 = H)
4d E = -21.11 (R^2 = p-Me)

5a E = -10.80

5b E = -17.33

Chart 4.1. Electrophiles employed in this work (electrophilicities E from refs. [15b,c, 16]).

4.2 Results and Discussion

4.2.1 Products

The pyridinium (**1(a−g)H$^+$X$^−$**), the isoquinolinium (**1hH$^+$Br$^−$**), and the quinolinium salts (**1iH$^+$Br$^−$**) were obtained by nucleophilic substitution from the corresponding pyridines, isoquinoline, or quinoline in tetrahydrofuran (THF) as described previously (Table 4.a).[9] As most ylides **1a−i** are unstable compounds, we made no attempts to isolate them but generated them in solution by treating their conjugate acids **1H$^+$X$^−$** (X$^−$ = Cl$^−$, Br$^−$) with a base.

Figure 4.1. ORTEP-drawing of the crystal structure of 6e-BF$_4$.

The benzhydrylium tetrafluoroborate **2a-BF$_4$** was chosen as representative to study the products of the reactions of the ylides **1** with the benzhydrylium ions **2**. Slow addition of a solution of potassium *tert*-butoxide (KO^{t}Bu) in THF to a suspension of equimolar amounts of benzhydrylium tetrafluoroborate **2a-BF$_4$** and **1(a−i)H$^+$X$^−$** in acetonitrile/dichloromethane (5:1)
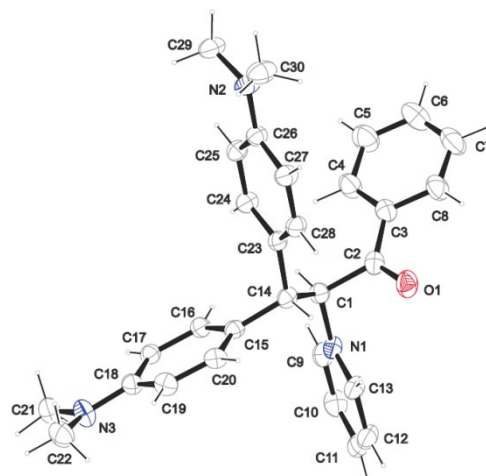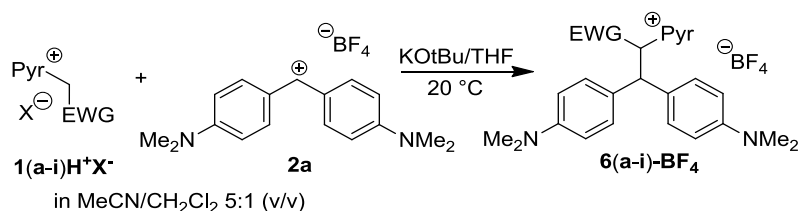
185

Table 4.2. Reactions of the ylides 1 with the benzhydrylium tetrafluoroborate 2a-BF₄.

Salt	Pyr	EWG	Product	Yield/%[a]
1aH⁺Br⁻	Pyridine	CO₂Et	**6a-BF₄**	39
1bH⁺Br⁻	Pyridine	CONEt₂	**6b-BF₄**	98
1cH⁺Br⁻	Pyridine	CN	**6c-BF₄**	88
1dH⁺Cl⁻	Pyridine	COMe	**6d-BF₄**	69
1eH⁺Br⁻	Pyridine	COPh	**6e-BF₄**	quant.[b]
1fH⁺Br⁻	4-NMe₂-Pyridine	COPh	**6f-BF₄**	quant.
1gH⁺Br⁻	3-Cl-Pyridine	COPh	**6g-BF₄**	(quant.)[c]
1hH⁺Br⁻	Isoquinoline	COPh	**6h-BF₄**	57
1iH⁺Br⁻	Quinoline	COPh	**6i-BF₄**	63

[a] After recrystallization from Et₂O/MeCN or MeCN. [b] **1eH⁺Br⁻** was dissolved in aq. KOH (0.1 M), and the resulting ylide **1e** was extracted with CHCl₃. The benzhydrylium tetrafluoroborate **2a-BF₄** (1 equiv) in CH₂Cl₂ was added to the CHCl₃ solution of **1e** at room temperature. [c] Yield of the crude product; purification by crystallization from Et₂O/MeCN failed due to decomposition of **6g-BF₄**.

at room temperature gave rise to the formation of the pyridinium salts **6(a−i)-BF₄**, which were purified by crystallization and isolated in 39% to quantitative yields (Table 4.2). The structures of the products were identified by NMR spectroscopy (^{1}H and ^{13}C) and HRMS as well as by the crystal structure of **6e-BF₄** (Figure 4.1).

Electrophile **3b** was chosen as a representative example for investigating the course of the reactions of the ylides **1** with the quinone methides **3**. The salts **1(a−i)H⁺X⁻** and quinone methide **3b** were suspended in acetonitrile at room temperature and treated with triethylamine (2.2 equiv). This procedure afforded the Michael adducts **7a−h** in excellent yields and modest diastereoselectivities (Table 4.3). The quinolinium derivative **7i** could not be isolated from the reaction of ylide **1i** with quinone methide **3b**, and only decomposition was observed.

As already mentioned above, we recently reported on the reactions of the ylides **1** with benzylidene malonates **4** (Scheme 4.2).[9] We observed that in polar solvents, such as dimethylsulfoxide (DMSO), addition of ylide **1a** to benzylidene malonate **4d** gave the Michael adduct **9a** via the intermediate betaine **8a**.[9] Carrying out the reaction of **1a** with **4d** in a non-

Table 4.3. Synthesis of the Michael adducts 7a−h.
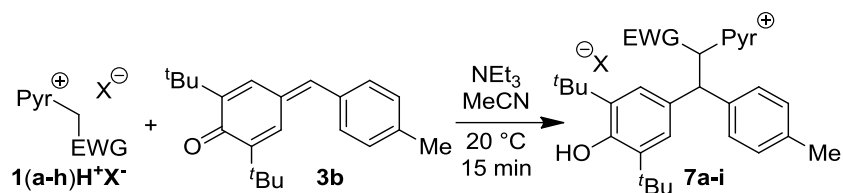
Salt	Pyr	EWG	Product	Yield/%	dr[a]
1aH⁺Br⁻	Pyridine	CO_2Et	**7a**	94	1:2
1bH⁺Br⁻	Pyridine	$CONEt^2$	**7b**	quant.	1:2
1cH⁺Br⁻	Pyridine	CN	**7c**	quant.	1:2
1dH⁺Cl⁻	Pyridine	COMe	**7d**	quant.	2:3
1eH⁺Br⁻	Pyridine	COPh	**7e**	quant.	1:7
1fH⁺Br⁻	4-NMe₂-Pyridine	COPh	**7f**	quant.	1:5
1gH⁺Br⁻	3-Cl-Pyridine	COPh	**7g**	quant.	1:5
1hH⁺Br⁻	Isoquinoline	COPh	**7h**	quant.	1:3
1iH⁺Br⁻	Quinoline	COPh	**7i**	0	-

[a] Determined by ¹H NMR of the isolated product.

polar solvent, such as CH_2Cl_2, led to the formation of the [3+2]-cycloadduct **10a**,[9] which was subsequently oxidized to the indolizine **11a**. The scope of this indolizine formation was tested for a broad variety of differently substituted pyridinium ylides (including **1a−e**) and Michael

Scheme 4.1. Solvent dependence of the reaction of the ylide 1a with benzylidene malonate 4d.[9]
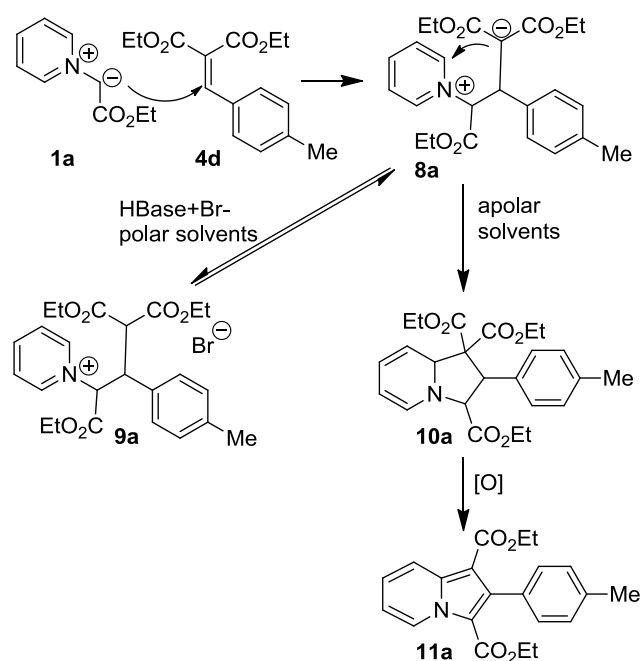
acceptors (including **4a−d**).[9] The reaction of isoquinolinium ylide **1h** with benzylidene malonate **4a** did not give a Michael adduct in DMSO but the [3+2]-cycloadduct, which was isolated in 75% yield.[9]

4.2.2 Kinetic Investigations

The kinetics of the reactions of the ylides **1** with the electrophiles **2−4** in DMSO at 20 °C were monitored photometrically by following the disappearance of one of the two reagents at or close to their absorption maxima (see Experimental Section). Because of the low stabilities of the ylides **1**, they were generated in solution by combining freshly prepared solutions of the salts **1(a−i)H⁺X⁻** and KO^{t}Bu (typically 1.05 equiv) in DMSO directly before the kinetic experiments. The formation of the ylides **1a−i** was confirmed by their UV−vis spectra (see Table 4.1 and Experimental Section). In order to ensure that the pyridinium ions **1(a−i)H⁺** were quantitatively deprotonated, the pyridinium ion with the highest pK_a value in the series (**1bH⁺**, Table 4.1) was titrated with a solution of KO^{t}Bu in DMSO, while the absorbance of the ylide **1b** was monitored by UV−vis spectroscopy at 425 nm. After the addition of 1 equiv. of KO^{t}Bu, addition of further portions of KO^{t}Bu did not lead to an increase of the absorbance of ylide **1b**, indicating the complete deprotonation of **1bH⁺** by 1 equiv. of KO^{t}Bu (see Experimental Section). To simplify the kinetics, one of the two components, nucleophile or electrophile, was used in high excess (≥ 10 equiv), which resulted in monoexponential decays of the UV−vis absorbances of the minor component. From the decays of the UV−vis absorbances, the first-order rate constants k_{obs} (s⁻¹) were derived by least-squares fitting of the exponential function $A_t = A_0 \exp(-k_{obs}t)$ to the time-dependent absorbances A_t of the minor component (Figure 4.2). Plots of k_{obs} against the concentrations of the excess compound were linear, mostly with negligible intercepts (Figure 4.2, insert). From the slopes of these plots, the second-order rate constants k_2 for the reactions of the ylides **1** with the reference electrophiles **2−4** could be derived as listed in Table 4.4. Errors given refer to standard deviations of the correlations k_{obs} versus concentration of the compounds used in excess.
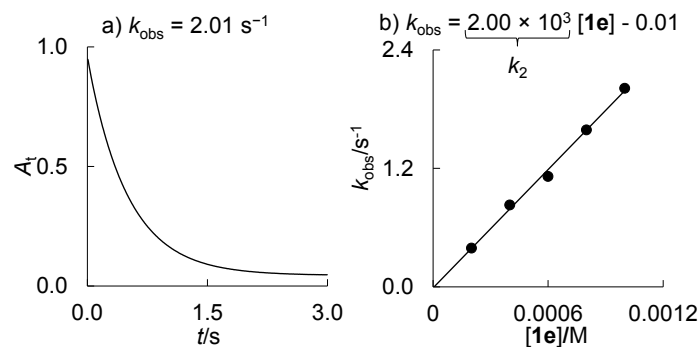
Figure 4.2. Decay of the absorbance of 3a ([3a]$_0$ = 2.00 × 10^{-5} M) at 533 nm during its reaction with 1e ([1e]$_0$ = 1.00 × 10^{-3} M) in DMSO at 20 °C. Insert: Linear correlation of k_{obs} with increasing concentration of 1e.

Table 4.4. Second-order rate constants k_2 for the reactions of the ylides 1 with the reference electrophiles 2(b−c)-BF$_4$, 3, and 4 in DMSO at 20 °C.
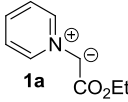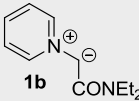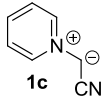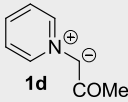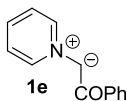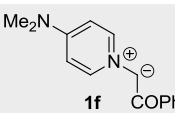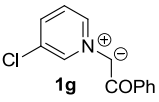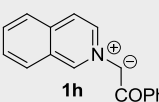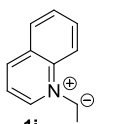
Nucleophile N/s_N	Electrophile	Excess of	λ/nm[a]	k_2(20 °C)/M^{-1} s^{-1}
	3a	**1a**	533	$(9.00 \pm 0.30) \times 10^4$
	3b	**1a**	371	$(9.68 \pm 0.37) \times 10^3$
	3e	**1a**	521	$(1.09 \pm 0.04) \times 10^3$
1a CO$_2$Et	**4a**	**1a**	302	$(1.37 \pm 0.09) \times 10^3$
	4b	**4b**	445	$(1.08 \pm 0.02) \times 10^3$
26.71/0.37	**4c**	**4c**	445	$(1.97 \pm 0.03) \times 10^2$
	4d	**4d**	445	$(1.13 \pm 0.01) \times 10^2$
	3a	**1b**	533	$(2.99 \pm 0.26) \times 10^{5, [b]}$
	3b	**1b**	371	$(3.21 \pm 0.23) \times 10^{4, [b]}$
1b CONEt$_2$	**3d**	**1b**	486	$(7.94 \pm 0.64) \times 10^{3, [b]}$
	3e	**1b**	521	$(3.79 \pm 0.26) \times 10^{3, [b]}$
27.45/0.38	**4a**	**4a**	425	$(4.23 \pm 0.30) \times 10^3$
	4c	**4c**	425	$(6.10 \pm 0.50) \times 10^2$
	3a	**1c**	533	$(2.34 \pm 0.10) \times 10^5$
	3b	**1c**	371	$(2.03 \pm 0.11) \times 10^4$
	3d	**1c**	486	$(2.67 \pm 0.09) \times 10^3$
1c CN	**3e**	**1c**	521	$(2.13 \pm 0.12) \times 10^3$
25.94/0.42	**4a**	**1c**	302	$(2.08 \pm 0.11) \times 10^3$
	4b	**1c**	277	$(6.26 \pm 0.49) \times 10^2$
	4c	**1c**	283	$(1.77 \pm 0.14) \times 10^2$
	4d	**1c**	295	$(1.77 \pm 0.05) \times 10^2$
	3a	**1d**	533	$(1.09 \pm 0.07) \times 10^4$
	3a	**1d**	533	$(1.07 \pm 0.08) \times 10^{4, [c]}$
1d COMe	**3b**	**1d**	371	$(5.02 \pm 0.30) \times 10^2$
	3c	**1d**	393	$(4.13 \pm 0.22) \times 10^2$
20.24/0.60	**3d**	**1d**	486	$(7.18 \pm 0.51) \times 10^1$
	4a	**4a**	425	$(2.26 \pm 0.01) \times 10^1$

Table 4.4. Continued.

Nucleophile N/s_N	Electrophile	Excess of	λ/nm[a]	k_2(20 °C)/M^{-1} s^{-1}
1e COPh 19.46/0.58	**2b-BF$_4$**	**1e**	635	$(7.08 \pm 0.31) \times 10^5$
	2c-BF$_4$	**1e**	630	$(3.85 \pm 0.14) \times 10^5$
	3a	**1e**	533	$(2.00 \pm 0.08) \times 10^3$
	3b	**1e**	371	$(1.29 \pm 0.10) \times 10^2$
	3e	**1e**	521	$(1.03 \pm 0.03) \times 10^1$
1f COPh 21.61/0.58	**3a**	**1f**	533	$(5.51 \pm 0.32) \times 10^4$
	4a	**4a**	425	$(1.77 \pm 0.09) \times 10^2$
	4b	**4b**	425	$(3.39 \pm 0.24) \times 10^1$
1g COPh 17.98/0.63	**2b-BF$_4$**	**1g**	630	$(2.49 \pm 0.13) \times 10^5$
	3a	**1g**	533	$(5.73 \pm 0.31) \times 10^2$
	4a	**4a**	476	1.78 ± 0.16
1h COPh 20.08/0.57	**2b-BF$_4$**	**1h**	630	$(1.51 \pm 0.11) \times 10^6$
	3a	**1h**	533	$(3.88 \pm 0.28) \times 10^3$
	4a	**4a**	482	$(3.05 \pm 0.12) \times 10^1$
1i COPh 19.38/0.50	**2b-BF$_4$**	**1i**	630	$(1.17 \pm 0.08) \times 10^5$
	3a	**1i**	533	$(7.54 \pm 0.31) \times 10^2$
	4a	**4a**	530	8.48 ± 0.43

[a] Monitored wavelength. [b] Excess of pyridinium salt, that is, **1bH$^+$Cl$^-$** : KO^{t}Bu = 1.9 : 1.0. [c] Reproduction with excess of pyridinium salt (**1dH$^+$Cl$^-$** : KO^{t}Bu = 1.9 : 1.0).

Plots of log k_2 for the reactions of the pyridinium ylides **1a,b** and **1d,e** with the reference electrophiles **2−4** against the corresponding electrophilicity parameters E are linear, as depicted for some representative examples in Figure 4.3 (for ylides **1c,f−i** see Experimental Section). From the linearity of these correlations one can deduce that the additions of pyridinium ylides to benzhydrylium ions **2**, quinone methides **3**, and benzylidene malonates **4** in DMSO have analogous rate-limiting steps despite leading to different reaction products. Since the E parameters for **2−4** were derived from reactions of benzhydrylium ions with $\pi_{C–C}$-nucleophiles and from reactions of quinone methides and benzylidene malonates with carbanions, i.e., reactions in which *one* new C−C-bond is formed in the rate-determining step, we conclude that the rate constants listed in Table 4.4 also correspond to the formation of *one* C−C-bond by attack of the ylides **1** at one carbon of the benzhydrylium ions **2** or the Michael acceptors **3,4**. From the slopes of the linear correlations, the nucleophile-specific slope parameters s_N can be derived, and the negative intercepts on the abscissa give the nucleophilicity parameter N of the pyridinium ylides **1** (Figure 4.3; Table 4.3).
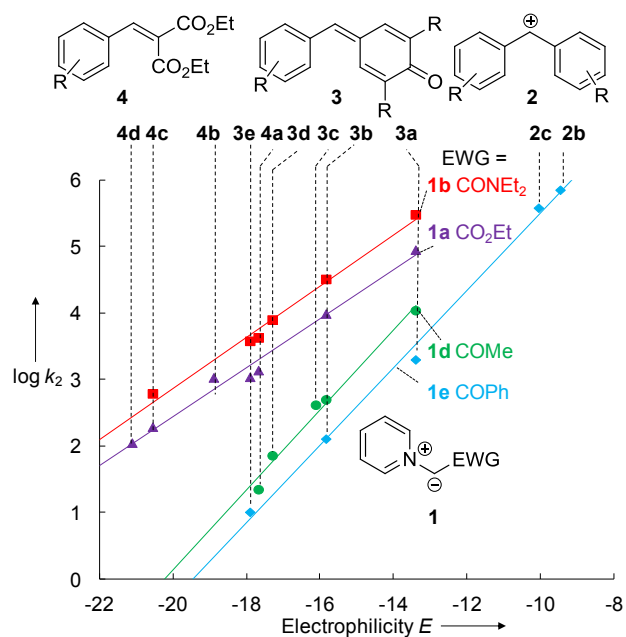
Figure 4.3. Plots of log k_2 (DMSO, 20°C) for the reactions of the pyridinium ylides 1a,b,d,e with the reference electrophiles 2–4 versus their electrophilicity parameters E. For the sake of clarity, the correlation lines for 1c and 1f–i are not shown (see Exerimental Section).
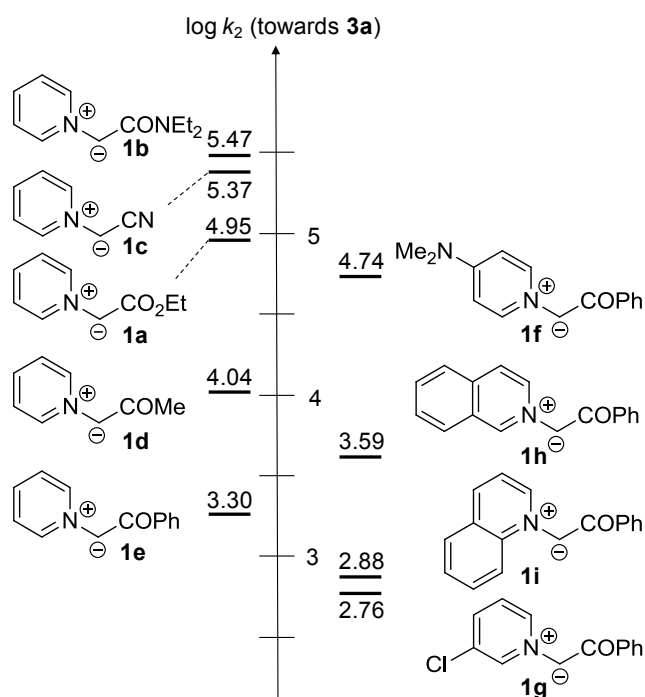
Figure 4.4. Reactivities (log k_2 towards 3a) for the reactions of ylides 1a−i with the quinone methide 3a in DMSO at 20 °C.

The different sensitivities s_N of the various ylides **1a−i** imply that their relative reactivities are significantly affected by the nature of the electrophilic reaction partner. As shown in Figure 4.4 for **3a** as reference electrophile, the reactivities of the ylides **1a−i** toward the quinone

191

methide **3a** differ by almost a factor of 500. While the pyridinium ylides **1a−c** with CO_2Et, $CONEt_2$, and CN substituents are the most reactive nucleophiles, the acetyl and benzoyl substituted ylides **1d,e** are 1 to 2 orders of magnitude less reactive. Comparison of the benzoyl substituted ylides **1e**, **1h**, and **1i** shows that variation of the heterocyclic ring has little influence on the nucleophilicity. Nevertheless, one can see that the isoquinolinium ylide **1h** is more reactive than the pyridinium ylide **1e** and the quinolinium ylide **1i**. An interpretation of this ranking will not be attempted because of the small differences in reactivity that can even be inverted when other electrophiles are used as references.

4.2.3 Applications to Mechanistic Analyses

To investigate the applicability of the N and s_N parameters in Table 4.4 to reactions with other types of electrophiles, the kinetics of the reactions of the ylides **1** with the benzylidene malononitrile **5a** and chalcone **5b** were studied.

4.2.3.1 Benzylidene Malononitrile 5a

Table 4.5 lists the experimental (k_{exp}) and calculated (k_{calcd} by eq 4.1) second-order rate constants for the reactions of the ylides **1d−i** with **5a**, which were determined by following the consumption of the ylides **1** in DMSO at 20 °C. While the experimental and calculated second-order rate constants for the reactions of ylides **1d,f,h,i** with **5a** agree within a factor of 7 (i.e., within the confidence limit of eq 4.1), **1e** and **1g** react 10^6 times more slowly than calculated (Table 4.5). This behavior prompted us to investigate the reactions of pyridinium ylides **1a−i** with the benzylidene malononitrile **5a** more closely.

The reactions of the ylides **1** with benzylidene malononitrile **5a** may either give the betaines **12**, the cyclopropanes **13**, or the tetrahydroindolizines **14**, as summarized in Scheme 4.2.

Table 4.5. Experimentally determined (k_{exp}) and calculated (k_{calcd}) second-order rate constants for the reactions of the ylides 1d−i with the electrophile 5a in DMSO at 20 °C.

Ylide	$k_{exp}/M^{-1} s^{-1}$	$k_{calcd}/M^{-1} s^{-1, [a]}$	k_{exp}/k_{calcd}	$k_{exp} =$
1d	$(2.14 \pm 0.07) \times 10^5$	4.86×10^5	0.44	k_2
1e	$(2.19 \pm 0.15) \times 10^{-1}$	1.05×10^5	2.09×10^{-6}	$K \cdot k_{rc}$
1f	$(4.27 \pm 0.25) \times 10^5$	1.70×10^6	0.25	k_2
1g	$(2.02 \pm 0.08) \times 10^{-1}$	3.11×10^4	6.50×10^{-6}	$K \cdot k_{rc}$
1h	$(2.95 \pm 0.06) \times 10^4$	1.96×10^5	0.15	k_2
1i	$(5.73 \pm 0.13) \times 10^3$	2.07×10^4	0.28	k_2

[a] Calculated by eq 4.1 from E (Chart 1) and N, s_N from Table 4.4.

Scheme 4.2. Reactions of ylides 1 with benzylidene malonate 5a in DMSO.
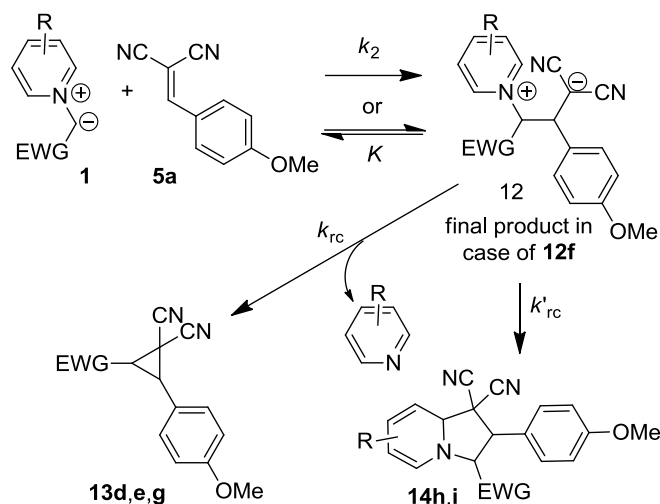
When an equimolar solution of the 4-dimethylaminosubstituted pyridinium salt **1fH⁺Br⁻** and benzylidene malononitrile **5a** in DMSO-d_6 was treated with 1,5,7-triazabicyclo- [4.4.0]dec-5-ene (TBD) as base, quantitative formation of the betaine **12f** was observed with moderate diastereoselectivity (Scheme 4.3). The structure of betaine **12f** could be assigned by 2D-NMR, but attempts to isolate **12f** failed. The ^{13}C NMR signal at $\delta = 16.0$ ppm was assigned to a carbanionic center, in agreement with published data for betaines derived from carboxamido-substituted pyridinium ylides and benzylidene malononitriles.[11a] As the pyridinium ring is stabilized by the dimethylamino group in 4-position, **12f** does not undergo subsequent cyclizations, and the measured rate constant corresponds to k_2.,

As expected from the large rate constant for the reaction of **1d** with **5a** reported in Table 4.5, complete consumption of the reactants was observed in the ^{1}H NMR spectrum taken immediately after mixing **1dH⁺Cl⁻** with benzylidene malononitrile **5a** and KO^{t}Bu in DMSO-d_6 at ambient temperature. ^{1}H NMR spectra taken after 5, 30, and 60 min showed 40/60, 21/79, and 0/100 mixtures of betaine **12d** and cyclopropane **13d**, respectively, indicating that the fast

Scheme 4.3. Reaction of the ylide 1f with benzylidene malononitrile 5a in DMSO-d_6.
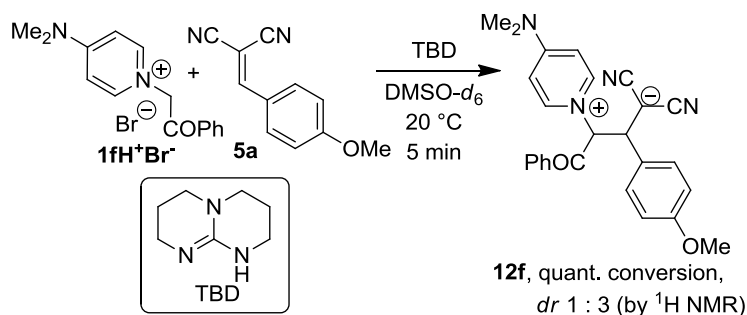
formation of the betaine **12d** is followed by a slow cyclization step. The cyclopropane **13d** was isolated in 53% yield when the mixture obtained from **1dH⁺Cl⁻**, **5a**, and KO^{t}Bu was worked up after a reaction time of 60 min (Table 4.6). The exclusive formation of *trans*-**13d** was derived from a NOESY experiment.[17]

A different behavior was observed for the ylides **1e**,**g**. When the reaction of **1eH⁺Br⁻** with **5a** and 1.8 equiv. triethyl-

Figure 4.5. ORTEP-drawing of the crystal structure of 13e. The asymmetric unit contains two formula units.

amine was monitored by ^{1}H NMR spectroscopy in DMSO-d_6, the intermedite betaine **12e** was not observable, and the reaction mixture showed signals of the reactants **1eH⁺Br⁻** and **5a**, the ylide **1e**, and the cyclopropane **13e**, the yield of which increased from 41% after 5 min to 81% after 30 min. Combination of **1eH⁺Br⁻** with benzylidene malononitrile **5a** and triethylamine in DMSO at ambient temperature yielded cyclopropane **13e** with complete trans-selectivity within 30 min (Table 4.6), as confirmed by the crystal structure of **13e** (Figure 4.5). Analogously, combination of the 3-chloro-substituted ylide **1g** with **5a** afforded cyclopropane **13g** (= **13e**) with complete trans-selectivity within 30 min.

The non-observance of the intermediate betaines **12e**,**g** in the reactions of **1e**,**g** with **5a** implies that in the reactions of these less Lewis-basic ylides (pK_a in Table 4.1), the equilibrium depicted on top of Scheme 4.2 is completely shifted to the left side, with the consequence that the experimentally determined rate constants k_{exp} correspond to $K \cdot k_{rc}$, which explains the large deviation of k_{exp} from k_{calcd} for these two combinations in Table 4.5.

The reactions of the ylides **1h**,**i** with benzylidene malononitrile **5a** in DMSO yielded 88% and 68% of the [3+2]-cycloadducts **14h**,**i**, respectively (Scheme 4.4). The stereochemistry of **14h**,**i** was assigned on the basis of NOESY correlations between the protons and the substituents of the pyrrolidine rings. From the stereochemistry of the [3+2]-cycloadducts one can deduce that the depicted major diastereoisomers of **14h**,**i** were formed via an endo approach of electrophiles to the anti ylides (Scheme 4.4), in agreement with literature reports for similar [3+2]-cycloadducts obtained from isoquinolinium ylides and benzylidene malononitriles.[7b,c] The stereochemistry of the minor diastereoisomers could not be assigned unambiguously.
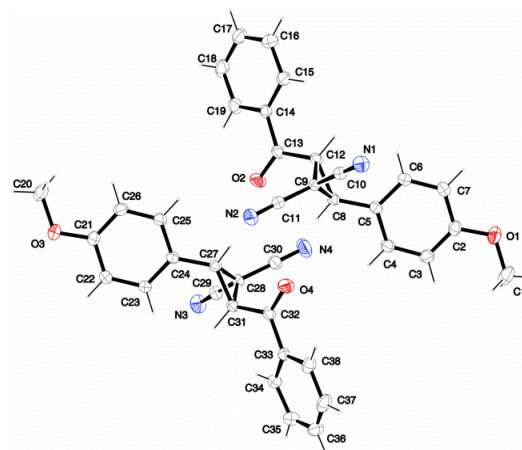
Table 4.6. Formation of the cyclopropanes 13 in DMSO.
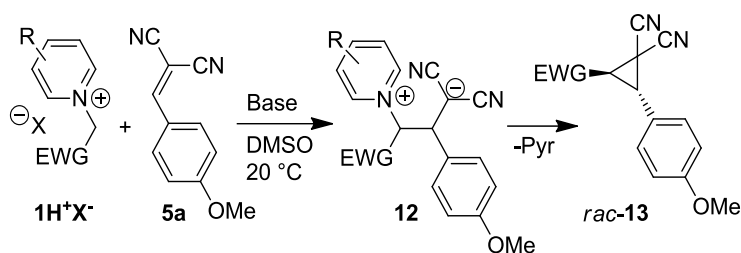
Salt	R	EWG	Base	Betaine	Cyclopropane	Yield/%
1dH⁺Cl⁻	H	COMe	KO^tBu	**12d**	**13d**	53[a]
1eH⁺Br⁻	H	COPh	NEt₃	**12e**	**13e**	67[b]
1gH⁺Br⁻	3-Cl	COPh	NEt₃	**12g**	**13g (= 13e)**	95[b]

[a] After column chromatography over silica (*n*-pentane : EtOAc ≅ 5 : 1). [b] After recrystallization from EtOH.

The formation of the [3 + 2]-cycloadducts **14h,i** from isoquinolinium and quinolinium ylides, instead of betaines or cyclopropanes as obtained with pyridinium ylides (see above), can be explained by the lower aromaticity of the heterocyclic ring of the bicyclic reactants **1h,i**, which facilitates the cyclization of the intermediate betaine.[5b]

In line with quantum chemical calculations by Matsumura, which indicated a barrier of only 2.9 kJ/mol for the cyclization of a betaine generated from an isoquinolinium ylide and 1,1-dicyanoethylene,[5b] one can conclude that the betaines formed from **5a** and **1h,i** undergo fast subsequent ring closures with formation of the [3+2]-adducts **14h,i** (Scheme 4.4), with the consequence that in these cases k_{exp} corresponds to k_2. The observation $k_{exp} \approx k_{calcd}$ also excludes concerted 1,3-dipolar cycloadditions **5a** + **1h,i** with a high energy of concert, because in this case k_{exp} should be considerably larger than k_{calcd}.[18]

Scheme 4.4. Formation of the tetrahydroindolizines 14h,i in DMSO.
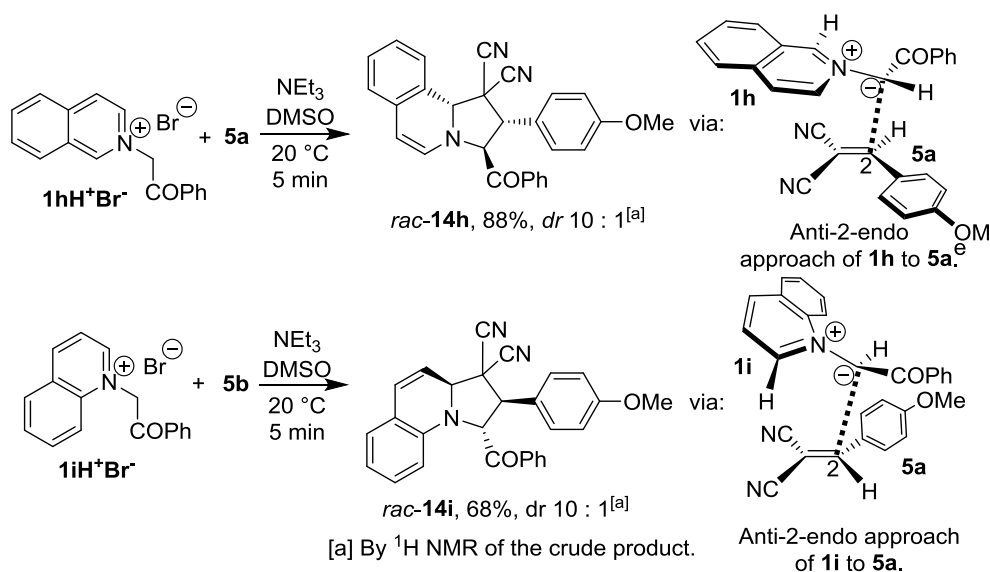
4.2.3.2 Chalcone 5b

All ylides **1** underwent [3+2]-cycloadditions with **5b**,[19] as evidenced by the isolation of the indolizines **16a−i**, obtained by oxidation of the initially generated tetrahydroindolizines **15a−i** with tetrakispyridinocobalto(II)-dichromate (TPCD; Table 4.7).

Because of the low stabilities of the initially formed tetrahydroindolizines **15a−i**, which were already reported in the literature,[7b] their isolation was generally not attempted. Only the tetrahydroindolizine **15i** was obtained in low yield by the reaction of ylide **1i** with chalcone **5b**, analyzed by 1H NMR spectroscopy, and identified as a 5:27:68 mixture of diastereoisomers. The stereochemistry of the depicted major diastereoisomer of **15i** (Scheme 4.5) was derived from the NOESY correlations between the protons and the substituents at the pyrrolidine ring. Its formation can be explained by the 1-endo-2-exo approach of the electrophile **5b** to the anti-configuration of ylide **1i**, in agreement with Tsuge's interpretation of the stereoselectivities of the reactions of isoquinolinium ylides with several different chalcones.[7b] The stereochemistry of the other diastereoisomers could not be assigned unambiguously. The purification of the

Table 4.7. Synthesis of the indolizines 16.

Salt	R	EWG	Product	Yield/%
1aH⁺Br⁻	H	CO₂Et	**16a**	54
1bH⁺Br⁻	H	CONEt₂	**16b**	63[a]
1cH⁺Br⁻	H	CN	**16c**	95
1dH⁺Cl⁻	H	COMe	**16d**	50
1eH⁺Br⁻	H	COPh	**16e**	93
1gH⁺Br⁻	3-Cl	COPh	**16g**	85[b]
1hH⁺Br⁻	Isoquinoline	COPh	**16h**	91
1iH⁺Br⁻	Quinoline	COPh	**16i**	77[a]

[a] 1. CH₂Cl₂/aq. NaOH (32%), 20°C; 2. Chloranil (2 equiv.), CH₂Cl₂, 20°C; [b] Mixture of isomers; **16g-(8-Cl)** : **16g-(6-Cl)** = 4 : 1.

Scheme 4.5. Reaction of salt 1iH⁺Br⁻ with chalcone 5b in DMSO.
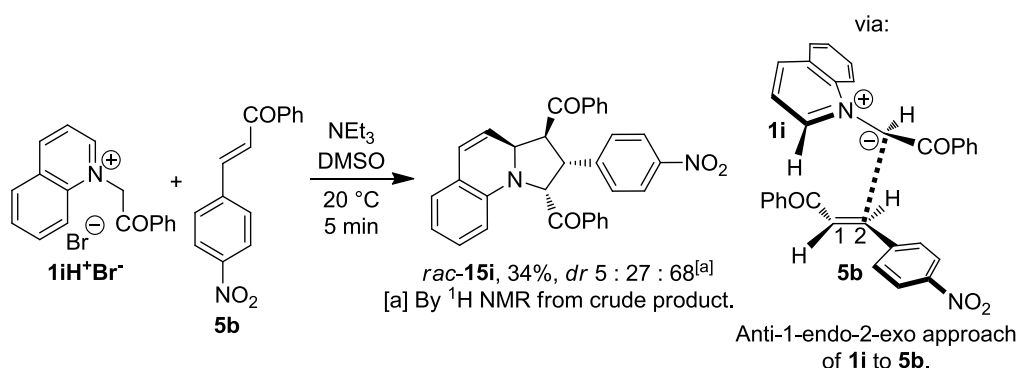
[3+2]-cycloadduct **15i** failed due to its decomposition during workup, which may also explain the low yield.

For the [3+2]-cycloadditions of the ylides **1** with the chalcone **5b**, concerted or stepwise mechanisms have to be considered (Scheme 4.6). In case of a stepwise mechanism with rate-determining formation of the intermediate betaine **18**, the experimentally determined rate constant k_{exp} should correspond to k_2 and agree with the calculated rate constant k_{calcd} within the general confidence limit of eq 4.1 (1−2 orders of magnitude).[15a,b]

The kinetics of the reactions of the ylides **1** with chalcone **5b** were studied by monitoring the consumption of the ylides **1a−i**. Table 4.8 lists the experimental (k_{exp}) and calculated second-order rate (k_{calcd} by eq 4.1) for these reactions in DMSO at 20 °C. For 7 of the 8 reactions of the ylides **1** with chalcone **5b** experimental and calculated second-order rate constants agree within a factor of 2.5, indicating a stepwise mechanism with rate-determining formation of the betaine **18** (Table 4.8). Only the reaction of ylide **1e** with chalcone **5b** proceeds 20 times more slowly than calculated by eq 4.1. This deviation might be due to a partial reversibility of the betaine
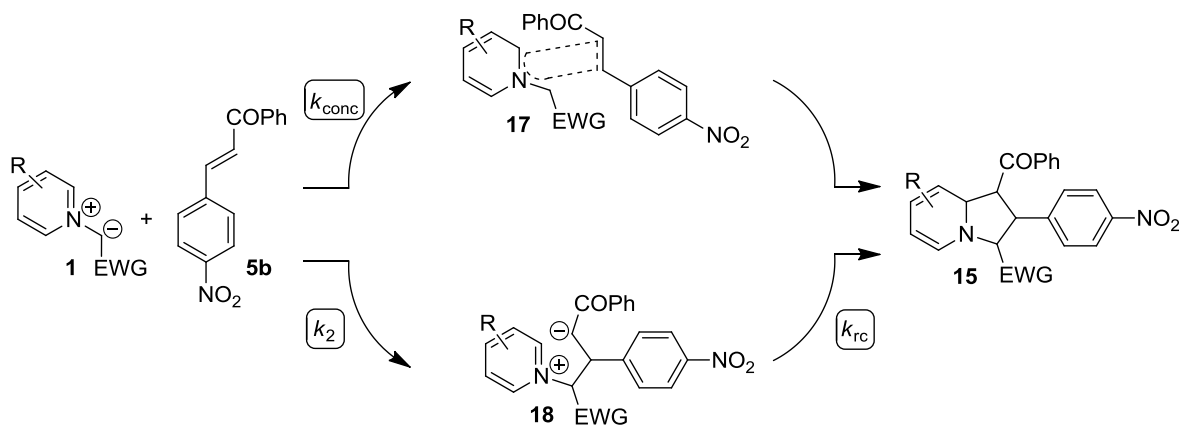
Scheme 4.6. Concerted and stepwise 1,3-dipolar cycloaddition of ylides 1 with chalcone 5b.

Table 4.8. Experimentally determined (k_{exp}) and calculated (k_{calcd}) second-order rate constants for the [3+2]-cycloadditions of the ylides 1a−i with the p-NO$_2$-chalcone 5b in DMSO at 20 °C.

Ylide	k_{exp}/M^{-1} s^{-1}	k_{calcd}/M^{-1} s^{-1} [a]	k_{exp}/k_{calcd}
1a	$(4.82 \pm 0.10) \times 10^3$	2.68×10^3	1.80
1b	$(6.12 \pm 0.28) \times 10^3$	7.80×10^3	0.78
1c	$(7.92 \pm 0.37) \times 10^3$	4.13×10^3	1.92
1d	$(2.55 \pm 0.09) \times 10^1$	5.61×10^1	0.45
1e	$(8.54 \pm 0.45) \times 10^{-1}$	1.72×10^1	0.05
1g	3.67 ± 0.12	2.56	1.43
1h	$(3.56 \pm 0.22) \times 10^1$	3.70×10^1	0.96
1i	$(1.64 \pm 0.05) \times 10^1$	1.08×10^1	1.52

[a] Calculated by eq 4.1 from E (Chart 1) and N, s_N from Table 4.4

formation followed by rate-determining cyclization, but since the deviation is within the confidence limit of eq 4.1, we do not want to speculate.

In case of concerted cycloadditions k_{exp}/k_{calcd} should be >1, depending on the degree of concertedness.[18] Because of the large error limits of eq 4.1, the kinetic data do not allow us to differentiate stepwise cycloadditions from concerted processes with highly unsymmetrical transition states and a small energy of concert. As none of the experimental rate constants k_{exp} in Table 4.8 is considerably faster than k_{calcd}, we conclude that none of these cycloadditions proceeds with a high energy of concert, which implies that eq 4.1, which has been derived for one-bond forming reactions of electrophiles with nucleophiles, can also be employed for predicting absolute rate constants for stepwise cycloadditions or concerted cycloadditions with highly unsymmetrical transition states. As the E parameters used for these calculations have previously been derived from the rate constants of carbanion additions (E for **5a**)[16a] or from stepwise cyclopropanations with sulfonium ylides (E for **5b**),[16c] the general power of this approach has thus been corroborated.

4.3   Conclusion

The rates of the reactions of the pyridinium ylides **1** with benzhydrylium ions **2**, quinone methides **3**, and arylidene malonates **4** follow the linear free-energy relationship (eq 4.1), which allows us to characterize the synthetically important pyridinium ylides by the reactivity parameters N and s_N and to include them in our comprehensive nucleophilicity scale.[15h]
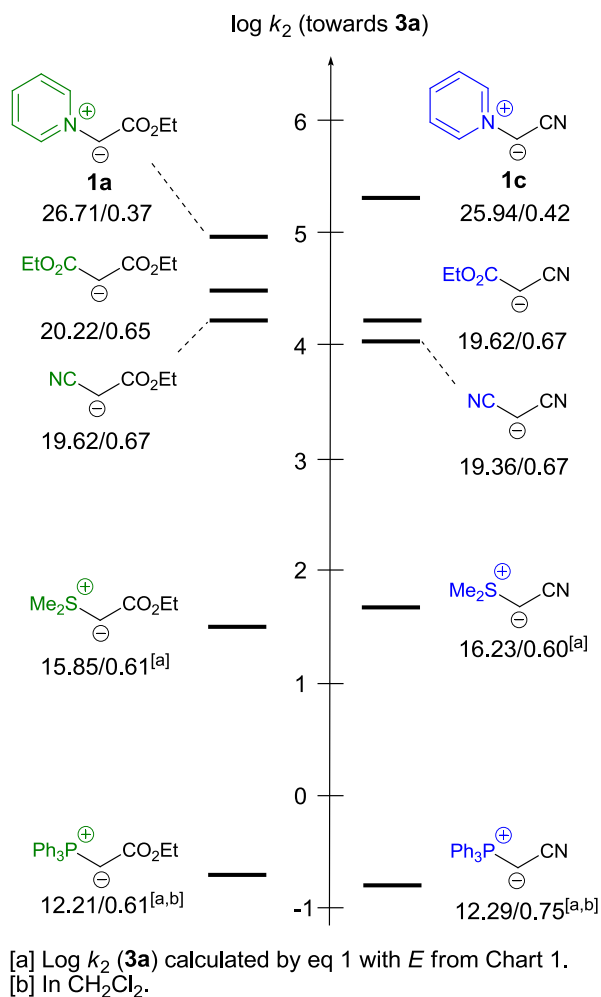
Figure 4.6. Comparison of the log k_2-values (towards 3a) of analogously substituted ylides[14a,c] and carbanions[15c] towards electrophile 3a. N and s_N-values are given below each nucleophile (reactivities refer to DMSO as solvent).

Figure 4.6 compares the reactivities of the ethoxycarbonyl-substituted pyridinium ylide **1a** (left) and the cyano-substituted pyridinium ylide **1c** (right) with those of analogously substituted carbanions as well as with those of phosphorus and sulfonium ylides. Both columns show that pyridinium ylides are approximately a million times more reactive than analogously substituted triphenylphosphonium ylides and about thousand times more reactive than the corresponding dimethylsulfonium ylides. The close similarity of the reactivities of the pyridinium ylides and of diethyl malonate and ethyl cyanoacetate anions shows that pyridinium substitution affects the reactivities of nucleophilic reaction centers to a similar extent as ethoxycarbonyl and cyano substitution. Because of the smaller sensitivities s_N of the pyridinium ylides compared to the other C-nucleophiles, the relative reactivities of the pyridinium ylides with respect to the other nucleophiles of Figure 4.6 will depend on the nature of the electrophilic reaction partner. Pyridinium ylides will show a lower relative reactivity toward reaction partners which are more

electrophilic than **3a** ($E > -13$), while they will show an even higher relative reactivity toward less reactive electrophiles ($E < -13$).

As correlation eq 4.1 allows one to calculate the rate constants for the formation of the zwitterions (betaines) from pyridinium ylides **1** and Michael acceptors, it can be employed for the analysis of reaction mechanisms. From the agreement between calculated (eq 4.1) and experimental rate constants for the 1,3-dipolar cycloadditions of the isoquinolinium (**1h**) and quinolinium ylide (**1i**) with the benzylidenemalononitrile **5a** and of all investigated ylides **1** with the chalcone **5b**, we have concluded that these cycloadditions proceed stepwise or in a concerted way with negligible energy of concert.

In two cases, i.e., in the reactions of the benzylidenemalononitrile **5a** with the pyridinium ylides **1e**,**g**, the experimental rate constants were found to be a million times smaller than calculated by eq 4.1. NMR spectroscopic monitoring of these reactions showed that they proceed with reversible formation of the intermediate betaines, which undergo subsequent slow, rate-determining ring-closure with formation of cyclopropanes. The large deviation between experimental and calculated rate constants thus was indicative of a change of the reaction mechanism, illustrating the value of eq 4.1 for mechanistic analyses.

The differentiation of concerted and stepwise 1,3-dipolar cycloadditions[20] has been a challenge for mechanistic chemistry for many decades.[21] While mechanistic investigations indicate a concerted pathway for most 1,3-dipolar cycloadditions,[22] stepwise processes via zwitterionic intermediates have been observed in reactions of thiocarbonyl ylides (electron-rich 1,3-dipoles) with electron-deficient dipolarophiles.[23]

Our observation that eq 4.1 allows one to predict absolute rate constants for 1,3-dipolar cycloadditions of pyridinium, isoquinolinium, and quinolinium ylides with the electron-poor dipolarophiles **4a−d** and **5a**,**b** implies a remarkable extension of the validity range of eq 4.1. It now appears feasible that eq 4.1 can generally be employed for predicting absolute rate constants of cycloadditions of highly nucleophilic 1,3-dipoles with highly electrophilic dipolarophiles as well as of electrophilic 1,3-dipoles with electron-rich dipolarophiles. In view of the great recent interest in the mechanisms of 1,3-dipolar cycloadditions using the distortion/interaction energy model[24] or activation strain model,[25] we expect that these data will significantly broaden the experimental basis of these models and assist the further development of this theoretical approach.

4.4 Addendum

The [3+2]-cycloaddition of ylide **1i** with nitrostyrene **5c** in DMSO gave the tetrahydroindolizine **19i** which was isolated in moderate yield as a single diastereoisomer after recrystallization (Scheme 4.7). The stereochemistry, assigned on basis of the NOESY correlations of the protons and substituents of the pyrrolidine ring, indicated that **19i** is formed by an anti-1-endo-2-exo approach of the ylide **1i** to nitrostyrene **5c** (Scheme 4.7), in agreement with Tsuge's[7b] report on the reactions of isoquinolinium ylides with nitrostyrenes.

Tetrahydroindolizines **19a−g**, the alleged initial adducts from ylides **1a−g** to nitrostyrene **5c**, could not be isolated by this method because they are too unstable. By subsequent oxidation of the product (**19c**) formed by the reaction of ylide **1c** with **5c**, using one equivalent of dichlordicyanobenzoquinone (DDQ) in air, we obtained 48% of the dihydroindolizine **20c** after 30 min (Scheme 4.7). The initial diastereomeric ratio after recrystallization of **20c** is *cis* : *trans* = 1 : 24, but **20c** epimerizes in CDCl$_3$ solution to give a 1 : 1 mixture within a day. Under the same conditions the reaction of ylide **1g** with nitrostyrene **5c** and subsequent oxidation by one equivalent of DDQ in air produced only the fully oxidized indolizine **19g** (Table 4.9).

Scheme 4.7. Synthesis of tetrahydroindolizine 19i and dihydroindolizine 20c in DMSO.
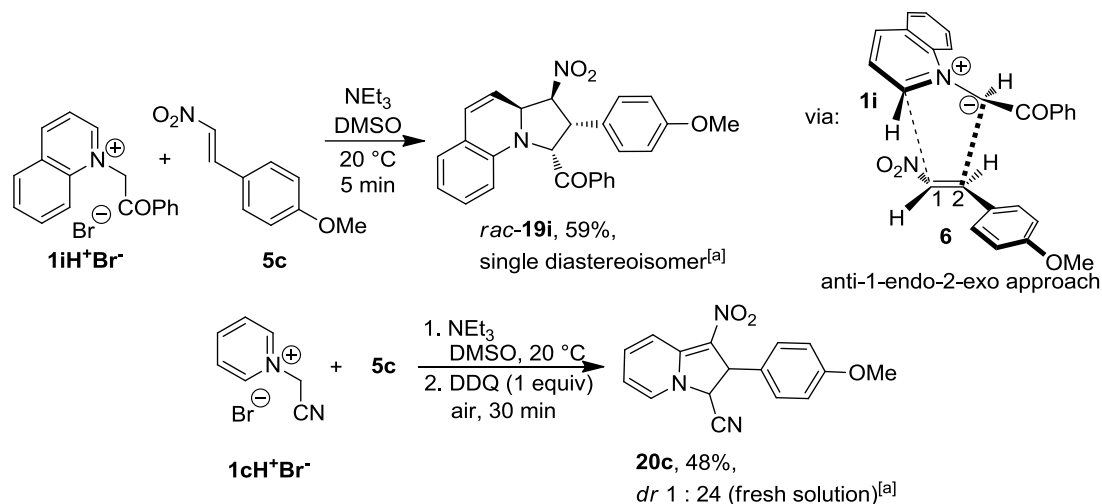
[a] Determined by ^{1}H NMR after recrystallization.

Table 4.9. Synthesis of the indolizines 21.

Salt	R	EWG	Solvent	Base	Oxidant	T/°C	Product	Yield/%
1aH⁺Br⁻	H	CO_2Et	DMSO	NEt_3	MnO_2	100[a]	**21a**	54
1bH⁺Br⁻	H	$CONEt_2$	CH_2Cl_2	aq. NaOH	Chloranil[b]	20	**21b**	10
1cH⁺Br⁻	H	CN	DMSO	NEt_3	MnO_2	100[a]	**21c**	64
1dH⁺Cl⁻	H	COMe	DMSO	NEt_3	MnO_2	100[a]	**21d**	70
1eH⁺Br⁻	H	COPh	DMSO	KO^{t}Bu	TPCD[c]	100[a]	**21e**	68
			DMSO	NEt_3	MnO_2	100[a]	**21e**	48
			DMSO	KO^{t}Bu	$KMnO_4/MnO_2$[d]	100[a]	**21e**	54
1gH⁺Br⁻	3-Cl	COPh	DMSO	NEt_3	MnO_2	100[a]	**21g**	67[e]
			DMSO	NEt_3	TPCD[c]	100[a]	**21g**	54[e]
			DMSO	NEt_3	DDQ[f]	20	**21g**	55[e]

[a] By microwave irradiation (5 W); [b] 2 equivalents; [c] Tetrakispyridinocobalto(II)dichromate; [d] Grounded $KMnO_4$: MnO_2 (1 : 3 by weight); [e] 4:1 mixtures of **21g**-(**8-Cl**) and **21g**-(**5c-Cl**); [f] 2,3-Dichloro-5,6-dicyano-1,4-benzoquinone.

As many of the tetrahydroindolizines **19** and dihydroindolizines **20** are unstable compounds, the crude cycloadducts **19a−i** were converted into the corresponding indolizines **21** by oxidation (Table 4.9). In a first step, the ylides **1** were generated by treating DMSO solutions of the salts **1H⁺X⁻** in the presence of nitrostyrene **5c** with a base, which led to the formation of the tetrahydroindolizines **19**. Their oxidation with MnO_2 or tetrakispyridinocobalto(II) dichromate (TPCD) at 100 °C (microwave irradiation, 5 W, 1 h) gave the indolizines **21** in moderate yields (Table 4.9). The carboxamido substituted **21b** could only be obtained in low yield by a biphasic generation of the tetrahydroindolizine **21b** and its subsequent oxidation by 2 equiv. of chloranil. The low yield may be due to a reaction of nitrostyrene **5c** with NaOH. The indolizine **21e** was obtained in 68% yield when the oxidation was performed with TPCD, while oxidations with MnO_2 or ground mixtures of $KMnO_4$: MnO_2 (1 : 3 by weight) resulted in lower yields of around 50%. Indolizine **21g** was obtained as 4 : 1 ratio of the 8-Cl over the 6-Cl regioisomer by oxidation of the tetrahydroindolizine **21g** by MnO_2 at 100 °C, TPCD or as 2 : 1 mixture by oxidation with one equiv. of DDQ in air at 20 °C (Table 4.9).

Scheme 4.8. Synthesis of the indolizines 21h,i and 22h,i.
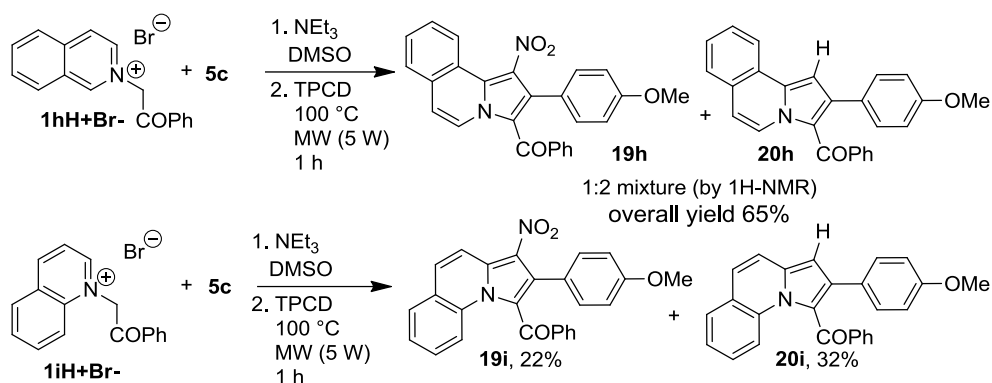
Indolizines derived from the ylides **1h**,**i** and the nitrostyrene **5c** were obtained as mixtures of the NO$_2$ substituted indolizines **21h**,**i** and the corresponding denitrated derivatives **22h**,**i** (Scheme 4.8). The indolizines **22h**,**i** may be formed by base-induced elimination of HNO$_2$ from the initially generated tetrahydroindolizines **19h**,**i** instead of oxidative removal of hydrogen from the 1-position and 3-position, respectively, which eventually yields the nitro-substituted indolizines **21h**,**i**. Pure **22h** was obtained in 11% yield by stirring **1hH$^+$Br$^-$** and **7** with 2.9 equiv. triethylamine at 20 °C for 5 h. Similar eliminations of HNO$_2$ from nitro-substituted tetrahydroindolizines have previously been employed to synthesize a broad variety of indolizines.[8c,26]

As illustrated in Schemes 4.7, 4.8 and Table 4.9 the ylides **1** exclusively underwent [3+2]-cycloadditions with nitrostyrene **5c**. As mentioned in the main section concerted or stepwise mechanisms have to be considered for such [3+2]-cycloadditions (Scheme 4.6). In case of a stepwise mechanism with rate-determining formation of the intermediate betaine, the observed rate constants k_2 and the calculated rate constants k_{calcd} should agree within the general confidence limit of equation 1 (one to two orders of magnitude).[15a,b]

For 6 of the 8 reactions of the ylides **1** with nitrostyrene **5c** experimental and calculated second-order rate constants agree within a factor of 3.5 indicating a rate-determining formation of a betaine (Table 4.10). The remaining 2 reactions proceed up to 12 times more slowly than calculated by equation 1. This deviation is within the confidence limit of equation 1, but might also be due to a partial reversibility of the betaine formation followed by rate-determining cyclization. In case of concerted cycloadditions k_{exp}/k_{calcd} should be greater than 1, depending on the degree of concertedness.[18b] As k_{exp} is never considerably faster than k_{calcd}, we conclude that all cycloadditions listed in Table 4.10 proceed stepwise or in a concerted manner with a negligible energy of concert.

Table 4.10. Observed (k_{exp}) and calculated (k_{calcd})[a] second-order rate constants for the [3+2]-cycloaddition reactions of the ylides 1a−i with the nitrostyrene 5c ($E = -14.70$)[27] in DMSO at 20 °C.

Ylide	$k_{exp}/M^{-1} s^{-1}$	$k_{calcd}/M^{-1} s^{-1}$	k_{exp}/k_{calcd}
1a	4.52×10^4	2.46×10^4	1.84
1b	9.90×10^3	8.01×10^4	0.12
1c	7.01×10^4	4.88×10^4	1.44
1d	8.02×10^2	2.13×10^3	0.38
1e	1.87×10^2	5.77×10^2	0.32
1g	4.78×10^1	1.13×10^2	0.42
1h	1.01×10^2	1.17×10^3	0.09
1i	9.66×10^1	2.27×10^2	0.43

[a] By eq. 1 using s_N and N for the ylides **1** from Table 4.4 and $E = -14.70$ of **5c** from ref. **[27]**.

4.5 Experimental Section

4.5.1 General

Chemicals. CH_2Cl_2 was dried over CaH_2 and freshly distilled prior to use; DMSO (99.7%, extra dry, over molecular sieves, AcroSeal) was purchased and used without further purification.

Devices. For the microwave assisted synthesis a CEM Discover 908010 microwave oven was used.

Analytics. ^{1}H- and ^{13}C NMR spectra were recorded in $CDCl_3$ (δ_H 7.26, δ_c 77.16),[28a] CD_2Cl_2 (δ_H 5.32, δ_c 53.84),[28b] or DMSO-d_6 (δ_H 2.50, δ_c 39.52)[28a] on 200, 300, 400, or 600 MHz NMR spectrometers and are given in ppm. The following abbreviations were used to designate chemical shift multiplicities: s = singlet, d = doublet, t = triplet, q = quartet, m = multiplet, br = broad. For reasons of simplicity, the ^{1}H NMR signals of AA'BB'-spin systems of *p*-disubstituted aromatic rings were treated as doublets. The assignments of individual NMR signals were based on additional 2D-NMR experiments (COSY, NOESY, HSQC, HMBC). Diastereomeric ratios (*dr*) were determined by ^{1}H NMR of the crude reaction products if not stated otherwise. Integrals for mixtures of diastereoisomers are set to 1.0 for one proton of the minor diastereoisomer. HRMS and MS were recorded on a Finnigan MAT 95 Q (EI) mass spectrometer or Thermo Finnigan LTQ FT Ultra (ESI). The melting points were recorded on a Büchi melting point B-540 device and are not corrected. The UV–vis spectra were recorded on a diode array-spectrophotometer system (J&M TIDAS DAD 2062) with 5 mm cuvette length

or a spectrophotometer (JASCO v630) with 1.0 cm cuvette length in DMSO by generating the ylides **1** from their corresponding salts **1H⁺X⁻** by deprotonation with 1.05 equiv. KO^{t}Bu.

Kinetics. The rates of all reactions were determined by UV-vis spectroscopy in DMSO at 20 °C by using stopped-flow spectrophotometer systems (Applied Photophysics SX.18MV-R and Hi-Tech SF-61DX2) as well as diode array-spectrometer systems (J&M TIDAS DAD 2062). The temperature of the solutions during the kinetic studies was maintained at 20 ± 0.2 °C by using circulating bath cryostats. The ylides were generated in DMSO at 20 °C immediately before each kinetic run by mixing DMSO solutions of the salts **1H⁺X⁻** and KO^{t}Bu (typically 1.00:1.05 equivalents). The kinetic runs were initiated by mixing DMSO solutions of the ylides and electrophiles under pseudo first-order conditions with one of the two reaction partners in large excess over the other ($\geq$10 equivalents). Pseudo first-order rate constants k_{obs} (s⁻¹) were obtained by fitting the single exponential $A_t = A_0 \exp(-k_{obs}t) + C$ (mono-exponential decrease) to the observed time-dependent absorbances (average of at least three kinetic runs for each concentration for the stopped-flow method) of the electrophiles or ylides. Second-order rate constants k_2 (L mol⁻¹ s⁻¹) were derived from the slopes of the linear correlations of the obtained k_{obs}-values against the concentrations of the excess reaction partner. Parts of the kinetics experiments have been performed during the master thesis of the author as indicated.[30]

4.5.2 Preparation of the Salts 1H⁺X⁻

General Procedure A for the Preparation of the Ylide Precursors. The salts **1aH⁺X⁻– 1iH⁺X⁻** were prepared from α-alkylhalides (10−16 mmol) and pyridines (10−16 mmol) in THF. The pyridine was dissolved in 5 − 15 mL of THF and the α-alkylhalide was added dropwise. After 30 min to 24h the resulting precipitate was filtered off, washed with 10 − 50 mL Et$_2$O and recrystallized from 5 − 10 mL methanol/toluene (1:1).

The synthesis of all other salts **1H⁺X⁻** listed in Scheme 1 has been reported in ref. [8e].

4-(Dimethylamino)-1-(2-oxo-2-phenylethyl)pyridin-1-ium bromide (1fH⁺Br⁻) was synthesized according to general procedure A from bromoacetophenone (2.0 g, 10 mmol) and 4-(dimethylamino)-pyridine (1.1 g, 9.2 mmol) by stirring for 30 min. **1fH⁺Br⁻** was obtained as
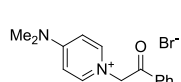
colorless solid (2.9 g, 9.0 mmol, 98%). **Mp** (MeOH:toluene 1:1): 227 °C; Lit: (MeOH) 228 − 229 °C.[29b] **¹H NMR** (400 MHz, DMSO-d_6) δ = 8.23 (d, $J = $ 7.8 Hz, 2 H, 2×C$_{ar}$-H), 8.07 − 8.02 (m, 2 H, 2× C$_{ar}$-H), 7.83 − 7.70 (m, 1 H, C$_{ar}$-H), 7.69 − 7.59 (m, 2 H, 2× C$_{ar}$-H), 7.14 (d, $J = $ 7.9 Hz, 2 H, 2× C$_{ar}$-H), 6.04 (s, 2 H, CH$_2$), 3.24 (s, 6 H, N(CH$_3$)$_2$). **¹³C NMR** (100 MHz, DMSO-d_6) δ = 192.3 (s, CO), 156.0 (s, C$_{ar}$), 143.2 (d, 2×C$_{ar}$-

H), 134.4 (d, C_{ar}-H), 133.8 (s, C_{ar}), 129.0 (d, 2×C_{ar}-H), 128.1 (d, 2×C_{ar}-H), 107.4 (d, 2×C_{ar}-H), 62.4 (t, CH_2), 39.8 (q, $N(CH_3)_2$, superimposed by solvent signal). **HRMS** (ESI+): *m/z* [$C_{15}H_{17}N_2O$]$^+$: calcd. 241.1335, found: 241.1334. DA201
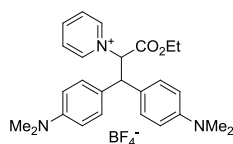
3-Chloro-1-(2-oxo-2-phenylethyl)pyridin-1-ium bromide (1gH$^+$Br$^-$) was synthesized according to general procedure A from bromoacetophenone (3.2 g, 16 mmol) and 3-chloro-pyridine (1.8 g, 16 mmol) by stirring for 24 h. **1gH$^+$Br$^-$** was obtained as colorless solid (4.3 g, 14 mmol, 88%). **Mp** (MeOH:toluene 1:1): 183 °C. **^{1}H NMR** (400 MHz, DMSO-d_6) δ = 9.46 (s, 1 H, C_{ar}-H), 9.09 (d, *J* = 6.1 Hz, 1 H, C_{ar}-H), 8.95 (dd, *J* = 8.5, 1.1 Hz, 1 H, C_{ar}-H), 8.35 (dd, *J* = 8.5, 6.1 Hz, 1 H, C_{ar}-H), 8.15 − 8.01 (m, 2 H, 2×C_{ar}-H), 7.80 (t, *J* = 7.4 Hz, 1 H, C_{ar}-H), 7.67 (t, *J* = 7.7 Hz, 2 H, 2×C_{ar}-H), 6.55 (s, 2 H, CH_2). **^{13}C NMR** (100 MHz, DMSO-d_6) δ = 190.1 (s, CO), 146.1 (d, C_{ar}-H), 145.5 (d, C_{ar}-H), 145.3 (d, C_{ar}-H), 134.8 (d, C_{ar}-H), 133.5 (s, C_{ar}), 133.4 (s, C_{ar}), 129.2 (d, 2×C_{ar}-H), 128.6 (d, C_{ar}-H), 128.3 (d, 2×C_{ar}-H), 66.4 (t, CH_2). **HRMS** (ESI+): *m/z* [$C_{13}H_{11}ClNO$]$^+$: calcd. 232.0524, found: 232.0523. DA277

1-(2-Oxo-2-phenylethyl)quinolin-1-ium bromide (1iH$^+$Br$^-$) was synthesized according to general procedure A from bromoacetophenone (2.6 g, 13 mmol) and quinoline (1.7 g, 13 mmol) by stirring for 24 h. **1iH$^+$Br$^-$** was obtained as light yellow solid (3.5 g, 11 mmol, 85%). **Mp** (MeOH:toluene 1:1): 195 °C; Lit: Mp (EtOH): 196 − 197 °C.[29a] **^{1}H NMR** (400 MHz, DMSO-d_6) δ = 9.56 (d, *J* = 5.8 Hz, 1 H, C_{ar}-H), 9.46 (d, *J* = 8.3 Hz, 1 H, C_{ar}-H), 8.56 (d, *J* = 7.6 Hz, 1 H, C_{ar}-H), 8.46 (d, *J* = 8.9 Hz, 1 H, C_{ar}-H), 8.34 (dd, *J* = 8.3, 5.9 Hz, 1 H, C_{ar}-H), 8.22 (t, *J* = 7.3 Hz, 1 H, C_{ar}-H), 8.17 (d, *J* = 7.3 Hz, 2 H, 2×C_{ar}-H), 8.07 (t, *J* = 7.6 Hz, 1 H, C_{ar}-H), 7.83 (t, *J* = 7.4 Hz, 1 H, C_{ar}-H), 7.70 (t, *J* = 7.7 Hz, 2 H, 2×C_{ar}-H), 7.06 (s, 2 H, CH_2). **^{13}C NMR** (100 MHz, DMSO-d_6) δ = 190.7 (s, CO), 151.0 (d, C_{ar}-H), 148.6 (d, C_{ar}-H), 138.6 (d, C_{ar}-H), 135.9 (s, C_{ar}), 134.8 (d, C_{ar}-H), 133.6 (s, C_{ar}), 130.59 (d, C_{ar}-H), 130.0 (d, C_{ar}-H), 129.4 (s, C_{ar}), 129.0 (d, 2×C_{ar}-H), 128.6 (d, 2×C_{ar}-H), 122.2 (d, C_{ar}-H), 119.1 (d, C_{ar}-H), 63.2 (t, CH_2). **HRMS** (ESI+): *m/z* [$C_{17}H_{14}NO$]$^+$: calcd. 248.1070, found: 248.1069. DA279

4.5.3 Product studies

General Procedure B for the Synthesis of 6-BF$_4$. The benzhydrylium tetrafluoroborate **2a** (147−294 µmol) was dissolved in dichloromethane (1 mL). Acetonitrile (5 mL) and pyridinium salt **1H$^+$X$^−$** (147−294 µmol) were added to the solution and the resulting suspension was titrated at room temperature with a solution of KO^{t}Bu (223−312 µmol) in THF (5 mL) till discoloration of the blue **2a**. The solvent was evaporated and the solid residue was dissolved in 10 mL of acetonitrile. Insoluble precipitates were removed by filtration. The solvent was evaporated, and the crude products were obtained. The crude products were recrystallized from Et$_2$O:acetonitrile (10:1) or pure acetonitrile to give the products **6-BF$_4$**. The products **6-BF$_4$** are very sensitive to moisture and acids, thus they decompose easily.

1-(1,1-Bis(4-(dimethylamino)phenyl)-3-ethoxy-3-oxopropan-2-yl)pyridin-1-ium tetra-fluoroborate (6a-BF$_4$) was synthesized according to general procedure B from **2a** (50.0 mg, 147 µmol), **1aH$^+$Br$^−$** (36.2 mg, 147 µmol), and KO^{t}Bu (25.0 mg, 223 µmol). Recrystallization from acetonitrile gave **6a-BF$_4$** as a green solid (29.4 mg, 58.2 µmol, 39%). **Mp** (Et$_2$O:MeCN 10:1): 148 °C. **^{1}H NMR** (400 MHz, DMSO-d_6) δ = 9.37 (d, J = 5.8 Hz, 2 H, 2×C$_{ar}$-H), 8.58 − 8.51 (m, 1 H, C$_{ar}$-H), 8.12 − 8.06 (m, 2 H, 2×C$_{ar}$-H), 7.30 (d, J = 8.9 Hz, 2 H, 2×C$_{ar}$-H), 7.22 (d, J = 8.9 Hz, 2 H, 2×C$_{ar}$-H), 6.68 (d, 2 H, J = 8.9 Hz, 2×C$_{ar}$-H), 6.65 (d, 1 H, J = 12.3 Hz, CH), 6.42 (d, J = 8.9 Hz, 2 H, 2×C$_{ar}$-H), 4.92 (d, J = 12.3 Hz, 1 H, CH), 3.99 − 3.82 (m, 2 H, CH$_2$), 2.82 (s, 6 H, N(CH$_3$)$_2$), 2.70 (s, 6 H, N(CH$_3$)$_2$), 0.81 (t, J = 7.1 Hz, 3 H, CH$_3$). **^{13}C NMR** (100 MHz, DMSO-d_6) δ = 167.3 (s, CO$_2$), 149.8 (s, C$_{ar}$), 149.1 (s, C$_{ar}$), 147.1 (d, C$_{ar}$-H), 145.0 (d, 2×C$_{ar}$-H), 128.6 (d, 2×C$_{ar}$-H), 128.2 (d, 2×C$_{ar}$-H), 127.9 (d, 2×C$_{ar}$-H), 126.6 (s, C$_{ar}$), 125.8 (s, C$_{ar}$), 112.4 (d, 2×C$_{ar}$-H), 112.2 (d, 2×C$_{ar}$-H), 73.0 (d, CH), 62.2 (t, CH$_2$), 52.3 (d, CH), 40.2 (q, N(CH$_3$)$_2$, superimposed by solvent signal), 39.8 (q, N(CH$_3$)$_2$, superimposed by solvent signal), 13.3 (q, CH$_3$). **HRMS** (ESI+): m/z [C$_{26}$H$_{32}$N$_3$O$_2$]$^+$: calcd. 418.2489, found 418.2487. DA162

1-(1-(Diethylamino)-3,3-bis(4-(dimethylamino)phenyl)-1-oxopropan-2-yl)pyridin-1-ium tetrafluoroborate (6b-BF$_4$) was synthesized according to general procedure B from **2a** (100 mg, 294 µmol), **1bH$^+$Br$^−$** (80.3 mg, 294 µmol), and KO^{t}Bu (35.0 mg, 312 µmol). The crude product was recrystallized from acetonitrile/Et$_2$O to furnish **6b-BF$_4$** as a red solid (154 mg, 253 µmol, 98%). **Mp** (Et$_2$O:MeCN 10:1): 155 °C. **^{1}H NMR** (400 MHz, DMSO-d_6) δ = 9.52 − 9.47 (m, 2 H, 2×C$_{ar}$-H), 8.54 − 8.48 (m, 1 H, C$_{ar}$-H), 8.10 − 8.03 (m, 2 H, 2× C$_{ar}$-H), 7.39 (d, J = 8.8 Hz, 2 H, 2×C$_{ar}$-H), 7.28 (d, J =
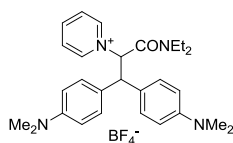
8.8 Hz, 2 H, 2×C_{ar}-H), 6.80 (d, J = 11.7 Hz, 1 H, CH), 6.66 (d, J = 8.9 Hz, 2 H, 2×C_{ar}-H), 6.46 (d, J = 8.9 Hz, 2 H, 2×C_{ar}-H), 4.94 (d, J = 11.6 Hz, 1 H, CH), 3.66 – 3.54 (m, 1 H, C*H*H^a), 3.42 – 3.27 (m, 1 H, C*H*H^b, superimposed by solvent signal), 3.20 – 3.12 (m, 1 H, CH*H*^{a}), 2.97 – 2.89 (m, 1 H, CH*H*^{b}), 2.82 (s, 6 H, N(CH₃)₂), 2.74 (s, 6 H, N(CH₃)₂), 0.88 (t, J = 7.0 Hz, 3 H, CH₃), 0.75 (t, J = 7.0 Hz, 3 H, CH₃). **¹³C NMR** (100 MHz, DMSO-d_6) δ = 164.9 (s, CON), 149.8 (s, C_{ar}), 149.0 (s, C_{ar}), 146.7 (d, C_{ar}-H), 144.7 (d, 2×C_{ar}-H), 129.0 (d, 2×C_{ar}-H), 128.9 (d, 2×C_{ar}-H), 127.8 (d, 2×C_{ar}-H), 126.1 (s, C_{ar}), 125.6 (s, C_{ar}), 112.3 (d, 2×C_{ar}-H), 112.0 (d, 2×C_{ar}-H), 68.8 (d, CH), 53.2 (d, CH), 41.7 (t, CH₂), 40.4 (t, CH₂, superimposed by solvent signal), 40.1 (q, N(CH₃)₂, superimposed by solvent signal), 39.9 (q, N(CH₃)₂, superimposed by solvent signal), 14.5 (q, CH₃), 12.0 (q, CH₃). **HRMS** (ESI+): m/z [$C_{28}H_{37}N_4O$]⁺: calcd. 445.2962, found 445.2961. DA199

1-(1-Cyano-2,2-bis(4-(dimethylamino)phenyl)ethyl)pyridin-1-ium   tetrafluoroborate (6c-BF₄) was synthesized according to general procedure B from **2a** (50.0 mg, 147 μmol), **1cH⁺Br⁻** (29.3 mg, 147 μmol), and KO^{t}Bu (25.0 mg, 223 μmol). The crude product was recrystallized from acetonitrile/Et₂O to give **6c-BF₄** as a yellow solid (59.0 mg, 129 μmol, 88%). **Mp** (Et₂O:MeCN 10:1): 211°C (decomp.). **¹H NMR** (400 MHz, DMSO-d_6) δ = 9.25 (d, J = 6.0 Hz, 2 H, 2×C_{ar}-H), 8.62 (t, J = 7.7 Hz, 1 H, C_{ar}-H), 8.17 (t, J = 7.0 Hz, 2 H, 2×C_{ar}-H), 7.39 (d, J = 8.6 Hz, 2 H, 2×C_{ar}-H), 7.25 (d, J = 11.7 Hz, 1 H, CH), 6.99 (d, J = 8.7 Hz, 2 H, 2×C_{ar}-H), 6.75 (d, J = 8.7 Hz, 2 H, 2×C_{ar}-H), 6.44 (d, J = 8.5 Hz, 2 H, 2×C_{ar}-H), 5.00 (d, J = 11.7 Hz, 1 H, CH), 2.88 (s, 6 H, N(CH₃)₂), 2.73 (s, 6 H, N(CH₃)₂). **¹³C NMR** (100 MHz, DMSO-d_6) δ = 150.4 (s, C_{ar}), 149.9 (s, C_{ar}), 148.6 (d, C_{ar}-H), 144.7 (d, 2×C_{ar}-H), 129.2 (d, 2×C_{ar}-H), 129.0 (d, 2×C_{ar}-H), 128.5 (d, 2×C_{ar}-H), 125.5 (s, C_{ar}), 124.1 (s, C_{ar}), 115.8 (s, CN), 113.0 (d, 2×C_{ar}-H), 112.6 (d, 2×C_{ar}-H), 63.1 (d, CH), 53.8 (d, CH), 40.2 (q, N(CH₃)₂, superimposed by solvent signal), 40.0 (q, N(CH₃)₂, superimposed by solvent signal). **HRMS** (ESI+): m/z [$C_{24}H_{27}N_4$]⁺: calcd. 371.2230, found 371.2229. DA166
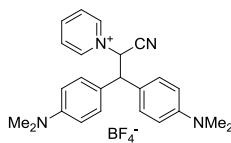
1-(1,1-Bis(4-(dimethylamino)phenyl)-3-oxobutan-2-yl)pyridin-1-ium tetrafluoroborate (6d-BF₄) was synthesized according to general procedure B from **2a** (100 mg, 294 μmol), **1dH⁺Cl⁻** (50.5 mg, 294 μmol) and KO^{t}Bu (34.6 mg, 308 μmol). The crude product was recrystallized from acetonitrile/Et₂O to give **6d-BF₄** as a green solid (96.3 mg, 203 μmol, 69%). **Mp** (Et₂O:MeCN): 197 °C (decomp.). **¹H NMR** (400 MHz, DMSO-d_6) δ = 9.27 (d, J = 6.0 Hz, 2 H, 2×C_{ar}-H), 8.46 (t, J = 7.8 Hz, 1 H, C_{ar}-H), 8.13 – 7.95 (m, 2 H, 2×C_{ar}-H), 7.39 (d, J = 8.5 Hz, 2 H, 2×C_{ar}-H),
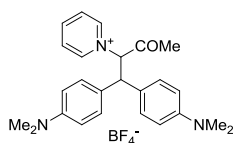
7.25 (d, J = 8.2 Hz, 2 H, 2×C_{ar}-H), 7.02 (d, J = 12.3 Hz, 1 H, CH), 6.71 (d, J = 8.8 Hz, 2 H, 2×C_{ar}-H), 6.42 (d, J = 8.8 Hz, 2 H, 2×C_{ar}-H), 4.82 (d, J = 12.3 Hz, 1 H, CH), 2.84 (s, 6 H, N(CH$_3$)$_2$), 2.69 (s, 6 H, N(CH$_3$)$_2$), 1.88 (s, 3 H, CH$_3$). **^{13}C NMR** (100 MHz, DMSO-d_6) δ = 202.1 (s, CO), 149.7 (s, C_{ar}), 149.0 (s, C_{ar}), 146.4 (d, C_{ar}-H), 145.2 (d, 2×C_{ar}-H), 128.7 (d, 2×C_{ar}-H), 128.1 (d, 2×C_{ar}-H), 127.3 (d, 2×C_{ar}-H), 126.5 (s, 2×C_{ar}), 112.7 (d, 2×C_{ar}-H), 112.2 (d, 2×C_{ar}-H), 77.3 (d, CH), 51.8 (d, CH), 40.0 (q, N(CH$_3$)$_2$, superimposed by solvent signal), 39.8 (q, N(CH$_3$)$_2$, superimposed by solvent signal), 31.0 (q, CH$_3$). **HRMS** (ESI+): m/z [C$_{25}$H$_{30}$N$_3$O]$^+$: calcd. 388.2383, found. 388.2383. DA172

1-(1,1-Bis(4-(dimethylamino)phenyl)-3-oxo-3-phenylpropan-2-yl)pyridin-1-ium tetra-fluoroborate (6e-BF$_4$). The pyridinium salt **1eH$^+$Br$^-$** (81.8 mg, 294 μmol) was added to aq. KOH (25 mL, 0.1 M) and the solution was stirred for 5 min. The resulting yellow ylide **1e** was extracted with 25 mL of chloroform. The benzhydrylium tetrafluoroborate **2a** (100 mg, 294 μmol) in CH$_2$Cl$_2$ (10 mL) was added to the solution of the ylide **1e** at room temperature, and immediate discoloration of **2a** was observed. The solvent was evaporated and the crude product was recrystallized from acetonitrile/Et$_2$O to give **6e-BF$_4$** as a green solid with a metallic luster (158 mg, 294 μmol, quant.). **Mp** (Et$_2$O:MeCN 10:1): 135 °C (decomp.). **^{1}H NMR** (400 MHz, DMSO-d_6) δ = 9.41 (d, J = 5.8 Hz, 2 H, 2×C_{ar}-H), 8.51 − 8.44 (m, 1 H, C_{ar}-H), 8.10 −

8.00 (m, 4 H, 4×C_{ar}-H), 7.61 − 7.55 (m, 1 H, C_{ar}-H), 7.51 (d, J = 12.0 Hz, 1 H, CH), 7.43 (t, J = 7.8 Hz, 2 H, 2×C_{ar}-H), 7.32 (d, J = 8.8 Hz, 2 H, 2×C_{ar}-H), 7.15 (d, J = 8.8 Hz, 2 H, 2×C_{ar}-H), 6.47 (d, J = 8.8 Hz, 2 H, 2×C_{ar}-H), 6.43 (d, J = 8.8 Hz, 2 H, 2×C_{ar}-H), 4.99 (d, J = 11.9 Hz, 1 H, CH), 2.74 (s, 6 H, N(CH$_3$)$_2$), 2.69 (s, 6 H, N(CH$_3$)$_2$). **^{13}C NMR** (100 MHz, DMSO-d_6) δ = 194.0 (s, CO), 149.5 (s, C_{ar}), 149.1 (s, C_{ar}), 146.7 (d, C_{ar}-H), 145.0 (d, 2×C_{ar}-H), 134.8 (s, C_{ar}), 134.5 (d, C_{ar}-H), 129.3 (d, 2×C_{ar}-H), 128.8 (d, 2×C_{ar}-H), 128.6 (d, 2×C_{ar}-H), 128.4 (d, 2×C_{ar}-H), 127.9 (d, 2×C_{ar}-H), 126.1 (s, C_{ar}), 125.7 (s, C_{ar}), 112.4 (d, 2×C_{ar}-H), 112.2 (d, 2×C_{ar}-H), 72.0 (d, CH), 52.9 (d, CH), 40.0 (q, N(CH$_3$)$_2$, superimposed by solvent signal), 39.9 (q, N(CH$_3$)$_2$, superimposed by solvent signal). **HRMS** (ESI+): m/z [C$_{30}$H$_{32}$N$_3$O]$^+$: calcd. 450.2540, found 450.2541. DA123
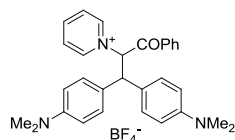
Table 4.11. Crystallographic data of 6e-BF₄·CH₂Cl₂.

net formula	$C_{30.50}H_{33}BClF_4N_3O$
M_r/g mol^{-1}	579.865
crystal size/mm	$0.17 \times 0.11 \times 0.06$
T/K	200(2)
radiation	MoKα
diffractometer	'KappaCCD'
crystal system	monoclinic
space group	$P2_1/c$
a/Å	10.9080(2)
b/Å	18.0229(3)
c/Å	30.2720(5)
α/°	90
β/°	98.2496(9)
γ/°	90
V/Å³	5889.71(17)
Z	8
calcd. density/g cm^{-3}	1.30791(4)
μ/mm^{-1}	0.184
absorption correction	none
refls. measured	37065
R_{int}	0.0582
mean σ(I)/I	0.0606
θ range	3.18–25.33
observed refls.	5645
x, y (weighting scheme)	0.1520, 4.0092
hydrogen refinement	constr
refls in refinement	10732
parameters	740
restraints	8
$R(F_{obs})$	0.0897
$R_w(F^2)$	0.3056
S	1.045
shift/error$_{max}$	0.001
max electron density/e Å^{-3}	1.228
min electron density/e Å^{-3}	−0.716

All B-F distances refined to 1.34 Å.
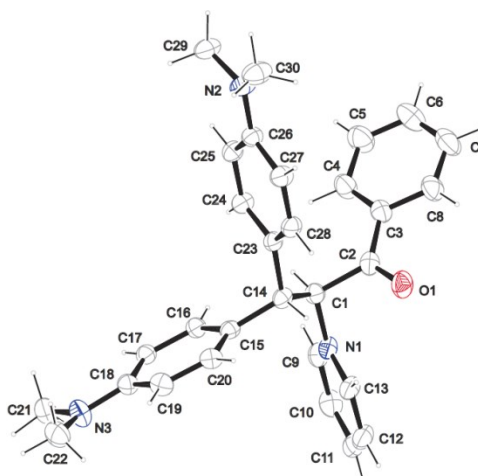
1-(1,1-Bis(4-(dimethylamino)phenyl)-3-oxo-3-phenylpropan-2-yl)-4-(dimethylamino) pyridin-1-ium tetrafluoroborate (6f-BF₄) was synthesized according to general procedure B from 2a (100 mg, 294 μmol), 1fH⁺Br⁻ (94.4 mg, 294 μmol), and KO^{t}Bu (34.6 mg, 308 μmol). The crude product was recrystallized from acetonitrile/Et₂O to give 6f-BF₄ as orange solid (170 mg, 293 μmol, quant.). The product decomposed to large degree in DMSO-d_6 at room temperature within a day. Mp. (Et₂O:MeCN): 114 °C. ¹H NMR (400 MHz, DMSO-d_6) δ = 8.60 (d, J = 7.9 Hz, 2 H, 2×C$_{ar}$-H), 8.19 − 8.13 (m, 2 H, 2×C$_{ar}$-H), 7.68 − 7.57 (m, 1 H, C$_{ar}$-H,

superimposed by decomposition product), 7.50–7.42 (m, 4 H, 4×C_{ar}-H), 7.24 (d, J = 8.8 Hz, 2 H, 2×C_{ar}-H), 7.17 (d, J = 12.0 Hz, 1 H, CH), 6.90 (d, J = 7.9 Hz, 2 H, 2×C_{ar}-H), 6.56 – 6.49 (m, 2 H, 2×C_{ar}-H), 6.47 (d, J = 8.9 Hz, 2 H, 2×C_{ar}-H), 4.96 (d, J = 12.0 Hz, 1 H, CH), 3.07 (s, 6 H, N(CH$_3$)$_2$), 2.78 (s, 6 H, N(CH$_3$)$_2$), 2.71 (s, 6 H, N(CH$_3$)$_2$). ^{13}C NMR (100 MHz, DMSO-d_6) δ = 195.1 (s, CO), 155.7 (s, C_{ar}), 149.2 (s, C_{ar}), 149.0 (s, C_{ar}), 141.1 (br d, 2×C_{ar}-H), 134.5 (d, C_{ar}-H), 134.4 (s, C_{ar}), 129.1 (d, 2×C_{ar}-H), 129.0 (d, 2×C_{ar}-H), 128.9 (d, 2×C_{ar}-H), 128.7 (d, 2×C_{ar}-H superimposed by decomposition product), 127.2 (s, C_{ar}), 127.2 (s, C_{ar}), 112.4 (d, 2×C_{ar}-H), 112.2 (d, 2×C_{ar}-H, superimposed by decomposition product), 107.7 (d, 2×C_{ar}-H), 67.7 (d, CH), 50.9 (d, CH), 40.0 (q, N(CH$_3$)$_2$, superimposed by solvent signal), 39.9 (q, N(CH$_3$)$_2$, superimposed by solvent signal), 39.8 (q, N(CH$_3$)$_2$, superimposed by solvent signal). HRMS (ESI+): m/z [C$_{32}$H$_{37}$N$_4$O]$^+$: calcd. 493.2962, found 493.2959. DA284
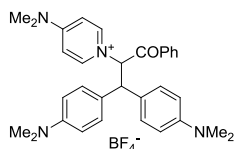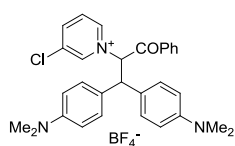
1-(1,1-Bis(4-(dimethylamino)phenyl)-3-oxo-3-phenylpropan-2-yl)-3-chloropyridin-1-ium tetrafluoroborate (6g-BF$_4$) was synthesized according to general procedure B from 2a (100 mg, 294 µmol), 1gH$^+$Br$^-$ (91.9 mg, 294 µmol), and KO^{t}Bu (34.6 mg, 308 µmol) to give 183 mg (320 µmol, quant) of the dark green crude product. A recrystallization of 6g-BF$_4$ from acetonitrile/Et$_2$O failed due to decomposition of 6g-BF$_4$. Therefore the crude material was used for spectroscopic characterization. ^{1}H NMR (400 MHz, DMSO-d_6) δ = 9.86 (s, 1 H, C_{ar}-H), 9.55 (d, J = 6.2 Hz, 1 H, C_{ar}-H), 8.70 (d, J = 9.5 Hz, 1 H, C_{ar}-H), 8.15 (dd, J = 8.5, 6.2 Hz, 1 H, C_{ar}-H), 8.05 (dd, J = 8.4, 1.1 Hz, 2 H, 2×C_{ar}-H), 7.64 – 7.55 (m, 2 H, CH, C_{ar}-H), 7.46 – 7.39 (m, 4 H, 4×C_{ar}-H), 7.15 (d, J = 8.7 Hz, 2 H, 2×C_{ar}-H), 6.52 (br, d, J = 8.0 Hz, 2 H, 2×C_{ar}-H), 6.43 (br d, J = 7.9 Hz, 2 H, 2×C_{ar}-H), 5.08 (d, J = 11.9 Hz, 1 H, CH), 2.78 (s, 6 H, N(CH$_3$)$_2$), 2.71 (s, 6 H, N(CH$_3$)$_2$). ^{13}C NMR (100 MHz, DMSO-d_6) δ = 193.5 (s, CO), 149.3 (br s, C_{ar}), 149.0 (br s, C_{ar}), 146.2 (d, C_{ar}-H), 144.5 (d, C_{ar}-H), 144.4 (d, C_{ar}-H), 134.9 (d, C_{ar}-H), 134.3 (s, C_{ar}), 133.5 (s, C_{ar}), 129.4 (d, 2×C_{ar}-H), 128.9 (d, 2×C_{ar}-H), 128.6 (s, C_{ar}), 128.5 (s, C_{ar}), 128.5 (d, 2×C_{ar}-H), 128.4 (d, 2×C_{ar}-H), 128.2 (d, C_{ar}-H), 112.5 (br d, 2×C_{ar}-H), 112.3 (br d, 2×C_{ar}-H), 72.4 (d, CH), 53.0 (d, CH), 40.0 (q, N(CH$_3$)$_2$, superimposed by solvent signal), 39.8 (q, N(CH$_3$)$_2$, superimposed by solvent signal). HRMS (ESI+): m/z [C$_{30}$H$_{31}$ClN$_3$O]$^+$: calcd. 484.2150, found 484.2148. DA285

2-(1,1-Bis(4-(dimethylamino)phenyl)-3-oxo-3-phenylpropan-2-yl)isoquinolin-2-ium

tetrafluoroborate (6h-BF₄) was synthesized according to general procedure B from 2a (100 mg, 294 μmol), 1hH⁺Br⁻ (96.5 mg, 294 μmol), and KO^{t}Bu (34.6 mg, 308 μmol). The crude product was recrystallized from acetonitrile/Et₂O to give 6h-BF₄ as dark green crystals (98.3 mg, 167 μmol, 57%). Mp. (Et₂O:MeCN): 180 °C. ^{1}H NMR (400 MHz, DMSO-d_6) δ = 10.62 (s, 1 H, C$_{ar}$-H), 9.21 (dd, J = 7.0, 1.2 Hz, 1 H, C$_{ar}$-H), 8.56 (d, J = 8.4 Hz, 1 H, C$_{ar}$-H), 8.52 (d, J = 7.0 Hz, 1 H, C$_{ar}$-H), 8.28 – 8.19 (m, 2 H, 15-H, C$_{ar}$-H), 8.17 (dd, J = 8.5, 1.2 Hz, 2 H, 2×C$_{ar}$-H), 8.05 (ddd, J = 8.2, 6.0, 2.2 Hz, 1 H, C$_{ar}$-H), 7.77 (d, J = 11.9 Hz, 1 H, CH), 7.64 – 7.57 (m, 1 H, C$_{ar}$-H), 7.50 – 7.42 (m, 4 H, 4×C$_{ar}$-H), 7.26 (d, J = 8.9 Hz, 2 H, 2×C$_{ar}$-H), 6.48 (d, J = 8.9 Hz, 2 H, 2×C$_{ar}$-H), 6.43 (d, J = 9.0 Hz, 2 H, 2×C$_{ar}$-H), 5.19 (d, J = 11.9 Hz, 1 H, CH), 2.71 (s, 6 H, N(CH₃)₂), 2.67 (s, 6 H, N(CH₃)₂). ^{13}C NMR (100 MHz, DMSO-d_6) δ = 194.0 (s, CO), 150.2 (d, C$_{ar}$-H), 149.5 (s, C$_{ar}$), 149.0 (s, C$_{ar}$), 137.6 (d, C$_{ar}$-H), 137.1 (s, C$_{ar}$), 135.1 (br d, C$_{ar}$-H), 134.7 (d, C$_{ar}$-H), 134.5 (s, C$_{ar}$), 131.4 (d, C$_{ar}$-H), 130.7 (d, C$_{ar}$-H), 129.4 (d, 2×C$_{ar}$-H), 128.8 (d, 2×C$_{ar}$-H), 128.6 (d, 2×C$_{ar}$-H), 128.5 (d, 2×C$_{ar}$-H), 127.2 (s, C$_{ar}$), 127.0 (d, C$_{ar}$-H), 126.2 (s, C$_{ar}$), 125.8 (s, C$_{ar}$), 125.4 (d, C$_{ar}$-H), 112.4 (d, 2×C$_{ar}$-H), 112.1 (d, 2×C$_{ar}$-H), 71.7 (d, CH), 53.1 (d, CH), 40.0 (q, N(CH₃)₂, superimposed by solvent signal), 39.8 (q, N(CH₃)₂, superimposed by solvent signal). HRMS (ESI+): m/z [C₃₄H₃₄N₃O]⁺: calcd. 500.2696, found 500.2701. DA478
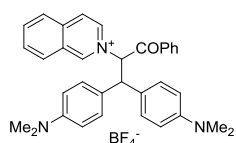
1-(1,1-Bis(4-(dimethylamino)phenyl)-3-oxo-3-phenylpropan-2-yl)quinolin-1-ium

tetra-fluoroborate (6i-BF₄) was synthesized according to general procedure B from 2a (100 mg, 294 μmol), 1iH⁺Br⁻ (96.5 mg, 294 μmol), and KO^{t}Bu (34.6 mg, 308 μmol). The crude product was recrystallized from acetonitrile/Et₂O to give 6i-BF₄ as brown solid (109 mg, 186 μmol, 63%). ^{1}H NMR (300 MHz, DMSO-d_6) δ = 10.07 (d, J = 5.4 Hz, 1 H, C$_{ar}$-H), 9.27 (t, J = 9.6 Hz, 2 H, 2×C$_{ar}$-H), 8.42 (d, J = 8.2 Hz, 1 H, C$_{ar}$-H), 8.32 (ddd, J = 8.7, 7.0, 1.4 Hz, 1 H, C$_{ar}$-H), 8.22 (dd, J = 8.2, 6.2 Hz, 1 H, C$_{ar}$-H), 8.16–8.07 (m, 3 H, 2×C$_{ar}$-H, CH), 8.05 – 7.97 (m, 1 H, C$_{ar}$-H), 7.60 (t, J = 7.3 Hz, 1 H, C$_{ar}$-H), 7.44 (d, J = 7.9 Hz, 2 H, 2×C$_{ar}$-H), 7.40 – 7.35 (m, 4 H, 4×C$_{ar}$-H), 6.49 (d, J = 8.8 Hz, 2 H, 2×C$_{ar}$-H), 6.40 (d, J = 8.8 Hz, 2 H, 2×C$_{ar}$-H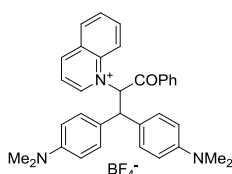), 5.28 (d, J = 11.5 Hz, 1 H, CH), 2.74 (s, 6 H, N(CH₃)₂), 2.69 (s, 6 H, N(CH₃)₂). ^{13}C NMR (75 MHz, DMSO-d_6) δ = 193.6 (s, CO), 149.7 (d, C$_{ar}$-H) 149.6 (s, C$_{ar}$), 149.2 (s, C$_{ar}$), 148.8 (br d, C$_{ar}$-H), 138.0 (s, C$_{ar}$), 136.5 (d, C$_{ar}$-H), 134.6 (d, C$_{ar}$-H), 134.3 (s, C$_{ar}$), 131.3 (d, C$_{ar}$-H), 129.9 (br, d, C$_{ar}$-H), 129.5 (d, 2×C$_{ar}$-H), 129.4 (s, C$_{ar}$), 129.3 (d, 2×C$_{ar}$-H), 128.7 (d, 2×C$_{ar}$-H), 128.3 (d, 2×C$_{ar}$-H), 125.9 (s, C$_{ar}$), 125.3 (s, C$_{ar}$), 121.7 (d, C$_{ar}$-H), 118.0 (d, C$_{ar}$-H), 112.3 (d, 2×C$_{ar}$-H), 112.1 (d,

2×C_{ar}-H), 66.3 (d, CH), 53.2 (d, CH), 40.0 (q, N(CH$_3$)$_2$, superimposed by solvent signal), 39.8 (q, N(CH$_3$)$_2$, superimposed by solvent signal). HRMS (ESI+): m/z [C$_{34}$H$_{34}$N$_3$O]$^+$: calcd. 500.2696, found 500.2693. DA286

4.5.4 Synthesis of the Michael Adducts 7

General Procedure C for the Synthesis of Michael Adducts 7. The quinone methide **3b** (1 equiv.) and the pyridinium salt (**1H$^+$X$^-$**, 1 equiv.) were mixed in dry acetonitrile (0.03 M). Triethylamine (2.2 equiv.) was added to the suspension and the mixture was stirred at room temperature till all **1H$^+$X$^-$** was dissolved (~15 min). The solvent was evaporated and the products **7** were obtained as colorless solids. In some cases the crude products **7** were dissolved in CH$_2$Cl$_2$, washed once with water and/or 2M HCl, and dried over Na$_2$SO$_4$. After removal of the solvent the products **7** were obtained.

Annotation for the NMR-analysis: # corresponds to signals of the major diastereoisomer, * to signals of the minor diastereoisomer. Integrals for mixtures of diastereoisomers are set to 1.0 for one proton of the minor diastereoisomer.

1-(1-(3,5-Di-*tert*-butyl-4-hydroxyphenyl)-3-ethoxy-3-oxo-1-(*p*-tolyl)propan-2-yl)pyridin-1-ium bromide (7a) was synthesized according to general procedure C from **3b** (50 mg, 0.16 mmol), **1aH$^+$Br$^-$** (40 mg, 0.16 mmol), and NEt$_3$ (50 µl, 0.36 mmol). The crude product was dissolved in CH$_2$Cl$_2$ (20 mL), and washed with water (1×20 mL). The solvent was evaporated and **7a** was obtained as colorless solid (82 mg, 0.15 mmol, 94%, *dr* 1:2). **^{1}H NMR** (300 MHz, CDCl$_3$) δ = 9.96# (d, J = 5.6 Hz, 4 H, 2×C_{ar}-H), 9.86* (d, J = 5.7 Hz, 2 H, 2×C_{ar}-H), 8.48 − 8.38#,* (m, 3 H, 2×C_{ar}-H), 8.03 − 7.96# (m, 4 H, 2×C_{ar}-H), 7.96 − 7.87* (m, 2 H, 2×C_{ar}-H), 7.63* (d, J = 8.2 Hz, 2 H, 2×C_{ar}-H), 7.50# (d, J = 8.1 Hz, 4 H, 2×C_{ar}-H), 7.45* (d, J = 12.0 Hz, 1 H; CH), 7.36# (s, 4 H, 2×C_{ar}-H), 7.31# (d, J = 12.2 Hz, 2 H, CH), 7.14* (d, J = 7.8 Hz, 2 H, 2×C_{ar}-H), 7.02* (s, 2 H, 2×C_{ar}-H), 6.97# (d, J = 7.9 Hz, 4 H, 2×C_{ar}-H), 5.21# (s, 2 H, OH), 5.09# (s, 1 H, OH), 4.64 − 4.52#,* (m, 3 H, 2×CH), 4.15 − 3.79#,* (m, 6 H, 2×CH$_2$), 2.27* (s, 3 H, CH$_3$), 2.12# (s, 6 H, CH$_3$), 1.42# (s, 36 H, 2×C(CH$_3$)$_3$), 1.28* (s, 18 H, 2×C(CH$_3$)$_3$), 0.88* (t, J = 7.1 Hz, 3 H, CH$_3$), 0.81# (t, J = 7.1 Hz, 6 H, CH$_3$). **^{13}C NMR** (75 MHz, CDCl$_3$) δ = 168.2# (s, CO$_2$), 167.8* (s, CO$_2$), 153.8# (s, C_{ar}), 153.4* (s, C_{ar}), 146.4# (d, C_{ar}-H), 146.0* (d, C_{ar}-H), 145.6* (d, 2×C_{ar}-H), 145.3# (d, 2×C_{ar}-H), 137.6* (s, C_{ar}), 137.6# (s, C_{ar}), 136.8* (s, 2×C_{ar}), 136.6# (s, 2×C_{ar}), 134.9* (s, C_{ar}), 134.2# (s, C_{ar}), 130.2# (d, 2×C_{ar}-H), 129.7* (d, 2×C_{ar}-H), 128.7* (d, 2×C_{ar}-H), 128.0# (d, 2×C_{ar}-H), 128.0# (d, 2×C_{ar}-H), 127.8# (s, C_{ar}), 127.8* (s, C_{ar}), 127.6* (d, 2×C_{ar}-H), 125.3# (d, 2×C_{ar}-H), 124.7* (d,
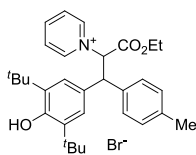
$2\times C_{ar}$-H), 73.3* (d, CH), 73.2$^\#$ (d, CH), 63.3* (t, CH_2), 63.1$^\#$ (t, CH_2), 57.7$^\#$ (d, CH), 57.5* (d, CH), 34.6$^\#$ (s, $2\times C(CH_3)_3$), 34.5* (s, $2\times C(CH_3)_3$), 30.5$^\#$ (q, $2\times C(CH_3)_3$), 30.4$^\#$ (q, $2\times C(CH_3)_3$), 21.1* (q, CH_3), 21.0$^\#$ (q, CH_3), 13.5* (q, CH_3), 13.4$^\#$ (q, CH_3). **HRMS** (ESI+): *m/z* [$C_{31}H_{40}NO_3$]$^+$: calcd. 474.3003, found 474.3006. DA601

1-(1-(3,5-Di-*tert*-butyl-4-hydroxyphenyl)-3-(diethylamino)-3-oxo-1-(*p*-tolyl)propan-2-yl)pyridin-1-ium bromide (7b) was synthesized according to general procedure C from **3b** (50 mg, 0.16 mmol), **1bH⁺Br⁻** (44 mg, 0.16 mmol), and NEt₃ (50 µl, 0.36 mmol). The crude product was dissolved in CH_2Cl_2 (20 mL), and washed with water (1×20 mL). The organic layer was dried over Na_2SO_4 and the solvent was evaporated. **7b** was obtained as colorless solid (92 mg, 0.16 mmol, quant., *dr* 1:2). **¹H NMR** (400 MHz, CDCl₃) δ = 10.19* (d, *J* = 6.1 Hz, 2 H, $2\times C_{ar}$-H), 10.12$^\#$ (d, *J* = 5.8 Hz, 4 H, $2\times C_{ar}$-H), 8.32 – 8.22$^{\#,*}$ (m, 3 H, $2\times C_{ar}$-H), 7.80 – 7.70$^{\#,*}$ (m, 6 H, $4\times C_{ar}$-H), 7.67* (d, *J* = 8.1 Hz, 2 H, $2\times C_{ar}$-H), 7.60$^\#$ (d, *J* = 8.1 Hz, 4 H, $2\times C_{ar}$-H), 7.51* (d, *J* = 11.5 Hz, 1 H, CH), 7.41$^\#$ (d, *J* = 11.3 Hz, 2 H, CH), 7.35* (s, 2 H, $2\times C_{ar}$-H), 7.13$^\#$ (d, *J* = 7.9 Hz, 4 H, $2\times C_{ar}$-H), 7.04$^\#$ (s, 4 H, $2\times C_{ar}$-H), 6.95* (d, *J* = 7.8 Hz, 2 H, $2\times C_{ar}$-H), 5.16* (s, 1 H, OH), 5.06$^\#$ (s, 2 H, OH), 4.76* (d, *J* = 11.6 Hz, 1 H, CH), 4.71$^\#$ (d, *J* = 11.3 Hz, 2 H, CH), 3.90$^\#$ (dq, *J* = 14.2, 7.0, Hz, 2 H, C*H*H^a), 3.84 – 3.72* (m, 1 H, C*H*H^a), 3.64 – 3.44$^{\#,*}$ (m, 3 H, $2\times$C*H*H^b), 3.36$^\#$ (dq, *J* = 14.2 Hz, 7.2, 2 H, CH*H*^{a}), 3.31 – 3.17* (m, 1 H, CH*H*^{a}), 3.13 – 3.94$^{\#,*}$ (m, 3 H, $2\times$CH*H*^{b}), 2.25$^\#$ (s, 6 H, CH_3), 2.09* (s, 3 H, CH_3), 1.38* (s, 18 H, $2\times C(CH_3)_3$), 1.27$^\#$ (s, 36 H, $2\times C(CH_3)_3$), 0.88* (t, *J* = 7.0 Hz, 6H, CH_3), 0.79$^\#$ (td, *J* = 7.1, 4.2 Hz, 12 H, CH_3). **¹³C NMR** (100 MHz, CDCl₃) δ = 165.8* (s, CO), 165.4$^\#$ (s, CO), 153.7* (s, C_{ar}), 153.2$^\#$ (s, C_{ar}), 145.6$^\#$ (d, $2\times C_{ar}$-H), 145.5* (d, $2\times C_{ar}$-H), 145.1$^{\#,*}$ (d, $2\times C_{ar}$-H), 137.7$^\#$ (s, C_{ar}), 137.1* (s, C_{ar}), 136.5$^\#$ (s, $2\times C_{ar}$), 136.5* (s, $2\times C_{ar}$), 134.8$^\#$ (s, C_{ar}), 134.3* (s, C_{ar}), 129.9* (d, $2\times C_{ar}$-H), 129.8$^\#$ (d, $2\times C_{ar}$-H), 129.0$^\#$ (d, $2\times C_{ar}$-H), 128.8* (d, $2\times C_{ar}$-H), 127.7* (s, C_{ar}), 127.5$^\#$ (s, C_{ar}), 127.1* (d, $2\times C_{ar}$-H), 126.8$^\#$ (d, $2\times C_{ar}$-H), 125.9* (d, $2\times C_{ar}$-H), 125.4$^\#$ (d, $2\times C_{ar}$-H), 69.3$^\#$ (d, CH), 68.9* (d, CH), 58.1$^\#$ (d, CH), 57.6* (d, CH), 43.7* (t, CH_2), 43.6$^\#$ (t, CH_2), 41.4* (t, CH_2), 41.3$^\#$ (t, CH_2), 34.6* (s, $2\times C(CH_3)_3$), 34.5$^\#$ (s, $2\times C(CH_3)_3$), 30.5$^\#$ (q, $2\times C(CH_3)_3$), 30.4* (q, $2\times C(CH_3)_3$), 21.1$^\#$ (q, CH_3), 21.0* (q, CH_3), 14.9$^\#$ (q, CH_3), 14.8* (q, CH_3), 12.5* (q, CH_3), 12.1$^\#$ (q, CH_3). **HRMS** (ESI+): *m/z* [$C_{33}H_{45}N_2O_2$]$^+$: calcd. 501.3476, found 501.3477. DA606
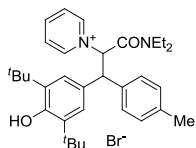
1-(1-Cyano-2-(3,5-di-*tert*-butyl-4-hydroxyphenyl)-2-(*p*-tolyl)ethyl)pyridin-1-ium bromide (7c) was synthesized according to general procedure C from **3b** (50 mg, 0.16 mmol), **1cH⁺Br⁻** (40 mg, 0.16 mmol), and NEt₃ (50 μl, 0.36 mmol). The crude product was dissolved in CH₂Cl₂ (20 mL), and washed with water (1×20 mL). The solvent was evaporated and **7c** was obtained as beige solid (81 mg, 0.16 mmol, quant., *dr* 1:2). **¹H NMR** (400 MHz, DMSO-d_6) δ = 9.36* (d, J = 5.7 Hz, 2 H, 2×C_{ar}-H), 9.23# (d, J = 5.8 Hz, 4 H, 2×C_{ar}-H), 8.69 – 8.64#,* (m, 3 H, 2×C_{ar}-H), 8.23 – 8.13#,* (m, 6 H, 4×C_{ar}-H), 7.62# (d, J = 8.1 Hz, 4 H, 2×C_{ar}-H), 7.57# (d, J = 11.8 Hz, 2 H, CH), 7.49* (d, J = 11.5 Hz, 1 H, CH), 7.33* (s, 2 H, 2×C_{ar}-H), 7.30# (d, J = 7.9 Hz, 4 H, 2×C_{ar}-H), 7.23* (d, J = 8.1 Hz, 2 H, 2×C_{ar}-H), 7.12* (s, 1 H, OH), 7.02* (d, J = 7.9 Hz, 2 H, 2×C_{ar}-H), 6.92# (s, 2 H, OH), 6.87# (s, 4 H, 2×C_{ar}-H), 5.23* (d, J = 11.4 Hz, 1 H, CH), 5.17# (d, J = 11.8 Hz, 2 H, CH), 2.33# (s, 6 H, CH₃), 2.15* (s, 3 H, CH₃), 1.40* (s, 18 H, 2×C(CH₃)₃),
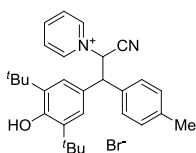
1.21# (s, 36 H, 2×C(CH₃)₃). **¹³C NMR** (100 MHz, DMSO-d_6) δ = 153.7* (s, C_{ar}), 153.3# (s, C_{ar}), 148.2* (d, C_{ar}-H), 147.9# (d, C_{ar}-H), 144.3# (d, 2×C_{ar}-H), 144.2* (d, 2×C_{ar}-H), 139.8* (s, 2×C_{ar}), 139.5# (s, 2×C_{ar}), 137.4# (s, C_{ar}), 137.1* (s, C_{ar}), 134.7# (s, C_{ar}), 133.8* (s, C_{ar}), 129.7# (d, 2×C_{ar}-H), 129.5* (d, 2×C_{ar}-

H), 128.8# (d, 2×C_{ar}-H), 128.5* (d, 2×C_{ar}-H), 128.0# (d, 2×C_{ar}-H), 128.0* (d, 2×C_{ar}-H), 127.6* (s, C_{ar}), 126.9# (s, C_{ar}), 124.6* (d, 2×C_{ar}-H), 124.1# (d, 2×C_{ar}-H), 115.1# (s, CN), 115.1* (s, CN), 62.5* (d, CH), 62.4# (d, CH), 54.6# (d, CH), 54.1* (d, CH), 34.7* (s, 2×C(CH₃)₃), 34.5# (s, 2×C(CH₃)₃), 30.4* (q, 2×C(CH₃)₃), 30.1# (q, 2×C(CH₃)₃), 20.6# (q, CH₃), 20.5* (q, CH₃). **HRMS** (ESI+): *m/z* [C₂₉H₃₅N₂O]⁺: calcd. 427.2744, found 427.2748. DA605

1-(1-(3,5-Di-*tert*-butyl-4-hydroxyphenyl)-3-oxo-1-(*p*-tolyl)butan-2-yl)pyridin-1-ium chloride (7d) was synthesized according to general procedure C from **3b** (50 mg, 0.16 mmol), **1dH⁺Cl⁻** (29 mg, 0.16 mmol), and NEt₃ (50 μl, 0.36 mmol). The solvent was evaporated and **7d** was obtained as colorless solid (79 mg, 0.16 mmol, quant., *dr* 2:3). **¹H NMR** (300 MHz, CDCl₃) δ = 9.91# (d, J = 5.1 Hz, 3 H, 2×C_{ar}-H), 9.84* (d, J = 5.4 Hz, 2 H, 2×C_{ar}-H), 8.50 – 8.23

#,* (m, 5 H, 2×C_{ar}-H, 2×CH), 7.88 − 7.73 #,* (m, 5 H, 4×C_{ar}-H), 7.69* (d, J = 8.1 Hz, 2 H, 2×C_{ar}-H), 7.46# (d, J = 8.1 Hz, 3 H, 2×C_{ar}-H), 7.39# (s, 3 H, 2×C_{ar}-H), 7.15* (d, J = 7.9 Hz, 2 H, 2×C_{ar}-H), 7.11# (s, 3 H, 2×C_{ar}-H), 6.93# (d, J = 7.9 Hz, 3 H, 2×C_{ar}-H), 5.25# (s, 2 H, OH), 5.05* (s, 1 H, OH), 4.51 − 4.32#,* (m, 2 H, 2×CH), 2.24* (s, 3 H, CH₃), 2.16# (s, 5 H, CH₃), 2.09* (s, 3 H, CH₃), 1.99# (s, 5 H, CH₃), 1.39# (s, 27 H, 2×C(CH₃)₃), 1.26* (s, 18 H, 2×C(CH₃)₃). **¹³C NMR** (75 MHz, CDCl₃) δ = 204.1# (s, CO), 203.7* (s, CO), 153.8# (s, C_{ar}), 153.0* (s, C_{ar}), 145.8* (d, 2×C_{ar}-H), 145.4# (d, 2×C_{ar}-H), 145.2* (d, 2×C_{ar}-H), 137.9* (s, C_{ar}), 137.3# (s, C_{ar}), 137.2# (s, 2×C_{ar}), 136.8* (s, 2×C_{ar}), 135.2* (s, C_{ar}),
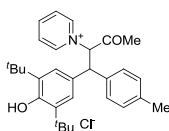
134.9$^\#$ (s, C_{ar}), 130.2* (d, 2×C_{ar}-H), 130.0$^\#$ (d, 2×C_{ar}-H), 128.6$^{*,\#}$ (s, 2×C_{ar}), 128.5* (d, 2×C_{ar}-H), 127.7$^\#$ (d, 2×C_{ar}-H), 127.3$^\#$ (d, 2×C_{ar}-H), 126.8* (d, 2×C_{ar}-H), 125.3$^\#$ (d, 2×C_{ar}-H), 124.5* (d, 2×C_{ar}-H), 76.3* (d, CH), 76.1$^\#$ (d, CH), 57.0$^\#$ (d, CH), 56.8* (d, CH), 34.6$^\#$ (s, 2×C(CH$_3$)$_3$), 34.4* (s, 2×C(CH$_3$)$_3$), 32.2* (q, CH$_3$), 31.7$^\#$ (q, CH$_3$), 30.4$^\#$ (q, 2×C(CH$_3$)$_3$), 30.3* (q, 2×C(CH$_3$)$_3$), 21.1* (q, CH$_3$), 20.9$^\#$ (q, CH$_3$). **HRMS** (ESI+): m/z [C$_{30}$H$_{38}$NO$_2$]$^+$: calcd. 444.2897, found 444.2899. DA604-2

1-(1-(3,5-Di-*tert*-butyl-4-hydroxyphenyl)-3-oxo-3-phenyl-1-(*p*-tolyl)propan-2-yl)pyridin-1-ium bromide (7e) was synthesized according to general procedure C from (**3b**) (50 mg, 0.16 mmol), **1eH$^+$Br$^-$** (47 mg, 0.15 mmol), and NEt$_3$ (50 µl, 0.36 mmol). The crude product was dissolved in CH$_2$Cl$_2$ (20 mL), and washed with water (1×20 mL). The solvent was evaporated, the residue was washed with diethyl ether, and **7e** was obtained as colorless solid (94 mg, 0.15 mmol, quant., *dr* 1:7). **^{1}H NMR** (400 MHz, CDCl$_3$) δ = 10.10$^\#$ (d, J = 5.9 Hz, 14 H, 2×C_{ar}-H), 9.98* (d, J = 5.8 Hz, 2 H, 2×C_{ar}-H), 8.49 – 8.40$^{\#,*}$ (m, 8 H, CH, 2×C_{ar}-H), 8.37 – 8.21$^{\#,*}$ (m, 8 H, CH, 2×C_{ar}-H), 8.30 – 8.25$^\#$ (m, 14 H, 2×C_{ar}-H), 7.89 – 7.80$^{\#,*}$ (m, 16 H, 6×C_{ar}-H), 7.72$^\#$ (d, J = 8.1 Hz, 14 H, 2×C_{ar}-H), 7.43 – 7.33$^{\#,*}$ (m, 8 H, 2×C_{ar}-H), 7.29* (t, J = 7.7 Hz, 2 H, 2×C_{ar}-H), 7.23$^\#$ (t, J = 7.8 Hz, 14 H, 2×C_{ar}-H, , superimposed by solvent signal), 7.16$^\#$ (s, 14 H, 2×C_{ar}-H), 7.08* (s, 2 H, 2×C_{ar}-H), 6.97$^\#$ (d, J = 7.9 Hz, 14 H, 2×C_{ar}-H), 6.88* (d, J = 7.9 Hz, 2 H, 2×C_{ar}-H), 5.08* (s, 1 H, OH), 4.91$^\#$ (s, 7 H, OH), 4.70* (d, J = 11.4 Hz, 1 H, CH), 4.64$^\#$ (d, J = 11.8 Hz, 7 H, CH), 2.09$^\#$ (s, 21 H, CH$_3$), 2.07* (s, 3 H, CH$_3$), 1.27* (s, 18 H, 2×C(CH$_3$)$_3$), 1.21$^\#$ (s, 126 H, 2×C(CH$_3$)$_3$). **^{13}C NMR** (100 MHz, CDCl$_3$) **Major$^\#$**: δ = 195.4 (s, CO), 153.3 (s, C_{ar}), 145.8 (d, C_{ar}-H), 145.4 (d, 2×C_{ar}-H), 137.3 (s, C_{ar}), 136.3 (s, 2×C_{ar}), 134.5 (d, 2×C_{ar}-H), 134.3 (s, C_{ar}), 130.3 (d, C_{ar}-H), 130.0 (d, 2×C_{ar}-H), 128.6 (d, 2×C_{ar}-H), 128.5 (s, 2×C_{ar}), 127.3 (d, 2×C_{ar}-H), 126.7 (d, 2×C_{ar}-H), 125.7 (d, 2×C_{ar}-H), 72.5 (d, CH), 58.0 (d, CH), 34.3 (s, 2×C(CH$_3$)$_3$), 30.1 (q, 2×C(CH$_3$)$_3$), 20.9 (q, CH$_3$). ^{13}C NMR-signals corresponding to the minor diastereoisomer* could not be assigned unambiguously due to their low intensity. **HRMS** (ESI+): m/z [C$_{35}$H$_{40}$NO$_2$]$^+$: calcd. 506.3054, found 506.3056. DA603-2

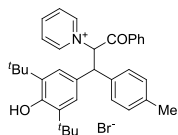**1-(1-(3,5-Di-*tert*-butyl-4-hydroxyphenyl)-3-oxo-3-phenyl-1-(*p*-tolyl)propan-2-yl)-4-di-methylamino)pyridin-1-ium bromide (7f)** was synthesized according to general procedure C from **3b** (50 mg, 0.16 mmol), **1fH⁺Br⁻** (47 mg, 0.16 mmol), and NEt₃ (50 µl, 0.36 mmol). The solvent was evaporated and **7f** was obtained as colorless solid (94 mg, 0.16 mmol, quant., *dr* 1:5). **¹H NMR** (400 MHz, CDCl₃) δ = 9.17# (d, *J* = 7.5 Hz, 10 H, 2×C$_{ar}$-H), 8.92* (d, *J* = 8.0 Hz, 2 H, 2×C$_{ar}$-H), 8.44* (d, *J* = 7.3 Hz, 2 H, 2×C$_{ar}$-H), 8.23 – 8.16# (m, 10 H, 2×C$_{ar}$-H), 7.66# (dd, *J* = 11.7, 8.1 Hz, 15 H, CH, 2×C$_{ar}$-H), 7.50 – 7.32#,* (m, 11 H, CH, 6×C$_{ar}$-H), 7.28 – 7.22# (m, 10 H, 2×C$_{ar}$-H, , superimposed by solvent signal), 7.05 – 6.98# (s, 10 H, 2×C$_{ar}$-H), 7.02#,* (m, 12 H, 4×C$_{ar}$-H), 6.88* (d, *J* = 8.1 Hz, 2 H, 2×C$_{ar}$-H), 6.63 – 6.57#,* (m, 12 H, 4×C$_{ar}$-H), 5.09 (s, 1 H, OH), 4.86# (s, 5 H, OH), 4.63* (d, *J* = 11.5 Hz, 1 H, CH), 4.53# (d, *J* = 11.9 Hz, 5 H, CH), 3.08* (s, 6 H, N(CH₃)₂), 3.04# (s, 30 H, N(CH₃)₂), 2.13# (s, 15 H, CH₃), 2.08* (s, 3 H, CH₃), 1.30* (s, 18 H, 2×C(CH₃)₃), 1.20# (s, 90 H, 2×C(CH₃)₃). **¹³C NMR** (100 MHz, CDCl₃) **Major**# δ = 197.4 (s, CO), 156.1 (s, C$_{ar}$), 153.0 (s, C$_{ar}$), 142.6 (d, 2×C$_{ar}$-H), 136.8 (s, C$_{ar}$), 136.2 (s, 2×C$_{ar}$), 135.3 (s, C$_{ar}$), 135.1 (s, C$_{ar}$), 134.0 (d, C$_{ar}$-H), 129.9 (d, 2×C$_{ar}$-H), 129.9 (d, 2×C$_{ar}$-H), 128.6 (d, 2×C$_{ar}$-H), 128.5 (d, 2×C$_{ar}$-H), 127.7 (s, C$_{ar}$), 125.6 (d, 2×C$_{ar}$-H), 107.1 (d, 2×C$_{ar}$-H), 68.8 (d, CH), 56.6 (d, CH), 40.2 (q, N(CH₃)₂), 34.3 (s, 2×*C*(CH₃)₃), 30.2 (q, 2×C(*C*H₃)₃), 21.0 (q, CH₃). ¹³C NMR-signals corresponding to the minor diastereoisomer* could not be assigned unambiguously due to their low intensity. **HRMS** (ESI+): *m/z* [C₃₇H₄₅N₂O₂]⁺: calcd. 549.3476, found 549.3479. DA608

3-Chloro-1-(1-(3,5-di-*tert*-butyl-4-hydroxyphenyl)-3-oxo-3-phenyl-1-(*p*-tolyl)propan-2-yl)pyridin-1-ium bromide (7g) was synthesized according to general procedure C from **3b** (50 mg, 0.16 mmol), **1gH⁺Br⁻** (51 mg, 0.16 mmol), and NEt₃ (50 µl, 0.36 µmol). The crude product was dissolved in CH₂Cl₂ (20 mL), and washed with water (1×20 mL). The solvent was evaporated and **7g** was obtained as colorless solid (100 mg, 0.16 mmol, quant., *dr* 1:5). **¹H NMR** (400 MHz, CDCl₃) δ = 10.54# (d, *J* = 5.3 Hz, 5 H, C$_{ar}$-H), 10.38* (d, *J* = 5.9 Hz, 1 H, C$_{ar}$-H), 9.96 – 9.83#,* (m, 6 H, 2×C$_{ar}$-H), 8.57# (d, *J* = 11.8 Hz, 5 H, CH), 8.51 – 8.43* (m, 2 H, CH, 2×C$_{ar}$-H), 8.33# (d, *J* = 8.3 Hz, 5 H, C$_{ar}$-H), 8.31 – 8.22# (m, 10 H, 2×C$_{ar}$-H), 7.96# (dd, *J* = 8.1, 6.4 Hz, 5 H, C$_{ar}$-H), 7.87* (dd, *J* = 8.0, 6.2 Hz, 1 H, C$_{ar}$-H), 7.74# (d, *J* = 8.0 Hz, 10 H, 2×C$_{ar}$-H), 7.52* (d, *J* = 8.1 Hz, 2 H, 2×C$_{ar}$-H), 7.42* (t, *J* = 7.3 Hz, 2 H, 2×C$_{ar}$-H), 7.37# (t, *J* = 7.4 Hz, 5 H, C$_{ar}$-H), 7.31# (d, *J* = 7.9 Hz, 5 H, C$_{ar}$-H), 7.27 – 7.18# (m, 5 H, C$_{ar}$-H, , superimposed by solvent signal), 7.19* (d, *J* = 8.1 Hz, 1H, 2×C$_{ar}$-H), 7.16# (s, 10 H, 2×C$_{ar}$-H), 7.12* (d, *J* = 6.5 Hz, 2 H, 2×C$_{ar}$-H), 7.02# (d, *J* = 8.0 Hz, 10 H, 2×C$_{ar}$-H), 6.92* (d, *J* = 8.0 Hz, 2 H, 2×C$_{ar}$-H), 5.13* (s, 1 H, OH), 4.93# (s, 5 H, OH),

4.63 – 4.55[#,*] (m, 6 H, 2×CH), 2.34[*] (s, 3 H, CH$_3$), 2.14[#] (s, 15 H, CH$_3$), 1.30[*] (s, 18 H, 2×C(CH$_3$)$_3$), 1.22[#] (s, 90 H, 2×C(CH$_3$)$_3$). ^{13}**C NMR** (100 MHz, CDCl$_3$) **Major**[#] δ = 195.0 (s, CO), 153.5 (s, C$_{ar}$), 145.7 (d, C$_{ar}$-H), 144.9 (d, C$_{ar}$-H), 143.6 (d, C$_{ar}$-H), 137.5 (s, C$_{ar}$), 136.5 (s, 2×C$_{ar}$), 135.1 (s, C$_{ar}$), 134.6 (s, C$_{ar}$), 134.4 (d, C$_{ar}$-H), 134.0 (s, C$_{ar}$), 130.5 (d, 2×C$_{ar}$-H), 130.2 (d, 2×C$_{ar}$-H), 128.6 (d, 2×C$_{ar}$-H), 128.5 (d, 2×C$_{ar}$-H), 128.1 (d, C$_{ar}$-H), 126.4 (s, C$_{ar}$), 125.8 (d, 2×C$_{ar}$-H), 72.9 (d, CH), 58.4 (d, CH), 34.3 (s, 2×C(CH$_3$)$_3$), 30.1 (q, 2×C(CH$_3$)$_3$), 21.0 (q, CH$_3$). ^{13}C NMR-signals corresponding to the minor diastereoisomer[*] could not be assigned unambiguously due to their low intensity. **HRMS** (ESI+): m/z [C$_{35}$H$_{39}$ClNO$_2$]$^+$: calcd. 540.2664, found 540.2674. DA607

2-(1-(3,5-Di-*tert*-butyl-4-hydroxyphenyl)-3-oxo-3-phenyl-1-(*p*-tolyl)propan-2-yl)isoquin-olin-2-ium bromide (7h) was synthesized according to general procedure C from **3b** (50 mg, 0.16 mmol), **1hH$^+$Br$^-$** (53 mg, 0.16 mmol), and NEt$_3$ (50 μl, 0.36 mmol). The crude product was dissolved in CH$_2$Cl$_2$ (20 mL), and washed with water (1×20 mL), and 2 N HCl (20 mL). The organic layer was dried over Na$_2$SO$_4$ and the solvent was evaporated. **7h** was obtained as colorless solid (103 mg, 0.16 mmol, quant., *dr* 1:3). ^{1}**H NMR** (300 MHz, CDCl$_3$) δ = 11.83[#,*] (d, J = 10.0 Hz, 4 H, 2×C$_{ar}$-H), 9.43[#] (d, J = 6.4 Hz, 3 H, C$_{ar}$-H), 9.00[*] (d, J = 6.8 Hz, 1 H, C$_{ar}$-H), 8.74[#] (d, J = 11.9 Hz, 3 H, CH), 8.66[*] (d, J = 7.0 Hz, 2 H, 2×C$_{ar}$-H), 8.55[*] (d, J = 8.3 Hz, 2 H, 2×C$_{ar}$-H), 8.51[*] (d, J = 11.7 Hz, 1 H, CH), 8.43[#] (d, J = 7.3 Hz, 6 H, 2×C$_{ar}$-H),
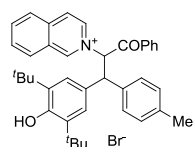
8.06 – 7.90[#,*] (m, 13 H, 5×C$_{ar}$-H), 7.86 – 7.74[#,*] (m, 11 H, 7×C$_{ar}$-H), 7.62[*] (d, J = 8.0 Hz, 2 H, 2×C$_{ar}$-H), 7.48 – 7.24[#,*] (m, 22 H, 8×C$_{ar}$-H, superimposed by solvent signal), 7.08[*] (s, 2 H, 2×C$_{ar}$-H), 7.01[*] (d, J = 8.5 Hz, 2 H, 2×C$_{ar}$-H), 6.97[#] (d, J = 8.0 Hz, 6 H, 2×C$_{ar}$-H), 5.27[*] (s, 1 H, OH), 4.94[#] (s, 3 H, OH), 4.83 – 4.72[#,*] (m, 4 H, 2×CH), 2.16[*] (s, 3 H, CH$_3$), 2.05[#] (s, 6 H, CH$_3$), 1.28[#] (s, 54 H, 2×C(CH$_3$)$_3$), 1.17[*] (s, 18 H, 2×C(CH$_3$)$_3$). ^{13}**C NMR** (75 MHz, CDCl$_3$) δ = 196.5[#] (s, CO), 195.0[*] (s, CO), 153.3[#] (s, C$_{ar}$), 153.1[*] (s, C$_{ar}$), 151.4[#] (br d, C$_{ar}$-H), 152.3[*] (br d, C$_{ar}$-H), 137.5[*] (s, C$_{ar}$), 137.4[#] (s, C$_{ar}$), 137.3[*] (d, C$_{ar}$-H), 137.1[*] (d, C$_{ar}$-H), 136.9[#] (s, C$_{ar}$), 136.4[#] (s, C$_{ar}$), 136.4[*] (s, C$_{ar}$), 136.3[*] (s, C$_{ar}$), 135.0[#] (s, C$_{ar}$), 135.0[*] (s, C$_{ar}$), 134.9[*] (d, C$_{ar}$-H), 134.9[#] (s, C$_{ar}$), 134.8[*] (s, C$_{ar}$), 134.4[#] (d, C$_{ar}$-H), 134.1[#] (br d, C$_{ar}$-H) , 132.3[*] (br d, C$_{ar}$-H), 131.8[#] (d, C$_{ar}$-H), 131.7[*] (d, C$_{ar}$-H), 131.1[*] (d, C$_{ar}$-H), 130.9[*] (d, 2×C$_{ar}$-H), 130.8[#] (d, C$_{ar}$-H), 130.5[*] (s, C$_{ar}$), 130.4[#] (d, 2×C$_{ar}$-H), 130.0[#] (d, 2×C$_{ar}$-H), 129.8[*] (d, 2×C$_{ar}$-H), 129.7[*] (s, C$_{ar}$), 129.2[#] (d, C$_{ar}$-H), 128.7[#] (d, 2×C$_{ar}$-H), 128.7[*] (d, 2×C$_{ar}$-H), 128.5[#] (d, 2×C$_{ar}$-H), 128.4[*] (d, 2×C$_{ar}$-H), 127.5[*] (s, C$_{ar}$), 127.4[#], (s, C$_{ar}$) 127.3[#,*] (s, 2×C$_{ar}$), 126.8[#] (d, C$_{ar}$-H), 126.6[*] (d, C$_{ar}$-H), 125.8[#] (d, 2×C$_{ar}$-H), 125.2[*] (d, 2×C$_{ar}$-H), 124.7[#] (d, C$_{ar}$-H) , 72.1[#] (d, CH), 71.9[*] (d, CH), 58.0[#] (d, CH), 57.3[*] (d, CH), 34.4[#] (s, 2×C(CH$_3$)$_3$), 34.3[*] (s, 2×C(CH$_3$)$_3$),

30.2# (q, 2×C(CH$_3$)$_3$), 30.2* (q, 2×C(CH$_3$)$_3$), 21.0* (q, CH$_3$), 20.9# (q, CH$_3$). **HRMS** (ESI+): *m/z* [C$_{39}$H$_{42}$NO$_2$]$^+$: calcd. 556.3210, found 556.3214. DA610

4.5.5 Reactions with Benzylidene Malononitrile 5a

1,1-Dicyano-3-(4-(dimethylamino)pyridin-1-ium-1-yl)-2-(4-methoxyphenyl)-4-oxo-4-phenylbutan-1-ide (12f) was generated by mixing from **5a** (46 mg, 0.25 mmol), **1fH$^+$Br$^-$** (80 mg, 0.25 mmol), and 1,5,7-triazabicyclo[4.4.0]dec-5-ene (TBD, 35 mg, 0.25 mmol) in DMSO-*d$_6$* at room temperature. The reaction mixture was analyzed by NMR. **12f** was obtained as a mixture of diastereoisomers (quant. conversion, *dr* 1:3). # corresponds to signals of the major diastereoisomer, * to signals of the minor diastereoisomer. Integrals for the minor diastereoisomer* are set to 1.0 for one proton of the minor diastereoisomer*. The Spectra are contaminated by traces of **1fH$^+$Br$^-$** and one equiv. of TBDH$^+$Br$^-$. **^{1}H NMR** (400 MHz, DMSO-*d$_6$*) δ = 3.03# (s, 18 H, N(CH$_3$)$_2$), 3.19* (s, 6 H, N(CH$_3$)$_2$, superimposed by TBDH$^+$Br$^-$ signal), 3.58* (s, 3 H, CH$_3$), 3.65# (s, 9 H, CH$_3$), 3.85* (d, *J* = 11.0 Hz, 1 H, CH), 4.00# (d, *J* = 11.9 Hz, 3 H, CH), 6.25* (d, *J* = 10.9 Hz, 1 H, CH), 6.49# (d, *J* = 11.9 Hz, 3 H, CH), 6.65* (d, *J* = 8.6 Hz, 2 H, 2×C$_{Ar}$-H), 6.75# (d, *J* = 8.6 Hz, 6 H, 2×C$_{Ar}$-H), 6.79# (d, *J* = 7.9 Hz, 6 H, 2×C$_{Ar}$-H), 7.10* (d, *J* = 7.8 Hz, 2 H, 2×C$_{Ar}$-H), 7.20* (d, *J* = 8.6 Hz, 2 H, 2×C$_{Ar}$-H), 7.34 − 7.40#,* (m, 8 H, 4×C$_{Ar}$-H), 7.58 − 7.63#,* (m, 8 H, 4×C$_{Ar}$-H), 7.69 − 7.74#,* (m, 4 H, 2×C$_{Ar}$-H), 8.34 − 8.40# (m, 6 H, 2×C$_{Ar}$-H), 8.53 − 8.59#,* (m, 8 H, 4×C$_{Ar}$-H). **^{13}C NMR** (100 MHz, DMSO-*d$_6$*) **Major**# δ = 16.0 (s, C$_q$$^-$), 39.7 (q, N(CH$_3$)$_2$, superimposed by TBDH$^+Br^-$ and solvent signal), 45.3 (d, CH), 54.9 (q, CH$_3$), 67.2 (d, CH), 107.3 (d, 2×C$_{Ar}$-H), 107.3 (s, 2×CN), 113.4 (d, 2×C$_{Ar}$-H), 128.3 (s, C$_{Ar}$), 128.7 (d, 2×C$_{Ar}$-H), 129.1 (d, 2×C$_{Ar}$-H), 129.5 (d, 2×C$_{Ar}$-H), 134.2 (s, C$_{Ar}$), 135.1 (d, C$_{Ar}$-H), 141.2 (d, 2×C$_{Ar}$-H), 155.5 (s, C$_{Ar}$), 157.6 (s, C$_{Ar}$-O), 195.6 (s, CO). ^{13}C NMR-signals corresponding to the minor diastereoisomer* could not be assigned unambiguously due to their low intensity. DA837
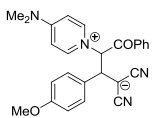
General Procedure D for the Synthesis of Products 13−14. Pyridinium salt **1** (0.25−0.50 mmol), benzylidene malononitrile **5a** (0.25−1.00 mmol), and base (0.721−1.00 mmol) were dissolved in DMSO (0.2 M) at room temperature and stirred for the time indicated. Brine (20 mL) was added to the reaction mixture and the aqueous layer was extracted with CH_2Cl_2 (3×15 mL). The combined organic layers were washed with brine (2×20 mL), dried over Na_2SO_4 and concentrated *in vacuo* to obtain the crude products. The products **13−14** were recrystallized from ethanol.

2-Acetyl-3-(4-methoxyphenyl)cyclopropane-1,1-dicarbonitrile (13d) was synthesized according to general procedure D from **5a** (184 mg, 1.00 mmol), **1dH⁺Cl⁻** (172 mg, 1.00 mmol), and KO^tBu (112 mg, 1.00 mmol) by stirring for 1 h. The crude product was purified by column chromatography (silica gel, *n*-pentane:EtOAc = 5:1). **13d** was obtained as colorless solid (128 mg, 533 μmol, 53%). A small sample of **13d** was recrystallized from EtOH for the determination of the melting point. **Mp** (EtOH): 161 °C. **¹H NMR** (400 MHz, CDCl₃) δ = 7.25 − 7.17 (m, 2 H, 2×C_Ar-H), 6.98 − 6.90 (m, 2 H, 2×C_Ar-H), 3.82 (s, 3 H, CH₃), 3.60 (d, *J* = 8.0 Hz, 1 H, CH), 3.33 (d, *J* = 8.0 Hz, 1 H, CH), 2.56 (s, 3 H, CH₃). **¹³C NMR** (100 MHz, CDCl₃) δ = 197.3 (s, CO), 160.7 (s, C_Ar), 129.6 (d, 2×C_ar-H), 120.9 (s, C_Ar), 114.8 (d, 2×C_ar-H), 112.3 (s, CN), 111.6 (s, CN), 55.5 (q, CH₃), 38.7 (d, CH), 38.6 (d, CH), 31.9 (q, CH₃), 15.3 (s, C_q). **HRMS** (EI): *m/z* [$C_{14}H_{12}N_2O_2$]: calcd. 240.0899, found 240.0904. **MS** (EI) *m/z* = 240 (2), 198 (24), 155 (8), 127 (7), 43 (100). DA839-3
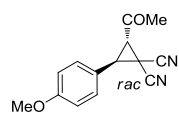
¹H NMR monitoring of the formation of 13d. 5a (46 mg, 0.25 mmol), **1dH⁺Cl⁻** (43 mg, 0.25 mmol), and KO^tBu (34.2 mg, 305 μmol) were combined in 2.5 mL DMSO-*d₆* at room temperature. The reaction mixture was analyzed by ¹H NMR after 5, 30, and 60 min with HO^tBu as internal standard. DA839-2

Conversion   5 min: **5a** 0%, **12d** ~40%, **13d** ~ 60%.

Conversion 30 min: **5a** 0%, **12d** ~21%, **13d** ~ 79%.

Conversion 60 min: **5a** 0%, **12d** ~0%,   **13d** ~100%.

2-Benzoyl-3-(4-methoxyphenyl)cyclopropane-1,1-dicarbonitrile (13e) was synthesized according to general procedure D from **5a** (92 mg, 0.50 mmol), **1eH⁺Br⁻** (140 mg, 503 μmol), and NEt₃ (100 μl, 721 μmol) by stirring for 30 min. **13e** was obtained as colorless needles (102 mg, 337 μmol, 67%). **Mp** (EtOH): 164°C. **¹H NMR** (300 MHz, CDCl₃) δ = 8.10 (dd, *J* = 8.4, 1.3 Hz, 2 H, 2×C_Ar-H), 7.78 − 7.68 (m, 1 H, C_Ar-H), 7.65 − 7.55 (m, 2 H, 2×C_Ar-H), 7.30 (dd, *J* = 9.3, 2.5 Hz, 2 H, 2×C_Ar-H), 7.01
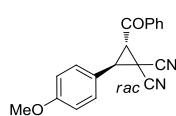
− 6.93 (m, 2 H, 2×C$_{Ar}$-H), 4.00 (d, J = 8.0 Hz, 1 H, CH), 3.86 (d, J = 8.1 Hz, 1 H, CH), 3.83 (s, 3 H, OCH$_3$). **^{13}C NMR** (75 MHz, CDCl$_3$) δ = 189.1 (s, CO), 160.8 (s, C$_{Ar}$), 135.6 (s, C$_{Ar}$), 135.2 (d, C$_{Ar}$-H), 129.7 (d, 2×C$_{Ar}$-H), 129.5 (d, 2×C$_{Ar}$-H), 128.9 (d, 2×C$_{Ar}$-H), 121.3 (s, C$_{Ar}$), 114.9 (d, 2×C$_{Ar}$-H), 112.5 (s, CN), 111.8 (s, CN), 55.5 (q, CH$_3$), 38.7 (s, CH), 35.9 (d, CH), 15.5 (s, C$_q$). **HRMS** (EI): m/z [C$_{19}$H$_{14}$N$_2$O$_2$]: calcd. 302.1055, found 302.1052. **MS** (EI) m/z = 302 (10), 105 (100), 77 (35). DA613

Table 4.12. Crystallographic data of 13e.

net formula	C$_{19}$H$_{14}$N$_2$O$_2$
M_r/g mol^{-1}	302.327
crystal size/mm	0.265 × 0.190 × 0.135
T/K	200(2)
radiation	'MoKα
diffractometer	'Bruker D8Quest'
crystal system	monoclinic
space group	$P2_1/c$
a/Å	15.3827(4)
b/Å	12.0666(3)
c/Å	17.7872(5)
α/°	90
β/°	107.919(2)
γ/°	90
V/Å^3	3141.45(14)
Z	8
calcd. density/g cm^{-3}	1.27847(6)
μ/mm^{-1}	0.084
absorption correction	multi-scan
transmission factor range	0.9053–0.9281
refls. measured	63848
R_{int}	0.0585
mean σ(I)/I	0.0312
θ range	2.28–27.52
observed refls.	4822
x, y (weighting scheme)	0.0542, 1.1648
hydrogen refinement	constr
refls in refinement	7220
parameters	417
restraints	0
$R(F_{obs})$	0.0486
$R_w(F^2)$	0.1343
S	1.012
shift/error$_{max}$	0.001
max electron density/e Å^{-3}	0.369
min electron density/e Å^{-3}	−0.229

^{1}H NMR monitoring of the formation of 13e. 5a (30 mg, 0.16 mmol), **1eH$^+$Br$^-$**(43 mg, 0.15 mmol), and NEt$_3$ (40 µl, 29 mg, 0.29 mmol) were dissolved in 1 mL DMSO-d_6 and the reaction was monitored by ^{1}H NMR after 5, and 30 min. The conversion was determined from the ratio of the integrals over the methoxy (OCH$_3$) ^{1}H NMR signals of **5a** and **13e**, respectively. DA591-2

Conversion 5 min: **5a** 59%, **13e** 41%.
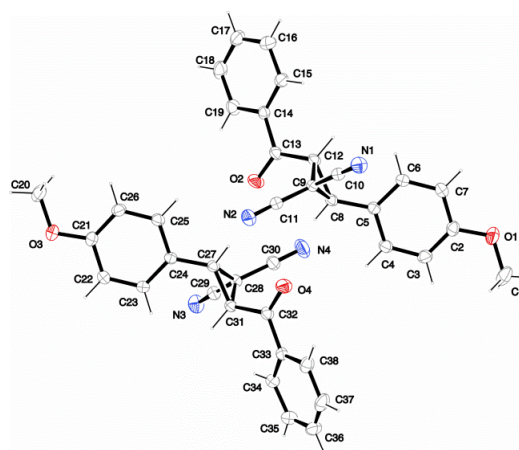Conversion 30 min: **5a** 18%, **13e** 82%.

2-Benzoyl-3-(4-methoxyphenyl)cyclopropane-1,1-dicarbonitrile (13g = 13e) was synthesized according to general procedure D from **5a** (92 mg, 0.50 mmol), **1gH$^+$Br$^-$**(140 mg, 448 µmol), and NEt$_3$ (100 µl, 721 µmol) by stirring for 30 min. **13g** (= **13e**) was obtained as colorless needles (128 mg, 424 µmol, 95%). DA620

Mp (EtOH): 164°C. (spectral data see above).

3-Benzoyl-2-(4-methoxyphenyl)-2,3-dihydropyrrolo[2,1-*a*]isoquinoline-1,1(10b*H*)-dicar-bonitrile (14h) was synthesized according to general procedure D from **5a** (46 mg, 0.25 mmol), **1hH$^+$Br$^-$**(82 mg, 0.25 mmol), and NEt$_3$ (100 µl, 721 µmol) by stirring for 5 min. **14h** was obtained as orange needles (94 mg, 0.22 mmol, 88%, *dr* 10:1). **14h** decomposes slowly in CDCl$_3$ at room temperature. **Mp.** (anti-endo-**14h**; EtOH): 130 − 132 °C. **^{1}H NMR** (300 MHz, CDCl$_3$) δ = 7.84 − 7.77 (m, 2 H, 2×C$_{ar}$-H), 7.62 − 7.53 (m, 1 H, C$_{ar}$-H), 7.49–7.39 (m, 5 H, 7-H, 4×C$_{ar}$-H), 7.30 (td, J = 7.6, 1.4 Hz, 1 H, 8-H), 7.19 (td, J = 7.5, 1.4 Hz, 1 H, 9-H), 7.07 (d, J = 7.6 Hz, 1 H, 10-H), 6.96 (d, J = 8.8 Hz, 2 H, 2×C$_{ar}$-H), 6.28 (d, J = 7.6 Hz, 1 H, 6-H), 5.58 (s, 1 H, 10^b-H), 5.48 (d, J = 7.6 Hz, 1 H, 5-H), 5.41 (d, J = 6.9 Hz, 1 H, 3-H), 4.33 (d, J = 6.8 Hz, 1 H, 2-H), 3.81 (s, 3 H, OCH$_3$). **^{13}C NMR** (75 MHz, CDCl$_3$) δ = 195.1 (s, CO), 160.7 (s, C$_{ar}$), 134.8 (s, C$_{ar}$), 134.4 (d, C$_{ar}$-H), 133.1 (d, C-5), 132.3 (s, C-6^a), 130.1 (d, C-8), 130.1 (d, 2×C$_{ar}$-H), 129.1 (d, 2×C$_{ar}$-H), 129.0 (d, 2×C$_{ar}$-H), 126.9 (d, C-9), 126.4 (d, C-7), 125.6 (d, C-10), 124.6 (s, C$_{ar}$), 123.6 (s, C-10^a), 115.0 (d, 2×C$_{ar}$-H), 114.6 (s, CN), 113.5 (s, CN), 101.6 (d, C-6), 70.6 (d, C-10^b), 70.6 (d, C-3), 55.5 (q, OCH$_3$), 54.3 (d, C-2), 50.1 (s, C-1). **HRMS** (EI): *m/z* (M–2 H) [C$_{28}$H$_{19}$N$_3$O$_2$]: calcd. 429.1477, found 429.1471. **MS** (EI) *m/z* = 429 (4), 247 (13), 246 (25), 185 (14), 184 (100), 141 (23), 129 (84), 105 (50), 77 (34). DA615
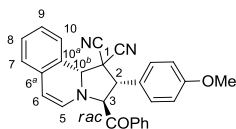
1-Benzoyl-2-(4-methoxyphenyl)-1,2-dihydropyrrolo[1,2-*a*]quinoline-3,3(3a*H*)-dicarbo-nitrile (14i) was synthesized according to general procedure D from **5a** (92 mg, 0.50 mmol), **1iH⁺Br⁻** (164 mg, 500 μmol), and NEt₃ (100 μl, 721 μmol) by stirring for 5 min. **14i** was obtained as red needles (146 mg, 338 μmol, 68%, *dr* 10:1). **Mp.** (anti-endo-**14i**; EtOH): 130 – 131 °C. **¹H NMR** (300 MHz, CDCl₃) δ = 7.75 – 7.67 (m, 2 H, 2×C_{ar}-H), 7.60 – 7.51 (m, 1 H, C_{ar}-H), 7.49 – 7.41 (m, 2 H, 2×C_{ar}-H), 7.39 – 7.31 (m, 2 H, 2×C_{ar}-H), 7.02 – 6.90 (m, 4 H, 7-H, 9-H, 2×C_{ar}-H), 6.78 – 6.65 (m, 2 H, 8-H, 4-H), 5.95 (d, *J* = 8.0 Hz, 1 H, 6-H), 5.80 (m, 2 H, 5-H, 3ᵃ-H), 5.52 (d, *J* = 8.0 Hz, 1 H, 1-H), 3.84 (s, 3 H, OCH₃), 3.74 (d, *J* = 8.0 Hz, 1 H, 2-H). **¹³C NMR** (75 MHz, CDCl₃) δ = 197.7 (s, CO), 161.0 (s, C_{ar}), 141.0 (s, C-9ᵃ), 134.6 (d, C_{ar}-H), 134.3 (s, C_{ar}), 131.1 (d, C-8), 130.3 (d, C-7), 130.1 (d, 2×C_{ar}-H), 129.1 (d, 2×C_{ar}-H), 128.8 (d, 2×C_{ar}-H), 128.5 (d, C-6), 123.5 (s, C_{ar}), 119.8 (s, C-5ᵃ), 119.4 (d, C-4), 115.7 (d, 2×C_{ar}-H), 115.1 (d, C-5), 112.9 (s, CN), 112.2 (s, CN), 109.9 (d, C-9), 70.5 (d, C-3ᵃ), 65.6 (d, C-1), 57.1 (d, C-2), 55.5 (q, OCH₃), 49.2 (s, C-3). **HRMS** (EI): *m/z* [$C_{28}H_{21}N_3O_2$]: calcd. 431.1634, found 431.1646. **MS** (EI) *m/z* = 246 (4), 185 (15), 184 (100), 141 (20), 129 (47), 114 (27), 105 (14), 43 (20). DA621-2
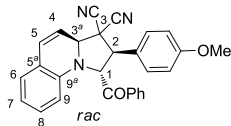
4.5.6 Reactions with *p*-NO₂-Chalcone 5b

2-(4-Nitrophenyl)-1,2,3,3a-tetrahydropyrrolo[1,2-*a*]quinoline-1,3-diyl)bis(phenylmeth-anone) (15i) was synthesized in analogy to procedure D from chalcone **5b** (127 mg, 504 μmol), pyridinium salt **1iH⁺Br⁻** (164 mg, 500 μmol), and NEt₃ (100 μl, 721 μmol) in DMSO (5 mL) at 20°C. **15i** was obtained as orange solid (68.9 mg, 138 μmol, 34% determined from ratio of **5b**:**15i** by ¹H NMR, *dr* 5:27:68 after recrystallization for anti-1-endo-2-exo adduct), but it partially decomposed to **5b** during work-up and recrystallization. Spectra are contaminated by **5b** due to the decomposition of **15i**. **¹H NMR** (600 MHz, CD₂Cl₂) δ = 8.02 – 7.97 (m, 2 H, 2×C_{ar}-H), 7.89 – 7.84 (m, 2 H, 2×C_{ar}-H), 7.72 – 7.70 (m, 2 H, 2×C_{ar}-H), 7.66 – 7.62 (m, 1 H, C_{ar}-H, superimposed by **5b**), 7.58 – 7.50 (m, 2 H, 2×C_{ar}-H, superimposed by **8**), 7.50 – 7.44 (m, 1 H, C_{ar}-H), 7.35 – 7.28 (m, 4 H, 4×C_{ar}-H), 6.94 (td, *J* = 7.8, 1.6 Hz, 1 H, 8-H), 6.88 (dd, *J* = 7.4, 1.5 Hz, 1 H, 6-H), 6.63 (td, *J* = 7.4, 1.0 Hz, 1 H, 7-H), 6.27 (dd, *J* = 9.7, 2.1 Hz, 1 H, 5-H), 6.15 (d, *J* = 8.3 Hz, 1 H, 9-H), 5.94 (dt, *J* = 8.4, 2.4 Hz, 1 H, 3ᵃ-H), 5.82 (d, *J* = 8.8 Hz, 1 H, 1-H), 5.25 (dd, *J* = 10.0, 2.3 Hz, 1 H, 4-H), 4.89 (dd, *J* = 8.4, 7.2 Hz, 1 H, 3-H), 4.61 (dd, *J* = 8.8, 7.2 Hz, 1 H, 2-H). **¹³C NMR** (100 MHz, CD₂Cl₂) δ = 200.3 (s, CO), 198.6 (s, CO), 145.2
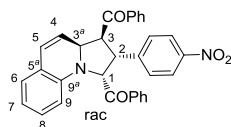
(s, C_{ar}), 142.3 (d, C-9^a), 137.6 (s, C_{ar}), 137.0 (s, C_{ar}), 136.1 (s, C_{ar}), 133.8 (d, C_{ar}-H), 133.6 (d, C_{ar}-H), 129.9 (d, 2×C_{ar}-H), 129.2 (d, C-8), 129.0 (d, 2×C_{ar}-H), 128.6 (d, 2×C_{ar}-H), 127.9 (d, 2×C_{ar}-H), 127.3 (d, C-6), 127.1 (d, C-5), 125.7 (d, 2×C_{ar}-H), 123.2 (d, 2×C_{ar}-H), 121.4 (s, C-5^a), 120.1 (d, C-4), 118.2 (d, C-7), 111.7 (d, C-9), 68.5 (d, C-1), 61.9 (d, C-3^a), 55.8 (d, C-3), 48.6 (d, C-2). **HRMS** (EI): m/z [M−H] [$C_{32}H_{23}N_2O_4$]$^-$: calcd. 499.1663, found 499.1644. **MS** (EI): m/z = 499 (8), 253 (59), 236 (38), 178 (25), 130 (17), 105 (100), 77 (77). DA886

General Procedure E for the Synthesis of Indolizines 16. Pyridinium salt **1H⁺X⁻** (500 μmol), chalcone **5b** (500 μmol), and Na_2CO_3 (1.75 mmol) were dissolved in DMSO (0.1 M) at room temperature and stirred for 5 min. TPCD (821 μmol) was added and the reaction mixture was heated at 100 °C for 3–4 h. The reaction mixture was cooled to room temperature and EtOAc (5 mL) was added. The resulting precipitate was filtered off and washed with EtOAc (20 mL). The filtrate was concentrated in vacuo and subjected to column chromatography (silica, *n*-pentane : EtOAc = 5 : 1). The products were recrystallized from Et₂O:EtOAc or Et₂O.

Ethyl 1-benzoyl-2-(4-nitrophenyl)indolizine-3-carboxylate (16a) was synthesized according to general procedure E from **1aH⁺Br⁻** (123 mg, 500 μmol), chalcone **5b** (128 mg, 505 μmol), Na_2CO_3 (186 mg, 1.75 mmol), and TPCD (500 mg, 821 μmol). **16a** was obtained as brownish solid (112 mg, 270 μmol, 54%). **Mp** (Et₂O): 154 °C. **¹H NMR** (300 MHz, CDCl₃) δ = 9.67 (dt, J = 7.2, 1.1 Hz, 1 H, 5-H), 8.02 – 7.94 (m, 3 H, 8-H, 2×C_{ar}-H), 7.47 (ddd, J = 7.1, 2.9, 1.6 Hz, 2 H, 2×C_{ar}-H), 7.40 – 7.27 (m, 4 H, 6-H, 3×C_{ar}-H), 7.20 – 7.13 (m, 2 H, 2×C_{ar}-H), 7.07 (td, J = 7.0 Hz, 1.4, 1 H, 7-H), 4.12 (q, J = 7.1 Hz, 2 H, CH₂), 0.94 (t, J = 7.1 Hz, 3 H, CH₃). **¹³C NMR** (75 MHz, CDCl₃) δ = 192.0 (s, CO), 161.4 (s, CO₂), 146.9 (s, C_{ar}), 142.3 (s, C_{ar}), 139.8 (s, C_{ar}), 138.9 (s, C-8^a), 136.5 (s, C-2), 131.9 (d, C_{ar}-H), 131.8 (d, 2×C_{ar}-H), 129.2 (d, 2×C_{ar}-H), 128.2 (d, C-5), 128.1 (d, 2×C_{ar}-H), 126.6 (d, C-7), 122.2 (d, 2×C_{ar}-H), 119.6 (d, C-8), 115.5 (d, C-6), 115.4 (br s, C-3), 114.8 (br s, C-1), 60.6 (t, CH₂), 13.9 (q, CH₃). **HRMS** (EI): m/z [$C_{24}H_{18}N_2O_5$]: calcd. 414.1216, found 414.1211. **MS** (EI): m/z = 415 (28), 414 (100), 342 (18), 337 (23), 309 (24), 265 (17), 263 (10), 77 (10). DA541
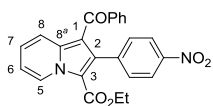
1-Benzoyl-*N*,*N*-diethyl-2-(4-nitrophenyl)indolizine-3-carboxamide (16b). The pyridinium salt **1bH⁺Br⁻** (150 mg, 549 μmol), and chalcone **5b** (128 mg, 505 μmol) were suspended in CH_2Cl_2 (5 mL), and aq. NaOH (32%, 1 mL) was added. The reaction mixture was stirred till **5b** was consumed (monitored by TLC, ~30 min), then water (20 mL) was added and the organic layer was separated. The aqueous layer was washed with CH_2Cl_2 (2×10 mL), and the combined organic layers were dried over Na_2SO_4. Chloranil (246 mg, 1.00 mmol) was added to the extracts and the reaction mixture was stirred for 3 h at 20 °C. The solvent was evaporated and the crude product was subjected to column chromatography (silica; *n*-pentane:EtOAc = 10:1). **16b** was obtained as yellow solid (140 mg, 317 μmol, 63%). **Mp** (Et₂O): 199 °C. **¹H NMR** (300 MHz, CDCl₃) δ = 8.18 (dt, *J* = 7.0, 1.1 Hz, 1 H, 5-H), 8.11 (dt, *J* = 9.1, 1.2 Hz, 1 H, 8-H), 7.99 – 7.86 (m, 2 H, 2×C$_{ar}$-H), 7.55 – 7.43 (m, 2 H, 2×C$_{ar}$-H), 7.37 – 7.31 (m, 2 H, 2×C$_{ar}$-H), 7.29 – 7.16 (m, 2 H, 7-H, C$_{ar}$-H, superimposed by solvent signal), 7.13 – 7.06 (m, 2 H, 2×C$_{ar}$-H), 6.90 (td, *J* = 6.9, 1.3 Hz, 1 H, 6-H), 3.72 (br s, 1 H, C*H*H^a), 3.26 (br s, 1 H, CH*H*^{a}), 3.01 (s, br, 1 H, C*H*H^b), 2.59 (br s, 1 H, CH*H*^{b}), 1.10 (br s, 3 H, CH₃), 0.60 (br s, 3 H, CH₃). **¹³C NMR** (75 MHz, CDCl₃) δ = 191.8 (s, CO), 162.4 (s, CON), 146.7 (s, C$_{ar}$), 140.6 (s, C$_{ar}$), 139.7 (s, C$_{ar}$), 137.3 (s, C-8^a), 131.8 (d, C$_{ar}$-H), 131.2 (d, 2×C$_{ar}$-H), 129.5 (d, 2×C$_{ar}$-H), 127.9 (d, 2×C$_{ar}$-H), 127.0 (s, C-2), 124.8 (d, C-7), 124.7 (d, C-5), 123.0 (d, 2×C$_{ar}$-H), 120.1 (d, C-8), 118.6 (s, C-3), 114.7 (d, C-6), 111.3 (s, C-1), 43.0 (br t, CH₂), 39.3 (br t, CH₂), 14.3 (br q, CH₃), 12.5 (br q, CH₃). **HRMS** (EI): *m/z* [C₂₆H₂₃N₃O₄]: calcd. 441.4785, found 441.1682. **MS** (EI): *m/z* = 442 (16), 441 (56), 369 (12), 343 (25), 342 (100), 336 (13), 266 (11), 265 (40), 246 (13), 219 (11), 105 (19). DA766
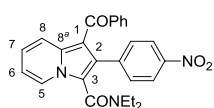
1-Benzoyl-2-(4-nitrophenyl)indolizine-3-carbonitrile hydrate (16c·H₂O) was synthesized according to general procedure E from **1cH⁺Br⁻** (100 mg, 502 μmol), chalcone **5b** (128 mg, 505 μmol), Na₂CO₃ (186 mg, 1.75 mmol), and TPCD (500 mg, 821 μmol). **16c** was obtained as yellow solid (183 mg, 475 μmol, 95%). **Mp** (Et₂O:EtOAc 2:1): 191 °C. **¹H NMR** (300 MHz, CDCl₃) δ = 9.72 (d, *J* = 7.0 Hz, 1 H, 5-H), 8.19 – 8.00 (m, 2 H, 2×C$_{ar}$-H), 7.84 (d, *J* = 8.1 Hz, 1 H, 8-H), 7.56 – 7.45 (m, 4 H, 4×C$_{ar}$-H), 7.38 – 7.31 (m, 1 H, C$_{ar}$-H), 7.31 – 7.16 (m, 3 H, 7-H, 2×C$_{ar}$-H, superimposed by solvent signal), 7.01 (t, *J* = 6.3 Hz, 1 H, 6-H), 5.33 (s, br, 2 H, H₂O). **¹³C NMR** 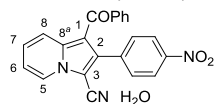(75 MHz, CDCl₃) δ = 191.6 (s, CO), 147.6 (s, C$_{ar}$), 140.9 (s, C$_{ar}$), 139.9 (s, C$_{ar}$), 138.3 (s, C-8^a), 132.6 (s, C-2), 132.0 (d, C$_{ar}$-H), 131.8 (d, 2×C$_{ar}$-H), 129.2 (d, 2×C$_{ar}$-H), 128.5 (d, C-5), 128.2 (d, 2×C$_{ar}$-H), 126.4 (d, C-7), 123.6 (d, 2×C$_{ar}$-H), 123.5 (br s, C-3), 119.4 (d, C-8), 115.2 (br s, C-1), 115.1 (d, C-6),

113.9 (s, CN). **HRMS** (EI): m/z [$C_{22}H_{15}N_3O_4$]: calcd. 385.1063, found 385.1059. **MS** (EI): m/z = 386 (24), 385 (100), 309 (12), 308 (60), 262 (18), 77 (11), 43 (13). DA540

1-(1-Benzoyl-2-(4-nitrophenyl)indolizin-3-yl)ethanone (16d) was synthesized according to general procedure E from **1dH$^+$Cl$^-$** (86 mg, 501 μmol), chalcone **5b** (128 mg, 505 μmol), Na$_2$CO$_3$ (186 mg, 1.75 mmol), and TPCD (500 mg, 821 μmol). **16d** was obtained as yellow, needle-shaped crystals (98 mg, 0.25 mmol, 50%). **Mp** (Et$_2$O): 168 °C. **^{1}H NMR** (300 MHz, CDCl$_3$) δ = 10.04 (dt, J = 7.2 Hz, 1.0, 1 H, 5-H), 8.15 − 8.07 (m, 2 H, 2×C$_{ar}$-H), 7.85 − 7.77 (m, 1 H, 8-H), 7.52 − 7.43 (m, 4 H, 4×C$_{ar}$-H), 7.41 − 7.33 (m, 2 H, 7-H, C$_{ar}$-H), 7.26 − 7.19 (m, 2 H, 2×C$_{ar}$-H), 7.10 (td, J = 7.0, 1.5 Hz, 1 H, 6-H), 1.95 (s, 3 H, CH$_3$). **^{13}C NMR** (75 MHz, CDCl$_3$) δ = 191.9 (s, CO), 189.4 (s, CO), 147.6 (s, C$_{ar}$), 142.2 (s, C$_{ar}$), 139.8 (s, C$_{ar}$), 138.5 (s, C-8^a), 137.3 (s, C-2), 132.2 (d, C$_{ar}$-H), 131.6 (d, 2×C$_{ar}$-H), 129.2 (d, 2×C$_{ar}$-H), 129.0 (d, C-5), 128.3 (d, 2×C$_{ar}$-H), 127.9 (d, C-7), 123.2 (d, 2×C$_{ar}$-H), 122.2 (s, C-3), 119.2 (d, C-8), 116.1 (d, C-6), 115.5 (s, C-1), 31.1 (q, CH$_3$). **HRMS** (EI): m/z [$C_{23}H_{16}N_2O_4$]: calcd. 384.1110, found 384.1105. **MS** (EI): m/z = 385 (24), 384 (100), 369 (17), 307 (41). DA538-2
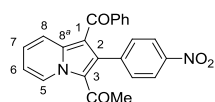
(2-(4-Nitrophenyl)indolizine-1,3-diyl)bis(phenylmethanone) (16e) was synthesized according to general procedure E from **1eH$^+$Br$^-$** (140 mg, 503 μmol), chalcone **5b** (128 mg, 505 μmol), Na$_2$CO$_3$ (186 mg, 1.75 mmol), and TPCD (500 mg, 821 μmol). **16e** was obtained as yellow solid (209 mg, 468 μmol, 93%). **Mp** (Et$_2$O): 225–226 °C. **^{1}H NMR** (300 MHz, CDCl$_3$) δ = 9.67 (d, J = 7.1 Hz, 1 H, 5-H), 8.10 (d, J = 9.0 Hz, 1 H, 8-H), 7.61 − 7.53 (m, 2 H, 2×C$_{ar}$-H), 7.49 − 7.38 (m, 3 H, 6-H, 2×C$_{ar}$-H), 7.38 − 7.30 (m, 2 H, 2×C$_{ar}$-H), 7.29 − 7.19 (m, 1 H, C$_{ar}$-H, superimposed by solvent signal), 7.19 − 6.94 (m, 8 H, 7-H, 7×C$_{ar}$-H). **^{13}C NMR** (75 MHz, CDCl$_3$) δ = 192.12 (s, CO), 187.9 (s, CO), 146.3 (s, C$_{ar}$), 140.9 (s, C$_{ar}$), 139.3 (s, C$_{ar}$), 139.1 (s, C$_{ar}$), 139.1 (s, C-8^a), 136.4 (s, C-2), 132.3 (d, C$_{ar}$-H), 132.2 (d, C$_{ar}$-H), 131.9 (d, 2×C$_{ar}$-H), 129.5 (d, 2×C$_{ar}$-H), 129.4 (d, 2×C$_{ar}$-H), 128.1 (d, 2×C$_{ar}$-H), 128.0 (d, C-5), 127.9 (d, 2×C$_{ar}$-H), 127.8 (d, C-7), 122.1 (d, 2×C$_{ar}$-H), 121.5 (s, C-3), 119.6 (d, C-8), 116.0 (d, C-6), 114.4 (s, C-1). **HRMS** (EI): m/z [$C_{28}H_{18}N_2O_4$]: calcd. 446.1267, found 446.1256. **MS** (EI): m/z = 447 (33), 446 (100), 369 (42), 341 (10), 105 (36), 58 (23). DA539
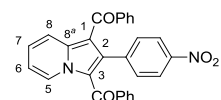
(8-Chloro-2-(4-nitrophenyl)indolizine-1,3-diyl)bis(phenylmethanone) **(16g)** was synthesized according to general procedure E from **1gH⁺Br⁻** (155 mg, 496 μmol), chalcone **5b** (128 mg, 505 μmol), Na₂CO₃ (186 mg, 1.75 mmol), and TPCD (500 mg, 821 μmol). **16g** was obtained in 85% yield (204 mg, 424 μmol, **16g-(8-Cl)**: **16g-(6-Cl)** 4:1 determined from crude product) after column chromatography. Pure **16g-(8-Cl)** was obtained as yellow solid after recrystallization (125 mg, 260 μmol, 52%). **Mp 16g-(8-Cl)** (Et₂O): 241 °C. **¹H NMR** (600 MHz, CDCl₃) δ = 9.65 (dd, J = 7.2, 0.7 Hz, 1 H, 5-H), 7.69 (d, J = 8.9 Hz, 2 H, 2×C_{ar}-H), 7.67 – 7.62 (m, 2 H, 2×C_{ar}-H), 7.47 – 7.41 (m, 1 H, C_{ar}-H), 7.41 – 7.36 (m, 2 H, 2×C_{ar}-H), 7.31 – 7.27 (m, 3 H, 7-H, 2×C_{ar}-H), 7.21 – 7.12 (m, 3 H, 3×C_{ar}-H), 7.03 (dd, J = 9.5, 6.0 Hz, 2 H, 2×C_{ar}-H), 6.97 (t, J = 7.3 Hz, 1 H, 6-H). **¹³C NMR** (150 MHz, CDCl₃) δ = 193.5 (s, CO), 187.4 (s, CO), 146.7 (s, C_{ar}), 140.1 (s, C-8^a), 139.0 (s, C_{ar}), 138.9 (s, C_{ar}), 135.0 (s, C-2), 133.7 (d, C_{ar}-H), 132.3 (s, C_{ar}), 132.0 (d, C_{ar}-H), 131.7 (d, 2×C_{ar}-H), 129.7 (d, 2×C_{ar}-H), 129.5 (d, 2×C_{ar}-H), 128.6 (d, 2×C_{ar}-H), 128.0 (d, 2×C_{ar}-H), 126.5 (d, C-5), 125.5 (d, C-7), 124.7 (s, C-8), 122.6 (d, 2×C_{ar}-H), 121.4 (s, C-3), 116.3 (s, C-1), 114.4 (d, C-6). **HRMS** (EI): m/z [$C_{28}H_{17}ClN_2O_4$]: calcd. 480.0877, found 480.0871. **MS** (EI): m/z = 482 (34), 481 (28), 480 (100), 405 (22), 404 (17), 403 (65), 331 (13), 231 (14), 181 (17), 119 (24), 105 (42), 44 (94). DA543

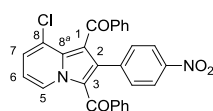**(2-(4-Nitrophenyl)pyrrolo[2,1-a]isoquinoline-1,3-diyl)bis(phenylmethanone) (16h)** was synthesized according to general procedure E from **1hH⁺Br⁻** (164 mg, 500 μmol), chalcone **5b** (128 mg, 505 μmol), Na₂CO₃ (186 mg, 1.75 mmol), and TPCD (500 mg, 821 μmol). **16h** was obtained as orange solid (227 mg, 457 μmol, 91%). **Mp** (Et₂O): 203 – 204 °C. **¹H NMR** (300 MHz, CDCl₃) δ = 9.22 (d, J = 7.6 Hz, 1 H, 5-H), 7.98 (d, J = 8.2 Hz, 1 H, 10-H), 7.78 – 7.63 (m, 5H, 7-H, 4×C_{ar}-H), 7.57 – 7.49 (m, 1 H, 8-H), 7.46 (dd, J = 8.3, 1.3 Hz, 2 H, 2×C_{ar}-H), 7.43–7.35 (m, 2 H, 9-H, C_{ar}-H), 7.27 – 7.10 (m, 6 H, 6-H, 5×C_{ar}-H, superimposed by solvent signal), 7.03 (dd, J = 10.5, 4.7 Hz, 2 H, 2×C_{ar}-H). **¹³C NMR** (75 MHz, CDCl₃) δ = 195.8 (s, CO), 187.7 (s, CO), 146.4 (s, C_{ar}), 140.7 (s, C-10^b), 139.0 (s, C_{ar}), 138.0 (s, C_{ar}), 134.0 (d, C_{ar}-H), 133.3 (s, C-2), 132.3 (d, C_{ar}-H), 132.2 (s, C_{ar}), 131.7 (d, 2×C_{ar}-H), 129.9 (d, 2×C_{ar}-H), 129.8 (s, C-10^a), 129.7 (d, 2×C_{ar}-H), 128.8 (d, C-8), 128.7 (d, 2×C_{ar}-H), 128.4 (d, C-9), 128.0 (d, 2×C_{ar}-H), 127.5 (d, C-7), 125.0 (d, C-10), 124.4 (d, C-5), 124.0 (s, C-6^a), 122.53 (d, 2×C_{ar}-H), 122.5 (s, C-3), 117.7 (s, C-1), 115.2 (d, C-6). **HRMS** (EI): m/z [$C_{32}H_{20}N_2O_4$]: calcd. 496.1423, found 496.1417. **MS** (EI): m/z = 497 (37), 496 (100), 466 (16), 419 (39), 105 (28), 77 (15). DA546
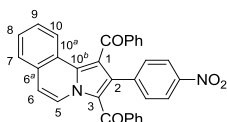
(2-(4-Nitrophenyl)pyrrolo[1,2-*a*]quinoline-1,3-diyl)bis(phenylmethanone) (16i). The pyridinium salt **1iH⁺Br⁻** (164 mg, 500 μmol), and chalcone **5b** (128 mg, 500 μmol) were suspended in CH$_2$Cl$_2$ (5 mL), and aq. NaOH (32%, 1 mL) was added. The reaction mixture was stirred till **5b** was consumed (monitored by TLC, ~ 30 min), then water (20 mL) was added and the organic layer was separated. The aqueous layer was washed with CH$_2$Cl$_2$ (2×10 mL) and the combined organic layers were dried over Na$_2$SO$_4$. Chloranil (246 mg, 1.00 mmol) was added to the extracts, and the mixture was stirred for 3 h at 20 °C. The solvent was evaporated, and the crude product was subjected to column chromatography (silica; *n*-pentane:EtOAc = 10:1). **16i** was obtained as yellow solid (192 mg, 387 μmol, 77%). **Mp** (Et$_2$O): 225 °C. **¹H NMR** (300 MHz, CDCl$_3$) δ = 7.84 (d, *J* = 9.4 Hz, 1 H, 4-H), 7.78 – 7.66 (m, 3 H, 3×C$_{ar}$-H), 7.64 – 7.49 (m, 5 H, 6-H or 9-H, 4×C$_{ar}$-H), 7.47 (d, *J* = 9.4 Hz, 1 H, 5-H), 7.40 – 7.29 (m, 3 H, 6-H or 9-H, 7-H or 8-H, C$_{ar}$-H), 7.28 – 7.06 (m, 7 H, 7-H or 8-H, 6×C$_{ar}$-H, superimposed by solvent signal). **¹³C NMR** (75 MHz, CDCl$_3$) δ = 192.2 (s, CO), 190.3 (s, CO), 146.7 (s, C$_{ar}$), 140.1 (s, C$_{ar}$), 139.3 (s, C-5^a or C-9^a), 137.6 (s, C-5^a or C-9^a), 136.6 (s, C-3^a), 134.2 (d, C-7 or C-8), 132.6 (s, C$_{ar}$), 132.4 (d, C-7 or C-8), 131.9 (d, 2×C$_{ar}$-H), 131.8 (s, C$_{ar}$), 129.8 (d, 2×C$_{ar}$-H), 129.6 (d, 2×C$_{ar}$-H), 129.4 (d, C$_{ar}$-H), 129.2 (d, C$_{ar}$-H), 128.9 (d, 2×C$_{ar}$-H), 128.2 (d, 2×C$_{ar}$-H), 127.1 (d, C-5), 125.6 (d, C-6 or C-9), 125.5 (s, C$_{ar}$), 125.5 (s, C$_{ar}$), 122.5 (d, 2×C$_{ar}$-H), 118.6 (d, C-6 or C-9), 118.0 (d, C-4), 115.8 (s, C$_{ar}$). C-1, C-2, and C-3 could not be assigned unambiguously and are therefore given as C$_{ar}$. **HRMS** (EI): *m/z* [C$_{32}$H$_{20}$N$_2$O$_4$]: calcd. 496.1423, found 496.1416. **MS** (EI): *m/z* = 497 (37), 496 (100), 420 (10), 419 (32), 391 (10), 315 (10), 105 (37), 77 (19), 44 (24), 43 (32). DA545-2
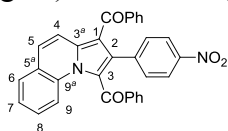
4.5.7   Reactions with Nitrostyrene 5c

(2-(4-Methoxyphenyl)-3-nitro-1,2,3,3a-tetrahydropyrrolo[1,2-*a*]quinolin-1-yl)(phenyl)methanone (19i). NEt$_3$ (160 μl, 1.15 mmol) was added to a solution of **1iH⁺Br⁻** (368 mg, 1.12 mmol) and nitrostyrene **5c** (200 mg, 1.12 mmol) in DMSO (5 mL) at 20 °C. The solution was stirred for 30 min, then water (20 mL) was added and the mixture was extracted with CH$_2$Cl$_2$ (3×10 mL). The combined organic layers were washed with water (2×10 mL), and dried over MgSO$_4$. The solvent was evaporated, and the resulting solid was recrystallized from CHCl$_3$. **19i** was obtained as yellow solid (280 mg, 655 μmol, 59%, single diastereoisomer). **Mp** (Et$_2$O): 166 − 167 °C. **¹H NMR** (400 MHz, DMSO-*d$_6$*) δ 7.76 (dd, *J* = 8.3, 1.2 Hz, 2 H, 2×C$_{ar}$-H), 7.55 – 7.45 (m, 1
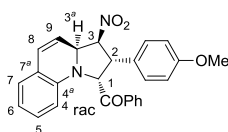
H, C_{ar}-H), 7.33 (t, J = 7.8 Hz, 2 H, 2×C_{ar}-H), 6.99 – 6.93 (m, 2 H, 2×C_{ar}-H), 6.92 – 6.84 (m, 2 H, 5-H, 6-H), 6.59 – 6.46 (m, 4 H, 7-H, 8-H, 2×C_{ar}-H), 6.05 (d, J = 9.8 Hz, 1 H, 1-H), 5.92 (d, J = 8.3 Hz, 1 H, 4-H), 5.88 – 5.80 (m, 1 H, 3^a-H), 5.59 (dd, J = 10.1, 2.5 Hz, 1 H, 9-H), 5.53 (dd, J = 5.5, 2.2 Hz, 1 H, 3-H), 4.76 (dd, J = 9.7, 2.1 Hz, 1 H, 2-H), 3.55 (s, 3 H, OCH_3). ^{13}C NMR (100 MHz, DMSO-d_6) δ 198.4 (s, CO), 158.3 (s, C_{ar}), 141.7 (s, C-4^a), 135.6 (s, C_{ar}), 133.4 (d, C_{ar}-H), 130.6 (d, 2×C_{ar}-H), 129.6 (d, C-6), 128.4 (d, 2×C_{ar}-H), 128.2 (d, C-7), 128.0 (d, 2×C_{ar}-H), 127.5 (d, C-7^a), 127.3 (s, C-8), 119.3 (s, C_{ar}), 117.6 (d, C-9), 117.2 (d, C-5), 113.4 (d, 2×C_{ar}-H), 109.8 (d, C-4), 95.5 (d, C-1), 66.8 (d, C-3), 64.4 (d, C-3^a), 55.0 (q, OCH_3), 47.9 (d, C-2). DA323

2-(4-Methoxyphenyl)-1-nitro-2,3-dihydroindolizine-3-carbonitrile (20c). NEt_3 (180 μl, 1.30 μmol) was added to a solution of **1cH$^+$Br$^-$** (245 mg, 1.23 μmol) and **5c** (200 mg, 1.12 mmol) in DMSO (5 mL) at 20 °C. The reaction mixture was stirred until **5c** was consumed (monitored by TLC; ~ 15 min). DDQ (280 mg, 1.23 mmol) was added and stirring was continued for 30 min at 20 °C. Water was added and the reaction mixture was extracted with CH_2Cl_2 (3×20mL). The combined organic layers were washed with water (2×20 ml), and dried over $MgSO_4$. The solvent was evaporated and the crude reaction product was recrystallized from $CHCl_3$. **20c** was obtained as yellow solid (159 mg, 538 μmol, 48%, dr 1:24 after crystallization). **20c** isomerized in DMSO-d_6:CDCl$_3$-solution (93:7) to dr 1:1. ^{1}H NMR (400 MHz, DMSO-d_6:CDCl$_3$ 100:7) δ = 8.24 – 8.19 (m, 2 H, 2×5-H), 8.11 – 8.05 (m, 2 H, 2×8-H), 7.99 – 7.92 (m, 2 H, 2×7-H), 7.18 – 7.13 (m, 2 H, 2×C_{ar}-H), 7.13 – 7.09 (m, 2 H, 2×C_{ar}-H), 7.00 − 6.94 (m, 2 H, 2×6-H), 6.90 − 6.87 (m, 4 H, 4×C_{ar}-H), 6.38 (d, J = 10.6 Hz, 1 H, 3-H), 5.90 (d, J = 4.3 Hz, 1 H, 3-H), 4.94 – 4.87 (m, 2 H, 2×2-H), 3.71 (s, 3 H, CH_3), 3.70 (s, 3 H, CH_3). ^{13}C NMR (100 MHz, DMSO-d_6:CDCl$_3$) δ = 158.9 (s, C_{ar}), 158.9 (s, C_{ar}), 148.7 (s, C-8^a), 148.6 (s, C-8^a), 143.9 (d, C-5), 143.6 (d, C-5), 137.5 (d, C-7), 137.4 (d, C-7), 130.9 (s, C_{ar}), 129.6 (s, C_{ar}), 129.2 (d, 2×C_{ar}-H), 128.9 (d, 2×C_{ar}-H), 117.8 (d, C-6), 117.6 (d, C-6), 116.4 (s, C-1), 115.7 (d, C-8), 115.5 (d, C-8), 114.3 (s, C-1), 114.1 (s, CN), 114.0 (s, CN), 113.7 (d, 4×C_{ar}-H), 60.6 (d, C-3), 59.8 (d, C-3), 55.1 (q, CH_3), 55.0 (q, CH_3), 48.3 (d, C-2), 45.5 (d, C-2). DA321
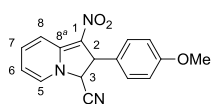
General Procedure E for the Synthesis of Indolizines 21. Pyridinium salt **1H$^+$X$^-$** (0.50−0.60 mmol), nitrostyrene **5c** (500 μmol), and NEt$_3$ (0.7 mmol) were dissolved in DMSO (0.1 M) at room temperature and stirred for 5 min. MnO$_2$ (1.25 mmol) or TPCD (821 μmol) were added and the suspension was heated in a microwave reactor at 100 °C (5 W) for 1 h. The reaction mixture was cooled to room temperature and EtOAc (5 mL) was added. The resulting precipitate was filtered off and washed with EtOAc (20 mL). Brine (50 mL) was added to the filtrate and the aqueous layer was extracted with EtOAc (3×20 mL). The combined organic layers were washed with brine (2×20 mL), dried over Na$_2$SO$_4$, concentrated in vacuo and subjected to a column chromatography (silica, *n*-pentane:EtOAc = 10:1). The products were recrystallized from Et$_2$O:EtOAc or Et$_2$O.

Ethyl 2-(4-methoxyphenyl)-1-nitroindolizine-3-carboxylate (21a). From **1aH$^+$Br$^-$** (123 mg, 500 μmol), nitrostyrene **5c** (90 mg, 0.50 mmol), NEt$_3$ (80 μl, 0.58 mmol), and MnO$_2$ (109 mg, 1.25 mmol) according to general procedure **E**. **21a** was obtained as orange needles (91 mg, 0.27 mmol, 54%). **Mp** (Et$_2$O) 142 °C. **^{1}H NMR** (300 MHz, CDCl$_3$) δ = 9.70 (dt, *J* = 7.1, 1.0 Hz, 1 H, 5-H), 8.59 (dt, *J* = 9.0, 1.2 Hz, 1 H, 8-H), 7.57 (ddd, *J* = 9.1, 6.9, 1.1 Hz, 1 H, 7-H), 7.29 – 7.19 (m, 2 H, 2×C$_{ar}$-H, superimposed by solvent signal), 7.15 (td, *J* = 7.0, 1.4 Hz, 1 H, 6-H), 7.01 – 6.92 (m, 2 H, 2×C$_{ar}$-H), 4.08 (q, *J* = 7.1 Hz, 2 H, CH$_2$), 3.87 (s, 3 H, CH$_3$), 0.92 (t, *J* = 7.1 Hz, 3 H, CH$_3$). **^{13}C NMR** (75 MHz, CDCl$_3$) δ = 161.6 (s, CO$_2$), 159.5 (s, C$_{ar}$), 134.4 (s, C$_{ar}$), 134.3(s, C-8^a), 130.5 (d, 2×C$_{ar}$-H), 129.4 (d, C-7), 128.4 (d, C-5), 125.0 (s, C-2), 124.8 (br s, C-1), 119.4 (d, C-8), 116.2 (d, C-6), 113.7 (s, C-3), 113.3 (d, 2×C$_{ar}$-H), 60.7 (t, CH$_2$), 55.5 (q, CH$_3$), 13.7 (q, CH$_3$). **HRMS** (EI): *m/z* [C$_{18}$H$_{16}$N$_2$O$_5$]: calcd. 340.1059, found 340.1054. **MS** (EI) *m/z* = 341 (18), 340 (100), 268 (10), 78 (11). DA575
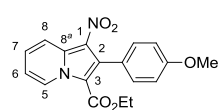
N,N-Diethyl-2-(4-methoxyphenyl)-1-nitroindolizine-3-carboxamide hydrate (21b·H$_2$O). Aq. NaOH (1 mL, 32%) was added to a suspension of **1bH$^+$Br$^-$** (150 mg, 550 μmol) and **5c** (90 mg, 0.50 mmol) in CH$_2$Cl$_2$ (5 mL) at ambient temperature. The reaction was stirred until **5c** was consumed (monitored by TLC, ~ 30 min). Water (20 mL) was added, the organic layer was separated, and the aqueous layer was washed twice with CH$_2$Cl$_2$ (2×10 mL). The combined organic layers were dried over Na$_2$SO$_4$. Chloranil (244 mg, 992 mmol) was added to the extract and the reaction was stirred for 3 h. The solvent was evaporated and the crude product was purified by column chromatography over silica (*n*-pentane:EtOAc = 10:1). **21b·H$_2$O** was obtained as red solid (20 mg, 52 μmol, 10%). **Mp** (Et$_2$O) 180 °C. **^{1}H NMR** (300 MHz, CDCl$_3$) δ = 8.54
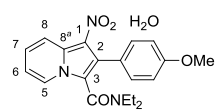
(dt, J = 9.1, 1.2 Hz, 1 H, 8-H), 8.26 (dt, J = 6.9, 1.1 Hz, 1 H, 5-H), 7.48 – 7.38 (m, 3 H, 7-H, 2×C_{ar}-H), 7.03 – 6.91 (m, 3 H, 6-H, 2×C_{ar}-H), 3.85 (s, 3 H, CH$_3$), 3.83 – 3.70 (m, 1 H, CHH^a), 3.27 – 3.05 (m, 2 H, CHH^a, CHH^b), 2.75 – 2.54 (m, 1 H, CHH^b), 1.70 (br s, 2 H, H$_2$O), 1.08 (t, J = 7.1 Hz, 3 H, CH$_3$), 0.66 (t, J = 7.1 Hz, 3 H, CH$_3$). **^{13}C NMR** (75 MHz, CDCl$_3$) δ = 161.7 (s, CON), 160.2 (s, C$_{ar}$), 133.6 (s, C-8^a), 131.9 (d, 2×C_{ar}-H), 128.1 (d, C-7), 125.9 (d, C-5), 125.7 (s, C$_{ar}$), 125.6 (br s, C-1), 123.1 (s, C-2), 120.0 (d, C-8), 118.6 (s, C-3), 115.5 (d, C-6), 113.9 (d, 2×C_{ar}-H), 55.6 (q, OCH$_3$), 43.0 (t, CH$_2$), 39.4 (t, CH$_2$), 14.3 (q, CH$_3$), 12.6 (q, CH$_3$). **HRMS** (EI): m/z [C$_{20}$H$_{21}$N$_3$O$_4$]: calcd. 367.1532, found 367.1546. **MS** (EI) m/z = 367 (51), 278 (32), 268 (100), 238 (15), 178 (9). DA768

2-(4-Methoxyphenyl)-1-nitroindolizine-3-carbonitrile (21c). From **1cH$^+$Br$^-$** (100 mg, 502 μmol), **5c** (90.0 mg, 0.50 mmol), NEt$_3$ (100 μl, 724 μmol), and MnO$_2$ (109 mg, 1.25 mmol) according to general procedure **E**. **21c** was obtained as beige solid (94 mg, 0.32 mmol, 64%). **Mp** (Et$_2$O) 175 °C (decomp.). **^{1}H NMR** (300 MHz, CDCl$_3$) δ = 8.59 (dt, J = 9.1, 1.2 Hz, 1 H, 8-H), 8.43 (dt, J = 6.8, 1.0 Hz, 1 H, 5-H), 7.62 (ddd, J = 9.1, 7.0, 1.1 Hz, 1 H, 7-H), 7.58 – 7.49 (m, 2 H, 2×C_{ar}-H), 7.27 – 7.19 (m, 1 H, 6-H, superimposed by solvent signal), 7.08 – 6.99 (m, 2 H, 2×C_{ar}-H), 3.89 (s, 3 H, CH$_3$). **^{13}C NMR** (75 MHz, CDCl$_3$) δ = 161.0 (s, C$_{ar}$), 136.3 (s, C$_{ar}$), 134.4 (s, C-8^a), 131.5 (d, 2× C$_{ar}$-H), 130.1 (d, C-7), 125.9 (d, C-5), 121.0 (br s, C-1), 120.7 (s, C-2), 120.4 (d, C-8), 116.9 (d, C-6), 114.2 (d, 2×C_{ar}-H), 112.0 (s, CN), 97.4 (s, C-3), 55.5 (q, CH$_3$). **HRMS** (EI): m/z [M+H]$^+$; [C$_{16}$H$_{12}$N$_3$O$_3$]: calcd. 294.0879, found 294.1815. **MS** (EI) m/z = 294 (21), 293 (100), 263 (31), 233 (20), 203 (22), 193 (14), 78 (21), 43 (15). DA581

1-(2-(4-Methoxyphenyl)-1-nitroindolizin-3-yl)ethanone (21d). From **1dH$^+$Cl$^-$** (86 mg, 0.50 mmol), nitrostyrene **5c** (90.0 mg, 0.50 mmol), NEt$_3$ (100 μl, 721 μmol), and MnO$_2$ (109 mg, 1.25 mmol) according to general procedure **E**. **21d** was obtained as yellow solid (108 mg, 0.35 mmol, 70%). **Mp** (Et$_2$O) 173 °C. **^{1}H NMR** (300 MHz, CDCl$_3$) δ = 10.07 (dt, J = 7.2, 1.0 Hz, 1 H, 5-H), 8.62 (dt, J = 9.0, 1.2 Hz, 1 H, 8-H), 7.64 (ddd, J = 8.9, 7.0, 1.1 Hz, 1 H, 7-H), 7.33 – 7.26 (m, 2 H, 2×C_{ar}-H), 7.18 (td, J = 7.0, 1.4 Hz, 1 H, 6-H), 7.07 – 7.00 (m, 2 H, 2×C_{ar}-H), 3.89 (s, 3 H, CH$_3$), 1.94 (s, 3 H, CH$_3$). **^{13}C NMR** (75 MHz, CDCl$_3$) δ = 191.0 (s, CO), 160.2 (s, C$_{ar}$), 135.2 (s, C$_{ar}$), 134.2 (s, C-8^a), 130.7 (d, C-7), 130.6 (d, 2×C_{ar}-H), 129.4 (d, C-5), 125.1 (br s, C-1), 124.7 (s, C-2), 121.9 (s, C-3), 119.1 (d, C-8), 116.9 (d, C-6), 114.3 (d, 2×C_{ar}-H), 55.5 (q, CH$_3$), 30.9 (q, CH$_3$). **HRMS** (EI): m/z [C$_{17}$H$_{14}$N$_2$O$_4$]: calcd. 310.0954, found 310.0947. **MS** (EI) m/z = 311 (20), 310 (100), 278 (34), 248 (10), 78 (10). DA580

(2-(4-Methoxyphenyl)-1-nitroindolizin-3-yl)(phenyl)methanone (21e). From **1eH⁺Br⁻** (140 mg, 503 µmol), nitrostyrene **5c** (90.0 mg, 0.50 mmol), NEt₃ (100 µl, 721 µmol), and TPCD (500 mg, 821 µmol) according to general procedure **E**. **21e** was obtained as orange solid (127 mg, 341 µmol, 68%). **Mp** (Et₂O) 147 °C. **¹H NMR** (300 MHz, CDCl₃) δ = 9.48 (d, *J* = 7.1 Hz, 1 H, 5-H), 8.65 (d, *J* = 8.8 Hz, 1 H, 8-H), 7.70 – 7.57 (m, 1 H, 7-H), 7.39 (d, *J* = 7.6 Hz, 2 H, 2×C$_{ar}$-H), 7.27 – 7.20 (m, 1 H, C$_{ar}$-H, , superimposed by solvent signal), 7.17 (t, *J* = 6.9 Hz, 1 H, 6-H), 7.11 – 7.03 (m, 4 H, 4×C$_{ar}$-H), 6.58 (d, *J* = 8.5 Hz, 2 H, 2×C$_{ar}$-H), 3.68 (s, 3 H, CH₃). **¹³C NMR** (75 MHz, CDCl₃) δ = 188.7 (s, CO), 159.7 (s, C$_{ar}$), 138.4 (s, C$_{ar}$), 134.9 (s, C$_{ar}$), 134.1 (s, C-8^a), 132.7 (d, 2×C$_{ar}$-H), 132.0 (d, C$_{ar}$-H), 130.4 (d, C-6), 129.4 (d, 2×C$_{ar}$-H), 128.2 (d, C-5), 127.9 (d, 2×C$_{ar}$-H), 124.0 (br s, C-1), 123.0 (s, C-2), 121.6 (s, C-3), 119.6 (d, C-8), 116.5 (d, C-7), 113.2 (d, 2×C$_{ar}$-H), 55.4 (q, CH₃). **HRMS** (EI): *m/z* [C₂₂H₁₆N₂O₄]: calcd. 372.1110, found 372.1104. **MS** (EI) *m/z* = 373 (26), 372 (100), 342 (22), 254 (11), 105 (31), 77 (19). DA578
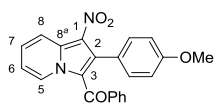
2-(4-Methoxyphenyl)-1-nitroindolizin-3-yl)(phenyl)methanone (21e). **21e** was also synthesized by employing MnO₂ (109 mg, 1.25 mmol, 2.5 equiv.; Yield **21e**: 90 mg, 0.24 mmol, 48%, 4:1 **21e**-(**8-Cl**): **21e**-(**6-Cl**)) or KMnO₄:MnO₂ (1:3 by weight, grounded, 150 mg; Yield **21e**: 99 mg, 0.27 mmol, 54%,4:1 **21e**-(**8-Cl**): **21e**-(**6-Cl**)) as oxidants according to procedure **E** with the same amounts of the reactants **1eH⁺Br⁻** and **5c** as above, but with KO^{t}Bu (57 mg, 0.51 mmol) as base. (Analytical data see above) DA578-2,3

(8-Chloro-2-(4-methoxyphenyl)-1-nitroindolizin-3-yl)(phenyl)methanone (21g-(8-Cl)) **and (6-chloro-2-(4-methoxyphenyl)-1-nitroindolizin-3-yl)(phenyl)methanone (21g-(6-Cl)).** **1gH⁺Br⁻** (375 mg, 1.20 mmol) and nitrostyrene **5c** (200 mg, 1.12 mmol) were dissolved in DMSO (5 mL), and NEt₃ (180 µl, 1.30 mmol) was added at ambient temperature. The mixture was stirred till the reaction was completed (~ 30 min; monitored by TLC), then DDQ (279 mg, 1.23 µmol) in DMSO (2 mL) was added and the reaction was stirred for 3 h. Water (10 mL) was added and the aqueous layer was extracted with CH₂Cl₂ (3×10 mL). The combined organic layers were washed with water (2×10 mL) and dried over MgSO₄. The solvent was evaporated and the crude material was subjected to a column chromatography (silica, *n*-pentane:EtOAc = 5:1). **21g** was obtained in two fractions in 55% over all yield. Fraction 1: **21g-(8-Cl)**, yellow solid (65.9 mg, 162 µmol, 14%); Fraction 2: ~ 1 : 1 mixture (by ¹H NMR) of **21g-(6-Cl)** and **21g-(8-Cl)**, red solid, (184 mg, 452 µmol, 41%). **Mp 21g-(8-Cl)** (Et₂O: EtOAc) 98 °C. Only NMR-signals of **21g-(8-Cl)** are given. **¹H NMR** (300 MHz, CDCl₃) δ = 9.48 (dd, *J* = 7.1, 0.8 Hz, 1 H, 5-H), 7.46 – 7.37 (m, 3
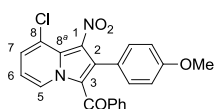
H, 7-H, 2×C$_{ar}$-H), 7.28 – 7.19 (m, 1 H, C$_{ar}$-H), 7.12 – 7.03 (m, 4 H, 4×C$_{ar}$-H), 6.97 (t, J = 7.3 Hz, 1 H, 6-H), 6.63 – 6.54 (m, 2 H, 2×C$_{ar}$-H), 3.69 (s, 3 H, CH$_3$). **^{13}C NMR** (75 MHz, CDCl$_3$) δ = 187.8 (s, CO), 159.8 (s, C$_{ar}$), 138.2 (s, C$_{ar}$), 132.2 (d, 2×C$_{ar}$-H), 132.0 (d, C$_{ar}$-H), 129.4 (d, 2×C$_{ar}$-H), 129.4 (s, C$_{ar}$), 128.1 (br s, C-1), 127.8 (d, C-7), 127.8 (d, 2×C$_{ar}$-H), 127.3 (s, C-8^a), 126.1 (d, C-5), 123.5 (s, C-8), 121.9 (s, C-2), 119.6 (s, C-3), 114.5 (d, C-6), 113.5 (d, 2×C$_{ar}$-H), 55.3 (q, OCH$_3$). **HRMS** (EI): m/z [C$_{22}$H$_{15}$ClN$_2$O$_4$]: calcd. 406.0720, found 406.0709. **MS** (EI) m/z = 409 (10), 408 (39), 406 (100), 376 (10), 105 (19), 77 (11). DA372

(8-Chloro-2-(4-methoxyphenyl)-1-nitroindolizin-3-yl)(phenyl)methanone (21g-(8-Cl)) and (6-chloro-2-(4-methoxyphenyl)-1-nitroindolizin-3-yl)(phenyl)methanone (21g-(6-Cl)). 21g was also synthesized by employing MnO$_2$ (109 mg, 1.25 mmol, 2.5 equiv.; Yield **21g**: 135 mg, 332 µmol, 67%, **21g(8-Cl)**: **21g(6-Cl)** 4:1) or TPCD (500 mg, 846 µmol; Yield: 109 mg, 268 µmol, 54%,**21g(8-Cl)**: **21g(6-Cl)** 4:1) as oxidants according to procedure E using **1gH$^+$Br$^−$** (155 mg, 496 µmol), **5c**: (90 mg, 0.50 mmol), and NEt$_3$: (100 µl, 721 µmol) as reactants in each experiment. (Analytical data see above) DA582-1+2

(2-(4-Methoxyphenyl)-1-nitropyrrolo[2,1-a]isoquinolin-3-yl)(phenyl)methanone (21h) & (2-(4-methoxyphenyl)pyrrolo[2,1-a]isoquinolin-3-yl)(phenyl)methanone (22h). From **1hH$^+$Br$^−$** (164 mg, 500 µmol), **5c** (90 mg, 0.50 mmol), NEt$_3$ (100 µl, 721 µmol), and TPCD (500 mg, 821 µmol) according to general procedure **E**. **21h** and **22h** were not separated and obtained as yellow solid in a 1:2 mixture (over all: 133 mg, 326 µmol, 65%). Signals marked with $^{\#}$ refer to **22h**, signals marked with * refer to **21h.** Integrals for **21h** are set to 1.0 for one proton of **21h**. **^{1}H NMR** (600 MHz, CDCl$_3$) δ = 9.29$^{\#}$ (d, J = 7.6 Hz, 2 H, 5-H), 9.02* (d, J = 7.5 Hz, 1 H, 5-H), 8.45* (d, J = 8.2 Hz, 1 H, 10-H), 8.17$^{\#}$ (d, J = 7.7 Hz, 2 H, 10-H), 7.78* (d, J = 7.5 Hz, 1 H, 7-H), 7.70$^{\#}$ (d, J = 7.3 Hz, 2 H, 7-H), 7.66* (td, J = 7.6, 1.1 Hz, 1 H, 8-H), 7.64 – 7.60* (m, 1 H, 9-H), 7.59 – 7.46$^{\#,*}$ (m, 10 H, 8-H, 9-H, 4×C$_{ar}$-H), 7.29 – 7.25* (m, 1 H, C$_{ar}$-H, superimposed by solvent signal), 7.25 – 7.18$^{\#,*}$ (m, 3 H, 6-H, C$_{ar}$-H), 7.13 – 7.01$^{\#,*}$ (m, 16 H, 1-H, 6-H, 8×C$_{ar}$-H), 6.65 – 6.53$^{\#,*}$ (m, 6 H, 4×C$_{ar}$-H), 3.71$^{\#}$ (s, 6 H, CH$_3$), 3.69* (s, 3 H, CH$_3$). **^{13}C NMR** (150 MHz, CDCl$_3$) δ = 188.2 (s), 187.7 (s), 159.6 (s), 158.6 (s), 139.8 (s), 138.3 (s), 138.0 (s), 134.9 (s), 132.3 (s), 132.2 (d), 131.3 (d, 3×C), 130.8 (d), 130.4 (d), 130.2 (br s), 130.0 (d), 129.8 (d), 129.7 (d), 129.0 (s), 128.6 (d), 128.3 (2×C, s), 128.0 (d), 127.9 (d), 127.8 (d), 127.6 (d), 127.6 (d), 127.0 (d), 125.5 (d), 125.1 (d), 124.7 (s), 123.8 (d), 123.6 (d), 122.7 (s), 122.3 (s), 122.0 (s), 115.6 (d), 113.5 (d), 113.4 (d), 112.9 (d), 103.5 (d), 55.4 (q), 55.3 (q). ^{13}C NMR signals could be assigned unambiguously. **21h. HRMS** (EI): m/z

[$C_{26}H_{18}N_2O_4$]: calcd. 422.1267, found 422.1263. **MS** (EI): m/z = 422 (12), 392 (17), 378 (29), 377 (100), 348 (28), 300 (26), 228 (14), 189 (18), 105 (10), 77 (12). DA584-2

(2-(4-Methoxyphenyl)pyrrolo[2,1-a]isoquinolin-3-yl)(phenyl)methanone (22h) was synthesized from **1hH⁺Br⁻** (164 mg, 500 µmol), nitrostyrene **5c** (90.0 mg, 0.50 mmol), NEt₃ (200 µl, 1.45 mmol) by stirring in DMSO (5 mL) in air at 20 °C for 5 h. **22h** was obtained as yellow solid (20 mg, 53 µmol, 11%). **Mp** (Et₂O) 185 − 186 °C. **¹H NMR** (300 MHz, CDCl₃) δ = 9.29 (d, J = 7.6 Hz, 1 H, 5-H), 8.17 (dd, J = 7.6, 1.7 Hz, 1 H, 10-H), 7.71 (dd, J = 7.3, 1.9 Hz, 1 H, 7-H), 7.61 − 7.47 (m, 4 H, 8-H, 9-H, 2×C_{ar}-H), 7.25 − 7.16 (m, 1 H, C_{ar}-H), 7.12 − 6.96 (m, 6 H, 1-H, 6-H, 4×C_{ar}-H), 6.66 − 6.51 (m, 2 H, 2×C_{ar}-H), 3.71 (s, 3 H, CH₃). **¹³C NMR** (75 MHz, CDCl₃) δ) = 187.7 (s, CO), 158.6 (s, C_{ar}), 139.8 (s, C-2), 138.0 (s, C_{ar}), 135.0 (s, C-10^a), 131.3 (d, 3×C_{ar}-H), 130.0 (d, 2×C_{ar}-H), 129.1 (s, C-6^a), 128.4 (s, C_{ar}), 128.0 (d, C-8 or -9), 127.8 (d, C-8 or -9), 127.6 (d, 2×C_{ar}-H), 127.0 (d, C-7), 125.5 (d, C-5), 124.8 (s, C-10^b), 123.6 (d, C-10), 122.0 (s, C-3), 113.4 (d, 2×C_{ar}-H), 112.9 (d, C-6), 103.5 (d, C-1), 55.4 (q, CH₃). **HRMS** (EI): m/z [$C_{26}H_{19}N_1O_2$]: calcd. 377.1416, found. 377.1397 **MS** (EI): m/z = 378 (28), 377 (100), 348 (23), 300 (22), 228 (12), 189 (14). DA584-3
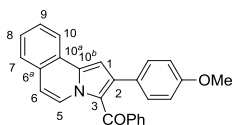
(2-(4-Methoxyphenyl)-3-nitropyrrolo[1,2-a]quinolin-1-yl)(phenyl)methanone (21i) & **(2-(4-Methoxyphenyl)pyrrolo[1,2-a]quinolin-1-yl)(phenyl)methanone (22i)** were synthesized according to general procedure E from **1iH⁺Br⁻** (164 mg, 500 µmol), nitrostyrene **5c** (90.0 mg, 0.50 mmol), NEt₃ (100 µl, 721 µmol), and TPCD (500 mg, 821 µmol). **22i** was eluted as first fraction and obtained as yellow solid (60 mg, 0.16 mmol, 32%). **21i** was eluted as second fraction and obtained as red solid (45 mg, 0.11 mmol, 22%). **21i. Mp** (Et₂O) 164 °C. **¹H NMR** (600 MHz, CDCl₃) δ = 8.52 (d, J = 9.5 Hz, 1 H, 6-H), 7.83 (dd, J = 7.7, 1.7 Hz, 1 H, 7-H), 7.79 (d, J = 9.2 Hz, 1 H, 9-H), 7.73 (dd, J = 8.3, 1.2 Hz, 2 H, 2×C_{ar}-H), 7.64 − 7.58 (m, 1 H, 4-H), 7.49 − 7.41 (m, 3 H, 5-H, 8-H, C_{ar}-H), 7.29 − 7.25 (m, 2 H, 2×C_{ar}-H), 7.17 (d, J = 8.8 Hz, 2 H, 2×C_{ar}-H), 6.70 (d, J = 8.8 Hz, 2 H, 2×C_{ar}-H), 3.71 (s, 3 H, CH₃). **¹³C NMR** (150 MHz, CDCl₃) δ = 190.1 (s, CO), 159.5 (s, C_{ar}), 137.4 (s, C_{ar}), 134.1 (d, C_{Ar}-H), 132.6 (s, C-5^a, C-9^a), 132.0 (s, C_{ar}), 131.8 (d, 2×C_{ar}-H), 130.5 (s, C-3), 130.1 (d, C-7), 130.0 (d, 2×C_{Ar}-H), 129.6 (d, C-9), 129.2 (d, C-8), 128.7 (d, 2×C_{ar}-H), 126.1 (d, C-5), 125.4 (s, C-3^a), 122.6 (d, C-2), 118.8 (d, C-4), 117.3 (d, C-6), 114.7 (s, C-1), 113.4 (d, 2×C_{ar}-H), 55.3 (q, OCH₃). **HRMS** (EI): m/z [$C_{26}H_{18}N_2O_4$]: calcd. 422.1267, found 422.1253. **MS** (EI) m/z = 423 (32), 422 (100), 105 (10). **22i. Mp** (Et₂O) 150 °C. **¹H NMR** (600 MHz, CDCl₃) δ =
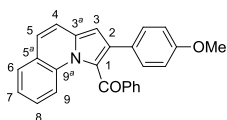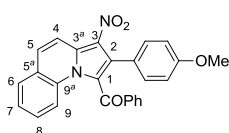
7.74 (dd, J = 8.4, 1.3 Hz, 2 H, 2×C_{ar}-H), 7.64 −7.62 (m, 1 H, 9-H), 7.60 (dd, J = 7.8, 1.1 Hz, 1 H, 6-H), 7.39 − 7.33 (m, 2 H, 4-H, C_{ar}-H), 7.30 − 7.18 (m, 7 H, 5-H, 7-H, 8-H, 4×C_{ar}-H, superimposed by solvent signal), 6.77 − 6.69 (m, 2 H, 2×C_{ar}-H), 6.65 (s, 1 H, 3-H), 3.72 (s, 3 H, OCH$_3$). **^{13}C NMR** (150 MHz, CDCl$_3$) δ = 190.0 (s, CO), 158.8 (s, C_{ar}), 138.8 (s, C_{ar}), 135.4 (s, C-2) , 134.6 (s, C-3^a), 133.5 (s, C-9^a), 133.0 (d, C_{ar}-H), 130.8 (d, 2×C_{ar}-H), 130.1 (d, 2×C_{ar}-H), 128.9 (d, C-9), 128.4 (d, 2×C_{ar}-H), 128.0 (d, C-8), 127.6 (s, C_{ar}), 125.0 (s, C-5^a), 124.1 (d, C-7 & br s, C-1), 123.3 (d, C-4), 118.6 (d, C-6), 118.2 (d, C-5), 113.5 (d, 2×C_{ar}-H), 105.0 (d, C-3), 55.3 (q, CH$_3$). **HRMS** (EI): m/z [C$_{26}$H$_{19}$NO$_2$]: calcd. 377.1416, found 377.0477. **MS** (EI) m/z = 378 (26), 377 (100), 348 (18), 300 (18), 228 (15), 188 (10). DA583-2

4.5.8   Kinetics

4.5.8.1   Kinetics of the Reactions of 1a with the Electrophiles 3−5
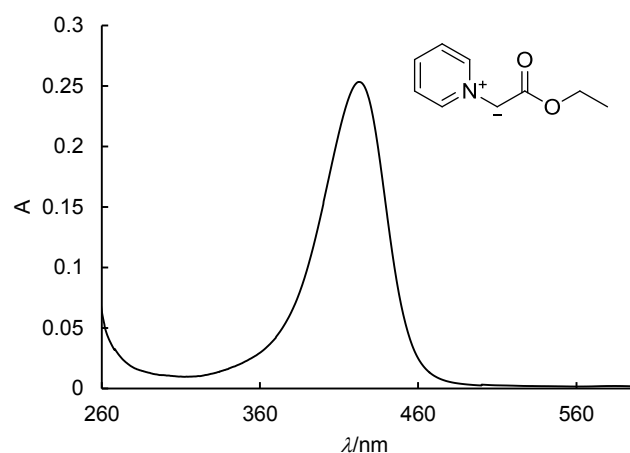
Figure 4.7. UV−Vis spectrum of 1a (c ~ 5 × 10^{-5} M) in DMSO at 20 °C.

Table 4.13. Determination of the nucleophilicity parameters N and s_N for 1a with the electrophiles 3,4 (filled dots) and 5 (open dot; not used for the determination of N and s_N).

Electrophile	E	log k_2
3a	−13.39	4.95
3b	−15.83	3.99
3e	−17.90	3.04
4a	−17.67	3.14
4b	−18.89	3.03
4c	−20.55	2.29
4d	−21.11	2.05
5b	−17.33	3.68

log k_2 = 0.3656 E + 9.7649
R² = 0.9807

N = 26.71; s_N = 0.37
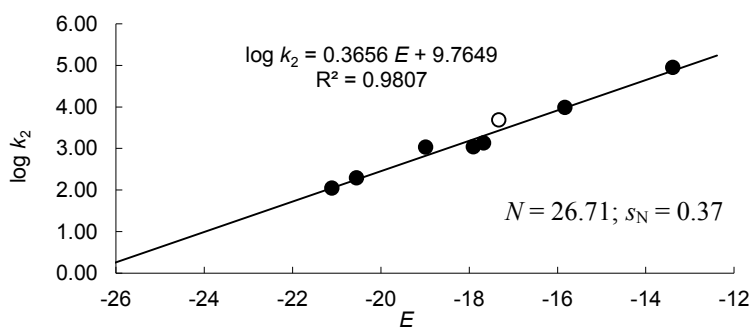
Table 4.14. Kinetics of the reaction of 1a with 3a (DMSO, 20 °C, Stopped-flow method, detection at 533 nm).[30]

No.	[3a]/mol L^{-1}	[1a]/mol L^{-1}	k_{obs}/s^{-1}
da79s1-1	4.00×10^{-5}	4.00×10^{-4}	4.80×10^{1}
da79s1-2	4.00×10^{-5}	8.00×10^{-4}	9.00×10^{1}
da79s1-3	4.00×10^{-5}	1.20×10^{-3}	1.26×10^{2}
da79s1-4	4.00×10^{-5}	1.60×10^{-3}	1.62×10^{2}
da79s1-5	4.00×10^{-5}	2.00×10^{-3}	1.92×10^{2}
k_2(20 °C) = 9.00×10^{4} L mol^{-1} s^{-1}			

y = 90000x + 15.6
R² = 0.9967
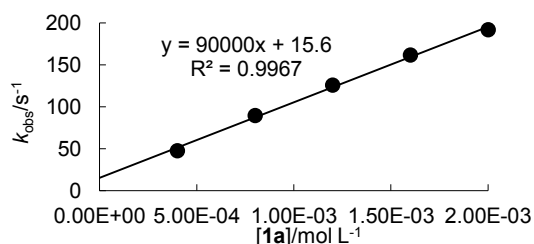
Table 4.15. Kinetics of the reaction of 1a with 3b (DMSO, 20 °C, Stopped-flow method, detection at 371 nm).[30]

No.	[3b]/mol L^{-1}	[1a]/mol L^{-1}	k_{obs}/s^{-1}
da79s2-1	4.00×10^{-5}	1.00×10^{-4}	6.64×10^{-1}
da79s2-2	4.00×10^{-5}	1.50×10^{-4}	1.02
da79s2-3	4.00×10^{-5}	2.00×10^{-4}	1.49
da79s2-2-1	4.00×10^{-5}	4.00×10^{-4}	3.09
da79s2-2-2	4.00×10^{-5}	5.00×10^{-4}	4.19
da79s2-2-3	4.00×10^{-5}	6.00×10^{-4}	5.57
da79s2-2-4	4.00×10^{-5}	7.00×10^{-4}	6.42
k_2(20 °C) = 9.68×10^{3} L mol^{-1} s^{-1}			

y = 9679.2x - 0.4577
R² = 0.9927

Table 4.16. Kinetics of the reaction of 1a with 3e (DMSO, 20 °C, Stopped-flow method, detection at 521 nm).[30]

No.	[3e]/mol L^{-1}	[1a]/mol L^{-1}	k_{obs}/s^{-1}
da79s3-1	2.00×10^{-5}	2.00×10^{-4}	1.80×10^{-1}
da79s3-2	2.00×10^{-5}	4.00×10^{-4}	3.71×10^{-1}
da79s3-3	2.00×10^{-5}	6.00×10^{-4}	6.23×10^{-1}
da79s3-4	2.00×10^{-5}	8.00×10^{-4}	8.59×10^{-1}
da79s3-5	2.00×10^{-5}	1.00×10^{-3}	1.03×10^{-1}
k_2(20 °C) = 1.09×10^{3} L mol^{-1} s^{-1}			

y = 1092.7x - 0.0433
R² = 0.9961
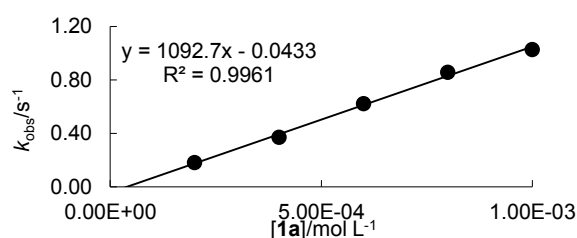
Table 4.17. Kinetics of the reaction of 1a with 4a (DMSO, 20 °C, Stopped-flow method, detection at 302 nm).

No.	[4a]/mol L^{-1}	[1a]/mol L^{-1}	k_{obs}/s^{-1}
da79s4-3	4.00×10^{-5}	8.00×10^{-4}	1.71
da79s43-4	4.00×10^{-5}	1.00×10^{-3}	1.86
da79s4-5	4.00×10^{-5}	1.20×10^{-3}	2.16
da79s4-1	4.00×10^{-5}	1.40×10^{-3}	2.51
da79s4-2	4.00×10^{-5}	1.60×10^{-3}	2.75
k_2(20 °C) = 1.37×10^{3} L mol^{-1} s^{-1}			

y = 1365x + 0.56
R² = 0.986
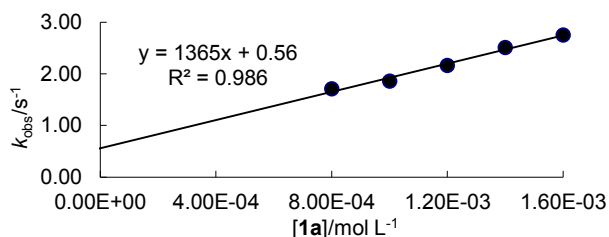
Table 4.18. Kinetics of the reaction of 1a with 4b (DMSO, 20 °C, Stopped-flow method, detection at 445 nm).

No.	[4b]/mol L^{-1}	[1a]/mol L^{-1}	k_{obs}/s^{-1}
da79s5-1	4.00×10^{-3}	4.00×10^{-4}	4.17
da79s5-2	5.00×10^{-3}	4.00×10^{-4}	5.41
da79s5-3	6.00×10^{-3}	4.00×10^{-4}	6.41
da79s5-4	7.00×10^{-3}	4.00×10^{-4}	7.51
da79s5-5	8.00×10^{-3}	4.00×10^{-4}	8.51
k_2(20 °C) = 1.08×10^{3} L mol^{-1} s^{-1}			

y = 1078x - 0.066
R² = 0.9986
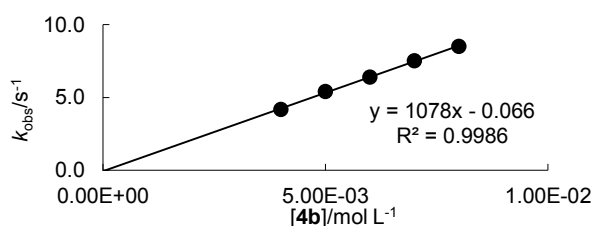
Table 4.19. Kinetics of the reaction of 1a with 4c (DMSO, 20 °C, Stopped-flow method, detection at 445 nm).

No.	[4c]/mol L^{-1}	[1a]/mol L^{-1}	k_{obs}/s^{-1}
da79s6-1	4.00×10^{-3}	4.00×10^{-4}	9.10×10^{-1}
da79s6-2	5.00×10^{-3}	4.00×10^{-4}	1.10
da79s6-3	6.00×10^{-3}	4.00×10^{-4}	1.29
da79s6-4	7.00×10^{-3}	4.00×10^{-4}	1.49
da79s6-5	8.00×10^{-3}	4.00×10^{-4}	1.69
k_2(20 °C) = 1.97×10^2 L mol^{-1} s^{-1}			

y = 197x + 0.116
R² = 0.9995

Table 4.20. Kinetics of the reaction of 1a with 4d (DMSO, 20 °C, Stopped-flow method, detection at 445 nm).

No.	[4d]/mol L^{-1}	[1a]/mol L^{-1}	k_{obs}/s^{-1}
da79s7-2	5.00×10^{-3}	4.00×10^{-4}	6.70×10^{-1}
da79s7-3	6.00×10^{-3}	4.00×10^{-4}	7.80×10^{-1}
da79s7-4	7.00×10^{-3}	4.00×10^{-4}	9.00×10^{-1}
da79s7-5	8.00×10^{-3}	4.00×10^{-4}	1.01
k_2(20 °C) = 1.13×10^2 L mol^{-1} s^{-1}			

y = 112.6x + 0.1101
R² = 0.9997

Table 4.21. Kinetics of the reaction of 1a with 5b (DMSO, 20 °C, Stopped-flow method, detection at 425 nm).

No.	[5b]/mol L^{-1}	[1a]/mol L^{-1}	k_{obs}/s^{-1}
da79s1-1	1.00×10^{-3}	1.00×10^{-4}	4.76
da79s1-2	1.50×10^{-3}	1.00×10^{-4}	7.18
da79s1-3	2.00×10^{-3}	1.00×10^{-4}	9.78
da79s1-4	2.50×10^{-3}	1.00×10^{-4}	1.22×10^1
da79s1-5	3.00×10^{-3}	1.00×10^{-4}	1.43×10^1
k_2(20 °C) = 4.82×10^3 L mol^{-1} s^{-1}			

y = 4820x + 0.004
R² = 0.9987
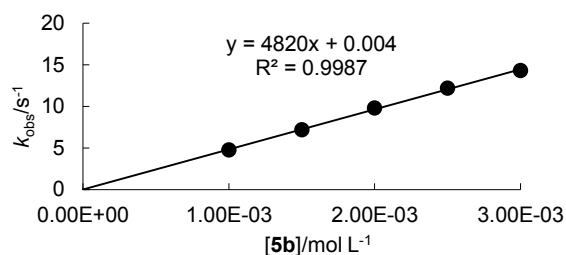
4.5.8.2 Kinetics of the Reactions of 1b with the Electrophiles 3−5
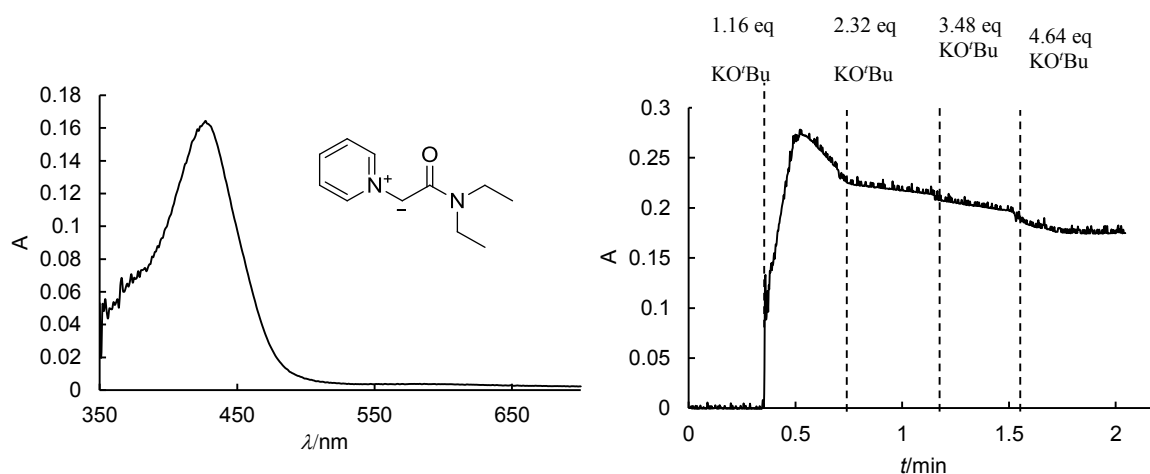
Figure 4.8. UV–Vis spectrum of 1b ($c \sim 1 \times 10^{-4}$ M) in DMSO at 20 °C (left). Monitoring of the UV–Vis absorption band (425 nm) of 1b during its generation from 1bH$^+$Br$^-$ by addition of KO^{t}Bu (right). The

experiment was performed by adding 250 µl portions of a solution of KO^{t}Bu in DMSO (dashed lines; [KO^{t}Bu] = 1.00 × 10^{-2} M) to an 8.61 × 10^{-5} M solution of 1bH$^+$Br$^-$ in DMSO (23.8 mL).

Table 4.22. Determination of the nucleophilicity parameters N and s_N for 1b with the electrophiles 3,4 (filled dots) and 5b (open dot; not used for the determination of N and s_N).

Electrophile	E	$\log k_2$
3a	−13.39	5.48
3b	−15.83	4.51
3d	−17.29	3.90
3e	−17.90	3.58
4a	−17.67	3.63
4c	−20.55	2.79
5b	−17.33	3.79

$\log k_2 = 0.3846\,E + 10.557$
$R^2 = 0.9881$

$N = 27.45; s_N = 0.38$

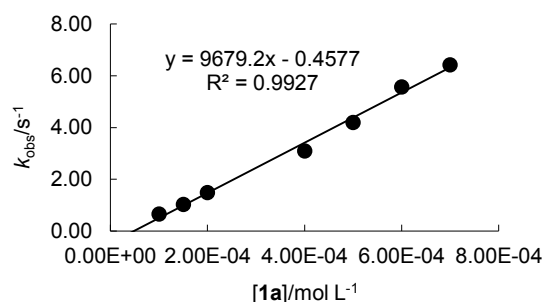**Table 4.23. Kinetics of the reaction of 1b with 3a (DMSO, 20 °C, Stopped-flow method, detection at 533 nm).**

No.	[3a]/mol L^{-1}	[KOtBu]/mol L^{-1}	[1bH$^+$Br$^-$]/mol L^{-1}	k_{obs}/s^{-1}
da191s1-4	4.00 × 10^{-5}	4.73 × 10^{-4}	8.80 × 10^{-4}	7.55 × 10^{1}
da191s1-2	4.00 × 10^{-5}	5.25 × 10^{-4}	1.00 × 10^{-3}	9.10 × 10^{1}
da191s1-5	4.00 × 10^{-5}	5.78 × 10^{-4}	1.08 × 10^{-3}	1.11 × 10^{2}
da191s1-3	4.00 × 10^{-5}	6.30 × 10^{-4}	1.20 × 10^{-3}	1.21 × 10^{2}
		k_2(20 °C) = 2.99 × 10^5 L mol^{-1} s^{-1}		

$y = 298765x - 65.144$
$R^2 = 0.9861$

Table 4.24. Kinetics of the reaction of 1b with 3b (DMSO, 20 °C, Stopped-flow method, detection at 371 nm).

No.	[3b]/mol L^{-1}	[KOtBu]/mol L^{-1}	[1bH$^+$Br$^-$]/mol L^{-1}	k_{obs}/s^{-1}
da191s2-1	4.00 × 10^{-5}	4.20 × 10^{-4}	8.00 × 10^{-4}	7.22
da191s2-3	4.00 × 10^{-5}	6.30 × 10^{-4}	1.20 × 10^{-3}	1.52 × 10^{1}
da191s2-4	4.00 × 10^{-5}	7.35 × 10^{-4}	1.40 × 10^{-3}	1.78 × 10^{1}
da191s2-5	4.00 × 10^{-5}	8.40 × 10^{-4}	1.60 × 10^{-3}	2.07 × 10^{1}
		k_2(20 °C) = 3.21 × 10^4 L mol^{-1} s^{-1}		

$y = 32131x - 5.8657$
$R^2 = 0.9902$
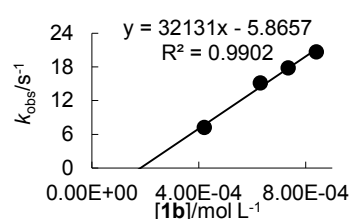
Table 4.25. Kinetics of the reaction of 1b with 3d (DMSO, 20 °C, Stopped-flow method, detection at 486 nm).

No.	[3d]/mol L^{-1}	[KOtBu]/mol L^{-1}	[1bH$^+$Br$^-$]/mol L^{-1}	k_{obs}/s^{-1}
da191s4-1	4.00 × 10^{-5}	4.20 × 10^{-4}	8.00 × 10^{-4}	1.62
da191s4-3	4.00 × 10^{-5}	6.30 × 10^{-4}	1.20 × 10^{-3}	3.17
da191s4-4	4.00 × 10^{-5}	7.35 × 10^{-4}	1.40 × 10^{-3}	4.35
da191s4-5	4.00 × 10^{-5}	8.40 × 10^{-4}	1.60 × 10^{-3}	4.84
		k_2(20 °C) = 7.94 × 10^3 L mol^{-1} s^{-1}		

$y = 7940.1x - 1.7157$
$R^2 = 0.9871$
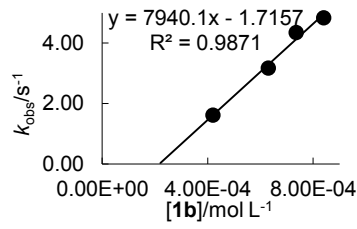
Table 4.26. Kinetics of the reaction of 1b with 3e (DMSO, 20 °C, Stopped-flow method, detection at 521 nm).

No.	[3e]/mol L^{-1}	[KOtBu]/mol L^{-1}	[1bH$^+$Br$^-$]/mol L^{-1}	k_{obs}/s^{-1}
da191s5-1	4.00 × 10^{-5}	4.20 × 10^{-4}	8.00 × 10^{-4}	1.45
da191s5-2	4.00 × 10^{-5}	5.25 × 10^{-4}	1.00 × 10^{-3}	1.69
da191s5-4	4.00 × 10^{-5}	7.35 × 10^{-4}	1.40 × 10^{-3}	2.63
da191s5-5	4.00 × 10^{-5}	8.40 × 10^{-4}	1.60 × 10^{-3}	2.97
		k_2(20 °C) = 3.79 × 10^3 L mol^{-1} s^{-1}		

$y = 3790.5x - 0.203$
$R^2 = 0.9903$
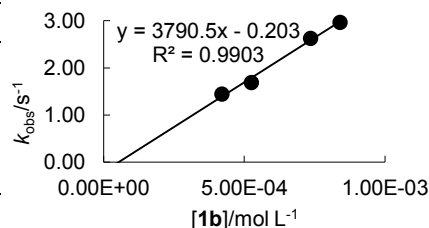
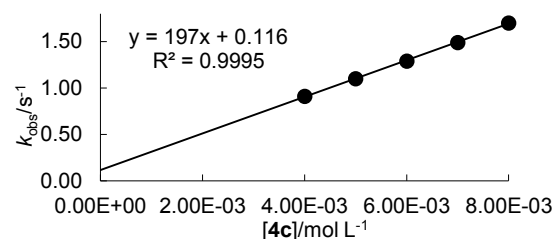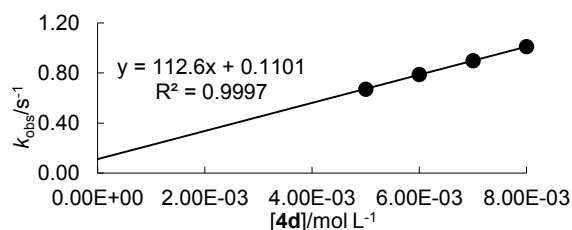**Table 4.27. Kinetics of the reaction of 1b with 4a (DMSO, 20 °C, Stopped-flow method, detection at 425 nm).**

No.	[4a]/mol L^{-1}	[1b]/mol L^{-1}	k_{obs}/s^{-1}
da191s10-1	2.00×10^{-3}	2.00×10^{-4}	1.20×10^{1}
da191s10-2	3.00×10^{-3}	2.00×10^{-4}	1.51×10^{1}
da191s10-4	4.00×10^{-3}	2.00×10^{-4}	1.95×10^{1}
da191s10-5	5.00×10^{-3}	2.00×10^{-4}	2.30×10^{1}
da191s10-5	6.00×10^{-3}	2.00×10^{-4}	2.92×10^{1}

$k_2(20 °C) = 4.23 \times 10^3$ L mol^{-1} s^{-1}

y = 4230x + 2.84, R² = 0.9852
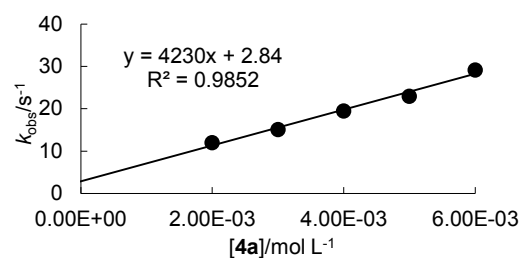
Table 4.28. Kinetics of the reaction of 1b with 4c (DMSO, 20 °C, Stopped-flow method, detection at 425nm).

No.	[4c]/mol L^{-1}	[1b]/mol L^{-1}	k_{obs}/s^{-1}
da191s12-1	2.00×10^{-3}	2.00×10^{-4}	5.17×10^{-1}
da191s12-2	3.00×10^{-3}	2.00×10^{-4}	9.47×10^{-1}
da191s12-4	4.00×10^{-3}	2.00×10^{-4}	1.66
da191s12-5	5.00×10^{-3}	2.00×10^{-4}	2.50
da191s12-5	6.00×10^{-3}	2.00×10^{-4}	2.79

$k_2(20 °C) = 6.10 \times 10^2$ L mol^{-1} s^{-1}

y = 609.9x - 0.7568, R² = 0.9803
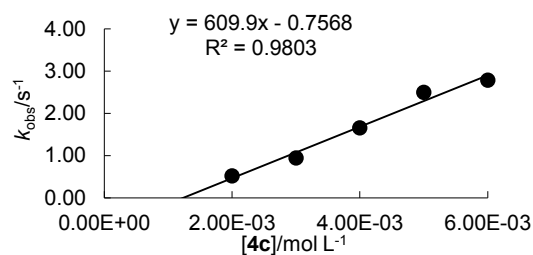
Table 4.29. Kinetics of the reaction of 1b with 5b (DMSO, 20 °C, Stopped-flow method, detection at 425 nm).

No.	[5b]/mol L^{-1}	[1b]/mol L^{-1}	k_{obs}/s^{-1}
da191s9-1	1.00×10^{-3}	1.00×10^{-4}	4.83
da191s9-2	1.50×10^{-3}	1.00×10^{-4}	7.66
da191s9-4	2.00×10^{-3}	1.00×10^{-4}	1.02×10^{1}
da191s9-5	2.50×10^{-3}	1.00×10^{-4}	1.43×10^{1}
da191s9-5	3.00×10^{-3}	1.00×10^{-4}	1.68×10^{1}

$k_2(20 °C) = 6.12 \times 10^3$ L mol^{-1} s^{-1}

y = 6116x - 1.474, R² = 0.9938
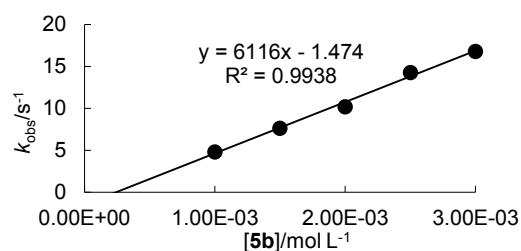
4.5.8.3 Kinetics of the Reactions of 1c with the Electrophiles 3−5
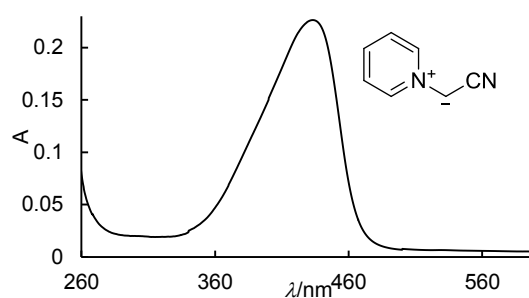
Figure 4.9. UV–Vis spectrum of 1c ($c \sim 5 \times 10^{-5}$ M) in DMSO at 20 °C.

239

Table 4.30. Determination of the nucleophilicity parameters N and s_N for 1c with the electrophiles 3,4 (filled dots) and 5 (open dot; not used for the determination of N and s_N)

Electrophile	E	$\log k_2$
3a	−13.39	5.37
3b	−15.83	4.31
3d	−17.29	3.43
3e	−17.90	3.33
4a	−17.67	3.32
4b	−18.89	2.80
4c	−20.55	2.25
4d	−21.11	2.25
5b	−17.33	3.90

$\log k_2 = 0.417\, E + 10.827$
$R^2 = 0.980$

$N = 25.94;\ s_N = 0.42$
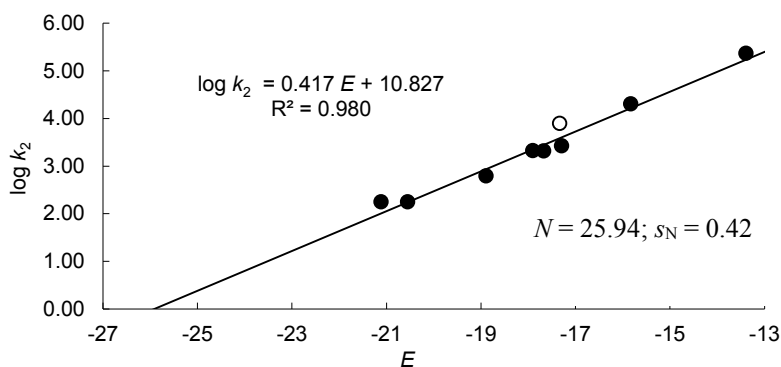
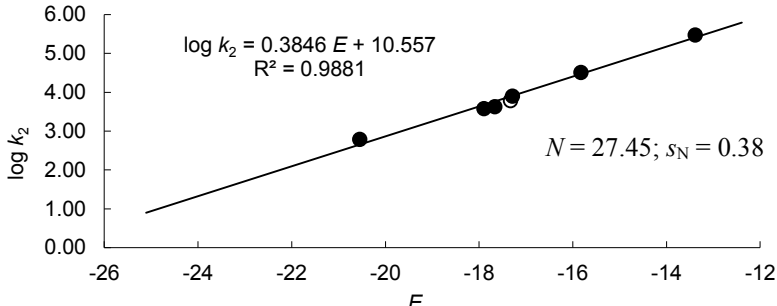**Table 4.31. Kinetics of the reaction of 1c with 3a (DMSO, 20 °C, Stopped-flow method, detection at 533 nm).**

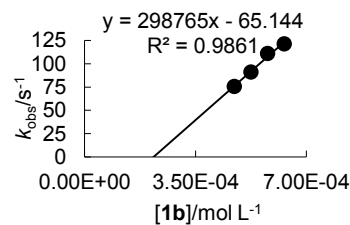| No.	[**3a**]/mol L^{-1}	[**1c**]/mol L^{-1}	k_{obs}/s^{-1}
da130s4-1	4.00×10^{-5}	4.00×10^{-4}	8.84×10^1
da130s4-3	4.00×10^{-5}	6.00×10^{-4}	1.40×10^2
da130s4-4	4.00×10^{-5}	7.00×10^{-4}	1.62×10^2
da130s4-5	4.00×10^{-5}	8.00×10^{-4}	1.81×10^2
k_2(20 °C) = 2.34×10^5 L mol^{-1} s^{-1}			

y = 233829x - 3.5429
R² = 0.9964
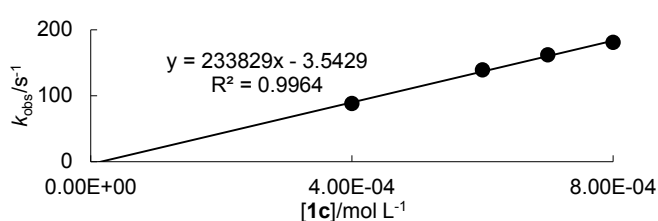
Table 4.32. Kinetics of the reaction of 1c with 3b (DMSO, 20 °C, Stopped-flow method, detection at 371 nm).

No.	[**3b**]/mol L^{-1}	[**1c**]/mol L^{-1}	k_{obs}/s^{-1}
da130s1-1	2.00×10^{-5}	2.00×10^{-4}	3.78
da130s1-2	2.00×10^{-5}	3.00×10^{-4}	6.00
da130s1-3	2.00×10^{-5}	4.00×10^{-4}	7.86
da130s1-4	2.00×10^{-5}	5.00×10^{-4}	1.05×10^1
da130s1-5	2.00×10^{-5}	6.00×10^{-4}	1.17×10^1
k_2(20 °C) = 2.03×10^4 L mol^{-1} s^{-1}			

y = 20340x - 0.168
R² = 0.9906
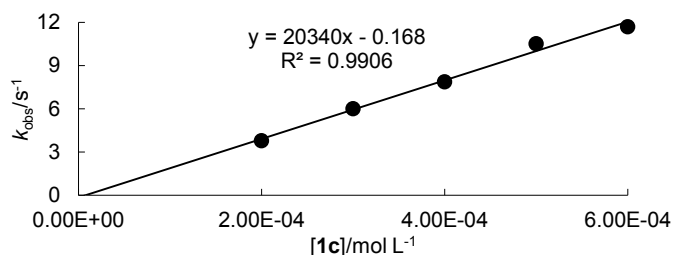
Table 4.33. Kinetics of the reaction of 1c with 3d (DMSO, 20 °C, Stopped-flow method, detection at 486 nm).

No.	[**3d**]/mol L^{-1}	[**1c**]/mol L^{-1}	k_{obs}/s^{-1}
da130s5-1	2.00×10^{-5}	1.72×10^{-4}	6.56×10^{-1}
da130s5-3	2.00×10^{-5}	3.45×10^{-4}	1.13
da130s5-4	2.00×10^{-5}	4.31×10^{-4}	1.32
da130s5-5	2.00×10^{-5}	5.17×10^{-4}	1.59
k_2(20 °C) = 2.67×10^3 L mol^{-1} s^{-1}			

y = 2669.9x + 0.1958
R² = 0.9977
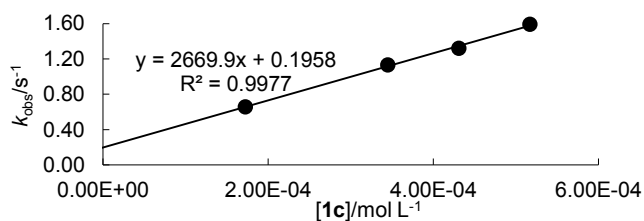
Table 4.34. Kinetics of the reaction of 1c with 3e (DMSO, 20 °C, Stopped-flow method, detection at 521 nm).

No.	[**3e**]/mol L^{-1}	[**1c**]/mol L^{-1}	k_{obs}/s^{-1}
da130s3-1	2.00×10^{-5}	2.00×10^{-4}	7.02×10^{-1}
da130s3-2	2.00×10^{-5}	4.00×10^{-4}	1.10
da130s3-3	2.00×10^{-5}	6.00×10^{-4}	1.40
da130s3-4	2.00×10^{-5}	8.00×10^{-4}	1.98
da130s3-5	2.00×10^{-5}	1.00×10^{-3}	2.39
k_2(20 °C) = 2.13×10^3 L mol^{-1} s^{-1}			

y = 2130x + 0.236
R² = 0.9908

Table 4.35. Kinetics of the reaction of 1c with 4a (DMSO, 20 °C, Stopped-flow method, detection at 302 nm).

No.	$[\mathbf{4a}]$/mol L^{-1}	$[\mathbf{1c}]$/mol L^{-1}	k_{obs}/s^{-1}
da130s2-1	2.00×10^{-5}	2.00×10^{-4}	6.40×10^{-4}
da130s2-2	2.00×10^{-5}	4.00×10^{-4}	1.14
da130s2-3	2.00×10^{-5}	6.00×10^{-4}	1.57
da130s2-4	2.00×10^{-5}	8.00×10^{-4}	1.85
da130s2-5	2.00×10^{-5}	1.00×10^{-3}	2.36
$k_2(20\ °C) = 2.08 \times 10^3$ L mol^{-1} s^{-1}			

$y = 2079x + 0.2638$
$R^2 = 0.9922$
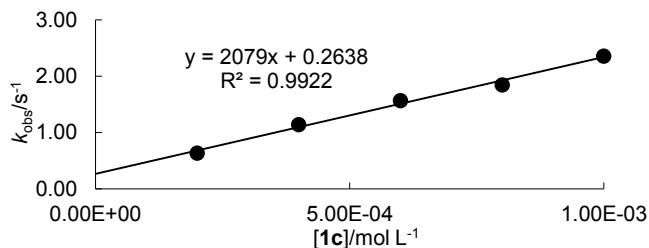
Table 4.36. Kinetics of the reaction of 1c with 4b (DMSO, 20 °C, Stopped-flow method, detection at 277 nm).

No.	$[\mathbf{4b}]$/mol L^{-1}	$[\mathbf{1c}]$/mol L^{-1}	k_{obs}/s^{-1}
da130s8-1	8.00×10^{-5}	8.00×10^{-4}	7.78×10^{-1}
da130s8-2	8.00×10^{-5}	1.00×10^{-3}	9.50×10^{-1}
da130s8-3	8.00×10^{-5}	1.20×10^{-3}	1.06
da130s8-5	8.00×10^{-5}	1.55×10^{-3}	1.26
$k_2(20\ °C) = 6.26 \times 10^2$ L mol^{-1} s^{-1}			

$y = 626.48x + 0.3004$
$R^2 = 0.9878$
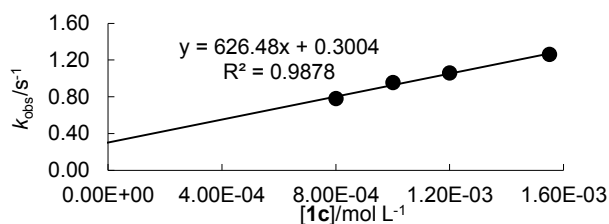
Table 4.37. Kinetics of the reaction of 1c with 4c (DMSO, 20 °C, Stopped-flow method, detection at 283 nm).

No.	$[\mathbf{4c}]$/mol L^{-1}	$[\mathbf{1c}]$/mol L^{-1}	k_{obs}/s^{-1}
da130s7-1	8.00×10^{-5}	8.00×10^{-4}	2.50×10^{-1}
da130s7-2	8.00×10^{-5}	1.00×10^{-3}	2.70×10^{-1}
da130s7-4	8.00×10^{-5}	1.40×10^{-3}	3.55×10^{-1}
da130s7-5	8.00×10^{-5}	1.60×10^{-3}	3.85×10^{-1}
$k_2(20\ °C) = 1.77 \times 10^2$ L mol^{-1} s^{-1}			

$y = 177x + 0.102$
$R^2 = 0.9884$
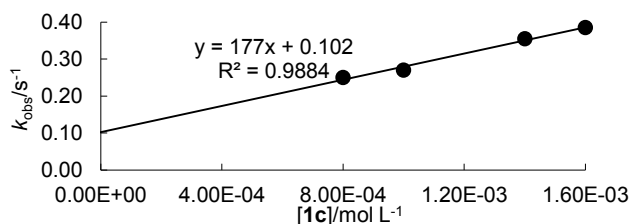
Table 4.38. Kinetics of the reaction of 1c with 4d (DMSO, 20 °C, Stopped-flow method, detection at 295 nm).

No.	$[\mathbf{4d}]$/mol L^{-1}	$[\mathbf{1c}]$/mol L^{-1}	k_{obs}/s^{-1}
da130s6-1	6.00×10^{-5}	6.00×10^{-4}	1.33×10^{-1}
da130s6-2	6.00×10^{-5}	7.50×10^{-4}	1.55×10^{-1}
da130s6-3	6.00×10^{-5}	9.00×10^{-4}	1.85×10^{-1}
da130s6-5	6.00×10^{-5}	1.20×10^{-3}	2.38×10^{-1}
$k_2(20\ °C) = 1.77 \times 10^2$ L mol^{-1} s^{-1}			

$y = 177.33x + 0.0248$
$R^2 = 0.9981$
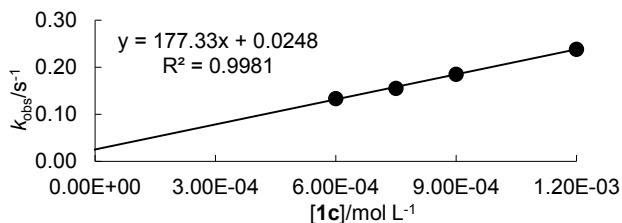
Table 4.39. Kinetics of the reaction of 1c with 5b (DMSO, 20 °C, Stopped-flow method, detection at 425 nm).

No.	$[\mathbf{5b}]$/mol L^{-1}	$[\mathbf{1c}]$/mol L^{-1}	k_{obs}/s^{-1}
da130s10-1	1.00×10^{-3}	1.00×10^{-4}	8.01
da130s10-2	1.50×10^{-3}	1.00×10^{-4}	1.33×10^1
da130s10-3	2.00×10^{-3}	1.00×10^{-4}	1.62×10^1
da130s10-4	2.50×10^{-3}	1.00×10^{-4}	2.03×10^1
da130s10-5	3.00×10^{-3}	1.00×10^{-4}	2.43×10^1
$k_2(20\ °C) = 7.92 \times 10^3$ L mol^{-1} s^{-1}			

$y = 7916x + 0.59$
$R^2 = 0.9936$

4.5.8.4 Kinetics of the Reactions of 1d with the Electrophiles 3−5
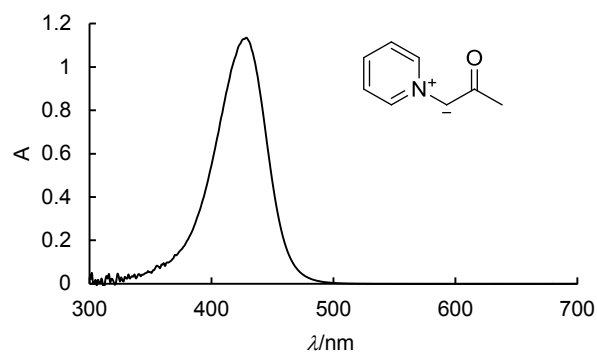
Figure 4.10. UV–Vis spectrum of 1d ($c \sim 1 \times 10^{-4}$ M) in DMSO at 20 °C.

Table 4.40. Determination of the nucleophilicity parameters N and s_N for 1d with the electrophiles 3,4 (filled dots) and 5 (open dots, not used to calculate N and s_N).

Electrophile	E	$\log k_2$
3a	−13.39	4.04
3b	−15.83	2.70
3d	−17.29	2.62
3e	−17.90	1.86
4a	−17.67	1.35
5a	−10.80	5.35
5b	−17.33	1.41

$\log k_2 = 0.6005\ E + 12.156$
$R^2 = 0.9831$

$N = 20.24$; $s_N = 0.60$
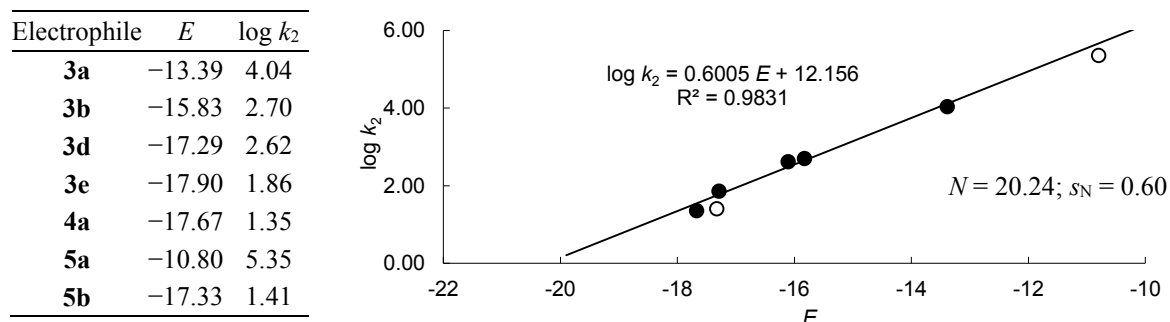
Table 4.41. Kinetics of the reaction of 1d with 3a (DMSO, 20 °C, Stopped-flow method, detection at 533 nm).

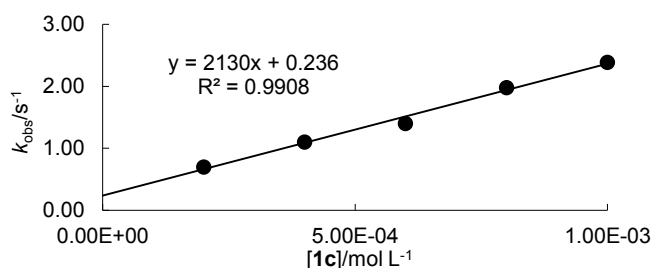| No.	[**3a**]/mol L^{-1}	[**1d**]/mol L^{-1}	k_{obs}/s^{-1}
da167s1-1	2.00×10^{-5}	2.00×10^{-4}	1.79
da167s1-2	2.00×10^{-5}	3.00×10^{-4}	2.57
da167s1-3	2.00×10^{-5}	4.00×10^{-4}	3.82
da167s1-4	2.00×10^{-5}	5.00×10^{-4}	5.00
k_2(20 °C) = 1.09×10^4 L mol^{-1} s^{-1}			

$y = 10880x - 0.513$
$R^2 = 0.9909$

Table 4.42. Kinetics of the reaction 1d with 3a (DMSO, 20 °C, Stopped-flow method, detection at 533 nm).

No.	[**3a**]/mol L^{-1}	[KOtBu]/mol L^{-1}	[**1d**H$^+$Cl$^-$]/mol L^{-1}	k_{obs}/s^{-1}
da167s1r-1	2.00×10^{-5}	1.05×10^{-4}	2.00×10^{-4}	1.00
da167s1r-2	2.00×10^{-5}	1.58×10^{-4}	3.00×10^{-4}	1.43
da167s1r-3	2.00×10^{-5}	2.10×10^{-4}	4.00×10^{-4}	2.01
da167s1r-4	2.00×10^{-5}	2.63×10^{-4}	5.00×10^{-4}	2.69
k_{2r}(20 °C) = 1.07×10^4 L mol^{-1} s^{-1}				
k_2/k_{2r} = 0.99				

$y = 10743x - 0.194$
$R^2 = 0.9895$

Table 4.43. Kinetics of the reaction of 1d with 3b (DMSO, 20 °C, Stopped-flow method, detection at 371 nm).

No.	[3b]/mol L^{-1}	[1d]/mol L^{-1}	k_{obs}/s^{-1}
da167s2-1	2.00×10^{-5}	4.00×10^{-4}	2.26×10^{-1}
da167s2-4	2.00×10^{-5}	5.00×10^{-4}	2.70×10^{-1}
da167s2-5	2.00×10^{-5}	7.00×10^{-4}	3.86×10^{-1}
da167s2-3	2.00×10^{-5}	8.00×10^{-4}	4.19×10^{-1}
k_2(20 °C) = 5.02×10^2 L mol^{-1} s^{-1}			
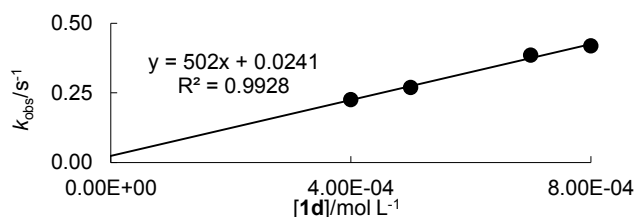
Table 4.44. Kinetics of the reaction of 1d with 3c (DMSO, 20 °C, Stopped-flow method, detection at 393 nm).

No.	[3c]/mol L^{-1}	[1d]/mol L^{-1}	k_{obs}/s^{-1}
da167s5-5	1.00×10^{-5}	2.00×10^{-4}	4.90×10^{-2}
da167s5-4	1.00×10^{-5}	3.00×10^{-4}	8.63×10^{-2}
da167s5-1	1.00×10^{-5}	4.00×10^{-4}	1.20×10^{-1}
da167s5-2	1.00×10^{-5}	6.00×10^{-4}	2.14×10^{-1}
k_2(20 °C) = 4.13×10^2 L mol^{-1} s^{-1}			
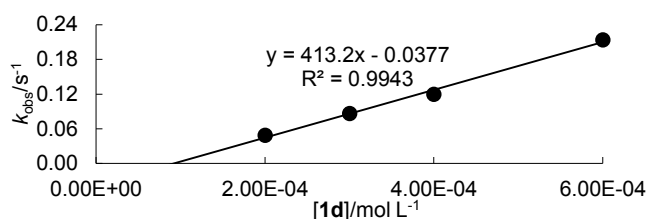
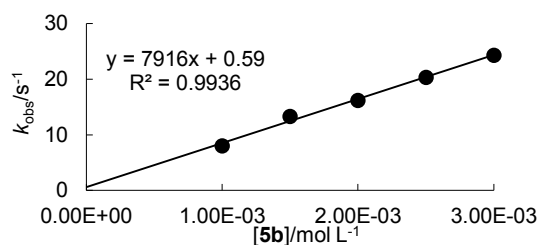**Table 4.45. Kinetics of the reaction of 1d with 3d (DMSO, 20 °C, Stopped-flow method, detection at 486 nm).**

No.	[3d]/mol L^{-1}	[1d]/mol L^{-1}	k_{obs}/s^{-1}
da167s4-1	2.00×10^{-5}	4.00×10^{-4}	2.86×10^{-2}
da167s4-2	2.00×10^{-5}	6.00×10^{-4}	3.65×10^{-2}
da167s4-3	2.00×10^{-5}	8.00×10^{-4}	5.48×10^{-2}
da167s4-4	2.00×10^{-5}	1.00×10^{-3}	7.21×10^{-2}
da167s4-5	2.00×10^{-5}	1.20×10^{-3}	8.26×10^{-2}
k_2(20 °C) = 7.18×10^1 L mol^{-1} s^{-1}			
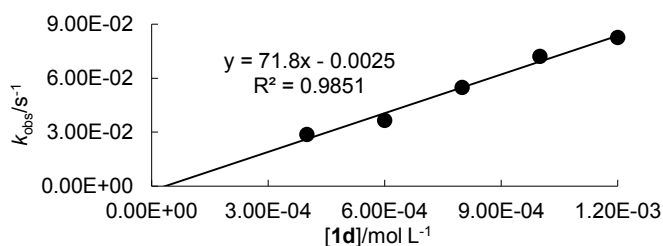
Table 4.46. Kinetics of the reaction of 1d with 4a (DMSO, 20 °C, Stopped-flow method, detection at 425 nm).

No.	[4a]/mol L^{-1}	[1d]/mol L^{-1}	k_{obs}/s^{-1}
da167s9-1	5.00×10^{-4}	5.00×10^{-5}	1.31×10^{-2}
da167s9-2	1.00×10^{-3}	5.00×10^{-5}	2.45×10^{-2}
da167s9-3	1.50×10^{-3}	5.00×10^{-5}	3.55×10^{-2}
da167s9-4	2.00×10^{-3}	5.00×10^{-5}	4.70×10^{-2}
da167s9-5	2.50×10^{-3}	5.00×10^{-5}	5.84×10^{-2}
k_2(20 °C) = 2.26×10^1 L mol^{-1} s^{-1}			
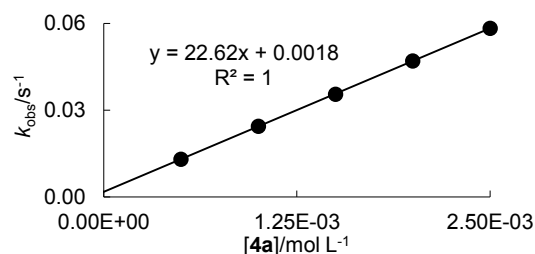
Table 4.47. Kinetics of the reaction of 1d with 5a (DMSO, 20 °C, Stopped-flow method, detection at 425 nm).

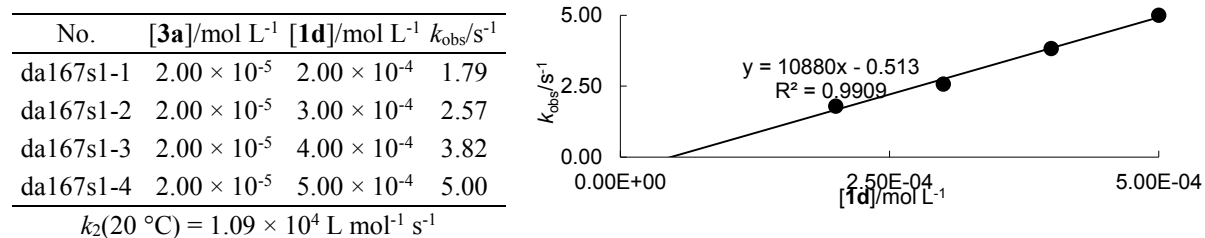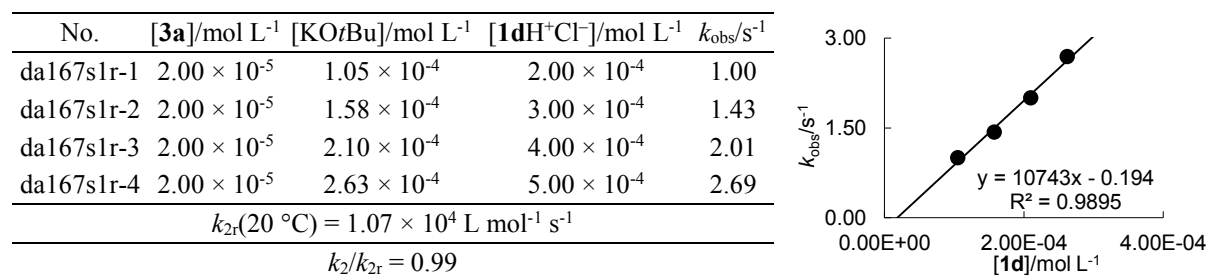| No.	[5a]/mol L^{-1}	[1d]/mol L^{-1}	k_{obs}/s^{-1}
da167s8-1	5.50×10^{-4}	5.00×10^{-5}	1.73×10^2
da167s8-2	6.00×10^{-4}	5.00×10^{-5}	1.84×10^2
da167s8-3	6.50×10^{-4}	5.00×10^{-5}	1.93×10^2
da167s8-5	7.50×10^{-4}	5.00×10^{-5}	2.16×10^2
k_2(20 °C) = 2.14×10^5 L mol^{-1} s^{-1}			
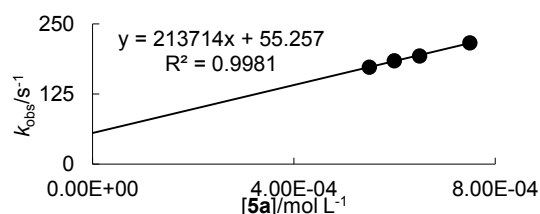
Table 4.48. Kinetics of the reaction of 1d with 5b (DMSO, 20 °C, Stopped-flow method, detection at 425 nm).

No.	$[5b]$/mol L^{-1}	$[1d]$/mol L^{-1}	k_{obs}/s^{-1}
da167s7-1	1.00×10^{-3}	5.00×10^{-5}	1.59×10^{-2}
da167s7-2	1.50×10^{-3}	5.00×10^{-5}	2.87×10^{-2}
da167s7-3	2.00×10^{-3}	5.00×10^{-5}	3.93×10^{-2}
da167s7-4	2.50×10^{-3}	5.00×10^{-5}	5.28×10^{-2}
da167s7-5	3.00×10^{-3}	5.00×10^{-5}	6.77×10^{-2}
k_2(20 °C) = 2.55×10^1 L mol^{-1} s^{-1}			

y = 25.54x − 0.0102
R² = 0.9966
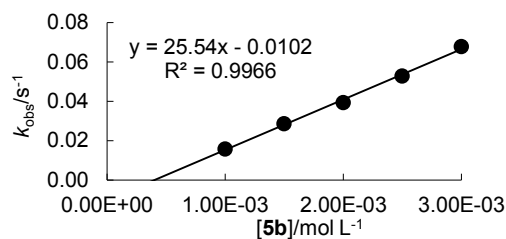
4.5.8.5 Kinetics of the Reactions of 1e with the Electrophiles 2−5
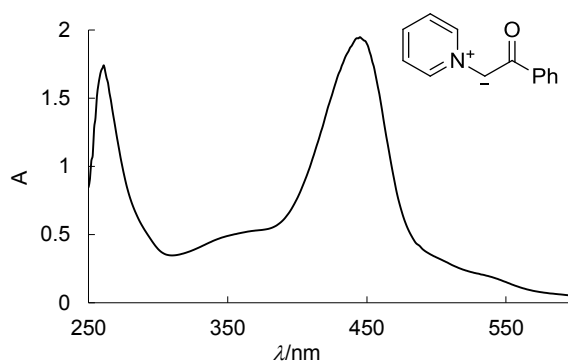
Figure 4.11. UV–Vis spectrum of 1e ($c \sim 1 \times 10^{-4}$ M) in DMSO at 20 °C.

Table 4.49. Determination of the nucleophilicity parameters N and s_N for 1e with the electrophiles 2,3 (filled dots) and 5 (open dots, not used to calculate N and s_N).

Electrophile	E	$\log k_2$
2b-BF₄	−9.45	5.85
2c-BF₄	−10.04	5.58
3a	−13.39	3.30
3b	−15.83	2.11
3e	−17.90	1.01
5a	−10.80	-0.66
5b	−17.33	-0.07

$\log k_2$ = 0.5813 E + 11.317
R² = 0.9958

N = 19.46; s_N = 0.58
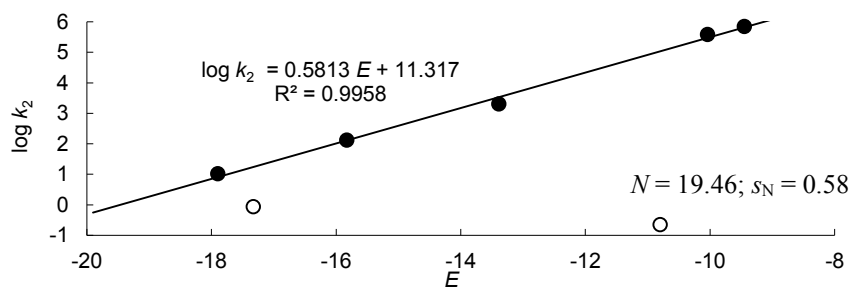
Table 4.50. Kinetics of the reaction of 1e with 2b-BF₄ (DMSO, 20 °C, Stopped-flow method, detection at 635 nm).[30]

No.	$[2b\text{-}BF_4]$/mol L^{-1}	$[1e]$/mol L^{-1}	k_{obs}/s^{-1}
da71s1-2	2.00×10^{-5}	2.00×10^{-4}	1.74×10^2
da71s1-3	2.00×10^{-5}	4.00×10^{-4}	3.18×10^2
da71s1-4	2.00×10^{-5}	6.00×10^{-4}	4.96×10^2
da71s1-5	2.00×10^{-5}	8.00×10^{-4}	6.08×10^2
da71s1-6	2.00×10^{-5}	1.00×10^{-3}	7.37×10^2
k_2(20 °C) = 7.08×10^5 L mol^{-1} s^{-1}			

y = 707980x + 41.834
R² = 0.9943

Table 4.51. Kinetics of the reaction of 1e with 2c-BF₄ (DMSO, 20 °C, Stopped-flow method, detection at 630 nm).[30]

No.	[2c-BF$_4$]/mol L^{-1}	[1e]/mol L^{-1}	k_{obs}/s^{-1}
da71s2-2	2.00×10^{-5}	1.00×10^{-4}	2.91×10^{1}
da71s2-1	2.00×10^{-5}	2.00×10^{-4}	6.43×10^{1}
da71s2-3	2.00×10^{-5}	3.00×10^{-4}	1.13×10^{2}
da71s2-4	2.00×10^{-5}	4.00×10^{-4}	1.43×10^{2}
da71s2-5	2.00×10^{-5}	5.00×10^{-4}	1.82×10^{2}
k_2(20 °C) = 3.85×10^{5} L mol^{-1} s^{-1}			

Plot: y = 384500x - 9.07, R² = 0.9958
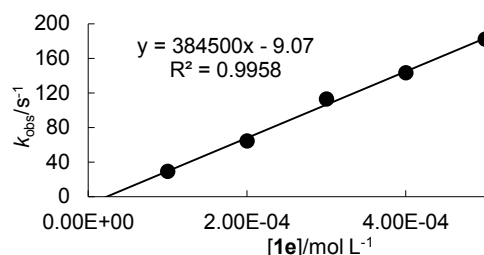
Table 4.52. Kinetics of the reaction of 1e with 3a (DMSO, 20 °C, Stopped-flow method, detection at 533 nm).[30]

No.	[3a]/mol L^{-1}	[1e]/mol L^{-1}	k_{obs}/s^{-1}
da71s3r-1	2.00×10^{-5}	2.00×10^{-4}	3.93×10^{-1}
da71s3r-2	2.00×10^{-5}	4.00×10^{-4}	8.29×10^{-1}
da71s3r-3	2.00×10^{-5}	6.00×10^{-4}	1.12
da71s3r-4	2.00×10^{-5}	8.00×10^{-4}	1.59
da71s3r-4	2.00×10^{-5}	1.00×10^{-3}	2.01
k_2(20 °C) = 2.00×10^{3} L mol^{-1} s^{-1}			

Plot: y = 1997.5x - 0.0103, R² = 0.9957
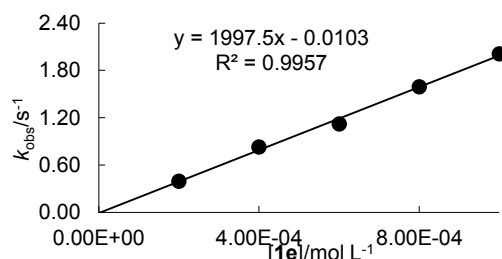
Table 4.53. Kinetics of the reaction of 1e with 3b (DMSO, 20 °C, Stopped-flow method, detection at 371 nm).[30]

No.	[3b]/mol L^{-1}	[1e]/mol L^{-1}	k_{obs}/s^{-1}
da71s4-1	1.00×10^{-5}	1.00×10^{-4}	9.92×10^{-3}
da71s4-2	1.00×10^{-5}	1.50×10^{-4}	1.72×10^{-2}
da71s4-3	1.00×10^{-5}	2.00×10^{-4}	2.53×10^{-2}
da71s4-5	1.00×10^{-5}	3.00×10^{-4}	3.58×10^{-2}
k_2(20 °C) = 1.29×10^{2} L mol^{-1} s^{-1}			

Plot: y = 129.41x - 0.0022, R² = 0.9893
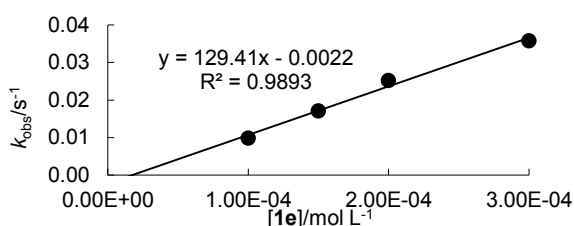
Table 4.54. Kinetics of the reaction of 1e with 3e (DMSO, 20 °C, J&M method, detection at 521 nm).[30]

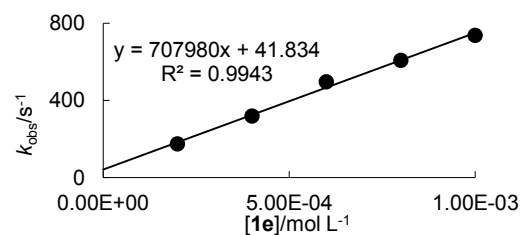| No.	[3e]/mol L^{-1}	[1e]/mol L^{-1}	k_{obs}/s^{-1}
da71j1-1	3.97×10^{-5}	4.17×10^{-4}	4.52×10^{-3}
da71j1-2	3.97×10^{-5}	8.33×10^{-4}	9.42×10^{-3}
da71j-3	3.97×10^{-5}	1.26×10^{-3}	1.41×10^{-2}
da71j1-4	4.01×10^{-5}	1.68×10^{-3}	1.75×10^{-2}
da71j1-5	4.00×10^{-5}	2.09×10^{-3}	2.20×10^{-2}
k_2(20 °C) = 1.03×10^{1} L mol^{-1} s^{-1}			

Plot: y = 10.303x + 0.0005, R² = 0.9972

Table 4.55. Kinetics of the reaction of 1e with 5a (DMSO, 20 °C, J&M method, detection at 445 nm).

No.	[5a]/mol L^{-1}	[1e]/mol L^{-1}	k_{obs}/s^{-1}
da71j10-1	7.37×10^{-4}	7.37×10^{-5}	1.34×10^{-4}
da71j10-5	1.46×10^{-3}	7.28×10^{-5}	3.54×10^{-4}
da71j10-4	2.19×10^{-3}	7.30×10^{-5}	5.13×10^{-4}
da71j10-3	2.83×10^{-3}	7.08×10^{-5}	6.02×10^{-4}
da71j10-2	3.63×10^{-3}	7.26×10^{-5}	7.92×10^{-4}
k_2(20 °C) = 2.19×10^{-1} L mol^{-1} s^{-1}			

Plot: y = 0.2186x + 5E-06, R² = 0.9864

Table 4.56. Kinetics of the reaction of 1e with 5b (DMSO, 20 °C, J&M method, detection at 445 nm).

No.	$[5b]$/mol L^{-1}	$[1e]$/mol L^{-1}	k_{obs}/s^{-1}
da71j9-5	2.17×10^{-3}	7.23×10^{-5}	2.78×10^{-3}
da71j9-4	2.54×10^{-3}	7.27×10^{-5}	3.05×10^{-3}
da71j9-3	2.83×10^{-3}	7.08×10^{-5}	3.34×10^{-3}
da71j9-2	3.28×10^{-3}	7.29×10^{-5}	3.79×10^{-3}
da71j9-1	3.68×10^{-3}	7.37×10^{-5}	4.02×10^{-3}
$k_2(20\ °C) = 8.54 \times 10^{-1}$ L mol^{-1} s^{-1}			
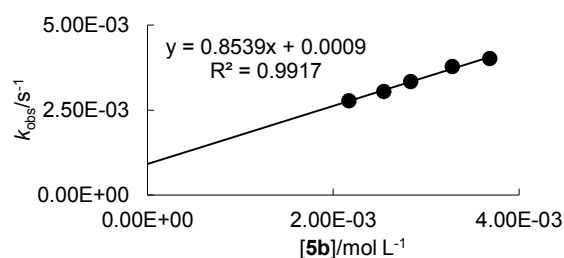
4.5.8.6 Kinetics of the Reactions of 1f with the Electrophiles 3−5
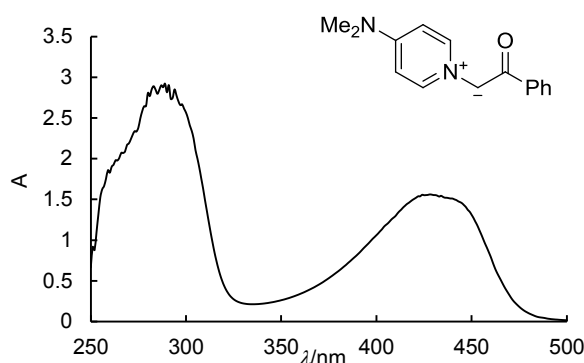
Figure 4.12. UV–Vis spectrum of 1f ($c \sim 1 \times 10^{-4}$ M) in DMSO at 20 °C.

Table 4.57. Determination of the nucleophilicity parameters N and s_N for 1f with the electrophiles 3,4 (filled dots) and 5 (open dot, not used to calculate N and s_N).

Electrophile	E	$\log k_2$
3a	-13.39	4.74
4a	-17.67	2.25
4b	-18.98	1.53
5a	-10.80	5.63

$\log k_2 = 0.5761\,E + 12.449$
$R^2 = 0.9999$

$N = 21.61;\ s_N = 0.58$
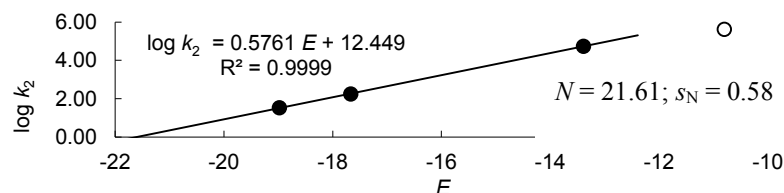
Table 4.58. Kinetics of the reaction of 1f with 3a (DMSO, 20 °C, Stopped-flow method, detection at 533 nm).

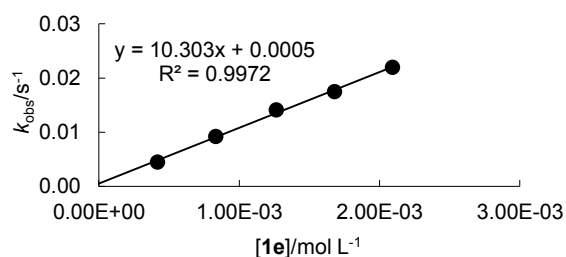| No.	$[3a]$/mol L^{-1}	$[1f]$/mol L^{-1}	k_{obs}/s^{-1}
da201s2-1	2.00×10^{-5}	2.00×10^{-4}	1.41×10^{1}
da201s2-2	2.00×10^{-5}	3.00×10^{-4}	1.79×10^{1}
da201s2-3	2.00×10^{-5}	4.00×10^{-4}	2.50×10^{1}
da201s2-5	2.00×10^{-5}	6.00×10^{-4}	3.56×10^{1}
$k_2(20\ °C) = 5.51 \times 10^{4}$ L mol^{-1} s^{-1}			
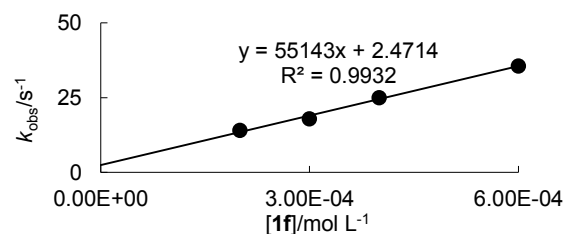
Table 4.59. Kinetics of the reaction of 1f with 4a (DMSO, 20 °C, Stopped-flow method, detection at 425 nm).

No.	[4a]/mol L^{-1}	[1f]/mol L^{-1}	k_{obs}/s^{-1}
da201s3-1	4.00×10^{-3}	1.00×10^{-4}	7.35×10^{-1}
da201s3-2	5.00×10^{-3}	1.00×10^{-4}	9.32×10^{-1}
da201s3-3	6.00×10^{-3}	1.00×10^{-4}	1.13
da201s3-4	7.00×10^{-3}	1.00×10^{-4}	1.31
da201s3-5	8.00×10^{-3}	1.00×10^{-4}	1.43
$k_2(20\ °C) = 1.77 \times 10^2$ L mol^{-1} s^{-1}			

$y = 177.1x + 0.0442$
$R^2 = 0.9928$
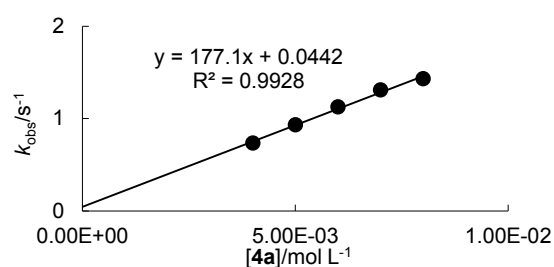
Table 4.60. Kinetics of the reaction of 1f with 4b (DMSO, 20 °C, Stopped-flow method, detection at 425 nm).

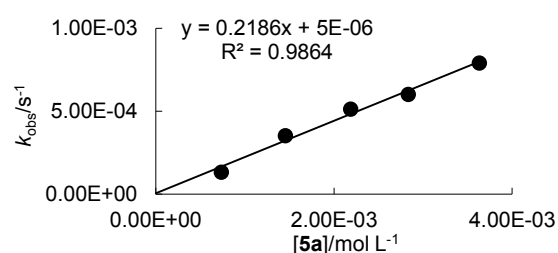| No.	[4b]/mol L^{-1}	[1f]/mol L^{-1}	k_{obs}/s^{-1}
da201s1-1	4.00×10^{-3}	1.00×10^{-4}	1.56×10^{-1}
da201s1-2	5.00×10^{-3}	1.00×10^{-4}	1.85×10^{-1}
da201s1-3	6.00×10^{-3}	1.00×10^{-4}	2.09×10^{-1}
da201s1-4	7.00×10^{-3}	1.00×10^{-4}	2.50×10^{-1}
da201s1-5	8.00×10^{-3}	1.00×10^{-4}	2.93×10^{-1}
$k_2(20\ °C) = 3.39 \times 10^1$ L mol^{-1} s^{-1}			

$y = 33.90x + 0.02$
$R^2 = 0.99$
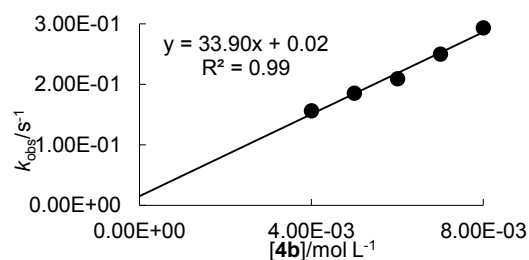
Table 4.61. Kinetics of the reaction of 1f with 5a (DMSO, 20 °C, Stopped-flow method, detection at 425 nm).

No.	[5a]/mol L^{-1}	[1f]/mol L^{-1}	k_{obs}/s^{-1}
da201s6-1	1.10×10^{-3}	1.00×10^{-4}	6.00×10^2
da201s6-2	1.20×10^{-3}	1.00×10^{-4}	6.45×10^2
da201s6-3	1.30×10^{-3}	1.00×10^{-4}	6.96×10^2
da201s6-4	1.40×10^{-3}	1.00×10^{-4}	7.20×10^2
da201s6-5	1.50×10^{-3}	1.00×10^{-4}	7.76×10^2
$k_2(20\ °C) = 4.27 \times 10^5$ L mol^{-1} s^{-1}			

$y = 427000x + 132.3$
$R^2 = 0.9897$
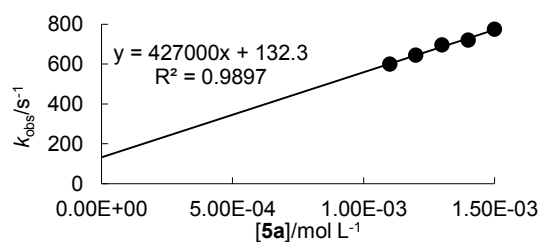
4.5.8.7 Kinetics of the Reactions of 1g with the Electrophiles 2−5
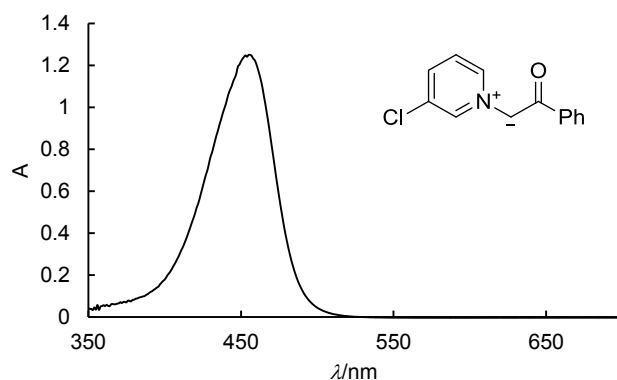
Figure 4.13. UV−Vis spectrum of 1g ($c \sim 1 \times 10^{-4}$ M) in DMSO at 20 °C.

Table 4.62. Determination of the nucleophilicity parameters N and s_N for 1g with the electrophiles 2−4 (filled dots) and 5 (open dots, not used to calculate N and s_N).

$$N = 17.98;\ s_N = 0.63$$

Electrophile	E	$\log k_2$
2b-BF$_4$	-9.45	5.40
3a	-13.39	2.76
4a	-17.67	0.25
5a	-10.80	-0.70
5b	-17.33	0.56

$\log k_2 = 0.6255\,E + 11.248$
$R^2 = 0.9985$
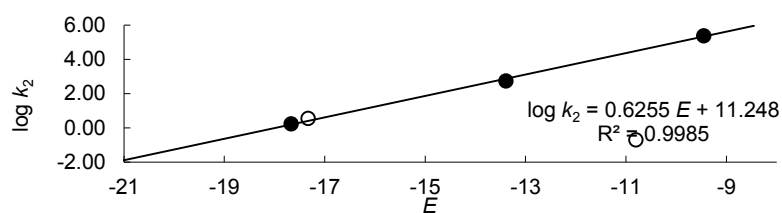
Table 4.63. Kinetics of the reaction of 1g with 2b-BF$_4$ (DMSO, 20 °C, Stopped-flow method, detection at 635 nm).

| No.	[**2b-BF$_4$**]/mol L^{-1}	[**1g**]/mol L^{-1}	k_{obs}/s^{-1}
da277s2-1	5.00×10^{-6}	5.00×10^{-5}	9.23
da277s2-2	5.00×10^{-6}	7.50×10^{-5}	1.41×10^1
da277s2-3	5.00×10^{-6}	1.00×10^{-4}	1.95×10^1
da277s2-4	5.00×10^{-6}	1.25×10^{-4}	2.69×10^1
da277s2-5	5.00×10^{-6}	1.50×10^{-4}	3.40×10^1
k_2(20 °C) = 2.49 × 10^5 L mol^{-1} s^{-1}			

y = 249280x - 4.202
$R^2 = 0.9915$
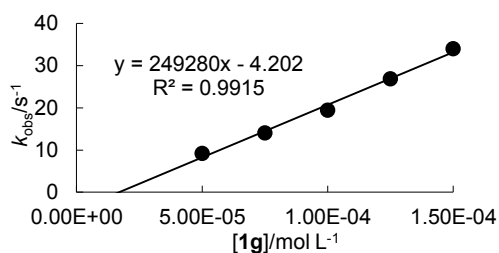
Table 4.64. Kinetics of the reaction of 1g with 3a (DMSO, 20 °C, Stopped-flow method, detection at 533 nm).

No.	[**3a**]/mol L^{-1}	[**1g**]/mol L^{-1}	k_{obs}/s^{-1}
da277s1-1	4.00×10^{-5}	4.00×10^{-4}	2.40×10^{-1}
da277s1-2	4.00×10^{-5}	6.00×10^{-4}	3.53×10^{-1}
da277s1-3	4.00×10^{-5}	8.00×10^{-4}	4.88×10^{-1}
da277s1-4	4.00×10^{-5}	1.00×10^{-3}	5.77×10^{-1}
k_2(20 °C) = 5.73 × 10^2 L mol^{-1} s^{-1}			

y = 573x + 0.0134
$R^2 = 0.9943$
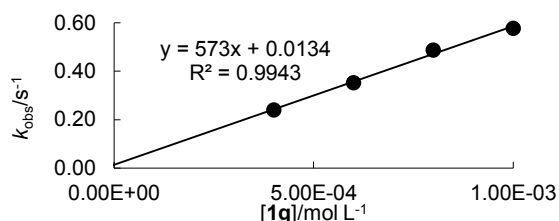
Table 4.65. Kinetics of the reaction of 1g with 4a (DMSO, 20 °C, J&M method, detection at 476 nm).

No.	[**4a**]/mol L^{-1}	[**1g**]/mol L^{-1}	k_{obs}/s^{-1}
da277j1-1	1.02×10^{-3}	1.02×10^{-4}	2.99×10^{-3}
da277j1-3	2.05×10^{-3}	8.22×10^{-5}	5.24×10^{-3}
da277j1-4	2.56×10^{-3}	8.13×10^{-5}	5.88×10^{-3}
da277j1-5	3.03×10^{-3}	8.08×10^{-5}	6.56×10^{-3}
k_2(20 °C) = 1.78 L mol^{-1} s^{-1}			

y = 1.7841x + 0.0013
$R^2 = 0.9841$
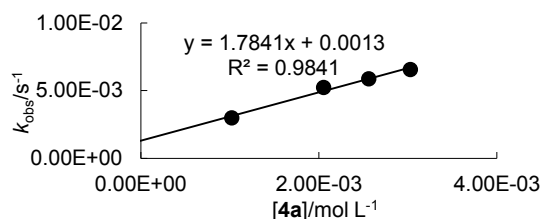
Table 4.66. Kinetics of the reaction of 1g with 5a (DMSO, 20 °C, J&M method, detection at 476 nm).

No.	[**5a**]/mol L^{-1}	[**1g**]/mol L^{-1}	k_{obs}/s^{-1}
da277j3-1	8.22×10^{-4}	8.22×10^{-5}	2.85×10^{-4}
da277j3-2	1.62×10^{-3}	8.10×10^{-5}	4.58×10^{-4}
da277j3-3	2.45×10^{-3}	8.18×10^{-5}	6.06×10^{-4}
da277j3-4	3.23×10^{-3}	8.07×10^{-5}	7.43×10^{-4}
da277j3-5	4.00×10^{-3}	8.00×10^{-5}	9.46×10^{-4}
k_2(20 °C) = 2.02 × 10^{-1} L mol^{-1} s^{-1}			

y = 0.2017x + 0.0001
$R^2 = 0.9947$
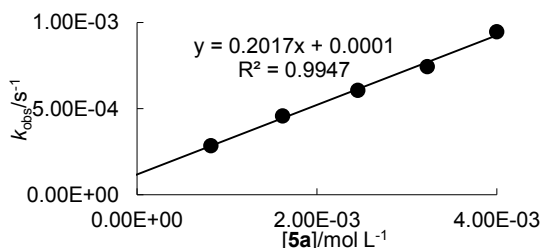
Table 4.67. Kinetics of the reaction of 1g with 5b (DMSO, 20 °C, J&M method, detection at 476 nm).

No.	$[\mathbf{5b}]$/mol L^{-1}	$[\mathbf{1g}]$/mol L^{-1}	k_{obs}/s^{-1}
da277j2-1	6.20×10^{-4}	6.20×10^{-5}	2.56×10^{-3}
da277j2-2	9.38×10^{-4}	6.12×10^{-5}	3.62×10^{-3}
da277j2-3	1.24×10^{-3}	6.21×10^{-5}	4.62×10^{-3}
da277j2-4	1.56×10^{-3}	6.16×10^{-5}	6.03×10^{-3}
da277j2-5	1.84×10^{-3}	6.13×10^{-5}	6.97×10^{-3}
k_2(20 °C) = 3.67 L mol^{-1} s^{-1}			
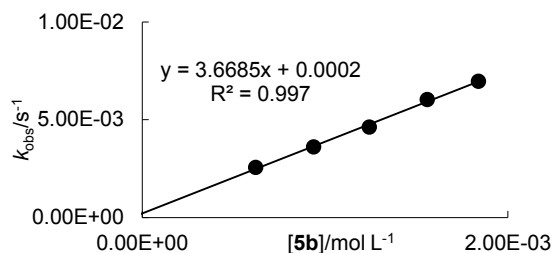
4.5.8.8 Kinetics of the Reactions of 1h with the Electrophiles 2−5
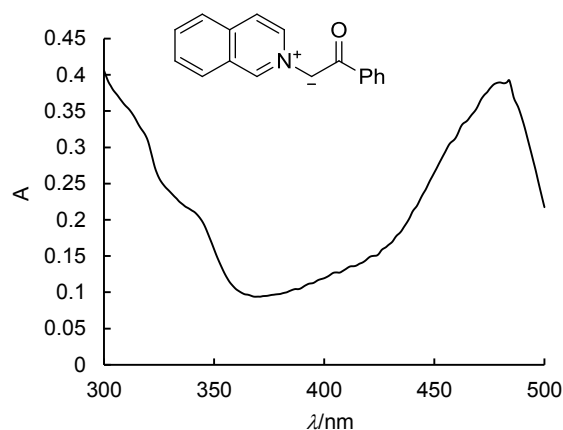
Figure 4.14. UV–Vis spectrum of 1h ($c \sim 5 \times 10^{-5}$ M) in DMSO at 20 °C.

Table 4.68. Determination of the nucleophilicity parameters N and s_N for 1h with the electrophiles 2−4 (filled dots) and 5 (open dots, not used to calculate N and s_N).

Electrophile	E	$\log k_2$
2b-BF$_4$	-9.45	6.18
3a	-13.39	3.59
4a	-17.67	1.48
5a	-10.80	4.47
5b	−17.33	1.55

$N = 20.08$; $s_N = 0.57$

$\log k_2 = 0.5703\,E + 11.451$
$R^2 = 0.9931$

Table 4.69. Kinetics of the reaction of 1h with 2b-BF$_4$ (DMSO, 20 °C, Stopped-flow method, detection at 635 nm).

| No.	$[\mathbf{2b\text{-}BF_4}]$/mol L^{-1}	$[\mathbf{1h}]$/mol L^{-1}	k_{obs}/s^{-1}
da448s1-1	2.00×10^{-5}	1.00×10^{-4}	1.06×10^{2}
da448s1-2	2.00×10^{-5}	1.25×10^{-4}	1.50×10^{2}
da448s1-3	2.00×10^{-5}	1.50×10^{-4}	1.73×10^{2}
da448s1-4	2.00×10^{-5}	1.75×10^{-4}	2.12×10^{2}
da448s1-5	2.00×10^{-5}	2.00×10^{-4}	2.64×10^{2}
k_2(20 °C) = 1.51 × 10^6 L mol^{-1} s^{-1}			

Table 4.70. Kinetics of the reaction of 1h with 3a (DMSO, 20 °C, Stopped-flow method, detection at 533 nm).

| No.	$[3a]/\text{mol L}^{-1}$	$[1h]/\text{mol L}^{-1}$	k_{obs}/s^{-1}
da448s2-1	2.00×10^{-5}	2.00×10^{-4}	8.57×10^{-1}
da448s2-2	2.00×10^{-5}	2.50×10^{-4}	9.74×10^{-1}
da448s2-3	2.00×10^{-5}	3.00×10^{-4}	1.18
da448s2-4	2.00×10^{-5}	3.50×10^{-4}	1.37
da448s2-5	2.00×10^{-5}	4.00×10^{-4}	1.63
$k_2(20\ °C) = 3.88 \times 10^3\ \text{L mol}^{-1}\ \text{s}^{-1}$			

y = 3884x + 0.037
R² = 0.9849

Table 4.71. Kinetics of the reaction of 1h with 4a (DMSO, 20 °C, J&M method, detection at 482 nm).

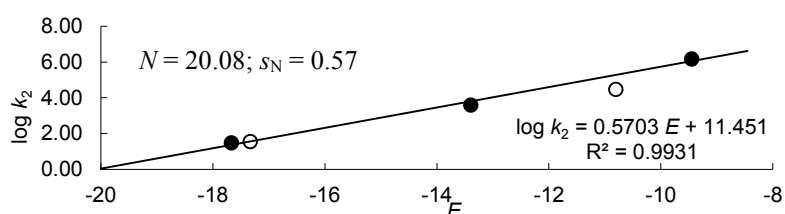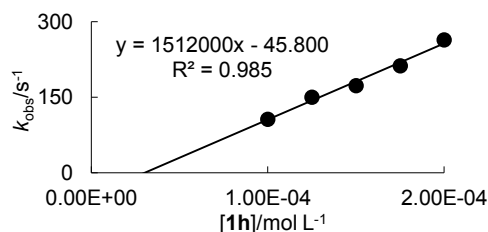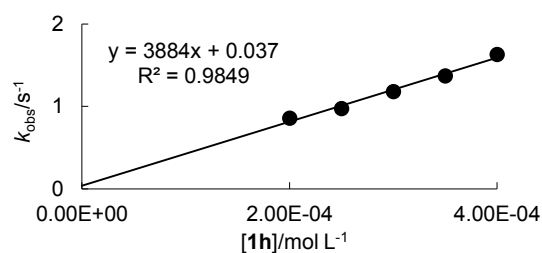| No.	$[4a]/\text{mol L}^{-1}$	$[1h]/\text{mol L}^{-1}$	k_{obs}/s^{-1}
da448j1-1	9.21×10^{-4}	9.21×10^{-5}	3.03×10^{-2}
da448j1-4	1.02×10^{-3}	9.12×10^{-5}	3.33×10^{-2}
da448j1-2	1.11×10^{-3}	9.22×10^{-5}	3.59×10^{-2}
da448j1-5	1.24×10^{-3}	9.65×10^{-5}	3.92×10^{-2}
da448j1-3	1.34×10^{-3}	9.61×10^{-5}	4.35×10^{-2}
$k_2(20\ °C) = 3.05 \times 10^1\ \text{L mol}^{-1}\ \text{s}^{-1}$			

y = 30.502x + 0.0021
R² = 0.9922
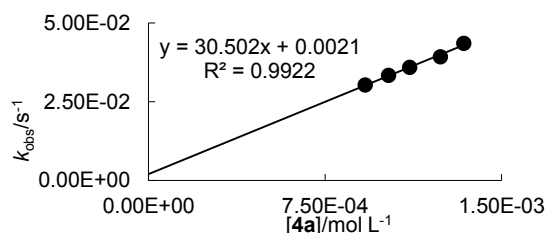
Table 4.72. Kinetics of the reaction of 1h with 5a (DMSO, 20 °C, Stopped-flow method, detection at 482 nm).

No.	$[5a]/\text{mol L}^{-1}$	$[1h]/\text{mol L}^{-1}$	k_{obs}/s^{-1}
da448s4-1	1.00×10^{-3}	1.00×10^{-4}	3.03×10^1
da448s4-2	1.50×10^{-3}	1.00×10^{-4}	4.47×10^1
da448s4-3	2.00×10^{-3}	1.00×10^{-4}	6.04×10^1
da448s4-4	2.50×10^{-3}	1.00×10^{-4}	7.58×10^1
da448s4-5	3.00×10^{-3}	1.00×10^{-4}	8.86×10^1
$k_2(20\ °C) = 2.95 \times 10^4\ \text{L mol}^{-1}\ \text{s}^{-1}$			

y = 29540x + 0.88
R² = 0.9989
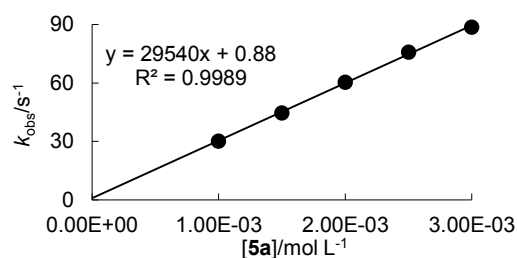
Table 4.73. Kinetics of the reaction of 1h with 5b (DMSO, 20 °C, J&M method, detection at 482 nm).

No.	$[5b]/\text{mol L}^{-1}$	$[1h]/\text{mol L}^{-1}$	k_{obs}/s^{-1}
da448j2-1	9.21×10^{-4}	9.21×10^{-5}	4.02×10^{-2}
da448j2-3	1.15×10^{-3}	9.62×10^{-5}	4.85×10^{-2}
da448j2-4	1.18×10^{-3}	9.10×10^{-5}	5.05×10^{-2}
da448j2-5	1.35×10^{-3}	9.64×10^{-5}	5.53×10^{-2}
$k_2(20\ °C) = 3.56 \times 10^1\ \text{L mol}^{-1}\ \text{s}^{-1}$			

y = 35.575x + 0.0077
R² = 0.9921
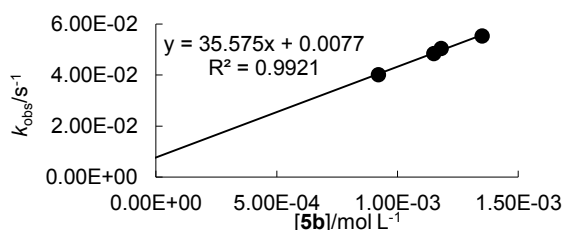
4.5.8.9 Kinetics of the Reactions of 1i with the Electrophiles 3−5
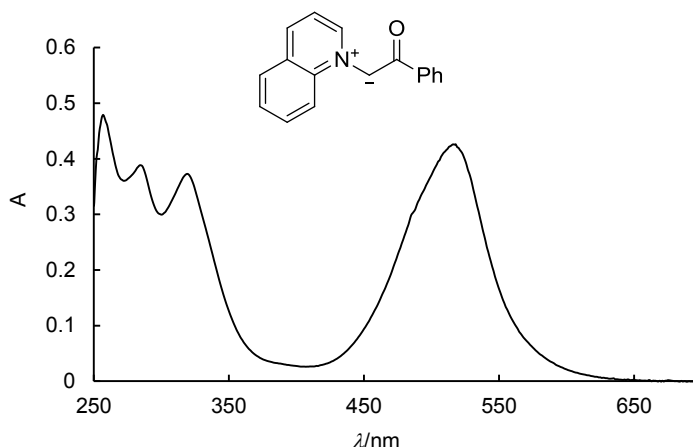
Figure 4.15. UV–Vis spectrum of **1i** ($c \sim 5 \times 10^{-5}$ M) in DMSO at 20 °C.

Table 4.74. Determination of the nucleophilicity parameters N and s_N for 1i with the electrophiles 2−4 (filled dots) and 5 (open dots, not used to calculate N and s_N).

Electrophile	E	$\log k_2$
2b-BF₄	-9.45	5.07
3a	-13.39	2.88
4a	-17.67	0.93
5a	-10.80	3.76
5b	−17.33	1.22

$N = 19.38$;

$s_N = 0.50$

$\log k_2 = 0.503\,E + 9.7489$
$R^2 = 0.9967$
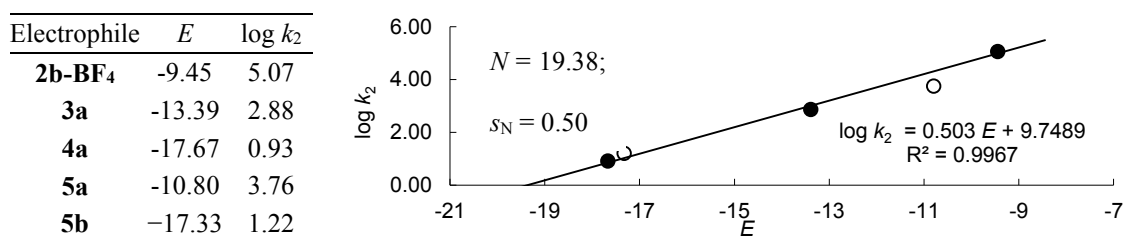
Table 4.75. Kinetics of the reaction of 1i with 2b-BF₄ (DMSO, 20 °C, Stopped-flow method, detection at 635 nm).

No.	[**2b-BF₄**]/mol L⁻¹	[**1i**]/mol L⁻¹	k_{obs}/s⁻¹
da279s2-1	2.00×10^{-5}	2.00×10^{-4}	2.51×10^{1}
da279s2-3	2.00×10^{-5}	3.00×10^{-4}	3.49×10^{1}
da279s2-4	2.00×10^{-5}	3.50×10^{-4}	4.31×10^{1}
da279s2-5	2.00×10^{-5}	4.00×10^{-4}	4.80×10^{1}
$k_2(20\ °C) = 1.17 \times 10^5$ L mol⁻¹ s⁻¹			

$y = 116703x + 1.3129$
$R^2 = 0.9896$
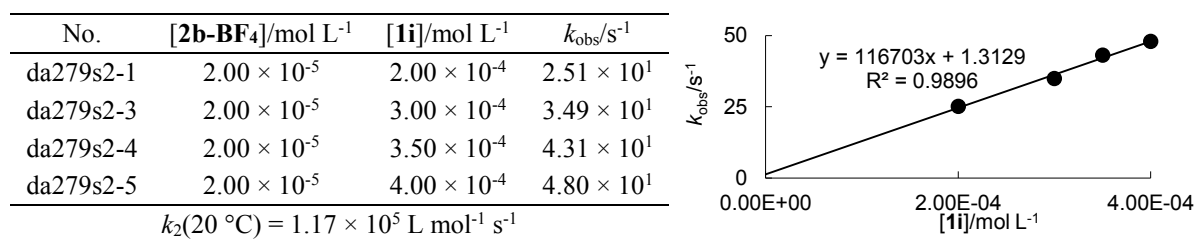
Table 4.76. Kinetics of the reaction of 1i with 3a (DMSO, 20 °C, Stopped-flow method, detection at 533 nm).

No.	[**3a**]/mol L⁻¹	[**1i**]/mol L⁻¹	k_{obs}/s⁻¹
da279s1-2	2.00×10^{-5}	3.00×10^{-4}	1.48×10^{-1}
da279s1-3	2.00×10^{-5}	3.50×10^{-4}	1.83×10^{-1}
da279s1-4	2.00×10^{-5}	4.00×10^{-4}	2.27×10^{-1}
da279s1-5	2.00×10^{-5}	4.50×10^{-4}	2.59×10^{-1}
$k_2(20\ °C) = 7.54 \times 10^2$ L mol⁻¹ s⁻¹			

$y = 754x - 0.0785$
$R^2 = 0.9966$

251
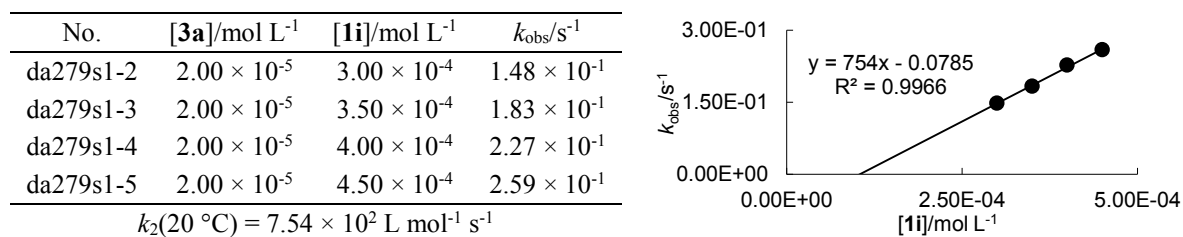
Table 4.77. Kinetics of the reaction of 1i with 4a (DMSO, 20 °C, J&M method, detection at 530 nm).

No.	$[4a]/mol\ L^{-1}$	$[1i]/mol\ L^{-1}$	k_{obs}/s^{-1}
da279j1-1	9.06×10^{-4}	9.06×10^{-5}	9.89×10^{-3}
da279j1-2	1.38×10^{-3}	9.07×10^{-5}	1.48×10^{-2}
da279j1-3	1.80×10^{-3}	9.02×10^{-5}	1.73×10^{-2}
da279j1-5	2.70×10^{-3}	9.01×10^{-5}	2.54×10^{-2}
$k_2(20\ °C) = 8.48\ L\ mol^{-1}\ s^{-1}$			

$y = 8.4791x + 0.0025$
$R^2 = 0.9948$
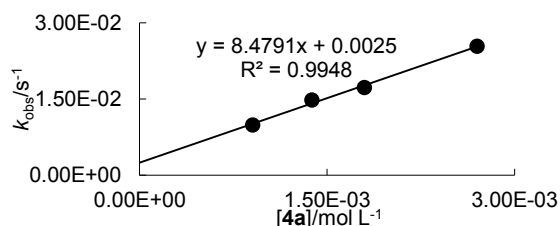
Table 4.78. Kinetics of the reaction of 1i with 5a (DMSO, 20 °C, Stopped-flow method, detection at 530 nm).

No.	$[5a]/mol\ L^{-1}$	$[1i]/mol\ L^{-1}$	k_{obs}/s^{-1}
da279s5-1	2.00×10^{-3}	1.00×10^{-4}	1.14×10^{1}
da279s5-2	3.00×10^{-3}	1.00×10^{-4}	1.69×10^{1}
da279s5-3	4.00×10^{-3}	1.00×10^{-4}	2.33×10^{1}
da279s5-4	5.00×10^{-3}	1.00×10^{-4}	2.90×10^{1}
da279s5-5	6.00×10^{-3}	1.00×10^{-4}	3.40×10^{1}
$k_2(20\ °C) = 5.73 \times 10^{3}\ L\ mol^{-1}\ s^{-1}$			

$y = 5730x$
$R^2 = 0.9985$
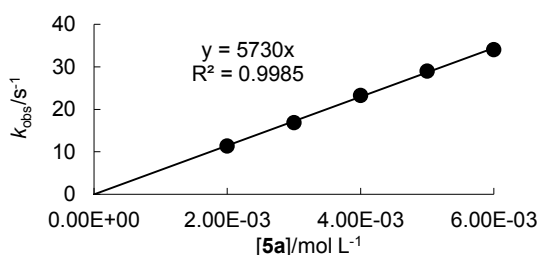
Table 4.79. Kinetics of the reaction of 1i with 5b (DMSO, 20 °C, J&M method, detection at 530 nm).

No.	$[5b]/mol\ L^{-1}$	$[1i]/mol\ L^{-1}$	k_{obs}/s^{-1}
da279j2-1	7.26×10^{-4}	9.07×10^{-5}	1.16×10^{-2}
da279j2-2	1.16×10^{-3}	9.09×10^{-5}	1.91×10^{-2}
da279j2-3	1.38×10^{-3}	9.06×10^{-5}	2.30×10^{-2}
da279j2-4	1.60×10^{-3}	9.11×10^{-5}	2.64×10^{-2}
da279j2-5	1.82×10^{-3}	9.09×10^{-5}	2.94×10^{-2}
$k_2(20\ °C) = 1.64 \times 10^{1}\ L\ mol^{-1}\ s^{-1}$			

$y = 16.428x - 8E-05$
$R^2 = 0.9977$
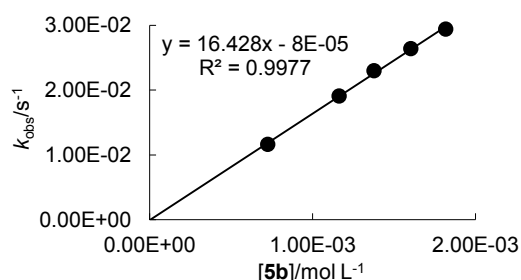
4.5.8.10 Kinetics of the Reactions of the Ylides 1 with Nitrostyrene 5c

Table 4.80. Kinetics of the reaction of 1a with 5c (DMSO, 20 °C, Stopped-flow method, detection at 425 nm).

No.	$[5c]/mol\ L^{-1}$	$[1a]/mol\ L^{-1}$	k_{obs}/s^{-1}
da79s8-4	5.00×10^{-4}	1.00×10^{-4}	3.02×10^{1}
da79s8-5	6.30×10^{-4}	1.00×10^{-4}	3.26×10^{1}
da79s8-1	2.00×10^{-3}	1.00×10^{-4}	8.89×10^{1}
da79s8-2	2.50×10^{-3}	1.00×10^{-4}	1.19×10^{2}
da79s8-3	3.00×10^{-3}	1.00×10^{-4}	1.43×10^{2}
$k_2(20\ °C) = 4.52 \times 10^{4}\ L\ mol^{-1}\ s^{-1}$			

$y = 45165x + 4.7858$
$R^2 = 0.9945$
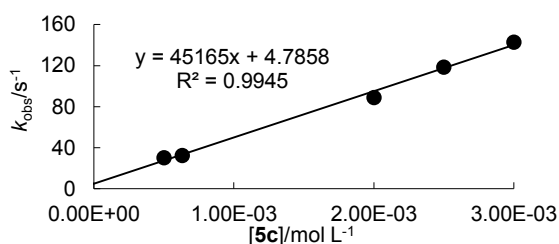
Table 4.81. Kinetics of the reaction of 1b with 5c (DMSO, 20 °C, Stopped-flow method, detection at 425 nm).

No.	$[5c]/mol\ L^{-1}$	$[1b]/mol\ L^{-1}$	k_{obs}/s^{-1}
da191s8-2	1.60×10^{-3}	1.00×10^{-4}	3.28×10^{1}
da191s8-4	2.40×10^{-3}	1.00×10^{-4}	4.02×10^{1}
da191s8-5	3.20×10^{-3}	1.00×10^{-4}	4.86×10^{1}
da191s8-5	4.00×10^{-3}	1.00×10^{-4}	5.64×10^{1}
$k_2(20\ °C) = 9.90 \times 10^{3}\ L\ mol^{-1}\ s^{-1}$			

$y = 9900x + 16.78$
$R^2 = 0.9995$

Table 4.82. Kinetics of the reaction of 1c with 5c (DMSO, 20 °C, Stopped-flow method, detection at 425 nm).

No.	$[5c]$/mol L^{-1}	$[1c]$/mol L^{-1}	k_{obs}/s^{-1}
da130s9-1	5.00×10^{-4}	1.00×10^{-4}	3.13×10^{1}
da130s9-2	6.30×10^{-4}	1.00×10^{-4}	4.00×10^{1}
da130s9-3	7.50×10^{-4}	1.00×10^{-4}	4.88×10^{1}
da130s9-4	8.80×10^{-4}	1.00×10^{-4}	5.78×10^{1}
$k_2(20\ °C) = 7.01 \times 10^{4}$ L mol^{-1} s^{-1}			

y = 70094x - 3.8902
R² = 0.9997

Table 4.83. Kinetics of the reaction of 1d with 5c (DMSO, 20 °C, Stopped-flow method, detection at 425 nm).

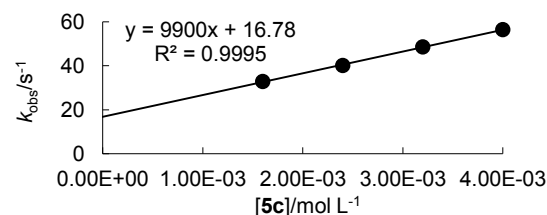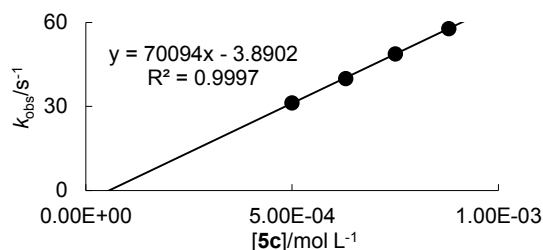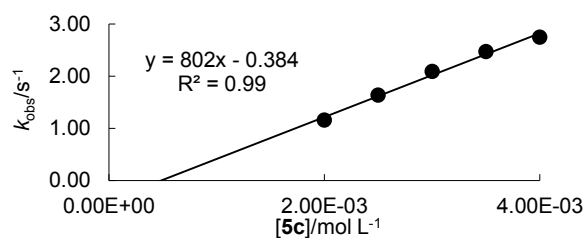| No.	$[5c]$/mol L^{-1}	$[1d]$/mol L^{-1}	k_{obs}/s^{-1}
da167s6-1	2.00×10^{-3}	1.00×10^{-4}	1.16
da167s6-2	2.50×10^{-3}	1.00×10^{-4}	1.64
da167s6-3	3.00×10^{-3}	5.00×10^{-5}	2.09
da167s6-4	3.50×10^{-3}	5.00×10^{-5}	2.47
da167s6-5	4.00×10^{-3}	5.00×10^{-5}	2.75
$k_2(20\ °C) = 8.02 \times 10^{2}$ L mol^{-1} s^{-1}			

y = 802x - 0.384
R² = 0.99

Table 4.84. Kinetics of the reaction of 1e with 5c (DMSO, 20 °C, Stopped-flow method, detection at 445 nm).

No.	$[5c]$/mol L^{-1}	$[1e]$/mol L^{-1}	k_{obs}/s^{-1}
da71s5-1	2.00×10^{-3}	5.00×10^{-5}	7.07×10^{-1}
da71s5-2	3.00×10^{-3}	5.00×10^{-5}	8.72×10^{-1}
da71s5-3	3.50×10^{-3}	5.00×10^{-5}	9.80×10^{-1}
da71s5-5	4.00×10^{-3}	5.00×10^{-5}	1.08
$k_2(20\ °C) = 1.87 \times 10^{2}$ L mol^{-1} s^{-1}			

y = 186.57x + 0.3267
R² = 0.996
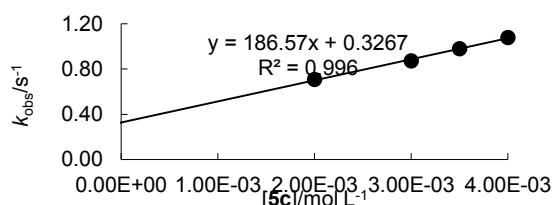
The positive intercept may be caused by a reversible betaine formation.

Table 4.85. Kinetics of the reaction of 1g with 5c (DMSO, 20 °C, Stopped-flow method, detection at 476 nm).

No.	$[5c]$/mol L^{-1}	$[1g]$/mol L^{-1}	k_{obs}/s^{-1}
da277s3-1	2.00×10^{-3}	1.00×10^{-4}	7.20×10^{-2}
da277s3-2	2.50×10^{-3}	1.00×10^{-4}	1.05×10^{-1}
da277s3-3	3.00×10^{-3}	1.00×10^{-4}	1.27×10^{-1}
da277s3-4	3.50×10^{-3}	1.00×10^{-4}	1.48×10^{-1}
da277s3-5	4.00×10^{-3}	1.00×10^{-4}	1.70×10^{-1}
$k_2(20\ °C) = 4.78 \times 10^{1}$ L mol^{-1} s^{-1}			

y = 47.8x - 0.019
R² = 0.9908
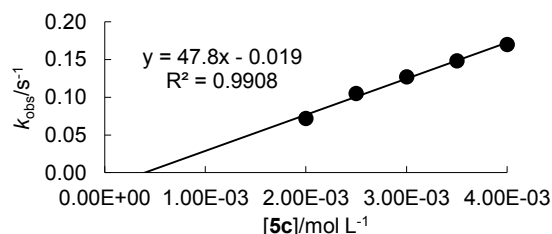
Table 4.86. Kinetics of the reaction of 1h with 5c (DMSO, 20 °C, Stopped-flow method, detection at 482 nm).

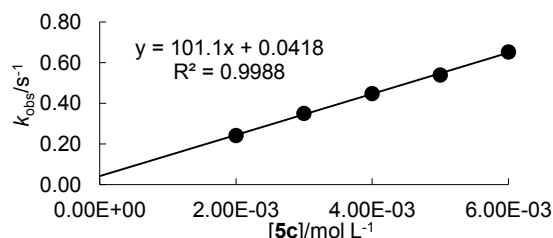| No.	$[5c]$/mol L^{-1}	$[1h]$/mol L^{-1}	k_{obs}/s^{-1}
da448s3-1	2.00×10^{-3}	1.00×10^{-4}	2.42×10^{-1}
da448s3-2	3.00×10^{-3}	1.00×10^{-4}	3.50×10^{-1}
da448s3-3	4.00×10^{-3}	1.00×10^{-4}	4.47×10^{-1}
da448s3-4	5.00×10^{-3}	1.00×10^{-4}	5.39×10^{-1}
da448s3-5	6.00×10^{-3}	1.00×10^{-4}	6.53×10^{-1}
$k_2(20\ °C) = 1.01 \times 10^{2}$ L mol^{-1} s^{-1}			

y = 101.1x + 0.0418
R² = 0.9988

Table 4.87. Kinetics of the reaction of 1i with 5c (DMSO, 20 °C, Stopped-flow method, detection at 530 nm).

No.	$[5c]/\text{mol L}^{-1}$	$[1i]/\text{mol L}^{-1}$	k_{obs}/s^{-1}
da279s4-1	2.00×10^{-3}	1.00×10^{-4}	1.35×10^{-1}
da279s4-2	2.50×10^{-3}	1.00×10^{-4}	1.92×10^{-1}
da279s4-3	3.00×10^{-3}	1.00×10^{-4}	2.41×10^{-1}
da279s4-4	3.50×10^{-3}	1.00×10^{-4}	2.83×10^{-1}
da279s4-5	4.00×10^{-3}	1.00×10^{-4}	3.31×10^{-1}
$k_2(20\,°C) = 9.66 \times 10^1 \text{ L mol}^{-1} \text{ s}^{-1}$			
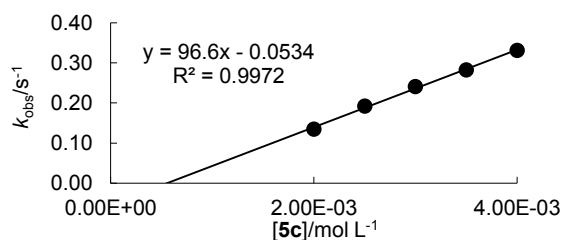
4.6 References

[1] For reviews see: (a) I. Zugravescu, M. Petrovanu, *N-Ylid Chemistry*, McGraw-Hill, New York, **1976**; (b) A. G. Mikhailovskii, V. S. Shklyaev, *Chem. Heterocycl. Compd.* **1997**, *33*, 243−265; (c) J. Jacobs, E. Van Hende, S. Claessens, N. De Kimpe, *Curr. Org. Chem.* **2011**, *15*, 1340−1362; (d) A. Kakehi, *Heterocycles* **2012**, *85*, 1529-1577.

[2] For pK_a studies see: (a) W. G. Phillips, K. W. Ratts, *J. Org. Chem.* **1970**, *35*, 3144-3147; (b) A. R. E. Carey, S. Al-Quatami, R. A. More O'Ferrall, B. A. Murray, *J. Chem. Soc., Chem. Commun.* **1988**, 1097−1098; (c) X.-M. Zhang, F. G. Bordwell, M. Van Der Puy, H. E. Fried, *J. Org. Chem.* **1993**, *58*, 3060−3066; (d) A. R. E. Carey, R. A. More O'Ferrall, B. A. Murray, *J. Chem. Soc., Perkin Trans. 2* **1993**, 2297−2302; (e) Y. Fu, H.-J. Wang, S.-S. Chong, Q.-X. Guo, L. Liu, *J. Org. Chem.* **2009**, *74*, 810−819.

[3] For deprotonation studies see: (a) Z. Dega-Szafran, G. Schroeder, M. Szafran, *J. Phys. Org. Chem.* **1999**, *12*, 39−46; (b) Z. Dega-Szafran, G. Schroeder, M. Szafran, A. Szwajca, B. Łeska, M. Lewandowska, *J. Mol. Struct.* **2000**, *555*, 31−42; (c) M. Szafran, A. Szwajca, B. Łęska, G. Schroeder, Z. Dega-Szafran, *J. Mol. Struct.* **2002**, *643*, 55−68; (d) A. Szwajca, B. Łęska, G. Schroeder, M. Szafran, *J. Mol. Struct.* **2004**, *708*, 87−95.

[4] For kinetic studies see: (a) J. E. Jackson, N. Soundararajan, M. S. Platz, M. T. H. Liu, *J. Am. Chem. Soc.* **1988**, *110*, 5595−5596; (b) R. Bonneau, M. T. H. Liu, R. Lapouyade, *J. Chem. Soc., Perkin Trans. 1* **1989**, 1547−1548.

[5] For computational studies see: (a) P. Karafiloglou, G. Surpateanu, *Int. J. Quantum Chem.* **2004**, *98*, 456−464; (b) S. Matsumura, R. Takagi, S. Kojima, K. Ohkata, M. Abe, *Heterocycles* **2010**, *81*, 2479−2495.

[6] Examples of dihydrofuran synthesis: (a) S. M. Rajesh, S. Perumal, J. C. Menendez, S. Pandian, R. Murugesan, *Tetrahedron* **2012**, *68*, 5631−5636; (b) P. Gunasekaran, K. Balamurugan, S. Sivakumar, S. Perumal, J. C. Menéndez, A. I. Almansour, *Green*

Chem. **2012**, *14*, 750−757; (c) V. A. Osyanin, D. V. Osipov, Y. N. Klimochkin, *J. Org. Chem.* **2013**, *78*, 5505−5520.

[7]   Examples of [3+2]-cycloadduct synthesis: (a) O. Tsuge, S. Kanemasa, S. Takenaka, *Bull. Chem. Soc. Jpn.* **1985**, *58*, 3137−3157; (b) O. Tsuge, S. Kanemasa, S. Takenaka, *Bull. Chem. Soc. Jpn.* **1985**, *58*, 3320−3336; (c) A. M. Shestopalov, Y. A. Sharanin, V. N. Nesterov, L. A. Rodinovskaya, V. E. Shklover, Y. T. Struchkov, V. P. Litvinov, *Chem. Heterocycl. Compd.* **1991**, *27*, 1006−1011; (d) N. Fernández, L. Carrillo, J. L. Vicario, D. Badía, E. Reyes, *Chem. Commun.* **2011**, *47*, 12313−12315.

[8]   Examples of indolizine synthesis: (a) A. R. Katritzky, G. Qiu, B. Yang, H.-Y. He, *J. Org. Chem.* **1999**, *64*, 7618−7621; (b) E. Kim, M. Koh, J. Ryu, S. B. Park, *J. Am. Chem. Soc.* **2008**, *130*, 12206–12207; (c) E. Kim, M. Koh, B. J. Lim, S. B. Park, *J. Am. Chem. Soc.* **2011**, *133*, 6642–6649; (d) Y. Yang, C. Xie, Y. Xie, Y. Zhang, *Org. Lett.* **2012**, *14*, 957−959; (e) M. Kucukdisli, T. Opatz, *Eur. J. Org. Chem.* **2012**, 4555–4564.

[9]   D. S. Allgäuer, H. Mayr, *Eur. J. Org. Chem.* **2013**, 6379–6388.

[10]   Examples for synthesis of stable betaines: (a) Y. Han, J. Chen, L. Hui, C.-G. Yan, *Tetrahedron* **2010**, *66*, 7743−7748; (b) Q.-F. Wang, L. Hui, H. Hou, C.-G. Yan, *J. Comb. Chem.* **2010**, *12*, 260–265; (c) A. Kumar, G. Gupta, S. Srivastava, *Org. Lett.* **2011**, *13*, 6366−6369.

[11]   Examples for cyclopropanations: (a) A. M. Shestopalov, V. P. Litvinov, L. A. Rodinovskaya, Y. A. Sharanin, *Bull. Acad. Sci. USSR, Div. Chem. Sci. (Engl. Transl.)* **1991**, *40*, 129−138; (b) N. H. Vo, C. J. Eyermann, C. N. Hodge, *Tetrahedron Letters* **1997**, *38*, 7951−7954; (c) S. Kojima, K. Fujitomo, Y. Shinohara, M. Shimizu, K. Ohkata, *Tetrahedron Lett.* **2000**, *41*, 9847–9851; (d) S. Yamada, J. Yamamoto, E. Ohta, *Tetrahedron Lett.* **2007**, *48*, 855–858; (e) Q.-F. Wang, X.-K. Song, J. Chen, C.-G. Yan, *J. Comb. Chem.* **2009**, *11*, 1007−1010; (f) N. Kanomata, R. Sakaguchi, K. Sekine, S. Yamashita, H. Tanaka, *Adv. Synth. Catal.* **2010**, *352*, 2966–2978.

[12]   (a) F. G. Bordwell, A. Cripe, D. L. Hughes, in *Nucleophilicity* (Eds.: J. M. Harris, S. P. McManus), American Chemical Society, Washington, DC, **1987**, p. 137−154; (b) W. P. Jencks, in *Nucleophilicity* (Eds.: J. M. Harris, S. P. McManus), American Chemical Society, Washington, DC, **1987**, p. 155−168.

[13]   (a) S. T. A. Berger, A. R. Ofial, H. Mayr, *J. Am. Chem. Soc.* **2007**, *129*, 9753–9761; (b) T. A. Nigst, A. Antipova, H. Mayr, *J. Org. Chem* **2012**, *77*, 8142−8155.

[14] (a) R. Appel, R. Loos, H. Mayr, *J. Am. Chem. Soc.* **2009**, *131*, 704−714; (b) S. Lakhdar, R. Appel, H. Mayr, *Angew. Chem., Int. Ed.* **2009**, *48*, 5034−5037; (c) R. Appel, H. Mayr, *Chem. Eur. J.* **2010**, *16*, 8610−8614; (d) R. Appel, N. Hartmann, H. Mayr, *J. Am. Chem. Soc.* **2010**, *132*, 17894−17900.

[15] For reviews see: (a) H. Mayr, M. Patz, *Angew. Chem., Int. Ed. Engl.* **1994**, *33*, 938−957; (b) H. Mayr, T. Bug, M. F. Gotta, N. Hering, B. Irrgang, B. Janker, B. Kempf, R. Loos, A. R. Ofial, G. Remennikov, H. Schimmel, *J. Am. Chem. Soc.* **2001**, *123*, 9500−9512; (c) R. Lucius, R. Loos, H. Mayr, *Angew. Chem., Int. Ed.* **2002**, *41*, 91−95; (d) H. Mayr, B. Kempf, A. R. Ofial, *Acc. Chem. Res.* **2003**, *36*, 66−77; (e) H. Mayr, A. R. Ofial, *Pure Appl. Chem.* **2005**, 1807−1821; (f) H. Mayr, A. R. Ofial, *J. Phys. Org. Chem.* **2008**, *21*, 584−595; (g) H. Mayr, S. Lakhdar, B. Maji, A. R. Ofial, *Beilstein J. Org. Chem.* **2012**, *8*, 1458−1478; (h) For a comprehensive database of nucleophilicity parameters N, s_N and electrophilicity parameters E, see http://www.cup.lmu.de/oc/mayr/.

[16] (a) T. Lemek, H. Mayr, *J. Org. Chem.* **2003**, *68*, 6880−6886; (b) O. Kaumanns, R. Lucius, H. Mayr, *Chem. Eur. J.* **2008**, *14*, 9675−9682; (c) R. Appel, H. Mayr, *J. Am. Chem. Soc.* **2011**, *113*, 8240−8251.

[17] The *trans*-selectivity of pyridinium ylide mediated cyclopropanations of a broad variety of benzylidene malononitriles and related Michael acceptors was already reported in different solvents, e.g. in MeCN or EtOH.[11]

[18] (a) Hartnagel, M.; Grimm, K.; Mayr, H. *Liebigs Ann.* **1997**, 71−80. (b) Mayr, H.; Ofial, A. R.; Sauer, J.; Schmied, B. *Eur. J. Org. Chem.* **2000**, 2013−2020. (c) Fichtner, C.; Mayr, H. *J. Chem. Soc., Perkin Trans. 2* **2002**, 1441−1444.

[19] In case of the reaction of chalcone **5b** with the 4-NMe$_2$ substituted pyridinium ylide **1f** complicated kinetics were observed, which may be caused by a reversible formation of the intermediate betaine (compare Scheme 4.3). As it is unclear, which reaction step was observed in the kinetic measurement, we excluded **1f** from the studies with chalcone **5b**.

[20] (a) R. Huisgen, *Angew. Chem., Int. Ed. Engl.* **1963**, *2*, 565−598; (b) R. Huisgen, *Angew. Chem., Int. Ed. Engl.* **1963**, *2*, 633−645.

[21] (a) R. A. Firestone, *J. Org. Chem.* **1968**, *33*, 2285−2290; (b) R. Huisgen, *J. Org. Chem.* **1968**, *33*, 2291−2297.

[22] R. Huisgen, in *1,3-Dipolar Cycloaddition Chemistry* (Ed.: A. Padwa), Wiley, New York, **1984**, p. 1−176.

[23]   (a) R. Huisgen, G. Mloston, E. Langhals, *J. Am. Chem. Soc.* **1986**, *108*, 6401−6402; (b) R. Huisgen, G. Mloston, E. Langhals, *Helvetica Chimica Acta* **2001**, *84*, 1805−1820; (c) R. Huisgen, G. Mloston, H. Giera, E. Langhals, *Tetrahedron* **2002**, *58*, 507−519; (d) G. Mloston, R. Huisgen, H. Giera, *Tetrahedron* **2002**, *58*, 4185−4193; (e) R. Huisgen, H. Giera, K. Polborn, *Tetrahedron* **2005**, *61*, 6143−6153; (f) R. Huisgen, P. Pöchlauer, G. Mlostoń, K. Polborn, *Helv. Chim. Acta* **2007**, *90*, 983−998.

[24]   (a) D. H. Ess, K. N. Houk, *J. Am. Chem. Soc.* **2007**, *129*, 10646−10647; (b) D. H. Ess, K. N. Houk, *J. Am. Chem. Soc.* **2008**, *130*, 10187−10198; (c) L. Xu, C. E. Doubleday, K. N. Houk, *J. Am. Chem. Soc.* **2010**, *132*, 3029−3037; (d) Y. Lan, L. Zou, Y. Cao, K. N. Houk, *J. Phys. Chem. A* **2011**, *115*, 13906–13920; (e) S. A. Lopez, M. E. Munk, K. N. Houk, *J. Org. Chem.* **2013**, *78*, 1576−1582.

[25]   (a) W.-J. van Zeist, F. M. Bickelhaupt, *Org. Biomol. Chem.* **2010**, *8*, 3118−3127; (b) I. Fernández, F. P. Cossío, F. M. Bickelhaupt, *J. Org. Chem.* **2011**, *76*, 2310−2314.

[26]   S. Muthusaravanan, S. Perumal, P. Yogeeswari, D. Sriram, *Tetrahedron Lett.* **2010**, *51*, 6439–6443.

[27]   I. Zenz, H. Mayr, *J. Org. Chem.* **2011**, *76*, 9370−9378.

[28]   a) H. E. Gottlieb, V. Kotlyar, A. Nudelman, *J. Org. Chem.* **1997**, *62*, 7512−7515; b) G. F. Fulmer, A. J. M. Miller, N. H. Sherden, H. E. Gottlieb, A. Nudelman, B. M. Stoltz, J. E. Bercaw, K. I. Goldberg, *Organometallics* **2010**, *29*, 2176−2179.

[29]   a) I. C. Calder, Q. N. Porter, C. M. Richards, *Aust. J. Chem.* **1972**, *25*, 345 – 351; b) A. Szwajca, B. Leska, G. Schroeder, M. Szafran, *J. Mol. Struct.* **2004** , *708*, 87 – 95.

[30]   D. S. Allgäuer, Master Thesis, Ludwig-Maximilian-Universität, München (Germany) **2009**.

5 Electrophilicities of 1,2-Disubstituted Ethylenes

Dominik S. Allgäuer and Herbert Mayr

5.1 Introduction

The acceptor-substituted ethylenes **1a−e** (Scheme 5.1) are frequently used in organic syntheses,[1] for example as reagents in Michael additions,[2] [3+2]-cycloadditions,[3, 4] and Diels-Alder reactions,[5, 6] which can be promoted by metals[7, 8] or organocatalysts.[9, 10]

Although the relative reactivities of the acceptor-substituted ethylenes **1a–e** in 1,3-dipolar cycloadditions[3, 4b, 11] and Diels-Alder reactions[6a, b, 12] have been correlated with their LUMO energies, a general quantification of their electrophilicities has, to the best of our knowledge, not been reported.

We have previously shown, that a multitude of reactions of nucleophiles with carbocations and Michael acceptors can be described by eq 5.1, in which electrophiles are characterized by one parameter E (electrophilicity), and nucleophiles are characterized by the solvent-dependent parameters s_N (sensitivity) and N (nucleophilicity).[13] From the linearity of the plots of the second-order rate constants log k_2 versus the electrophilicity parameters E, and from the plots of (log k_2)/s_N versus the nucleophilicity parameters N, reactivity parameters for many types of nucleophiles and electrophiles were derived.[13]

We recently quantified the nucleophilic reactivities N and s_N of colored pyridinium ylides **2**[14] (Table 5.1) and sulfonium ylides **3**[15] (Table 5.2) based on the kinetics of their reactions with benzhydrylium ions, quinone methides, and benzylidene malonates. These N and s_N parameters will now be used to quantify the electrophilic reactivities of colorless Michael acceptors, such as **1**, so that these synthetically important electrophiles may be included into our comprehensive reactivity scale.

$$\log k_2 = s_N(N + E) \qquad (5.1)$$

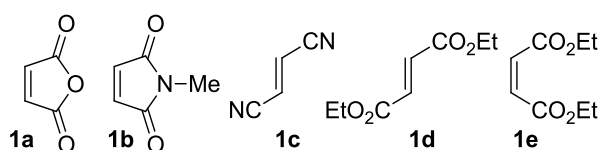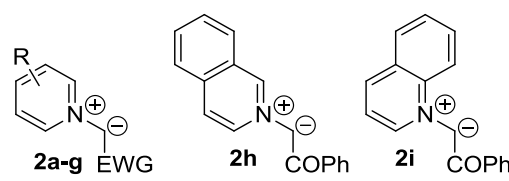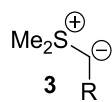**Scheme 5.1. Michael acceptors 1a−e investigated in this work.**

Table 5.1. Pyridinium ylides 2 employed in this work (N and s_N parameters in DMSO from ref. [14]).

Ylide	R	EWG	N/s_N
2a	H	CO_2Et	26.71/0.37
2b	H	$CONEt_2$	27.45/0.38
2c	H	CN	25.94/0.42
2d	H	COMe	20.24/0.60
2e	H	COPh	19.46/0.58
2f	p-NMe$_2$	COPh	21.61/0.58
2g	m-Cl	COPh	17.98/0.63
2h			20.08/0.57
2i			19.38/0.50

Table 5.2. Sulfonium ylides 3 employed in this work (N and s_N parameters in DMSO from ref. [15b]).

Ylide	R	N/s_N
3a	p-CN-C$_6$H$_4$	21.07/0.68
3b	p-NO$_2$-C$_6$H$_4$	18.42/0.65
3c	p-Me$_2$N-C$_6$H$_4$CO	15.68/0.65
3d	p-MeO-C$_6$H$_4$CO	14.48/0.71

5.2 Results and Discussion

5.2.1 General

Pyridinium ylides **2** undergo [3+2]-cycloadditions with dipolarophiles **1** (Scheme 5.2).[16, 17] These reactions can either be concerted (k_{conc}) or stepwise via intermediate betaines (k_2) with a subsequent ring closure (k_{rc}) to the tetrahydroindolizines (Scheme 5.2). For certain substitution patterns, stepwise mechanisms via diradical intermediates have also to be considered.[4c, 18, 19] We recently reported that the 1,3-dipolar cycloadditions of pyridinium ylides with substituted benzylidene malononitriles and chalcones proceed in a stepwise manner via zwitterionic intermediates.[14]

Sulfonium ylides **3** generally react in a stepwise manner with Michael acceptors, with initial irreversible formation of intermediate betaines (k_2), which usually undergo a fast subsequent ring closure (k'_{rc}) to cyclopropanes (Scheme 5.3).[15, 20]

Scheme 5.2. Concerted (upper path) and stepwise cycloadditions (lower path) of the pyridinium ylides 2 with the dipolarophiles 1.
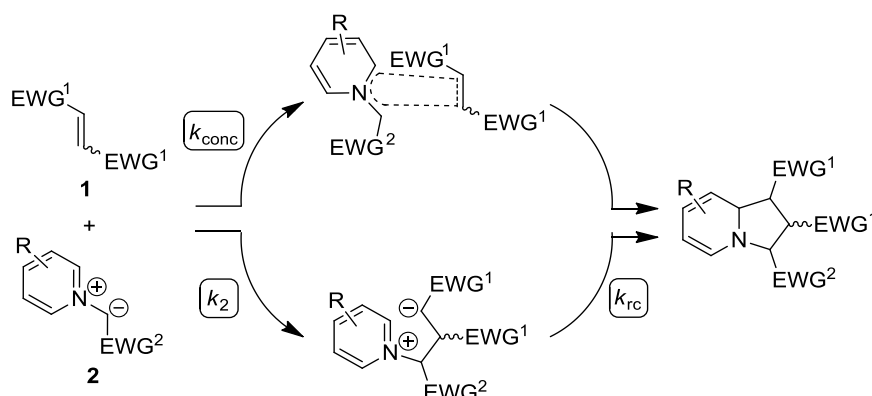
In reactions of alkoxycarbonyl-substituted sulfonium ylides with cyclopentenone, the intermediate betaines are formed irreversibly, and may undergo base-mediated epimerization before they cyclize to cyclopropanes.[21] In contrast, the formation of cyclopropanes from Michael acceptors and aminosulfoxonium ylides was concluded to proceed via reversible formation of the intermediate betaines as di-

Scheme 5.3. Schematic mechanism for the reaction of sulfonium ylides 3 with the Michael acceptors 1.

ethyl maleate was observed to isomerize to diethyl fumarate when combined with the ylide.[22]
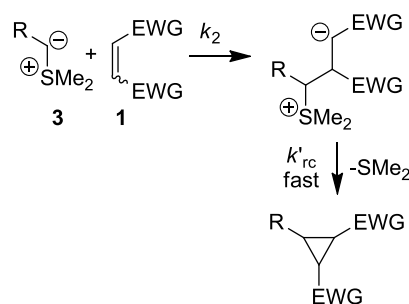
5.2.2 Products

The products of the reactions of the dipolarophiles **1** with isoquinolinium, quinolinium, and pyridinium ylides were studied with **2h** and **2e** as representative examples.

Treatment of DMSO solutions of the dipolarophiles **1a−e** and the isoquinolinium salt **2hH⁺Br⁻** with NEt₃ at ambient temperature gave the tetrahydroindolizines **4a−e** in 65−94% yield with variable diastereoselectivities (Scheme 5.4). The stereochemistry of the products was assigned on the basis of NOESY correlations of the protons and substituents at the pyrrolidine ring, and was found to be consistent with previous investigations of similar tetrahydroindolizines.[17] The major diastereoisomers of **4a−e** shown in Scheme 5.4 originate from 1-*endo* approach of **1a−e** to the *anti*-form of the ylide **2h** (Figure 5.1). The selectivity for this approach is higher for the 1,2-*cis* disubstituted ethylenes **1a,b,e** than for the *trans*-com-

Scheme 5.4. Formation of the tetrahydroindolizines 4a−e in DMSO.

rac-**4a** X = O; 65%, *dr* 7:1[a]
rac-**4b** X = NMe; 90%, *dr* >95:5[a]

rac-**4c** EWG = CN; 66%, *dr* 4:1[a]
rac-**4d** EWG = CO$_2$Et; 66%, *dr* 3:1[a]

rac-**4e** 94%, *dr* >95:5[a]

[a] By ^{1}H-NMR of the crude products.

anti-endo approach
1a X = O
1b X = NMe

anti-1-*endo*-2-*exo* approach
1c EWG = CN
1d EWG = CO$_2$Et

anti-endo approach
1e
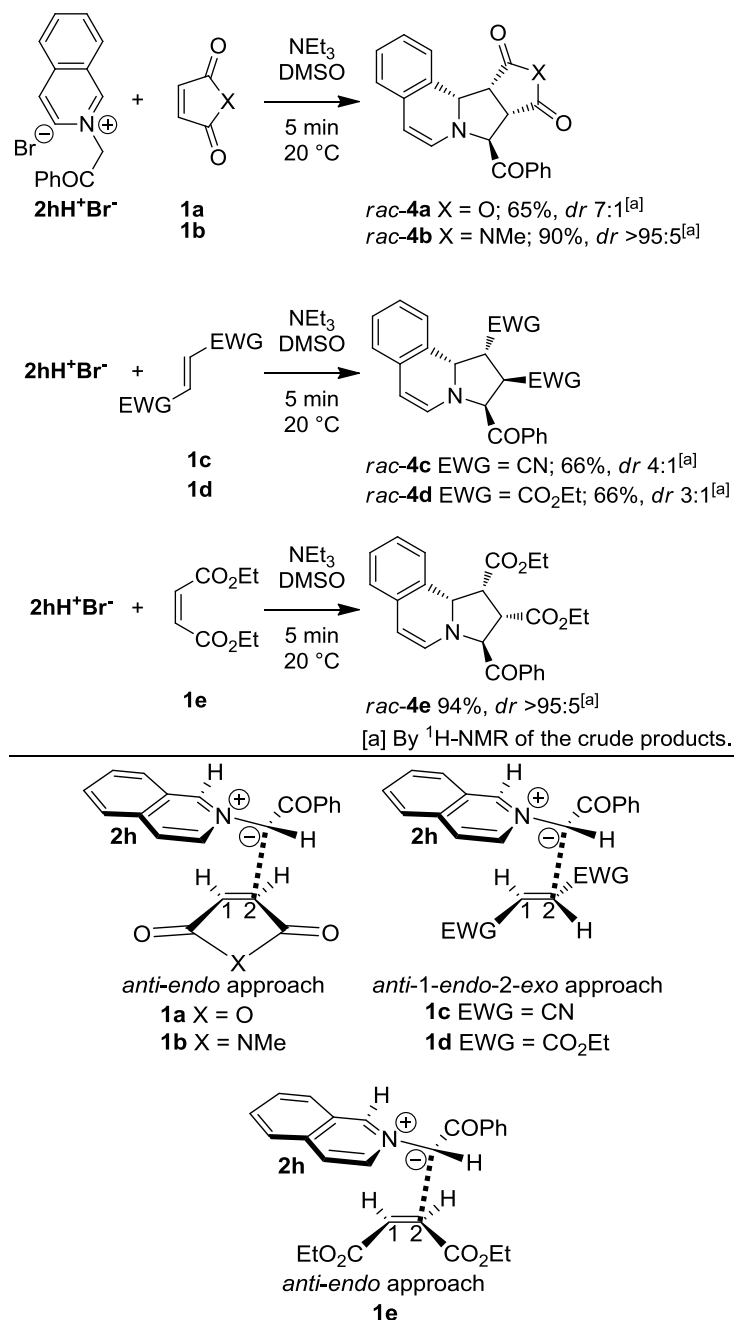
Figure 5.1. *Endo*-**approaches of 1a−e to the ylide 2h.**

pounds **1c** and **1d**; *anti*-endo-tetrahydroindolizines **4b** and **4e** were even formed exclusively.

The reaction of **2eH$^+$Br$^−$** with maleic anhydride (**1a**) in DMF in presence of tetrakispyridinocobalto(II) dichromate (TPCD) was recently reported to give indolizine **6a** by oxidative decarboxylation of the intermediate tetrahydroindolizine (i.e., **5a**; Scheme 5.5).[23] Our attempts to perform this synthesis in DMSO under otherwise identical conditions failed.

**Scheme 5.5. Reaction of maleic anhydride 1a with 2eH⁺Br⁻ under oxidative conditions (from ref. [23]).**
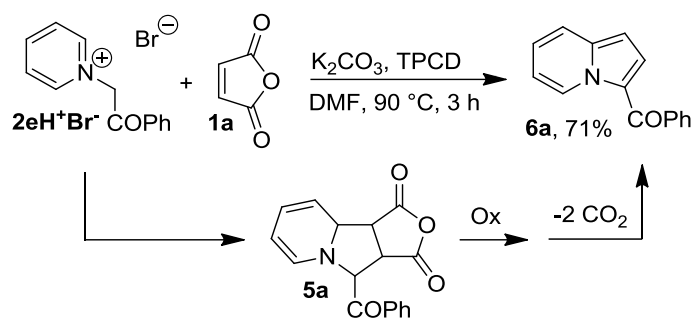
When we treated a mixture of the pyridinium bromide **2eH⁺Br⁻** and maleimide **1b** with triethylamine in DMSO at 20 °C, the tetrahydroindolizine **5b** was obtained as a single diastereoisomer in quantitative yield, as shown by ^{1}H NMR spectroscopy of the crude reaction mixture (Scheme 5.6). The formation of **5b** has previously been reported by Tsuge and co-workers,[24] who also determined the stereochemistry of **5b** to be that shown in Scheme 5.6.[24a]

Our attempts to purify **5b** by chromatography on silica gel with chloroform as eluent led to the formation of (*E*)-itaconimide **7b** in 51% yield. The configuration of the double bond was verified by the NOESY correlation of the protons and substituents at the double bond, and is in agreement with reported data.[24] The formation of **7b** can be rationalized by the mechanism shown in Scheme 5.6. In this mechanism, the weak bond between C-9a and C-9b in tetrahydroindolizine **5b** cleaves to regenerate the betaine **8b**, which is protonated to give Michael adduct **9b**. Elimination of a proton and pyridine from **9b** by an E2 or E1cB mechanism gives the *E*-itaconimide **7b**.

Combination of the Michael acceptors **1c−e** with the pyridinium salt **2eH⁺Br⁻** and base led to the formation of the tetrahydroindolizines **5c−e**, which were not characterized but were oxidized in a one-pot procedure by 2 equiv. of chloranil to the indolizines **10c−d** in 63−88% yield (Scheme 5.7). The cycloaddition of **2e** with **1c** was achieved by treatment of a mixture of **2eH⁺Br⁻** and **1c** with NEt₃, whereas attempts to perform this reaction under biphasic conditions [CH₂Cl₂/aq. NaOH (32%)][25] only led to polymerization of **1c**. However, biphasic conditions were successfully used for the reactions of **2eH⁺Br⁻** with **1d** and **1e** to give indolizine **10d** after oxidation.

The reaction of the sulfonium ylides **3c,d** with **1b,c** as representative examples resulted in the formation of the cyclopropanes **11b** and **11c** with complete stereocontrol in 46% and 62% yields, respectively (Scheme 5.8).[26] The stereochemistry of the cyclopropanes **11b,c** was assigned on basis of NOESY correlations of the protons and substituents at the cyclopropane ring.

Scheme 5.6. Base induced reaction of 2eH⁺Br⁻ with *N*-Mmethylmaleimide 1b. Stereochemistry of 5b according to ref. [24a].
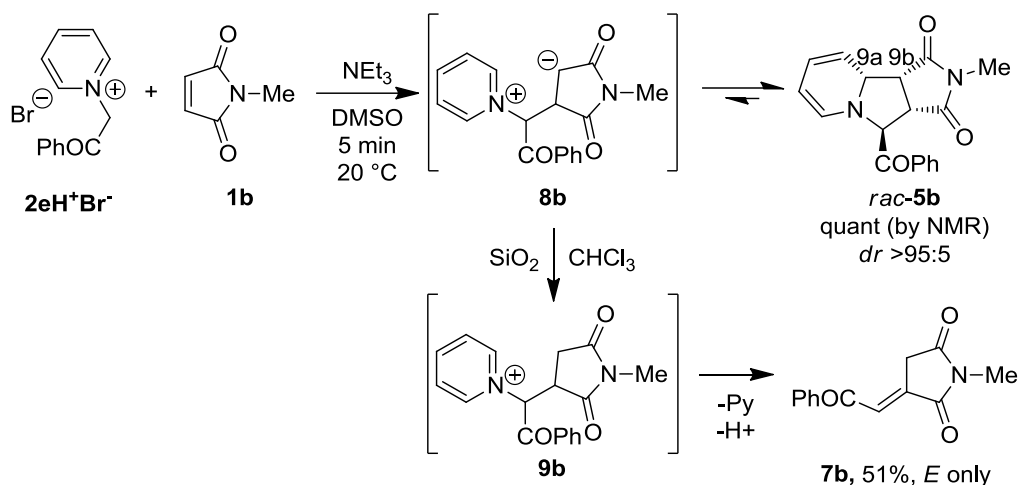
Scheme 5.7. Synthesis of indolizines 10c−d.
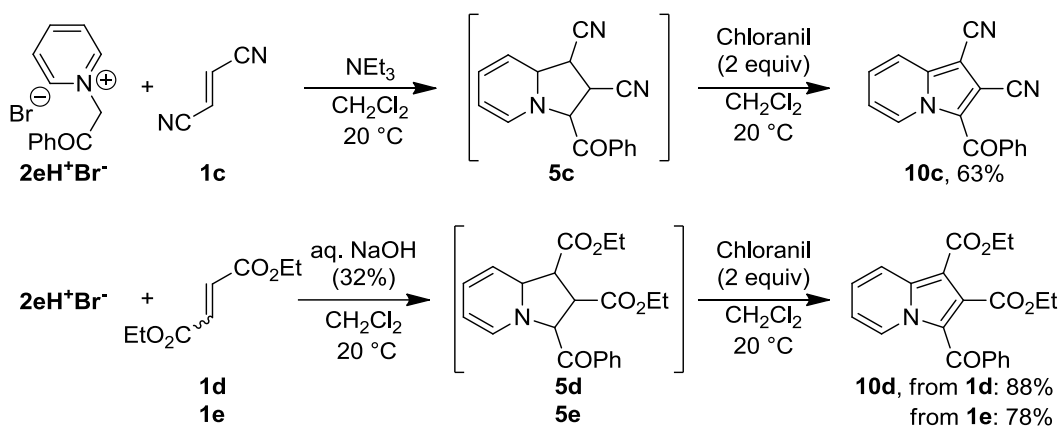
The reactions of the sulfonium ylides **3a**,**b** with **1b**,**c** did not lead to isolable products, possibly due to polymerization of **1b**,**c** initiated by the high KO^{t}Bu concentrations required to generate the ylides **3a**,**b**. For the kinetic investigations of these reactions dilute solutions of the ylides **3a**,**b** and the ethylenes **1b**,**c** were used. Clean second-order reactions were observed under these conditions, possibly because in highly dilute solutions the base induced polymerization of the ethylenes was suppressed. The kinetics of the reaction of maleic anhydride **1a** with the sulfonium ylide **3b** followed a second-order rate law, but we were not able to isolate a product from the reaction. Thus a definite interpretation of the determined second-order rate constant k_2^{exp} (see below) will not be attempted.

The reaction of diethyl fumarate **1d** with sulfonium ylide **3a** gave the cyclopropane **11d** in 81% yield with exclusive formation of the diastereoisomer with the ester groups *trans* to each other (stereochemistry verified by NOESY as described above; Scheme 5.8). The preferred formation of the cyclopropane **11d** with the ester groups in a *trans* configuration to each other

was also found inthe reaction of diethyl maleate **1e** with sulfonium ylide **3a** (Scheme 5.8), which indicates that the *cis*-configuration of the double bond of diethyl maleate **1e** was eroded during the cyclopropanation process. This observation can be rationalized by the intermediate formation of the betaine **12e**, which has sufficient life-time for the rotation around the σ bond between C-1 and C-2 to take place before cyclization with elimination of dimethyl sulfide leads to the diastereoisomer of cyclopropane **11d** shown in Scheme 5.9.[20a, 22a] Non-stereospecific cyclopropanations have previously been observed in the reaction of diethyl maleate **1e** with aminosulfoxonium ylides.[22a] As diethyl maleate **1e** isomerized to diethyl fumarate **1d** in the presence of aminosulfoxonium ylides it was concluded that the betaine formation from diethyl maleate **1e** and aminosulfoxonium ylides was a reversible process.[22a] To clarify, whether the formation of betaine **12e** from diethyl maleate **1e** and the sulfonium ylide **3a** is a reversible or irreversible process, the reaction was monitored by ^{1}H NMR in DMSO-d_6 at ambient temperature.

Scheme 5.8. Cyclopropanations of the Michael acceptors 1b−e with the sulfonium ylides 3a−d.
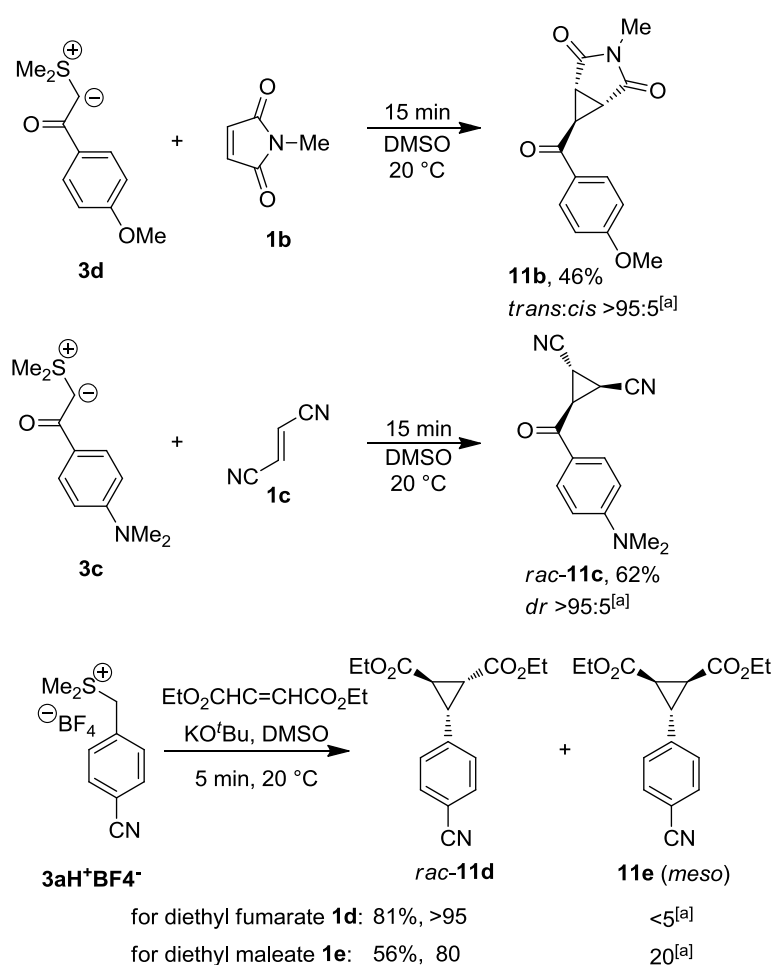
[a] Determined by ^{1}H NMR of the crude product.
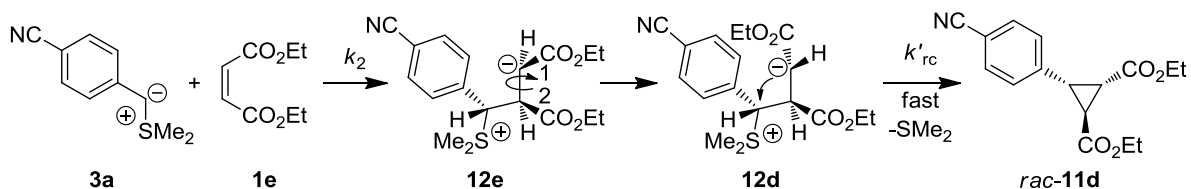
Scheme 5.9. Mechanism of the cyclopropanation reaction of diethyl maleate 1e with 3a.

When 1 equiv. of KO^{t}Bu in DMSO-d_6 was added to a solution of **3aH$^+$BF$_4^-$** and **1e** in DMSO-d_6 the cyclopropane **11d**, SMe$_2$, ^{t}BuOH and decomposition products of the ylide **3a**, but also non-converted **3aH$^+$BF$_4^-$**, **1e**, and traces of **11e** were observed in the ^{1}H NMR spectrum taken immediately after mixing the reagents. The ^{1}H NMR spectrum did not change during 13 min (for details see Experimental Section). As betaines **12d** and **12e** were not observable, one can exclude fast formation of **12d** and **12e**, which would then undergo subsequent slow cyclization. The ^{1}H NMR spectra of the reaction mixture also allowed excluding reversible formation of the betaines **12d** and **12e**, because diethyl fumarate **1d** was not observed in the reaction mixture.

5.2.3 Kinetic Investigations

The kinetics of the reactions of **1a−e** with the ylides **2** and **3** were investigated in DMSO solution at 20 °C and monitored photometrically by following the disappearance of the ylides **2** and **3** at or close to their absorption maxima. Due to their low stabilities, the ylides **2a−i** and **3a,b** were generated directly before each kinetic experiment in the flask used for the kinetic experiment by combining DMSO solutions of the salts **2(a−i)H$^+$X$^-$** or **3(a,b)H$^+$BF$_4^-$** with KO^{t}Bu (typically 1.05 equivalents). To perform the kinetic measurements under pseudo-first-order conditions an excess of at least 10 equivalents of the Michael acceptors **1a−e** with respect to the ylides **2** and **3** was used.
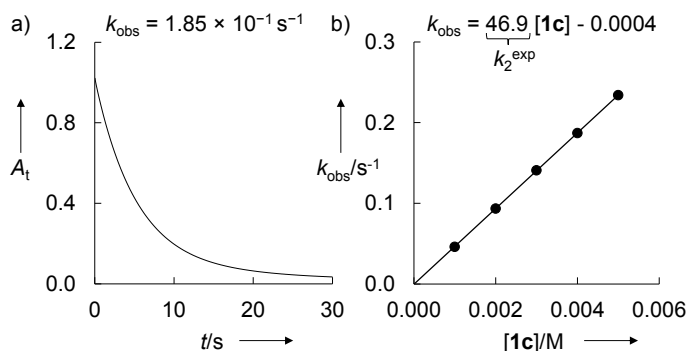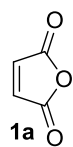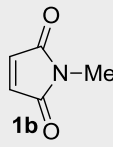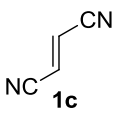

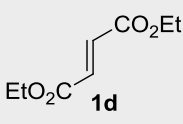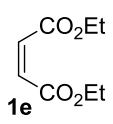**Figure 5.2. a) Decay of the absorbance of 2e ([2e]$_0$ = 5 × 10^{-5} M) at 445 nm during its reaction with 1c ([1c]$_0$ = 4.00 × 10^{-3} M) in DMSO at 20°C. b) Correlation of k_{obs} with the concentration of 1c.**

Table 5.3. Experimental (k_2^{exp}) and calculated (k_2^{calcd})[a] second-order rate constants for the reactions of the Michael acceptors 1a−e with the ylides 2a−i and 3a,b in DMSO at 20 °C.

Electrophile	Ylide	k_2^{exp}/M^{-1} s^{-1}	k_2^{calcd}/M^{-1} s^{-1}	k_2^{exp}/k_2^{calcd}
	2d	3.69×10^5	2.27×10^5	1.6
	2e	4.74×10^4	5.32×10^4	0.89
1a	**2g**	1.16×10^4	1.59×10^4	0.73
	2h	$\approx 2.1 \times 10^5$ [b]	9.94×10^4	2.1
	2i	$\approx 1.8 \times 10^4$ [b]	1.08×10^4	1.7
$E = -11.31$	**3b**	4.00×10^4	4.17×10^4	1.0
	2d	7.84×10^3	5.04×10^3	1.6
	2e	1.15×10^3	1.34×10^3	0.86
1b N−Me	**2f**	2.07×10^4	2.37×10^4	0.88
	2h	1.81×10^4 [c]	2.67×10^3	6.8
	2i	2.44×10^4 [c]	4.53×10^2	54
$E = -14.07$	**3b**	5.80×10^2	6.74×10^2	0.86
	2a	$\approx 1.6 \times 10^5$ [b]	1.17×10^4	14
	2c	$\approx 1.5 \times 10^5$ [b]	2.51×10^4	5.9
1c	**2d**	6.18×10^2	5.22×10^2	1.2
	2e	4.69×10^1	1.50×10^2	0.31
	2g	2.29×10^1	2.69×10^1	0.85
$E = -15.71$	**2h**	4.73×10^2	3.10×10^2	1.5
	3a	8.42×10^3	4.41×10^3	1.9
	2a	8.83×10^3 [c]	1.99×10^3	4.4
	2b	$\approx 7.1 \times 10^3$ [b]	4.67×10^3	1.5
1d	**2c**	$\approx 1.4 \times 10^4$ [b]	2.64×10^3	5.3
	2d	4.73×10^1	2.93×10^1	1.6
	2e	4.54	9.25	0.49
$E = -17.79$	**2h**	5.68×10^2 [c]	2.01×10^1	28
	3a	2.03×10^2	1.69×10^2	1.2
	2c	9.28×10^2	5.09×10^2	1.8
1e	**2d**	3.12 [d]	2.80	1.1
	2e	5.53×10^{-1}	9.54×10^{-1}	0.58
	2h	1.47×10^1 [c]	2.05	7.2
$E = -19.49$	**3a**	(≈ 3.4) [e]	1.18×10^1	0.29

[a] Calculated by eq 1 using the N and s_N parameters from Tables 1 and 2 and E in this Table; [b] As the k_{obs} versus [**1**] plots for these reactions, which proceed on the <10 ms time scale, do not have negligible intercepts, these data are considered to be less reliable and were not used for the determination of E(**1a,c,d**) according to eq 1; [c] These rate constants possibly correspond to concerted, but highly unsymmetrical processes and were thus exempted from the determination of E; [d] By stopped-flow method; reproduction by a spectrometer using fiber optics gave k_2^{exp} = 3.48 M^{-1} s^{-1} (details see Supporting Information); [e] Kinetics deviate slightly from second-order rate law, and thus k_2 not employed for the determination of E.

The first-order rate constants k_{obs} were obtained by least squares fitting of the exponential function $A_t = A_0 \exp(-k_{obs}t) + C$ (mono-exponential decrease) to the observed time-dependent absorbances (Figure 5.2a). Most of the Correlations of k_{obs} with the concentrations of the Michael acceptors **1a−e** were linear with negligible intercepts, as required by the relation $k_{obs} = k_2[\mathbf{1}]$ (Figure 5.2b). From the slopes of the linear correlations, the second-order rate constants for the reactions of the Michael acceptors **1a−e** with the ylides **2,3** were obtained (Table 5.3).

When the reactions of the pyridinium ylides **2** and the sulfonium ylides **3** with the acceptor-substituted ethylenes **1** proceed stepwise with rate-determining formation of the zwitterionic intermediates **8** and **12**, the measured rate constants correspond to k_2, as specified in Schemes 5.2 and 5.3. As k_2 refers to the formation of one new CC-bond without breaking a σ-bond, as the reactions employed for the parameterization of eq 5.1, this correlation may also apply for the rate constants listed in Table 5.3. A linear correlation was found (Figure 5.3) when (log k_2^{exp})/s_N was plotted against the previously published nucleophilicity parameters N, which had been derived from the reactions of the ylides **2** and **3** with benzhydrylium ions, quinone methides, and benzylidene malonates.

Using the constants from Table 5.3, which could unambiguously be assigned to k_2 (see footnotes of Table 5.3 and the text below) the electrophilicity parameters E of the 1,2-disubstituted ethylenes **1a−e** were calculated by least square-fitting, i.e., by minimizing $\Delta^2 = \sum(\log k_2 - s_N(N + E))^2$ (Table 5.3).
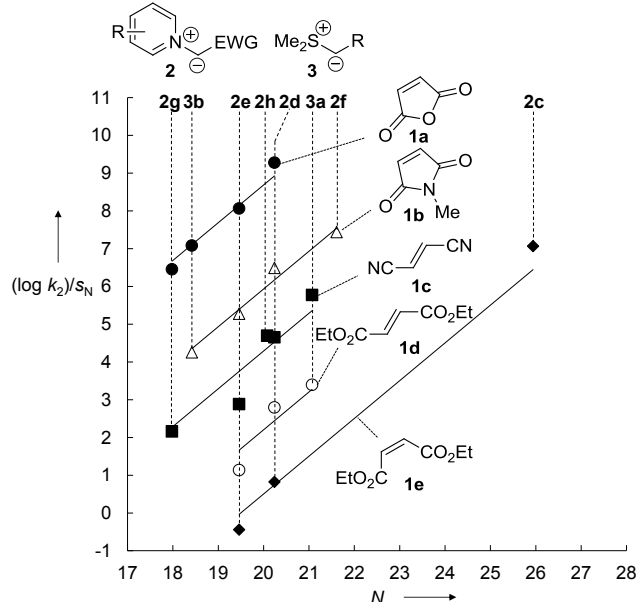

Figure 5.3. Correlation of (log k_2)/s_N-values derived from the reactions of the dipolarophiles 1 with the ylides 2,3 against the corresponding nucleophilicity parameters N of the ylides 2,3 (the slopes are fixed to 1.0 as required by eq 5.1). k_2 Values not used for the determination of E are not shown but are listed in Table 5.3.

Table 5.3 compares the experimental rate-constants for the reactions of the ylides **2** and **3** with the acceptor-substituted ethylenes **1** with the values calculated by eq 5.1 using the nucleophile-specific parameters s_N and N from Tables 5.1 and 5.2, and the electrophilicity parameters E listed in Table 5.3, which were obtained by the described least-squares minimization. The 19 second-order rate constants used to derive the electrophilicity parameters E of the activated ethylenes **1**, as well as four rate constants which were not used for the parameterization because of their lower precision, agreed with the calculated values within a factor of 3.

The remaining eight reactions proceed 4 to 54 times faster than calculated by equation 1. Though these deviations are within the confidence limit of equation 1, these rate constants have not been used for deriving the electrophilicity parameter E, as the positive deviations might also be due to a low degree of concertedness of these [3+2]-cycloaddition reactions.

The fact that all rate constants listed in Table 5.3 agree with the values calculated by eq 5.1 within two orders of magnitude, 28 out of the 31 values even within one order of magnitude, indicates that all reactions, even though they led to different final products – tetrahydroindolizines (from **2**) and cyclopropanes (from **3**) – share a common rate determining step, i.e., formation of one new CC-bond with generation of an intermediate betaines. However, as discussed above, concerted processes with highly unsymmetrical transition states cannot be excluded for some 1,3-dipolar cycloadditions.

5.3 Conclusion

The correlation (5.1), $\log k_2 = s_N(N + E)$, where electrophiles are characterized by one (E), and nucleophiles are characterized by two parameters (N, s_N) was found to describe the rates of the stepwise 1,3-dipolar cycloadditions of pyridinium ylides **2** with the 1,2-diacceptor substituted ethylenes **1a−e** as well as the rates of the stepwise cyclopropanations of **1a−e** with the sulfonium ylide **3**. From the fact that the same electrophilicity parameters E can be used for both types of reaction of the acceptor-substituted ethylenes **1a−e**, we conclude that all reactions proceed with analogous rate-determining steps, i.e., formation of one new CC-bond leading to a zwitterionic intermediate, that subsequently undergoes fast reactions to give either [3+2]-cycloadducts or cyclopropanes.
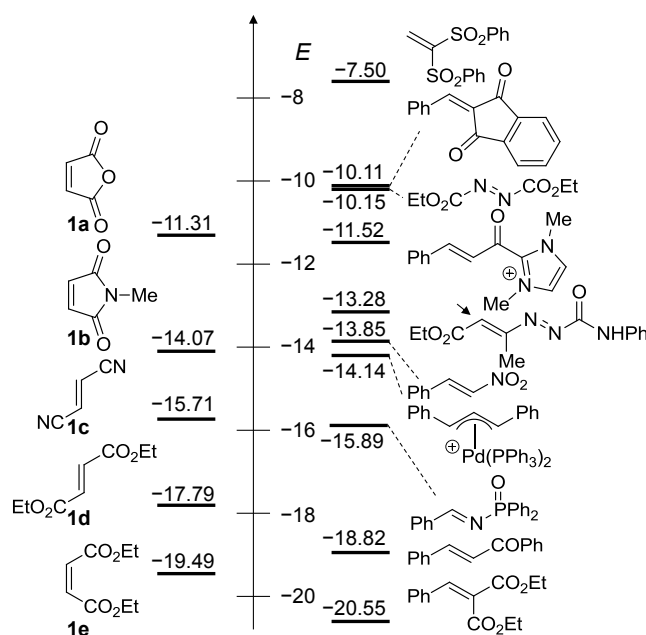
Figure 5.4. Comparison of the electrophilicity parameters *E* of the 1,2-disubstituted ethylenes 1a–e (Table 5.3) and other Michael acceptors (*E* from refs. [27-30, 32-35]).

For that reason, the Michael acceptors **1a–e** can be integrated in our comprehensive electrophilicity scale (Figure 5.4), which shows that the electrophilicity parameters *E* for the dipolarophiles **1** cover almost 9 orders of magnitude. The most reactive Michael acceptor in this series, maleic anhydride **1a**, has a similar electrophilic reactivity as diethyl azodicarboxylate,[27] benzylidene indandione,[28] or acylazolium ions,[29] but it is less electrophilic than the *gem*-substituted di(phenylsulfonyl)ethene.[30] The reactivity of the double bond decreases by approximately 3 orders of magnitude, when the bridging oxygen in **1a** is substituted by a methylimino group in *N*-methyl maleimide **1b**, that has a similar reactivity as palladium-stabilized arylallyl cations,[31] 1,2-diaza-1,3-diene,[32] or β-nitrostyrene.[33] Fumaronitrile **1c** is approximately 2 orders of magnitude less reactive than **1b** with an electrophilicity similar to that of a phosphinoyl-substituted imine.[34] Exchanging the cyano groups in fumaronitrile **1c** by ethoxy carbonyl groups (**1d**) decreases the electrophilic reactivity by two more orders of magnitude, making **1d** similarly reactive as chalcone.[34] The activated C=C-double bond in ethyl fumarate **1d** is almost 8 orders of magnitude less electrophilic, than the analogously substituted N=N-double bond in diethyl azodicarboxylate. A change of the double bond geometry of the dipolarophile from *trans* (**1d**) to *cis* in diethyl maleate **1e** decreases the reactivity by 2 orders of magnitude,[4a] that **1e** adopts a similar electrophilicity as diethyl benzylidenemalonate.[35] Attempts to rationalize this nucleophile-independent order of electrophilicities are in progress.[36]

5.4 Experimental Section

5.4.1 General

Chemicals. The pyridinium salts **2H⁺X⁻** were synthesized as described in ref. [25]; the sulfonium salts **3(a,b)H⁺BF₄⁻** were synthesized as described in ref. [15b], and the sulfonium ylides **3c,d** as described in ref. [15a].

Analytics. ^{1}H and ^{13}C NMR spectra were recorded in CDCl$_3$ (δ_H 7.26, δ_c 77.16),[37a] CD$_3$CN (δ_H 1.94, δ_c 118.26),[37b] or DMSO-d_6 (δ_H 2.50, δ_c 39.52)[37a] on 200, 300, 400, or 600 MHz NMR spectrometers. The following abbreviations were used to designate chemical shift multiplicities: s = singlet, d = doublet, t = triplet, q = quartet, m = multiplet, br = broad. For reasons of simplicity, the ^{1}H NMR signals of AA'BB'-spin systems of *p*-disubstituted aromatic rings were treated as doublets. The assignments of individual NMR signals were based on additional 2D NMR experiments (COSY, NOESY, HSQC, HMBC). Diastereomeric ratios (*dr*) were determined by ^{1}H NMR of the crude reaction products if not stated otherwise. HRMS and MS were recorded on a Finnigan MAT 95 Q (EI) mass spectrometer or Thermo Finnigan LTQ FT Ultra (ESI). The melting points were recorded on a Büchi Melting Point B-540 device and are not corrected.

Kinetics. DMSO (99.7%, extra dry, over molecular sieves, AcroSeal) was purchased and used without further purification. The rates of all reactions were determined by UV-vis spectroscopy in DMSO at 20 °C by using stopped-flow spectrophotometer systems (Applied Photophysics SX.18MV-R and Hi-Tech SF-61DX2) as well as diodearray-spectrophotometer systems (J&M TIDAS DAD 2062). The temperature of the solutions during the kinetic studies was maintained at 20 ± 0.2 °C by using circulating bath cryostats. The ylides were generated in DMSO at 20 °C immediately before each kinetic run by mixing DMSO solutions of the pyridinium **2H⁺X⁻** or sulfonium salts **3H⁺BF₄⁻**, and KO^{t}Bu (typically 1.05 equiv). The kinetic runs were initiated by mixing DMSO solutions of the Michael acceptors **1** and the ylides **2,3** under first-order conditions with **1** in large excess over **2,3** (>10 equiv). First-order rate constants k_{obs} (s^{-1}) were obtained by fitting the single exponential $A_t = A_0 \exp(-k_{obs}t) + C$ (mono-exponential decrease) to the observed time-dependent absorbances (average of at least three kinetic runs for each concentration for the stopped-flow method) of the electrophiles or ylides. Second-order rate constants k_2 (L mol^{-1} s^{-1}) were derived from the slopes of the linear plots of k_{obs} against the concentrations of the Michael acceptors **1a−e** used in excess.

5.4.2 Product Studies

5.4.2.1 Syntheses of the [3+2]-Cycloadducts 4

Procedure A for the Synthesis of [3+2]-Cycloadducts 4. NEt$_3$ (0.72 mmol) was added to a solution of **2hH$^+$Br$^-$** (0.50 mmol) and **1a−e** (0.50 mmol) in DMSO (5 mL) at room temperature. The mixture was stirred for 5 min, then CH$_2$Cl$_2$ (15 mL) and water (25 mL) were added and the organic layer was separated. The aqueous layer was extracted with CH$_2$Cl$_2$ (2 × 15 mL), the combined organic layers were washed with brine (2 × 25 mL) and dried over Na$_2$SO$_4$. The solvent was evaporated at room temperature and the residue was recrystallized from ethanol, ethanol/Et$_2$O, or Et$_2$O. Solutions of all [3+2]-cycloadducts **4** in CDCl$_3$ or DMSO-d_6 are slowly oxidized by air when stored at room temperature.

8-Benzoyl-8,8a-dihydrofuro[3',4':3,4]pyrrolo[2,1-*a*]isoquinoline-9,11(11a*H*,11b*H*)-dione (*rac*-**4a**). From **2hH$^+$Br$^-$** (164 mg, 500 μmol), **1a** (49 mg, 0.50 mmol) and NEt$_3$ (0.10 mL, 73 mg, 0.72 mmol) according to procedure **A**: 113 mg (327 μmol, 65%, *dr* 7:1, major diastereoisomer is depicted), yellow solid (**Mp** (Et$_2$O) 157−159 °C). The NMR-signals of the minor diastereoisomer could not be assigned unambiguously due to overlap with the major diastereoisomer. **^{1}H NMR** (400 MHz, DMSO-d_6) δ = 3.81 (t, J = 8.3 Hz, 1 H, 11^a-H), 4.22 (d, J = 8.4 Hz, 1 H, 8^a-H), 4.67 (d, J = 8.1 Hz, 1 H, 11^b-H), 5.37 (d, J = 7.6 Hz, 1 H, 5-H), 5.97 (s, 1 H, 8-H), 6.62 (d, J = 7.6 Hz, 1 H, 6-H), 6.91 (d, J = 7.44 Hz, 1 H, 4-H), 7.05 (t, J = 7.3 Hz, 1 H, 2-H), 7.13 (t, J = 7.6 Hz, 1 H, 3-H), 7.23 (d, J = 7.4 Hz, 1 H, 1-H), 7.54 (t, J = 7.7 Hz, 2 H, 2×C$_{Ar}$-H), 7.64 (t, J = 7.3 Hz, 1 H, C$_{Ar}$-H), 8.09 (d, J = 7.5 Hz, 2 H, 2×C$_{Ar}$-H). **^{13}C NMR** (100 MHz, DMSO-d_6) δ = 46.3 (d, C-8^a), 51.9 (d, C-11^a), 61.7 (d, C-11^b), 72.3 (d, C-8), 102.1 (d, C-5), 124.1 (d, C-4), 125.6 (d, C-2), 125.6 (s, C-1^a), 127.7 (d, C-1), 128.3 (d, C-3), 128.7 (d, (d, 2×C$_{Ar}$-H), 129.2 (d, 2×C$_{Ar}$-H), 130.9 (s, C-4^a), 133.8 (d, C$_{Ar}$-H), 133.8 (s, C$_{Ar}$), 135.3 (d, C-6), 170.3 (s, C-9), 173.8 (s, C-11), 194.0 (s, CO). **HRMS** (EI): calcd. for C$_{21}$H$_{15}$NO$_4$ 345.1001, found 345.0991. DA845

8-Benzoyl-10-methyl-11a,11b-dihydro-8H-pyrrolo[3',4':3,4]pyrrolo[2,1-*a*]isoquinoline-9,11(8a*H*,10*H*)-dione (*rac*-**4b**). From **2hH$^+$Br$^-$** (164 mg, 500 μmol), **1b** (56 mg, 0.50 mmol) and NEt$_3$ (0.10 mL, 73 mg, 0.72 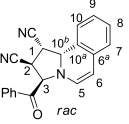mmol) according to procedure **A**: 162 mg (452 μmol, 90%, *dr* >95:5, major diastereoisomer is depicted), yellow solid (**Mp** (EtOH) 105−106 °C). **^{1}H NMR** (300 MHz, CDCl$_3$) δ = 2.81 (s, 3 H, CH$_3$), 3.44 (t, J = 7.9 Hz, 1 H, 11^a-H), 3.97 (d, J = 7.5 Hz, 1 H, 8^a-H), 4.80 (d, J = 8.0 Hz,
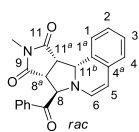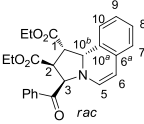
1 H, 11^b-H), 5.37 (d, J = 7.6 Hz, 1 H, 5-H), 5.44 (s, 1 H, 8-H), 6.14 (d, J = 7.5 Hz, 1 H, 6-H), 6.93 (ddd, J = 7.6, 1.7, 0.9 Hz, 1 H, 4-H), 7.11 – 7.23 (m, 3 H, 1-H, 2-H, 3-H), 7.43 – 7.56 (m, 2 H, 2×C$_{Ar}$-H), 7.57 – 7.65 (m, 1 H, C$_{Ar}$-H), 8.06 – 8.13 (m, 2 H, 2×C$_{Ar}$-H). ^{13}C NMR (75 MHz, CDCl$_3$) δ = 25.6 (q, CH$_3$), 46.0 (d, C-8^a), 51.4 (d, C-11^a), 62.1 (d, C-11^b), 72.8 (d, C-8), 102.8 (d, C-5), 124.8 (d, C-4), 126.1 (s, C-1^a), 126.4 (d, C-1, or C-2, or C-3), 127.6 (d, C-1, or C-2, or C-3), 128.8 (d, C-1, or C-2, or C-3), 129.0 (d, 2×C$_{Ar}$-H), 129.4 (d, 2×C$_{Ar}$-H), 131.1 (s, C-4^a), 134.1 (s, C$_{Ar}$), 134.2 (d, C$_{Ar}$-H), 135.0 (d, C-6), 175.2 (s, C-11), 178.3 (s, C-9), 193.8 (s, CO). HRMS (EI): calcd. for C$_{22}$H$_{18}$N$_2$O$_3$ 358.1317, found 358.3118. MS (EI) m/z: 359 (5), 358 (21), 357 (7), 253 (64), 246 (34), 239 (15), 168 (35), 167 (27), 105 (11), 77 (15), 58 (22), 43 (100). DA831

3-Benzoyl-1,2,3,10b-tetrahydropyrrolo[2,1-*a*]isoquinoline-1,2-dicarbonitrile (*rac*-**4c**). From **2hH$^+$Br$^−$** (164 mg, 500 μmol), **1c** (39 mg, 0.50 mmol) and NEt$_3$ (0.10 mL, 73 mg, 0.72 mmol) according to procedure **A**: 108 mg (332 μmol, 66%, *dr* 4:1, major diastereoisomer is depicted), yellow solid (**Mp** (EtOH) 179−181 °C; lit 179−182 °C[17]). The NMR-signals of the minor diastereoisomer could not be assigned unambiguously due to overlap with the major diastereoisomer. Major: ^{1}H NMR (400 MHz, DMSO-d_6) δ = 4.32 (dd, J = 7.9, 4.6 Hz, 1 H, 2-H), 4.45 (dd, J = 6.6, 4.5 Hz, 1 H, 1-H), 5.07 (d, J = 6.5 Hz, 1 H, 10^b-H), 5.40 (d, J = 7.5 Hz, 1 H, 6-H), 6.03 (d, J = 7.9 Hz, 1 H, 3-H), 6.47 (d, J = 7.6 Hz, 1 H, 5-H), 7.00 (dd, J = 7.6, 1.4 Hz, 1 H, 7-H), 7.11 (dd, J = 7.5, 1.3 Hz, 1 H, 9-H), 7.17 – 7.25 (m, 2 H, 8-H, 10-H), 7.55 – 7.64 (m, 2 H, 2×C$_{Ar}$-H), 7.69 – 7.76 (m, 1 H, C$_{Ar}$-H), 8.08 – 8.18 (m, 2 H, 2×C$_{Ar}$-H). Major: ^{13}C NMR (100 MHz, DMSO-d_6) δ = 32.6 (d, C-2), 40.3 (d, C-1), 61.1 (d, C-10^b), 67.7 (d, C-3), 100.2 (d, C-6), 117.5 (s, CN), 118.1 (s, CN), 124.1 (d, C-7), 125.5 (s, C-10^a), 125.7 (d, C-9), 126.9 (d, C-8 or C-10), 128.7 (d, C-8 or C-10), 128.9 (d, 2×C$_{Ar}$-H), 128.9 (d, 2×C$_{Ar}$-H), 131.8 (s, C-6^a), 134.1 (d, C-5), 134.3 (d, C$_{Ar}$-H), 134.3 (s, C$_{Ar}$), 193.6 (s, CO). HRMS (ESI): calcd. for [C$_{21}$H$_{16}$N$_3$O]$^+$ 326.1288, found 326.1286. DA780

Diethyl 3-benzoyl-1,2,3,10b-tetrahydropyrrolo[2,1-*a*]isoquinoline-1,2-dicarboxylate (*rac*-**4d**). From **2hH$^+$Br$^−$** (164 mg, 500 μmol), **1d** (86 mg, 0.50 mmol), and NEt$_3$ (0.10 mL, 73 mg, 0.72 mmol) according to procedure **A**: 139 mg (331 μmol, 66%, *dr* 3:1 decreases upon standing to 2:1, major diastereoisomer is depicted), yellow solid (**Mp** (EtOH) 119−123 °C). The NMR-signals of the minor diastereoisomer could not be assigned unambiguously due to overlap with the major diastereoisomer. Major: ^{1}H NMR (300 MHz, CDCl$_3$) δ = 0.81 − 0.89 (m, 3 H, CH$_3$), 1.19 − 1.29 (m, 3 H, CH$_3$), 3.77 − 3.84 (m, 1 H, 2-H, superimposed by minor diastereoisomer), 3.90 (dd, J = 8.8, 6.6 Hz,

1 H, 1-H), 4.08 (q, J = 7.1 Hz, 2 H, CH$_2$), 4.13 – 4.27 (m, 2 H, CH$_2$), 5.07 (d, J = 8.8 Hz, 1 H, 10^b-H), 5.38 (dd, J = 7.5, 0.5 Hz, 1 H, 6-H), 5.52 (d, J = 7.3 Hz, 1 H, 3-H), 6.22 (d, J = 7.5 Hz, 1 H, 5-H, superimposed by minor diastereoisomer), 6.84 – 6.88 (m, 1 H, 7-H), 6.89 – 7.19 (m, 3 H, 8-H, 9-H, 10-H, superimposed by minor diastereoisomer), 7.43 – 7.52 (m, 2 H, 2×C$_{Ar}$-H, superimposed by minor diastereoisomer), 7.55 – 7.62 (m, 1 H, C$_{Ar}$-H), 7.98 – 8.04 (m, 2 H, 2×C$_{Ar}$-H, superimposed by minor diastereoisomer). Major: **^{13}C NMR** (75 MHz, CDCl$_3$) δ = 13.7 (q, CH$_3$), 14.1 (q, CH$_3$), 47.8 (d, C-2), 53.8 (d, C-1), 61.0 (t, CH$_2$), 61.1 (t, CH$_2$), 61.9 (d, 10^b-H), 70.8 (d, C-3), 102.5 (d, C-6), 124.5 (d, C-7), 125.5 (d, C-8 or C-9 or C-10), 126.9 (s, C-10^a), 128.3 (d, C-8 or C-9 or C-10), 128.4 (d, C-8 or C-9 or C-10), 128.9 (d, 2×C$_{Ar}$-H), 129.0 (d, 2×C$_{Ar}$-H), 131.9 (s, C-6^a), 133.7 (d, C$_{Ar}$-H), 134.8 (d, C-5), 135.4 (s, C$_{Ar}$), 170.9 (s, CO$_2$), 173.5 (s, CO$_2$), 194.1 (s, CO). **HRMS** (ESI): calcd. for [C$_{25}$H$_{26}$NO$_5$]$^+$ 420.1805, found 420.1804. DA778

Diethyl 3-benzoyl-1,2,3,10b-tetrahydropyrrolo[2,1-a]isoquinoline-1,2-dicarboxylate (*rac*-**4e**). From **2hH$^+$Br$^-$** (164 mg, 500 µmol), **1e** (86 mg, 0.50 mmol), and NEt$_3$ (0.10 mL, 73 mg, 0.72 mmol) according to procedure **A**: 198 mg (472 µmol, 94%, *dr* >95:5, major diastereoisomer is depicted), yellow solid (**Mp** (EtOH: Et$_2$O) 91−92 °C). **^{1}H NMR** (300 MHz, CDCl$_3$) δ = 0.75 – 0.81 (m, 3 H, CH$_3$), 1.05 – 1.12 (m, 3 H, CH$_3$), 3.52 – 3.59 (m, 1 H, 1-H), 3.68 – 3.83 (m, 2 H, CH$_2$), 3.88 (t, J = 7.0 Hz, 1 H, 2-H), 3.95 – 4.16 (m, 2 H, CH$_2$), 4.94 (d, J = 7.6 Hz, 1 H, 6-H), 5.25 (d, J = 5.4 Hz, 1 H, 10^b-H), 5.64 (d, J = 6.6 Hz, 1 H, 3-H), 6.01 (d, J = 7.6 Hz, 1 H, 5-H), 6.69 (d, J = 7.3 Hz, 1 H, 7-H or 10-H), 6.93 – 6.87 (m, 2 H, 8-H, 9-H), 6.93 – 7.01 (m, 1 H, 7-H or 10-H), 7.40 – 7.50 (m, 2 H, 2×C$_{Ar}$-H), 7.50 – 7.58 (m, 1 H, C$_{Ar}$-H), 7.98 – 8.09 (m, 2 H, 2×C$_{Ar}$-H). **^{13}C NMR** (75 MHz, CDCl$_3$) δ = 13.7 (q, CH$_3$), 14.1 (q, CH$_3$), 45.3 (d, C-2), 53.9 (d, C-1), 60.8 (t, CH$_2$), 61.5 (t, CH$_2$), 64.5 (d, C-10^b), 66.6 (d, C-3), 97.6 (d, C-6), 124.1 (d, C-7 or C-10), 125.2 (d, C-8 or C-9), 126.3 (s, C-10^a), 127.3 (d, C-8 or C-9), 128.2 (d, C-7 or C-10), 129.0 (d, 2×C$_{Ar}$-H), 129.1 (d, 2×C$_{Ar}$-H), 132.5 (s, C-6^a), 133.8 (d, C$_{Ar}$-H), 135.4 (d, C-5), 136.4 (s, C$_{Ar}$), 170.8 (s, CO$_2$), 171.8 (s, CO$_2$), 197.5 (s, CO). **HRMS** (EI): calcd. for C$_{25}$H$_{25}$NO$_5$ 419.1733, found 419.1722. **MS** (EI) *m/z*: 417 (4), 314 (10), 215 (19), 194 (12), 167 (12), 105 (33), 77 (12), 58 (33), 43 (100). DA779
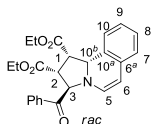
5.4.2.2 Synthesis of (*E*)-1-methyl-3-(2-oxo-2-phenylethylidene)pyrrolidine-2,5-dione (7b)
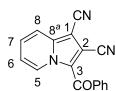
NEt$_3$ (0.10 mL, 73 mg, 0.72 mmol) was added to a solution of **2eH$^+$Br$^-$** (139 mg, 500 µmol) and **1b** (55 mg, 0.50 mmol) in DMSO (5 mL) at room temperature. After 5 min water (20 mL) was added and the mixture was extracted with CH$_2$Cl$_2$ (3×15 mL). The combined organic layers were washed with water (2×20 mL) and dried over Na$_2$SO$_4$. The solvent was evaporated and the residue, which is **5b** (quant. conversion, *dr* >95:5, ^{1}H NMR in agreement with ref. [24b]), was subjected to a column chromatography (silica; CHCl$_3$). After recrystallization from Et$_2$O/*i*-hexane **7b** was obtained (59 mg, 0.26 mmol, 51%, *E*-configuration) as colorless solid (**Mp** (Et$_2$O/*i*-hexane) 144−146 °C, lit 144 °C[25b]). R_f (silica, CHCl$_3$) = 0.69. ^{1}H NMR (300 MHz, CDCl$_3$) δ = 3.16 (s, 3 H, CH$_3$), 3.80 (d, *J* = 2.5 Hz, 2 H, 3-H), 7.49 – 7.57 (m, 2 H, 2×C$_{Ar}$-H), 7.60 – 7.68 (m, 1 H, C$_{Ar}$-H), 7.92 (t, *J* = 2.6 Hz, 1 H, CH), 8.04 (dt, *J* = 8.6, 1.8 Hz, 2 H, 2×C$_{Ar}$-H). ^{13}C NMR (75 MHz, CDCl$_3$) δ = 25.3 (q, CH$_3$), 34.9 (t, C-3), 123.3 (d, CH), 128.7 (d, 2×C$_{Ar}$-H), 129.2 (d, 2× C$_{Ar}$-H), 134.2 (d, C$_{Ar}$-H), 137.4 (s, C$_{Ar}$), 139.8 (s, C-4), 170.0 (s, C-2), 174.3 (s, C-5), 189.8 (s, CO). **HRMS** (ESI): calcd. for [C$_{13}$H$_{10}$NO$_3$]$^-$ 228.0666, found 228.0667. DA868
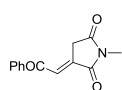
5.4.2.3 Syntheses of the Indolizines 10
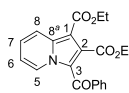
Procedure B for the Synthesis of the Indolizines 10. Aq. NaOH (1 mL, 30%) or NEt$_3$ (0.72 mmol) was added to suspensions of **1c−e** (0.50 mmol) and **2eH$^+$X$^-$** (0.50−0.75 mmol) in CH$_2$Cl$_2$ (10 mL) and the mixture was stirred for 30–60 min at room temperature. Water (30 mL) was added, and the reaction mixture was extracted with CH$_2$Cl$_2$ (3 × 5 mL). The combined organic layers were dried over Na$_2$SO$_4$. Chloranil (1.00 mmol) was added to the solution and stirring at room temperature was continued for 30−60 min until all chloranil was consumed as monitored by TLC. The solvent was evaporated and the residue was subjected to column chromatography (*n*-pentane:EtOAc = 15:1–3:1, depending on R_f). The resulting solids were dissolved in CHCl$_3$ and insoluble precipitates were removed by filtration. After evaporation, the products were further purified by recrystallization from Et$_2$O.

3-Benzoylindolizine-1,2-dicarbonitrile (10c). From **2eH$^+$Br$^-$** (139 mg, 500 µmol), **1c** (78 mg, 0.50 mmol), NEt$_3$ (0.10 mL, 73 mg, 0.72 mmol), and chloranil (246 mg, 1.00 mmol) according to procedure **B**: 86 mg (0.32 mmol, 63%), colorless solid (**Mp** (Et$_2$O) 215−216 °C). R_f (silica, *n*-pentane:EtOAc 2:1) 0.14. ^{1}H NMR (400 MHz, DMSO-

d_6) δ = 7.47 (td, J = 7.0, 1.3 Hz, 1 H, 6-H), 7.60 (t, J = 7.7 Hz, 2 H, 2×C_{Ar}-H), 7.70 − 7.80 (m, 2 H, 7-H, C_{Ar}-H), 7.81 − 7.90 (m, 2 H, 2×C_{Ar}-H), 8.05 (dt, J = 9.0, 1.2 Hz, 1 H, 8-H), 9.42 (dt, J = 7.2, 1.1 Hz, 1 H, 5-H). S   The signals of the quaternary carbons C-1, C-2, C-3, and the cyano groups were not assigned, as these nuclei show no correlations in the HMBC spectra. **^{13}C NMR** (100 MHz, DMSO-d_6) δ = 87.8 (s), 107.2 (s), 111.8 (s), 112.8 (s), 117.8 (d, C-8), 118.1 (d, C-6), 125.3 (s), 128.6 (d, 2×C_{Ar}-H), 128.9 (d, C-5), 129.4 (d, 2×C_{Ar}-H), 130.0 (d, C-7), 133.4 (d, C_{Ar}-H), 137.5 (s, C_{Ar}), 139.1 (s, C-8^a), 184.2 (s, CO). **HRMS** (EI): calcd. for $C_{17}H_9N_3O$ 271.0746, found 271.0748. **MS** (EI) m/z: 272 (20), 271 (100), 243 (24), 194 (10), 105 (83), 77 (67), 43 (23). DA776

Diethyl 3-benzoylindolizine-1,2-dicarboxylate (10d). From **2eH$^+$Br$^−$** (167 mg, 600 µmol), **1d** (86 mg, 0.50 mmol), aq. NaOH (1 mL, 32%), and chloranil (246 mg, 1.00 mmol) according to procedure **B**: 161 mg (441 µmol, 88%), colorless solid (**Mp** (Et$_2$O) 110–111 °C). **R_f** (silica, n-pentane:EtOAc 5:1) 0.22. **^{1}H NMR** (300 MHz, CDCl$_3$) δ = 1.06 (t, J = 7.2 Hz, 3 H, CH$_3$), 1.34 (t, J = 7.1 Hz, 3 H, CH$_3$), 3.65 (q, J = 7.2 Hz, 2 H, CH$_2$), 4.34 (q, J = 7.1 Hz, 2 H, CH$_2$), 7.08 (td, J = 7.0, 1.4 Hz, 1 H, 6-H), 7.38 − 7.51 (m, 3 H, 7-H, 2×C_{Ar}-H), 7.51 − 7.59 (m, 1 H, C_{Ar}-H), 7.64 − 7.77 (m, 2 H, 2×C_{Ar}-H), 8.41 (dt, J = 9.1, 1.2 Hz, 1 H, 8-H), 9.62 (dt, J = 7.2, 1.1 Hz, 1 H, 5-H). **^{13}C NMR** (75 MHz, CDCl$_3$) δ = 13.7 (q, CH$_3$), 14.4 (q, CH$_3$), 60.6 (t, CH$_2$), 61.8 (t, CH$_2$), 104.4 (s, C-1, or C-2, or C-3), 116.0 (d, C-6), 120.1 (d, C-8), 120.8 (s, C-1, or C-2, or C-3), 128.0 (d, C-5), 128.2 (d, 2×C_{Ar}-H), 128.6 (d, C-7), 128.9 (d, 2×C_{Ar}-H), 131.9 (s, C-1, or C-2, or C-3), 132.0 (d, C_{Ar}-H), 138.6 (s, C-8^a), 139.8 (s, C_{Ar}), 163.1 (s, CO$_2$), 165.0 (s, CO$_2$), 186.9 (s, CO). **HRMS** (ESI): calcd. for [C$_{21}$H$_{19}$NO$_5$Na]$^+$ 388.1155, found 388.1154. DA769

Diethyl 3-benzoylindolizine-1,2-dicarboxylate (10d): From **2eH$^+$Br$^−$** (167 mg, 750 µmol), **1e** (86 mg, 0.50 mmol), aq. NaOH (1 mL, 32%,), and chloranil (246 mg, 1.00 mmol) according to procedure **B**: 142 mg, (389 µmol, 78%), colorless solid (**Mp** (Et$_2$O): 110–111 °C). (analytical data see above). DA773

5.4.2.4 Syntheses of the Cyclopropanes 11

Procedure C for the Synthesis of Cyclopropanes 11. 1b,c (0.50−0.60 mmol) in DMSO (5 mL) was added dropwise to a solution of **3c,d** (0.41−0.47 mmol) in DMSO (5 mL) over 5–10 min at room temperature. The reaction mixture was stirred for additional 5 min then aq. sat. NH$_4$Cl (25 mL) was added. The aqueous layer was extracted with CH$_2$Cl$_2$ (3×15 mL), the combined organic layers were washed with brine (2×20 mL), and dried over Na$_2$SO$_4$. The

solvent was evaporated and the residue was purified by column chromatography over silica (**11b**) or alox (**11c**) with *n*-pentane:EtOAc = 3:1–2:1, and recrystallized from EtOH.

6-(4-Methoxybenzoyl)-3-methyl-3-azabicyclo[3.1.0]hexane-2,4-dione (**11b**). From **1b** (55 mg, 0.50 mmol) and **3d** (87 mg, 0.41 mmol) according to procedure **C**: 49 mg (0.19 mmol, 46%, *dr* >95:5); colorless solid (**Mp** (EtOH) 156−157 °C). **^{1}H NMR** (300 MHz, CDCl$_3$) δ = 2.93 (s, 3 H, CH$_3$), 3.00 (d, *J* = 2.8 Hz, 2 H, 2×CH), 3.31 (t, *J* = 2.8 Hz, 1 H, CHCO), 3.89 (s, 3 H, CH$_3$), 6.89 − 7.03 (m, 2 H, 2×C$_{Ar}$-H), 8.05 − 7.87 (m, 2 H, 2×C$_{Ar}$-H). **^{13}C NMR** (75 MHz, CDCl$_3$) δ = 24.7 (q, CH$_3$), 28.1 (d, 2×CH), 35.7 (d, CH), 55.8 (q, CH$_3$), 114.3 (d, 2×C$_{Ar}$-H), 128.8 (s, C$_{Ar}$), 131.1 (d, 2×C$_{Ar}$-H), 164.7 (s, C$_{Ar}$), 173.3 (s, 2×CO), 190.2 (s, CO). **HRMS** (ESI): calcd. for [C$_{14}$H$_{12}$NO$_4$]$^-$ 258.0772, found 258.0774. DA864
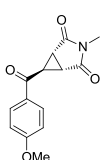
3-(4-(Dimethylamino)benzoyl)cyclopropane-1,2-dicarbonitrile (rac-**11c**). From **1c** (44 mg, 0.56 mmol) and **3c** (105 mg, 470 μmol) according to procedure **C**: 70 mg (292 μmol, 62%, *dr* >95:5), colorless solid (**Mp** (EtOH) 188−189 °C). **^{1}H NMR** (400 MHz, CD$_3$CN) δ = 2.75 (dd, *J* = 9.0, 5.9 Hz, 1 H, CH), 2.86 (t, *J* = 5.9 Hz, 1 H, CH), 3.07 (s, 6 H, N(CH$_3$)$_2$), 3.73 − 3.84 (m, 1 H, CH), 6.71 − 6.81 (m, 2 H, 2×C$_{Ar}$-H), 7.89 − 7.97 (m, 2 H, 2×C$_{Ar}$-H). **^{13}C NMR** (100 MHz, CD$_3$CN) δ = 12.0 (d, CH), 14.3 (d, CH), 28.9 (d, CH), 40.3 (q, 2×CH$_3$), 111.9 (d, 2×C$_{Ar}$-H), 116.3 (s, CN), 118.1 (s, CN), 124.0 (s, C$_{Ar}$), 131.9 (d, 2×C$_{Ar}$-H), 155.5 (s, C$_{Ar}$), 187.6 (s, CO). **HRMS** (ESI): calcd. for [C$_{14}$H$_{14}$N$_3$O]$^+$ 240.1131, found 240.1130. DA863
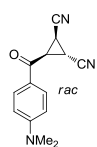
Procedure D for the Synthesis of Cyclopropanes 11. KO^{t}Bu (0.75 mmol) in DMSO (5 mL) was added dropwise to a solution of **3aH$^+$BF$_4^-$** (0.75 mmol) and **1** (0.50 mmol) in DMSO (5 mL) over 5–10 min at room temperature. The reaction mixture was stirred for additional 5 min and quenched with aq. sat. NH$_4$Cl (25 mL). The aqueous layer was extracted with CH$_2$Cl$_2$ (3×15 mL). The combined organic layers were washed with brine (2×20 mL) and dried over Na$_2$SO$_4$. The solvent was evaporated and the residue was purified by column chromatography over silica (*n*-pentane:EtOAc = 20:1–10:1).

Diethyl 3-(4-cyanophenyl)cyclopropane-1,2-dicarboxylate (*rac*-**11d**). From **1d** (86 mg, 0.50 mmol), **3aH$^+$BF$_4^-$** (200 mg, 754 μmol), and KO^{t}Bu (84 mg, 0.75 mmol) according to procedure **D**: 116 mg (404 μmol, 81%, **11d:11e** >95:5), colorless oil. **^{1}H NMR** (300 MHz, CDCl$_3$) δ = 1.03 (t, *J* = 7.1 Hz, 3 H, CH$_3$), 1.30 (t, *J* = 7.1 Hz, 3 H, CH$_3$), 2.65 (dd, *J* = 10.0, 4.8 Hz, 1 H, CH), 2.84 (dd, *J* = 6.4, 4.9 Hz, 1 H, CH), 3.07 (dd, *J* = 10.0, 6.4 Hz, 1 H, CH), 3.89 − 3.99 (m, 2 H, CH$_2$), 4.16 − 4.26 (m, 2 H, CH$_2$),
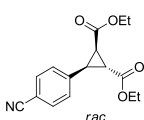
7.35 – 7.40 (m, 2 H, 2×C_{Ar}-H), 7.54 – 7.60 (m, 2 H, 2×C_{Ar}-H). **^{13}C NMR** (75 MHz, CDCl$_3$) δ = 14.1 (q, CH$_3$), 14.3 (q, CH$_3$), 26.1 (d, CH), 30.1 (d, CH), 32.2 (d, CH), 61.2 (t, CH$_2$), 61.7 (t, CH$_2$), 111.3 (s, C_{Ar}), 118.7 (s, CN), 129.9 (d, 2×C_{Ar}-H), 132.0 (d, 2×C_{Ar}-H), 139.9 (s, C_{Ar}), 168.0 (s, CO$_2$), 170.9 (s, CO$_2$). **HRMS** (EI): calcd. for C$_{16}$H$_{17}$NO$_4$ 287.1158, found 287.1147. **MS** (EI) *m/z*: 287 (2), 242 (8), 215 (15), 214 (100), 186 (60), 158 (24), 140 (64). DA666

Diethyl 3-(4-cyanophenyl)cyclopropane-1,2-dicarboxylate (*rac*-**11d** + **11e**). From **1e** (86 mg, 0.50 mmol), **3aH$^+$BF$_4^-$** (200 mg, 754 µmol), and KO^{t}Bu (84 mg, 0.75 mmol) according to procedure **D**: 81 mg (0.28 mmol, 56%, **11d**:**11e** 80:20), colorless oil. The amount of **11e** obtained after purification was too small to be reliably analyzed by NMR. Analytical data of *rac*-**11d** see above. DA669

^{1}H NMR-Monitoring. A solution (1.00 mL, 1.0 equiv) of KO^{t}Bu in DMSO-d_6 (253 mM) was added in one portion to a solution of **3aH$^+$BF$_4^-$** (73.0 mg, 275 µmol) and **1e** (42.7 mg, 248 µmol) in DMSO-d_6 (2.00 mL) at ambient temperature. A sample was taken, which was monitored by ^{1}H NMR for 13 min. Another 0.5 equiv., and after 28 min additional 0.3 equiv. of KO^{t}Bu solution were added (dashed lines in Figure 5.5), and the reaction was monitored for 6 h. The time-dependent concentrations of SMe$_2$, **11d**, **1e**, and **3aH$^+$BF$_4^-$** were derived by using ^{t}BuOH as internal standard (Table 5.5, Figure 5.5). The spectra show traces of cyclopropane **11e** which were not analyzed due to their low intensity.

50% of **1e** was isomerized to **1d** the by excess of base after 6 h. To have a reliable measure of the stability of sulfonium ylide **3a** its decomposition was monitored by ^{1}H NMR by generating **3a** from **3aH$^+$BF$_4^-$** (29 mg, 0.11 mmol) and KO^{t}Bu (11 mg, 98 µmol) in DMSO-d_6. After 15 min the ^{1}H NMR spectrum showed no ylide **3a**, but only decomposition products which were not identified.

Table 5.4. Time-dependent concentrations of KO^{t}Bu, SMe$_2$, 11d, 1e, and 3aH$^+$BF$_4^-$ during the reaction of 3a with 1e in DMSO-d_6 at ambient temperature.

t/min	[KO^{t}Bu]/M	[SMe$_2$]/M	[11d]/M	[1e]/M	[3aH$^+$BF$_4^-$]/M
2	8.42×10^{-2}	2.65×10^{-2}	2.27×10^{-2}	5.85×10^{-2}	3.66×10^{-2}
5	8.42×10^{-2}	2.67×10^{-2}	2.27×10^{-2}	5.85×10^{-2}	3.66×10^{-2}
7	8.42×10^{-2}	2.64×10^{-2}	2.27×10^{-2}	5.81×10^{-2}	3.62×10^{-2}
9	8.42×10^{-2}	2.68×10^{-2}	2.27×10^{-2}	5.81×10^{-2}	3.62×10^{-2}
13	8.42×10^{-2}	2.68×10^{-2}	2.27×10^{-2}	5.81×10^{-2}	3.62×10^{-2}
20	1.08×10^{-1}	3.32×10^{-2}	2.60×10^{-2}	3.36×10^{-2}	1.73×10^{-2}
28	1.20×10^{-1}	3.61×10^{-2}	2.99×10^{-2}	1.50×10^{-2}	5.98×10^{-2}
31	1.20×10^{-1}	3.61×10^{-2}	2.99×10^{-2}	1.50×10^{-2}	5.98×10^{-2}
297	1.20×10^{-1}	3.61×10^{-2}	3.11×10^{-2}	4.79×10^{-2}	2.99×10^{-2}
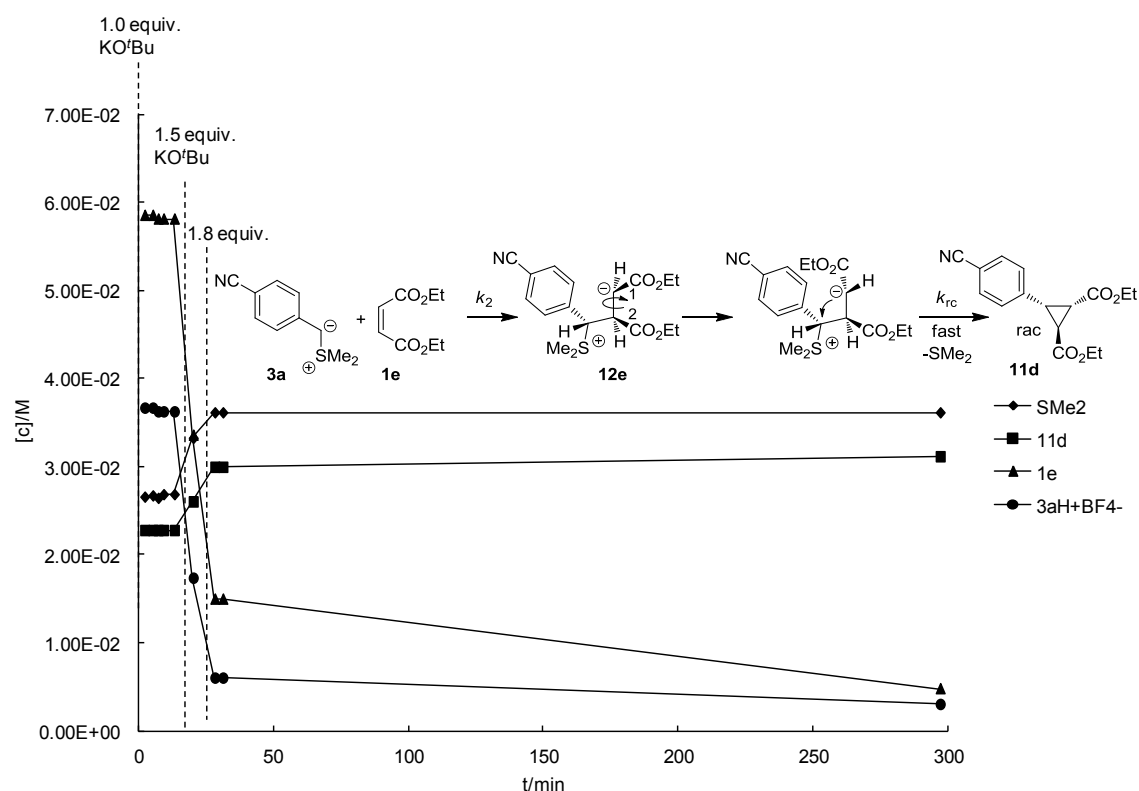
Figure 5.5. Plot of the time-dependent concentrations of SMe$_2$, 11d, 1e, and 3aH$^+$BF4$^-$ during the reaction of 3a with 1e in DMSO-d_6 at ambient temperature. Above each dashed line the equivalents of KO^{t}Bu regarding to 3aH$^+$BF4$^-$ at the corresponding time are given.

5.4.3 Kinetics of the Reactions of Electrophiles 1a−e with Ylides 2,3

5.4.3.1 Kinetics of Reactions of Maleic Anhydride 1a

Table 5.5. Kinetics of the reaction of 1a with 2d (DMSO, 20 °C, Stopped-flow method, detection at 425 nm).

No.	$[1a]$/mol L^{-1}	$[2d]$/mol L^{-1}	k_{obs}/s^{-1}
MAN2-1	1.06×10^{-3}	1.00×10^{-4}	3.69×10^{2}
MAN2-4	1.27×10^{-3}	1.00×10^{-4}	4.35×10^{2}
MAN2-2	1.59×10^{-3}	1.00×10^{-4}	5.63×10^{2}
k_2(20 °C) = 3.69×10^{5} L mol^{-1} s^{-1}			

y = 368718x − 26.632
R² = 0.9955
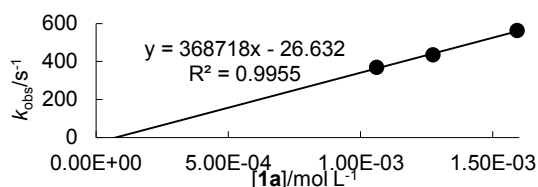
Table 5.6. Kinetics of the reaction of 1a with 2e (DMSO, 20 °C, Stopped-flow method, detection at 445 nm).

No.	$[1a]$/mol L^{-1}	$[2e]$/mol L^{-1}	k_{obs}/s^{-1}
MAN1-1	1.06×10^{-3}	5.00×10^{-5}	4.81×10^{1}
MAN1-2	1.59×10^{-3}	5.00×10^{-5}	7.58×10^{1}
MAN1-3	2.12×10^{-3}	5.00×10^{-5}	9.79×10^{1}
MAN1-4	2.65×10^{-3}	5.00×10^{-5}	1.23×10^{2}
MAN1-5	3.18×10^{-3}	5.00×10^{-5}	1.50×10^{2}
k_2(20 °C) = 4.74×10^{4} L mol^{-1} s^{-1}			

y = 47358x − 1.44
R² = 0.9989
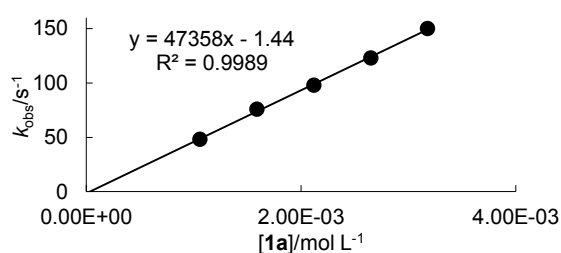
Table 5.7. Kinetics of the reaction of 1a with 2g (DMSO, 20 °C, Stopped-flow method, detection at 476 nm).

No.	$[1a]$/mol L^{-1}	$[2g]$/mol L^{-1}	k_{obs}/s^{-1}
MAN3-1	1.06×10^{-3}	5.00×10^{-5}	1.38×10^{1}
MAN3-2	1.59×10^{-3}	5.00×10^{-5}	2.10×10^{1}
MAN3-3	2.12×10^{-3}	5.00×10^{-5}	2.68×10^{1}
MAN3-4	2.65×10^{-3}	5.00×10^{-5}	3.32×10^{1}
MAN3-5	3.18×10^{-3}	5.00×10^{-5}	3.83×10^{1}
k_2(20 °C) = 1.16×10^{4} L mol^{-1} s^{-1}			

y = 11569x + 2.076
R² = 0.9968
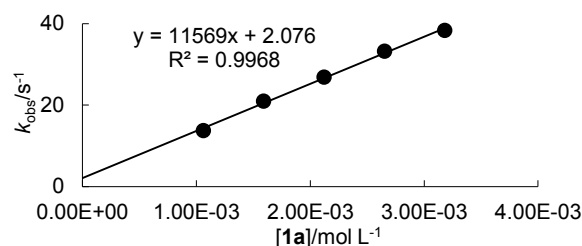
Table 5.8. Kinetics of the reaction of 1a with 2h (DMSO, 20 °C, Stopped-flow method, detection at 480 nm).

No.	$[1a]$/mol L^{-1}	$[2h]$/mol L^{-1}	k_{obs}/s^{-1}
MAN9-1	1.11×10^{-3}	1.00×10^{-4}	3.69×10^{2}
MAN9-2	1.39×10^{-3}	1.00×10^{-4}	4.08×10^{2}
MAN9-3	1.67×10^{-3}	1.00×10^{-4}	4.73×10^{2}
MAN9-4	1.94×10^{-3}	1.00×10^{-4}	5.41×10^{2}
k_2(20 °C) ≈ 2.1×10^{5} L mol^{-1} s^{-1}			
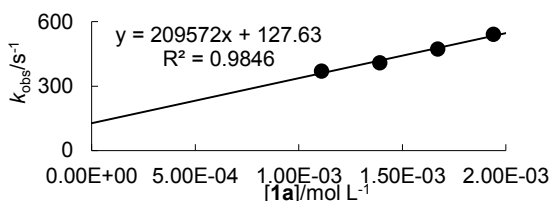
y = 209572x + 127.63
R² = 0.9846

The positive intercept may be due to the fact that the reaction is very fast and the solutions are not homogenous after 5 ms.

Table 5.9. Kinetics of the reaction of 1a with 2i (DMSO, 20 °C, Stopped-flow method, detection at 530 nm).

No.	[**1a**]/mol L^{-1}	[**2i**]/mol L^{-1}	k_{obs}/s^{-1}
MAN4-1	1.06×10^{-3}	1.00×10^{-4}	1.26×10^2
MAN4-2	1.59×10^{-3}	1.00×10^{-4}	1.33×10^2
MAN4-3	2.12×10^{-3}	1.00×10^{-4}	1.42×10^2
MAN4-4	2.65×10^{-3}	1.00×10^{-4}	1.54×10^2
k_2(20 °C) ≈ 1.8×10^4 L mol^{-1} s^{-1}			
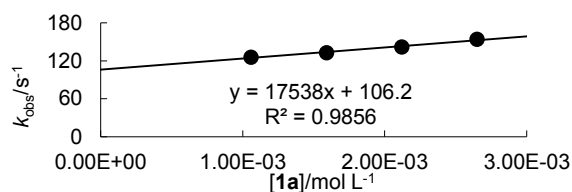
y = 17538x + 106.2
R² = 0.9856

The positive intercept may be due to the fact that the reaction is very fast and the solutions are not homogenous after 5 ms.

Table 5.10. Kinetics of the reaction of 1a with 3b (DMSO, 20 °C, Stopped-flow method, detection at 520 nm).

No.	[**1a**]/mol L^{-1}	[**3b**]/mol L^{-1}	k_{obs}/s^{-1}
MAN7r-1	1.00×10^{-3}	5.00×10^{-5}	3.98×10^1
MAN7r-2	1.25×10^{-3}	5.00×10^{-5}	4.98×10^1
MAN7r-3	1.50×10^{-3}	5.00×10^{-5}	5.99×10^1
MAN7r-4	1.75×10^{-3}	5.00×10^{-5}	6.93×10^1
MAN7r-5	2.00×10^{-3}	5.00×10^{-5}	8.01×10^1
k_2(20 °C) = 4.00×10^4 L mol^{-1} s^{-1}			

y = 40040x - 0.28
R² = 0.9997
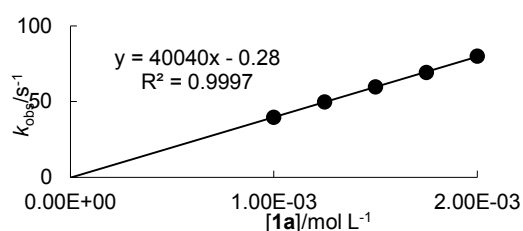
Table 5.11. Calculation of the Electrophilicity Parameter E for 1a using the N and s_N Parameters of 2,3, eq 5.1, and the Second-Order Rate Constants for the Reactions of 1a with 2,3 (filled dots).

Nucleophile	N/s_N	k_2/ L mol^{-1} s^{-1}
2d	20.24/0.60	3.69×10^5
2e	19.46/0.58	4.74×10^4
2g	17.98/0.63	1.16×10^4
3b	18.42/0.65	4.00×10^4
$E^{[a]}$ = −11.31		
2h	19.38/0.50	2.10×10^5
2i	20.08/0.57	1.75×10^4

log k_2/s_N = N - 11.31
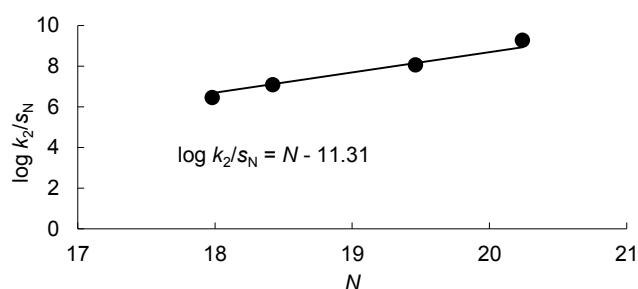
[a] Calculated by least square minimization according to eq 5.1.

5.4.3.2 Kinetics of Reactions of *N*-Methylmaleimide 1b

Table 5.12. Kinetics of the reaction of 1b with 2d (DMSO, 20 °C, Stopped-flow method, detection at 425 nm).

| No.	[**1b**]/mol L^{-1}	[**2d**]/mol L^{-1}	k_{obs}/s^{-1}
MMI2-1	2.53×10^{-4}	5.00×10^{-5}	1.88
MMI2-2	3.84×10^{-4}	5.00×10^{-5}	2.84
MMI2-3	5.05×10^{-4}	5.00×10^{-5}	3.72
MMI2-4	6.37×10^{-4}	5.00×10^{-5}	4.84
MMI2-5	7.58×10^{-4}	5.00×10^{-5}	5.83
k_2(20 °C) = 7.84×10^3 L mol^{-1} s^{-1}			

y = 7838.4x - 0.1552
R² = 0.9988

Table 5.13. Kinetics of the reaction of 1b with 2e (DMSO, 20 °C, Stopped-flow method, detection at 445 nm).

No.	[**1b**]/mol L^{-1}	[**2e**]/mol L^{-1}	k_{obs}/s^{-1}
MMI1-1	2.53×10^{-4}	5.00×10^{-5}	2.64×10^{-1}
MMI1-2	3.84×10^{-4}	5.00×10^{-5}	4.08×10^{-1}
MMI1-3	5.05×10^{-4}	5.00×10^{-5}	5.42×10^{-1}
MMI1-4	6.37×10^{-4}	5.00×10^{-5}	7.02×10^{-1}
MMI1-5	7.58×10^{-4}	5.00×10^{-5}	8.42×10^{-1}
$k_2(20\ °C) = 1.15 \times 10^3$ L mol^{-1} s^{-1}			

y = 1147.6x - 0.0307
R² = 0.9996
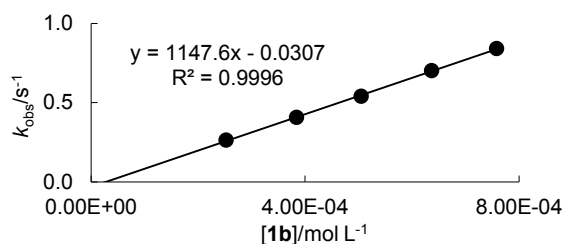
Table 5.14. Kinetics of the reaction of 1b with 2f (DMSO, 20 °C, Stopped-flow method, detection at 456 nm).

No.	[**1b**]/mol L^{-1}	[**2f**]/mol L^{-1}	k_{obs}/s^{-1}
MMI3-1	2.53×10^{-4}	5.00×10^{-5}	5.34
MMI3-2	3.84×10^{-4}	5.00×10^{-5}	7.86
MMI3-3	5.05×10^{-4}	5.00×10^{-5}	1.01×10^1
MMI3-4	6.37×10^{-4}	5.00×10^{-5}	1.29×10^1
MMI3-5	7.58×10^{-4}	5.00×10^{-5}	1.59×10^1
$k_2(20\ °C) = 2.07 \times 10^4$ L mol^{-1} s^{-1}			

y = 20698x - 0.0826
R² = 0.9965
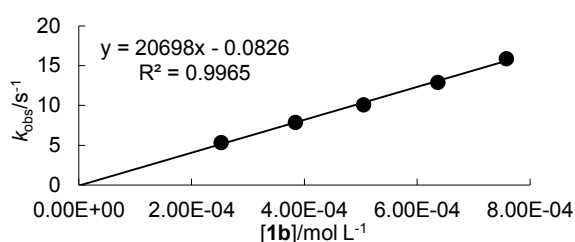
Table 5.15. Kinetics of the reaction of 1b with 2h (DMSO, 20 °C, Stopped-flow method, detection at 480 nm).

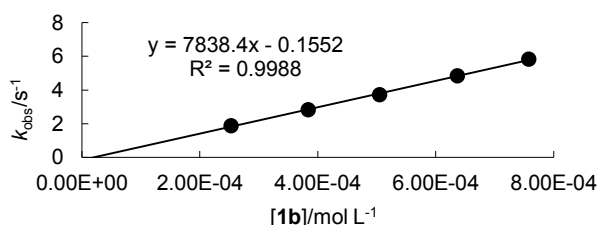| No.	[**1b**]/mol L^{-1}	[**2h**]/mol L^{-1}	k_{obs}/s^{-1}
MMI4-1	2.53×10^{-4}	5.00×10^{-5}	4.45
MMI4-2	3.84×10^{-4}	5.00×10^{-5}	6.70
MMI4-3	5.05×10^{-4}	5.00×10^{-5}	8.83
MMI4-4	6.37×10^{-4}	5.00×10^{-5}	1.13×10^1
MMI4-5	7.58×10^{-4}	5.00×10^{-5}	1.36×10^1
$k_2(20\ °C) = 1.81 \times 10^4$ L mol^{-1} s^{-1}			

y = 18107x - 0.2119
R² = 0.9995
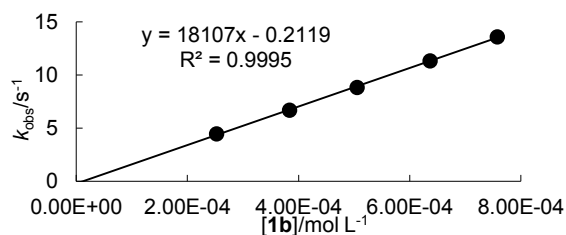
Table 5.16. Kinetics of the reaction of 1b with 2i (DMSO, 20 °C, Stopped-flow method, detection at 530 nm).

No.	[**1b**]/mol L^{-1}	[**2i**]/mol L^{-1}	k_{obs}/s^{-1}
MMI6-1	5.00×10^{-4}	5.00×10^{-5}	1.05×10^1
MMI6-2	7.50×10^{-4}	5.00×10^{-5}	1.62×10^1
MMI6-3	1.00×10^{-3}	5.00×10^{-5}	2.27×10^1
MMI6-4	1.25×10^{-3}	5.00×10^{-5}	2.89×10^1
MMI6-5	1.50×10^{-3}	5.00×10^{-5}	3.47×10^1
$k_2(20\ °C) = 2.44 \times 10^4$ L mol^{-1} s^{-1}			

y = 24440x - 1.84
R² = 0.9996
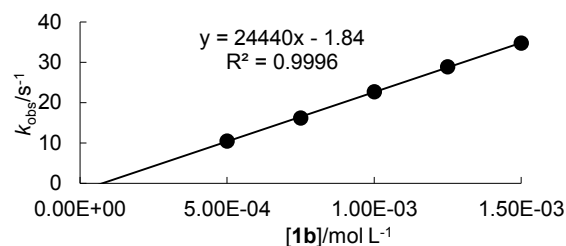
Table 5.17. Kinetics of the reaction of 1b with 3b (DMSO, 20 °C, Stopped-flow method, detection at 520 nm).

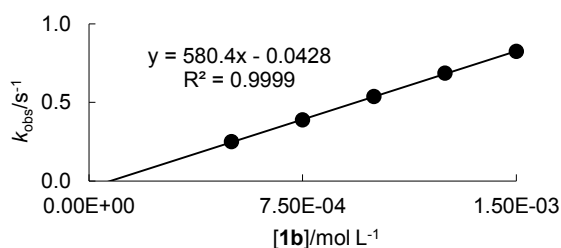| No.	[**1b**]/mol L^{-1}	[**3b**]/mol L^{-1}	k_{obs}/s^{-1}
MMI5-1	5.00×10^{-4}	5.00×10^{-5}	2.49×10^{-1}
MMI5-2	7.50×10^{-4}	5.00×10^{-5}	3.89×10^{-1}
MMI5-3	1.00×10^{-3}	5.00×10^{-5}	5.38×10^{-1}
MMI5-4	1.25×10^{-3}	5.00×10^{-5}	6.86×10^{-1}
MMI5-5	1.50×10^{-3}	5.00×10^{-5}	8.26×10^{-1}
$k_2(20\ °C) = 5.80 \times 10^2$ L mol^{-1} s^{-1}			

y = 580.4x - 0.0428
R² = 0.9999

Table 5.18. Calculation of the Electrophilicity Parameter *E* for 1b using the *N* and *s*$_N$ Parameters of 2,3, eq 5.1, and the Second-Order Rate Constants for the Reactions of 1b with 2,3 (filled dots; open dots refer to rate constants not used for the determination of *E*).

| Nucleophile	N/s_N	k_2/ L mol^{-1} s^{-1}
2d	20.24/0.60	7.84×10^3
2e	19.46/0.58	1.15×10^3
2f	21.61/0.58	2.06×10^4
3b	18.42/0.65	5.80×10^2
	$E^{[a]} = -14.07$	
2h	20.08/0.57	1.81×10^4
2i	19.38/0.50	2.45×10^4
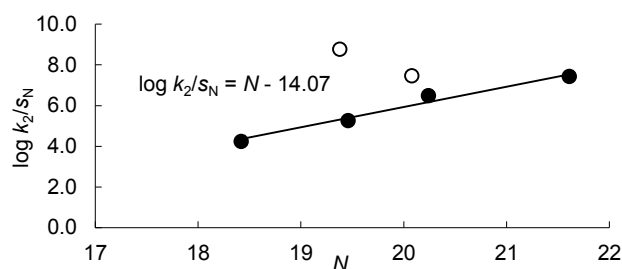
[a] Calculated by least square minimization according to eq 5.1.

5.4.3.3   Kinetics of Reactions of Fumaronitrile 1c

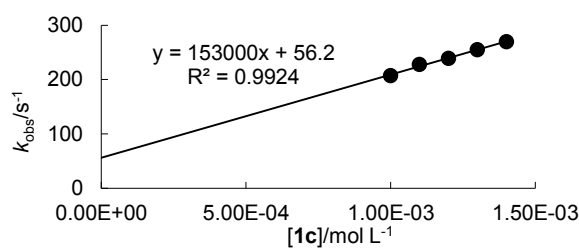**Table 5.19. Kinetics of the reaction of 1c with 2a (DMSO, 20 °C, Stopped-flow method, detection at 425 nm).**

No.	[**1c**]/mol L^{-1}	[**2a**]/mol L^{-1}	k_{obs}/s^{-1}
FN1-1	1.00×10^{-3}	1.00×10^{-4}	1.32×10^2
FN1-2	1.10×10^{-3}	1.00×10^{-4}	1.52×10^2
FN1-3	1.20×10^{-3}	1.00×10^{-4}	1.67×10^2
FN1-4	1.30×10^{-3}	1.00×10^{-4}	1.79×10^2
	$k_2(20\ °C) \approx 1.6 \times 10^5$ L mol^{-1} s^{-1}		
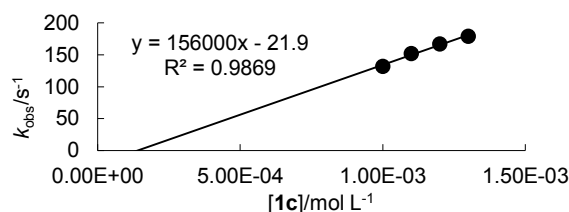
The positive intercept may be due to the fact that the reaction is very fast and the solutions are not homogenous after 5 ms.

Table 5.20. Kinetics of the reaction of 1c with 2c (DMSO, 20 °C, Stopped-flow method, detection at 425 nm).

No.	[**1c**]/mol L^{-1}	[**2c**]/mol L^{-1}	k_{obs}/s^{-1}
FN2-1	1.00×10^{-3}	1.00×10^{-4}	2.07×10^2
FN2-2	1.10×10^{-3}	1.00×10^{-4}	2.28×10^2
FN2-3	1.20×10^{-3}	1.00×10^{-4}	2.39×10^2
FN2-4	1.30×10^{-3}	1.00×10^{-4}	2.55×10^2
FN2-5	1.40×10^{-3}	1.00×10^{-4}	2.70×10^2
	$k_2(20\ °C) \approx 1.5 \times 10^5$ L mol^{-1} s^{-1}		

The positive intercept may be due to the fact that the reaction is very fast and the solutions are not homogenous after 5 ms.

Table 5.21. Kinetics of the reaction of 1c with 2d (DMSO, 20 °C, Stopped-flow method, detection at 425 nm).

No.	[**1c**]/mol L^{-1}	[**2d**]/mol L^{-1}	k_{obs}/s^{-1}
FN4-1	1.00×10^{-3}	5.00×10^{-5}	5.87×10^{-1}
FN4-2	1.10×10^{-3}	5.00×10^{-5}	6.47×10^{-1}
FN4-3	1.20×10^{-3}	5.00×10^{-5}	6.94×10^{-1}
FN4-4	1.30×10^{-3}	5.00×10^{-5}	7.67×10^{-1}
FN4-5	1.40×10^{-3}	5.00×10^{-5}	8.36×10^{-1}
	$k_2(20\ °C) = 6.18 \times 10^2$ L mol^{-1} s^{-1}		

Table 5.22. Kinetics of the reaction of 1c with 2e (DMSO, 20 °C, Stopped-flow method, detection at 445 nm).

No.	$[\mathbf{1c}]$/mol L^{-1}	$[\mathbf{2e}]$/mol L^{-1}	k_{obs}/s^{-1}
FN5-1	1.00×10^{-3}	5.00×10^{-5}	4.62×10^{-2}
FN5-2	2.00×10^{-3}	5.00×10^{-5}	9.35×10^{-2}
FN5-3	3.00×10^{-3}	5.00×10^{-5}	1.41×10^{-1}
FN5-4	4.00×10^{-3}	5.00×10^{-5}	1.87×10^{-1}
FN5-5	5.00×10^{-3}	5.00×10^{-5}	2.34×10^{-1}
$k_2(20\ °C) = 4.69 \times 10^{1}$ L mol^{-1} s^{-1}			

y = 46.91x - 0.0004
R² = 1
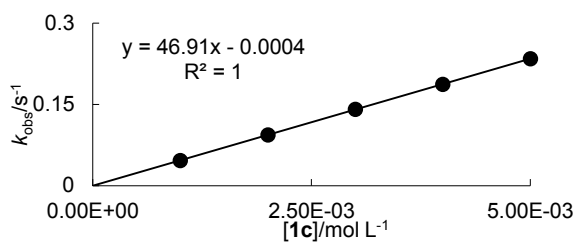
Table 5.23. Kinetics of the reaction of 1c with 2g (DMSO, 20 °C, diode array-spectometer method, detection at 476 nm).

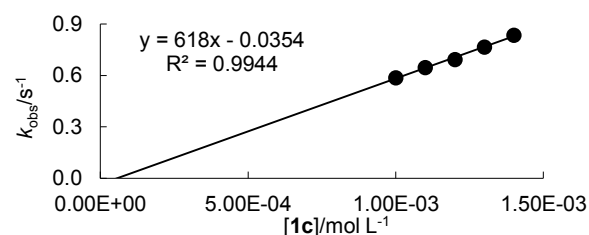| No.	$[\mathbf{1c}]$/mol L^{-1}	$[\mathbf{2g}]$/mol L^{-1}	k_{obs}/s^{-1}
FN8-1	1.89×10^{-3}	9.37×10^{-5}	4.92×10^{-2}
FN8-2	2.40×10^{-3}	9.29×10^{-5}	5.91×10^{-2}
FN8-3	2.89×10^{-3}	9.41×10^{-5}	7.13×10^{-2}
FN8-4	3.20×10^{-3}	9.01×10^{-5}	8.06×10^{-2}
FN8-5	3.74×10^{-3}	9.26×10^{-5}	9.02×10^{-2}
$k_2(20\ °C) = 2.29 \times 10^{1}$ L mol^{-1} s^{-1}			

y = 22.904x + 0.0053
R² = 0.9942
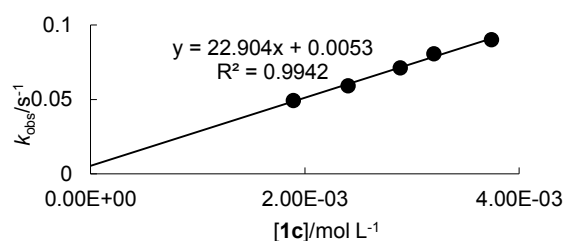
Table 5.24. Kinetics of the reaction of 1c with 2h (DMSO, 20 °C, Stopped-flow method, detection at 480 nm).

No.	$[\mathbf{1c}]$/mol L^{-1}	$[\mathbf{2h}]$/mol L^{-1}	k_{obs}/s^{-1}
FN6-1	1.00×10^{-3}	1.00×10^{-4}	5.07×10^{-1}
FN6-2	2.00×10^{-3}	1.00×10^{-4}	9.67×10^{-1}
FN6-3	3.00×10^{-3}	1.00×10^{-4}	1.42
FN6-4	4.00×10^{-3}	1.00×10^{-4}	1.91
FN6-5	5.00×10^{-3}	1.00×10^{-4}	2.40
$k_2(20\ °C) = 4.73 \times 10^{2}$ L mol^{-1} s^{-1}			

y = 472.9x + 0.0221
R² = 0.9997
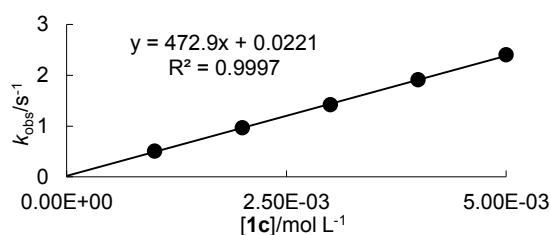
Table 5.25. Kinetics of the reaction of 1c with 3a (DMSO, 20 °C, Stopped-flow method, detection at 379 nm).

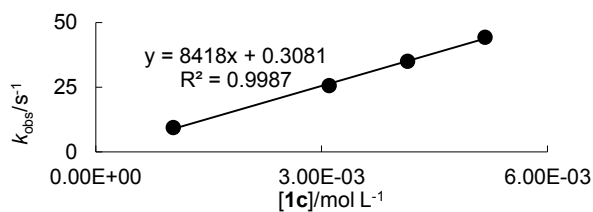| No.	$[\mathbf{1c}]$/mol L^{-1}	$[\mathbf{3a}]$/mol L^{-1}	k_{obs}/s^{-1}
FN7r-1	1.03×10^{-3}	5.00×10^{-5}	9.37
FN7r-3	3.10×10^{-3}	6.00×10^{-5}	2.57×10^{1}
FN7r-4	4.14×10^{-3}	6.00×10^{-5}	3.50×10^{1}
FN7r-5	5.17×10^{-3}	6.00×10^{-5}	4.43×10^{1}
$k_2(20\ °C) = 8.42 \times 10^{3}$ L mol^{-1} s^{-1}			

y = 8418x + 0.3081
R² = 0.9987

Table 5.26. Calculation of the Electrophilicity Parameter *E* for 1c using the *N* and s_N Parameters of 2,3, eq 5.1, and the Second-Order Rate Constants for the Reactions of 1c with 2,3 (filled dots; open dots refer to rate constants not used for the determination of *E*).

Nucleophile	N/s_N	$k_2/$ L mol^{-1} s^{-1}
2d	20.24/0.60	6.18×10^2
2e	19.46/0.58	4.69×10^1
2g	17.98/0.63	2.29×10^1
2h	19.38/0.50	4.73×10^2
3a	21.07/0.68	8.42×10^3
$E^{[a]} = -15.71$		
2a	26.71/0.37	1.6×10^5
2c	25.94/0.42	1.5×10^5

$\log k_2/s_N = N - 15.71$
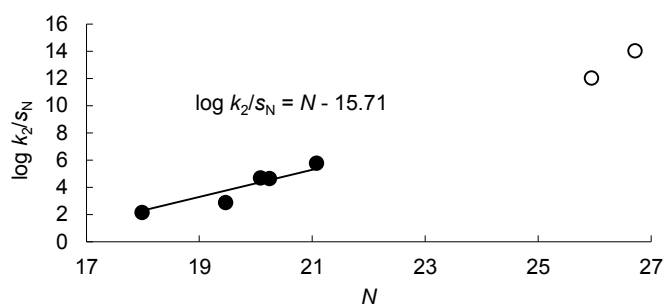
[a] Calculated by least square minimization according to eq 5.1.

5.4.3.4 Kinetics of Reactions of Diethyl Fumarate 1d

Table 5.27. Kinetics of the reaction of 1d with 2a (DMSO, 20 °C, Stopped-flow method, detection at 425 nm).

No.	[**1d**]/mol L^{-1}	[**2a**]/mol L^{-1}	k_{obs}/s^{-1}
FU2-1	1.05×10^{-3}	5.00×10^{-5}	9.10
FU2-2	1.57×10^{-3}	5.00×10^{-5}	1.36×10^1
FU2-3	2.09×10^{-3}	5.00×10^{-5}	1.77×10^1
FU2-4	2.61×10^{-3}	5.00×10^{-5}	2.35×10^1
FU2-5	3.14×10^{-3}	5.00×10^{-5}	2.72×10^1
$k_2(20 °C) = 8.83 \times 10^3$ L mol^{-1} s^{-1}			

y = 8830.4x - 0.2532
R² = 0.9961

Table 5.28. Kinetics of the reaction of 1d with 2b (DMSO, 20 °C, Stopped-flow method, detection at 425 nm).

No.	[**1d**]/mol L^{-1}	[**2b**]/mol L^{-1}	k_{obs}/s^{-1}
FU8-1	8.12×10^{-3}	4.00×10^{-4}	1.26×10^2
FU8-2	8.93×10^{-3}	4.00×10^{-4}	1.34×10^2
FU8-3	9.74×10^{-3}	4.00×10^{-4}	1.38×10^2
FU8-4	1.06×10^{-2}	4.00×10^{-4}	1.44×10^2
FU8-5	1.14×10^{-2}	4.00×10^{-4}	1.50×10^2
$k_2(20 °C) \approx 7.1 \times 10^3$ L mol^{-1} s^{-1}			

y = 7045.1x + 69.654
R² = 0.9912

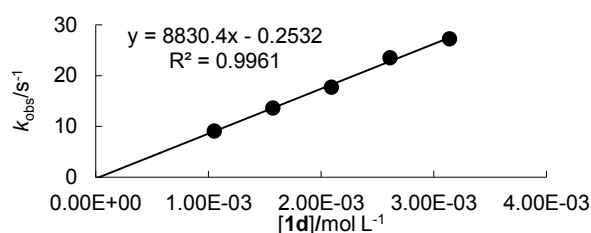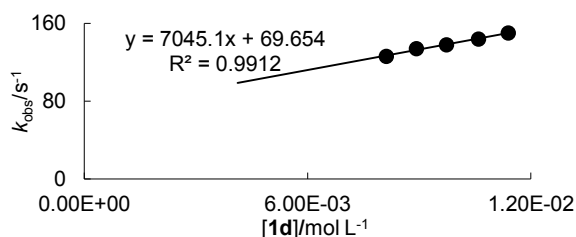The positive intercept may be due to the fact that the reaction is very fast and the solutions are not homogenous after 5 ms.

Table 5.29. Kinetics of the reaction of 1d with 2c (DMSO, 20 °C, Stopped-flow method, detection at 425 nm).

No.	[**1d**]/mol L^{-1}	[**2c**]/mol L^{-1}	k_{obs}/s^{-1}
FU9-1	8.12×10^{-3}	4.00×10^{-4}	1.47×10^2
FU9-2	8.93×10^{-3}	4.00×10^{-4}	1.64×10^2
FU9-3	9.74×10^{-3}	4.00×10^{-4}	1.72×10^2
FU9-4	1.06×10^{-2}	4.00×10^{-4}	1.83×10^2
FU9-5	1.14×10^{-2}	4.00×10^{-4}	1.94×10^2
$k_2(20 °C) \approx 1.4 \times 10^4$ L mol^{-1} s^{-1}			
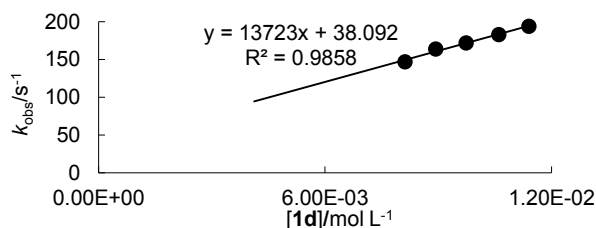
y = 13723x + 38.092
R² = 0.9858

The positive intercept may be due to the fact that the reaction is very fast and the solutions are not homogenous after 5 ms.

Table 5.30. Kinetics of the reaction of 1d with 2d (DMSO, 20 °C, Stopped-flow method, detection at 425 nm).

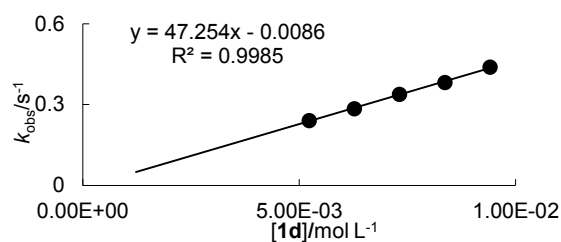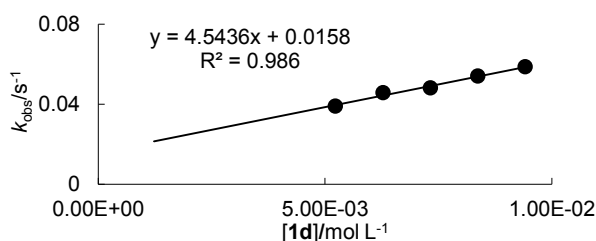| No.	$[\mathbf{1d}]$/mol L^{-1}	$[\mathbf{2d}]$/mol L^{-1}	k_{obs}/s^{-1}
FU3-1	5.23×10^{-3}	5.00×10^{-5}	2.41×10^{-1}
FU3-2	6.27×10^{-3}	5.00×10^{-5}	2.85×10^{-1}
FU3-3	7.32×10^{-3}	5.00×10^{-5}	3.38×10^{-1}
FU3-4	8.36×10^{-3}	5.00×10^{-5}	3.83×10^{-1}
FU3-5	9.41×10^{-3}	5.00×10^{-5}	4.39×10^{-1}
k_2(20 °C) = 4.73×10^1 L mol^{-1} s^{-1}			

y = 47.254x - 0.0086
R² = 0.9985

Table 5.31. Kinetics of the reaction of 1d with 2e (DMSO, 20 °C, Stopped-flow method, detection at 445 nm).

No.	$[\mathbf{4}]$/mol L^{-1}	$[\mathbf{6e}]$/mol L^{-1}	k_{obs}/s^{-1}
FU1-1	5.23×10^{-3}	5.00×10^{-5}	3.90×10^{-2}
FU1-2	6.27×10^{-3}	5.00×10^{-5}	4.57×10^{-2}
FU1-3	7.32×10^{-3}	5.00×10^{-5}	4.81×10^{-2}
FU1-4	8.36×10^{-3}	5.00×10^{-5}	5.40×10^{-2}
FU1-5	9.41×10^{-3}	5.00×10^{-5}	5.86×10^{-2}
k_2(20 °C) = 4.54 L mol^{-1} s^{-1}			

y = 4.5436x + 0.0158
R² = 0.986

The positive intercept may be caused by a slightly reversible betaine formation.

Table 5.32. Kinetics of the reaction of 1d with 2h (DMSO, 20 °C, diode array-spectometer method, detection at 480 nm).

No.	$[\mathbf{1d}]$/mol L^{-1}	$[\mathbf{2h}]$/mol L^{-1}	k_{obs}/s^{-1}
FU5-3	4.53×10^{-4}	9.32×10^{-5}	2.93×10^{-1}
FU5-2	5.27×10^{-4}	9.28×10^{-5}	3.25×10^{-1}
FU5-5	6.10×10^{-4}	9.40×10^{-5}	3.76×10^{-1}
FU5-4	6.77×10^{-4}	9.28×10^{-5}	4.19×10^{-1}
k_2(20 °C) = 5.68×10^2 L mol^{-1} s^{-1}			

y = 567.85x + 0.0314
R² = 0.9931
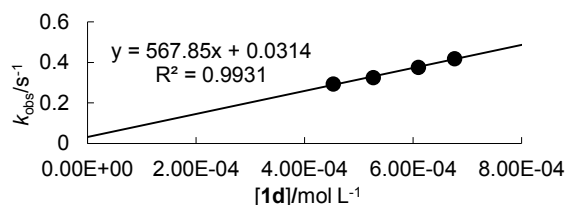
Table 5.33. Kinetics of the reaction of 1d with 3a (DMSO, 20 °C, Stopped-flow method, detection at 379 nm).

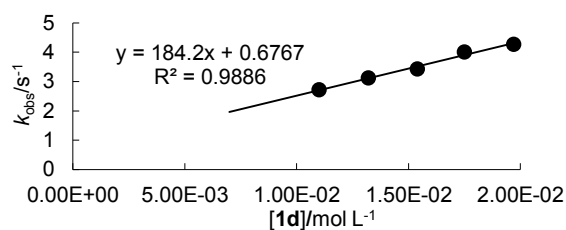| No.	$[\mathbf{1d}]$/mol L^{-1}	$[\mathbf{3a}]$/mol L^{-1}	k_{obs}/s^{-1}
FU6-1	1.10×10^{-2}	2.00×10^{-4}	2.80 ± 0.02
FU6-2	1.32×10^{-2}	2.00×10^{-4}	3.31 ± 0.02
FU6-3	1.54×10^{-2}	2.00×10^{-4}	3.58 ± 0.02
FU6-4	1.75×10^{-2}	2.00×10^{-4}	4.07
FU6-5	1.97×10^{-2}	2.00×10^{-4}	4.34
k_2(20 °C) = 1.84×10^2 L mol^{-1} s^{-1}			

y = 184.2x + 0.6767
R² = 0.9886

Table 5.34. Calculation of the Electrophilicity Parameter *E* for 1d using the *N* and *s*$_N$ Parameters of 2,3, eq 5.1, and the Second-Order Rate Constants for the Reactions of 1d with 2,3 (filled dots; open dots refer to rate constants not used for the determination of *E*).

Nucleophile	*N*/*s*$_N$	k_2/ L mol^{-1} s^{-1}
2d	20.24/0.60	4.73×10^1
2e	19.46/0.58	4.54
3a	21.07/0.68	1.84×10^2
	$E^{[a]} = -17.76$	
2a	26.71/0.37	8.83×10^3
2b	27.45/0.38	7.05×10^3
2c	25.94/0.42	1.39×10^4
2h	20.08/0.57	5.68×10^2

$\log k_2/s_N = N - 17.76$
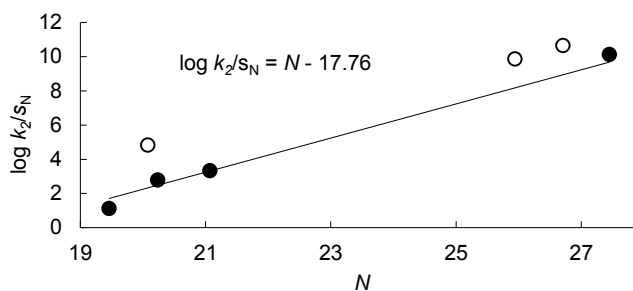
[a] Calculated by least square minimization according to eq 5.1.

5.4.3.5 Kinetics of Reactions of Diethyl Maleate 1e

Table 5.35. Kinetics of the reaction of 1e with 2c (DMSO, 20 °C, Stopped-flow method, detection at 425 nm).

No.	[**1e**]/mol L^{-1}	[**2c**]/mol L^{-1}	k_{obs}/s^{-1}
MA2-1	1.00×10^{-3}	1.00×10^{-4}	7.79×10^{-1}
MA2-2	2.00×10^{-3}	1.00×10^{-4}	1.73
MA2-3	3.01×10^{-3}	1.00×10^{-4}	2.59
MA2-4	4.01×10^{-3}	1.00×10^{-4}	3.52
MA2-5	5.01×10^{-3}	1.00×10^{-4}	4.43
	k_2(20 °C) = 9.28×10^2 L mol^{-1} s^{-1}		

y = 928.16x + 0.064
R² = 0.9979

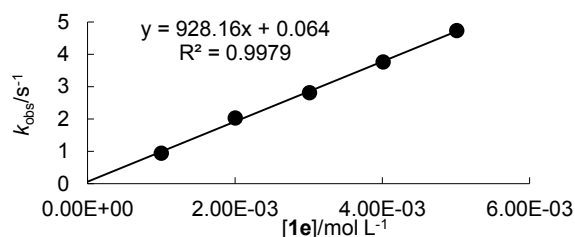**Table 5.36. Kinetics of the reaction of 1e with 2d (DMSO, 20 °C, Stopped-flow method, detection at 425 nm).**

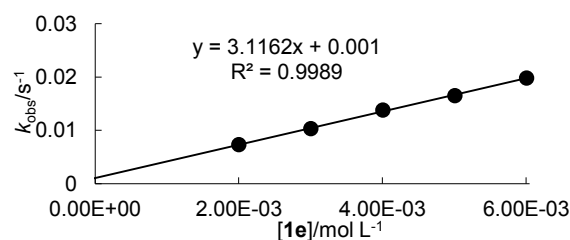| No.	[**1e**]/mol L^{-1}	[**2d**]/mol L^{-1}	k_{obs}/s^{-1}
MA4-1	2.00×10^{-3}	2.50×10^{-5}	7.29×10^{-3}
MA4-2	3.01×10^{-3}	2.50×10^{-5}	1.03×10^{-2}
MA4-3	4.01×10^{-3}	2.50×10^{-5}	1.38×10^{-2}
MA4-4	5.01×10^{-3}	2.50×10^{-5}	1.65×10^{-2}
MA4-5	6.01×10^{-3}	2.50×10^{-5}	1.98×10^{-2}
	k_2(20 °C) = 3.12 L mol^{-1} s^{-1}		

y = 3.1162x + 0.001
R² = 0.9989

Table 5.37. Reproduction of the Kinetics of the reaction of 1e with 2d (DMSO, 20 °C, diode array-spectometer method, detection at 425 nm).

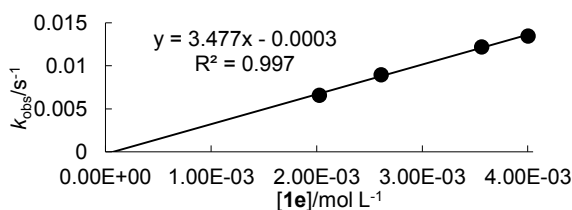| No.	[**1e**]/mol L^{-1}	[**2d**]/mol L^{-1}	k_{obs}/s^{-1}
MA8-5	2.02×10^{-3}	9.32×10^{-5}	6.60×10^{-3}
MA8-4	2.61×10^{-3}	9.39×10^{-5}	8.98×10^{-3}
MA8-2	3.56×10^{-3}	9.32×10^{-5}	1.22×10^{-2}
MA8-1	4.00×10^{-3}	9.22×10^{-5}	1.35×10^{-2}
	k_2(20 °C) = 3.48 L mol^{-1} s^{-1}		

y = 3.477x - 0.0003
R² = 0.997

Table 5.38. Kinetics of the reaction of 1e with 2e (DMSO, 20 °C, diode array-spectometer method, detection at 445 nm).

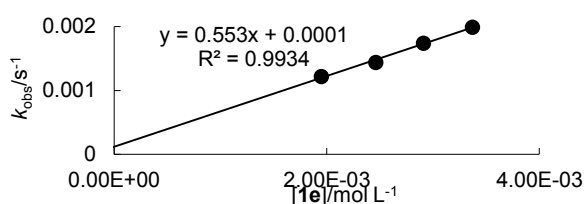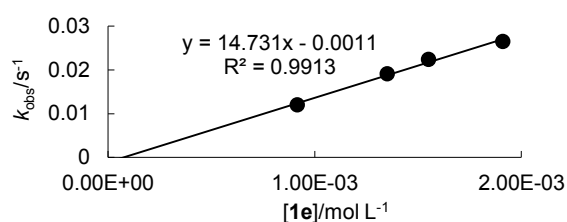| No.	[1e]/mol L^{-1}	[2e]/mol L^{-1}	k_{obs}/s^{-1}
MA7-5	1.95×10^{-3}	9.41×10^{-5}	1.22×10^{-3}
MA7-4	2.46×10^{-3}	9.27×10^{-5}	1.44×10^{-3}
MA7-3	2.91×10^{-3}	9.23×10^{-5}	1.74×10^{-3}
MA7-2	3.37×10^{-3}	9.23×10^{-5}	1.99×10^{-3}
k_2(20 °C) = 5.53×10^{-1} L mol^{-1} s^{-1}			

y = 0.553x + 0.0001
R² = 0.9934

**Table 5.39. Kinetics of the reaction of 1e with 2h (DMSO, 20 °C, diode array-spectometer method, detection at 480 nm).**

No.	[1e]/mol L^{-1}	[2h]/mol L^{-1}	k_{obs}/s^{-1}
MA5-2	9.16×10^{-4}	9.21×10^{-5}	1.20×10^{-2}
MA5-4	1.35×10^{-3}	9.35×10^{-5}	1.91×10^{-2}
MA5-5	1.55×10^{-3}	9.20×10^{-5}	2.24×10^{-2}
MA5-1	1.91×10^{-3}	9.51×10^{-5}	2.65×10^{-2}
k_2(20 °C) = 1.47×10^{1} L mol^{-1} s^{-1}			

y = 14.731x - 0.0011
R² = 0.9913

Table 5.40. Kinetics of the reaction of 1e with 3a (DMSO, 20 °C, diode array-spectometer method, detection at 379 nm).

| No.	[1e]/mol L^{-1}	[3a]/mol L^{-1}	k_{obs}/s^{-1}
MA9-1	1.03×10^{-3}	9.30×10^{-5}	4.37×10^{-3}
MA9-2	1.53×10^{-3}	9.44×10^{-5}	5.38×10^{-3}
MA9-3	2.00×10^{-3}	9.36×10^{-5}	6.92×10^{-3}
MA9-4	2.46×10^{-3}	9.32×10^{-5}	8.84×10^{-3}
MA9-5	3.03×10^{-3}	9.34×10^{-5}	1.09×10^{-2}
k_2(20 °C) ≈ 3.4 L mol^{-1} s^{-1}			

y = 3.3535x + 0.0005
R² = 0.9865
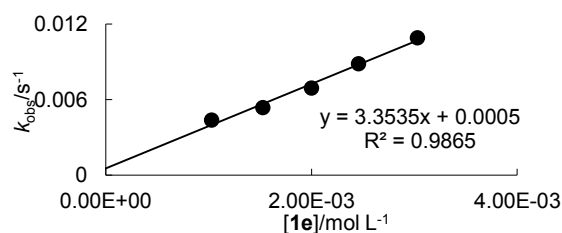
Estimated k_2 value; the decays of the absorption of ylide **3a** deviate from pseudo-first-order kinetics.

Table 5.41. Calculation of the Electrophilicity Parameter E for 1e using the N and s_N Parameters of 2,3, eq 5.1, and the Second-Order Rate Constants for the Reactions of 1e with 2,3 (filled dots; open dots refer to rate constants not used for the determination of E).

Nucleophile	N/s_N	k_2/ L mol^{-1} s^{-1}
2c	25.94/0.42	9.28×10^{2}
2d	20.24/0.60	3.12
2e	19.46/0.58	5.53×10^{-1}
$E^{[a]}$ = − 19.49		
2h	20.08/0.57	1.47×10^{1}
3a	21.07/0.68	(≈3.4)

log k_2/s_N = N - 19.49
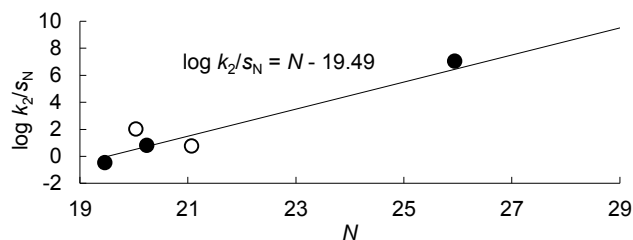
[a] Calculated by least square minimization according to eq 5.1.

5.5 References

[1]   For reviews see: (a) S. Patai, Z. Rappoport, in *The Chemistry of Alkenes* (Eds.: S. Patai, Z. Rappoport), Wiley, New York, **1964**, p. 469−584; (b) C. Bianchi, C. De Micheli, R. Gandolfi, in *The Chemistry of Double-Bonded Functional Groups, Vol. 1* (Eds.: S. Patai, Z. Rappoport), Wiley, London, **1977**, p. 369−533; (c) Z. Rappoport, in *Nucleophilicity* (Eds.: J. M. Harris, S. P. McManus), American Chemical Society, Washington, DC, **1987**, p. 399−424; (d) D. A. Oare, C. H. Heathcock, in *Topics in Stereochemistry, Vol. 20* (Eds.: E. L. Eliel, S. H. Wilen), Wiley-Interscience, Hoboken, NJ **1991**, p. 87−170; (e) I. Chataigner, A. Harrison-Marchand, J. Maddaluno, in *Science of Synthesis, Vol. 26* (Ed.: J. Cossy), Georg Thieme Verlag, Stuttgart, Germany, **2005**, p. 1123−1286; (f) F. Fringuelli, O. Piermatti, F. Pizzo, L. Vaccaro, in *Science of Synthesis, Vol. 47b* (Ed.: A. de Meijere), Georg Thieme Verlag, Stuttgart, Germany, **2010**, p. 561−722.

[2]   For reviews on conjugate additions see: (a) W. Nagata, M. Yoshioka, *Org. React.* **1977**, *25*, 255−476; (b) P. Perlmutter, *Conjugate Addition Reactions in Organic Synthesis, Vol. 9*, Pergamon, Oxford, **1992**; (c) A. Córdova, *Catalytic asymmetric conjugate reactions*, Wiley-VCH, Weinheim, **2010**.

[3]   A. Padwa, *1,3-Dipolar Cycloaddition Chemistry*, John Wiley and Sons, New York, **1985**.

[4]   For reviews on 1,3-dipolar cycloadditions see: (a) R. Huisgen, *Angew. Chem. Int. Ed. Engl.* **1963**, *2*, 565−598; (b) R. Huisgen, *Angew. Chem. Int. Ed. Engl.* **1963**, *2*, 633−645; (c) R. Huisgen, *J. Org. Chem.* **1976**, *41*, 403−419; (d) G. Pandey, P. Banerjee, S. R. Gadre, *Chem. Rev.* **2006**, *106*, 4484−4517.

[5]   F. Fringuelli, A. Taticchi, *The Diels-Alder Reaction: Selected Practical Methods*, Wiley, Chichester, **2002**.

[6]   For reviews on Diels-Alder reactions see: (a) R. Sustmann, *Pure Appl. Chem.* **1974**, *40*, 569-593; (b) J. Sauer, R. Sustmann, *Angew. Chem. Int. Ed. Engl.* **1980**, *19*, 779−807; (c) H. B. Kagan, O. Riant, *Chem. Rev.* **1992**, *92*, 1007-1019; (d) K. C. Nicolaou, S. A. Snyder, T. Montagnon, G. Vassilikogiannakis, *Angew. Chem., Int. Ed.* **2002**, *41*, 1668−1698.

[7]   D. A. Oare, C. H. Heathcock, in *Topics in Stereochemistry, Vol. 18* (Eds.: E. L. Eliel, S. H. Wilen), Wiley-Interscience, New York, **1989**, p. 227−407.

[8]   (a) W. Zeng, G.-Y. Chen, Y.-G. Zhou, Y.-X. Li, *J. Am. Chem. Soc.* **2007**, *129*, 750−751; (b) I. López, G. Silvero, M. J. Arévalo, R. Babiano, J. C. Palacios, J. L. Bravo, *Tetrahedron* **2007**, *63*, 2901−2906.

[9]   (a) A. Berkessel, H. Gröger, *Asymmetric Organocatalysis*, Wiley-VCH, Weinheim **2005**; (b) A. Ting, J. M. Goss, N. T. McDougal, S. E. Schaus, in *Asymmetric Organocatalysis, Top. Curr. Chem. Vol. 291* (Ed.: B. List), Springer, Berlin, **2010**, p. 145−201; (c) J. L. Vicario, *Organocatalytic enantioselective conjugate addition reactions - A powerful tool for the stereocontrolled synthesis of complex molecules Vol. 5*, RCS Publ., Cambridge **2010**.

[10]   For organo catalytic applications see: (a) J. L. Vicario, D. Badía, L. Carrillo, *Synthesis* **2007**, 2065−2092; (b) D. Almasi, D. A. Alonso, C. Nájera, *Tetrahedron: Asymmetry* **2007**, *18*, 299–365; (c) Z.-W. Ma, Y. Wu, B. Sun, H.-L. Du, W.-M. Shi, J.-C. Tao, *Tetrahedron: Asymmetry* **2013**, *24*, 7−13.

[11]   (a) W. Bihlmaier, R. Huisgen, H.-U. Reissig, S. Voss, *Tetrahedron Lett.* **1979**, *20*, 2621−2624; (b) R. Huisgen, L. Xingya, *Tetrahedron Lett.* **1983**, *24*, 4185−4188.

[12]   B. Blankenburg, H. Fiedler, M. Hampel, H. G. Hauthal, G. Just, K. Kahlert, J. Korn, K. H. Müller, W. Pritzkow, Y. Reinhold, M. Röllig, E. Sauer, D. Schnurpfeil, G. Zimmermann, *J. Prakt. Chem.* **1974**, *316*, 804−816.

[13]   For reviews see: (a) H. Mayr, M. Patz, *Angew. Chem. Int. Ed. Engl.* **1994**, *33*, 938−957; (b) H. Mayr, T. Bug, M. F. Gotta, N. Hering, B. Irrgang, B. Janker, B. Kempf, R. Loos, A. R. Ofial, G. Remennikov, H. Schimmel, *J. Am. Chem. Soc.* **2001**, *123*, 9500−9512; (c) R. Lucius, R. Loos, H. Mayr, *Angew. Chem. Int. Ed.* **2002**, *41*, 91−95; (d) H. Mayr, B. Kempf, A. R. Ofial, *Acc. Chem. Res.* **2003**, *36*, 66−77; (e) H. Mayr, A. R. Ofial, *Pure Appl. Chem.* **2005**, 1807−1821; (f) H. Mayr, A. R. Ofial, *J. Phys. Org. Chem.* **2008**, *21*, 584−595; (g) H. Mayr, S. Lakhdar, B. Maji, A. R. Ofial, *Beilstein J. Org. Chem.* **2012**, *8*, 1458−1478; (h) For a comprehensive database of nucleophilicity parameters N, s_N and electrophilicity parameters E, see http://www.cup.lmu.de/oc/mayr/.

[14]   D. S. Allgäuer, P. Mayer, H. Mayr, *J. Am. Chem. Soc.* **2013**, *135*, 15216–15224.

[15]   (a) R. Appel, H. Mayr, *Chem. Eur. J.* **2010**, *16*, 8610−8614; (b) R. Appel, N. Hartmann, H. Mayr, *J. Am. Chem. Soc.* **2010**, *132*, 17894−17900.

[16]   For reviews on pyridinium ylide chemistry see: (a) I. Zugravescu, M. Petrovanu, *N-Ylid Chemistry*, McGraw-Hill, New York, **1976**; (b) A. G. Mikhailovskii, V. S. Shklyaev, *Chem. Heterocycl. Compd.* **1997**, *33*, 243−265; (c) J. Jacobs, E. Van Hende, S.

Claessens, N. De Kimpe, *Curr. Org. Chem.* **2011**, *15*, 1340−1362; (d) A. Kakehi, *Heterocycles* **2012**, *85*, 1529-1577.

[17]   O. Tsuge, S. Kanemasa, S. Takenaka, *Bull. Chem. Soc. Jpn.* **1985**, *58*, 3137−3157.

[18]   (a) R. A. Firestone, *J. Org. Chem.* **1968**, *33*, 2285−2290; (b) R. A. Firestone, *J. Org. Chem.* **1972**, *37*, 2181−2191.

[19]   R. Huisgen, *J. Org. Chem.* **1968**, *33*, 2291−2297.

[20]   For articels on sulfonium ylide chemistry see: (a) A.-H. Li, L.-X. Dai, V. K. Aggarwal, *Chem. Rev.* **1997**, *97*, 2341−2372; (b) S. L. Riches, C. Saha, N. F. Filgueira, E. Grange, E. M. McGarrigle, V. K. Aggarwal, *J. Am. Chem. Soc.* **2010**, *132*, 7626−7630.

[21]   V. K. Aggarwal, E. Grange, *Chem. Eur. J.* **2006**, *12*, 568−575.

[22]   (a) C. R. Johnson, C. W. Schroeck, *J. Am. Chem. Soc.* **1968**, *90*, 6852−6854; (b) C. R. Johnson, C. W. Schroeck, *J. Am. Chem. Soc.* **1971**, *93*, 5303−5305; (c) C. R. Johnson, C. W. Schroeck, J. R. Shanklin, *J. Am. Chem. Soc.* **1973**, *95*, 7424−7431.

[23]   Y. Liu, Y. Zhang, Y.-M. Shen, H.-W. Hua, J.-H. Xu, *Org. Biomol. Chem.* **2010**, *8*, 2449–2456.

[24]   (a) O. Tsuge, S. Kanemasa, S. Takenaka, S. Kuraoka, *Chem. Lett.* **1984**, 465−468; (b) O. Tsuge, S. Kanemasa, S. Takenaka, *Bull. Chem. Soc. Jpn.* **1987**, *60*, 1489−1495.

[25]   D. S. Allgäuer, H. Mayr, *Eur. J. Org. Chem.* **2013**, 6379–6388.

[26]   The kinetics of the reactions of the sulfonium ylides **3c**,**d** with **1b**,**c** could not be investigated photometrically because of overlapping UV−vis absorptions of reactants and products.

[27]   T. Kanzian, H. Mayr, *Chem. Eur. J.* **2010**, *16*, 11670−11677.

[28]   S. T. A. Berger, F. H. Seeliger, F. Hofbauer, H. Mayr, *Org. Biomol. Chem.* **2007**, *5*, 3020−3026.

[29]   R. C. Samanta, B. Maji, S. De Sarkar, K. Bergander, R. Fröhlich, C. Mück-Lichtenfeld, H. Mayr, A. Studer, *Angew. Chem. Int. Ed.* **2012**, *51*, 5234−5238.

[30]   H. Asahara, H. Mayr, *Chem. Asian J.* **2012**, *7*, 1401−1407.

[31]   K. Troshin, P. Mayer, H. Mayr, *Organometallics* **2012**, *31*, 2416-2424.

[32]   T. Kanzian, S. Nicolini, L. De Crescentini, O. A. Attanasi, A. R. Ofial, H. Mayr, *Chem. Eur. J.* **2010**, *16*, 12008−12016.

[33]   I. Zenz, H. Mayr, *J. Org. Chem.* **2011**, *76*, 9370−9378.

[34]   R. Appel, H. Mayr, *J. Am. Chem. Soc.* **2011**, *113*, 8240−8251.

[35]   O. Kaumanns, R. Lucius, H. Mayr, *Chem. Eur. J.* **2008**, *14*, 9675−9682.

[36]   For previous theoretical approaches to electrophilicity and nucleophilicity parameters, as defined by eq 5.1 see: (a) P. Pérez, A. Toro-Labbé, A. Aizman, R. Contreras, *J. Org. Chem.* **2002**, *67*, 4747−4752; (b) L. R. Domingo, P. Pérez, R. Contreras, *Tetrahedron* **2004**, *60*, 6585−6591; (c) E. Chamorro, M. Duque-Noreña, P. Pérez, *J. Mol. Struct. THEOCHEM* **2009**, *896*, 73−79; (d) E. Chamorro, M. Duque-Noreña, P. Pérez, *J. Mol. Struct. THEOCHEM* **2009**, *901*, 145−152; (e) C. Wang, Y. Fu, Q.-X. Guo, L. Liu, *Chem. Eur. J.* **2010**, *16*, 2586−2598; (f) L.-G. Zhuo, W. Liao, Z.-X. Yu, *Asian J. Org. Chem.* **2012**, *1*, 336−345; (g) S.-i. Kiyooka, D. Kaneno, R. Fujiyama, *Tetrahedron* **2013**, *69*, 4247−4258; (h) E. Chamorro, M. Duque-Noreña, R. Notario, P. Pérez, *J. Phys. Chem. A* **2013**, *117*, 2636−2643.

[37]   a) H. E. Gottlieb, V. Kotlyar, A. Nudelman, *J. Org. Chem* **1997**, *62*, 7512−7515; b) G. F. Fulmer, A. J. M. Miller, N. H. Sherden, H. E. Gottlieb, A. Nudelman, B. M. Stoltz, J. E. Bercaw, K. I. Goldberg, *Organometallics* **2012**, *29*, 2176−2179.

6 Quantification of the Ambient Electrophilicities of α,β-Unsaturated Aldehydes

Dominik S. Allgäuer and Herbert Mayr

6.1 Introduction

α,β-Unsaturated aldehydes like acrolein (**1a**), crotonaldehyde (**1b**), and cinnamaldehyde (**1c**) (Chart 6.1) are common building blocks in organic synthesis,[1] which are frequently activated by secondary amines (iminium catalysis).[1-h] Various kinetic studies on the electrophilic reactivities of α,β-unsaturated aldehydes are available, which focus on their reactions with biomimetic sulfur nucleophiles[2] and their hydrogenation using metal catalysts.[3] Only recently the kinetics of iminium activated reactions of α,β-unsaturated aldehydes with cyclopentadiene were reported.[4] Some kinetic studies also compare 1,2 versus 1,4 reactivity[5] of the α,β-unsaturated aldehydes **1**, others the addition of nucleophiles to their conjugate position.[6]

Our earlier investigations of ambient systems focused on ambient nucleophilicity.[7, 8] In these studies we used eq 6.1, in which the nucleophile is described by two solvent-dependent parameters s_N (sensitivity) and N (nucleophilicity),[9] and the electrophile is described by one parameter E (electrophilicity). We now report on the determination of the electrophilicity parameters E of the β-positions and the carbonyl groups of the α,β-unsaturated aldehydes **1** and include them into our comprehensive electrophilicity scale.[9h] In this way we are able to quantify the magnitude of iminium activation of α,β-unsaturated aldehydes as of the electrophilicities of several iminium ions derived from cinnamaldehyde **1c** were already described by our group.[9g, 10]

$$\log k_2 = s_N(N + E) \qquad (6.1)$$

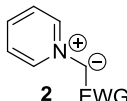**Chart 6.1. α,β-Unsaturated aldehydes 1a−c investigated in this work.**

The electrophilicity of the formyl group of cinnamaldehyde **1c** was recently quantified along with the electrophilicities of other aldehydes through their reactions with sulfur ylides,[11] but the electrophilicity of its β-position is still unknown as appropriate reference nucleophiles for its determination have not been available.

The recently described colored pyridinium ylides **2** (Table 6.1)[12] prefer the 1,4 over the 1,2-addition to α,β-unsaturated aldehydes **1**,[13] a behavior which has been utilized in Kröhnke condensations.[14] As pyridinium ylides only rarely react with the formyl groups of aldehydes, they are ideal candidates for studying the electrophilicities of the β-position of the enals **1**.[15]

The outcome of the reactions of sulfonium ylides **3** (Table 6.2) with α,β-unsaturated aldehydes **1** strongly depends on the substituent of ylide **3**. Semi-stabilized sulfonium ylides (R = aryl), like **3a,b**, preferentially add to the carbonyl group of α,β-unsaturated aldehydes to form epoxides,[16] while stabilized sulfonium ylides (R = EWG), like **3c**, add to the β-position to form cyclopropanes.[17] In contrast, stabilized sulfonium ylides rarely react with aliphatic and aromatic aldehydes.[18] In recent years the mechanism of epoxide formation in the reactions of sulfonium ylides and aldehydes has been studied in detail,[16a, c-e, h, i, 19] and was used for the determination of the electrophilic reactivities of aldehydes and imines.[11]
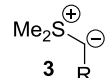
Combination of the α,β-unsaturated aldehydes **1** with either pyridinium ylides **2** or semi-stabilized sulfonium ylides **3** allowed us to address the conjugate position and the carbonyl moiety of the α,β-unsaturated aldehydes **2** individually. In this way, we were able to derive the electrophilicity parameters E for both reaction sites from the second order-rate constants of their reactions with the ylides **2** and **3** and the corresponding nucleophilicity parameters N and s_N.

Table 6.1. Pyridinium Ylides 2 used as reference nucleophiles in this Study and their N and s_N parameters in DMSO at 20 °C.

Ylide	EWG	N/s_N[a]
2a	CO$_2$Et	26.71/0.37
2b	CN	25.92/0.42
2c	COMe	20.24/0.60
2d	COPh	19.47/0.60

[a] From ref. [12].

Table 6.2. Sulfonium ylides 3 used as reference nucleophiles in this Study and their N and s_N parameters in DMSO at 20 °C.

| Ylide	R	N/s_N[a]
3a	p-CN-C$_6$H$_4$	21.07/0.68
3b	p-NO$_2$-C$_6$H$_4$	18.42/0.65
3c	p-Me$_2$N-	15.68/0.65

[a] From ref. [20].

6.2 Results and Discussion

6.2.1 General

The pyridinium ylides **2** can add to the CC-double bond of the α,β-unsaturated aldehydes **1** either in a concerted way or stepwise via betaine **4**. Both pathways result in the formation of the tetrahydroindolizines **5** (Scheme 6.1). A stepwise formation of tetrahydroindolizines with rate determining betaine formation was found for the reactions of pyridinium ylides **2** with various acceptor-substituted olefins.[12, 22, 23]

As outlined above, the reactions of sulfonium ylides **3** with the α,β-unsaturated aldehydes **1** can either lead to epoxides **7** or cyclopropanes **9**, depending on the stabilization of the ylide. The different pathways for the formation of these two types of products are depicted in Scheme 6.2. The formation of the *anti*-betaine **6** formed by 1,2-attack and the formation of the *syn*-betaine **8** formed by 1,4-attack are presumably only slightly reversible or irreversible, as these betaines should be stabilized through attractive ionic interactions.[16f, g, j, 17, 24] The subsequent ring-closures ($k_{rc}^{1,4}$) are reported to be fast processes for the *anti*-betaine **6** and for the *syn*-betaine **8**, but may be slower for the *syn*-betaine **6** and the *anti*-betaine **8** ($k_{rc}^{2,3}$, Scheme 6.2).[16]

Scheme 6.1. Concerted and stepwise [3+2]-cycloaddition of pyridinium ylides 2 with the α,β-unsaturated aldehydes 1.
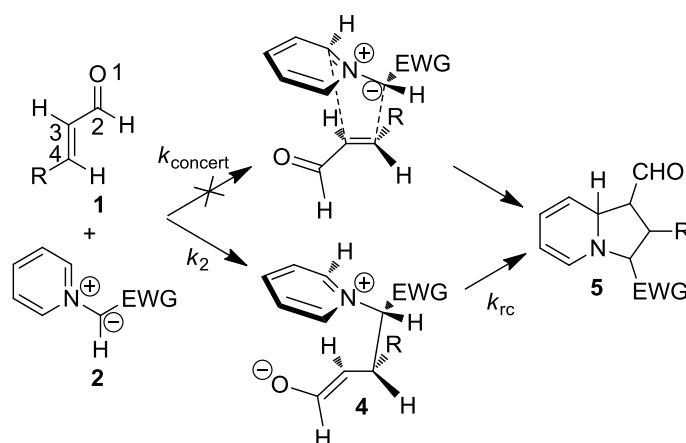
Scheme 6.2. Schematic mechanisms for the reactions of sulfonium ylides 3 with the α,β-unsaturated aldehydes 1. *Syn* **and** *anti* **terminology in the intermediate betaines 6 and 8 refers to the relations of the substituents around the newly formed CC-bond.**
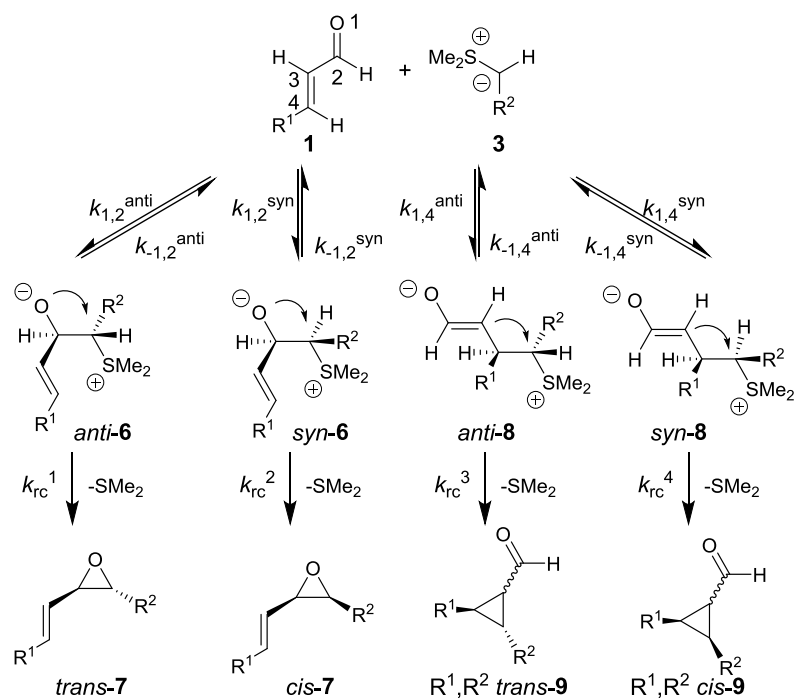

6.2.2 Products

Combination of the Michael acceptors **1a−c** with the pyridinium ylides **2** under basic conditions leads to the formation of tetrahydroindolizines **5** (Scheme 6.1). As the corresponding cycloadducts derived from isoquinolinium ylides and α,β-unsaturated aldehydes, including crotonaldehyde **1b** and cinnamaldehyde **1c** were reported to be unstable,[13] we made no attempts to isolate the tetrahydroindolizines **5** and oxidized them to indolizines instead.

The reaction of acrolein **1a** with **2dH⁺Br⁻** under basic conditions afforded two different products after oxidation, the 3-benzoyl-substituted indolizine **10d** and the 3-alkyl-substituted indolizine **11**. Their ratio depended on the quantity of acrolein **1a** employed in the reaction (Scheme 6.3).

With one equivalent of acrolein **1a** the reaction with ylide **2d** gave the indolizine **10d** in 58% yield after oxidation (Scheme 6.3). Indolizine **10d** is formed by conjugate addition of the ylide **2d** to acrolein **1a**, giving the intermediate betaine **4d** which cyclizes to the tetrahydroindolizine **5d**, and its oxidation results in the formation of indolizine **10d** (Scheme 6.3).

Scheme 6.3. Proposed mechanism for the formation of the indolizines 10d and 11.
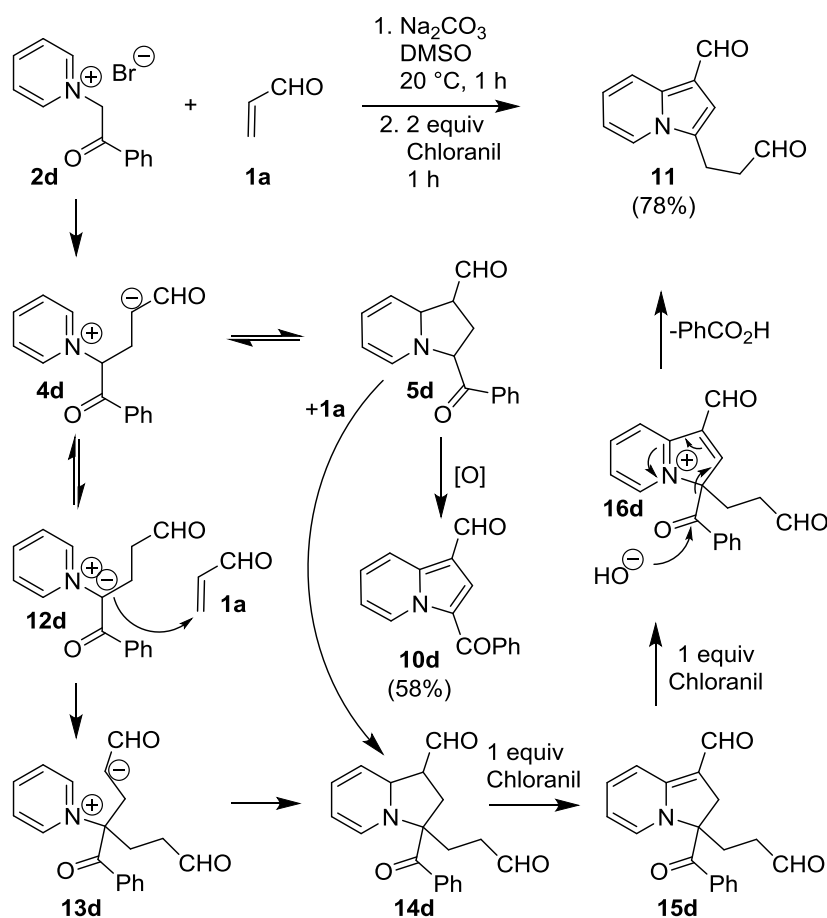
When two equivalents of acrolein **1a** were used in the reaction with ylide **2d**, the indolizine **11** (identified by ^{1}H-,^{13}C-, 2D-NMR, HRMS) was obtained in 78% yield. The formation of **11** can be rationalized by the mechanism depicted in Scheme 6.3. The initially formed betaine **4d** must be in equilibrium with the tetrahydroindolizine **5d** (gives indolizine **10d** after oxidation) and with the ylide **12d**.[25, 26] Ylide **12d** can add to a second molecule of acrolein **1a** to form the betaine **13d**, which cyclizes to the [3+2]-cycloadduct **14d**. The cycloadduct **14d** may also be formed by deprotonation of the tetrahydroindolizine **5d** and subsequent Michael addition of the formed carbanion to acrolein (**1a**). Hydride abstraction from the [3+2]-cycloadduct **14d** by one equivalent of chloranil gives the dihydroindolizine **15d**, which is oxidized by a second equivalent of chloranil to the pyridinium ion **16d**. The benzoyl group of the pyridinium ion **16d** is attacked by OH$^-$ and the subsequent elimination of benzoic acid gives the indolizine **11**. A similar base-induced elimination of an acyl-group from a pyridinium ion resulting in the formation of an indolizine was recently reported by our group.[27]

Table 6.3. Synthesis of the indolizines 10 and 11.
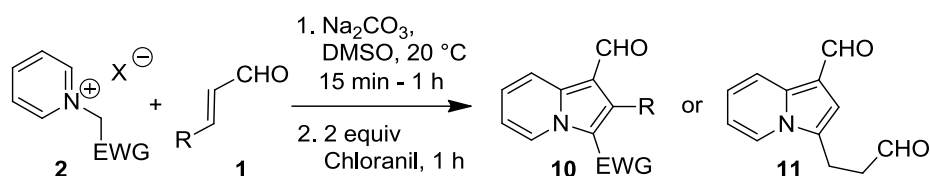
Aldehyde	Salt	EWG	Equiv. 1	Product	Yield/%
1a (R = H)	**2aH⁺Br⁻**	CO₂Et	2	**10a**	32
	2bH⁺Br⁻	CN	2	**10b**	36
	2cH⁺Cl⁻	COMe	1	**10c**	40
			2	**11**	86
	2dH⁺Br⁻	COPh	1	**10d**	58
			2	**11**	78
1b (R = Me)	**2aH⁺Br⁻**	CO₂Et	2	**10e**	56
	2dH⁺Br⁻	COPh	2	**10f**	88
1c (R = Ph)	**2bH⁺Br⁻**	CN	2	**10g**	41
	2cH⁺Cl⁻	COMe	1.5	**10h**	54

Table 6.3 shows that all tested combinations of the α,β-unsaturated aldehydes **1a−c** with the pyridinium ylides **2a−d** resulted in the formation of indolizines **10** in 32–88% yield. The [2:1]-product **11** was only obtained when the acyl-substituted pyridinium ylides **2c** and **2d** were combined with an excess of acrolein.

A [2:1]-product, analogous to **11**, was neither observed in the reactions of crotonaldehyde (**1b**) and cinnamaldehyde (**1c**) with the ylides **2c** and **2d** nor in the reactions of the ester and cyano-substituted ylides **2a** and **2b** with 2 equiv. of acrolein (**1a**). The reactions of equimolar mixtures of acrolein (**1a**) and crotonaldehyde (**1b**), or acrolein (**1a**) and cinnamaldehyde (**1c**) and one of the pyridinium ylides **2c** or **2d** did not lead to indolizines corresponding to **11**. The limitations in the formation of the indolizine **11** may be caused by an unfavorable equilibrium between the betaines **4** and the tetrahydroindolizines **5** (Scheme 6.3).

In line with earlier findings the regioselectivity of the attack of sulfonium ylides **3a−c** at acrolein (**1a**) was found to be strongly dependent on the nature of the employed ylide. Furthermore the regioselectivity of the attack of the sulfonium ylide was found to be influenced by the employed solvent. As shown in Table 6.4 the reaction of acrolein **1a** with the semi-stabilized *p*-cyano-benzyl-substituted sulfonium ylide **3a** preferentially gave the 1,2-adduct, epoxide **7a**, under biphasic reaction conditions (Conditions A), while the corresponding reaction in DMSO (Conditions B) preferentially gave cyclopropane **9a**. The reaction of acrolein (**1a**) with the less nucleophilic *p*-nitro-benzyl-substituted ylide **3b** gave the 1,4-adduct, cyclopropane **9b** preferentially, even under biphasic reaction conditions.[28] The reaction of

acrolein **1a** with the stabilized ylide **3c** resulted in the exclusive formation of cyclopropane **9c**. On the other hand, the reactions of ylide **3a** with crotonaldehyde **1b** and cinnamaldehyde **1c** led to the formation of the *trans*-epoxides **7d** and **7e** selectively, regardless of the employed solvent. A concurrence of epoxidation and cyclopropanation in reactions of α,β-unsaturated aldehydes with semi-stabilized sulfonium ylides was recently reported for a similar series α,β-unsaturated aldehydes in THF at −78 °C.[16d]

The stereochemistry of the *trans*-epoxides **7** and the cyclopropanes **9** was assigned on basis of NOESY correlations of the protons and substituents of the three-membered rings. The epoxides **7** were exclusively obtained as the *trans*-isomers. The cyclopropanes **9** were preferentially formed with a *trans*-configuration between the carbonyl group and R^2.

In all cases ^{1}H NMR monitoring of the reactions of ylide **3a** with the enals **1a–c** in DMSO-d_6 showed a complete conversion of the reactants immediately after mixing. While in the reaction of **3a** with acrolein (**1a**) 1:4 mixtures of epoxide **7a** and cyclopropane **9a** were formed, the corresponding reaction of **3a** with crotonaldehyde (**1b**) and cinnamaldehyde (**1c**) resulted in the exclusive formation of the epoxides **9d** and **9e**. As the betaines **6** and **8** (Scheme 6.2) were not observable, rapid formations of **6** and **8** with slow subsequent ring-closures can be ruled out.

Table 6.4. Synthesis of the epoxides 7 and the cyclopropanes 9 in DMSO.

Aldehyde	Yli-de	R^2	Condi-tions[a]	*trans*-Epoxide 7	Yield 7/%	Cyclopro-pane 9	Yield 9/%	*trans:cis* 9 (R^1 = H)[b]
1a (R^1 = H)	**3a**	C$_6$H$_4$-*p*-CN	A	**7a**	54	**9a**	(25)[c]	6:1
	3a	C$_6$H$_4$-*p*-CN	B	**7a**	(20)[d]	**9a**	68	3:1
	3b	C$_6$H$_4$-*p*-NO$_2$	A	**7b**	36	**9b**	60	5:1
	3c	COC$_6$H$_4$-*p*-OMe	C	**7c**	0	**9c**	70	5:1
1b (R^1 = Me)	**3a**	C$_6$H$_4$-*p*-CN	A	**7d**	70	**9d**	0	-
	3a	C$_6$H$_4$-*p*-CN	B	**7d**	quant.[e]	**9d**	0	-
1c (R^1 = Ph)	**3a**	C$_6$H$_4$-*p*-CN	A	**7e**	93	**9e**	0	-
	3a	C$_6$H$_4$-*p*-CN	B	**7e**	quant.[e]	**9e**	0	-

[a] Conditions A: CHCl$_3$/aq. K$_2$CO$_3$ (sat.), 2 h; Conditions B: KO^{t}Bu (1.1 equiv), DMSO, 5 min; Conditions C: DMSO, 15 min; [b] The diastereoselectivities were determined by ^{1}H NMR of the crude products; [c] Calculated from the 3:1 ratio of **7a**:**9a** in the crude reaction mixture; **7a** was not isolated; [d] From the 1:4 Ratio of **7a**:**9a** in the crude product; **9a** was not isolated; [e] Determined by ^{1}H NMR of the crude reaction mixture.

6.2.3 Kinetic Investigations and Discussion

The kinetics of the reactions of the α,β-unsaturated aldehydes **1a−c** with the pyridinium ylides **2a−d** and the sulfonium ylides **3a,c** were studied in DMSO solution at 20 °C and monitored photometrically by following the disappearance of the ylides **2** and **3** at or close to their absorption maxima. Due to their low stabilities the ylides **2a−d** and **3a** were generated in DMSO by combining DMSO solutions of the salts **2(a−d)H$^+$X$^−$** or **3aH$^+$BF$_4^−$** and KO^{t}Bu (typically 1.05 equivalents) directly before each kinetic experiment. The sulfonium ylide **3c** is a stable compound and thus stock solutions of this ylide were prepared. For the kinetic measurements 10 or more equivalents (pseudo first-order conditions) of the enals **1a−c** over the ylides **2** and **3** were used. First-order rate constants k_{obs} were obtained by least-squares fitting of the single exponential function $A_t = A_0 \exp(-k_{obs}t)$ (mono-exponential decay) to the observed time-dependent absorbances (Figure 6.1a). Plots of k_{obs} versus the concentrations of the Michael acceptors **1a−c** were linear with negligible intercepts in most cases, as required by $k_{obs} = k_2[\mathbf{1}]$ (Figure 6.1b). From the slopes of the linear correlations the second-order rate constants of the reactions of the Michael acceptors **1a−c** with the ylides **2** and **3** were obtained (Table 6.5).

Equation 1 implies a slope of 1.0 for the plots of $(\log k_2)/s_N$ versus the nucleophilicity parameters N. Figure 6.2 shows that this requirement is roughly fulfilled for the reactions of the α,β-unsaturated aldehydes **1a−c** with pyridinium ylides **2a−d** and the sulfonium ylide **3c**. The reaction of acrolein (**1a**) with the ethoxy carbonyl-substituted pyridinium ylide **2a** proceeds 4.5 times faster than expected from the correlation. This deviation is small and within the limit of confidence of eq 6.1 (two orders of magnitude), but might also be due to a low degree of concertedness of the [3+2]-cycloaddition reaction. Therefore, the rate constant of the reaction of acrolein (**1a**) with pyridinium ylide **2a** was excluded for the determination of the electrophilicity parameter E. The deviations of the other rate constants for the reactions of the pyridinium ylides **2a−d** and the sulfonium ylide **3c** with the enals **1a−c** from the correlation lines stay below a factor of four, thus they were used to determine the electrophilicity parameter E by least squares-fitting, i.e., minimization of $\Delta^2 = \sum(\log k_2 - s_N(N + E)^2)$ (Table 6.5).
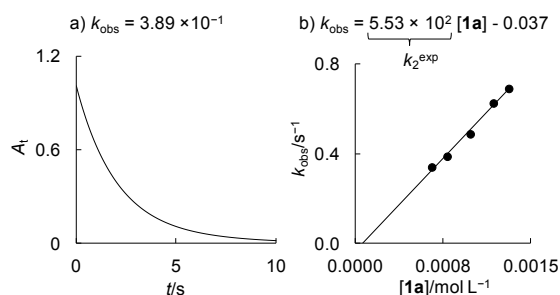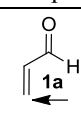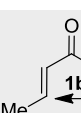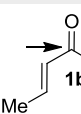
a) $k_{obs} = 3.89 \times 10^{-1}$

b) $k_{obs} = 5.53 \times 10^2$ [1a] - 0.037

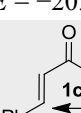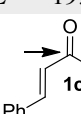**Figure 6.1. a) Decay of the absorbance of 2d ([2d]$_0$ ~ 5 × 10^{-5} M) at 445 nm during its reaction with 1a ([1a]$_0$ = 7.89 × 10^{-4} M) in DMSO at 20°C. b) Plot of the k_{obs}-values versus the concentration of 1a.**

Table 6.5. Experimental (k_2^{exp}) and calculated (k_2^{calcd})[a] second-order rate constants for the 1,2- and 1,4-additions of the ylides 2,3 to the α,β-unsaturated aldehydes 1a−c in DMSO at 20 °C.

Electrophile/E	Ylide	k_2^{exp}/M^{-1} s^{-1}	k_2^{calcd}/M^{-1} s^{-1}	k_2^{exp}/k_2^{calcd}
1a $E = -14.65$	**2a**	1.25 × 10^5 [b]	2.9 × 10^4	4.5
	2b	1.08 × 10^5 [c]	5.51 × 10^4	2.22
	2c	2.86 × 10^3	2.26 × 10^3	1.27
	2d	5.53 × 10^2	6.15 × 10^2	0.90
	3a	9.73 × 10^{2} [d]	2.30 × 10^4	0.04
	3c	2.46	4.66	0.53
1b Me $E = -19.10$	**2b**	2.86 × 10^3	7.48 × 10^2	3.83
	2c	4.01	4.85	0.83
	2d	7.47 × 10^{-1}	1.62	0.46
1b Me $E = -20.52$	**3a**	2.35	Identical[e]	-
1c Ph $E = -19.66$	**2a**	4.11 × 10^2	4.06 × 10^2	1.01
	2b	1.16 × 10^3	4.34 × 10^2	2.67
	2c	1.11	2.23	0.50
1c Ph $E = -19.92$[f]	**3a**	6.03[f]	Identical[e]	-

[a] Calculated by eq 6.1 using N and s_N from Tables 7.1, 7.2 and E; [b] Exempted from the determination of E due to a possible small degree of concertedness; [c] The k_{obs} vs. [1a] plot for this reaction, which proceeds on the >20 ms timescale, does not have a negligible intercept; [d] Bisexponential decays of the absorbance of ylide **3a** at low concentrations of acrolein **1a** were observed; the second-order rate constant corresponding to the slow decays of **3a** measured at high concentrations of **1a** must refer to more complex kinetics; Not used for the determination of E; [e] Only one k_2-value used for the determination of E; [f] E and k_2 value from ref. [11].
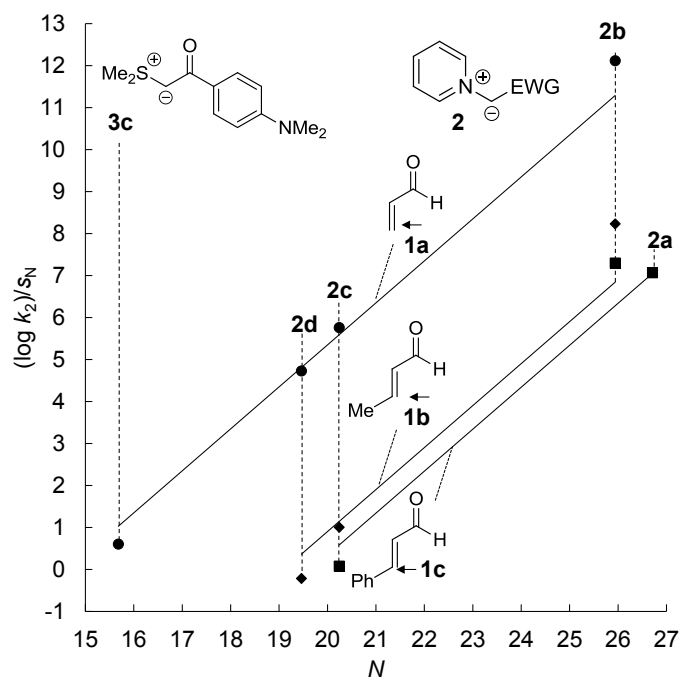
Figure 6.2. Plots of the (log k_2)/s_N-values derived from the reactions of the α,β-unsaturated aldehydes 1 with the ylides 2a−d and 3c versus the corresponding nucleophilicity parameters N (the slopes are fixed to 1.0 as required by eq 6.1). The rate of the reaction of 1a with 2a was not used for the determination of E and is thus not displayed.

The four experimental second-order rate constants for the reactions of the acrolein (**1a**) with the pyridinium ylides **2b−d** and the sulfonium ylide **3c** agree with those calculated by eq 6.1 within a factor of two, indicating a common rate-determining step, i.e., the formation of the intermediate betaines **4** and **6**.

In the reaction of acrolein **1a** with the ylide **3a** the epoxide **7a** and the cyclopropane **9a** were formed (Table 6.4). The kinetics of the reaction showed bisexponential decays at low concentrations of acrolein **1a**, which are suppressed at higher concentrations. The second-order rate constant k_2^{exp} in Table 6.5 was derived from the k_{obs} values measured at higher concentrations of **1a**. As it is unclear, which reaction step was followed in this case the derived second-order rate constant was not used for the calculation of E of acrolein (**1a**).

The rates of the reactions of the enals **1b** and **1c** with the sulfonium ylide **3a** only deviate slightly from the correlation lines of the corresponding reactions with pyridinium ylides **2**. However, considering the exclusive formations of the epoxides in the product studies (Table 6.4), the measured rate constants of the reactions of the aldehydes **1b** and **1c** with the sulfonium

Scheme 6.4. Transformation of hydroxy sulfides 16 to epoxides 19.[29]
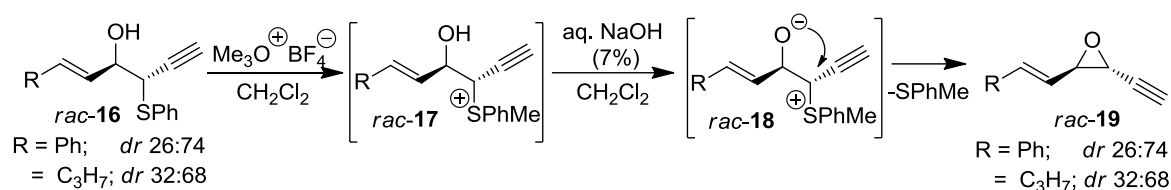
ylide **3a** can be assigned to the attack of **3a** at the formyl-group, what would allow us to derive the corresponding electrophilicity parameters *E*.

In a previous investigation,[29] the hydroxysulfides **16** were S-alkylated to give the sulfonium salts **17**. Its treatment with a base gave the intermediate betaines **18** which cyclized to the epoxides **19** (Scheme 6.4). This reaction sequence proceeded without erosion of the diastereomeric ratios of the starting materials **16**, indicating that the intermediate betaines **18**, which are closely related to the betaines **6** formed from the aldehydes **1b** and **1c** and ylide **3a**, do not undergo retroaddition. The irreversible formation of betaine **18** in combination with the non-observance of the betaines **6** by ¹H NMR monitoring allows one to conclude that the intermediate betaines **6** must be formed irreversible and the subsequent ring-closures are fast processes. Therefore, the observed second-order rate constants k_2^{exp} for the reactions of ylide **3a** with the aldehydes **1b** and **1c** can be assigned to the 1,2-addition and the electrophilicity parameter *E* of the carbonyl group of crotonaldehyde (**1b**) and cinnamaldehyde (**1c**)[11] can be derived as given in Table 6.5 using eq 6.1.

Reported rate constants for reactions of acrolein (**1a**), crotonaldehyde (**1b**), and cinnamaldehyde (**1c**) with substituted pyridines, morpholine, and cysteine dianion in H₂O or MeOH, were collected from the literature (Table 6.7).[3a, 5b, 6b] The nucleophilicity parameters *N* and s_N of these nucleophiles in the solvents employed for the kinetic measurements are known (Table 6.6), what allows a comparison of the experimental rate constants (k_2^{exp}) and those calculated by eq 6.1 using *E* from Table 6.5 and the *N* and s_N values of the nucleophiles listed in Table 6.6. The small differences between the temperatures used to determine the rate constants and the reactivity parameters s_N, *N*, and *E* are neglected in this comparison.

The observed (k_2^{exp}) and calculated (k_2^{calcd}) rate constants agree within two orders of magnitude, which is within the limit of confidence of eq 6.1. In four of eight cases the rate constants agree with a factor better than four, supporting the derived electrophilicity parameters *E* for the β-position of the α,β-unsaturated aldehydes **1**. The assumption of a stepwise addition of the pyridinium ylides **2** to the α,β-unsaturated aldehydes **1** is also verified in this way

Table 6.6. *N* and *s*$_N$-parameters of substituted pyridines, morpholine, and cysteine dianion at 20 °C.[30]

Nucleophile	Abbreviation	Solvent	*N*/*s*$_N$	
4-Pyridone anione	4-PyO$^-$	H$_2$O	14.76/0.48	[a]
4-NMe$_2$-Pyridine	DMAP	H$_2$O	13.19/0.56	[b]
4-Morpolino-Pyridine	MorAP	H$_2$O	12.39/0.66	[b]
4-NH$_2$-Pyridine	AP	H$_2$O	12.19/0.66	[b]
3-Br-4-NH$_2$-Pyridine	3-BrAP	MeCN	12.96/0.67	[c]
Morpholine	Mor	MeOH/MeCN	15.40/0.64	[d]
Cysteine Dianion	Cys^{2-}	H$_2$O	23.43/0.42	[e]

[a] From ref. [31d]; [b] From ref. [31b]; [c] From ref. [31e]; [d] From ref. [31a]; [e] From ref. [31c].

Table 6.7. Rates of the Michael addition of nucleophiles to the 4-positions of 1a−c (from refs. [3a, 5b, 6b]).

Elec.	Nuc.	Solvent	*T*/°C	k_2^{exp}/M^{-1} s^{-1}	k_2^{calcd}/M^{-1} s^{-1} [a]	k_2^{exp}/k_2^{calcd}	
1a	4-PyO$^-$	H$_2$O	25	0.96	1.12	0.86	[b]
	DMAP	H$_2$O	25	2.39	1.51×10^{-1}	15.8	[b]
	MorAP	H$_2$O	25	1.04	3.19×10^{-2}	32.6	[b]
	AP	H$_2$O	25	1.65	2.36×10^{-2}	83.2	[b]
	3-BrAP	H$_2$O	25	1.10×10^{-1}	7.51×10^{-2}	1.51	[b]
	Mor	MeOH	30	1.25	2.99	0.42	[c]
1b	DMAP	H$_2$O	25	8×10^{-3}	4.92×10^{-4}	16.3	[b]
1c	Cys^{2-}	H$_2$O	25	1.22×10^1	3.83×10^1	0.32	[d]

[a] Calculated by eq. 1 from *N*, *s*$_N$ in Table 6.6 and *E* in Table 6.5; [b] From ref. [6b]; [c] From ref. [5b] [d] From ref. [3a].

(Scheme 6.1). The remaining four rate constants of the reactions of acrolein **1a** and crotonaldehyde **1b** with 4-amino-pyridines proceed 16 to 83 times faster than calculated what is within the limit of confidence of eq 6.1 of two orders of magnitude.

6.3   Conclusion

In this work we present the first access to 1-carbaldehyde substituted indolizines synthesized by a [3+2]-cycloaddition/oxidation-protocol from pyridinium ylides and α,β-unsaturated aldehydes under mild conditions.[31] The addition of two molecules of the Michael acceptor to one pyridinium ylide giving a 3-alkyl substituted indolizine[32] after oxidation has, to our knowledge, not been reported before. Both methods, the single and double addition of α,β-unsaturated aldehydes to pyridinium ylides, provide a simple access to 1-carbaldehyde substituted indolizines from readily accessible materials.

The linear free-energy correlation eq 6.1 was found to describe the rates of reactions of the α,β-unsaturated aldehydes acrolein **1a**, crotonaldehyde **1b**, and cinnamaldehyde **1c** with pyrid-
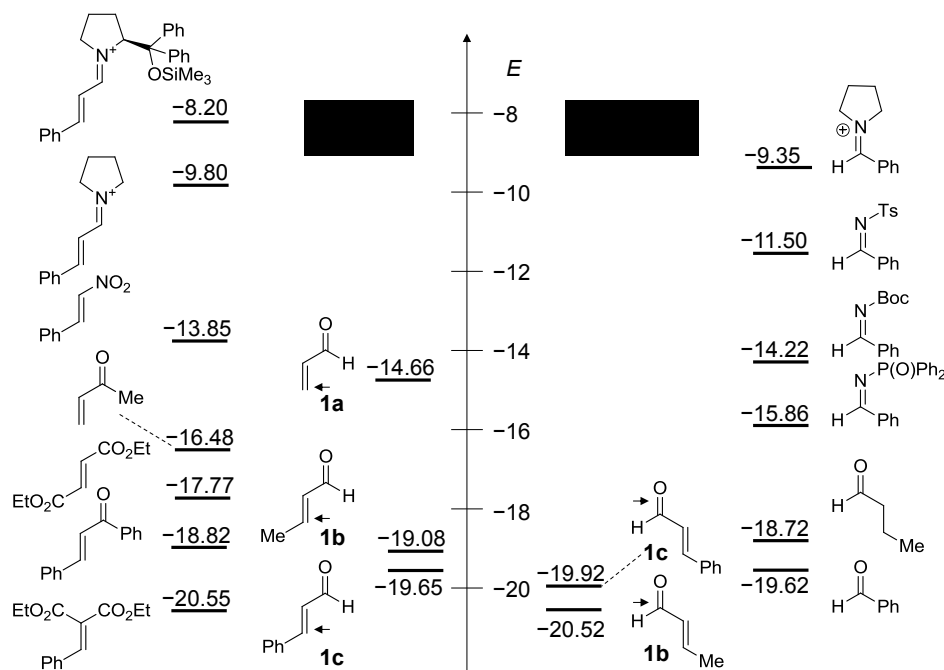
Figure 6.3. Comparison of the electrophilicity parameters of the α,β-unsaturated aldehydes 1 with other related Michael acceptors and aldehydes.[10a, 11, 23, 33-35]

inium ylides **2** and sulfonium ylides **3**. From these rate constants the electrophilicity parameters for the β-position and the carbonyl carbon of the enals **1a−c** could be derived, what allowed us to include them into our comprehensive reactivity scale. The fair agreement of the previously reported rate constants for the addition of amines, pyridines, and cysteine to the α,β-unsaturated aldehydes **1** with those calculated by eq 6.1, demonstrates the general utility of the electrophilicity parameters E for predicting reactivities towards a wide variety of nucleophiles.

The ambient reactivities of α,β-unsaturated aldehydes can now be compared to the electrophilicities of other acceptor substituted C=C-double (Figure 6.3, left) and carbon heteroatom (C=Het) double bonds (Figure 6.3, right).

The reactivity of the C=C-double bond of acrolein (**1a**) is similar to that of nitrostyrene[33] while the related methylvinylketone[23] is 66 times less reactive (Figure 6.3; left). Addition of a methyl-group in the 4-position of acrolein (**1a**) decreases the reactivity by a factor of ~26,000, so that crotonaldehyde (**1b**) is less reactive than chalcone[11] or diethyl fumarate.[22] Exchanging the methyl (**1b**) by a phenyl group (**1c**) leads to a slight decrease of reactivity by a factor of 4.

The carbonyl groups of the investigated α,β-unsaturated aldehydes **1b** and **1c** have a similar reactivity as the corresponding conjugated double bonds (Figure 6.3; right). The reduction of the conjugated double bond in crotonaldehyde (**1b**) to *n*-butanal[11] increases the reactivity of the carbonyl group by a factor of 63. The formyl group of cinnamaldehyde **1c** is two times less

reactive than benzaldehyde.[11] Iminium activation of cinnamaldehyde and benzaldehyde leads to a ~10^{10} fold increase of the reactivity in both cases,[10a, 35] so that the reactivity of the iminium activated cinnamaldehyde towards 1,4-attack is similar to the reactivity of iminium activated benzaldehyde towards 1,2-attack.

One major drawback of the derived reactivity parameters for the carbonyl groups of α,β-unsaturated aldehydes is that they may only be representative for their reactions with carbon-centered nucleophiles. In reactions with oxygen- or nitrogen-centered nucleophiles, the anomeric stabilization[36] of the resulting products may probably affect the transition state of the reaction resulting in an enhanced reaction rate which cannot be described by eq 6.1.[11] Furthermore the electrophilicity parameters E determined in this work might not be independent from the solvent, as found for benzhydrylium ions.[9]

6.4 Experimental Section

6.4.1 General

Chemicals. The pyridinium salts **2H⁺X⁻** were synthesized according to ref. [12], the sulfonium salts **3H⁺X⁻** according to ref. [20], and the sulfonium ylides **3c,d** according to ref. [21].

Analytics. ^{1}H- and ^{13}C NMR spectra were recorded in CDCl$_3$ (δ_H 7.26, δ_c 77.16),[37a] CD$_2$Cl$_2$ (δ_H 7.26, δ_c 77.16), [37b] or DMSO-d_6 (δ_H 2.50, δ_c 39.52)[37a] on 200, 300, 400, or 600 MHz NMR spectrometers and are given in ppm. The following abbreviations were used to designate chemical shift multiplicities: s = singlet, d = doublet, t = triplet, q = quartet, m = multiplet, br = broad. For reasons of simplicity, the ^{1}H NMR signals of AA'BB'-spin systems of *p*-disubstituted aromatic rings were treated as doublets. The assignments of individual NMR signals were based on additional 2D-NMR experiments (COSY, NOESY, HSQC, HMBC). Diastereomeric ratios (*dr*) were determined by ^{1}H NMR of the crude reaction products if not stated otherwise. HRMS and MS were recorded on a Finnigan MAT 95 Q (EI) mass spectrometer or Thermo Finnigan LTQ FT Ultra (ESI). The melting points were recorded on a Büchi Melting Point B-540 device and are not corrected.

Kinetics. DMSO (99.7%, extra dry, over molecular sieves, AcroSeal) was purchased and used without further purification. The rates of all reactions were determined by UV-vis spectroscopy in DMSO at 20 °C by using stopped-flow spectrophotometer systems (Applied

Photophysics SX.18MV-R and Hi-Tech SF-61DX2) as well as diodearray-spectrophotometer systems (J&M TIDAS DAD 2062). The temperature of the solutions during the kinetic studies was maintained at 20 ± 0.2 °C by using circulating bath cryostats. The ylides were generated in DMSO at 20 °C immediately before each kinetic run by mixing DMSO solutions of the salts **2H⁺X⁻** or **3aH⁺BF₄⁻** and KO′Bu (typically 1.00:1.05 equivalents). Ylide **3c** is a stable compound and thus stock solutions of it were prepared. The kinetic runs were initiated by mixing DMSO solutions of the ylides and electrophiles under pseudo first-order conditions with one of the two reaction partners in large excess over the other (>10 equivalents). Pseudo first-order rate constants k_{obs} (s⁻¹) were obtained by fitting the single exponential $A_t = A_0 \exp(-k_{obs}t) + C$ (mono-exponential decrease) to the observed time-depended absorbances (average of at least three kinetic runs for each concentration for the stopped-flow method) of the electrophiles or ylides. Second-order rate constants k_2 (L mol⁻¹ s⁻¹) were derived from the slopes of the linear correlations of the obtained k_{obs}-values against the concentrations of the excess reaction partner.

6.4.2 Product Studies

6.4.2.1 Reactions of the α,β-Unsaturated Aldehydes 1 with the Pyridinium Ylides 2

Procedure A for the Synthesis of the Indolizines 10 and 11. Na₂CO₃ (0.50 mmol) was added to a solution of **1** (0.50 – 1.00 mmol) and **2H⁺X⁻** (500 μmol) in DMSO (0.2 M) at room temperature. The reaction was stirred until **1** was completely consumed as monitored by TLC (15 min–1 h). Chloranil (2 equiv) was added and the solution was stirred at room temperature for 30 min–1 h until all chloranil was consumed as monitored by TLC. The reaction was quenched with 2 M HCl and extracted with CHCl₃ (3×15mL). The combined organic layers were washed with brine (2×25 mL) and dried over Na₂SO₄. The solvent was evaporated and the residue was subjected to a column chromatography (silica; *n*-pentane:EtOAc 15:1–3:1, depending on R_f). The products were subsequently recrystallized from Et₂O.

Ethyl 1-formylindolizine-3-carboxylate (10a). From **1a** (56 mg, 1.0 mmol), **2aH⁺Br⁻** (123 mg, 500 μmol), Na₂CO₃ (53 mg, 0.50 mmol), and chloranil (246 mg, 1.00 mmol) according to procedure **A**. **10a** was obtained as colorless solid (35 mg, 0.16 mmol, 32%). The product is contaminated by traces of 2,3,5,6-tetrachlorobenzene-1,4-diol (reduced chloranil). **Mp** (Et₂O) 138 − 139 °C. **¹H NMR** (600 MHz, CDCl₃) δ 1.42 (t, *J* = 7.1 Hz, 3H, CH₃), 4.41 (q, *J* = 7.1 Hz, 2H, CH₂), 7.09 (td, *J* = 7.0, 1.4 Hz, 1H, 6-H), 7.43 (ddd, *J* = 8.8, 6.9, 1.1 Hz, 1H, 7-H), 7.94 (s, 1H, 2-H), 8.43 (dt, *J* = 9.0, 1.2 Hz, 1H, 8-H), 9.56
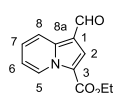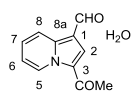
(dt, J = 7.0, 1.1 Hz, 1H, 5-H), 10.01 (s, 1H, CHO). ^{13}C NMR (150 MHz, CDCl$_3$) δ 14.4 (q, CH$_3$), 60.5 (t, CH$_2$), 114.5 (s, C-1), 115.8 (d, C-6), 116.1 (s, C-3), 119.6 (d, C-8), 125.7 (d, C-2), 127.5 (d, C-7), 128.2 (d, C-5), 138.3 (s, C-8a), 161.0 (s, CO$_2$), 184.7 (s, CHO). **HRMS** (EI): calcd. for [C$_{12}$H$_{11}$NO$_3$]$^+$ 217.0733, found 217.0734. DA909

1-Formylindolizine-3-carbonitrile (**10b**). From **1b** (56 mg, 1.0 mmol), **2bH$^+$Br$^-$** (123 mg, 500 μmol), Na$_2$CO$_3$ (53 mg, 0.50 mmol), and chloranil (246 mg, 1.00 mmol) according to procedure **A**. **10b** was obtained as colorless solid (30 mg, 0.18 mmol, 36%). ^{1}**H NMR** (300 MHz, CDCl$_3$) δ 7.16 (td, J = 6.9, 1.3 Hz, 1H, 6-H), 7.47 (dddd, J = 9.0, 7.0, 1.1, 0.5 Hz, 1H, 7-H), 7.75 (s, 1H, 2-H), 8.36 – 8.49 (m, 2H, 5,8-H), 9.99 (d, J = 0.5 Hz, 1H, CHO). ^{13}**C NMR** (75 MHz, CDCl$_3$) δ 105.6 (s, CN), 112.2 (s, C-3), 115.0 (s, C-1), 116.4 (d, C-6), 120.4 (d, C-8), 125.8 (d, C-5), 126.3 (d, C-2)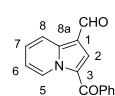, 127.9 (d, C-7), 137.0 (s, C-8a), 183.8 (s, CHO). **HRMS** (EI): calcd. for [C$_{10}$H$_6$N$_2$O]$^+$ 170.0475, found 170.0477. **MS** (EI) m/z: 170 (71), 169 (100), 141 (12), 89 (24). DA905

3-Acetylindolizine-1-carbaldehyde hydrate (**10c·H$_2$O**). From **1a** (27 mg, 0.5 mmol), **2cH$^+$Cl$^-$** (139 mg, 500 μmol), Na$_2$CO$_3$ (53 mg, 0.50 mmol),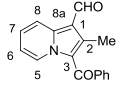 and chloranil (246 mg, 1.00 mmol) according to procedure **A**. **10c** was obtained as brown solid (40 mg, 0.20 mmol, 40%). The product is contaminated by traces of an unknown by-product. R_f (n-pentane:EtOAc 10:1) = 0.8. **Mp** (Et$_2$O) 109 − 110 °C. ^{1}**H NMR** (400 MHz, CDCl$_3$) δ 1.71 (br s, 2H, H$_2$O), 2.62 (s, 3H, CH$_3$), 7.14 (td, J = 7.0, 1.4 Hz, 1H, 6-H), 7.52 (ddd, J = 8.8, 6.9, 1.2 Hz, 1H, 7-H), 7.93 (s, 1H, 2-H), 8.45 (dt, J = 8.9, 1.2 Hz, 1H, 8-H), 9.93 (dt, J = 7.0, 1.1 Hz, 1H, 6-H), 10.04 (s, 1H, CHO). ^{13}**C NMR** (100 MHz, CDCl$_3$) δ 27.3 (q, CH$_3$), 114.9 (s, C-1), 116.6 (d, C-6), 119.2 (d, C-8), 123.8 (s, C-3), 127.2 (d, C-2), 129.0 (d, C-7), 129.4 (br d, C-5), 138.7 (s, C-8a) 184.4 (s, CHO), 187.9 (s, CO). **HRMS** (EI): calcd. for [C$_{11}$H$_9$NO$_2$]$^+$ 187.0628, found 187.0624. **MS** (EI) m/z: 188 (12), 187 (100), 172 (91), 121 (33), 105 (30), 77 (13), 43 (38). DA906

3-Benzoylindolizine-1-carbaldehyde (**10d**). From **1a** (29 mg, 0.53 mmol), **2dH$^+$Br$^-$** (139 mg, 500 μmol), Na$_2$CO$_3$ (53 mg, 0.50 mmol), and chloranil (246 mg, 1.00 mmol) according to procedure **A**. **10d** was obtained as colorless solid (71 mg, 0.29 mmol, 58%). R_f (n-pentane:EtOAc 5:1) = 0.12. **Mp** (Et$_2$O) 129 − 130 °C. ^{1}**H NMR** (300 MHz, CDCl$_3$) δ 7.14 (t, J = 6.4 Hz, 1H, 6-H), 7.40 – 7.57 (m, 4H, 7-H, 3×C$_{Ar}$-H), 7.69 (s, 1H, 2-H), 7.76 (ddd, J = 3.7, 1.8, 1.2 Hz, 2H, 2×C$_{Ar}$-H), 8.43 (d, J = 8.8 Hz, 1H, 8-H), 9.81 − 10.04 (m, 2H, 5-H, CHO). ^{13}**C NMR** (75 MHz, CDCl$_3$) δ 115.5 (s, C-1), 116.9 (d, C-6), 119.6 (d, C-8), 123.8 (d, C-3), 128.6 (d, 2×C$_{Ar}$-H), 129.1 (d, 2×C$_{Ar}$-H), 129.6 (d, C-5 or C-7),

129.6 (br d, C-5 or C-7), 130.5 (d, C-2), 131.9 (d, C_{Ar}-H), 139.3 (s, C-8^a), 139.8 (s, C_{Ar}), 184.8 (d, CHO), 185.9 (s, CO). **HRMS** (ESI): calcd. for $[C_{16}H_{12}NO_2]^+$ 250.0863, found 250.0860. DA800-3

Ethyl 1-formyl-2-methylindolizine-3-carboxylate (**10e**). From **1b** (70 mg, 1.0 mmol), **2aH⁺Br⁻** (123 mg, 500 μmol), Na_2CO_3 (53 mg, 0.50 mmol), and chloranil (246 mg, 1.00 mmol) according to procedure **A**. **10e** was obtained as a colorless solid (64 mg, 0.28 mmol, 56%). R_f (*n*-pentane:EtOAc 5:1) = 0.39. **Mp** (Et₂O) 140 − 141 °C. **¹H NMR** (300 MHz, CDCl₃) δ 1.45 (t, *J* = 7.1 Hz, 3 H, CH₃), 2.81 (s, 3 H, CH₃), 4.44 (q, *J* = 7.1 Hz, 2 H, CH₂), 7.02 (td, *J* = 7.0, 1.4 Hz, 1 H, 6-H), 7.40 (ddd, *J* = 8.8, 6.9, 1.1 Hz, 1 H, 7-H), 8.45 (dt, *J* = 8.9, 1.2 Hz, 1 H, 8-H), 9.62 (dt, *J* = 7.1, 1.0 Hz, 1 H, 5-H), 10.21 (s, 1 H, CHO). **¹³C NMR** (75 MHz, CDCl₃) δ = 11.6 (q, CH₃), 14.6 (q, CH₃), 60.5 (t, CH₂), 113.3 (s, C-3), 114.2 (s, C-2), 115.4 (d, C-6), 118.8 (d, C-8), 127.9 (d, C-7), 128.5 (d, C-5), 138.5 (s, C-1), 138.9 (s, C-8^a), 162.3 (s, CO₂), 184.4 (d, CHO). **HRMS** (EI): calcd. for $[C_{13}H_{13}NO_3]^{+}$ 231.0890, found 231.0890. **MS** (EI) *m/z*: 231 (15), 202 (15), 159 (10), 58 (32), 43 (100). DA791
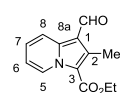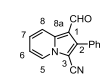
3-Benzoyl-2-methylindolizine-1-carbaldehyde (**10f**). From **1b** (70 mg, 1.0 mmol), **2dH⁺Br⁻** (139 mg, 500 μmol), Na_2CO_3 (53 mg, 0.50 mmol), and chloranil (246 mg, 1.00 mmol) according to procedure **A**. **10f** was obtained as colorless solid (116 mg, 441 μmol, 88%). R_f (*n*-pentane:EtOAc 1:1) = 0.24. **Mp** (Et₂O) 108 − 110 °C. **¹H NMR** (300 MHz, CDCl₃) δ = 2.13 (d, *J* = 2.3 Hz, 3 H, CH₃), 6.99 (tdd, *J* = 7.0 Hz, 2.1, 1.5, 1 H, 6-H), 7.35 − 7.46 (m, 3 H, 7-H, 2×C_{Ar}-H), 7.47 − 7.55 (m, 1 H, C_{Ar}-H), 7.62 (ddd, *J* = 6.8, 3.4, 1.5 Hz, 2 H, 2×C_{Ar}-H), 8.30 − 8.43 (m, 1 H, 8-H), 9.47 (ddt, *J* = 7.0, 2.1, 1.1 Hz, 1 H, 5-H), 10.10 (d, *J* = 2.3 Hz, 1 H, CHO). **¹³C NMR** (75 MHz, CDCl₃) δ = 12.5 (q, CH₃), 113.8 (s, C-1), 115.8 (d, C-6), 118.7 (d, C-8), 122.9 (s, C-2), 128.7 (d, C-5), 128.7 (d, 2× C_{Ar}-H), 128.8 (d, 2× C_{Ar}-H), 129.2 (d, C-7), 132.2 (d, C_{Ar}-H), 137.8 (s, C-3), 139.4 (s, C-8^a), 140.9 (s, C_{Ar}), 184.3 (d, CHO), 187.8 (s, CO). **HRMS** (EI): calcd. for $C_{17}H_{13}NO_2$ 263.0946, found 263.0944. **MS** (EI) *m/z*: 264 (20), 263 (83), 262 (100), 234 (49), 186 (15), 158 (10), 105 (10), 77 (21), 43 (53). DA848

1-Formyl-2-phenylindolizine-3-carbonitrile (**10g**). From **1c** (99 mg, 0.75 mmol), **2bH⁺Br⁻** (86 mg, 0.50 mmol), Na_2CO_3 (53 mg, 0.50 mmol), and chloranil (246 mg, 1.00 mmol) according to procedure **A**. **10g** was obtained as a brown solid (50 mg, 0.20 mmol, 51%). **¹H NMR** (300 MHz, CDCl₃) δ 7.18 (td, *J* = 6.9, 1.3 Hz, 1H, 6-H), 7.44 − 7.67 (m, 6H, 7-H, 5×C_{ar}-H), 8.42 (dt, *J* = 6.8, 1.1 Hz, 1H, 5-H), 8.58 (dt, *J* = 8.9, 1.2 Hz, 1H, 8-H), 9.94 (s, 1H, CHO). **¹³C NMR** (75 MHz, CDCl₃) δ 96.3 (s, CN), 112.1 (s, C-1), 112.6 (s, C-3), 116.5 (d, C-5), 120.8 (d, C-8), 125.6 (d, C-5), 128.5 (d, C-7) , 129.1 (d, 2×C_{ar}-H), 129.3 (s, C_{ar}),

129.5 (d, C_{ar}-H), 130.2 (d, 2×C_{ar}-H), 137.6 (s, C-8a), 142.7 (s, C-2), 185.2 (s, CHO). **HRMS** (EI): calcd. for $[C_{16}H_{10}N_2O]^{+}$ 246.0788, found 246.0772. **MS** (EI) *m/z*: 264 (18), 263 (95), 248 (35), 187 (14), 186 (100), 105.15 (11), 89 (15), 58 (14), 43 (42). DA904
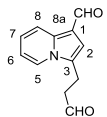
3-Acetyl-2-phenylindolizine-1-carbaldehyde (**10h**). From **1c** (99 mg, 0.75 mmol), **2cH⁺Cl⁻** (86 mg, 0.50 mmol), Na_2CO_3 (53 mg, 0.50 mmol), and chloranil (246 mg, 1.00 mmol) according to procedure A. **10h** was obtained as brown solid (78 mg, 0.27 mmol, 54%). R_f (*n*-pentane:EtOAc 5:1) = 0.33. **Mp** (Et$_2$O) 96 − 97 °C. **¹H NMR** (300 MHz, CDCl$_3$) δ 1.98 (s, 3 H, CH$_3$), 7.16 (td, *J* = 7.0, 1.5 Hz, 1 H, 6-H), 7.41 − 7.61 (m, 7 H, 2-H, 7-H, 5×C_{Ar}-H), 8.60 (dt, *J* = 8.9, 1.3 Hz, 1 H, 8-H), 9.53 (s, 1 H, CHO), 10.07 (dt, *J* = 7.2, 1.1 Hz, 1 H, 5-H). **¹³C NMR** (75 MHz, CDCl$_3$) δ 30.5 (q, CH$_3$), 114.8 (d, C-1), 116.9 (d, C-6), 119.6 (d, C-8), 122.3 (s, C-3), 128.6 (d, 2×C_{Ar}-H), 129.0 (d, C-7), 129.6 (d, C-5), 129.8 (d, C_{Ar}-H), 130.3 (d, 2×C_{Ar}-H), 133.0 (s, C_{Ar}), 137.7 (s, C-8^a), 143.1, 186.3 (d, CHO), 189.8 (s, CO). **HRMS** (EI): calcd. for $[C_{17}H_{13}NO_2]^{+}$ 263.0941, found 263.0943. **MS** (EI) *m/z*: 264 (18), 263 (95), 248 (35), 187 (14), 186 (100), 105.15 (11), 89 (15), 58 (14), 43 (42). DA797
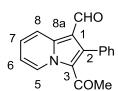
3-(3-Oxopropyl)indolizine-1-carbaldehyde (**11**). From **1a** (56 mg, 1.0 mmol), **2dH⁺Br⁻** (139 mg, 500 µmol), Na_2CO_3 (53 mg, 0.50 mmol), and chloranil (246 mg, 1.00 mmol) according to procedure **A**. **11** was obtained as a brown solid (79 mg, 0.39 mmol, 78%). (Analytical data see below). DA800-2

3-(3-Oxopropyl)indolizine-1-carbaldehyde (**11**). From **1a** (56 mg, 1.0 mmol), **2cH⁺Cl⁻** (86 mg, 0.50 mmol), Na_2CO_3 (53 mg, 0.50 mmol), and chloranil (246 mg, 1.00 mmol) according to procedure **A**. **11** was obtained as a brown solid (86 mg, 0.43 mmol, 86%). R_f (*n*-pentane:EtOAc 1:1) = 0.20. **Mp** (Et$_2$O) 148 − 149 °C. **¹H NMR** (300 MHz, CDCl$_3$) δ 2.97 − 3.07 (m, 2 H, C*H$_2$*CHO), 3.13 (t, *J* = 7.2 Hz, 2 H, CH$_2$), 6.92 (t, *J* = 6.9 Hz, 1 H, 6-H), 6.99 (s, 1 H, 2-H), 7.15 − 7.24 (m, 1 H, 7-H), 7.95 (d, *J* = 7.0 Hz, 1 H, 5-H), 8.22 (br, d, *J* = 9.0 Hz, 1 H, 8-H), 9.93 (s, 1 H, CH$_2$C*HO*), 9.99 (s, 1 H, CHO). **¹³C NMR** (75 MHz, CDCl$_3$) δ 18.2 (t, CH$_2$), 41.2 (t, CH$_2$CHO), 113.7 (s, C-1), 114.2 (d, C-6), 119.2 (br, d, C-8), 123.1 (d, C-5), 123.9 (d, C-2, C-7), 125.4 (s, C-3), 136.8 (br, s, C-8^a), 183.4 (d, CHO), 200.2 (d, CH$_2$C*HO*). **HRMS** (EI): calcd. for $[C_{12}H_{11}NO_2]^{+}$ 201.0784, found 201.0783. **MS** (EI) *m/z*: 201 (28), 159 (11), 158 (100), 145 (18), 58 (20), 43 (60). DA847

6.4.2.2 Reactions of the α,β-Unsaturated Aldehydes 1 with the Sulfonium Ylides 3

Procedure B for the Synthesis of the Epoxides 7. Aq. K_2CO_3 (5 mL, sat.) was added to solutions of **1** (2.5–5.0 mmol) and **3aH⁺BF₄⁻** (500 μmol) dissolved in $CHCl_3$ (0.1 M). The emulsion was stirred for 2 h, then water (20 mL) was added and the organic layer was separated. The aqueous layer was successively washed with $CHCl_3$ (2×20 mL), the combined organic layers were washed with water (20 mL) and dried over Na_2SO_4. The solvent was evaporated and the residues were subjected to a column chromatography (Alox, neutral, activity III; *n*-pentane:EtOAc) according to their R_f-value.

trans-**4-(3-Vinyloxiran-2-yl)benzonitrile** (*trans*-**7a**). From **1a** (280 mg, 5.00 mmol) and **3aH⁺BF₄⁻** (132 mg, 500 μmol) according to procedure **B**. **7a** was obtained as a yellow oil (67 mg, 0.27 mmol, 54%, *trans*). The spectrum of the crude product showed signals of cyclopropane **9a** (*dr* 6:1; ratio **7a**:**9a** ~3:1). R_f (*n*-pentane:EtOAc 5:1) = 0.23. **¹H NMR** (300 MHz, CDCl₃) δ = 3.28 – 3.39 (m, 1 H, CH), 3.80 (d, *J* = 1.9 Hz, 1 H, CH-C$_{ar}$), 5.33 – 5.42 (m, 1 H, CH=CH*H*), 5.47 – 5.59 (m, 1 H, CH=C*H*H), 5.72 (ddd, *J* = 17.4, 10.2, 7.2 Hz, 1 H, C*H*=CHH), 7.35 – 7.41 (m, 2 H, 2×C$_{Ar}$-H), 7.59 – 7.67 (m, 2 H, 2×C$_{Ar}$-H). **¹³C NMR** (75 MHz, CDCl₃) δ = 59.4 (d, CH-C$_{Ar}$), 63.4 (d, CH), 112.1 (s, C$_{Ar}$), 118.7 (s, CN), 120.6 (d, CH=*C*HH), 126.2 (d, 2×C$_{Ar}$-H), 132.4 (d, 2×C$_{Ar}$-H), 134.3 5569(d, *C*H=CHH), 142.6 (s, C$_{Ar}$). **HRMS** (EI): calcd. for [C₁₁H₉NO]⁺ 171.0679, found 171.0679. **MS** (EI) *m/z*: 171 (14), 170 (29), 143 (12), 142 (61), 115 (39), 102 (15), 85 (65), 83 (100), 54.98 (10), 44 (22). DA856

4-(2-Formylcyclopropyl)benzonitrile (*trans*-**9a**). A solution of KO*t*Bu (29 mg, 0.26 mmol) in 2.6 mL of DMSO was added dropwise to a solution of **1a** (45 mg, 0.80 mmol) and **3aH⁺BF₄⁻** (66 mg, 0.25 mmol) in 10 mL of DMSO at 20 °C. After the addition was completed brine (40 mL) was added and the mixture was extracted with CH_2Cl_2 (3×20 mL). The organic layer was wahed with water (3×20 mL) and brine (3×20 mL) and subsequently dried over Na_2SO_4. The solvent was removed and the crude product was purified by column chromatography (silica; *n*-pentane:EtOAc 5:1). **9a** was obtained as yellow oil (29 mg, 0.17 mmol, 68%, *trans*:*cis* 3:1). The spectrum of the crude product showed signals of epoxide **7a** (*trans*; ratio **7a**:**9a** 1:4). R_f (*n*-pentane:EtOAc 5:1) = 0.15. **¹H NMR** (400 MHz, CDCl₃) δ 1.50 – 1.57 (m, 1H, C*H*H), 1.80 – 1.86 (m, 1H, CH*H*), 2.24 (dddd, *J* = 8.8, 5.1, 2.7, 2.0 Hz, 1H, CH), 2.63 – 2.67 (m, CH), 7.17 – 7.22 (m, 2H, C$_{ar}$-H), 7.55 – 7.61 (m, 3H, C$_{ar}$-H, superimposed by minor diastereoisomer), 9.41 (dd, *J* = 4.1, 0.7 Hz, 1H, CHO). Only signals of

the major diastereoisomer are given due to overlapping. #-major diastereoisomer, *-minor diastereoisomer; **^{13}C NMR** (100 MHz, CDCl$_3$) δ 12.0 (t, CH$_2$),* 17.2 (t, CH$_2$),# 26.4 (d, CH),# 27.0 (d, CH),* 30.1 (d, CH),* 34.0 (d, CH),# 110.7 (s, CN),# 111.2 (s, CN),* 118.7 (s, C$_{ar}$)*, 118.8 (s, C$_{ar}$),# 127.0 (d, 2×C$_{ar}$-H),# 130.1 (d, 2×C$_{ar}$-H),* 132.3 (d, 2×C$_{ar}$-H),* 132.5 (d, 2×C$_{ar}$-H),# 141.5 (s, C$_{ar}$),* 144.9 (s, C$_{ar}$),# 198.8 (d, CHO),# 199.5 (d, CHO).* **HRMS** (EI): calcd. for [C$_{11}$H$_9$NO]$^+$ 171.0679, found 171.0629. **MS** (EI) *m/z*: 171 (40), 170 (38), 142 (100), 141 (36), 116 (52), 115 (63), 89 (21), 63 (16), 55 (20). DA920

NMR-Monitoring of the reaction of 1a with 3a. A solution of KO^{t}Bu (37 mg, 0.33 mmol) in 1.0 mL of DMSO-d_6 was added to a solution of **1a** (22 mg, 0.39 mmol) and **3aH$^+$BF$_4^-$** (66 mg, 0.25 mmol) in 2.0 mL of DMSO-d_6 at 20 °C. The spectra taken immediately after mixing of the reactants showed complete conversion of the reactants to epoxide **7a** and cyclopropane **9d** (**7a**:**9a** 1:4; *trans*:*cis* (**7a**) 3:1).

***trans*-2-(4-Nitrophenyl)-3-vinyloxirane** (**7b**) and **2-(4-nitrophenyl)cyclopropane-carbaldehyde (9b)**. From **1a** (280 mg, 5.00 mmol) and **3bH$^+$BF$_4^-$** (143 mg, 500 μmol) according to procedure **B**. **7b** was obtained as a colorless oil (34 mg, 0.18 mmol, 36%, *trans*). **9b** was obtained as yellow oil (57 mg, 0.30 mmol, 60%, *trans*:*cis* 5:1). The ratio of **7b**:**9b** in the crude product was 3:2. **7b.** **R_f** (*n*-pentane:EtOAc 5:1) = 0.23. **^{1}H NMR** (300 MHz, CDCl$_3$) δ = 3.34 (ddd, *J* = 7.1, 1.9, 0.5 Hz, 1 H, CH), 3.87 (d, *J* = 1.9 Hz, 1 H, CH-C$_{ar}$), 5.35 – 5.46 (m, 1 H, =CHH), 5.50 – 5.63 (m, 1 H, =CHH), 5.74 (dddd, *J* = 17.3, 10.1, 7.2, 0.5 Hz, 1 H, CH=), 7.39 – 7.51 (m, 2 H, 2×C$_{ar}$-H), 8.15 – 8.27 (m, 2 H, 2×C$_{ar}$-H). **^{13}C NMR** (75 MHz, CDCl$_3$) δ = 59.3 (d, *C*H-C$_{ar}$), 63.5 (d, CH), 120.8 (t, C=*C*HH), 124.0 (d, 2×C$_{ar}$-H), 126.4 (d, 2×C$_{ar}$-H), 134.3 (d, CH=), 144.7 (s br, C$_{ar}$), 148.0 (s, C$_{ar}$). **MS** (EI) *m/z*: 191 (4), 178 (11), 175 (17), 174 (35), 162 (10), 145 (13), 144 (48), 117 (16), 116 (100), 115 (48), 91 (15), 89 (43), 70 (17), 63 (24), 55 (18). **9b.** Only signals of the major diastereoisomer are given due to overlapping. **^{1}H NMR** (300 MHz, CDCl$_3$) δ = 1.52 (ddd, *J* = 8.4, 6.6, 5.1 Hz, 1H, C*H*H), 1.78 (dt, *J* = 9.1, 5.3 Hz, 1H, CH*H*), 2.15 – 2.29 (m, 1H, C*H*-CHO), 2.64 (ddd, *J* = 9.1, 6.5, 4.0 Hz, 1H, CH-C$_{ar}$), 7.13 – 7.24 (m, 2H, 2×C$_{ar}$-H, superimposed by solvent), 8.04 – 8.14 (m, 2H, 2×C$_{ar}$-H), 9.37 (d, *J* = 4.0 Hz, 1H, CHO). **^{13}C NMR** (75 MHz, CDCl$_3$) δ = 17.5 (t, CHH), 26.2 (d, CH-C$_{ar}$), 34.1 (d, *C*H-CHO), 124.0 (d, 2×C$_{ar}$-H), 127.0 (d, 2×C$_{ar}$-H), 146.9 (br s, C$_{ar}$) , 147.1 (s, C$_{ar}$), 198.7 (d, CHO). **HRMS** (EI): calcd. for [C$_{10}$H$_9$NO$_3$]$^+$ 191.0577, found 191.0579. **MS** (EI) *m/z*: 191 (13), 174 (35), 162 (14), 144 (33), 115 (100), 91 (11), 63 (12). DA889

***trans*-4-(3-((*E*)-Prop-1-en-1-yl)oxiran-2-yl)benzonitrile** (**7d**). From **1b** (350 mg, 5.00 mmol) and **3aH⁺BF₄⁻** (132 mg, 500 µmol) according to procedure **B**. **7d** was obtained as a yellow oil (64 mg, 0.35 µmol, 70%, *trans*). No formation of the corresponding cyclopropane **9d** was observed. R_f (*n*-pentane:EtOAc 5:1) = 0.41. **¹H NMR** (300 MHz, CDCl₃) δ = 1.70 (dd, J = 6.6, 1.7 Hz, 3 H, CH₃), 3.20 (dd, J = 8.0, 1.9 Hz, 1 H, CH), 3.72 (d, J = 1.9 Hz, 1 H, CH-C$_{ar}$), 5.26 (ddq, J = 15.4, 8.0, 1.6 Hz, 1 H, CH=C*H*-CH), 5.85 – 6.00 (m, 1 H, C*H*=CH-CH), 7.27 – 7.34 (m, 2 H, 2×C$_{Ar}$-H), 7.51 – 7.58 (m, 2 H, 2×C$_{Ar}$-H). **¹³C 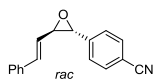NMR** (75 MHz, CDCl₃) δ = 18.0 (q, CH₃), 59.3 (d, CH-C$_{Ar}$), 63.5 (d, CH), 111.9 (s, C$_{Ar}$), 118.7 (s, CN), 126.2 (d, 2×C$_{Ar}$-H), 127.5 (d, CH=*C*H-CH), 132.4 (d, 2×C$_{Ar}$-H), 133.1 (d, *C*H=CH-CH), 143.0 (s, C$_{Ar}$). **HRMS** (EI): calcd. for [C₁₂H₁₁NO]⁺ 185.0835, found 185.0836. **MS** (EI) *m/z*: 184 (10), 170 (18), 156 (100), 130 (55), 129 (26), 102 (22), 83 (31), 69 (12). DA854
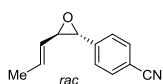
NMR-Monitoring of the reaction of 1b with 3a. A solution of KO*ᵗ*Bu (40 mg, 0.36 mmol) in 2.0 mL of DMSO-d_6 was added to a solution of **1b** (18 mg, 0.25 mmol) and **3aH⁺BF₄⁻** (66 mg, 0.25 mmol) in 2.0 mL of DMSO-d_6 at 20 °C. The spectra taken immediately after mixing of the reactants showed complete conversion of the reactants to epoxide **7d** without formation of cyclopropane **9d**. DA918

***trans*-4-(3-((*E*)-Styryl)oxiran-2-yl)benzonitrile** (**7e**): From **1c** (360 mg, 2.50 mmol) and **3aH⁺BF₄⁻** (132 mg, 500 µmol) according to procedure **B**. After recrystallization from *n*-pentane:EtOAc **7e** was obtained as yellow needles (115 mg, 465 µmol, 93%, *trans*). No formation of the corresponding cyclopropane **9e** was observed. R_f (*n*-pentane:EtOAc 25:1) = 0.40. **Mp** (*n*-pentane:EtOAc): 130 °C. **¹H NMR** (300 MHz, CDCl₃) δ = 3.41 (ddd, J = 7.6, 1.9, 0.6 Hz, 1 H, CH), 3.85 (d, J = 1.8 Hz, 1 H, CH-C$_{Ar}$), 5.97 (dd, J = 16.0, 7.7 Hz, 1 H, CH=C*H*-CH), 6.76 (d, J = 16.0 Hz, 1 H, C*H*=CH-CH), 7.16 – 7.38 (m, 7 H, 7×C$_{Ar}$-H, superimposed by solvent), 7.53 – 7.62 (m, 2 H, 2×C$_{Ar}$-H). **¹³C NMR** (75 MHz, CDCl₃) δ = 60.0 (d, *C*H-C$_{Ar}$), 63.7 (d, CH), 112.1 (s, C$_{Ar}$), 118.7 (s, CN), 125.3 (d, CH=*C*H-CH), 126.2 (d, 2×C$_{Ar}$-H), 126.7 (d, 2×C$_{Ar}$-H), 128.6 (d, C$_{Ar}$-H), 128.9 (d, 2×C$_{Ar}$-H), 132.5 (d, 2×C$_{Ar}$-H), 135.5 (d, *C*H=CH-CH), 135.8 (s, C$_{Ar}$), 142.7 (s, C$_{Ar}$). **HRMS** (EI): calcd. for [C₁₇H₁₃NO]⁺ 247.0992, found 247.0990. **MS** (EI) *m/z*: 247 (19), 218 (39), 140 (12), 130 (35), 117 (45), 115 (100), 102 (10), 43 (18). DA855
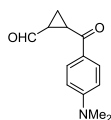
NMR-Monitoring of the reaction of 1c with 3a. A solution of KO*ᵗ*Bu (40 mg, 0.36 mmol) in 2.0 mL of DMSO-d_6 was added to a solution of **1c** (32 mg, 0.24 mmol) and **3aH⁺BF₄⁻** (67 mg, 0.25 mmol) in 2.0 mL of DMSO-d_6 at 20 °C. The spectra taken immediately after mixing of the

reactants showed complete conversion of the reactants to epoxide **7e** without formation of cyclopropane **9e**. DA919

2-(4-(Dimethylamino)benzoyl)cyclopropanecarbaldehyde (9c). **3c** (97.2 mg, 435 µmol) in DMSO (5 mL) was added dropwise to a solution of **1a** (29 mg, 525 µmol) in DMSO (5 mL) at ambient temperature. The solution was stirred for 30 min and quenched with sat. aq. NH$_4$Cl (20 mL). The mixture was extracted with CH$_2$Cl$_2$ (3×15 mL), the combined organic layers were washed with brine (2×20 mL) and dried over Na$_2$SO$_4$. The solvent was evaporated and the residue was subjected to a column chromatography (Silica; *n*-pentane:EtOAc 5:1). **9c** was obtained as a yellow oil (76 mg, 0.35 mmol, 70 %, *trans*:*cis* 5:1). **R**$_f$ (*n*-pentane:EtOAc 5:1) = 0.16. #-major diastereoisomer, *-minor diastereoisomer; integral of one proton of the minor diastereoisomer is set to 1.0 (*dr* 1:2 for this spectrum). No formation of the corresponding epoxide **7c** was observed. **^{1}H NMR** (300 MHz, CDCl$_3$) δ = 1.50 – 1.62 (m, 3 H, C*H*H, CH),[#,*] 1.76 (ddd, *J* = 8.5, 6.0, 3.6 Hz, 2 H, CH*H*),[#] 2.13 – 2.22 (m, 2 H, CH$_2$),[*] 2.59 (ddt, *J* = 8.4, 5.6, 3.8 Hz, 2 H, C*H*CHO),[#] 3.07 (s, 18 H, N(CH$_3$)$_2$),[#,*] 3.10 – 3.19 (m, 1 H, CH),[*] 3.23 (ddd, *J* = 8.7, 6.0, 3.8 Hz, 2 H, CHCO),[#] 6.61 – 6.69 (m, 6 H, 4×C$_{Ar}$-H),[#,*] 7.86 – 7.98 (m, 6 H, 4×C$_{Ar}$-H),[#,*] 9.24 (d, *J* = 6.5 Hz, 1 H, CHO),[*] 9.50 (d, *J* = 3.8 Hz, 2 H, CHO)[#]. **^{13}C NMR** (75 MHz, CDCl$_3$) δ = 13.5 (t, CHH),[*] 17.1 (t, CHH),[#] 25.6 (d, *C*HCO),[#] 26.8 (d, *C*HCO),[*] 32.1 (d, *C*HCHO),[*] 32.6 (d, *C*HCHO),[#] 40.1 (q, N(CH$_3$)$_2$),[#,*] 110.8 (d, 2×C$_{Ar}$-H),[*] 110.9 (d, 2×C$_{Ar}$-H),[#] 124.8 (s, C$_{Ar}$),[#] 125.0 (s, C$_{Ar}$),[*] 130.7 (d, 2×C$_{Ar}$-H),[#] 130.8 (d, 2×C$_{Ar}$-H),[*] 153.9 (s, C$_{Ar}$),[#,*] 193.1 (s, CO),[*] 193.4 (s, CO),[#] 199.6 (d, CHO),[#] 200.6 (d, CHO).[*] **HRMS** (ESI): calcd. for [C$_{13}$H$_{16}$NO$_2$]$^+$ 218.1176, found 218.1174. DA849

6.4.3 Kinetics of the Reactions of the α,β-Unsaturated Aldehydes 1 with the Ylides 2,3

6.4.3.1 Kinetics of the Reactions of Acrolein 1a

Table 6.8. Kinetics of the reaction of 1a with 2a (DMSO, 20 °C, Stopped-flow method, detection at 425 nm).

No.	[**1a**]/ mol L^{-1}	[**2a**]/mol L^{-1}	k_{obs}/s^{-1}
Ac1-2	7.23×10^{-4}	$\sim 5 \times 10^{-5}$	9.85×10^{1}
Ac1-3	7.89×10^{-4}	$\sim 5 \times 10^{-5}$	1.06×10^{2}
Ac1-4	8.54×10^{-4}	$\sim 5 \times 10^{-5}$	1.14×10^{2}
Ac1-5	9.20×10^{-4}	$\sim 5 \times 10^{-5}$	1.23×10^{2}
k_2(20 °C) = 1.25×10^{5} L mol^{-1} s^{-1}			

y = 125248x + 7.524
R² = 0.9978
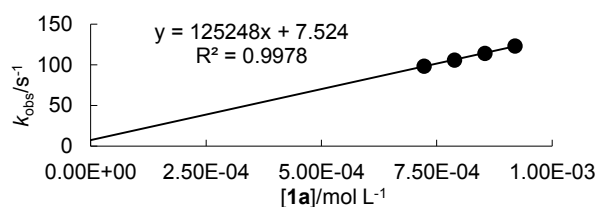
Table 6.9. Kinetics of the reaction of 1a with 2b (DMSO, 20 °C, Stopped-flow method, detection at 425 nm).

No.	$[\mathbf{1a}]$/ mol L^{-1}	$[\mathbf{2b}]$/mol L^{-1}	k_{obs}/s^{-1}
Ac7-1	1.01×10^{-3}	$\sim 1 \times 10^{-4}$	1.87×10^2
Ac7-2	1.12×10^{-3}	$\sim 1 \times 10^{-4}$	2.00×10^2
Ac7-3	1.22×10^{-3}	$\sim 1 \times 10^{-4}$	2.11×10^2
Ac7-4	1.32×10^{-3}	$\sim 1 \times 10^{-4}$	2.20×10^2
Ac7-5	1.42×10^{-3}	$\sim 1 \times 10^{-4}$	2.31×10^2
k_2(20 °C) = 1.08×10^5 L mol^{-1} s^{-1}			
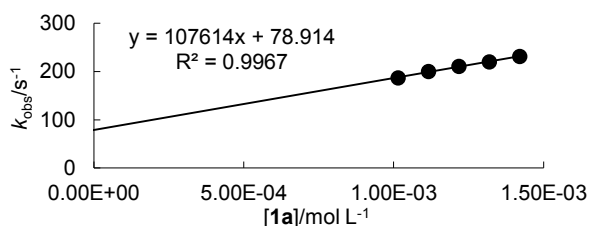
y = 107614x + 78.914
R² = 0.9967

The positive intercept may be due to the fact that the reaction is very fast and the solutions are not homogenous after 5 ms.

Table 6.10. Kinetics of the reaction of 1a with 2c (DMSO, 20 °C, Stopped-flow method, detection at 425 nm).

No.	$[\mathbf{1a}]$/ mol L^{-1}	$[\mathbf{2c}]$/mol L^{-1}	k_{obs}/s^{-1}
Ac2-1	6.57×10^{-4}	$\sim 5 \times 10^{-5}$	1.70
Ac2-2	8.54×10^{-4}	$\sim 5 \times 10^{-5}$	2.16
Ac2-3	9.86×10^{-4}	$\sim 5 \times 10^{-5}$	2.47
Ac2-4	1.18×10^{-3}	$\sim 5 \times 10^{-5}$	3.16
Ac2-5	1.31×10^{-3}	$\sim 5 \times 10^{-5}$	3.55
k_2(20 °C) = 2.86×10^3 L mol^{-1} s^{-1}			

y = 2859.8x - 0.2485
R² = 0.9918
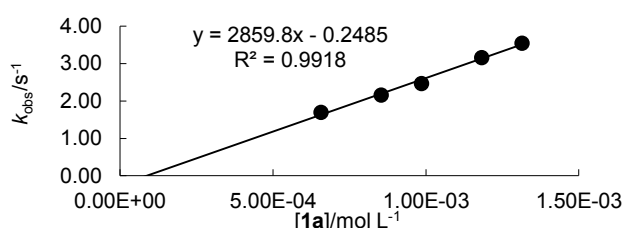
Table 6.11. Kinetics of the reaction of 1a with 2d (DMSO, 20 °C, Stopped-flow method, detection at 445 nm).

No.	$[\mathbf{1a}]$/ mol L^{-1}	$[\mathbf{2d}]$/mol L^{-1}	k_{obs}/s^{-1}
Ac3-1	6.57×10^{-4}	$\sim 5 \times 10^{-5}$	3.41×10^{-1}
Ac3-2	7.89×10^{-4}	$\sim 5 \times 10^{-5}$	3.89×10^{-1}
Ac3-3	9.86×10^{-4}	$\sim 5 \times 10^{-5}$	4.89×10^{-1}
Ac3-4	1.18×10^{-3}	$\sim 5 \times 10^{-5}$	6.27×10^{-1}
Ac3-5	1.31×10^{-3}	$\sim 5 \times 10^{-5}$	6.92×10^{-1}
k_2(20 °C) = 5.53×10^2 L mol^{-1} s^{-1}			

y = 552.52x - 0.037
R² = 0.9914
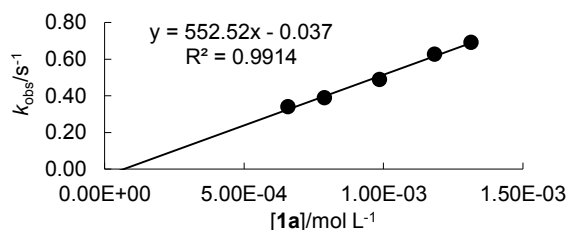
Table 6.12. Kinetics of the reaction of 1a with 3a (DMSO, 20 °C, Stopped-flow method, detection at 379 nm).

No.	$[\mathbf{1a}]$/ mol L^{-1}	$[\mathbf{3a}]$/mol L^{-1}	k_{obs}/s^{-1}
Ac8r-6	3.97×10^{-3}	$\sim 5 \times 10^{-5}$	3.25
Ac8r-7	4.96×10^{-3}	$\sim 5 \times 10^{-5}$	4.23
Ac8r-8	5.95×10^{-3}	$\sim 5 \times 10^{-5}$	5.03
Ac8r-9	6.94×10^{-3}	$\sim 5 \times 10^{-5}$	6.15
Ac8r-10	7.93×10^{-3}	$\sim 5 \times 10^{-5}$	7.12
k_2(20 °C) = 9.73×10^2 L mol^{-1} s^{-1}			

y = 972.88x - 0.6352
R² = 0.9979
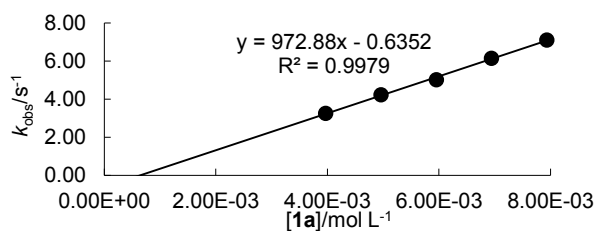
Table 6.13. Kinetics of the reaction of 1a with 3c (DMSO, 20 °C, J&M method, detection at 279 nm).

No.	$[\mathbf{1a}]$/ mol L^{-1}	$[\mathbf{3c}]$/mol L^{-1}	k_{obs}/s^{-1}
Ac9-2	2.51×10^{-3}	1.01×10^{-4}	5.70×10^{-3}
Ac9-3	2.99×10^{-3}	9.82×10^{-5}	6.92×10^{-3}
Ac9-4	3.64×10^{-3}	1.03×10^{-4}	8.51×10^{-3}
Ac9-5	3.92×10^{-3}	9.80×10^{-5}	9.17×10^{-3}
k_2(20 °C) = 2.46 L mol^{-1} s^{-1}			

y = 2.4632x - 0.0005
R² = 0.9997
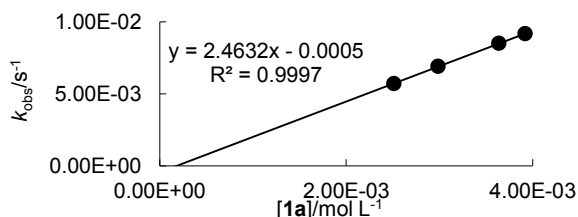
Table 6.14. Calculation of the Electrophilicity Parameter *E* for 1a using the *N* and s_N Parameters of 2,3, Eq 6.1, and the Second-Order Rate Constants for the Reactions of 1a with 2,3 (filled dots *E*(C=C), open dots were not used for the determination of *E*).

Nucleophile	N/s_N	k_2
2c	25.94/0.42	1.08×10^5
2d	20.24/0.60	2.86×10^3
2e	19.46/0.58	5.53×10^2
3c	15.68/0.65	2.46
E(C=C)[a] = −14.65		
2a	26.71/0.37	1.25×10^5
3a	21.07/0.68	9.73×10^2

[a] Calculated by least square minimization according to eq 6.1.

6.4.3.2 Kinetics of the Reactions of Crotonaldehyde 1b

Table 6.15. Kinetics of the reaction of 1b with 2b (DMSO, 20 °C, Stopped-flow method, detection at 425 nm).

| No.	[**1b**]/ mol L^{-1}	[**2b**]/mol L^{-1}	k_{obs}/s^{-1}
Ca2-1	1.03×10^{-3}	$\sim 1 \times 10^{-4}$	2.84
Ca2-2	2.06×10^{-3}	$\sim 1 \times 10^{-4}$	6.08
Ca2-3	3.10×10^{-3}	$\sim 1 \times 10^{-4}$	8.85
Ca2-4	4.13×10^{-3}	$\sim 1 \times 10^{-4}$	1.20×10^1
Ca2-5	5.16×10^{-3}	$\sim 1 \times 10^{-4}$	1.47×10^1
k_2(20 °C) = 2.86×10^3 L mol^{-1} s^{-1}			
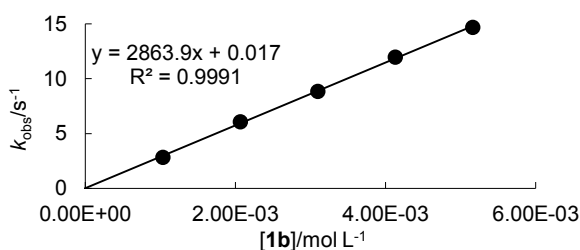
Table 6.16. Kinetics of the reaction of 1b with 2c (DMSO, 20 °C, J&M method, detection at 425 nm).

No.	[**1b**]/ mol L^{-1}	[**2c**]/mol L^{-1}	k_{obs}/s^{-1}
Ca6-1	8.19×10^{-4}	$\sim 4 \times 10^{-5}$	3.99×10^{-3}
Ca6-2	1.20×10^{-3}	$\sim 4 \times 10^{-5}$	5.35×10^{-3}
Ca-4	1.99×10^{-3}	$\sim 4 \times 10^{-5}$	8.42×10^{-3}
Ca6-5	2.49×10^{-3}	$\sim 4 \times 10^{-5}$	1.07×10^{-2}
k_2(20 °C) = 4.01 L mol^{-1} s^{-1}			
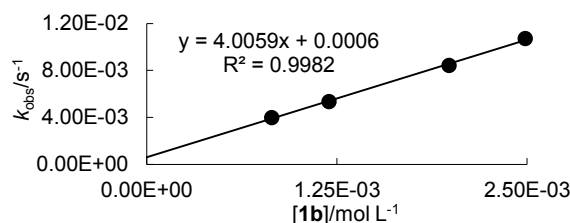
Table 6.17. Kinetics of the reaction of 1b with 2d (DMSO, 20 °C, J&M method, detection at 445 nm).

No.	[**1b**]/ mol L^{-1}	[**2d**]/mol L^{-1}	k_{obs}/s^{-1}
Ca7-1	2.03×10^{-3}	$\sim 4 \times 10^{-5}$	1.99×10^{-3}
Ca7-2	2.39×10^{-3}	$\sim 4 \times 10^{-5}$	2.42×10^{-3}
Ca7-3	2.83×10^{-3}	$\sim 4 \times 10^{-5}$	2.70×10^{-3}
Ca7-4	3.25×10^{-3}	$\sim 4 \times 10^{-5}$	2.96×10^{-3}
Ca7-5	3.67×10^{-3}	$\sim 4 \times 10^{-5}$	3.27×10^{-3}
k_2(20 °C) = 7.47×10^{-1} L mol^{-1} s^{-1}			
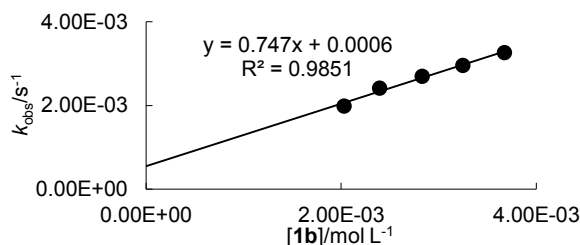
Table 6.18. Kinetics of the reaction of 1b with 3a (DMSO, 20 °C, J&M method, detection at 379 nm).

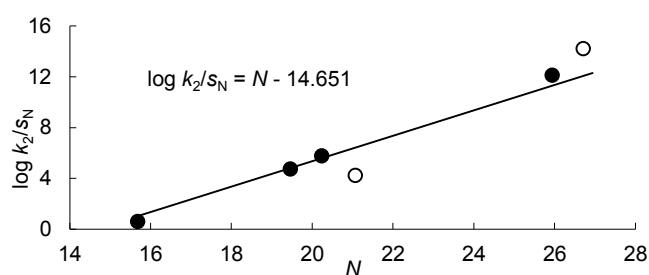| No.	[1b]/ mol L^{-1}	[3a]/mol L^{-1}	k_{obs}/s^{-1}
Ca5-2	2.68×10^{-3}	$\sim 3 \times 10^{-5}$	7.38×10^{-3}
Ca5-3	5.25×10^{-3}	$\sim 2 \times 10^{-5}$	1.48×10^{-2}
Ca5-4	7.91×10^{-3}	$\sim 1 \times 10^{-4}$	2.05×10^{-2}
Ca5-5	1.02×10^{-2}	$\sim 1 \times 10^{-4}$	2.51×10^{-2}
k_2(20 °C) = 2.35 L mol^{-1} s^{-1}			

y = 2.3495x + 0.0017
R² = 0.9931
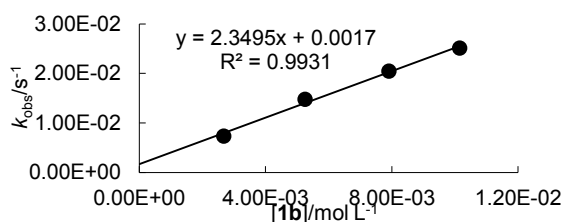
Table 6.19. Calculation of the Electrophilicity Parameter *E* for 1b using the *N* and *s*$_N$ Parameters of 2,3, Eq 6.1, and the Second-Order Rate Constants for the Reactions of 1b with 2,3 (filled dots *E*(C=C); open dots *E*(C=O)).

Nucleophile	N/s_N	k_2
2c	25.94/0.42	2.86×10^3
2d	20.24/0.60	4.01
2e	19.46/0.58	7.47×10^{-1}
E(C=C)$^{[a]}$ = −19.10		
3a	21.07/0.68	2.35
E(C=O)$^{[b]}$ = −20.52		

log k_2/s_N = *N* - 19.098
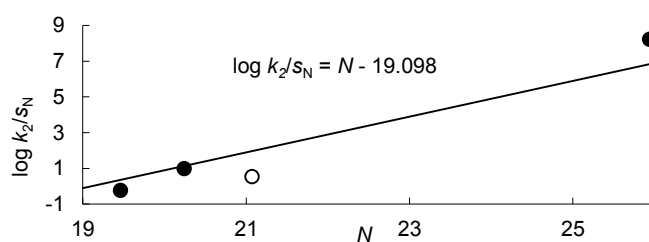
[a] Calculated by least square minimization according to eq 6.1; [b] Calculated from eq 6.1.

6.4.3.3 Kinetics of the Reactions of Cinnamaldehyde 1c

Table 6.20. Kinetics of the reaction of 1c with 2a (DMSO, 20 °C, Stopped-flow method, detection at 425 nm).

No.	[1c]/ mol L^{-1}	[2a]/mol L^{-1}	k_{obs}/s^{-1}
Za1-1	2.00×10^{-3}	$\sim 1 \times 10^{-4}$	8.15×10^{-1}
Za1-2	3.00×10^{-3}	$\sim 1 \times 10^{-4}$	1.27
Za1-3	4.00×10^{-3}	$\sim 1 \times 10^{-4}$	1.69
Za1-4	5.00×10^{-3}	$\sim 1 \times 10^{-4}$	2.09
Za1-5	6.00×10^{-3}	$\sim 1 \times 10^{-4}$	2.46
k_2(20 °C) = 4.11 × 10² L mol^{-1} s^{-1}			

y = 411x + 0.021
R² = 0.9985
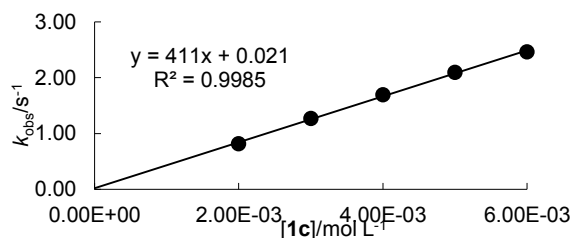
Table 6.21. Kinetics of the reaction of 1c with 2b (DMSO, 20 °C, Stopped-flow method, detection at 425 nm).

No.	[1c]/ mol L^{-1}	[2b]/mol L^{-1}	k_{obs}/s^{-1}
Za2-1	2.00×10^{-3}	$\sim 1 \times 10^{-4}$	2.46
Za2-2	3.00×10^{-3}	$\sim 1 \times 10^{-4}$	3.44
Za2-3	4.00×10^{-3}	$\sim 1 \times 10^{-4}$	4.88
Za2-4	5.00×10^{-3}	$\sim 1 \times 10^{-4}$	6.05
Za2-5	6.00×10^{-3}	$\sim 1 \times 10^{-4}$	6.95
k_2(20 °C) = 1.16 × 10³ L mol^{-1} s^{-1}			

y = 1159x + 0.12
R² = 0.9945
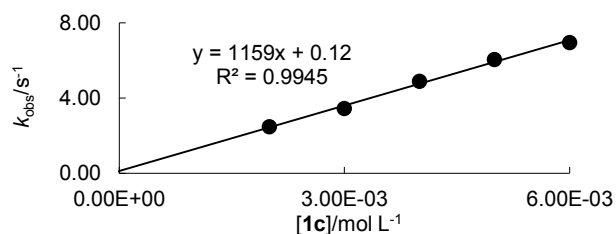
Table 6.22. Kinetics of the reaction of 1c with 2c (DMSO, 20 °C, J&M method, detection at 425 nm).

No.	[1c]/ mol L^{-1}	[2c]/mol L^{-1}	k_{obs}/s^{-1}
Za5-1	1.89×10^{-3}	$\sim 4 \times 10^{-5}$	3.57×10^{-3}
Za5-2	2.25×10^{-3}	$\sim 4 \times 10^{-5}$	3.78×10^{-3}
Za5-3	3.05×10^{-3}	$\sim 4 \times 10^{-5}$	4.78×10^{-3}
Za5-4	3.26×10^{-3}	$\sim 4 \times 10^{-5}$	4.97×10^{-3}
Za5-5	3.69×10^{-3}	$\sim 4 \times 10^{-5}$	5.53×10^{-3}
k_2(20 °C) = 1.11 L mol^{-1} s^{-1}			
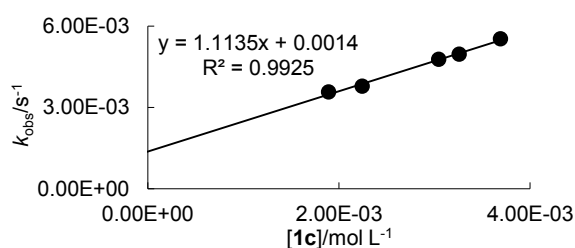
Table 6.23. Calculation of the Electrophilicity Parameter *E* for 1c using the *N* and *s*$_N$ Parameters of 2,3, Eq 6.1, and the Second-Order Rate Constants for the Reactions of 1c with 2,3 (filled dots *E*(C=C); open dots *E*(C=O)).

Nucleophile	N/s_N	k_2
2a	26.71/0.37	4.11×10^2
2b	27.45/0.38	1.16×10^3
2c	25.94/0.42	1.11
E(C=C)[a] = −19.66		
3a	21.07/0.68	6.03[b]
E (C=O) = −19.92[b]		
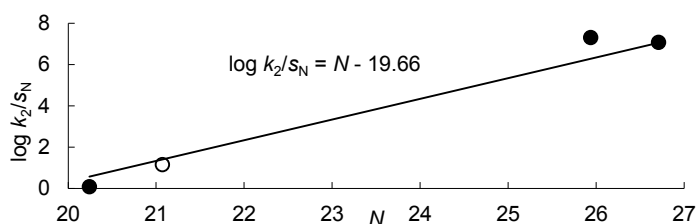
[a] Calculated by least square minimization according to eq 6.1; [b] From ref. [11]

6.5 References

[1] (a) E. D. Bergmann, D. Ginsburg, R. Pappo, in *Organic Reactions*, Wiley, New York, **1959**, pp. 179-555; (b) P. Perlmutter, *Conjugate Addition reactions in Organic Synthesis, Vol. 9*, Pergamon, Oxford, **1992**; (c) A. Erkkila, I. Majander, P. M. Pihko, *Chem. Rev.* **2007**, *107*, 5416-5470; (d) S. Mukherjee, J. W. Yang, S. Hoffmann, B. List, *Chem. Rev.* **2007**, *107*, 5471-5569; (e) D. Almasi, D. A. Alonso, C. Nájera, *Tetrahedron: Asymmetry* **2007**, *18*, 299–365; (f) A. Ting, J. M. Goss , N. T. McDougal, S. E. Schaus, in *Asymmetric Organocatalysis, Vol. 291* (Ed.: B. List), Springer, Berlin, **2010**, pp. 145−201; (g) Wiley-VCH Weinheim, **2010**; (h) *Organocatalytic enantioselective conjugate addition reactions Vol. 5*, RCS Publ., Cambridge **2010**.

[2] (a) T.-R. Kim, S.-J. Yun, B.-B. Park, *Bull. Kor. Chem. Soc.* **1986**, *7*, 25-29; (b) D. W. Roberts, A. Natsch, *Chem. Res. Toxicol.* **2009**, *22*, 592-603; (c) J. A. H. Schwöbel, D. Wondrousch, Y. K. Koleva, J. C. Madden, M. T. D. Cronin, G. Schüürmann, *Chem. Res. Toxicol.* **2010**, *23*, 1576-1585; (d) S. Amslinger, N. Al-Rifai, K. Winter, K. Wörmann, R. Scholz, B. Paul, M. Wild, *Org. Biomol. Chem.* **2013**, *11*, 549-554.

[3] (a) G. Scibona, P. R. Danesi, F. Orlandini, *J. Phys. Chem.* **1966**, *70*, 3403-3407; (b) F. D'Souza, G. R. Deviprasad, *J. Org. Chem.* **2001**, *66*, 4601-4609.

[4]   G. Evans, T. J. K. Gibbs, R. L. Jenkins, S. J. Coles, M. B. Hursthouse, J. A. Platts, N. C. O. Tomkinson, *Angew. Chem. Int. Ed.* **2008**, *47*, 2820-2823.

[5]   (a) S. Patai, Z. Rappoport, in *The Chemistry of Alkenes* (Eds.: S. Patai, Z. Rappoport), Wiley, New York, **1964**, p. 469−584; (b) H. Shenhav, Z. Rappoport, S. Patai, *J. Chem. Soc. B* **1970**, 469-476; (c) A. F. Noels, J. N. Braham, A. J. Hubert, P. Teyssié, *Tetrahedron* **1978**, *34*, 3495-3497; (d) L. Wartski, M. El Bouz, J. Seyden-Penne, W. Dumont, A. Krief, *Tetrahedron Lett.* **1979**, *20*, 1543-1546; (e) J. P. Guthrie, K. J. Cooper, J. Cossar, B. A. Dawson, K. F. Taylor, *Can. J. Chem.* **1984**, *62*, 1441-1445; (f) T. Strzalko, J. Seyden-Penne, L. Wartski, J. Corset, M. Castella-Ventura, F. Froment, *J. Org. Chem.* **1998**, *63*, 3295-3301.

[6]   (a) J. W. Bunting, A. Toth, C. K. M. Heo, R. G. Moors, *J. Am. Chem. Soc.* **1990**, *112*, 8878-8885; (b) C. K. M. Heo, J. W. Bunting, *J. Org. Chem.* **1992**, *57*, 3570-3578.

[7]   (a) R. Loos, S. Kobayashi, H. Mayr, *J. Am. Chem. Soc.* **2003**, *125*, 14126-14132; (b) A. A. Tishkov, H. Mayr, *Angew. Chem. Int. Ed* **2005**, *44*, 142-145; (c) A. A. Tishkov, U. Schmidhammer, S. Roth, E. Riedle, H. Mayr, *Angew. Chem. Int. Ed.* **2005**, *44*, 4623-4626; (d) H. F. Schaller, U. Schmidhammer, E. Riedle, H. Mayr, *Chem. Eur. J.* **2008**, *14*, 3866-3868; (e) M. Breugst, H. Mayr, *J. Am. Chem. Soc.* **2010**, *132*, 15380-15389; (f) M. Breugst, H. Zipse, J. P. Guthrie, H. Mayr, *Angew. Chem. Int. Ed.* **2010**, *49*, 5165-5169; (g) M. Baidya, S. Kobayashi, H. Mayr, *J. Am. Chem. Soc.* **2010**, *132*, 4796-4805; (h) H. Mayr, M. Breugst, A. R. Ofial, *Angew. Chem.* **2011**, *123*, 6598−6634; (i) T. A. Nigst, J. Ammer, H. Mayr, *Angew. Chem. Int. Ed.* **2012**, *51*, 1353-1356; (j) B. Maji, H. Mayr, *Angew. Chem. Int. Ed.* **2013**, *52*, 11163-11167; (k) B. Maji, K. Troshin, H. Mayr, *Angew. Chem. Int. Ed.* **2013**, *52*, 11900-11904.

[8]   X. Guo, H. Mayr, *J. Am. Chem. Soc.* **2013**, 12377-12387.

[9]   (a) H. Mayr, M. Patz, *Angew. Chem., Int. Ed. Engl.* **1994**, *33*, 938−957; (b) H. Mayr, T. Bug, M. F. Gotta, N. Hering, B. Irrgang, B. Janker, B. Kempf, R. Loos, A. R. Ofial, G. Remennikov, H. Schimmel, *J. Am. Chem. Soc.* **2001**, *123*, 9500−9512; (c) R. Lucius, R. Loos, H. Mayr, *Angew. Chem., Int. Ed.* **2002**, *41*, 91−95; (d) H. Mayr, B. Kempf, A. R. Ofial, *Acc. Chem. Res.* **2003**, *36*, 66−77; (e) H. Mayr, A. R. Ofial, *Pure Appl. Chem.* **2005**, 1807−1821; (f) H. Mayr, A. R. Ofial, *J. Phys. Org. Chem.* **2008**, *21*, 584−595; (g) H. Mayr, S. Lakhdar, B. Maji, A. R. Ofial, *Beilstein J. Org. Chem.* **2012**, *8*, 1458−1478; (h) For a comprehensive database of nucleophilicity parameters N, s_N and electrophilicity parameters E, see http://www.cup.lmu.de/oc/mayr/.

[10] (a) S. Lakhdar, T. Tokuyasu, H. Mayr, *Angew. Chem. Int. Ed.* **2008**, *47*, 8723−8726; (b) S. Lakhdar, R. Appel, H. Mayr, *Angew. Chem., Int. Ed.* **2009**, *48*, 5034−5037; (c) S. Lakhdar, J. Ammer, H. Mayr, *Angew. Chem., Int. Ed.* **2011**, *50*, 9953-9956; (d) M. C. Holland, S. Paul, W. B. Schweizer, K. Bergander, C. Mück-Lichtenfeld, S. Lakhdar, H. Mayr, R. Gilmour, *Angew. Chem., Int. Ed.* **2013**, *52*, 7967-7971.

[11] R. Appel, H. Mayr, *J. Am. Chem. Soc.* **2011**, *113*, 8240−8251.

[12] D. S. Allgäuer, P. Mayer, H. Mayr, *J. Am. Chem. Soc.* **2013**, *135*, 15216–15224.

[13] O. Tsuge, S. Kanemasa, S. Takenaka, *Bull. Chem. Soc. Jpn.* **1985**, *58*, 3320−3336.

[14] (a) J. H. van Esch, M. A. M. Hoffmann, R. J. M. Nolte, *J. Org. Chem.* **1995**, *60*, 1599-1610; (b) M. S. Lowry, W. R. Hudson, R. A. Pascal, S. Bernhard, *J. Am. Chem. Soc.* **2004**, *126*, 14129-14135; (c) I. Sasaki, L. Vendier, A. Sournia-Saquet, P. G. Lacroix, *Eur. J. Inorg. Chem.* **2006**, *2006*, 3294-3302; (d) S. Verma, P. Kar, A. Das, D. K. Palit, H. N. Ghosh, *Chem. Eur. J.* **2010**, *16*, 611−619.

[15] (a) F. Kröhnke, *Ber. dt. chem. Ges.* **1934**, *67*, 656-667; (b) J. Àlvarez-Builla, J. L. Novella, E. Gálvez, P. Smith, F. Florencio, S. Garciá-Blanco, J. Bellanato, M. Santos, *Tetrahedron* **1986**, *42*, 699-708; (c) Z. Mao, X. Li, X. Lin, P. Lu, Y. Wang, *Tetrahedron* **2012**, *68*, 85-91.

[16] (a) Y. L. Stanc, M. L. Corre, *Can. J. Chem.* **1985**, *63*, 2958-2960; (b) V. K. Aggarwal, S. Calamai, J. Gair Ford, *J. Chem. Soc., Perkin Trans. 1* **1997**, 593−600; (c) A. Solladié-Cavallo, A. Diep-Vohuule, T. Isarno, *Angew. Chem. Int. Ed.* **1998**, *37*, 1689-1691; (d) A. Solladié-Cavallo, L. Bouérat, M. Roje, *Tetrahedron Lett.* **2000**, *41*, 7309-7312; (e) V. K. Aggarwal, I. Bae, H.-Y. Lee, J. Richardson, D. T. Williams, *Angew. Chem., Int. Ed.* **2003**, *42*, 3274−3278; (f) D. R. Edwards, P. Montoya-Peleaz, C. M. Crudden, *Org. Lett.* **2007**, *9*, 5481-5484; (g) E. M. McGarrigle, E. L. Myers, O. Illa, M. A. Shaw, S. L. Riches, V. K. Aggarwal, *Chem. Rev.* **2007**, *107*, 5841−5883; (h) O. Illa, M. Arshad, A. Ros, E. M. McGarrigle, V. K. Aggarwal, *J. Am. Chem. Soc.* **2010**, *132*, 1828−1830; (i) D. J. Phillips, A. E. Graham, *Synlett* **2010**, *2010*, 769-773; (j) D. Janardanan, R. B. Sunoj, *Org. Biomol. Chem.* **2011**, *9*, 1642-1652.

[17] (a) T. Kajiwara, T. Nakatomi, Y. Sasaki, A. Hatanaka, *Agric. Biol. Chem.* **1980**, *44*, 2099-2104; (b) J. W. Bode, S. S. Sohn, *J. Am. Chem. Soc.* **2007**, *129*, 13798-13799.

[18] (a) K. W. Ratts, A. N. Yao, *J. Org. Chem.* **1966**, *31*, 1689-1693; (b) A. W. Johnson, R. T. Amel, *J. Org. Chem.* **1969**, *34*, 1240−1247; (c) V. K. Aggarwal, C. Hebach, *Org. Biomol. Chem.* **2005**, *3*, 1419−1427.

[19]   V. K. Aggarwal, J. N. Harvey, J. Richardson, *J. Am. Chem. Soc.* **2002**, *124*, 5747−5756.

[20]   R. Appel, N. Hartmann, H. Mayr, *J. Am. Chem. Soc.* **2010**, *132*, 17894−17900.

[21]   R. Appel, H. Mayr, *Chem. Eur. J.* **2010**, *16*, 8610−8614.

[22]   D. S. Allgäuer, H. Mayr, *Eur. J. Org. Chem.* **2013**, *submitted*.

[23]   D. S. Allgäuer, H. Asahara, H. Mayr, **2013**, *unpublished results*.

[24]   The formation of *anti* betaines from benzaldehyde and dimethylsulfonium benzylidene was found to be irreversible, whereas the *syn*-betaine formation was reversible, as previously demonstrated in the solvents DMSO, CD$_3$CN and CH$_2$Cl$_2$ by cross-over experiments and kinetic isotope effect studies.[16b, f]

[25]   X.-M. Zhang, F. G. Bordwell, M. Van Der Puy, H. E. Fried, *J. Org. Chem.* **1993**, *58*, 3060−3066.

[26]   A reaction of a carbanion derived from the tetrahydroindolizine **5** seems unlikely, as the pK_a value of the corresponding CH-acid is much higher (> 25;   For a comprehensive database of pK_a-values in DMSO see http://www.chem.wisc.edu/areas/reich/pka-table/) than the pK_a value of **13a** (~ 12; F. G. Bordwell, X. M. Zhang, M. Van Der Puy, H. E. Fried, *J. Org. Chem.* **1993**, *58*, 3060-3066).

[27]   D. S. Allgäuer, H. Mayr, *Eur. J. Org. Chem.* **2013**, 6379–6388.

[28]   The kinetics of the reaction of **1a** with **3b** were not investigated as complex kinetics were expected.

[29]   T. M. Mitzel, C. Palomo, K. Jendza, *J. Org. Chem.* **2001**, *67*, 136-145.

[30]   (a) H. Mayr, A. R. Ofial, *Angew. Chem.* **2006**, *118*, 1844−1854; (b) F. Brotzel, B. Kempf, T. Singer, H. Zipse, H. Mayr, *Chem. Eur. J.* **2007**, *13*, 336−345; (c) F. Brotzel, H. Mayr, *Org. Biomol. Chem.* **2007**, *5*, 3814−3820; (d) M. Breugst, H. Mayr, *J. Am. Chem. Soc.* **2010**, *132*, 15380−15389; (e) T. A. Nigst, J. Ammer, H. Mayr, *J. Phys. Chem. A* **2012**, *116*, 8494−8499.

[31]   Currently there is only one report (X. Zhang, W. Cao, X. Wei, H. Hu, *Syn. Comm.* **1997**, *27*, 1395-1403) on a synthesis of 1-carbaldehyde substituted indolizine by a [3+2]-cycloaddition/oxidation-protocol from pyridinium ylides and α,β-unsaturated aldehydes, but this method requires harsh conditions (95 °C/DMF/Co-Cr-oxidant).

[32]   (a) M. Kucukdisli, T. Opatz, *Eur. J. Org. Chem.* **2012**, 4555–4564; (b) A. Kakehi, *Heterocycles* **2012**, *85*, 1529-1577.

[33]   I. Zenz, H. Mayr, *J. Org. Chem.* **2011**, *76*, 9370−9378.

[34]   O. Kaumanns, R. Lucius, H. Mayr, *Chem. Eur. J.* **2008**, *14*, 9675−9682.

[35]   R. Appel, S. Chelli, T. Tokuyasu, K. Troshin, H. Mayr, *J. Am. Chem. Soc.* **2013**, *135*, 6579−6587.

[36]   (a) P. v. R. Schleyer, E. D. Jemmis, G. W. Spitznagel, *J. Am. Chem. Soc.* **1985**, *107*, 6393-6394; (b) J. P. Richard, T. L. Amyes, D. J. Rice, *J. Am. Chem. Soc.* **1993**, *115*, 2523-2524; (c) K. Rakus, S. P. Verevkin, W.-H. Peng, H.-D. Beckhaus, C. Rüchardt, *Liebigs Ann.* **1995**, *1995*, 2059-2067.

[37]   (a) H. E. Gottlieb, V. Kotlyar, A. Nudelman, *J. Org. Chem.* **1997**, *62*, 7512−7515; (b) G. F. Fulmer, A. J. M. Miller, N. H. Sherden, H. E. Gottlieb, A. Nudelman, B. M. Stoltz, J. E. Bercaw, K. I. Goldberg *Organometallics* **2012**, *29*, 2176−2179.

7 Electrophilicities of Acceptor-Substituted Olefins

Dominik S. Allgäuer, Haruyasu Asahara, and Herbert Mayr

7.1 Introduction

Acceptor-substituted olefins, like the activated ethylenes, propylenes, and styrenes depicted in Chart 7.1, are important substrates in organic reactions[1] and can combine with nucleophiles, e.g. in Michael additions,[1a-e, 2] addition-elimination sequences,[3] [3+2]-cycloadditions,[4] or Diels-Alder reactions.[5]

Many kinetic studies, especially between 1950 and 1970, tried to describe the electrophilic reactivities of such activated double bonds with C,[6] N,[7-10] O,[11], [12, 13] S,[10, 14] and P[15] nucleophiles. In the 1960s, a two-parameter Hammett-Taft-type free-energy relationship was derived from linear Brønsted plots of the rate constants of reactions of α,β-unsaturated compounds with amines and thiols in water.[10] The relation provided the relative rates of the reactivities of a rather narrow set of compounds with respect to the reaction of glycine with acrylonitrile.

We have previously shown that a multitude of combinations of nucleophiles with electrophiles can be described by the linear free-energy relationship eq 7.1, where the nucleophile is described by two solvent-dependent parameters, s_N (sensitivity) and N (nucleophilicity), and the electrophile by one parameter E (electrophilicity).
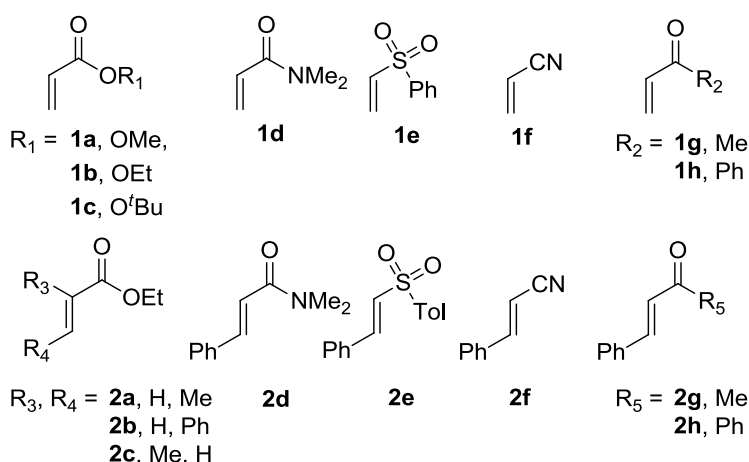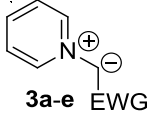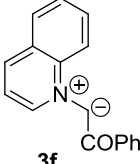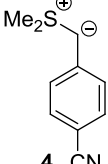
Chart 7.1. Acceptor-substituted olefins 1 and 2 investigated in this work.

$$\log k_2 = s_N(N + E) \qquad (7.1)$$

Table 7.1. Pyridinium Ylides[19] 3a−f and the sulfonium Ylide[20a] 4 used as reference nucleophiles (N and s_N parameters in DMSO, 20 °C).

Ylide	EWG	N/s_N
3a	CO_2Et	26.71/0.37
3b	$CONEt_2$	27.45/0.38
3c	CN	25.94/0.42
3d	COMe	20.24/0.60
3e	COPh	19.46/0.58

3f
19.38/0.50[a]

4 CN
21.07/0.68[b]

[a] From ref. [19]; [b] From ref. [20a].

We already quantified the electrophilic reactivities of many Michael acceptors,[16] but until now the studies were restricted to systems having absorption maxima in the visible or near UV region, as no appropriate colored reference nucleophiles were available. Recently we have developed an approach to quantify the electrophilic reactivities of colorless 1,2-disubstituted ethylenes[17] and α,β-unsaturated aldehydes[18] using colored pyridinium ylides 3[19] and sulfonium ylide 4[20] as reference nucleophiles (Table 7.1). The rates of the reactions of the Michael acceptors **1** and **2** with the ylides **3** and **4** in combination with their nucleophilicity parameters N and s_N will be used to derive the electrophilicity parameters E of the Michael acceptors **1** and **2** according to eq 7.1.[21] In this way we can include these synthetically important electrophiles into our comprehensive reactivity scale.[16-18, 22]

7.2   Results and Discussion

7.2.1   General

The [3+2]-cycloadditions of the acceptor-substituted olefins **1** and **2** with pyridinium ylides 3[3a, 23, 24] can either follow a concerted (k_{conc}, Scheme 7.1 top), or stepwise (k_2, Scheme 7.1 bottom) mechanism. The stepwise addition of the ylides **3** to the CC-double bonds of the dipolarophiles **1** and **2** proceeds via an intermediate betaine which cyclizes (k_{rc}) to give a tetrahydroindolizine (Scheme 7.1). For certain substitution patterns, stepwise mechanisms via diradical intermediates have also to be considered.[4e, 25, 26] We recently reported that the 1,3-dipolar cycloadditions of pyridinium ylides with substituted benzylidene malononitriles and chalcones proceed stepwise via zwitterionic intermediates.[19]

Scheme 7.1. Concerted and stepwise cycloadditions of pyridinium ylides 3 with the acceptor-substituted olefins 1,2.
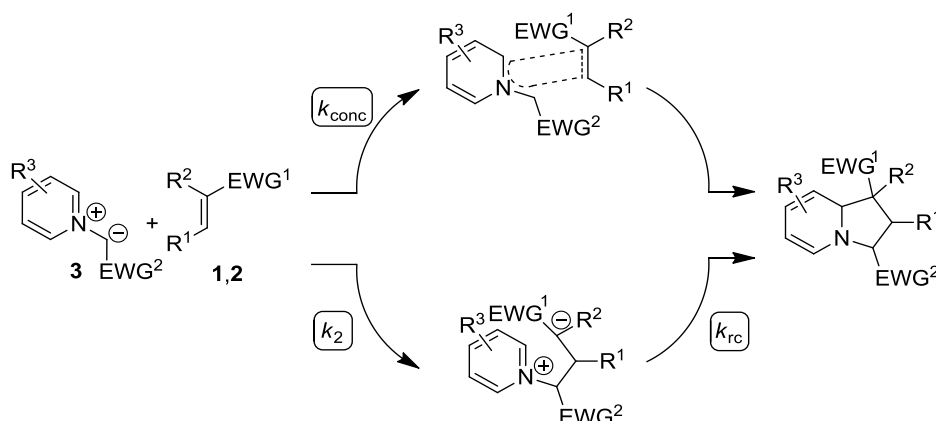
Scheme 7.2. Schematic mechanism for the reaction of sulfonium ylide 4 with the acceptor-substituted olefins 1.
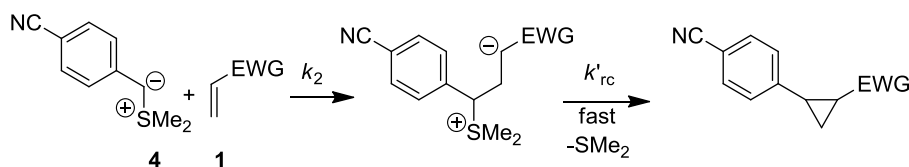
The reactions of the sulfonium ylides **3** with Michael acceptors proceed stepwise, with initial irreversible formation of intermediate betaines (k_2; Scheme 7.2).[3b, 20, 27] The subsequent ring closure (k'_{rc}) to cyclopropanes is usually a fast process.[3b, 20, 27]

7.2.2 Products

The reactions of the pyridinium ylides **3**, generated by deprotonation of their parent salts **3H$^+$X$^-$** with Na$_2$CO$_3$, with the Michael acceptors **1** in DMSO give the tetrahydroindolizines **5** as initial products (Table 7.2) As [3+2]-adducts derived from isoquinolinium ylides and the activated ethylenes **1a** and **1f** had been reported to be unstable at ambient temperature,[28] a one-pot procedure was developed to oxidize the tetrahydroindolizines **5** to the corresponding indolizines **6** using chloranil. The indolizines **6** were obtained in 52−98% yield after purification (Table 7.2).

We recently reported on a one-pot synthesis of indolizine **8** from ethyl methacrylate **2c** and pyridinium salt **3eH$^+$Br$^-$** under basic, oxidative conditions (Scheme 7.3).[29] In this synthesis the initially generated tetrahydroindolizine **7** was oxidized by 1 equiv. of chloranil in the presence of air. A base-induced elimination of the ethoxycarbonyl group resulted in the formation of indolizine **8** in 20% yield.

Table 7.2. Synthesis of the indolizines 6.
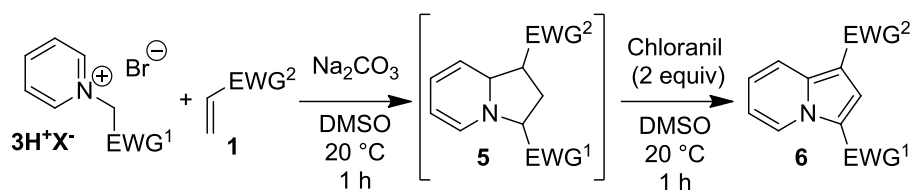
Salt	EWG^1	Ethylene **1**	EWG^2	Product	Yield/%
3bH$^+$Br$^-$	CO$_2$Me	**1a**	CONEt$_2$	**6a**	52
3cH$^+$Br$^-$	CO$_2$Et	**1b**	CN	**6b**	58
3dH$^+$Cl$^-$	CO$_2^t$Bu	**1c**	COMe	**6c**	96
3cH$^+$Br$^-$	CONMe$_2$	**1d**	CN	**6d**	64
3dH$^+$Cl$^-$	SO$_2$Ph	**1e**	COMe	**6e**	98
3aH$^+$Br$^-$	CN	**1f**	CO$_2$Et	**6f**	58
3eH$^+$Br$^-$	COMe	**1g**	COPh	**6g**	74
3dH$^+$Cl$^-$	COPh	**1h**	COMe	**6h**	97

Scheme 7.3. Reaction of 1eH$^+$Br$^-$ and ethyl methacrylate 2c.
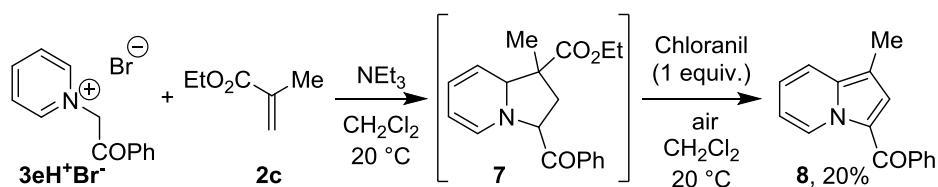
Combination of the Michael acceptors **2** with the pyridinium salts **3H$^+$X$^-$** under biphasic conditions (CH$_2$Cl$_2$/aq. NaOH (32%)) resulted in the formation of the tetrahydroindolizines **9** which were not isolated due to their low stability.[19]

Oxidation of the [3+2]-cycloadducts **9** by 1 equiv. of chloranil gave the dihydroindolizines **10** in variable yields with moderate diastereoselectivities (Table 7.3). The yields of **10** were strongly dependent on the electron-withdrawing group of the Michael acceptors. The ester or cyano-substituted dihydroindolizines **10b** and **10f** were obtained in 89% and 90% yield, while acetyl-substitution diminished the yield (**10g**). The sulfonyl-substituted dihydroindolizine **10e** could not be isolated as it decomposed during the purification. The synthesis of dihydroindolizines **10** derived from the Michael acceptors **2a**,d,h was not attempted.

Oxidation of the tetrahydroindolizines **9** by 2 equiv. of chloranil resulted in the formation of the indolizines **11** in 50−90% yield (Table 7.3). The outcome of the [3+2]-cycloaddition/oxidation-sequence seemed to be slightly dependent on the on the electron-withdrawing groups of the reactants, as acetyl-substitution decreased the yield of the indolizines **11**, like observed for the dihydroindolizines **10**. In the reaction of *N,N*-dimethyl cinnamamide **2d** with pyridinium ylide **3d** the indolizine **11d** was not formed and instead **2d** was reisolated.[30]

Table 7.3. Reactions of the Michael acceptors 2 with the pyridinium ylides 3.
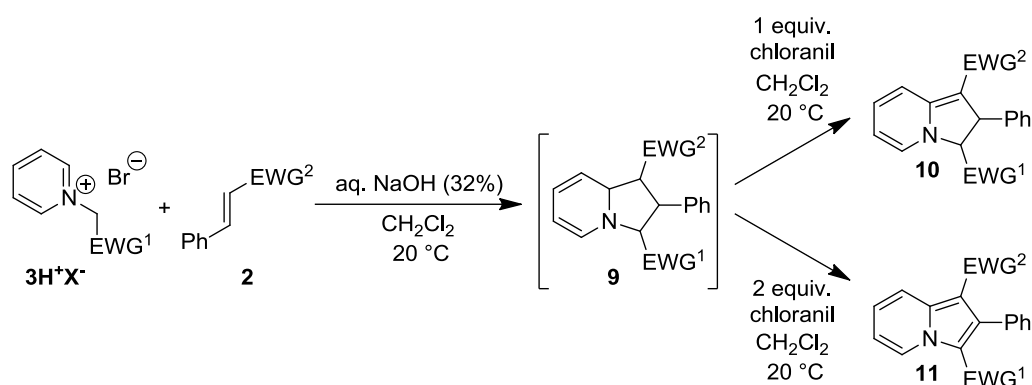
Salt	EWG[1]	Olefin 2	EWG[2]	R	Product	Yield/%	dr[a]
3cH$^+$Br$^-$	CN	**2a**	CO$_2$Et	Me	**11a**	84[b]	-
3aH$^+$Br$^-$	CO$_2$Et	**2b**	CO$_2$Et	Ph	**11b**	89	-
3cH$^+$Br$^-$	CN	**2b**	CO$_2$Et	Ph	**10c**	89	3:1
					11c	85	-
3dH$^+$Cl$^-$	COMe	**2d**	CONMe$_2$	Ph	**10d**	-	-
3cH$^+$Br$^-$	CN	**2e**	Tos	Ph	**10e**	decomp.	-
					11e	90	-
3aH$^+$Br$^-$	CO$_2$Et	**2f**	CN	Ph	**10f**	90	8:1
					11f	90	-
3cH$^+$Br$^-$	CN	**2g**	COMe	Ph	**10g**	18	2:1
					11g	50	-
3dH$^+$Cl$^-$	COMe	**2h**	COPh	Ph	**11h**	67	-

[a] By ^{1}H NMR after column chromatography; [b] DMSO, 20 °C, 1. Na$_2$CO$_3$, 2. Chloranil (2 equiv.).

Table 7.4. Reactions of the sulfonium ylide 4 with the Michael acceptors 1.
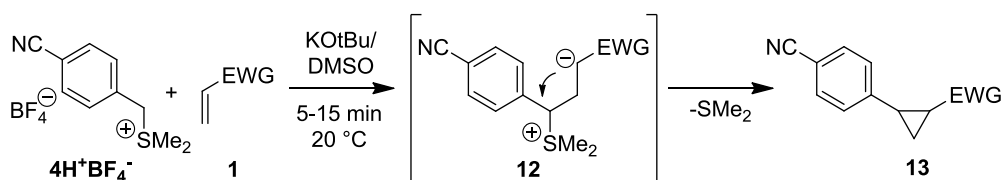
Electrophile 1	EWG	Product	Yield/%	dr[a]
1a	CO$_2$Me	**13a**	64	2:1
1b	CO$_2$Et	**13b**	66	7:1
1c	CO$_2^t$Bu	**13c**	60	5:1[b]
1e	SO$_2$Ph	**13e**	88	single
1f	CN	**13f**	42	single[b]
1g	COMe	**13g**	68	3:1
1h	COPh	**13h**	83	3:1

[a] Determined by ^{1}H NMR of the crude product; [b] After column chromatography.

The reactions of the acceptor-substituted ethylenes **1a–c** and **1e–h** with the sulfonium ylide **4** in DMSO at ambient temperature gave the cyclopropanes **13** in 42−88% yield with variable diastereoselectivities. The diastereomeric ratio of the cyclopropanes **13** depends on the nature of the electron-withdrawing group of the Michael acceptor **1**. While cyclopropane **13a** is formed with low diastereoselectivity, the selectivity increases with the size of the ester substituent in **1** (**13a→13b,c**). The diastereoselectivities for the formation of the acyl-substituted cyclopropanes **13g,h** are, instead, independent of the substituent size (Me versus Ph). For the sulfonyl-substituted cyclopropane **13e** and the cyano-substituted cyclopropane **13f** only one diastereoisomer was observed. The configuration of the substituents of the two diastereoisomers of the cyclopropanes **13** could not be assigned unambiguously.

7.2.3 Kinetic Studies and Discussion

The kinetics of the reactions of the acceptor-substituted olefins **1** and **2** with the pyridinium ylides **3** and the sulfonium ylide **4** in DMSO at 20 °C were monitored photometrically by following the disappearance of the absorbances of the ylides **3** and **4** at or close to their absorption maxima. Due to the low stabilities of the ylides **3** and **4**, they were generated in solution by combining freshly prepared solutions of the salts $\mathbf{3H^{+}X^{-}}$ or $\mathbf{4H^{+}BF_4^{-}}$ and KO^tBu (typically 1.05 eq) in DMSO directly before each kinetic experiment. To perform the kinetic experiments under pseudo-first-order conditions the electrophiles **1** and **2** were used in high excess (≥ 10 equivalents) over the ylides **3** and **4**, which resulted in monoexponential decays of their UV–vis absorbances. From the decays of the UV–Vis absorbances of the ylides **3** and **4** the first-order rate constants k_{obs} (s^{-1}) were derived by least-squares fitting of the exponential function $A_t = A_0 \exp(-k_{obs}t) + C$ to the time-dependent absorbances A_t (Figure 7.1a). Correlations of k_{obs} versus the concentration of the Michael acceptors **1** and **2** (Figure 7.1b) were linear and from their slopes the second order rate constants k_2 listed in Table 7.5 were derived.

a) $k_{obs} = 1.10 \times 10^{-1}$ b) $k_{obs} = 1.94 \times 10^{1}$ [1e] + 0.001
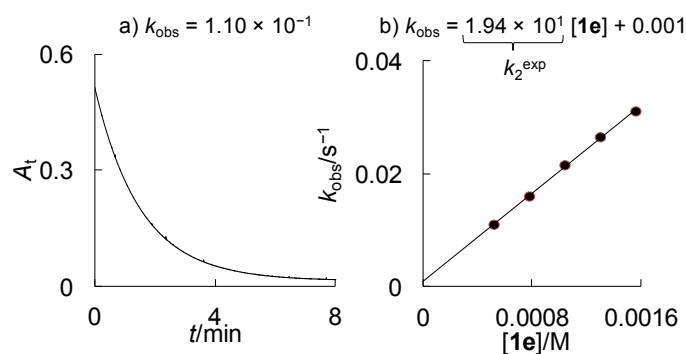
Figure 7.1. a) Decay of the absorbance of 3d ([3d]$_0 \sim 5 \times 10^{-5}$ M) at 427 nm during the reaction with 1e ([1e]$_0$ = 5.22 × 10^{-4} M) in DMSO at 20°C. b) Linear correlation of k_{obs} with the concentration of 1e.

Table 7.5. Experimental (k_2^{exp}) and calculated (k_2^{calcd})[a] second-order rate constants for the reactions of the Michael acceptors 1 and 2 with the ylides 3 and 4 in DMSO at 20 °C.
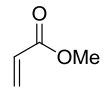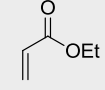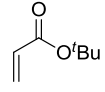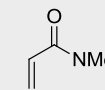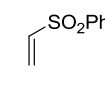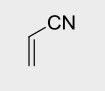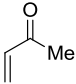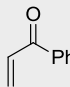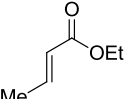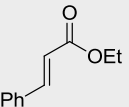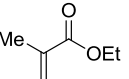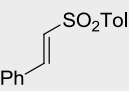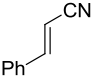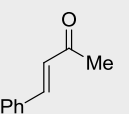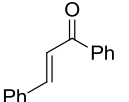
	Electrophile	Nucleophile	k_2^{exp}/M^{-1} s^{-1}	k_2^{calcd}/M^{-1} s^{-1}	k_2^{exp}/k_2^{calcd}
1a	O OMe $E = -18.92$	3a	1.10×10^3	7.60×10^2	1.44
		3b	6.91×10^3 [b]	1.74×10^3	3.98
		3c	2.01×10^3	8.85×10^2	2.28
		3d	1.37×10^1	6.16	2.22
		4	3.25	2.88×10^1	0.11
1b	O OEt $E = -19.16$	3a	1.07×10^3	6.23×10^2	1.71
		3c	1.67×10^3	7.05×10^2	2.36
		3d	1.12×10^1	4.46	2.50
		4	3.89	2.00×10^1	0.20
1c	O O^{t}Bu $E = -20.28$	3a	2.61×10^2	2.40×10^2	1.09
		3b	3.40×10^2 [b]	5.32×10^2	0.64
		3c	2.94×10^2	2.39×10^2	1.23
		3d	2.05	9.50×10^{-1}	2.17
		4	1.89	3.46	0.55
1d	O NMe$_2$ $E = -23.54$	3a	1.12×10^1	1.49×10^1	0.75
		3b	1.39×10^1	3.07×10^1	0.45
		3c	2.68×10^1	1.02×10^1	2.63
1e	SO$_2$Ph $E = -18.36$	3a	1.60×10^3	1.53×10^3	1.66
		3b	5.56×10^3 [b]	2.86×10^3	1.95
		3c	2.55×10^3	1.71×10^3	1.49
		3d	1.94×10^1	1.35×10^1	1.44
		3e	4.10	4.37	0.94
		4	2.36×10^1	7.02×10^1	0.34
1f	CN $E = -19.06$	3a	1.89×10^3	6.78×10^2	2.79
		3b	3.79×10^3 [b]	1.55×10^3	2.45
		3c	3.64×10^3	7.77×10^2	4.69
		3d	2.36	5.12	0.46
		3e	2.25	1.71	1.31
		3f	2.56×10^1 [c]	1.45	17.6
		4	4.90	2.33×10^1	0.21

Table 7.5. Continued.

	Electrophile	Nucleophile	k_2^{exp}/M^{-1} s^{-1}	k_2^{calcd}/M^{-1} s^{-1}	k_2^{exp}/k_2^{calcd}
1g	(structure) O, Me $E = -16.48$	**3a**	6.84×10^3	6.09×10^3	1.12
		3c	7.99×10^3	9.40×10^3	0.85
		3d	1.24×10^2	1.80×10^2	0.69
		3e	2.74×10^1	5.35×10^1	0.51
		4	$(\sim 4.25 \times 10^1)^{[d]}$	1.39×10^3	0.03
1h	(structure) O, Ph $E = -15.27$	**3a**	3.43×10^4	1.71×10^4	2.01
		3b	2.55×10^4	4.25×10^4	0.60
		3c	4.89×10^4	3.03×10^4	1.61
		3d	8.00×10^2	9.61×10^2	0.83
		3e	2.07×10^2	2.70×10^2	0.77
		4	$(\sim 7.21 \times 10^2)^{[d]}$	8.80×10^3	0.08
2a	(structure) O, OEt, Me $E = -23.73$	**3a**	4.14	1.27×10^1	0.33
		3c	2.87×10^1	8.16	3.57
2b	(structure) O, OEt, Ph $E = -24.51$	**3a**	3.08	6.60	0.47
		3c	7.77	3.97	1.96
2c	(structure) O, Me, OEt $E = -22.78$	**3a**	1.50×10^1	2.85×10^1	0.53
		3c	3.76×10^1	2.13×10^1	1.76
2e	(structure) SO$_2$Tol, Ph $E = -24.69$	**3a**	2.36	5.59	0.42
		3c	7.17	3.35	2.14
2f	(structure) CN, Ph $E = -24.57$	**3a**	6.15	identical	-
2g	(structure) O, Me, Ph $E = -22.99$	**3a**	1.77×10^1	2.37×10^1	0.75
		3b	2.66×10^1	2.37×10^1	0.54
		3c	3.91×10^1	1.73×10^1	2.26
2h	(structure) O, Ph, Ph $E = -19.37^{[e]}$	**3a**	3.31×10^2	5.19×10^2	0.64
		3b	3.20×10^2	1.18×10^3	0.27
		3c	6.17×10^2	5.21×10^2	1.18
		4	$3.41 \times 10^{1, [f]}$	1.43×10^1	2.38

[a] Calculated by eq 7.1 from N, s_N from Table 7.1 and E from this Table; [b] Bis-exponential decay of the absorbance was observed and only the initial rate was used to determine k_2; [c] Not used for the determination of E as the reaction rate may already be enhanced by a partially concerted cycloaddition;[17] [d] Bis-exponential decay of the absorbance was observed and the second-order rate constant can only be estimated from the initial decay of the absorption; not used for the determination of E; [e] The electrophilicity value of $E = -18.82$ for **2h** reported in ref. [16h] had to be corrected, as it was derived only from the reaction of **2h** with **4**; [f] k_2 Value from ref. [16h].

If the reactions of the Michael acceptors **1** and **2** with the pyridinium ylides **3** proceed stepwise with rate-determining formation of the intermediate betaines, the measured second-order rate constants equal k_2 as defined in Scheme 7.1. As k_2 refers to the attack of a nucleophile at an electron-deficient π-system, which generally follow eq 7.1, this equation may also be used to correlate the rate constants listed in Table 7.5. The correlations of (log k_2)/s_N for the reactions of the electrophiles **1** and **2** with the ylides **3** and **4** versus the corresponding nucleophilicity parameters N are linear with a slope of roughly 1.0 as required by eq 7.1 (Figure 7.2). The rate constant for the reaction of acrylonitrile **1f** with the quinolinium ylide **3f** (marked by footnote [c] in Table 7.5) deviates by a factor of 18 from the correlation line, which is still within the limit of confidence of eq 7.1 (two orders of magnitude), but might also be due to a low degree of concertedness of the reaction. Therefore, this reaction was not considered for the determination of the electrophilicity parameter E of acrylonitrile **1f**.

In the reactions of methylvinylketone (**1g**) and phenylvinylketone (**1h**) with the sulfonium ylide **4** bisexponential decays of the absorbance of **4** were observed, so that the second-order rate constants could only be estimated from the initial decays of the absorbance. The rate constants deviate from the correlation line and the reactions proceed 13 and 33 times slower than calculated, indicating a change of mechanism. Thus, these rate constants were not considered for the determination of the electrophilicity parameters of the acyl-substituted ethylenes **1g,h**.
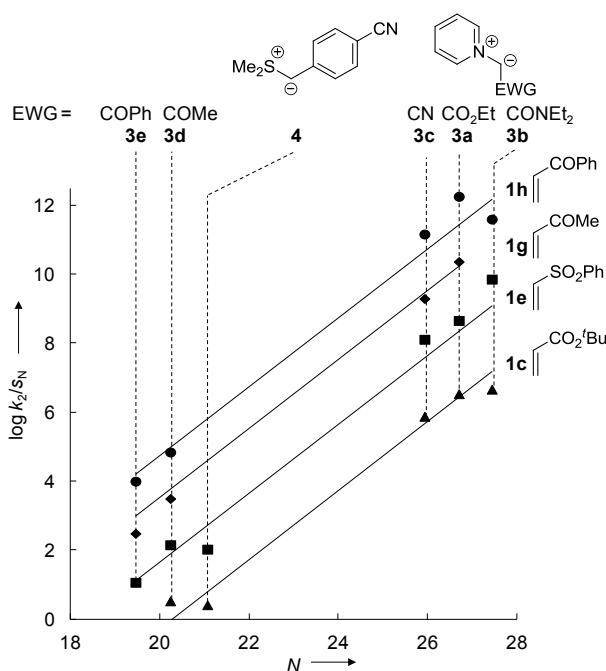
Figure 7.2. Correlation of (log k_2)/s_N (DMSO, 20 °C) for the reactions of the Michael acceptors 1c−h with the ylides 3 and 4 against the nucleophilicity parameters N of the ylides. For the sake of clarity the correlation lines of the other electrophiles 1 and 2 are not shown (for details see Experimental Section).

The electrophilicity parameters E for the acceptor-substituted olefins **1** and **2** were determined by least-squares minimization (minimization of $\Delta^2 = \sum(\log k_2 - s_N(N + E)^2)$) considering the rate constants of their reactions with pyridinium ylides **3a−e** and the sulfonium ylide **4** (Table 7.5).

In all 57 investigated reactions of the acceptor-substituted π-systems **1** and **2** with the pyridinium ylides **3** and sulfonium ylide **4** the experimental and calculated second-order rate constants agree within a factor of 33, which is within the limit of confidence of eq 7.1. For the 54 rate constants used to derive the electrophilicity parameters E the agreement between experimental and calculated rate constants is better than a factor of 5. The published E parameter of chalcone **2h**[16h] had to be corrected slightly as it can now be based on four rate constants and not only on the rate of its reaction with ylide **4**.

As all measured rate constants in Table 7.5 agree within two orders of magnitude with the rate constants calculated by eq 7.1 this indicates that despite the different reaction products, the tetrahydroindolizines **5,7,9** on one hand (Tables 7.2, 7.3 and Scheme 7.3) and the cyclopropanes **13** on the other (Table 7.4), all investigated reactions proceed via a common rate-determining step, the initial CC-bond formation to the intermediate betaines.

7.3   Conclusion

The rates of the stepwise [3+2]-cycloaddition of the pyridinium ylides **3** with the acceptor-substituted ethylenes **1** and **2**, as well as their stepwise cyclopropanations by the sulfonium ylide **4**, were found to follow the linear free-energy relationship (eq 7.1). As the derived electrophilicity parameters E describe both types of reactions of the Michael acceptors **1** and **2**, it is likely that both reactions proceed via initial formation of a zwitterion, which undergoes a fast subsequent ring closure to the [3+2]-adducts or cyclopropanes.

Therefore, the electrophilicities E of the acceptor-substituted olefins **1** and **2** can be included into our comprehensive electrophilicity scale.[21g] The electrophilicity parameters E of the activated ethylenes **1** (including acrolein)[18] cover almost nine orders of magnitude (Figure 7.3). An amido-substituted ethylene ($E = -23.54$) is a weak electrophile. In comparison, the acrylic ester **1c** which is substituted with a sterically demanding *tert*-butoxy group is more than 1,800 times more reactive. Exchanging the *tert*-butoxy by an ethoxy group (**1b**) or methoxy group (**1a**) increases the reactivity by approximately a factor of 14−23 compared to *tert*-butyl acrylate **1c**. Substituting the methoxycarbonyl group (**1a**) by a cyano group (**1f**) has almost no effect on

the reactivity, whereas a phenylsulfonyl group (**1e**) activates of the double bond by a factor of four in comparison to methoxycarbonyl (**1a**). Acyl groups increase the reactivity of the CC-double bond significantly as methylvinylketone (**1g**) is 275 times, phenylvinylketone (**1h**) is ~4,500 times, and acrolein is ~18,000 times more reactive than methyl acrylate **1a**.

The addition of a methyl group in 2-position of ethyl acrylate **1b** (→**2c**) decreases the reactivity by a factor of ~4,200, while adding a methyl group in the conjugate-position (→**2a**) leads to a ~37,000 fold decrease of the reactivity, and the ethyl cinnamate (**2b**) is even ~220,000 times less reactive than **1b**. Phenyl groups in the conjugate position (**2b,e−h**) generally deactivate the double bond of the activated ethylene **1** by a factor of $10^4–10^6$, probably due to steric inhibition of the nucleophilic attack and the associated disruption of phenyl conjugation. All investigated activated styrenes **2** are rather weak electrophiles as their electrophilicities range from $–24.7 < E < –19.3$.
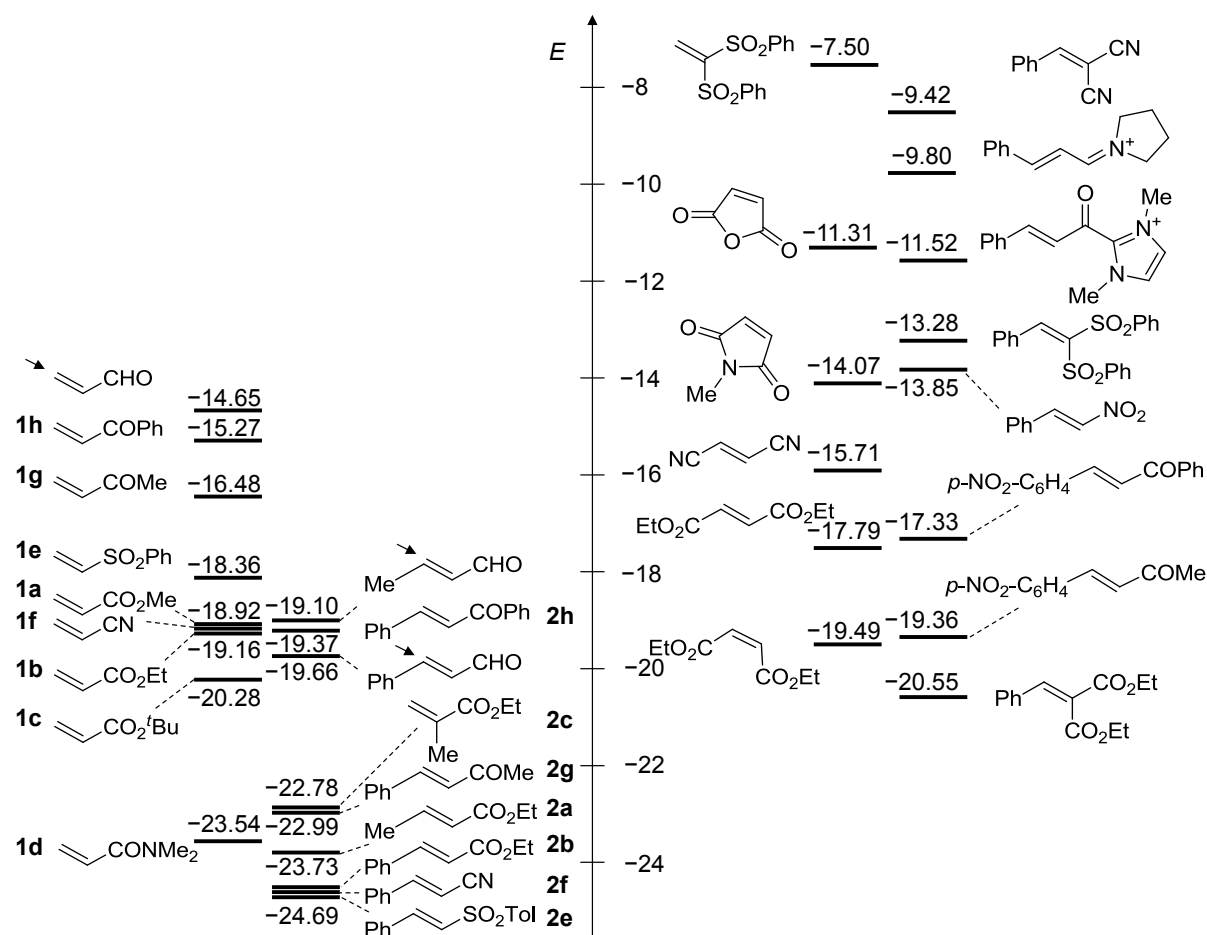
Figure 7.3. Comparison of the electrophilic reactivities of the Michael acceptors 1 and 2 with α,β-unsaturated aldehydes,[18] different disubstituted ethylenes,[16f, j, 17] other Michael acceptors,[16b, d, h-j] and azolium[22] and iminium[16e] ions.

Besides the reactivity comparisons which can be made within the series of the acceptor-substituted olefins **1** and **2**, comparisons with other Michael systems are possible:

When one compares the reactivities of the recently characterized β-nitro-styrenes[16i] with those of the activated styrenes **2**, one can see that a β-nitro-group increases the reactivity of the CC-double bond by 330,000 fold relative to a benzoyl group. In contrast, a *p*-nitro-substituent at the aromatic ring increases the reactivity of the CC-double bond of chalcone **2h** only by a factor of 100 and by a factor of ~4,300 for benzylidene acetone **2g**.[16h]

Addition of a second ethoxycarbonyl group to ethyl acrylate **1b** in *trans*-configuration (diethyl fumarate)[17] increases the reactivity of the double bond by a factor of 32, while a second ethoxycarbonyl group in *cis*-configuration (diethyl maleate)[17] leads to a three times lower reactivity. In contrast, a second electron-withdrawing group in 2-position[16j] of (vinyl)sulfonylbenzene (**1e**) or β-tosyl-styrene (**2e**) leads to an tremendous increase of the reactivity of the double bond by a factor of ~10^{11}. 2-Substitution of cinnamonitrile **2f** with a second cyano group even increases the reactivity of the CC-double bond by a factor of 10^{15},[16b] whereas diethyl benzylidene malonate[16d] is only ~9,100 times more reactive than the parent ethyl cinnamate **2b**. Activation of ethyl cinnamate **2b** by substituting the ethoxy by an azolium group[22] increases the reactivity of the CC-double bond 10^{13} fold, so that the magnitude of azolium activation of ethyl cinnamate is in the range of the activation of cinnamaldehyde[16e] by iminium-substitution.[18]

As this study gives electrophilicity parameters for many important Michael systems it can help to increase the understanding of the nucleophile-independent order of electrophilicities, which is currently investigated.[31] Our results may also be helpful to develop new tools for the analysis of the mechanism of concerted cycloaddition reactions.[4h, i, 5a, 32] The electrophilicities of the acceptor-substituted olefins investigated in this work may also broaden the experimental basis for the ongoing development of the distortion/interaction energy model[33] or activation strain model.[34]

7.4 Experimental Section

7.4.1 General

Chemicals. DMSO (99.7%, extra dry, over molecular sieves, AcroSeal) was purchased and used without further purification. The pyridinium salts **3H⁺X⁻** were synthesized according to ref. [19], the sulfonium salt **4H⁺BF₄⁻** according to ref. [20].

Analytics. ¹H- and ¹³C NMR spectra were recorded in CDCl₃ (δ_H 7.26, δ_c 77.16)[35] on 200, 300, 400, or 600 MHz NMR spectrometers and are given in ppm. The following abbreviations were used to designate chemical shift multiplicities: s = singlet, d = doublet, t = triplet, q = quartet, m = multiplet, br = broad. For reasons of simplicity, the ¹H NMR signals of AA'BB'-spin systems of *p*-disubstituted aromatic rings were treated as doublets. The assignments of individual NMR signals were based on additional 2D-NMR experiments (COSY, NOESY, HSQC, HMBC). Diastereomeric ratios (*dr*) were determined by ¹H NMR of the crude reaction products if not stated otherwise. HRMS and MS were recorded on a Finnigan MAT 95 Q (EI) mass spectrometer or Thermo Finnigan LTQ FT Ultra (ESI). The melting points were recorded on a Büchi Melting Point B-540 device and are not corrected.

Kinetics. The rates of all reactions were determined by UV-vis spectroscopy in DMSO at 20 °C by using stopped-flow spectrophotometer systems (Applied Photophysics SX.18MV-R and Hi-Tech SF-61DX2) as well as diode array-spectrophotometer systems (J&M TIDAS DAD 2062). The temperature of the solutions during the kinetic studies was maintained at 20 ± 0.2 °C by using circulating bath cryostats. The ylides were generated in DMSO at 20 °C immediately before each kinetic run by mixing DMSO solutions of the salts **3H⁺X⁻** or **4H⁺BF₄⁻** and KO^{t}Bu (typically 1.00:1.05 equivalents). The kinetic runs were initiated by mixing DMSO solutions of the ylides and electrophiles under pseudo first-order conditions with one of the two reaction partners in large excess over the other (>10 equivalents). Pseudo first-order rate constants k_{obs} (s⁻¹) were obtained by fitting the single exponential $A_t = A_0 \exp(-k_{obs}t) + C$ (mono-exponential decrease) to the observed time-depended absorbances (average of at least three kinetic runs for each concentration for the stopped-flow method) of the electrophiles or ylides. Second-order rate constants k_2 (L mol⁻¹ s⁻¹) were derived from the slopes of the linear correlations of the obtained k_{obs}-values against the concentrations of the excess reaction partner. Some kinetics have been performed by H. Asahara as indicated.

7.4.2 Product Studies

7.4.2.1 Synthesis of the Indolizines 6

Procedure A for the Synthesis of the Indolizines 6. The Michael-acceptor **1** (1.00 mmol) and the salt **3H$^+$X$^-$** (500 μmol) and Na$_2$CO$_3$ (500 μmol) were dissolved in DMSO (5 mL) and stirred until for 30–60 min at ambient temperature. Chloranil (1.00 mmol) was added to the solution and stirring was continued for 0.5–3 h until the oxidant was consumed as monitored by TLC. The reaction was treated with 2M HCl and extracted with CHCl$_3$ (3×15mL). The combined organic layers were washed with 2M NaOH (25 mL) and brine (25 mL) and dried over Na$_2$SO$_4$. The solvent was evaporated and the residue was subjected to a column chromatography (*n*-pentane:EtOAc 15:1–3:1, depending on R_f). The products were further purified by recrystallization from Et$_2$O.

Methyl 3-(diethylcarbamoyl)indolizine-1-carboxylate (6a). From **3bH$^+$Br$^-$** (137 mg, 500 μmol), **1a** (86, 1.00 mmol), Na$_2$CO$_3$ (53 mg, 0.50 mmol), and chloranil (246 mg, 1.00 mmol) according to procedure **A**. **6a** was obtained as colorless solid (72 mg, 0.26 mmol, 52%, *cis*:*trans*-amide 1:3). R_f (*n*-pentane:EtOAc 5:1) = 0.08. **Mp.** (Et$_2$O): 55 °C. **^{1}H NMR** (300 MHz, CDCl$_3$) δ = 1.30 (t, *J* = 7.0 Hz, 6 H, CH$_3$), 3.61 (q, *J* = 7.1 Hz, 4 H, CH$_2$), 3.90 (s, 3 H, CH$_3$), 6.82 (td, *J* = 7.2, 1.4 Hz, 1 H, 6-H), 7.18 (ddd, *J* = 9.0, 6.7, 1.0 Hz, 1 H, 7-H), 7.45 (s, 1 H, 2-H), 8.18 – 8.28 (m, 1 H, 8-H), 8.94 (dt, *J* = 7.2, 1.0 Hz, 1 H, 5-H). **^{13}C NMR** (75 MHz, CDCl$_3$) δ = 13.9 (q, CH$_3$), 41.7 (br, t, CH$_2$), 51.2 (t, CH$_3$), 103.4 (s, C-3), 113.4 (d, C-6), 117.9 (s, C-1), 118.8 (d, C-2), 119.4 (d, C-8), 124.6 (d, C-7), 127.9 (d, C-5), 137.7 (s, C-8a), 162.7 (s, CON), 165.1 (s, CO$_2$). **HRMS** (ESI): calcd. for [C$_{15}$H$_{19}$N$_2$O$_3$]$^+$ 275.1390, found 275.1390.   DA832

Ethyl 3-cyanoindolizine-1-carboxylate (6b). From **3cH$^+$Br$^-$** (100 mg, 500 μmol), **1b** (100 mg, 1.00 mmol), Na$_2$CO$_3$ (53 mg, 0.50 mmol), and chloranil (246 mg, 1.00 mmol) according to procedure **A**. **6b** was obtained as colorless solid (61 mg, 0.29 mmol, 58%). R_f (*n*-pentane:EtOAc 5:1) = 0.29. **Mp.** (Et$_2$O): 103 °C. **^{1}H NMR** (300 MHz, CDCl$_3$) δ = 1.41 (t, *J* = 7.1 Hz, 3 H, CH$_3$), 4.38 (q, *J* = 7.1 Hz, 2 H, CH$_2$), 7.03 (td, *J* = 7.0, 1.1 Hz, 1 H, 6-H), 7.33 (ddd, *J* = 9.3, 6.9, 1.1 Hz, 1 H, 7-H), 7.79 (s, 1 H, 2-H), 8.27 – 8.39 (m, 2 H, 5-H, 8-H). **^{13}C NMR** (75 MHz, CDCl$_3$) δ = 14.6 (q, CH$_3$), 60.4 (t, CH$_2$), 96.8 (s, CN), 106.2 (s, C-1), 112.8 (s, C-3), 115.1 (d, C-6), 120.6 (d, C-8), 125.3 (d, C-2), 125.8 (d, C-5), 126.1 (d, C-7), 137.9 (s, C-8a), 163.4 (s, CO$_2$). **HRMS** (EI): calcd. for [C$_{12}$H$_{10}$N$_2$O$_2$]$^+$

335

214.0737, found 214.0743. **MS** (EI) *m/z*: 215 (7), 214 (52), 186 (30), 169 (100), 142 (14), 89 (12), 58 (10), 43 (29). DA782

tert-**Butyl 3-acetylindolizine-1-carboxylate (6c).** From **3dH⁺Cl⁻** (86 mg, 500 μmol), **1c** (128, 1.00 mmol), Na₂CO₃ (53 mg, 0.50 mmol), and chloranil (246 mg, 1.00 mmol) according to procedure **A**. **6c** was obtained as yellow solid (124 mg, 479 μmol, 96%). *R*f (*n*-pentane:EtOAc 5:1) = 0.34. **Mp**. (Et₂O): 150 °C. **¹H NMR** (300 MHz, CDCl₃) δ = 1.64 (s, 9 H, 3×CH₃), 2.58 (s, 3 H, CH₃), 6.99 (td, *J* = 7.0, 1.4 Hz, 1 H, 6-H), 7.36 (dddd, *J* = 9.0, 6.8, 1.2, 0.4 Hz, 1 H, 7-H), 7.93 (s, 1 H, 2-H), 8.30 (dddd, *J* = 9.0, 1.1, 0.4 Hz, 1 H, 8-H), 9.88 (dtd, *J* = 7.1, 1.1, 0.5 Hz, 1 H, 5-H). **¹³C NMR** (75 MHz, CDCl₃) δ = 27.4 (q, CH₃), 28.7 (q, 3×CH₃), 80.7 (s, C_q), 107.5 (s, C-1), 115.1 (d, C-6), 119.6 (d, C-8), 122.6 (s, C-3), 126.5 (d, C-2), 127.0 (d, C-7), 129.2 (d, C-5), 139.2 (s, C-8a), 163.7 (s, CO₂), 187.8 (s, CO). **HRMS** (EI): calcd. for [C₁₅H₁₇NO₃]⁺ 259.1203, found 259.1205. **MS** (EI) *m/z*: 260 (2), 259 (12), 204 (6), 203 (65), 188 (66), 186 (13), 58 (44), 43 (100). DA789

3-Cyano-*N*,*N*-dimethylindolizine-1-carboxamide (6d). From **3cH⁺Br⁻** (99 mg, 0.50 mmol), **1d** (127 mg, 1.00 mmol), Na₂CO₃ (53 mg, 0.50 mmol), and chloranil (246 mg, 1.00 mmol) according to procedure **A**. **6d** was obtained as yellowish solid (68 mg, 0.32 mmol, 64%). *R*f (*n*-pentane:EtOAc 1:1) = 0.16. **Mp.** (Et₂O): 72 °C. **¹H NMR** (300 MHz, CDCl₃) δ = 3.17 (s, 6 H, 2×CH₃), 6.96 (td, *J* = 6.9, 1.3 Hz, 1 H, 6-H), 7.20 (ddd, *J* = 9.1, 6.8, 1.1 Hz, 1 H, 7-H), 7.43 (s, 1 H, 2-H), 8.05 (dt, *J* = 9.1, 1.2 Hz, 1 H, 8-H), 8.28 (dt, *J* = 7.0, 1.1 Hz, 1 H, 5-H). **¹³C NMR** (75 MHz, CDCl₃) δ = 37.8 (q, 2×CH₃), 95.3 (s, C-3), 109.1 (s, C-1), 113.2 (s, CN), 114.8 (d, C-6), 120.7 (d, C-8), 122.7 (d, C-2), 124.5 (d, C-7), 125.3 (d, C-5), 137.4 (s, C-8a), 165.6 (s, CON). **HRMS** (ESI): calcd. for [C₁₂H₁₂N₃O]⁺ 214.0975, found 214.0974. DA799

1-(1-(Phenylsulfonyl)indolizin-3-yl)ethanone (6e). From **3dH⁺Cl⁻** (86 mg, 0.50 mmol), **1e** (168 mg, 1.00 mmol), Na₂CO₃ (53 mg, 0.50 mmol), and chloranil (246 mg, 1.00 mmol) according to procedure **A**. **6e** was obtained as colorless solid (147 mg, 491 μmol, 98%). *R*f (*n*-pentane:EtOAc 5:1) = 0.16. **Mp.** (Et₂O): 173 °C. **¹H NMR** (300 MHz, CDCl₃) δ = 2.58 (s, 3 H, CH₃), 7.06 (td, *J* = 7.0, 1.4 Hz, 1 H, 6-H), 7.39 – 7.58 (m, 4 H, 7-H, 3×C_Ar-H), 7.95 (s, 1 H, 2-H), 7.96 – 8.02 (m, 2 H, 2×C_Ar-H), 8.18 (dt, *J* = 9.0, 1.2 Hz, 1 H, 8-H), 9.87 (dt, *J* = 7.1, 1.1 Hz, 1 H, 5-H). **¹³C NMR** (75 MHz, CDCl₃) δ = 27.5 (s, CH₃), 113.6 (s, C-1), 115.9 (d, C-6), 117.7 (d, C-8), 123.1 (d, C-3), 124.9 (d, C-2), 126.6 (d, 2×C_Ar-H), 128.0 (d, C-7), 129.4 (d, 2×C_Ar-H), 129.4 (d, C-5), 132.9 (d, C_Ar-H), 136.7 (s, C-8a), 143.4 (s, C_Ar), 187.9 (s, CO). **HRMS** (EI): calcd. for [C₁₆H₁₃NO₃S]⁺ 299.0611, found 299.0611. **MS** (EI) *m/z*: 302

(1), 301 (7), 300 (20), 299 (100), 284 (63), 220 (10), 174 (20), 78.12 (12), 58 (15), 43 (48). DA796

Ethyl 1-cyanoindolizine-3-carboxylate (6f). From **3aH⁺Br⁻** (123 mg, 500 μmol), **1f** (53 mg, 1.0 mmol), Na_2CO_3 (53 mg, 0.50 mmol), and chloranil (246 mg, 1.00 mmol) according to procedure **A**. **6f** was obtained as colorless solid (63 mg, 0.29 mmol, 58%). R_f (*n*-pentane:EtOAc 5:1) = 0.28. **Mp.** (Et₂O): 70 °C. **¹H NMR** (300 MHz, CDCl₃) δ = 1.41 (t, *J* = 7.1 Hz, 3 H, CH₃), 4.40 (q, *J* = 7.1 Hz, 2 H, CH₂), 7.03 (td, *J* = 7.0, 1.3 Hz, 1 H, 6-H), 7.34 (ddd, *J* = 8.9, 6.9, 1.1 Hz, 1 H, 7-H), 7.71 – 7.81 (m, 2 H, 2-H, 8-H), 9.53 (dt, *J* = 7.1, 1.1 Hz, 1 H, 5-H). **¹³C NMR** (75 MHz, CDCl₃) δ = 14.6 (q, CH₃), 60.9 (t, CH₂), 83.9 (s, CN), 115.1 (d, C-6), 115.6 (s, C-1), 115.6 (s, C-3), 117.8 (d, C-8), 124.9 (d, C-2), 125.9 (d, C-7), 128.4 (d, C-5), 140.7 (s, C-8a), 160.5 (s, CO₂). **HRMS** (EI): calcd. for $[C_{12}H_{10}N_2O_2]^+$ 214.0737, found 214.0729. **MS** (EI) *m/z*: 214 (89), 186.05 (100), 169 (46), 142 (37), 114 (24), 58 (11), 43 (31). DA783
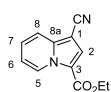
1-(3-Benzoylindolizin-1-yl)ethanone (6g). From **3eH⁺Br⁻** (139 mg, 0.50 mmol), **1g** (70 mg, 1.0 mmol), Na_2CO_3 (53 mg, 0.50 mmol), and chloranil (246 mg, 1.00 mmol) according to procedure **A**. **6g** was obtained as colorless solid (98 mg, 0.37 mmol, 74%). R_f (*n*-pentane:EtOAc 5:1) = 0.17. **Mp.** (Et₂O): 145 °C. **¹H NMR** (300 MHz, CDCl₃) δ = 2.51 (s, 3 H, CH₃), 7.16 (td, *J* = 7.0, 1.4 Hz, 1 H, 6-H), 7.48 – 7.65 (m, 4 H, 7-H, 3×C_Ar-H), 7.70 (s, 1 H, 2-H), 7.78 – 7.88 (m, 2 H, 2×C_Ar-H), 8.66 (dt, *J* = 8.9, 1.2 Hz, 1 H, 8-H), 9.98 (dt, *J* = 7.0, 1.1 Hz, 1 H, 5-H). **¹³C NMR** (75 MHz, CDCl₃) δ = 27.9 (q, CH₃), 115.0 (s, C-1), 116.3 (d, C-6), 120.6 (d, C-8), 122.5 (s, C-3), 128.6 (d, 2×C_Ar-H), 129.0 (d, 2×C_Ar-H), 129.1 (d, C-5), 129.1 (d, C-2), 129.2 (d, C-7), 131.7 (d, C_Ar-H), 139.7 (s, C-8a), 140.1 (s, C_Ar), 185.7 (s, CO), 193.2 (s, CO). **HRMS** (EI): calcd. for $[C_{17}H_{13}NO_2]^+$ 263.0941, found 263.0941. **MS** (EI) *m/z*: 263 (50), 248 (100), 105 (18), 77 (16), 43 (18). DA784
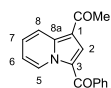
1-(1-Benzoylindolizin-3-yl)ethanone (6h). From **3dH⁺Cl⁻** (86 mg, 500 μmol), **1h** (132 mg, 1.00 mmol), Na_2CO_3 (53 mg, 0.50 mmol), and chloranil (246 mg, 1.00 mmol) according to procedure **A**. **6h** was obtained as colorless solid (127 mg, 482 μmol, 97%). R_f (*n*-pentane:EtOAc 5:1) = 0.61. **Mp.** (Et₂O): 113 °C. **¹H NMR** (300 MHz, CDCl₃) δ = 2.56 (s, 3 H, CH₃), 7.14 (td, *J* = 7.0, 1.4 Hz, 1 H, C-6), 7.48 – 7.65 (m, 4 H, C-7, 3×C_Ar-H), 7.78 (s, 1 H, 2-H), 7.81 – 7.89 (m, 2 H, 2×C_Ar-H), 8.64 (dt, *J* = 9.0, 1.2 Hz, 1 H, 8-H), 9.98 (dtd, *J* = 7.0, 1.2, 0.5 Hz, 1 H, 5-H). **¹³C NMR** (75 MHz, CDCl₃) δ = 27.5 (q, CH₃), 113.4 (s, C-1), 116.5 (d, C-6), 120.5 (d, C-8), 122.9 (s, C-3), 128.0 (C-7), 128.0 (d, C-2), 128.6 (d, 2×C_Ar-H), 128.8 (s, C_Ar), 129.0 (d, C-5), 129.0 (d, 2×C_Ar-H), 131.7 (d, C_Ar-H), 140.3 (s, C_Ar),
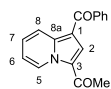
140.5 (s, C-8a), 188.0 (s, CO), 190.6 (s, CO). **HRMS** (EI): calcd. for $[C_{17}H_{13}NO_2]^{+\cdot}$ 263.0941, found 263.0940. **MS** (EI) m/z: 264 (17), 263 (100), 262 (31), 248 (35), 234 (50), 204 (47), 191 (31). DA785

7.4.2.2 Synthesis of the Dihydroindolizines 10

Procedure B for the Synthesis of the Dihydroindolizines 10. NaOH (1 mL, aq. 30%) was added under intense stirring to a suspension of **2** (0.50 mmol) and **3H⁺Br⁻** (500−750 µmol) in CH_2Cl_2 (5 mL) at room-temperature. The suspension was stirred until **2** was completely consumed as monitored by TLC (30 min–60 min). Water (30 mL) was added and the reaction mixture was extracted with CH_2Cl_2 (3×5 mL). The combined organic layers were dried over Na_2SO_4 before chloranil (500 µmol) was added. The solution was stirred at room temperature for 5−30 min until the oxidant was consumed. The solvent was evaporated and the residue was subjected to a column chromatography (n-pentane:EtOAc 3:1–1:1, depending on R_f). The products were further purified by recrystallization from EtOH.

Ethyl 3-cyano-2-phenyl-2,3-dihydroindolizine-1-carboxylate (10b). From **3cH⁺Br⁻** (119 mg, 600 µmol), **2b** (88 mg, 0.50 mmol) and chloranil (123 mg, 500 µmol) according to procedure **B**. **10b** was obtained as orange solid (130 mg, 445 µmol, 89%, dr 3:1). R_f (n-pentane:EtOAc 5:1) = 0.14. *major-, #minor diastereoisomer; no integrals given due the odd ratio of major and minor diastereoisomer. Tentative assignment of the NMR-signals, as no 2D NMR spectra are available. **¹H NMR** (300 MHz, CDCl₃) δ = 0.93−1.14 (m, 2×CH₃),*,# 3.88−4.14 (m, 2×CH₂),*,# 4.53 (d, J = 11.2 Hz, CH),# 4.64 (d, J = 5.4 Hz, CH),# 4.76 (d, J = 5.4 Hz, CH),* 5.32 (d, J = 11.3 Hz, CH),# 5.88−6.00 (m, 2×C-H),*,# 6.90 – 6.98 (m, 3×C-H),*,#

6.99 – 7.07 (m, C-H),# 7.17 – 7.41 (m, 9×C_Ar-H, superimposed by solvent),*,# 7.41 – 7.50 (m, 2×C-H, C_Ar-H).*,# **¹³C NMR** (75 MHz, CDCl₃) δ = 14.6 (q, CH₃),* 14.6 (q, CH₃),# 48.9 (d, C-2),# 51.9 (d, C-2),* 58.7 (d, C-3),* 59.7 (d, C-3),# 60.3 (t, CH₂),* 60.3 (t, CH₂),# 90.2 (s, CN),* 90.6 (s, CN),# 107.8 (d, C-6 or C-7),# 108.1 (d, C-6 or C-7),* 114.3 (d, C-5 or C-8),# 116.8 (d, C-5 or C-8),* 118.1 (s, C-1),* 118.7 (s, C-1),# 127.1 (d, 2×C_ar-H),* 127.9 (d, C_ar-H),* 128.3 (d, C_ar-H),# 128.3 (d, 2×C_ar-H),# 128.8 (d, 2×C_ar-H),# 129.1 (d, 2×C_ar-H),* 132.5 (d, C-6 or C-7),# 132.7 (d, C-6 or C-7),* 136.1 (d, C-5 or C-8),* 136.3 (d, C-5 or C-8),# 139.2 (s, C_ar),# 142.2 (s, C_ar),* 152.3 (br s, 2×C-8a),*,# 165.4 (s, CO₂),# 165.4 (s, CO₂)*. **HRMS** (EI): calcd. for $[C_{18}H_{16}N_2O_2]^{+\cdot}$ 292.1206, found 292.1208. **MS** (EI) m/z: 293 (12), 292 (49), 247 (20), 220 (26), 219 (100), 218 (22), 192 (16), 143 (16), 43 (16). DA762
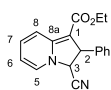
Ethyl 1-cyano-2-phenyl-2,3-dihydroindolizine-3-carboxylate (10f). From **3aH⁺Br⁻** (148 mg, 600 µmol), **2f** (65 mg, 0.50 mmol) and chloranil (123 mg, 500 µmol) according to procedure **B**. **10f** was obtained as orange solid (132 mg, 452 µmol, 90%, *dr* 8:1). R_f (*n*-pentane:EtOAc 5:1) = 0.12. *major-, #minor diastereoisomer; signal of one proton of the minor diastereoisomer was set to 1.0. **¹H NMR** (300 MHz, CDCl₃) δ = 0.85 (t, *J* = 7.2 Hz, 3 H, CH₃),# 1.35 (t, *J* = 7.1 Hz, 25 H, CH₃),* 3.46 – 3.62 (m, 1 H, C*H*H),# 3.76 (dq, *J* = 10.7, 7.1 Hz, 1 H, CH*H*),# 4.21 – 4.44 (m, 18 H, CH₂),* 4.47 (d, *J* = 5.4 Hz, 8 H, 2-H),* 4.56 (d, *J* = 5.4 Hz, 8 H, 3-H),* 4.68 (d, *J* = 12.5 Hz, 1 H, 2-H),# 5.08 (d, *J* = 12.5 Hz, 1 H, C-3),# 5.73 – 5.84 (m, 9 H, 2×(6-H or 7-H)),*,# 6.63 (dt, *J* = 9.4, 1.2 Hz, 8 H, 5-H or 8-H),* 6.77 (d, *J* = 7.0 Hz, 1 H, 5-H or 8-H),# 6.80 – 6.93 (m, 17 H, 2×(5-H or 8-H) and 2×(6-H or 7-H), superimposed by solvent),*,# 7.21 – 7.44 (m, 49 H, 10×C$_{Ar}$-H).*,# The intensities for most signals of the carbon atoms of the minor diastereoisomer # in the ¹³C NMR were too low or too broad to give visible peaks, therefore only the signals of the major diastereoisomer are given. **¹³C NMR** (75 MHz, CDCl₃) δ = 14.3 (q, CH₃),* 50.2 (d, C-2),* 62.8 (d, CH₂),* 65.5 (s, C-1),* 72.5 (d, C-3),* 105.9 (d, C-6 or C-7),* 115.5 (d, C-5 or C-8),* 120.6 (s, CN),* 127.2 (d, 2×C$_{Ar}$-H),* 128.0 (d, C$_{Ar}$-H),* 129.2 (d, 2×C$_{Ar}$-H),* 135.1 (d, C-6 or C-7),* 135.9 (d, C-5 or C-8),* 141.9 (s, C$_{Ar}$),* 155.4 (s, C-8a),* 169.3 (s, CO₂).* **HRMS** (EI): calcd. for [C$_{18}$H$_{16}$N₂O₂]⁺ 292.1206, found 292.1206. **MS** (EI) *m/z*: 293 (15), 292 (70), 291 (38), 263 (14), 219 (100), 218 (41), 192 (18), 142 (25). DA763

1-Acetyl-2-phenyl-2,3-dihydroindolizine-3-carbonitrile dihydrate (10g·2H₂O). From **3cH⁺Br⁻** (149 mg, 750 µmol), **2g** (73 mg, 0.50 mmol) and chloranil (123 mg, 500 µmol) according to procedure **B**. **10g·2H₂O** was obtained as red solid (23 mg, 88 µmol, 18%, *dr* 2:1, isomerization upon standing in CDCl₃-solution to 3:1). R_f (*n*-pentane:EtOAc 5:1)= 0.11. *major-, #minor diastereoisomer; signal of one proton of the minor diastereoisomer was set to 1.0. **¹H NMR** (300 MHz, CDCl₃) δ = 1.79 (br, s, 9 H, CH₃),* 2.02 (br, s, 3 H, CH₃),# 4.60 (d, *J* = 10.8 Hz, 1 H, C-2),# 4.71 (d, *J* = 5.1 Hz, 3 H, 2-H),* 4.83 (d, *J* = 5.1 Hz, 3 H, 3-H),# 5.54 (d, *J* = 10.7 Hz, 1 H, C-3), 6.21 (t, *J* = 6.7 Hz, 3 H, 6-H or 7-H),* 6.23 – 6.35 (m, 1 H, 6-H or 7-H),# 7.10 (d, *J* = 6.9 Hz, 3 H, 5-H or 8-H),* 7.13 – 7.22 (m, 3 H, 5-H or 8-H),* 7.23 – 7.41 (m, 28 H, 2×(6-H or 7-H), 2×(5-H or 8-H), 10×C$_{Ar}$-H, superimposed by solvent), 8.03 (s, 4 H, 2×H₂O). The intensities for some signals of the carbon atoms of the minor diastereoisomer # in the ¹³C NMR were too low or too broad to give visible peaks, therefore only the signals of the major diastereoisomer are given. **¹³C NMR** (100 MHz, CDCl₃) δ = 28.2 (br, q, CH₃),* 52.5 (d, C-2),* 61.2 (d, C-3),* 110.8 (br d, C-6 or C-7),* 116.4
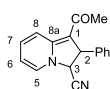
(s, C-1),* 120.0 (br s, CN),* 127.3 (d, 2×C$_{Ar}$-H),* 128.5 (d, C-5 or C-8),* 129.4 (d, C$_{Ar}$-H),* 129.6 (d, 2×C$_{Ar}$-H),* 132.7 (br d, C-5 or C-8),* 138.3 (br d, C-6 or C-7),* 141.6 (s, C$_{Ar}$),* 152.8 (s, C-8a),* 186.9 (s, CO).* **HRMS** (EI): calcd. for [C$_{17}$H$_{14}$N$_2$O]$^{+}$ 262.1101, found 262.1105. **MS** (EI) *m/z*: 263 (20), 262 (99), 261 (29), 260 (30), 247 (60), 219 (100), 192 (32), 143 (30), 78 (16), 43 (44). DA770

7.4.2.3 Synthesis of the Indolizines 11

Procedure C for the Synthesis of the Indolizines 11. NaOH (aq. 30%, 1 mL) was added under intense stirring to suspensions of **2** (500 µmol) and **3H$^+$X$^-$** (500−750 µmol) in CH$_2$Cl$_2$ (5 mL) at room-temperature. The mixture was stirred until the Michael acceptor was completely consumed as monitored by TLC (30–60 min). Water (30 mL) was added and the reaction mixture was extracted with CH$_2$Cl$_2$ (3×5 mL). The combined organic layers were dried over Na$_2$SO$_4$, before chloranil (1.00 mmol) was added. The solution was stirred at room temperature for 30−60 min until all chloranil was consumed. The solvent was evaporated and the residue was subjected to a column chromatography (*n*-pentane:EtOAc 15:1–3:1, depending on R_f). The resulting solids were taken up in CHCl$_3$ and insoluble precipitates were removed by filtration. After evaporation the products were further purified by recrystallization from Et$_2$O.

Ethyl 3-cyano-2-methylindolizine-1-carboxylate (11a). From **3cH$^+$Br$^-$** (100 mg, 500 µmol), **2a** (114 mg, 1.00 mmol), Na$_2$CO$_3$ (53 mg, 0.50 mmol), and chloranil (246 mg, 1.00 mmol) according to procedure **A**. **11a** was obtained as colorless solid (96 mg, 0.42 mmol, 84%). R_f (*n*-pentane:EtOAc 5:1) = 0.61. **Mp.** (Et$_2$O): 124 °C. **^{1}H NMR** (300 MHz, CDCl$_3$) δ = 1.43 (t, *J* = 7.1 Hz, 3 H, CH$_3$), 2.65 (s, 3 H, CH$_3$), 4.39 (q, *J* = 7.1 Hz, 2 H, CH$_2$), 6.97 (td, *J* = 6.9, 1.6 Hz, 1 H, 6-H), 7.25 − 7.33 (m, 1 H, 7-H, superimposed by solvent), 8.17 − 8.38 (m, 2 H, 5-H, 8-H). **^{13}C NMR** (75 MHz, CDCl$_3$) δ = 12.9 (q, CH$_3$), 14.7 (q, CH$_3$), 60.1 (t, CH$_2$), 97.8 (s, CN), 104.5 (s, C-1), 112.9 (br, s, C-3), 114.6 (d, C-6), 120.3 (d, C-5 or C-8), 125.5 (d, C-5 or C-8), 126.1 (d, C-7), 138.6 (s, C-8a), 139.1 (s, C-2), 164.3 (s, CO$_2$). **HRMS** (EI): calcd. for [C$_{13}$H$_{12}$N$_2$O$_2$]$^{+}$ 228.0893, found 228.0895. **MS** (EI) *m/z*: 229 (15), 228 (94), 200 (48), 183 (100), 156 (31), 155 (21), 78 (10), 58. (29), 43 (79). DA788
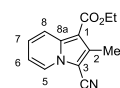
Diethyl 2-phenylindolizine-1,3-dicarboxylate (11b). From **3aH$^+$Br$^-$** (138 mg, 500 µmol), **2b** (88 mg, 0.50 mmol) and chloranil (246 mg, 1.00 mmol) according to procedure **C**. **11b** was obtained as colorless solid (150 mg, 445 µmol, 89%). R_f (*n*-pentane:EtOAc 5:1) = 0.50. **Mp.** (Et$_2$O): 87 °C. **^{1}H NMR** (300 MHz, CDCl$_3$) δ = 0.84 (t, *J* = 7.1 Hz, 3 H, CH$_3$), 1.00 (t, *J* = 7.1 Hz, 3 H, CH$_3$), 4.01 (q, *J* = 7.2 Hz, 2 H, CH$_2$), 4.08 (q, *J* = 7.2 Hz, 2 H,
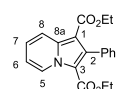
CH$_2$) 6.98 (ddd, J = 6.8, 1.4 Hz, 1 H, 6-H), 7.22 – 7.39 (m, 6 H, 7-H, 5×C$_{Ar}$-H), 8.41 (ddd, J = 9.0, 1.4, 1.0 Hz, 1 H, 8-H), 9.62 (dt, J = 7.1, 1.1 Hz, 1 H, 5-H). ^{13}C NMR (75 MHz, CDCl$_3$) δ = 13.5 (q, CH$_3$), 13.9 (q, CH$_3$), 59.6 (t, CH$_2$), 59.9 (t, CH$_2$), 105.2 (s, C-1 or C-3), 113.7 (s, C-1 or C-3), 114.5 (d, C-6), 119.8 (s, C-8), 125.9 (s, C-7), 126.8 (d, C$_{Ar}$-H), 127.0 (d, 2×C$_{Ar}$-H), 128.0 (s, C-5), 129.3 (d, 2×C$_{Ar}$-H), 136.4 (s, C$_{Ar}$), 138.8 (s, C-8a), 140.0 (s, C-2), 162.0 (s, CO$_2$), 164.5 (s, CO$_2$). **HRMS** (EI): calcd. for [C$_{20}$H$_{19}$NO$_4$]$^+$ 337.1309, found 337.1304. **MS** (EI) m/z: 338 (19), 337 (100), 292 (14), 265 (24), 264 (18), 193 (14). DA708

Ethyl 3-cyano-2-phenylindolizine-1-carboxylate (11c). From **3cH$^+$Br$^-$** (149 mg, 750 µmol), **2b** (88 mg, 0.50 mmol) and chloranil (246 mg, 1.00 mmol) according to procedure **C**. **11c** was obtained as colorless solid (123 mg, 424 µmol, 85%). R_f (n-pentane:EtOAc 5:1) = 0.70. **Mp.** (Et$_2$O): 122 °C. ^{1}**H NMR** (300 MHz, CDCl$_3$) δ = 1.18 (t, J = 7.1 Hz, 3 H, CH$_3$), 4.23 (q, J = 7.1 Hz, 2 H, CH$_2$), 7.05 (td, J = 6.9, 1.3 Hz, 1 H, 6-H), 7.36 (ddd, J = 9.1, 6.9, 1.1 Hz, 1 H, 7-H), 7.41 – 7.59 (m, 5 H, 5×C$_{Ar}$-H), 8.29 – 8.49 (m, 2 H, 5-H, 8-H). ^{13}**C NMR** (75 MHz, CDCl$_3$) δ = 14.2 (q, CH$_3$), 60.1 (t, CH$_2$), 97.4 (s, CN), 103.9 (s, C-1 or C-3), 113.0 (s, C-1 or C-3), 115.2 (d, C-6), 120.9 (d, C-5 or C-8), 125.6 (d, C-5 or C-8), 126.4 (d, C-7), 128.0 (d, 2×C$_{Ar}$-H), 128.8 (d, C$_{Ar}$-H), 130.1 (d, 2×C$_{Ar}$-H), 131.7 (s, C$_{Ar}$), 138.7 (s, C-8a), 141.3 (s, C-2), 163.7 (s, CO$_2$). **HRMS** (ESI): calcd. for [C$_{18}$H$_{15}$N$_2$O$_2$]$^+$ 291.1128, found 291.1129. DA771

2-Phenyl-1-tosylindolizine-3-carbonitrile (11e). From **3cH$^+$Br$^-$** (149 mg, 750 µmol), **2e** (129 mg, 500 µmol) and chloranil (246 mg, 1.00 mmol) according to procedure **C**. **11e** was obtained as colorless solid (168 mg, 450 µmol, 90%).

R_f (n-pentane:EtOAc 5:1) = 0.18. **Mp.** (Et$_2$O): 200 °C. ^{1}**H NMR** (300 MHz, CDCl$_3$) δ = 2.31 (s, 3 H, CH$_3$), 7.01 – 7.07 (m, 2 H, 2×C$_{Ar}$-H), 7.11 (td, J = 6.9, 1.3 Hz, 1 H, 6-H), 7.30 – 7.52 (m, 8 H, 7-H, 7×C$_{Ar}$-H), 8.33 (dt, J = 6.9, 1.1 Hz, 1 H, 5-H), 8.59 (dt, J = 9.2, 1.2 Hz, 1 H, 8-H). ^{13}**C NMR** (75 MHz, CDCl$_3$) δ = 21.6 (q, CH$_3$), 98.3 (s, CN), 112.0 (s, C-1), 112.6 (s, C-3), 115.7 (d, C-6), 119.9 (d, C-8), 125.6 (d, C-5), 126.7 (d, 2×C$_{Ar}$-H), 127.0 (d, C-7), 128.2 (d, 2×C$_{Ar}$-H), 129.3 (s, C$_{Ar}$), 129.4 (d, 2×C$_{Ar}$-H), 129.4 (d, C$_{Ar}$-H), 130.6 (d, 2×C$_{Ar}$-H), 136.4 (s, C-8a), 139.5 (s, C-2), 140.2 (s, C$_{Ar}$), 143.7 (s, C$_{Ar}$). **HRMS** (ESI): calcd. for [C$_{22}$H$_{17}$N$_2$O$_2$S]$^+$ 373.1005, found 373.1005. DA774

Ethyl 1-cyano-2-phenylindolizine-3-carboxylate (11f). From **3aH$^+$Br$^-$** (148 mg, 600 µmol), **2f** (65 mg, 0.50 mmol) and chloranil (246 mg, 1.00 mmol) according to procedure **C**. **11f** was obtained as colorless solid (131 mg, 450 µmol, 90%). R_f (n-pentane:EtOAc 5:1) = 0.31. **Mp.** (Et$_2$O): 136 °C. ^{1}**H NMR** (300 MHz, CDCl$_3$) δ =
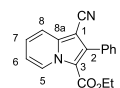
1.02 (t, J = 7.1 Hz, 3 H, CH$_3$), 4.17 (q, J = 7.1 Hz, 2 H, CH$_2$), 7.04 (td, J = 7.0, 1.4 Hz, 1 H, 6-H), 7.37 (ddd, J = 8.9, 6.8, 1.1 Hz, 1 H, 7-H), 7.41 – 7.53 (m, 5 H, 5×C$_{Ar}$-H), 7.76 (dt, J = 8.9, 1.2 Hz, 1 H, 8-H), 9.62 (dt, J = 7.2, 1.1 Hz, 1 H, 5-H). **^{13}C NMR** (75 MHz, CDCl$_3$) δ = 13.8 (q, CH$_3$), 60.6 (t, CH$_2$), 86.4 (s, CN), 112.7 (s, C-1 or C-3), 115.1 (d, C-6), 115.4 (s, C-1 or C-3), 117.4 (d, C-8), 126.3 (d, C-7), 127.9 (d, 2×C$_{Ar}$-H), 128.5 (C$_{Ar}$-H), 128.8 (d, C-5), 130.0 (2×C$_{Ar}$-H), 132.7 (s, C$_{Ar}$), 139.9 (s, C-8a), 140.7 (s, C-2), 161.2 (s, CO$_2$). **HRMS** (ESI): calcd. for [C$_{18}$H$_{15}$N$_2$O$_2$]$^+$ 291.1128, found 291.1128. DA772

3-Acetyl-2-phenylindolizine-1-carbonitrile (11g). From **3eH$^+$Br$^-$** (149 mg, 750 µmol), **2g** (73 mg, 0.50 mmol) and chloranil (246 mg, 1.00 mmol) according to procedure **C**. **11g** was obtained as colorless solid (66 mg, 0.25 mmol, 50%). R_f (*n*-pentane:EtOAc 5:1) = 0.20. **Mp.** (Et$_2$O): 161 °C. **^{1}H NMR** (300 MHz, CDCl$_3$) δ = 2.01 – 1.91 (m, 3 H, CH$_3$), 7.04 (t, J = 6.9, 1 H, 6-H), 7.39 – 7.30 (m, 1 H, 7-H), 7.49 – 7.38 (m, 5 H, 5×C$_{Ar}$-H), 8.28 (dd, J = 6.8, 0.9, 1 H, 5-H), 8.52 (dd, J = 9.1, 0.8, 1 H, 8-H). **^{13}C NMR** (75 MHz, CDCl$_3$) δ = 30.7 (q, CH$_3$), 97.5 (s, CN), 112.8 (s, C-1), 114.2 (d, C-3), 116.0 (d, C-6), 121.6 (d, C-8), 125.3 (d, C-5), 127.6 (d, C-7), 128.9 (d, 2× C$_{Ar}$-H), 129.4 (d, C$_{Ar}$-H), 129.9 (d, 2×C$_{Ar}$-H), 132.2 (s, C$_{Ar}$), 138.2 (s, C-8a), 140.7 (s, C-2), 194.3 (s, CO). **HRMS** (EI): calcd. for [C$_{17}$H$_{12}$N$_2$O]$^+$ 260.0944, found 260.0943. **MS** (EI) *m/z*: 261 (9), 260 (56), 245 (100), 216 (30), 190 (12), 130 (10), 58 (23), 43 (72). DA846

1-(1-Benzoyl-2-phenylindolizin-3-yl)ethanone (11h). From **3dH$^+$Cl$^-$** (128 mg, 750 µmol), **2h** (104 mg, 500 µmol) and chloranil (246 mg, 1.00 mmol) according to procedure **C**. **11h** was obtained as colorless solid (116 mg, 336 µmol, 67%). R_f (*n*-pentane:EtOAc 5:1) = 0.46. **Mp.** (Et$_2$O): 154 °C. **^{1}H NMR** (300 MHz, CDCl$_3$) δ = 1.95 (s, 3 H, CH$_3$), 7.05 (td, J = 7.0, 1.5 Hz, 1 H, 6-H), 7.10 – 7.33 (m, 9 H, 8×C$_{Ar}$-H, superimposed by solvent), 7.36 (ddd, J = 8.9, 6.8, 1.2 Hz, 1 H, 7-H), 7.42 – 7.55 (m, 2 H, 2×C$_{Ar}$-H), 7.96 (dt, J = 9.0, 1.3 Hz, 1 H, 8-H), 10.04 (dt, J = 7.2, 1.1 Hz, 1 H, 5-H). **^{13}C NMR** (75 MHz, CDCl$_3$) δ = 30.8 (q, CH$_3$), 115.5 (s, C-1), 115.6 (d, C-6), 119.1 (d, C-8), 122.2 (s, C-3), 127.5 (d, C-7), 127.9 (d, 2×C$_{Ar}$-H), 128.0 (d, 2×C$_{Ar}$-H), 128.1 (d, C$_{Ar}$-H), 129.0 (d, C-5), 129.2 (d, 2×C$_{Ar}$-H), 130.8 (d, 2×C$_{Ar}$-H), 131.6 (d, C$_{Ar}$-H), 134.7 (s, C$_{Ar}$), 138.7 (s, C-8a), 139.9 (s, C$_{Ar}$), 140.0 (s, C-2), 190.4 (s, CO), 192.8 (s, CO). **HRMS** (ESI): calcd. for [C$_{23}$H$_{18}$NO$_2$]$^+$ 340.1332, found 340.1331. DA781

7.4.2.4 Synthesis of the Cyclopropanes 13

General Procedure D for the Synthesis of Cyclopropanes 13. KO^{t}Bu (750 µmol) in DMSO (2 mL) was added dropwise to solutions of **1** (0.50 mmol) and **4H$^+$BF$_4^-$** (600−750 µmol) in DMSO (5 mL) at room temperature over 1–5 min. The solution was stirred for additional 5 min then sat. aq. NH$_4$Cl (25 mL) was added. The aqueous layer was extracted with CH$_2$Cl$_2$ (3×15 mL), the combined organic layers were washed with brine (2×20 mL), and dried over Na$_2$SO$_4$. The solvent was evaporated and the residue was purified by column chromatography over silica (*n*-pentane:EtOAc 20:1–10:1).

Methyl 2-(4-cyanophenyl)cyclopropanecarboxylate (13a). From **4H$^+$BF$_4^-$** (200 mg, 750 µmol), **1a** (43 mg, 0.50 mmol), and KO^{t}Bu (84 mg, 0.75 mmol) according to procedure **D**. **13a** was obtained as colorless oil which solidified slowly at ambient temperature (64 mg, 0.32 mmol, 64%, *dr* 2:1 in the crude product, 5:1 after column chromatography). *major-, #minor diastereoisomer; signal of one proton of the minor diastereoisomer was set to 1.0. **¹H NMR** (300 MHz, CDCl$_3$) δ = 1.35 (ddd, *J* = 8.5, 6.4, 4.8 Hz, 5 H, C*H*H),* 1.43 (ddd, *J* = 8.6, 8.0, 5.3 Hz, 1 H, C*H*H),# 1.62–1.77 (m, 6 H, 2×CH*H*),*,# 1.96 (ddd, *J* = 8.5, 5.5, 4.2 Hz, 5 H, CH),* 2.18 (ddd, *J* = 9.2, 8.0, 5.7 Hz, 1 H, CH),# 2.64 – 2.49 (m, 6 H, 2×CH),*,# 3.47 (s, 3 H, CH$_3$),# 3.72 (s, 15 H, CH$_3$),* 7.13 – 7.20 (m, 11 H, 2×C$_{Ar}$-H, superimposed by solvent),* 7.36 (d, *J* = 8.0 Hz, 2 H, 2×C$_{Ar}$-H),# 7.52 – 7.60 (m, 12 H, 4× C$_{Ar}$-H).*,# **¹³C NMR** (75 MHz, CDCl$_3$) δ = 11.9 (t, CHH),# 17.6 (t, CHH),* 22.2 (d, CH),# 24.7 (d, CH),* 25.5 (d, CH),# 26.1 (d, CH),* 51.8 (q, CH$_3$),# 52.2 (q, CH$_3$),* 110.4 (s, C$_{Ar}$),# 110.6 (s, C$_{Ar}$),* 118.9 (s, CN),# 119.0 (s, CN),* 126.9 (d, C$_{Ar}$-H),* 130.1 (d, C$_{Ar}$-H),# 131.8 (d, C$_{Ar}$-H),# 132.4 (d, 2× C$_{Ar}$-H),* 142.3 (s, C$_{Ar}$),# 145.9 (s, C$_{Ar}$),* 171.0 (s, CO$_2$),# 173.1 (s, CO$_2$).* **HRMS** (EI): calcd. for [C$_{12}$H$_{11}$NO$_2$]$^+$ 201.0784, found 201.0781. **MS** (EI) *m/z*: 201 (6), 169 (4), 142 (11), 115 (5), 58 (32), 43 (100). DA834-2

Ethyl 2-(4-cyanophenyl)cyclopropanecarboxylate (13b). From **4H$^+$BF$_4^-$** (159 mg, 600 µmol), **1b** (50 mg, 0.50 mmol), and KO^{t}Bu (67 mg, 0.60 mmol) according to procedure **D**. **13b** was obtained as colorless oil (71 mg, 0.33 mmol, 66%, *dr*~7:1 in the crude product, 4:1 after column chromatography). *major-, #minor diastereoisomer; signal of one proton of the minor diastereoisomer was set to 1.0. **¹H NMR** (300 MHz, CDCl$_3$) δ = 1.00 (t, *J* = 7.1 Hz, 3 H, CH$_3$),# 1.20 – 1.48 (m, 17 H, CH$_3$, 2×C*H*H),*,# 1.62 – 1.76 (m, 5 H, 2×CH*H*),*,# 1.94 (ddd, *J* = 8.4, 5.5, 4.2 Hz, 4 H, CH),* 2.09 – 2.22 (m, 1 H, CH),# 2.47 – 2.57 (m, 5 H, 2×CH),*,# 3.88 (q, *J* = 7.1 Hz, 2 H, CH$_2$),# 4.16 (q, *J* = 7.1 Hz, 8 H, CH$_2$),* 7.16 (d,

J = 8.3 Hz, 8 H, 2×C$_{Ar}$-H),* 7.33 – 7.38 (m, 2 H, 2×C$_{Ar}$-H),# 7.50 – 7.59 (m, 10 H, 4×C$_{Ar}$-H).*,# **^{13}C NMR** (75 MHz, CDCl$_3$) δ = 11.6 (t, CH$_2$),# 14.2 (q, CH$_3$),* 14.3 (q, CH$_3$),* 17.6 (t, CH$_2$),* 22.4 (d, CH),# 24.9 (d, CH),* 25.4 (d, CH),# 25.9 (d, CH),* 60.6 (d, CH$_2$),# 61.1 (d, CH$_2$),* 110.3 (s, C$_{Ar}$),* 110.5 (s, C$_{Ar}$),# 118.9 (s, CN),* 119.0 (s, CN),# 126.9 (d, 2×C$_{Ar}$-H),* 130.2 (d, 2×C$_{Ar}$-H),# 131.7 (d, 2×C$_{Ar}$-H),# 132.3 (d, 2×C$_{Ar}$-H),* 142.4 (s, C$_{Ar}$)#, 146.0 (s, C$_{Ar}$),* 170.5 (s, CO$_2$),# 172.6 (s, CO$_2$).* **HRMS** (EI): calcd. for [C$_{13}$H$_{13}$NO$_2$]$^+$ 215.0941, found 215.0935. **MS** (EI) m/z: 216 (10), 215 (66), 187 (27), 170 (37), 142 (100), 140 (34), 115 (25). DA658

tert-**Butyl 2-(4-Cyanophenyl)cyclopropanecarboxylate (13c).** From **4H$^+$BF$_4$$^−$** (200 mg, 750 μmol), **1c** (64 mg, 0.50 mmol), and KO^{t}Bu (84 mg, 0.75 mmol) according to procedure **D**. **13c** was obtained as colorless oil (73 mg, 0.30 mmol, 60%, *dr* 5:1 after column chromatography). Only signals of the major diastereoisomer given. **^{1}H NMR** (400 MHz, CDCl$_3$) δ = 1.17 (s, 9 H, C(CH$_3$)$_3$), 1.33 (ddd, J = 8.5, 7.9, 5.2 Hz, 1 H, C*H*H), 1.69 – 1.62 (m, 1 H, CH*H*), 2.03 – 2.11 (m, 1 H, CH), 2.48 – 2.57 (m, 1 H, CH), 7.39 – 7.35 (m, 2 H, 2×C$_{Ar}$-H), 7.57 – 7.54 (m, 2 H, 2×C$_{Ar}$-H). **^{13}C NMR** (100 MHz, CDCl$_3$) δ = 11.1 (t, CHH), 23.4 (d, CH), 25.1 (d, CH), 28.0 (q, C(*C*H$_3$)$_3$), 80.8 (s, *C*(CH$_3$)$_3$), 110.4 (s, C$_{Ar}$), 119.2 (s, CN), 130.4 (d, 2×C$_{Ar}$-H), 131.7 (d, 2×C$_{Ar}$-H), 142.9 (s, C$_{Ar}$), 169.6 (s, CO$_2$). **HRMS** (EI): calcd. for [C$_{11}$H$_9$NO$_2$]$^+$ (M–C$_4$H$_8$) 187.0628, found 187.0634. **MS** (EI) m/z: 187 (100), 170 (44), 142 (44), 85 (63), 83 (100), 57 (62). DA833-2

4-(2-(Phenylsulfonyl)cyclopropyl)benzonitrile (13e). From **4H$^+$BF$_4$$^−$** (200 mg, 750 μmol), **1e** (84 mg, 0.50 mmol), and KO^{t}Bu (84 mg, 0.75 mmol) according to procedure **D**. **13e** was obtained as colorless oil, which solidified slowly at ambient temperature (130 mg, 430 μmol, 88%, single diastereoisomer). **Mp**. 127 °C. **^{1}H NMR** (300 MHz, CDCl$_3$) δ = 1.50 (ddd, J = 8.4, 6.6, 5.9 Hz, 1 H C*H*H), 1.88 – 1.98 (m, 1 H, CH*H*), 2.72 (ddd, J = 8.5, 5.5, 4.5 Hz, 1 H, CH), 2.87 – 3.01 (m, 1 H, CH), 7.08 – 7.16 (m, 2 H, 2×C$_{Ar}$-H), 7.49 – 7.62 (m, 2 H, 4×C$_{Ar}$-H), 7.63 – 7.71 (m, 1 H, C$_{Ar}$-H), 7.88 – 7.96 (m, 2 H, 2×C$_{Ar}$-H). **^{13}C NMR** (75 MHz, CDCl$_3$) δ = 14.5 (t, CH$_2$), 23.4 (d, CH), 42.3 (d, CH), 111.0 (s, C$_{Ar}$), 118.4 (s, CN), 127.3 (d, 2×C$_{Ar}$-H), 127.6 (d, 2×C$_{Ar}$-H), 129.4 (d, 2×C$_{Ar}$-H), 132.4 (d, 2×C$_{Ar}$-H), 133.8 (d, C$_{Ar}$-H), 140.0 (s, C$_{Ar}$), 143.0 (s, C$_{Ar}$). **HRMS** (EI): calcd. for [C$_{16}$H$_{13}$NO$_2$S]$^+$ 283.0662, found 283.0667. **MS** (EI) m/z: 283 (3), 143 (8), 142 (100), 140 (12). DA662

4-(2-Cyanocyclopropyl)benzonitrile (13f). From **4H⁺BF₄⁻** (200 mg, 750 μmol), , **1f** (24 mg, 0.50 mmol), and KO^{t}Bu (84 mg, 0.75 mmol) according to procedure **D**. **9f** was obtained as colorless solid (35 mg, 0.21 mmol, 42%, single diastereoisomer after column). **Mp**. 81 °C. **¹H NMR** (300 MHz, CDCl₃) δ = 1.50 (ddd, J = 8.8, 6.6, 5.4 Hz, 1 H, CHH), 1.59 – 1.77 (m, 2 H, CH, CHH), 2.67 (ddd, J = 9.1, 6.6, 4.8 Hz, 1 H, CH), 7.24 – 7.16 (m, 2 H, 2×C$_{Ar}$-H), 7.66 – 7.56 (m, 2 H, 2×C$_{Ar}$-H). **¹³C NMR** (75 MHz, CDCl₃) δ = 7.6 (d, CH), 15.9 (d, CH₂), 24.8 (d, CH), 111.6 (s, C$_{Ar}$), 118.5 (s, CN), 120.2 (s, CN), 127.2 (d, 2×C$_{Ar}$-H), 132.7 (d, 2×C$_{Ar}$-H), 143.2 (s, C$_{Ar}$). **HRMS** (EI): calcd. for [C₁₁H₈N₂]⁺ 168.0682, found 168.0680. **MS** (EI) m/z: 169 (12), 168 (100), 167 (14), 141 (61), 140 (54), 114 (20). DA661-2
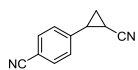
4-(2-Acetylcyclopropyl)benzonitrile (13g). From **4H⁺BF₄⁻** (159 mg, 0.60 mmol), **1g** (35 mg, 0.50 mmol) and KO^{t}Bu (67 mg, 0.60 mmol) according to procedure **D**. **13g** was obtained as colorless oil (62 mg, 0.34 mmol, 68%, dr 3:1). The signals of the minor diastereoisomer could not be assigned in the ¹H NMR due to overlap with the major diastereoisomer. Major: **¹H NMR** (300 MHz, CDCl₃) δ = 1.38 (ddd, J = 8.3, 6.4, 4.4 Hz, 1 H, CHH), 1.71 (ddd, J = 9.0, 5.4, 4.4 Hz, 1 H, CHH), 2.21 – 2.29 (m, 1 H, CH), 2.31 (s, 3 H, CH₃), 2.53 (ddd, J = 9.1, 6.4, 4.1 Hz, 1 H, CH), 7.12 – 7.19 (m, 2 H, 2×C$_{Ar}$-H), 7.53 – 7.60 (m, 2 H, 2×C$_{Ar}$-H). *major-, #minor diastereoisomer. **¹³C NMR** (75 MHz, CDCl₃) δ = 12.5 (t CH₂),# 19.7 (t, CH₂),* 28.4 (d, CH),# 28.4 (d, CH),* 30.4 (d, CH),# 31.0 (q, CH₃),* 31.8 (q, CH₃),# 33.2 (d, CH),* 110.3 (s, C$_{Ar}$),* 110.6 (s, C$_{Ar}$),# 118.9 (s, 2×CN),*,# 126.8 (d, 2×C$_{Ar}$-H),* 130.0 (d, 2×C$_{Ar}$-H),# 131.8 (d, 2×C$_{Ar}$-H),# 132.4 (d, 2×C$_{Ar}$-H),* 141.9 (s, C$_{Ar}$),# 146.2 (s, C$_{Ar}$),* 203.6 (s, CO),# 205.9 (s, CO).* **HRMS** (EI): calcd. for [C₁₂H₁₁NO]⁺ 185.0835, found 185.0837. **MS** (EI) m/z: 186 (13), 185 (95), 170 (34), 143 (59), 142 (64), 115 (31), 89 (12), 43 (100). DA655
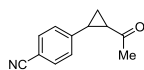
4-(2-Benzoylcyclopropyl)benzonitrile (13h). From **4H⁺BF₄⁻** (200 mg, 750 μmol), **1h** (66 mg, 0.50 μmol), and KO^{t}Bu (84 mg, 0.75 mmol) according to procedure **D**. The diastereoisomers of **13h** were obtained as colorless oils (over all: 103 mg, 417 μmol, 83%, dr 3:1). **Major**: **¹H NMR** (300 MHz, CDCl₃) δ = 1.34 – 1.70 (m, 1 H, CHH), 1.97 (ddd, J = 8.9, 5.4, 4.3 Hz, 1 H, CHH), 2.74 (ddd, J = 8.9, 6.5, 4.0 Hz, 1 H, CH), 2.89 – 3.01 (m, 1 H, CH), 7.22 – 7.29 (m, 2 H, 2×C$_{Ar}$-H, superimposed by solvent), 7.44 – 7.51 (m, 2 H, 2×C$_{Ar}$-H), 7.54 – 7.63 (m, 3 H, 3×C$_{Ar}$-H), 7.92 – 8.03 (m, 2 H, 2×C$_{Ar}$-H). **¹³C NMR** (75 MHz, CDCl₃) δ = 19.8 (t, CH₂), 29.3 (s, CH), 29.7 (s, CH), 110.4 (s, CN), 118.9 (s, C$_{Ar}$), 127.0 (d, 2×C$_{Ar}$-H), 128.2 (d, 2×C$_{Ar}$-H), 128.8 (d, 2×C$_{Ar}$-H), 132.5 (d, 2×C$_{Ar}$-H), 133.4 (d, C$_{Ar}$-H), 137.5 (s, C$_{Ar}$), 146.4 (s, C$_{Ar}$), 197.7 (s, CO). **HRMS** (EI): calcd. for [C₁₇H₁₃NO]⁺ 247.0992,
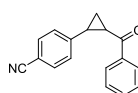
found 247.0978. **MS** (EI) m/z: 248, (19), 247 (100), 246 (31), 232 (10), 140 (10), 115 (11), 105 (72), 77 (32). **Minor**: ^{1}**H NMR** (300 MHz, CDCl$_3$) δ = 1.53 – 1.61 (m, 1 H, C*H*H), 2.05 – 2.15 (m, 1 H, CH*H*), 2.92 – 2.99 (m, 1 H, CH, superimposed by major diastereoisomer), 3.12 – 3.34 (m, 1 H, CH), 7.23 – 7.33 (m, 2 H, 2×C$_{Ar}$-H, superimposed by solvent), 7.36 – 7.57 (m, 3 H, 3×C$_{Ar}$-H, superimposed by major diastereoisomer), 7.57 – 7.64 (m, 2 H, 2×C$_{Ar}$-H), 7.84 – 7.91 (m, 2 H, 2×C$_{Ar}$-H). ^{13}**C NMR** (75 MHz, CDCl$_3$) δ 12.4 (t, CH$_2$), 27.3 (d, CH), 29.1 (d, CH), 110.5 (s, C$_{Ar}$), 119.0 (s, CN), 128.1 (d, 2×C$_{Ar}$-H), 128.7 (d, 2×C$_{Ar}$-H), 129.9 (d, 2×C$_{Ar}$-H), 131.8 (d, 2×C$_{Ar}$-H), 132.5 (d, C$_{Ar}$-H), 138.3 (s, C$_{Ar}$), 142.0 (s, C$_{Ar}$), 195.6 (s, CO). **HRMS** (EI): calcd. for [C$_{17}$H$_{13}$NO]$^{.+}$ 247.0992, found 247.1001. **MS** (EI) m/z: 248, (20), 247 (100), 246 (48), 232 (10), 140 (11), 116 (27), 105 (78), 77 (37). DA691

7.4.3   Kinetics of the Reactions of the Michael Acceptors 1 and 2 with the Ylides 3 and 4

7.4.3.1   Reactions with Methyl acrylate 1a

Table 7.6. Kinetics of the reaction of 1a with 3a (DMSO, 20 °C, Stopped-flow method, detection at 425 nm).

No.	[3a]/mol L^{-1}	[1a]/ mol L^{-1}	k_{obs}/s^{-1}
MEA1-1	1×10^{-4}	2.08×10^{-3}	2.69
MEA1-2	1×10^{-4}	3.12×10^{-3}	3.39
MEA1-3	1×10^{-4}	4.16×10^{-3}	4.88
MEA1-4	1×10^{-4}	5.20×10^{-3}	6.16
MEA1-5	1×10^{-4}	6.24×10^{-3}	7.00
k_2(20 °C) = 1.10 × 10^3 L mol^{-1} s^{-1}			

y = 1095.4x + 0.268
R² = 0.9878
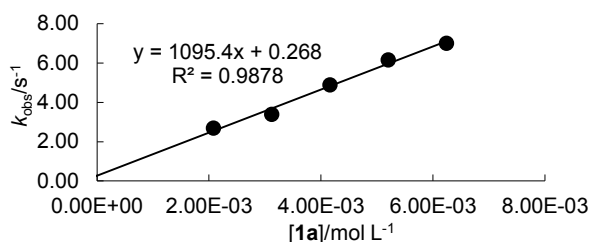
Table 7.7. Kinetics of the reaction of 1a with 3b (DMSO, 20 °C, Stopped-flow method, detection at 425 nm).

No.	[3b]/mol L^{-1}	[1a]/ mol L^{-1}	k_{obs}/s^{-1}
MEA3-1	2×10^{-4}	2.08×10^{-3}	1.26×10^1
MEA3-2	2×10^{-4}	3.12×10^{-3}	1.80×10^1
MEA3-3	2×10^{-4}	4.16×10^{-3}	2.55×10^1
MEA3-4	2×10^{-4}	5.20×10^{-3}	3.31×10^1
MEA3-5	2×10^{-4}	6.24×10^{-3}	4.10×10^1
k_2(20 °C) = 6.91 × 10^3 L mol^{-1} s^{-1}			
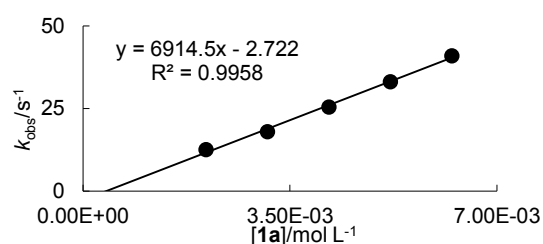
y = 6914.5x - 2.722
R² = 0.9958

Bisexponential decays. The initial rate is assigned to the betaine formation. The bisexponential decays may be caused by a rate determining ring-closure.

Table 7.8. Kinetics of the reaction of 1a with 3c (DMSO, 20 °C, Stopped-flow method, detection at 425 nm).

No.	$[3c]$/mol L^{-1}	$[1a]$/ mol L^{-1}	k_{obs}/s^{-1}
MEA2-1	1×10^{-4}	2.08×10^{-3}	4.99
MEA2-2	1×10^{-4}	3.12×10^{-3}	6.18
MEA2-3	1×10^{-4}	4.16×10^{-3}	8.90
MEA2-4	1×10^{-4}	5.20×10^{-3}	1.13×10^1
MEA2-5	1×10^{-4}	6.24×10^{-3}	1.29×10^1
k_2(20 °C) = 2.01×10^3 L mol^{-1} s^{-1}			

y = 2013.8x + 0.478
R² = 0.9868
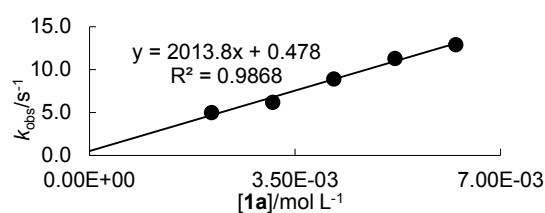
Table 7.9. Kinetics of the reaction of 1a with 3d (DMSO, 20 °C, Stopped-flow method, detection at 425 nm).

No.	$[3c]$/mol L^{-1}	$[1a]$/ mol L^{-1}	k_{obs}/s^{-1}
MEA2-1	1×10^{-4}	2.08×10^{-3}	3.11×10^{-2}
MEA2-2	1×10^{-4}	3.12×10^{-3}	4.02×10^{-2}
MEA2-3	1×10^{-4}	4.16×10^{-3}	5.75×10^{-2}
MEA2-4	1×10^{-4}	5.20×10^{-3}	7.52×10^{-2}
MEA2-5	1×10^{-4}	6.24×10^{-3}	8.48×10^{-2}
k_2(20 °C) = 1.37×10^1 L mol^{-1} s^{-1}			

y = 13.694x + 0.0008
R² = 0.987
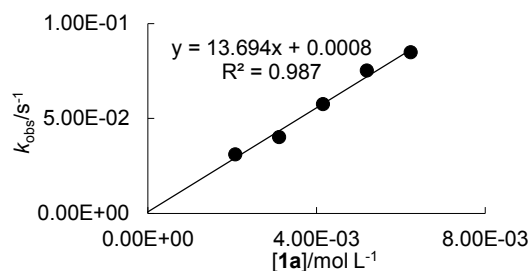
Table 7.10. Kinetics of the reaction of 1a with 4 (DMSO, 20 °C, J&M method, detection at 371 nm).

No.	$[4]$/mol L^{-1}	$[1a]$/ mol L^{-1}	k_{obs}/s^{-1}
MEA5-1	1×10^{-4}	5.19×10^{-3}	1.99×10^{-2}
MEA5-2	1×10^{-4}	4.19×10^{-3}	1.60×10^{-2}
MEA5-3	1×10^{-4}	3.13×10^{-3}	1.32×10^{-2}
MEA5-5	1×10^{-4}	3.98×10^{-3}	1.56×10^{-2}
k_2(20 °C) = 3.25 L mol^{-1} s^{-1}			

y = 3.2461x + 0.0028
R² = 0.9866
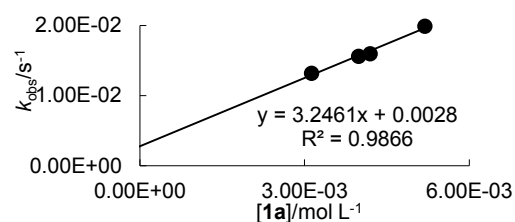
Table 7.11. Calculation of the Electrophilicity Parameter E for 1a using the N and sN Parameters of 3,4, Eq 7.1, and the Second-Order Rate Constants for the Reactions of 1a with 3,4.

Nucleophile	N/s_N	k_2/ L mol^{-1} s^{-1}
3a	26.71/0.37	1.10×10^3
3b	27.45/0.38	6.91×10^3
3c	25.94/0.42	2.01×10^3
3d	20.24/0.60	1.37×10^1
4	21.07/0.68	3.25
E (**1a**)$^{[a]}$ = $-$ 18.92		

log k_2/s_N = N - 18.923
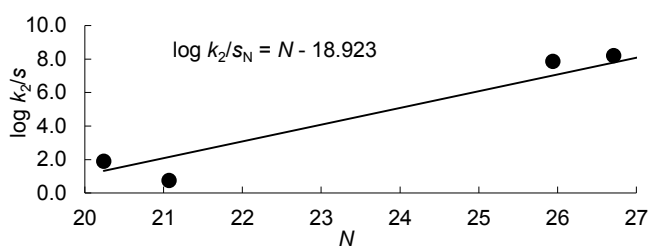
[a] Calculated by least square minimization according to eq 7.1 using N, s_N from Table 7.1.

7.4.3.2 Reactions with Ethyl acrylate (1b)

Table 7.12. Kinetics of the reaction of 1b with 3a (DMSO, 20 °C, Stopped-flow method, detection at 425 nm).

No.	[3a]/mol L^{-1}	[1b]/ mol L^{-1}	k_{obs}/s^{-1}
EA1-1	1×10^{-4}	1.00×10^{-3}	8.52×10^{-1}
EA1-2	1×10^{-4}	2.00×10^{-3}	1.76
EA1-3	1×10^{-4}	3.00×10^{-3}	2.82
EA1-4	1×10^{-4}	4.00×10^{-3}	3.74
EA1-5	1×10^{-4}	5.00×10^{-3}	5.20
k_2(20 °C) = 1.07×10^3 L mol^{-1} s^{-1}			

$y = 1067.6x - 0.3284$
$R^2 = 0.9917$

Table 7.13. Kinetics of the reaction of 1b with 3c (DMSO, 20 °C, Stopped-flow method, detection at 425 nm).

No.	[3c]/mol L^{-1}	[1b]/ mol L^{-1}	k_{obs}/s^{-1}
EA2-1	1×10^{-4}	1.00×10^{-3}	1.63
EA2-2	1×10^{-4}	2.00×10^{-3}	3.60
EA2-3	1×10^{-4}	3.00×10^{-3}	5.10
EA2-4	1×10^{-4}	4.00×10^{-3}	6.38
EA2-5	1×10^{-4}	5.00×10^{-3}	8.57
k_2(20 °C) = 1.67×10^3 L mol^{-1} s^{-1}			

$y = 1665.6x + 0.06$
$R^2 = 0.9926$
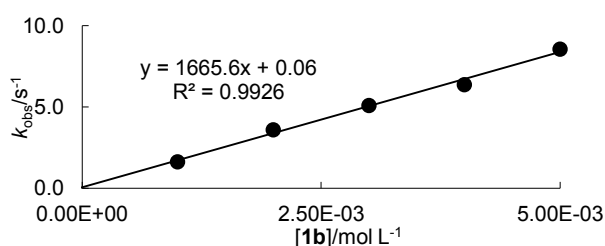
Table 7.14. Kinetics of the reaction of 1b with 3d (DMSO, 20 °C, Stopped-flow method, detection at 425 nm).

No.	[3d]/mol L^{-1}	[1b]/ mol L^{-1}	k_{obs}/s^{-1}
EA4-1	3×10^{-5}	2.00×10^{-3}	2.08×10^{-2}
EA4-2	3×10^{-5}	3.00×10^{-3}	3.30×10^{-2}
EA4-3	3×10^{-5}	4.00×10^{-3}	4.54×10^{-2}
EA4-4	3×10^{-5}	5.00×10^{-3}	5.60×10^{-2}
EA4-5	3×10^{-5}	6.00×10^{-3}	6.51×10^{-2}
k_2(20 °C) = 1.12×10^1 L mol^{-1} s^{-1}			

$y = 11.16x - 0.0006$
$R^2 = 0.9961$
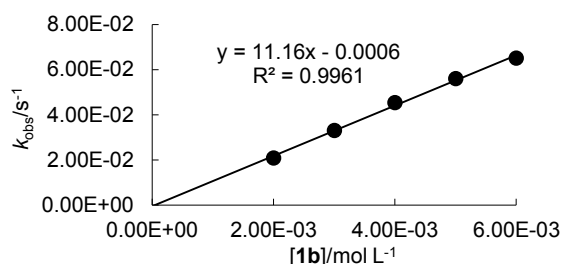
Table 7.15. Kinetics of the reaction of 1b with 4 (DMSO, 20 °C, J&M method, detection at 371 nm).

No.	[4]/mol L^{-1}	[1b]/ mol L^{-1}	k_{obs}/s^{-1}
EA9-1	9×10^{-5}	4.94×10^{-3}	1.74×10^{-2}
EA9-2	9×10^{-5}	4.25×10^{-3}	1.54×10^{-2}
EA9-3	9×10^{-5}	3.75×10^{-3}	1.32×10^{-2}
EA9-4	9×10^{-5}	3.32×10^{-3}	1.13×10^{-2}
EA9-5	9×10^{-5}	2.93×10^{-3}	9.74×10^{-3}
k_2(20 °C) = 3.89 L mol^{-1} s^{-1}			

$y = 3.8944x - 0.0015$
$R^2 = 0.9927$
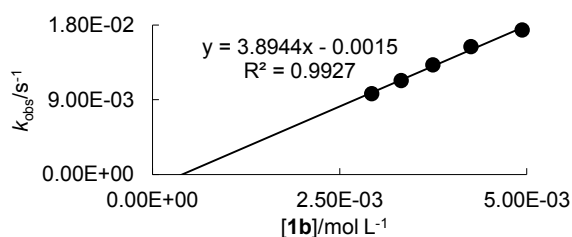
Table 7.16. Calculation of the Electrophilicity Parameter E for 1b using the N and s_N Parameters of 3,4, Eq 7.1, and the Second-Order Rate Constants for the Reactions of 1b with 3,4.

Nucleophile	N/s_N	k_2/ L mol^{-1} s^{-1}
3a	26.71/0.37	1.07×10^3
3c	25.94/0.42	1.67×10^3
3d	20.24/0.60	1.12×10^1
4	21.07/0.68	3.89
E (**1b**) [a] = − 19.16		

log $k_2/s_N = N - 19.158$
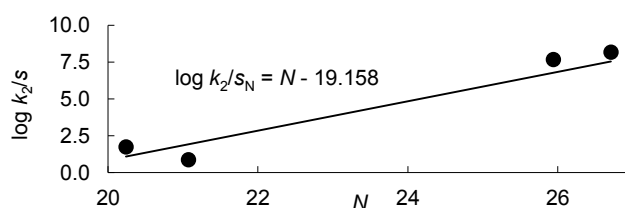
[a] Calculated by least square minimization according to eq 7.1 using N, s_N from Table 7.1.

### 7.4.3.3 Reactions with *tert*-Butyl acrylate (1c)

Table 7.17. Kinetics of the reaction of 1c with 3a (DMSO, 20 °C, Stopped-flow method, detection at 425 nm).

No.	[3a]/mol L^{-1}	[1c]/ mol L^{-1}	k_{obs}/s^{-1}
tBuAA1-1	4×10^{-4}	4.00×10^{-3}	1.12
tBuAA1-2	4×10^{-4}	6.00×10^{-3}	1.68
tBuAA1-3	4×10^{-4}	8.00×10^{-3}	2.26
tBuAA1-4	4×10^{-4}	1.00×10^{-2}	2.76
tBuAA1-5	4×10^{-4}	1.20×10^{-2}	3.19
k_2(20 °C) = 2.61 × 10^2 L mol^{-1} s^{-1}			

y = 261x + 0.114
R² = 0.9966

Table 7.18. Kinetics of the reaction of 1c with 3b (DMSO, 20 °C, Stopped-flow method, detection at 427 nm).

No.	[3b]/mol L^{-1}	[1c]/ mol L^{-1}	k_{obs}/s^{-1}
tBuAA5-1	8×10^{-4}	8.00×10^{-3}	1.72
tBuAA5-2	8×10^{-4}	1.20×10^{-2}	2.58
tBuAA5-3	8×10^{-4}	1.60×10^{-2}	4.12
tBuAA5-4	8×10^{-4}	2.00×10^{-2}	5.47
tBuAA5-5	8×10^{-4}	2.40×10^{-2}	7.08
k_2(20 °C) = 3.40 × 10^2 L mol^{-1} s^{-1}			

y = 340.25x - 1.25
R² = 0.9912
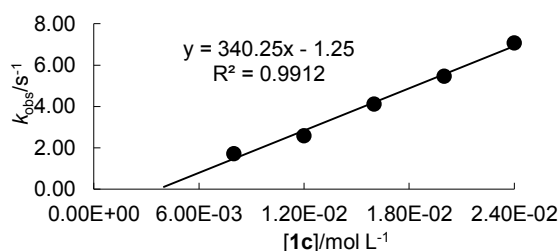
Table 7.19. Kinetics of the reaction of 1c with 3c (DMSO, 20 °C, Stopped-flow method, detection at 445 nm).

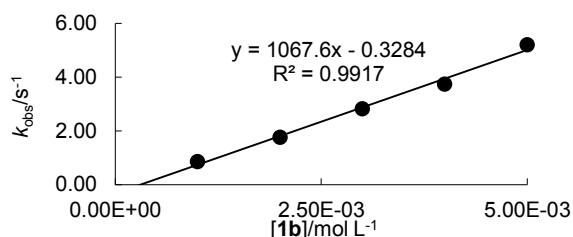| No.	[3c]/mol L^{-1}	[1c]/ mol L^{-1}	k_{obs}/s^{-1}
tBuAA4-1	4×10^{-4}	4.00×10^{-3}	9.57×10^{-1}
tBuAA4-2	4×10^{-4}	8.00×10^{-3}	2.17
tBuAA4-3	4×10^{-4}	1.20×10^{-2}	3.31
tBuAA4-4	4×10^{-4}	1.60×10^{-2}	4.45
tBuAA4-5	4×10^{-4}	2.00×10^{-2}	5.69
k_2(20 °C) = 2.94 × 10^2 L mol^{-1} s^{-1}			

y = 293.65x - 0.2084
R² = 0.9998
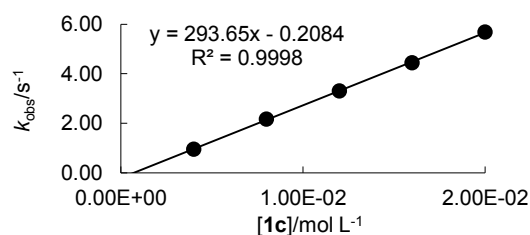
Table 7.20. Kinetics of the reaction of 1c with 3d (DMSO, 20 °C, J&M method, detection at 427 nm).

No.	[3d]/mol L^{-1}	[1c]/ mol L^{-1}	k_{obs}/s^{-1}
tBuAA2-2	3×10^{-4}	4.38×10^{-3}	1.20×10^{-2}
tBuAA2-3	3×10^{-4}	5.93×10^{-3}	1.60×10^{-2}
tBuAA2-4	3×10^{-4}	7.55×10^{-3}	1.90×10^{-2}
tBuAA2-5	3×10^{-4}	8.60×10^{-3}	2.07×10^{-2}
k_2(20 °C) = 2.05 L mol^{-1} s^{-1}			

y = 2.0506x + 0.0034
R² = 0.9896
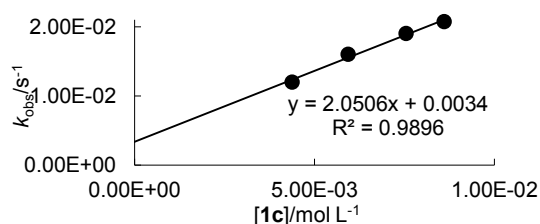
Table 7.21. Kinetics of the reaction of 1c with 4 (DMSO, 20 °C, J&M method, detection at 379 nm).

No.	[4]/mol L^{-1}	[1c]/ mol L^{-1}	k_{obs}/s^{-1}
tBuAA6-1	1×10^{-4}	1.02×10^{-3}	2.63×10^{-3}
tBuAA6-2	1×10^{-4}	1.48×10^{-3}	3.56×10^{-3}
tBuAA6-3	1×10^{-4}	2.01×10^{-3}	4.25×10^{-3}
tBuAA6-5	1×10^{-4}	2.98×10^{-3}	6.39×10^{-3}
k_2(20 °C) = 1.89 L mol^{-1} s^{-1}			

y = 1.8931x + 0.0007
R² = 0.9918
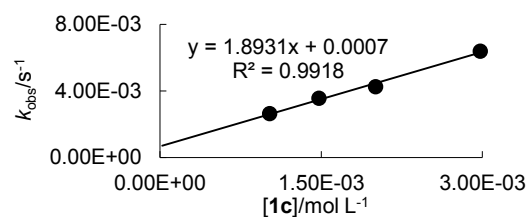
Table 7.22. Calculation of the Electrophilicity Parameter E for 1c using the N and s_N Parameters of 3,4, Eq 7.1, and the Second-Order Rate Constants for the Reactions of 1c with 3,4.

Nucleophile	N/s_N	k_2/ L mol^{-1} s^{-1}
3a	26.71/0.37	2.61×10^2
3c	25.94/0.42	3.40×10^2
3d	20.24/0.60	2.94×10^2
4	21.07/0.68	2.05
E (**1c**) [a] = $-$ 20.28		

$\log k_2/s_N = N - 20.277$
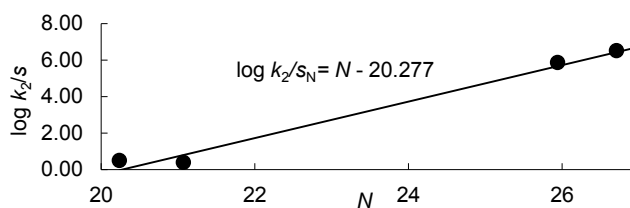
[a] Calculated by least square minimization according to eq 7.1 using N, s_N from Table 7.1.

7.4.3.4 Reactions with *N,N*-Dimethylacrylamide (1d)

Table 7.23. Kinetics of the reaction of 1d with 3a (DMSO, 20 °C, Stopped-flow method, detection at 425 nm).

No.	[**3a**]/mol L^{-1}	[**1d**]/ mol L^{-1}	k_{obs}/s^{-1}
AM4-1	5×10^{-5}	2.68×10^{-3}	2.90×10^{-2}
AM4-2	5×10^{-5}	4.01×10^{-3}	4.23×10^{-2}
AM4-3	5×10^{-5}	5.35×10^{-3}	5.47×10^{-2}
AM4-4	5×10^{-5}	6.69×10^{-3}	7.40×10^{-2}
AM4-5	5×10^{-5}	8.03×10^{-3}	8.83×10^{-2}
k_2(20 °C) = 1.12×10^1 L mol^{-1} s^{-1}			

y = 11.232x - 0.0025
R² = 0.9943
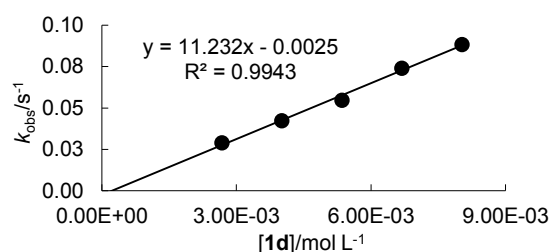
Table 7.24. Kinetics of the reaction of 1d with 3b (DMSO, 20 °C, Stopped-flow method, detection at 425 nm).
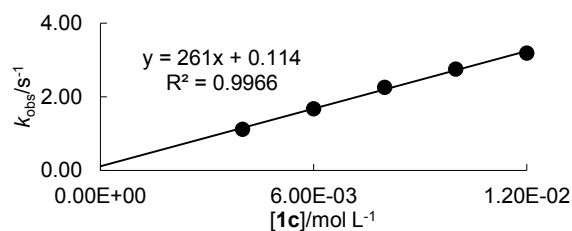
No.	[**3b**]/mol L^{-1}	[**1d**]/ mol L^{-1}	k_{obs}/s^{-1}
AM2-1	5×10^{-5}	2.68×10^{-3}	4.61×10^{-2}
AM2-2	5×10^{-5}	4.01×10^{-3}	6.40×10^{-2}
AM2-3	5×10^{-5}	5.35×10^{-3}	7.85×10^{-2}
AM2-4	5×10^{-5}	6.69×10^{-3}	1.02×10^{-2}
AM2-5	5×10^{-5}	8.03×10^{-3}	1.20×10^{-2}
k_2(20 °C) = 1.39×10^1 L mol^{-1} s^{-1}			

y = 13.885x + 0.0078
R² = 0.9952
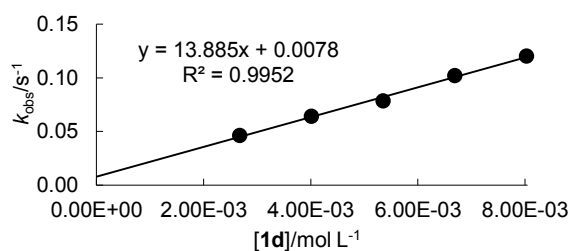
Table 7.25. Kinetics of the reaction of 1d with 3c (DMSO, 20 °C, Stopped-flow method, detection at 425 nm).

No.	[**3c**]/mol L^{-1}	[**1d**]/ mol L^{-1}	k_{obs}/s^{-1}
AM3-1	5×10^{-5}	2.68×10^{-3}	8.24×10^{-2}
AM3-2	5×10^{-5}	4.01×10^{-3}	1.13×10^{-1}
AM3-3	5×10^{-5}	5.35×10^{-3}	1.46×10^{-1}
AM3-4	5×10^{-5}	6.69×10^{-3}	1.85×10^{-1}
AM3-5	5×10^{-5}	8.03×10^{-3}	2.26×10^{-1}
k_2(20 °C) = 2.68×10^1 L mol^{-1} s^{-1}			

y = 26.843x + 0.0068
R² = 0.996
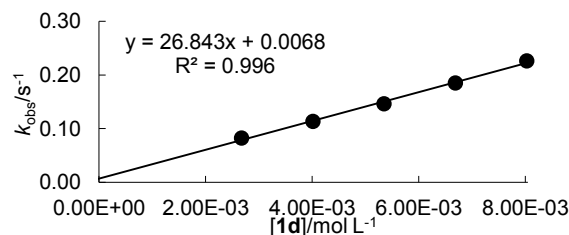
Table 7.26. Calculation of the Electrophilicity Parameter E for 1d using the N and s_N Parameters of 3, Eq 7.1, and the Second-Order Rate Constants for the Reactions of 1d with 3.

Nucleophile	N/s_N	$k_2^{exp}/M^{-1}\,s^{-1}$	$k_2^{calcd}/M^{-1}\,s^{-1}$	k_2^{exp}/k_2^{calcd}
3a	26.71/0.37	1.12×10^1	1.49×10^1	0.75
3b	27.45/0.38	1.39×10^1	3.07×10^1	0.45
3c	25.94/0.42	2.68×10^1	1.02×10^1	2.63
		E (**1d**) [b] $= -23.54$		

[a] By eq 7.1 using N, s_N and E from this Table; [b] Calculated by least square minimization according to eq 7.1 N, s_N and E from this Table.

log $k_2/s_N = N - 23.538$

7.4.3.5 Reactions with (Vinylsulfonyl)benzene (1e)

Table 7.27. Kinetics of the reaction of 1e with 3a (DMSO, 20 °C, Stopped-flow method, detection at 425 nm; from ref. [36]).

No.	[3a]/mol L^{-1}	[1e]/ mol L^{-1}	k_{obs}/s^{-1}
VS4-2	5×10^{-5}	5.12×10^{-4}	7.87×10^{-1}
VS4-3	5×10^{-5}	7.68×10^{-4}	1.18
VS4-4	5×10^{-5}	1.02×10^{-4}	1.60
VS4-6	5×10^{-5}	1.54×10^{-3}	2.42
VS4-8	5×10^{-5}	2.05×10^{-3}	3.23
	$k_2(20\,°C) = 1.60 \times 10^3$ L mol^{-1} s^{-1}		

y = 1595.3x - 0.0363
R² = 0.9999
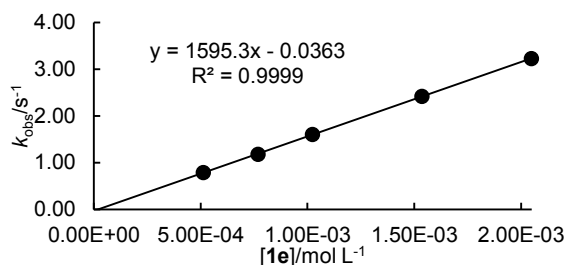
Table 7.28. Kinetics of the reaction of 1e with 3b (DMSO, 20 °C, Stopped-flow method, detection at 425 nm).

No.	[3b]/mol L^{-1}	[1e]/ mol L^{-1}	k_{obs}/s^{-1}
VS4-1	4×10^{-4}	5.02×10^{-3}	3.54×10^1
VS4-2	4×10^{-4}	6.02×10^{-3}	4.08×10^1
VS4-3	4×10^{-4}	7.03×10^{-3}	4.75×10^1
VS4-4	4×10^{-4}	8.03×10^{-3}	5.26×10^1
VS4-5	4×10^{-4}	9.04×10^{-3}	5.74×10^1
	$k_2(20\,°C) = 5.56 \times 10^3$ L mol^{-1} s^{-1}		

y = 5564.2x + 7.615
R² = 0.9969
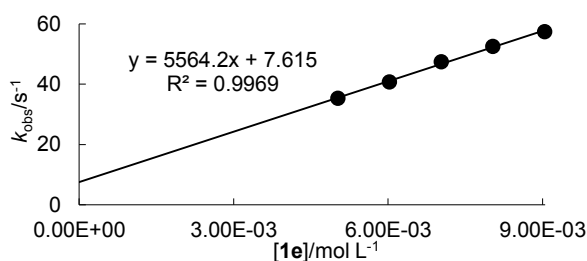
Table 7.29. Kinetics of the reaction of 1b with 3c (DMSO, 20 °C, Stopped-flow method, detection at 425 nm).

No.	[3c]/mol L^{-1}	[1e]/ mol L^{-1}	k_{obs}/s^{-1}
VS4-1	2×10^{-4}	5.02×10^{-3}	1.18×10^1
VS4-2	2×10^{-4}	6.02×10^{-3}	1.41×10^1
VS4-3	2×10^{-4}	7.03×10^{-3}	1.68×10^1
VS4-4	2×10^{-4}	8.03×10^{-3}	1.90×10^1
VS4-5	2×10^{-4}	9.04×10^{-3}	2.22×10^1
k_2(20 °C) = 2.55×10^3 L mol^{-1} s^{-1}			
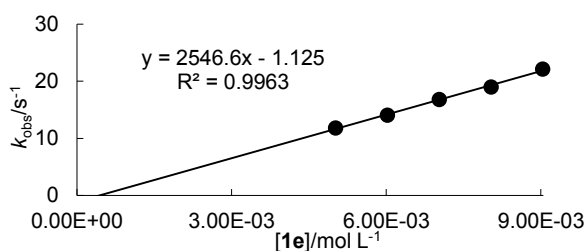
y = 2546.6x - 1.125
R² = 0.9963

Bisexponential decays. The initial rate is assigned to the betaine formation. The bisexponential decays may be caused by a rate determining ring-closure.

Table 7.30. Kinetics of the reaction of 1d with 3d (DMSO, 20 °C, J&M method, detection at 427 nm; from ref. [36]).

No.	[3d]/mol L^{-1}	[1d]/ mol L^{-1}	k_{obs}/s^{-1}
VS5-2	5×10^{-5}	5.22×10^{-4}	1.10×10^{-2}
VS5-3	5×10^{-5}	7.83×10^{-4}	1.60×10^{-2}
VS5-4	5×10^{-5}	1.04×10^{-3}	2.16×10^{-2}
VS5-5	5×10^{-5}	1.30×10^{-3}	2.65×10^{-2}
VS5-6	5×10^{-5}	1.57×10^{-3}	3.11×10^{-2}
k_2(20 °C) = 1.94×10^1 L mol^{-1} s^{-1}			

y = 19.432x + 0.001
R² = 0.999
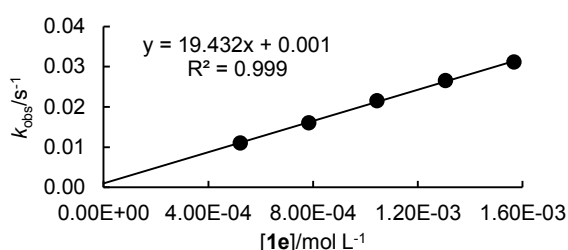
Table 7.31. Kinetics of the reaction of 1e with 3e (DMSO, 20 °C, J&M method, detection at 445 nm ; from ref. [36]).

No.	[3e]/mol L^{-1}	[1e]/ mol L^{-1}	k_{obs}/s^{-1}
VS5-2	6×10^{-5}	7.83×10^{-4}	3.32×10^{-3}
VS5-3	6×10^{-5}	1.04×10^{-3}	4.21×10^{-3}
VS5-4	6×10^{-5}	1.30×10^{-3}	5.15×10^{-3}
VS5-5	6×10^{-5}	1.57×10^{-3}	6.41×10^{-3}
VS5-6	6×10^{-5}	2.09×10^{-3}	8.61×10^{-3}
k_2(20 °C) = 4.10 L mol^{-1} s^{-1}			

y = 4.1019x - 3E-05
R² = 0.9967
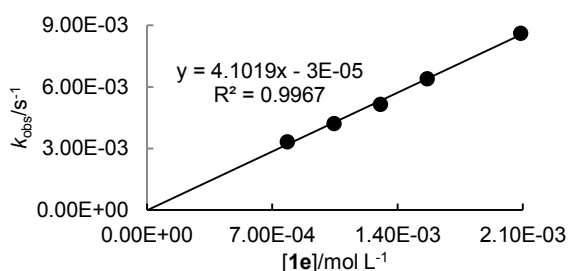
Table 7.32. Kinetics of the reaction of 1e with 4 (DMSO, 20 °C, Stopped-flow method, detection at 379 nm).

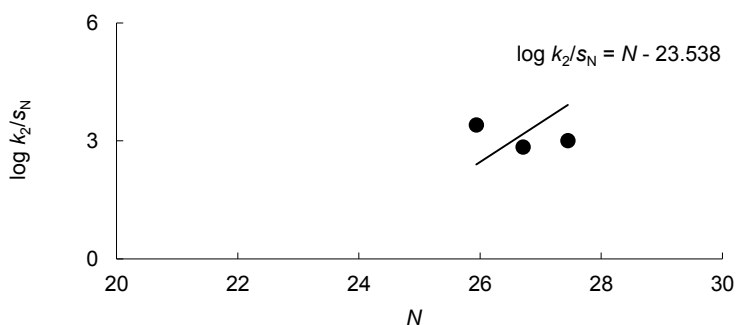| No.	[4]/mol L^{-1}	[1e]/ mol L^{-1}	k_{obs}/s^{-1}
VS4-1	1×10^{-4}	5.02×10^{-3}	1.11×10^{-1}
VS4-2	1×10^{-4}	6.02×10^{-3}	1.39×10^{-1}
VS4-3	1×10^{-4}	7.03×10^{-3}	1.59×10^{-1}
VS4-4	1×10^{-4}	8.03×10^{-3}	1.80×10^{-1}
VS4-5	1×10^{-4}	9.04×10^{-3}	2.09×10^{-1}
k_2(20 °C) = 2.36×10^1 L mol^{-1} s^{-1}			

y = 23.603x - 0.0063
R² = 0.9953
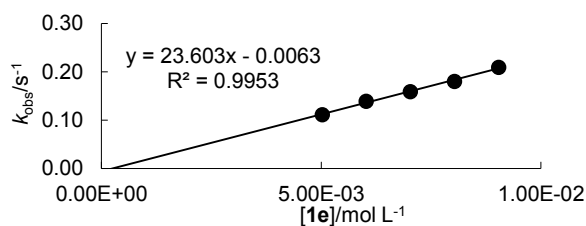
Table 7.33. Calculation of the Electrophilicity Parameter E for 1e using the N and s_N Parameters of 3,4, Eq 7.1, and the Second-Order Rate Constants for the Reactions of 1e with 3,4.

Nucleophile	N/s_N	k_2/ L mol^{-1} s^{-1}
3a	26.71/0.37	1.60×10^3
3b	27.45/0.38	5.56×10^3
3c	25.94/0.42	2.55×10^3
3d	20.24/0.60	1.94×10^1
3e	19.46/0.58	4.10
4	21.07/0.68	2.36×10^1
E (**1e**)$^{[a]}$ = $-$ 18.36		

$$\log k_2/s_N = N - 18.355$$

[a] Calculated by least square minimization according to eq 7.1 using N, s_N from Table 7.1.

7.4.3.6 Reactions with Acrylonitrile (1f)

Table 7.34. Kinetics of the reaction of 1f with 3a (DMSO, 20 °C, Stopped-flow method, detection at 425 nm).

No.	[**3a**]/mol L^{-1}	[**1f**]/ mol L^{-1}	k_{obs}/s^{-1}
AN7-1	5×10^{-5}	1.00×10^{-3}	1.94
AN7-2	5×10^{-5}	1.50×10^{-3}	3.09
AN7-3	5×10^{-5}	2.00×10^{-3}	3.79
AN7-4	5×10^{-5}	2.50×10^{-3}	4.58
AN7-5	5×10^{-5}	3.00×10^{-3}	5.92
k_2(20 °C) = 1.89×10^3 L mol^{-1} s^{-1}			

y = 1890x + 0.084
R² = 0.9872
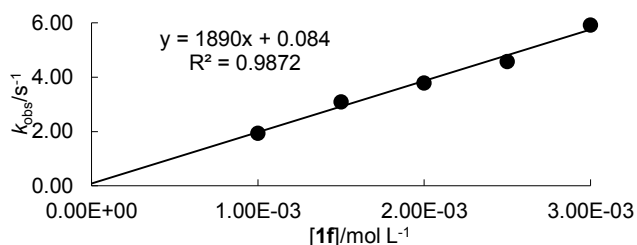
Table 7.35. Kinetics of the reaction of 1f with 3b (DMSO, 20 °C, Stopped-flow method, detection at 425 nm).

No.	[**3b**]/mol L^{-1}	[**1f**]/ mol L^{-1}	k_{obs}/s^{-1}
AN9-2	1×10^{-4}	1.50×10^{-3}	4.71
AN9-3	1×10^{-4}	2.00×10^{-3}	6.71
AN9-4	1×10^{-4}	2.50×10^{-3}	8.36
AN9-5	1×10^{-4}	3.00×10^{-3}	1.05×10^1
k_2(20 °C) = 3.79×10^3 L mol^{-1} s^{-1}			
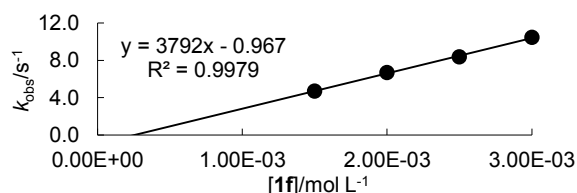
y = 3792x - 0.967
R² = 0.9979

Bisexponential decays. The initial rate is assigned to the betaine formation. The bisexponential decays may be caused by a rate determining ring-closure.

Table 7.36. Kinetics of the reaction of 1f with 3c (DMSO, 20 °C, Stopped-flow method, detection at 425 nm).

No.	[**3c**]/mol L^{-1}	[**1f**]/ mol L^{-1}	k_{obs}/s^{-1}
AN7-1	1×10^{-4}	1.00×10^{-3}	3.73
AN7-2	1×10^{-4}	1.50×10^{-3}	6.17
AN7-3	1×10^{-4}	2.00×10^{-3}	7.02
AN7-4	1×10^{-4}	2.50×10^{-3}	9.36
AN7-5	1×10^{-4}	3.00×10^{-3}	1.12×10^1
k_2(20 °C) = 3.64×10^3 L mol^{-1} s^{-1}			

y = 3642x + 0.22
R² = 0.9852
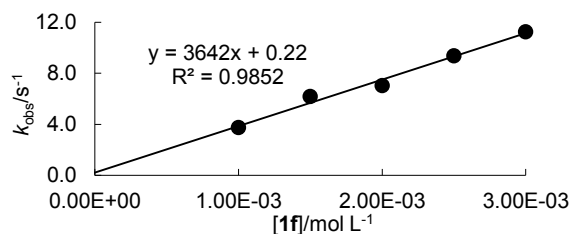
Table 7.37. Kinetics of the reaction of 1f with 3d (DMSO, 20 °C, J&M method, detection at 425 nm).

No.	[3d]/mol L^{-1}	[1f]/ mol L^{-1}	k_{obs}/s^{-1}
AN4-1	1×10^{-4}	9.89×10^{-3}	1.98×10^{-2}
AN4-2	1×10^{-4}	1.55×10^{-2}	3.15×10^{-2}
AN4-3	1×10^{-4}	2.02×10^{-2}	3.91×10^{-2}
AN4-4	1×10^{-4}	2.51×10^{-2}	5.58×10^{-2}
AN4-5	1×10^{-4}	3.01×10^{-2}	6.68×10^{-2}
k_2(20 °C) = 2.36 L mol^{-1} s^{-1}			

y = 2.3628x - 0.0049
R² = 0.9887
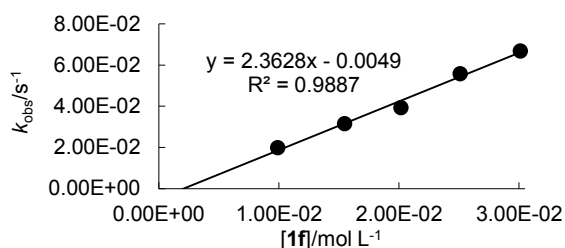
Table 7.38. Kinetics of the reaction of 1f with 3e (DMSO, 20 °C, J&M method, detection at 445 nm).

No.	[3e]/mol L^{-1}	[1f]/ mol L^{-1}	k_{obs}/s^{-1}
AN3-1	1×10^{-4}	1.02×10^{-3}	3.60×10^{-3}
AN3-3	1×10^{-4}	2.04×10^{-3}	6.07×10^{-3}
AN3-4	1×10^{-4}	2.57×10^{-3}	6.82×10^{-3}
AN3-5	1×10^{-4}	2.96×10^{-3}	8.13×10^{-3}
k_2(20 °C) = 2.25 L mol^{-1} s^{-1}			

y = 2.2492x + 0.0013
R² = 0.989
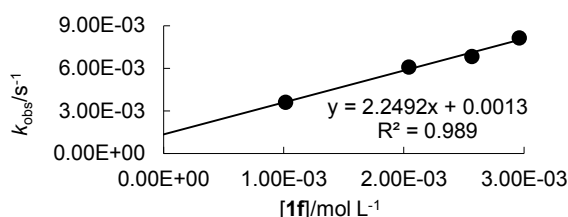
Table 7.39. Kinetics of the reaction of 1f with 3f (DMSO, 20 °C, J&M method, detection at 476 nm).

No.	[3f]/mol L^{-1}	[1f]/ mol L^{-1}	k_{obs}/s^{-1}
AN5-1	1×10^{-4}	1.02×10^{-3}	2.79×10^{-2}
AN5-2	1×10^{-4}	1.54×10^{-3}	4.30×10^{-2}
AN5-3	1×10^{-4}	2.02×10^{-3}	5.59×10^{-2}
AN5-4	1×10^{-4}	2.52×10^{-3}	6.90×10^{-2}
AN5-5	1×10^{-4}	3.07×10^{-3}	8.00×10^{-2}
k_2(20 °C) = 2.56 × 10^1 L mol^{-1} s^{-1}			

y = 25.561x + 0.0032
R² = 0.9955
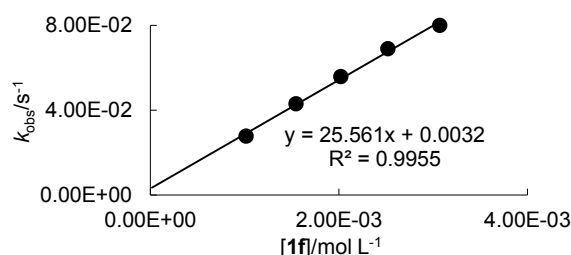
Table 7.40. Kinetics of the reaction of 1f with 4 (DMSO, 20 °C, J&M method, detection at 379 nm).

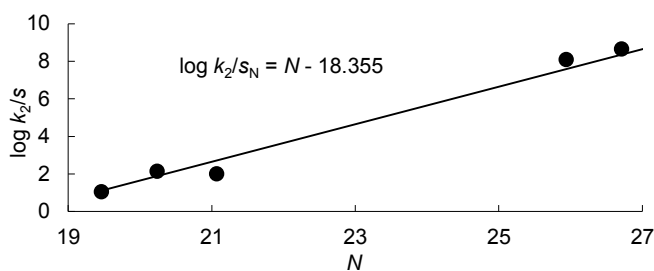| No.	[4]/mol L^{-1}	[1f]/ mol L^{-1}	k_{obs}/s^{-1}
AN6-1	1×10^{-4}	1.03×10^{-3}	7.30×10^{-3}
AN6-2	1×10^{-4}	1.54×10^{-3}	9.50×10^{-3}
AN6-3	1×10^{-4}	2.04×10^{-3}	1.13×10^{-2}
AN6-5	1×10^{-4}	3.00×10^{-3}	1.70×10^{-2}
k_2(20 °C) = 4.90 L mol^{-1} s^{-1}			

y = 4.9023x + 0.002
R² = 0.9881
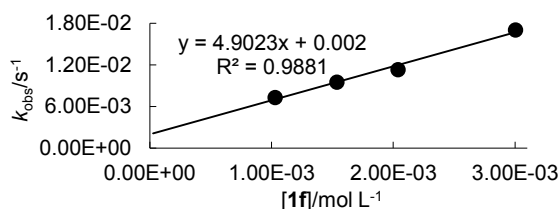
Table 7.41. Calculation of the Electrophilicity Parameter E for 1f using the N and s_N Parameters of 3,4, Eq 7.1, and the Second-Order Rate Constants for the Reactions of 1f with 3,4.

Nucleophile	N/s_N	k_2/ L mol^{-1} s^{-1}
3a	26.71/0.37	1.89×10^3
3b	27.45/0.38	3.79×10^3
3c	25.94/0.42	3.64×10^3
3d	20.24/0.60	2.36
3e	19.46/0.58	2.25
4	21.07/0.68	4.90
E (1f)[a] = − 19.06		
3f	19.38/0.50	2.56×10^1 [b]
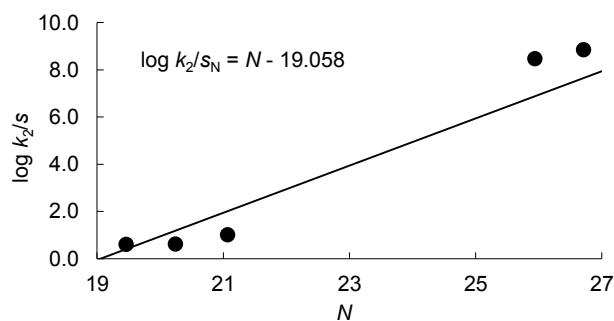
log k_2/s_N = N - 19.058

[a] Calculated by least square minimization according to eq 7.1 using N, s_N from Table 7.1; [b] Not used for the determination of E.

7.4.3.7 Reactions with Methylvinylketone (1g)

Table 7.42. Kinetics of the reaction of 1g with 3a (DMSO, 20 °C, Stopped-flow method, detection at 425 nm).

No.	[3a]/mol L^{-1}	[1g]/ mol L^{-1}	k_{obs}/s^{-1}
MVK3-1	2×10^{-4}	3.00×10^{-3}	1.99×10^1
MVK3-2	2×10^{-4}	3.30×10^{-3}	2.21×10^1
MVK3-3	2×10^{-4}	3.60×10^{-3}	2.32×10^1
MVK3-4	2×10^{-4}	3.90×10^{-3}	2.61×10^1
MVK3-5	2×10^{-4}	4.20×10^{-3}	2.81×10^1
k_2(20 °C) = 6.84×10^3 L mol^{-1} s^{-1}			

y = 6843.3x - 0.74
R² = 0.9853
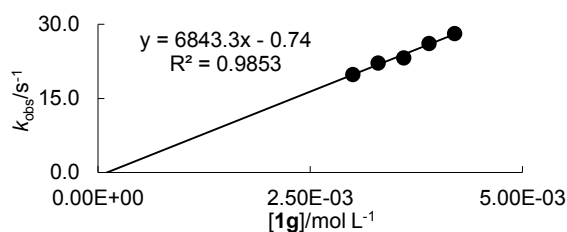
Table 7.43. Kinetics of the reaction of 1g with 3c (DMSO, 20 °C, Stopped-flow method, detection at 425 nm).

| No.	[3c]/mol L^{-1}	[1g]/ mol L^{-1}	k_{obs}/s^{-1}
MVK4-1	2×10^{-4}	3.00×10^{-3}	2.46×10^1
MVK4-2	2×10^{-4}	3.30×10^{-3}	2.65×10^1
MVK4-3	2×10^{-4}	3.60×10^{-3}	2.89×10^1
MVK4-4	2×10^{-4}	3.90×10^{-3}	3.19×10^1
MVK4-5	2×10^{-4}	4.20×10^{-3}	3.39×10^1
k_2(20 °C) = 7.99×10^3 L mol^{-1} s^{-1}			

y = 7993.3x + 0.374
R² = 0.9937
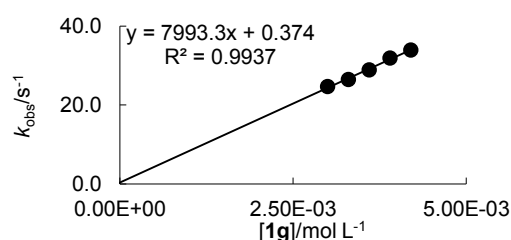
Table 7.44. Kinetics of the reaction of 1g with 3d (DMSO, 20 °C, Stopped-flow method, detection at 425 nm).

No.	[3d]/mol L^{-1}	[1g]/ mol L^{-1}	k_{obs}/s^{-1}
MVK5-1	1×10^{-4}	3.00×10^{-3}	3.28×10^{-1}
MVK5-2	1×10^{-4}	3.30×10^{-3}	3.55×10^{-1}
MVK5-3	1×10^{-4}	3.60×10^{-3}	3.99×10^{-1}
MVK5-4	1×10^{-4}	3.90×10^{-3}	4.47×10^{-1}
MVK5-5	1×10^{-4}	4.20×10^{-3}	4.68×10^{-1}
k_2(20 °C) = 1.24×10^2 L mol^{-1} s^{-1}			

y = 124x - 0.047
R² = 0.9856

Table 7.45. Kinetics of the reaction of 1g with 3e (DMSO, 20 °C, Stopped-flow method, detection at 445 nm).

No.	[3e]/mol L^{-1}	[1g]/ mol L^{-1}	k_{obs}/s^{-1}
MVK6-1	1×10^{-4}	3.00×10^{-3}	7.48×10^{-2}
MVK6-2	1×10^{-4}	3.30×10^{-3}	8.13×10^{-2}
MVK6-3	1×10^{-4}	3.60×10^{-3}	9.07×10^{-2}
MVK6-4	1×10^{-4}	3.90×10^{-3}	1.01×10^{-1}
MVK6-5	1×10^{-4}	4.20×10^{-3}	1.06×10^{-1}
k_2(20 °C) = 2.74×10^1 L mol^{-1} s^{-1}			

y = 27.367x - 0.0078
R² = 0.9893
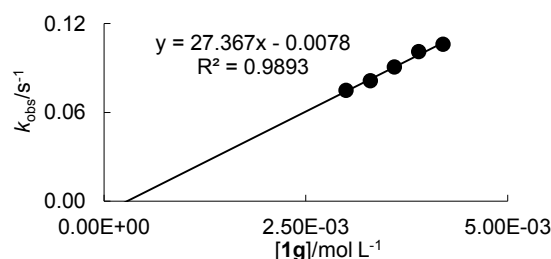
Table 7.46. Kinetics of the reaction of 1g with 4 (DMSO, 20 °C, Stopped-flow method, detection at 379 nm).

No.	[4]/mol L^{-1}	[1g]/ mol L^{-1}	k_{obs}/s^{-1}
MVK7-1	1×10^{-4}	3.00×10^{-3}	9.67×10^{-2}
MVK7-2	1×10^{-4}	3.30×10^{-3}	1.06×10^{-1}
MVK7-3	1×10^{-4}	3.60×10^{-3}	1.23×10^{-1}
MVK7-4	1×10^{-4}	3.90×10^{-3}	1.37×10^{-1}
MVK7-5	1×10^{-4}	4.20×10^{-3}	1.45×10^{-1}
k_2(20 °C) = 4.25×10^1 L mol^{-1} s^{-1}			

y = 42.533x - 0.0316
R² = 0.9868
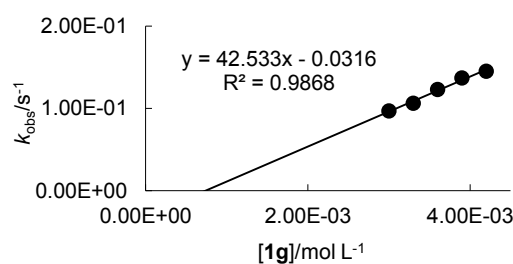
Table 7.47. Calculation of the Electrophilicity Parameter E for 1g using the N and s_N Parameters of 3,4, Eq 7.1, and the Second-Order Rate Constants for the Reactions of 1g with 3,4.

| Nucleophile	N/s_N	$k_2/$ L mol^{-1} s^{-1}
3a	26.71/0.37	6.84×10^3
3c	25.94/0.42	7.99×10^3
3d	20.24/0.60	1.24×10^2
3e	19.46/0.58	2.74×10^1
E (**1g**)[a] = -16.48		
4	21.07/0.68	4.25×10^1 [b]
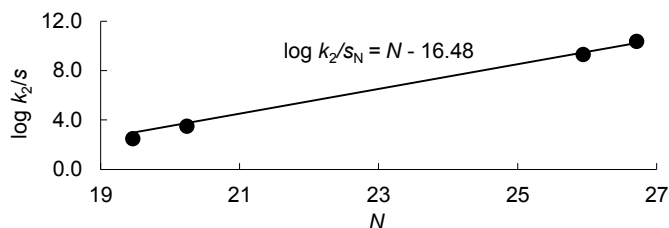
log $k_2/s_N = N$ - 16.48

[a] Calculated by least square minimization according to eq 7.1 using N, s_N from Table 7.1; [b] Not used for the determination of E.

7.4.3.8 Reactions with Phenylvinylketone (1h)

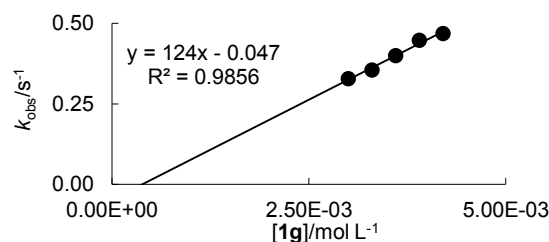**Table 7.48. Kinetics of the reaction of 1h with 3a (DMSO, 20 °C, Stopped-flow method, detection at 425 nm).**

No.	[**3a**]/mol L^{-1}	[**1h**]/ mol L^{-1}	$k_{obs}/$s^{-1}
PVK3-1	1×10^{-4}	1.02×10^{-3}	3.79×10^1
PVK3-2	1×10^{-4}	1.12×10^{-3}	4.10×10^1
PVK3-3	1×10^{-4}	1.22×10^{-3}	4.49×10^1
PVK3-4	1×10^{-4}	1.32×10^{-3}	4.80×10^1
PVK3-5	1×10^{-4}	1.42×10^{-3}	5.18×10^1
k_2(20 °C) = 3.43×10^4 L mol^{-1} s^{-1}			

y = 34310x + 2.894
R² = 0.9987
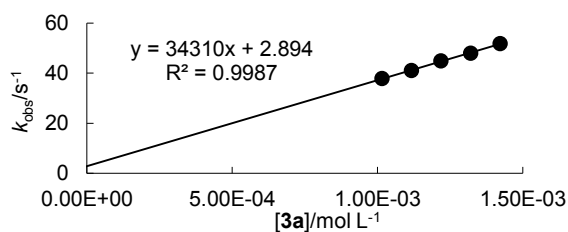
Table 7.49. Kinetics of the reaction of 1h with 3b (DMSO, 20 °C, Stopped-flow method, detection at 425 nm).

No.	[**3b**]/mol L^{-1}	[**1h**]/ mol L^{-1}	$k_{obs}/$s^{-1}
PVK3-1	4×10^{-4}	4.06×10^{-3}	1.38×10^2
PVK3-2	4×10^{-4}	4.47×10^{-3}	1.46×10^2
PVK3-3	4×10^{-4}	4.87×10^{-3}	1.56×10^2
PVK3-4	4×10^{-4}	5.28×10^{-3}	1.70×10^2
PVK3-5	4×10^{-4}	5.69×10^{-3}	1.77×10^2
k_2(20 °C) = 2.55×10^4 L mol^{-1} s^{-1}			

y = 25531x + 33.06
R² = 0.9906
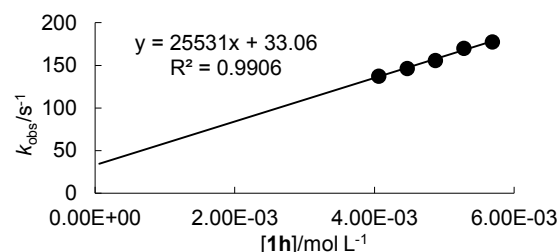
Table 7.50. Kinetics of the reaction of 1h with 3c (DMSO, 20 °C, Stopped-flow method, detection at 425 nm).

No.	[**3c**]/mol L^{-1}	[**1h**]/ mol L^{-1}	$k_{obs}/$s^{-1}
PVK2-1	4×10^{-4}	4.06×10^{-3}	1.76×10^2
PVK2-2	4×10^{-4}	4.47×10^{-3}	2.01×10^2
PVK2-3	4×10^{-4}	4.87×10^{-3}	2.22×10^2
PVK2-4	4×10^{-4}	5.28×10^{-3}	2.40×10^2
PVK2-5	4×10^{-4}	5.69×10^{-3}	2.56×10^2
k_2(20 °C) = 4.89×10^4 L mol^{-1} s^{-1}			

y = 48858x - 19.392
R² = 0.9918

The positive intercept may be due to the fact that the reaction is very fast and the solutions are not homogenous after 5 ms.

Table 7.51. Kinetics of the reaction of 1h with 3d (DMSO, 20 °C, Stopped-flow method, detection at 425 nm).

No.	$[3d]/mol\ L^{-1}$	$[1h]/mol\ L^{-1}$	k_{obs}/s^{-1}
PVK4-1	5×10^{-5}	1.02×10^{-3}	8.89×10^{-1}
PVK4-2	5×10^{-5}	1.12×10^{-3}	9.52×10^{-1}
PVK4-3	5×10^{-5}	1.22×10^{-3}	1.04
PVK4-4	5×10^{-5}	1.32×10^{-3}	1.12
PVK4-5	5×10^{-5}	1.42×10^{-3}	1.21
$k_2(20\ °C) = 8.00 \times 10^2\ L\ mol^{-1}\ s^{-1}$			

y = 799.66x + 0.069
R² = 0.9973
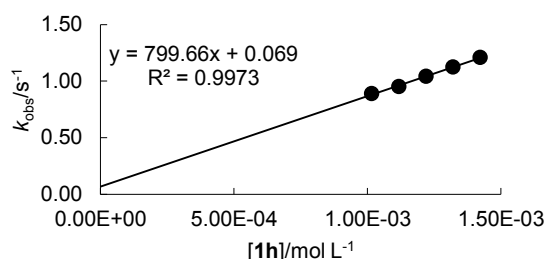
Table 7.52. Kinetics of the reaction of 1h with 3e (DMSO, 20 °C, Stopped-flow method, detection at 445 nm).

No.	$[3e]/mol\ L^{-1}$	$[1h]/mol\ L^{-1}$	k_{obs}/s^{-1}
PVK5-1	5×10^{-5}	1.02×10^{-3}	2.18×10^{-1}
PVK5-2	5×10^{-5}	1.12×10^{-3}	2.38×10^{-1}
PVK5-3	5×10^{-5}	1.22×10^{-3}	2.58×10^{-1}
PVK5-4	5×10^{-5}	1.32×10^{-3}	2.78×10^{-1}
PVK5-5	5×10^{-5}	1.42×10^{-3}	3.03×10^{-1}
$k_2(20\ °C) = 2.07 \times 10^2\ L\ mol^{-1}\ s^{-1}$			

y = 206.81x + 0.007
R² = 0.9977
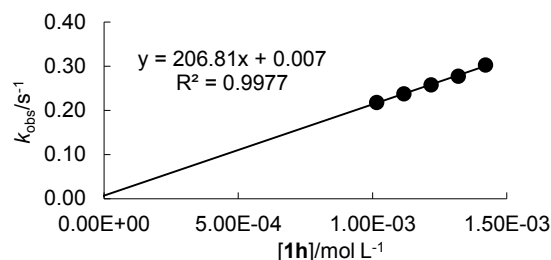
Table 7.53. Kinetics of the reaction of 1h with 4 (DMSO, 20 °C, Stopped-flow method, detection at 379 nm).

| No.	$[4]/mol\ L^{-1}$	$[1h]/mol\ L^{-1}$	k_{obs}/s^{-1}
PVK6-1	1×10^{-4}	1.02×10^{-3}	6.35×10^{-1}
PVK6-2	1×10^{-4}	1.12×10^{-3}	7.17×10^{-1}
PVK6-3	1×10^{-4}	1.22×10^{-3}	8.02×10^{-1}
PVK6-4	1×10^{-4}	1.32×10^{-3}	8.75×10^{-1}
PVK6-5	1×10^{-4}	1.42×10^{-3}	9.22×10^{-1}
$k_2(20\ °C) = 7.21 \times 10^2\ L\ mol^{-1}\ s^{-1}$			

y = 720.87x - 0.0882
R² = 0.9896
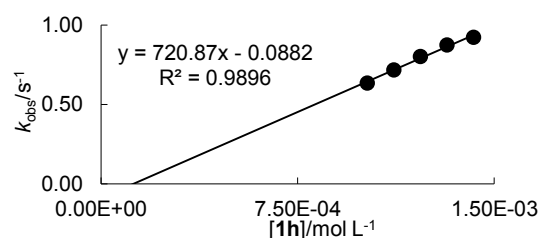
Table 7.54. Calculation of the Electrophilicity Parameter E for 1h using the N and s_N Parameters of 3,4, Eq 7.1, and the Second-Order Rate Constants for the Reactions of 1h with 3,4.

| Nucleophile	N/s_N	$k_2/\ L\ mol^{-1}\ s^{-1}$
3a	26.71/0.37	3.43×10^4
3b	27.45/0.38	2.55×10^4
3c	25.94/0.42	4.89×10^4
3d	20.24/0.60	8.00×10^2
3e	19.46/0.58	2.07×10^2
$E\ (\mathbf{1h})^{[a]} = -15.27$		
4	21.07/0.68	$7.21 \times 10^{2\ [b]}$
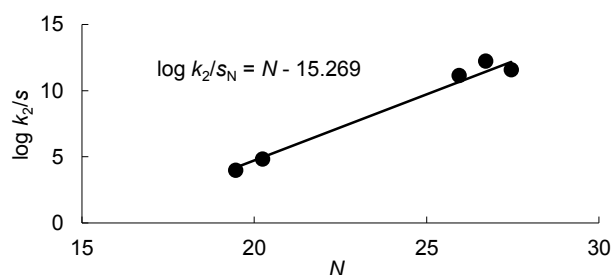
log $k_2/s_N = N$ - 15.269

[a] Calculated by least square minimization according to eq 7.1 using N, s_N from Table 7.1; [b] Not used for the determination of E.

7.4.3.9 Reactions with Ethyl crotonate (2a)

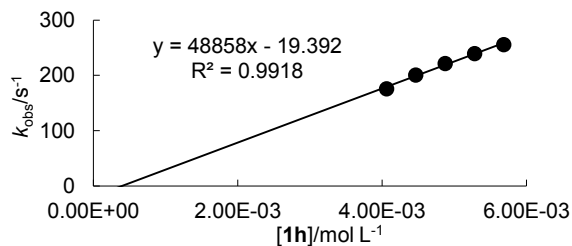**Table 7.55. Kinetics of the reaction of 2a with 3a (DMSO, 20 °C, Stopped-flow method, detection at 425 nm).**

No.	$[3a]/mol\ L^{-1}$	$[2a]/mol\ L^{-1}$	k_{obs}/s^{-1}
CEE1-1	1×10^{-4}	2.01×10^{-3}	8.49×10^{-3}
CEE1-2	1×10^{-4}	4.02×10^{-3}	1.59×10^{-2}
CEE1-3	1×10^{-4}	6.03×10^{-3}	2.50×10^{-2}
CEE1-4	1×10^{-4}	8.04×10^{-3}	3.26×10^{-2}
CEE1-5	1×10^{-4}	1.00×10^{-2}	4.17×10^{-2}
$k_2(20\ °C) = 4.14\ L\ mol^{-1}\ s^{-1}$			

$y = 4.1368x - 0.0002$
$R^2 = 0.9988$
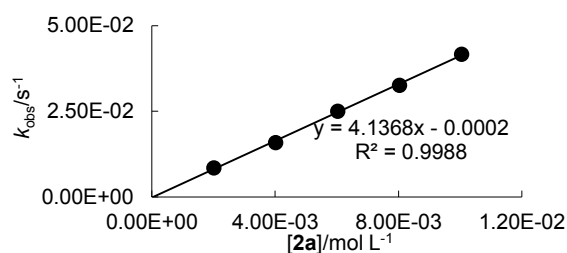
Table 7.56. Kinetics of the reaction of 2a with 3c (DMSO, 20 °C, Stopped-flow method, detection at 425 nm).

No.	$[3c]/mol\ L^{-1}$	$[2a]/mol\ L^{-1}$	k_{obs}/s^{-1}
CEE3-1	1×10^{-4}	1.97×10^{-3}	5.49×10^{-2}
CEE3-2	1×10^{-4}	9.98×10^{-4}	2.74×10^{-2}
CEE3-3	1×10^{-4}	1.29×10^{-3}	3.52×10^{-2}
CEE3-4	1×10^{-4}	1.52×10^{-3}	4.18×10^{-2}
CEE3-5	1×10^{-4}	1.79×10^{-3}	5.03×10^{-2}
$k_2(20\ °C) = 2.87 \times 10^1\ L\ mol^{-1}\ s^{-1}$			

$y = 28.741x - 0.0016$
$R^2 = 0.9988$
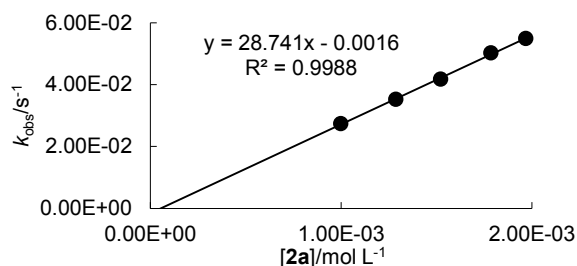
Table 7.57. Calculation of the Electrophilicity Parameter E for 2a using the N and s_N Parameters of 3, Eq 7.1, and the Second-Order Rate Constants for the Reactions of 2a with 3.

Nucleophile	N/s_N	$k_2^{exp}/L\ mol^{-1}\ s^{-1}$	$k_2^{calcd}/L\ mol^{-1}\ s^{-1}$	k_2^{exp}/k_2^{calcd}
3a	26.71/0.37	4.14	1.27×10^1	0.33
3c	25.94/0.42	2.87×10^1	8.16	3.57
$E\ (\mathbf{2a})^{[a]} = -\ 23.73$				

[a] Calculated by least square minimization according to eq 7.1 using N, s_N from Table 7.1.

7.4.3.10 Reactions with Ethyl cinnamate (2b)

Table 7.58. Kinetics of the reaction of 2b with 3a (DMSO, 20 °C, Stopped-flow method, detection at 425 nm).

No.	$[3a]/mol\ L^{-1}$	$[2b]/mol\ L^{-1}$	k_{obs}/s^{-1}
ZE1-1	1×10^{-4}	1.02×10^{-3}	2.67×10^{-3}
ZE1-2	1×10^{-4}	1.51×10^{-3}	3.81×10^{-3}
ZE1-3	1×10^{-4}	2.03×10^{-3}	5.61×10^{-3}
ZE1-4	1×10^{-4}	2.58×10^{-3}	7.30×10^{-3}
ZE1-5	1×10^{-4}	2.97×10^{-3}	8.57×10^{-3}
$k_2(20\ °C) = 3.08\ L\ mol^{-1}\ s^{-1}$			

$y = 3.0769x - 0.0006$
$R^2 = 0.9971$
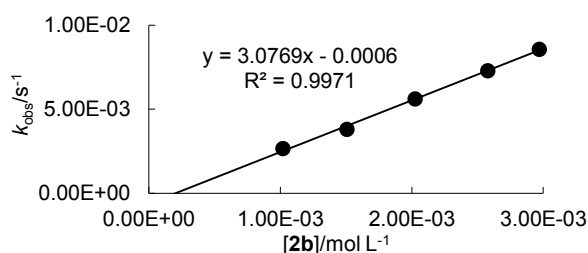
Table 7.59. Kinetics of the reaction of 2b with 3c (DMSO, 20 °C, Stopped-flow method, detection at 425 nm).

No.	[3c]/mol L^{-1}	[2b]/ mol L^{-1}	k_{obs}/s^{-1}
ZE1-1	2×10^{-4}	1.98×10^{-3}	1.76×10^{-2}
ZE1-2	2×10^{-4}	2.41×10^{-3}	2.07×10^{-2}
ZE1-3	2×10^{-4}	2.78×10^{-3}	2.33×10^{-2}
ZE1-4	2×10^{-4}	3.13×10^{-3}	2.65×10^{-2}
ZE1-5	2×10^{-4}	3.55×10^{-3}	2.98×10^{-2}
k_2(20 °C) = 7.77 L mol^{-1} s^{-1}			
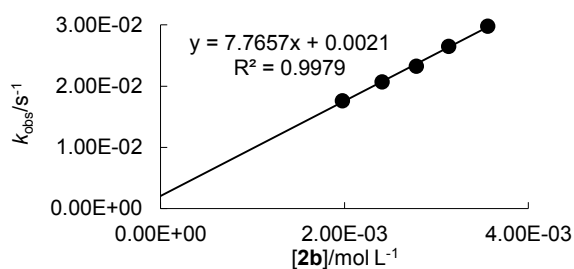
Table 7.60. Calculation of the Electrophilicity Parameter E for 2b using the N and s_N Parameters of 3, Eq 7.1, and the Second-Order Rate Constants for the Reactions of 2b with 3.

Nucleophile	N/s_N	k_2^{exp}/L mol^{-1} s^{-1}	k_2^{calcd}/L mol^{-1} s^{-1}	k_2^{exp}/k_2^{calcd}
3a	26.71/0.37	3.08	6.53	0.47
3c	25.94/0.42	7.77	4.00	1.94
E (**2b**)[a] = − 24.51				

[a] Calculated by least square minimization according to eq 7.1 using N, s_N from Table 7.1.

## 7.4.3.11 Reactions with Ethyl methycrylate (2c)

Table 7.61. Kinetics of the reaction of 2c with 3a (DMSO, 20 °C, Stopped-flow method, detection at 425 nm).

| No.	[3a]/mol L^{-1}	[2c]/ mol L^{-1}	k_{obs}/s^{-1}
EMA1-1	1×10^{-4}	1.00×10^{-3}	1.55×10^{-2}
EMA1-2	1×10^{-4}	2.01×10^{-3}	3.08×10^{-2}
EMA1-3	1×10^{-4}	3.01×10^{-3}	4.39×10^{-2}
EMA1-4	1×10^{-4}	4.01×10^{-3}	6.22×10^{-2}
EMA1-5	1×10^{-4}	5.01×10^{-3}	7.50×10^{-2}
k_2(20 °C) = 1.50 × 10^1 L mol^{-1} s^{-1}			
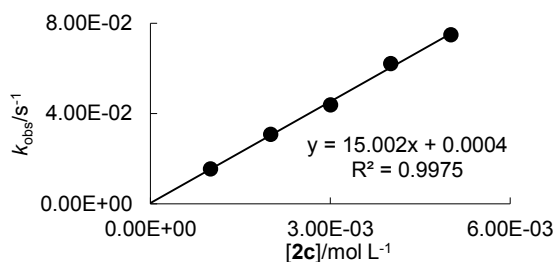
Table 7.62. Kinetics of the reaction of 2c with 3c (DMSO, 20 °C, Stopped-flow method, detection at 425 nm).

No.	[3c]/mol L^{-1}	[2c]/ mol L^{-1}	k_{obs}/s^{-1}
EMA2-1	2×10^{-4}	2.01×10^{-3}	7.88×10^{-2}
EMA2-2	2×10^{-4}	4.01×10^{-3}	1.45×10^{-1}
EMA2-3	2×10^{-4}	6.02×10^{-3}	2.24×10^{-1}
EMA2-4	2×10^{-4}	8.02×10^{-3}	3.00×10^{-1}
EMA2-5	2×10^{-4}	1.00×10^{-2}	3.78×10^{-1}
k_2(20 °C) = 3.76 × 10^1 L mol^{-1} s^{-1}			
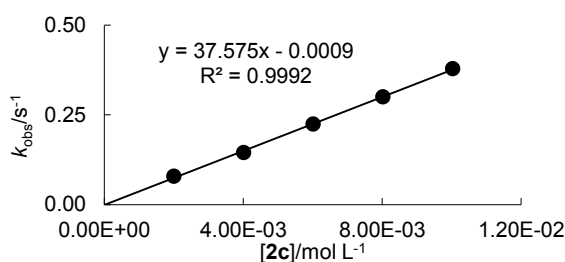
Table 7.63. Calculation of the Electrophilicity Parameter E for 2c using the N and s_N Parameters of 3, Eq 7.1, and the Second-Order Rate Constants for the Reactions of 2c with 3.

Nucleophile	N/s_N	k_2^{exp}/L mol^{-1} s^{-1}	k_2^{calcd}/L mol^{-1} s^{-1}	k_2^{exp}/k_2^{calcd}
3a	26.71/0.37	1.50 × 10^1	2.85 ×10^1	0.53
3c	25.94/0.42	3.76 × 10^1	2.13 × 10^1	1.76
E (**2c**)[a] = − 22.78				

[a] Calculated by least square minimization according to eq 7.1 using N, s_N from Table 7.1.

7.4.3.12 Reactions with (*E*)-1-Methyl-4-(styrylsulfonyl)benzene (2e)

Table 7.64. Kinetics of the reaction of 2e with 3a (DMSO, 20 °C, Stopped-flow method, detection at 425 nm).

No.	$[3a]$/mol L^{-1}	$[2e]$/ mol L^{-1}	k_{obs}/s^{-1}
STS1-1	1×10^{-4}	1.02×10^{-3}	2.40×10^{-3}
STS1-2	1×10^{-4}	1.50×10^{-3}	3.44×10^{-3}
STS1-3	1×10^{-4}	1.99×10^{-3}	4.57×10^{-3}
STS1-4	1×10^{-4}	2.59×10^{-3}	6.00×10^{-3}
STS1-5	1×10^{-4}	3.02×10^{-3}	7.10×10^{-3}
k_2(20 °C) = 2.36 L mol^{-1} s^{-1}			

y = 2.3549x - 7E-05
R² = 0.9993
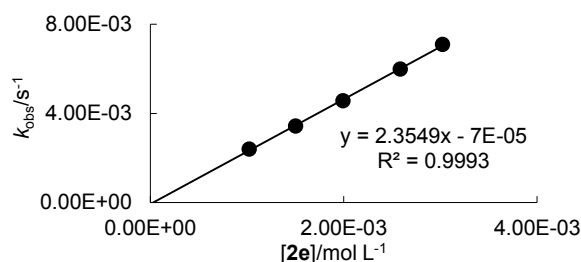
Table 7.65. Kinetics of the reaction of 2e with 3c (DMSO, 20 °C, Stopped-flow method, detection at 425 nm).

No.	$[3c]$/mol L^{-1}	$[2e]$/ mol L^{-1}	k_{obs}/s^{-1}
STS2-1	1×10^{-4}	1.04×10^{-3}	8.73×10^{-3}
STS2-2	1×10^{-4}	1.44×10^{-3}	1.14×10^{-2}
STS2-3	1×10^{-4}	2.01×10^{-3}	1.49×10^{-2}
STS2-5	1×10^{-4}	3.07×10^{-3}	2.33×10^{-2}
k_2(20 °C) = 7.17 L mol^{-1} s^{-1}			

y = 7.1701x + 0.001
R² = 0.9964
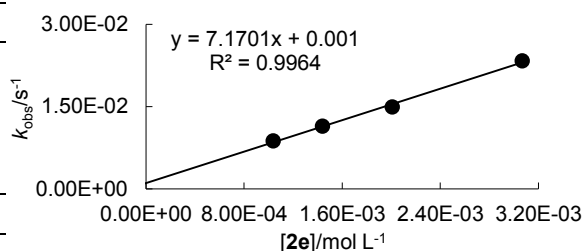
Table 7.66. Calculation of the Electrophilicity Parameter *E* for 2e using the *N* and *s*$_N$ Parameters of 3, Eq 7.1, and the Second-Order Rate Constants for the Reactions of 2e with 3.

Nucleophile	N/s_N	k_2^{exp}/L mol^{-1} s^{-1}	k_2^{calcd}/L mol^{-1} s^{-1}	k_2^{exp}/k_2^{calcd}
3a	26.71/0.37	2.36	5.59	0.42
3c	25.94/0.42	7.17	3.35	2.14
E (**2e**)$^{[a]}$ = − 24.69				

[a] Calculated by least square minimization according to eq 7.1 using N, s_N from Table 7.1.

7.4.3.13 Reactions with Cinnamonitrile (2f)

Table 7.67. Kinetics of the reaction of 2f with 3a (DMSO, 20 °C, Stopped-flow method, detection at 425 nm).

| No.	$[3a]$/mol L^{-1}	$[2f]$/ mol L^{-1}	k_{obs}/s^{-1}
ZN1-1	1×10^{-4}	2.47×10^{-3}	1.58×10^{-2}
ZN1-2	1×10^{-4}	4.94×10^{-3}	3.11×10^{-2}
ZN1-3	1×10^{-4}	7.40×10^{-3}	4.66×10^{-2}
ZN1-4	1×10^{-4}	9.87×10^{-3}	6.14×10^{-2}
ZN1-5	1×10^{-4}	1.23×10^{-2}	7.66×10^{-2}
k_2(20 °C) = 6.15 L mol^{-1} s^{-1}			

y = 6.1541x + 0.0007
R² = 0.9999
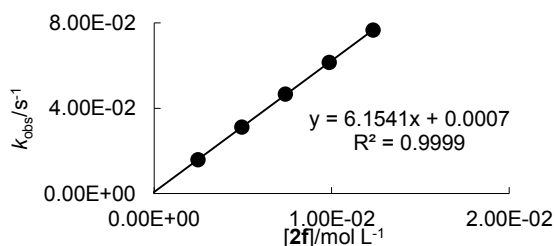
able 7.68. Calculation of the Electrophilicity Parameter *E* for 2f using the *N* and *s*$_N$ Parameters of 3, Eq 7.1, and the Second-Order Rate Constants for the Reactions of 2f with 3.

Nucleophile	N/s_N	k_2/ L mol^{-1} s^{-1}
3a	26.71/0.37	6.15
E (**2f**)$^{[a]}$ = −24.57		

[a] Calculated by eq 7.1 using N, s_N from Table 7.1.

7.4.3.14 (*E*)-4-phenylbut-3-en-2-one (2g)

Table 7.69. Kinetics of the reaction of 2g with 3a (DMSO, 20 °C, Stopped-flow method, detection at 425 nm).

No.	[3a]/mol L^{-1}	[2g]/ mol L^{-1}	k_{obs}/s^{-1}
PBO3-1	1×10^{-4}	2.01×10^{-3}	4.03×10^{-2}
PBO3-2	1×10^{-4}	4.01×10^{-3}	7.84×10^{-2}
PBO3-3	1×10^{-4}	6.02×10^{-3}	1.19×10^{-1}
PBO3-4	1×10^{-4}	8.03×10^{-3}	1.51×10^{-1}
PBO3-5	1×10^{-4}	1.00×10^{-2}	1.82×10^{-1}
	k_2(20 °C) = 1.77×10^1 L mol^{-1} s^{-1}		

y = 17.738x + 0.0073
R² = 0.9966
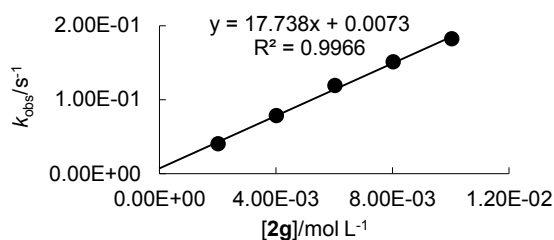
Table 7.70. Kinetics of the reaction of 2g with 3b (DMSO, 20 °C, Stopped-flow method, detection at 425 nm).

No.	[3b]/mol L^{-1}	[2g]/ mol L^{-1}	k_{obs}/s^{-1}
PBO2-1	4×10^{-4}	4.01×10^{-3}	1.20×10^{-1}
PBO2-2	4×10^{-4}	8.03×10^{-3}	2.02×10^{-1}
PBO2-3	4×10^{-4}	1.20×10^{-2}	3.32×10^{-1}
PBO2-4	4×10^{-4}	1.61×10^{-2}	4.19×10^{-1}
PBO2-5	4×10^{-4}	2.01×10^{-2}	5.45×10^{-1}
	k_2(20 °C) = 2.66×10^1 L mol^{-1} s^{-1}		

y = 26.582x + 0.0035
R² = 0.9949
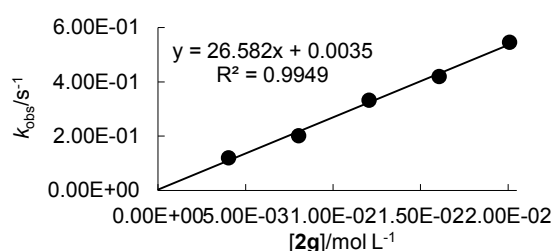
Table 7.71. Kinetics of the reaction of 2g with 3c (DMSO, 20 °C, Stopped-flow method, detection at 425 nm).

No.	[3c]/mol L^{-1}	[2g]/ mol L^{-1}	k_{obs}/s^{-1}
PBO1-1	4×10^{-4}	4.01×10^{-3}	2.19×10^{-1}
PBO1-2	4×10^{-4}	8.03×10^{-3}	4.34×10^{-1}
PBO1-4	4×10^{-4}	1.61×10^{-2}	6.95×10^{-1}
PBO1-5	4×10^{-4}	2.01×10^{-2}	8.74×10^{-1}
	k_2(20 °C) = 3.91×10^1 L mol^{-1} s^{-1}		

y = 39.138x + 0.0842
R² = 0.9916
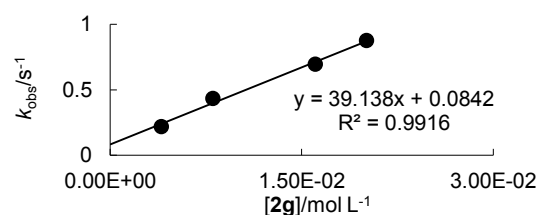
Table 7.72. Calculation of the Electrophilicity Parameter *E* for 2g using the *N* and s_N Parameters of 3, Eq 7.1, and the Second-Order Rate Constants for the Reactions of 2g with 3.

Nucleophile	N/s_N	k_2^{exp}/M^{-1} s^{-1}	k_2^{calcd}/M^{-1} s^{-1} [a]	k_2^{exp}/k_2^{calcd}
3a	26.71/0.37	1.77×10^1	2.37×10^1	0.75
3b	27.45/0.38	2.66×10^1	2.37×10^1	0.54
3c	25.94/0.42	3.91×10^1	1.73×10^1	2.26
	E (2g)[a] = − 22.99			

[a] From eq 7.1 using *N*, s_N and *E* from this Table; [b] Calculated by least square minimization according to eq 7.1 using *N*, s_N from Table 7.1.

log k_2/s_N = *N* - 22.993
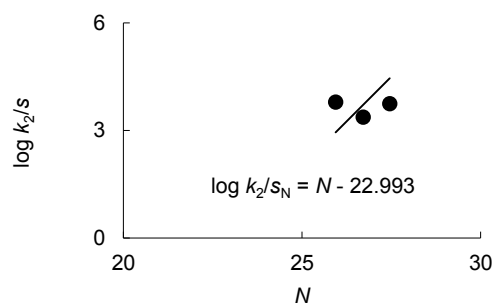
7.4.3.15 Reactions with Chalcone (2h)

Table 7.73. Kinetics of the reaction of 2h with 3a (DMSO, 20 °C, Stopped-flow method, detection at 425 nm).

| No.	[3a]/mol L^{-1}	[2h]/ mol L^{-1}	k_{obs}/s^{-1}
CHA3-1	1×10^{-4}	2.00×10^{-3}	6.44×10^{-1}
CHA3-2	1×10^{-4}	3.00×10^{-3}	9.57×10^{-1}
CHA3-3	1×10^{-4}	4.00×10^{-3}	1.28
CHA3-4	1×10^{-4}	5.00×10^{-3}	1.63
CHA3-5	1×10^{-4}	6.00×10^{-3}	1.96
$k_2(20\ °C) = 3.31 \times 10^2$ L mol^{-1} s^{-1}			

y = 330.5x - 0.0278
R² = 0.9996
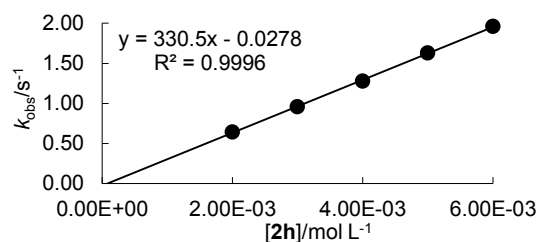
Table 7.74. Kinetics of the reaction of 2h with 3b (DMSO, 20 °C, Stopped-flow method, detection at 425 nm).

| No.	[3b]/mol L^{-1}	[2h]/ mol L^{-1}	k_{obs}/s^{-1}
CHA3-1	2×10^{-4}	2.00×10^{-3}	7.04×10^{-1}
CHA3-2	2×10^{-4}	3.00×10^{-3}	1.07
CHA3-3	2×10^{-4}	4.00×10^{-3}	1.26
CHA3-4	2×10^{-4}	5.00×10^{-3}	1.74
CHA3-5	2×10^{-4}	6.00×10^{-3}	1.97
$k_2(20\ °C) = 3.20 \times 10^2$ L mol^{-1} s^{-1}			

y = 320.2x + 0.068
R² = 0.9856
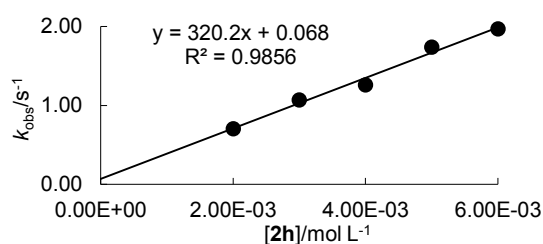
Table 7.75. Kinetics of the reaction of 2h with 3c (DMSO, 20 °C, Stopped-flow method, detection at 425 nm).

No.	[3c]/mol L^{-1}	[2h]/ mol L^{-1}	k_{obs}/s^{-1}
CHA3-1	2×10^{-4}	2.00×10^{-3}	1.24
CHA3-2	2×10^{-4}	3.00×10^{-3}	1.80
CHA3-3	2×10^{-4}	4.00×10^{-3}	2.44
CHA3-4	2×10^{-4}	5.00×10^{-3}	3.13
CHA3-5	2×10^{-4}	6.00×10^{-3}	3.66
$k_2(20\ °C) = 6.17 \times 10^2$ L mol^{-1} s^{-1}			

y = 617x - 0.014
R² = 0.9984
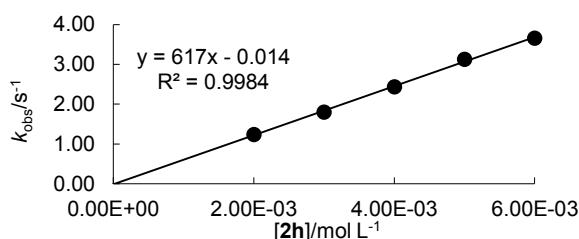
Table 7.76. Comparison of the Experimental Rate Constants for the reactions of 2h with 3,4 and the Rate Constants Calculated by Eq 7.1from the Reported E-parameter of 2h.

Nucleophile	N/s_N	k_2/ L mol^{-1} s^{-1}
3a	26.71/0.37	3.31×10^2
3b	27.45/0.38	3.20×10^2
3c	25.94/0.42	6.17×10^2
4	21.07/0.68	$3.41 \times 10^{1\ [a]}$
E (**2h**)$^{[a]} = -19.37$		

log $k_2/s_N = N - 19.371$
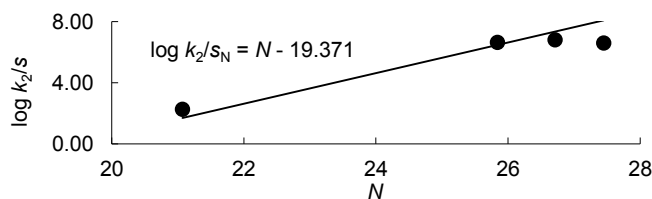
[a] Calculated by least square minimization according to eq 7.1 using N, s_N from Table 7.1.

7.5 References

[1] (a) S. Patai, Z. Rappoport, in *The Chemistry of Alkenes* (Eds.: S. Patai, Z. Rappoport), Wiley, New York, **1964**, p. 469−584; (b) W. Nagata, M. Yoshioka, *Org. React.* **1977**, *25*, 255−476; (c) D. A. Oare, C. H. Heathcock, in *Topics in Stereochemistry, Vol 18*

(Eds.: E. L. Eliel, S. H. Wilen), Wiley-Interscience, New York, **1989**, p. 227−407; (d) Z. Rappoport, in *Nucleophilicity* (Eds.: J. M. Harris, S. P. McManus), American Chemical Society, Washington, DC, **1987**, p. 399−424; (e) D. A. Oare, C. H. Heathcock, in *Topics in Stereochemistry, Vol. 20* (Eds.: E. L. Eliel, S. H. Wilen), Wiley-Interscience Hoboken, NJ **1991**, p. 87−170; (f) I. Chataigner, A. Harrison-Marchand, J. Maddaluno, in *Science of Synthesis, Vol. 26* (Ed.: J. Cossy), Georg Thieme Verlag, Stuttgart, Germany, **2005**, p. 1123−1286; (g) F. Fringuelli, O. Piermatti, F. Pizzo, L. Vaccaro, in *Science of Synthesis, Vol. 47b* (Ed.: A. de Meijere), Georg Thieme Verlag, Stuttgart, **2010**, p. 561−722.

[2]   (a) E. D. Bergmann, D. Ginsburg, R. Pappo, in *Organic Reactions*, Wiley, New York, **1959**, pp. 179-555; (b) P. Perlmutter, *Conjugate Addition Reactions in Organic Synthesis, Vol. 9*, Pergamon, Oxford, **1992**.

[3]   (a) I. Zugravescu, M. Petrovanu, *N-Ylid Chemistry*, McGraw-Hill, New York, **1976**; (b) A.-H. Li, L.-X. Dai, V. K. Aggarwal, *Chem. Rev.* **1997**, *97*, 2341−2372; (c) E. M. McGarrigle, E. L. Myers, O. Illa, M. A. Shaw, S. L. Riches, V. K. Aggarwal, *Chem. Rev.* **2007**, *107*, 5841−5883; (d) M. J. Gaunt, C. C. C. Johanson, *Chem. Rev.* **2007**, *107*, 5596−5605.

[4]   (a) R. Huisgen, H. Stangl, H. J. Sturm, H. Wagenhofer, *Angew. Chem.* **1961**, *73*, 170; (b) R. Huisgen, *Angew. Chem., Int. Ed. Engl.* **1963**, *2*, 565−598; (c) A. Ledwith, Y. Shih-Lin, *J. Chem. Soc. B* **1967**, 83−84; (d) R. Huisgen, G. Szeimies, L. Möbius, *Chem. Ber.* **1967**, *100*, 2494−2507; (e) R. Huisgen, *J. Org. Chem.* **1976**, *41*, 403−419; (f) A. Eckell, M. V. George, R. Huisgen, A. S. Kende, *Chem. Ber.* **1977**, *110*, 578−595; (g) L. Fisera, J. Geittner, R. Huisgen, H.-U. Reissig, *Heterocycles* **1978**, *10*, 153−158; (h) R. Huisgen, L. Xingya, *Tetrahedron Lett.* **1983**, *24*, 4185−4188; (i) A. Padwa, *1,3-Dipolar Cycloaddition Chemistry*, John Wiley and Sons, New York, **1985**; (j) R. Huisgen, E. Langhals, *Tetrahedron Lett.* **1989**, *30*, 5369−5372.

[5]   (a) J. Sauer, R. Sustmann, *Angew. Chem.* **1980**, *92*, 773-801; (b) J. Sauer, D. Lang, H. Wiest, *Chem. Ber.* **1964**, *97*, 3208−3218; (c) J. Sauer, H. Wiest, A. Mielert, *Chem. Ber.* **1964**, *97*, 3183−3207; (d) N. K. Sangwan, H.-J. Schneider, *J. Chem. Soc., Perkin Trans. 2* **1989**, 1223-1227; (e) A. Berkessel, H. Gröger, *Asymmetric Organocatalysis*, Wiley-VCH Weinheim **2005**.

[6]   (a) Y. Ogata, M. Okano, Y. Furuya, I. Tabushi, *J. Am. Chem. Soc.* **1956**, *78*, 5426-5428; (b) K. T. Finley, D. R. Call, G. W. Sovocool, W. J. Hayles, *Can. J. Chem.* **1967**, *45*, 571-573.

[7]   (a) N. Ogata, T. Asahara, *Bull. Chem. Soc. Jap.* **1966**, *39*, 1486-1490; (b) I. Šestáková, V. Horák, P. Zuman, *Collect. Czech. Chem. Commun.* **1966**, *31*, 3889-3902; (c) G. J. Dienys, L. J. J. Kunskaite, A. K. Vaitkevicius, A. V. Klimavicius, *Org. Reactiv., Engl. Ed.* **1975**, *12*, 275-282; (d) O. Adomeniene, G. Dienys, Z. Stumbreviciute, *Org. Reactiv., Engl. Ed.* **1978**, *15*, 38-44.

[8]   (a) K. L. Mallik, M. N. Das, *Z. Phys. Chem.* **1960**, *25*, 205-216; (b) K. Sanui, N. Ogata, *Bull. Chem. Soc. Jap.* **1967**, *40*, 1727-1727; (c) H. Shenhav, Z. Rappoport, S. Patai, *J. Chem. Soc. B* **1970**, 469-476; (d) J. Szczesna, M. Kostecki, S. Kinastowski, *Rocz. Akad. Roln. Poznaniu* **1988**, *192*, 99-104; (e) M. Kostecki, J. Szczesna, S. Kinastowski, *Rocz. Akad. Roln. Poznaniu* **1993**, *256*, 25-32.

[9]   (a) J. W. Bunting, A. Toth, C. K. M. Heo, R. G. Moors, *J. Am. Chem. Soc.* **1990**, *112*, 8878-8885; (b) C. K. M. Heo, J. W. Bunting, *J. Org. Chem.* **1992**, *57*, 3570-3578.

[10]   (a) M. Friedman, J. S. Wall, *J. Am. Chem. Soc.* **1964**, *86*, 3735-3741; (b) M. Friedman, J. F. Cavins, J. S. Wall, *J. Am. Chem. Soc.* **1965**, *87*, 3672-3682; (c) M. Friedman, J. S. Wall, *J. Org. Chem.* **1966**, *31*, 2888-2894; (d) M. Friedman, J. A. Romersberger, *J. Org. Chem.* **1968**, *33*, 154-157.

[11]   (a) P. Carsky, P. Zuman, V. Horvak, *Collect. Czech. Chem. Commun.* **1965**, *30*, 4316-4336; (b) B. A. Feit, R. Pazhenchevsky, B. Pazhenchevsky, *J. Org. Chem.* **1976**, *41*, 3246-3250.

[12]   (a) N. Ferry, F. J. McQuillin, *J. Chem. Soc.* **1962**, 103-113; (b) B.-A. Feit, A. Zilkha, *J. Org. Chem.* **1963**, *28*, 406-410; (c) R. N. Ring, G. C. Tesoro, D. R. Moore, *J. Org. Chem.* **1967**, *32*, 1091−1094.

[13]   (a) M. Morton, H. Landfield, *J. Am. Chem. Soc.* **1952**, *74*, 3523-3526; (b) W. G. Davies, E. W. Hardisty, T. P. Nevell, R. H. Peters, *J. Chem. Soc. B, Phys. Org.* **1970**, 998-1004.

[14]   (a) D. W. Roberts, A. Natsch, *Chem. Res. Toxicol.* **2009**, *22*, 592-603; (b) J. A. H. Schwöbel, D. Wondrousch, Y. K. Koleva, J. C. Madden, M. T. D. Cronin, G. Schüürmann, *Chem. Res. Toxicol.* **2010**, *23*, 1576-1585; (c) S. Amslinger, N. Al-Rifai, K. Winter, K. Wörmann, R. Scholz, B. Paul, M. Wild, *Org. Biomol. Chem.* **2013**, *11*, 549-554.

[15]   I. Petnehazy, G. Clementis, Z. M. Jaszay, L. Toke, C. D. Hall, *J. Chem. Soc., Perkin Trans. 2* **1996**, 2279-2284.

[16]   (a) R. Lucius, R. Loos, H. Mayr, *Angew. Chem., Int. Ed.* **2002**, *41*, 91−95; (b) T. Lemek, H. Mayr, *J. Org. Chem.* **2003**, *68*, 6880−6886; (c) S. T. A. Berger, F. H. Seeliger, F. Hofbauer, H. Mayr, *Org. Biomol. Chem.* **2007**, *5*, 3020−3026; (d) O. Kaumanns, R. Lucius, H. Mayr, *Chem. Eur. J.* **2008**, *14*, 9675−9682; (e) S. Lakhdar, T. Tokuyasu, H. Mayr, *Angew. Chem. Int. Ed.* **2008**, *47*, 8723−8726; (f) T. Kanzian, H. Mayr, *Chem. Eur. J.* **2010**, *16*, 11670−11677; (g) T. Kanzian, S. Nicolini, L. De Crescentini, O. A. Attanasi, A. R. Ofial, H. Mayr, *Chem. Eur. J.* **2010**, *16*, 12008−12016; (h) R. Appel, H. Mayr, *J. Am. Chem. Soc.* **2011**, *113*, 8240−8251; (i) I. Zenz, H. Mayr, *J. Org. Chem.* **2011**, *76*, 9370−9378; (j) H. Asahara, H. Mayr, *Chem. Asian J.* **2012**, *7*, 1401−1407.

[17]   D. S. Allgäuer, H. Mayr, *Eur. J. Org. Chem.* **2013**, *submitted*.

[18]   D. S. Allgäuer, H. Mayr, **2013**, *unpublished results*.

[19]   D. S. Allgäuer, P. Mayer, H. Mayr, *J. Am. Chem. Soc.* **2013**, *135*, 15216–15224.

[20]   (a) R. Appel, N. Hartmann, H. Mayr, *J. Am. Chem. Soc.* **2010**, *132*, 17894−17900; (b) R. Appel, H. Mayr, *Chem. Eur. J.* **2010**, *16*, 8610−8614.

[21]   (a) H. Mayr, M. Patz, *Angew. Chem., Int. Ed. Engl.* **1994**, *33*, 938−957; (b) H. Mayr, T. Bug, M. F. Gotta, N. Hering, B. Irrgang, B. Janker, B. Kempf, R. Loos, A. R. Ofial, G. Remennikov, H. Schimmel, *J. Am. Chem. Soc.* **2001**, *123*, 9500−9512; (c) H. Mayr, B. Kempf, A. R. Ofial, *Acc. Chem. Res.* **2003**, *36*, 66−77; (d) H. Mayr, A. R. Ofial, *Pure Appl. Chem.* **2005**, 1807−1821; (e) H. Mayr, A. R. Ofial, *J. Phys. Org. Chem.* **2008**, *21*, 584−595; (f) H. Mayr, S. Lakhdar, B. Maji, A. R. Ofial, *Beilstein J. Org. Chem.* **2012**, *8*, 1458−1478; (g) For a comprehensive database of nucleophilicity parameters N, s_N and electrophilicity parameters E, see http://www.cup.lmu.de/oc/mayr/.

[22]   R. C. Samanta, B. Maji, S. De Sarkar, K. Bergander, R. Fröhlich, C. Mück-Lichtenfeld, H. Mayr, A. Studer, *Angew. Chem., Int. Ed.* **2012**, *51*, 5234−5238.

[23]   (a) A. G. Mikhailovskii, V. S. Shklyaev, *Chem. Heterocycl. Compd.* **1997**, *33*, 243−265; (b) J. Jacobs, E. Van Hende, S. Claessens, N. De Kimpe, *Curr. Org. Chem.* **2011**, *15*, 1340−1362; (c) A. Kakehi, *Heterocycles* **2012**, *85*, 1529-1577.

[24]   O. Tsuge, S. Kanemasa, S. Takenaka, *Bull. Chem. Soc. Jpn.* **1985**, *58*, 3137−3157.

[25]   (a) R. A. Firestone, *J. Org. Chem.* **1968**, *33*, 2285−2290; (b) R. A. Firestone, *J. Org. Chem.* **1972**, *37*, 2181−2191.

[26]   R. Huisgen, *J. Org. Chem.* **1968**, *33*, 2291−2297.

[27]   S. L. Riches, C. Saha, N. F. Filgueira, E. Grange, E. M. McGarrigle, V. K. Aggarwal, *J. Am. Chem. Soc.* **2010**, *132*, 7626−7630.

[28]   O. Tsuge, S. Kanemasa, S. Takenaka, *Bull. Chem. Soc. Jpn.* **1985**, *58*, 3320−3336.

[29]   D. S. Allgäuer, H. Mayr, *Eur. J. Org. Chem.* **2013**, 6379–6388.

[30]   The kinetics of the reactions of *N,N*-dimethyl cinnamamide with the pyridinium ylides **3** showed bisexponential decays of the absorbances of the ylides **3**. As no reaction product could be obtained, it is unclear to which reaction these decays refer. Thus, the kinetics were not evaluated.

[31]   (a) P. Pérez, A. Toro-Labbé, A. Aizman, R. Contreras, *J. Org. Chem.* **2002**, *67*, 4747−4752; (b) L. R. Domingo, P. Pérez, R. Contreras, *Tetrahedron* **2004**, *60*, 6585−6591; (c) E. Chamorro, M. Duque-Noreña, P. Pérez, *J. Mol. Struct. THEOCHEM* **2009**, *896*, 73−79; (d) E. Chamorro, M. Duque-Noreña, P. Pérez, *J. Mol. Struct. THEOCHEM* **2009**, *901*, 145−152; (e) C. Wang, Y. Fu, Q.-X. Guo, L. Liu, *Chem. Eur. J.* **2010**, *16*, 2586−2598; (f) L.-G. Zhuo, W. Liao, Z.-X. Yu, *Asian J. Org. Chem.* **2012**, *1*, 336−345; (g) S.-i. Kiyooka, D. Kaneno, R. Fujiyama, *Tetrahedron* **2013**, *69*, 4247−4258; (h) E. Chamorro, M. Duque-Noreña, R. Notario, P. Pérez, *J. Phys. Chem. A* **2013**, *117*, 2636−2643.

[32]   (a) R. Huisgen, *Angew. Chem., Int. Ed. Engl.* **1963**, *2*, 633−645; (b) R. Sustmann, *Pure Appl. Chem.* **1974**, *40*, 569-593; (c) B. Blankenburg, H. Fiedler, M. Hampel, H. G. Hauthal, G. Just, K. Kahlert, J. Korn, K. H. Müller, W. Pritzkow, Y. Reinhold, M. Röllig, E. Sauer, D. Schnurpfeil, G. Zimmermann, *J. Prakt. Chem.* **1974**, *316*, 804−816; (d) W. Bihlmaier, R. Huisgen, H.-U. Reissig, S. Voss, *Tetrahedron Lett.* **1979**, *20*, 2621−2624.

[33]   (a) D. H. Ess, K. N. Houk, *J. Am. Chem. Soc.* **2007**, *129*, 10646−10647; (b) D. H. Ess, K. N. Houk, *J. .Am. Chem. Soc.* **2008**, *130*, 10187−10198; (c) L. Xu, C. E. Doubleday, K. N. Houk, *J. Am. Chem. Soc.* **2010**, *132*, 3029−3037; (d) Y. Lan, L. Zou, Y. Cao, K. N. Houk, *J. Phys. Chem. A* **2011**, *115*, 13906–13920; (e) S. A. Lopez, M. E. Munk, K. N. Houk, *J. Org. Chem.* **2013**, *78*, 1576−1582.

[34]   (a) W.-J. van Zeist, F. M. Bickelhaupt, *Org. Biomol. Chem.* **2010**, *8*, 3118−3127; (b) I. Fernández, F. P. Cossío, F. M. Bickelhaupt, *J. Org. Chem.* **2011**, *76*, 2310−2314.

[35]   H. E. Gottlieb, V. Kotlyar, A. Nudelman, *J. Org. Chem.* **1997**, *62*, 7512−7515.

[36]   H. Asahara *unpublished results*. **2012**.

8 Applications of the Linear Free-Energy Relationship log $k_2 = s_N(N + E)$

Dominik S. Allgäuer and Herbert Mayr

8.1 Introduction

In chapters 5–7 we have derived the electrophilicity parameters E for a variety of acceptor-substituted olefins, like the ethylenes **1** and **3**,[1] the propylenes **2a,c,i**[1b, 2] and the styrenes **2b,2e−h,j**[1b, 2] (Chart 8.1) from the rate constants of their reactions with pyridinium[3] and sulfonium ylides[4] using eq 8.1, in which k_2 is the second-order rate constant at 20 °C, s_N is a nucleophile specific slope parameter, N is a nucleophilicity parameter, and E is an electrophilicity parameter.

Rate constants for a large number of reactions of the Michael acceptors **1−3** with nucleophiles with known nucleophilicity parameters (N and s_N) were determined over the last decades (Scheme 8.1).[5-9] In order to examine the general applicability of the E parameters determined in this work for predicting rate constants of Michael reactions, we collected rate constants[5-9] for the additions of C,[5] N,[6] O,[7] S,[8] and P[9] nucleophiles to the Michael acceptors **1–3** from the literature and compared them with those calculated by eq 8.1 using the previously reported s_N and N parameters of these nucleophiles[10-15] and the E parameters of the acceptor-substituted olefins **1–3** from Chart 8.1. In order to avoid ambiguities, we did not correct the reported rate constants for small changes in temperature or solvent polarity and just discuss when large deviations arise.

Many rate constants for the reactions of the activated olefins **1−3** with diazomethanes ([3+2]-cycloadditions)[16] and dienes (Diels-Alder reactions)[17] have been reported previously (k_2^{exp}; Scheme 8.2). The nucleophilicity parameters N and s_N of these diazomethanes[18] and dienes[19] have been derived from their stepwise reactions with benzhydrylium ions in preceding studies. In recent reports we have shown that eq 8.1 allows to predict the second-order rate constants for a large variety of polar nucleophile electrophile combinations, while concerted reactions do not follow eq 1.[20]

$$\log k_2 = s_N(N + E) \qquad (8.1)$$
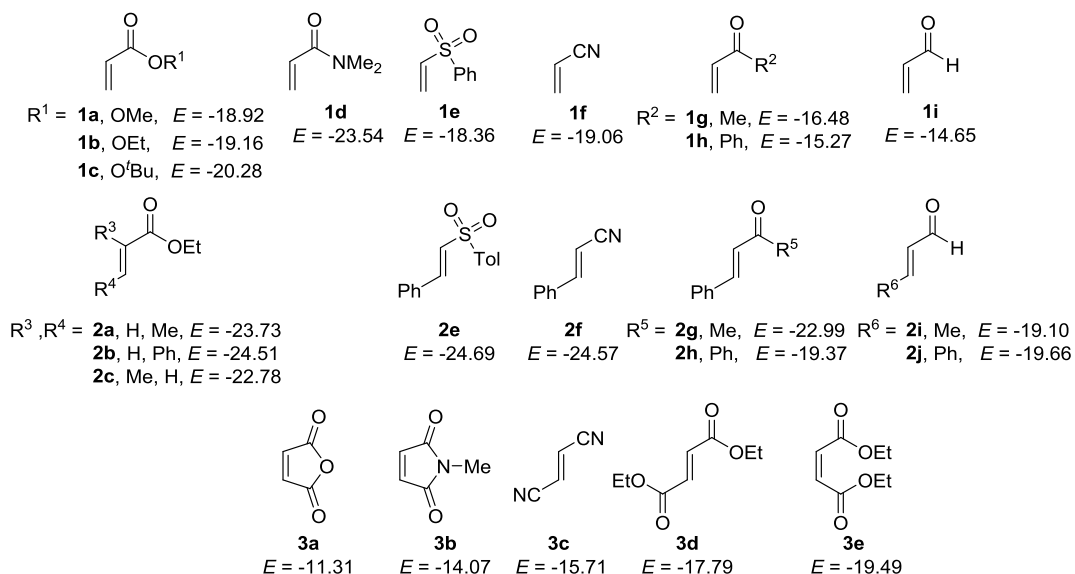
Chart 8.1. Structures and electrophilicity parameters E of the acceptor-substituted Olefins $1{-}3$ (E from refs. [1-2]).

The experimental rate constants (k_2^{exp}) for the reactions of diazomethanes and dienes with the Michael acceptors $1{-}3$ correspond to concerted processes, while the rate con-

Scheme 8.1. Addition of nucleophiles to the acceptor-substituted olefins $1{-}3$.

constants calculated by eq 8.1 (k_2^{calcd}) describe the corresponding stepwise additions. The deviation between these calculated rate constants (k_2^{calcd}) and the experimental rate constants (k_2^{exp}) can be used to derive the "free enthalpy of concert" $\Delta G_{concert}$ according to eq 8.2.[21]

Although the conditions (temperature, solvent) under which many of these rate-constants were obtained, differ from those used to derive E, N and s_N, we did not correct the reported rate constants for changes in temperature or solvent polarity to avoid ambiguities.

Scheme 8.2. a) 1,3-Dipolar cycloaddition of a diazomethane to the acceptor-substituted olefins $1{-}3$. b) Diels-Alder reaction of a diene with the acceptor-substituted olefins $1{-}3$.

$$\Delta G_{concert} = RT\ln(k_2^{exp}/k_2^{calcd}) \qquad (8.2)$$
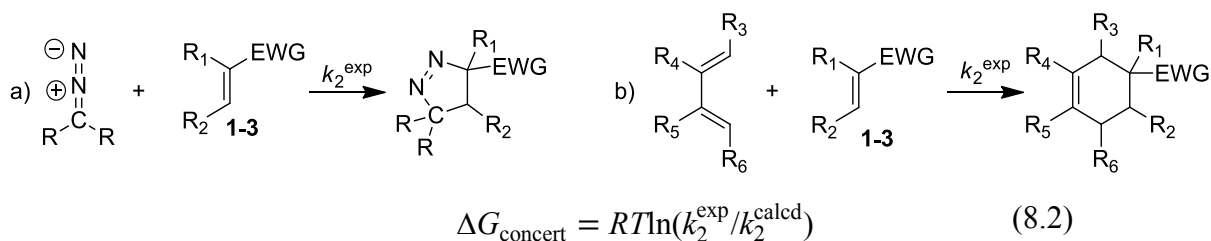
8.2 Testing the Applicability of log $k_2 = s_N(N + E)$

8.2.1 General

Table 8.1 lists the nucleophilicity parameters N and s_N of various C,[10] N,[11-13] O,[14] S,[12a, 13] and P[15] nucleophiles, for which rate constants for reactions with the Michael acceptors **1−3** are available, and the solvent in which these parameters were determined. In the following Figures and Tables, we will refer to the corresponding nucleophiles using the abbreviation given in Table 8.1.

Table 8.1. N and s_N parameters of C,[10] N,[11-13] O,[14] S,[12a, 13] and P [15] nucleophiles at 20 °C.

Nucleophile	Abbreviation	Solvent	N/s_N	Ref.
Acetylacetone anion	Acac⁻	H_2O	13.73/0.64	[10b]
Diethylmalonate anion	Ma⁻	DMSO	20.22/0.65	[10a]
4-Pyridone anion	4-PyO⁻	H_2O	14.76/0.48	[11b]
2-Pyridone anion	2-PyO⁻	H_2O	12.47/0.52	[11b]
4-Dimethylaminopyridine	DMAP	H_2O	13.19/0.56	[11a]
4-Morpholinoaminopyridine	MorAP	H_2O	12.39/0.66	[11a]
4-Aminopyridine	AP	H_2O	12.19/0.66	[11a]
3-Br-4-Aminopyridine	BrAP	MeCN	12.96/0.67	[11c]
Piperidine	Pip	MeOH/MeCN[a]	15.63/0.64	[12b]
		H_2O	18.13/0.43	[12c]
		DMSO	17.19/0.71	[12a]
Pyrrolidine	Pyr	MeCN	18.64/0.60	[12d]
		H_2O	17.21/0.49	[12c]
Morpholine	Mor	MeOH/MeCN[a]	15.40/0.64	[12b]
Dimethylamine	Me₂NH	H_2O	15.62/0.54	[12c]
Diethylamine	Et₂NH	H_2O	14.68/0.53	[12c]
Dipropylamine	nPr₂NH	MeCN	14.51/0.80	[12d]
Dibutylamine	nBu₂NH	MeCN	(~14.35/0.80)[b]	
NH₃	NH₃	H_2O	9.48/0.59	[12c]
Methylamine	MeNH₂	H_2O	13.85/0.53	[12c]
Ethylamine	EtNH₂	H_2O	12.87/0.58	[12c]
n-Propylamine	nPrNH₂	H_2O	13.33/0.56	[12c]
		MeCN	15.11/0.63	[12d]
iso-Propylamine	iPrNH₂	MeCN	13.77/0.70	[12d]
		H_2O	12.00/0.56	[12c]
n-Butylamine	nBuNH₂	MeCN	15.27/0.63	[12d]
$tert$-Butylamine	tBuNH₂	MeCN	12.35/0.67	[12d]
Benzylamine	BnNH₂	MeCN	14.29/0.67	[12d]
Allylamine	AllylNH₂	MeCN	14.37/0.66	[12d]
		H_2O	13.21/0.54	[12c]
Aniline	Aniline	MeCN	12.67/0.68	[12c]

Table 8.1. Continued.

Nucleophile	Abbreviation	Solvent	N/s_N	Ref.
Ethanolamine	HOEtNH$_2$	H$_2$O	12.61/0.58	[12c]
		MeCN	14.11/0.71	[12d]
Diethanolamine	(HOEt)$_2$NH	DMSO	15.51/0.70	[12c]
Glycine	Gly	H$_2$O	13.51/0.58	[13]
Diglycine	GlyGly	H$_2$O	12.91/0.58	[13]
Alanine	Ala	H$_2$O	13.01/0.58	[13]
β-Alanine	β-Ala	H$_2$O	13.26/0.58	[13]
Phenylalanine	Phe	H$_2$O	14.12/0.53	[13]
Methionine	Met	H$_2$O	13.16/0.58	[13]
OH$^-$	OH$^-$	H$_2$O	10.47/0.61	[12a]
MeO	MeO	MeOH	15.78/0.56	[14]
EtO$^-$	EtO$^-$	EtOH	15.78/0.65	[14]
nPrO$^-$	nPrO$^-$	nPrOH	16.03/0.70	[14]
iPrO$^-$	iPrO$^-$	iPrOH	17.03/0.63	[14]
Cysteine dianion	Cys^{2-}	H$_2$O	23.43/0.42	[13]
Mercaptoacetic acid dianion	SAc^{2-}	H$_2$O	22.62/0.43	[12a]
SO$_3^{2-}$	SO$_3^{2-}$	H$_2$O	16.83/0.56	[12a]
P(OMe)$_3$	P(OMe)$_3$	MeOH/MeCN[a]	9.05/0.70	[15]

[a] MeOH/MeCN 91/9; [b] Estimated from the reactivity of nPr$_2$NH using the reactivity difference of nPrNH$_2$ and nBuNH$_2$ of $\Delta N = 0.16$; as nPrNH$_2$ and nBuNH$_2$ have the same s_N parameter, the same s_N parameters are also assumed for nPr$_2$NH and nBu$_2$NH.

Table 8.2 lists the experimental rate constants (k_2^{exp}) collected from the literature,[5-9] as well as the rate constants calculated by eq 8.1 (k_2^{calcd}) using the electrophilicity parameters E of the acceptor-substituted olefins **1−3** from Chart 8.1 and nucleophilicity parameters N, s_N of the nucleophiles from Table 8.1. The solvents and temperatures employed in the measurements of k_2^{exp} sometimes differ from those used to determine N, s_N, and E. The effects of these differences are in many cases negligible and will only be discussed if large deviations arise.[19a, 20a, b]

The reported experimental second-order rate constants (k_2^{exp}) for the additions of carbanions,[5-6] pyridines (exceptions are discussed below),[6j, k] pyridones,[6j, k] amines (exceptions are discussed below),[6a-i, 6l] OH$^-$ (exceptions are discussed below),[7c, f, 7h-j] and alkoxides,[6b, 7a, b, d, e, g] SO$_3^{2-}$,[8a] mercapto acid dianions,[8b, c] and P(OMe$_3$)[9] agree fairly well with the k_2^{calcd} calculated by eq 8.1. The deviations between k_2^{exp} and k_2^{calcd} are small, in comparison to the big reactivity range of 18 orders of magnitude which is covered by the comparison. Of the 110 experimental and calculated rate constants listed in Table 8.2 for the additions of C, N, O, S, and P nucleophiles to the acceptor-substituted olefins **1−3,** 96 agree within the limit of confidence of eq 8.1 (two orders of magnitude), and 52 agree with a factor better than 10.

Table 8.2. Experimental (k_2^{exp}) [5-9] and calculated (k_2^{calcd})[a] second-order rate constants of the reactions of C, N, O, S, and P nucleophiles with the acceptor-substituted olefins 1−3.
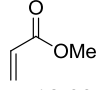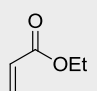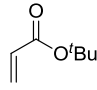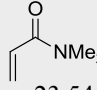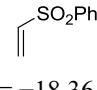
Electro-phile	Nucleo-phile	$T/$ °C	$k_2^{exp}/M^{-1}\,s^{-1}$	Ref.	k_2^{calcd} (20 °C)/$M^{-1}\,s^{-1}$	$k_2^{exp}/$ k_2^{calcd}
1a	DMAP	25	1.46×10^{-2} (H_2O)	[6k]	6.16×10^{-4} (H_2O)	23.7
	Mor	30	1.07×10^{-2} (MeOH)	[6g]	5.56×10^{-3} (MeOH)	1.92
	Pip	45	2.67×10^{-1} (MeOH)[b]	[6m]	7.80×10^{-3} (MeOH/MeCN)	34.2
$E = -18.92$	HOEtNH₂	20	7×10^{-3} (MeCN)	[6b]	3.82×10^{-4} (MeCN)	1.83
	Gly	30	1.82×10^{-2} (H_2O)	[6c]	7.25×10^{-4} (H_2O)	25.1
	GlyGly	30	4.60×10^{-3} (H_2O)	[6c]	3.25×10^{-4} (H_2O)	14.1
	Ala	30	1.11×10^{-2} (H_2O)	[6c]	3.72×10^{-4} (H_2O)	29.7
	β-Ala	30	2.84×10^{-2} (H_2O)	[6c]	5.19×10^{-4} (H_2O)	54.7
	Phe	30	6.40×10^{-3} (H_2O)	[6c]	2.85×10^{-3} (H_2O)	2.25
	Met	30	6.90×10^{-3} (H_2O)	[6c]	4.54×10^{-4} (H_2O)	15.1
	MeO⁻	24	2.1×10^{-1} (MeOH)	[7d]	1.74×10^{-2} (MeOH)	12.1
	SO₃²⁻	25	2.9×10^{-1} (H_2O)[b]	[8a]	6.72×10^{-2} (H_2O)	4.31
1b	Mor	45	1.3×10^{-2} (MeOH)[b]	[6m]	3.93×10^{-3} (MeOH/MeCN)	3.30
	n-BuNH₂	20	3.5×10^{-5} (THF)	[6f]	3.55×10^{-3} (MeCN)	0.01
	BnNH₂	20	8.30×10^{-7} (THF)	[6b]	5.47×10^{-4} (MeCN)	0.002
	AllylNH₂	20	2.66×10^{-6} (THF)	[6b]	6.92×10^{-4} (MeCN)	0.004
$E = -19.16$	Aniline	20	no reaction (THF)	[6b]	3.53×10^{-5} (MeCN)	-
	HOEtNH₂	20	4.0×10^{-4} (THF)	[6f]	2.61×10^{-4} (MeCN)	1.54
	(HOEt)₂NH	20	1.5×10^{-3} (THF)	[6b]	2.79×10^{-3} (DMSO)	0.54
	EtO⁻	20	2.0×10^{-3} (EtOH)	[6b]	6.37×10^{-3} (EtOH)	0.31
1c	nBu₂NH	25	3.18×10^{-6} (neat)	[6o]	1.81×10^{-5} (MeCN)	0.18
$E = -20.28$						
1d	DMAP	25	1.82×10^{-4} (H_2O)	[6k]	1.60×10^{-6} (H_2O)	113
	Gly	30	2.9×10^{-5} (H_2O/DMSO)	[6n]	1.53×10^{-6} (H_2O)	19.0
	GlyGly	30	2.0×10^{-5} (H_2O/DMSO)	[6n]	6.85×10^{-7} (H_2O)	29.2
$E = -23.54$	iPrO⁻	24	1.17×10^{-3} (iPrOH)	[7d]	7.94×10^{-5} (iPrOH)	14.7
1e	MeO⁻	25	8.0×10^{-2} (MeOH)	[7e]	3.61×10^{-2} (MeOH)	2.21
	EtO⁻	25	4.90×10^{-1} (EtOH)	[7e]	2.12×10^{-2} (EtOH)	23.1
	nPrO⁻	25	8.62×10^{-1} (nPrOH)	[7e]	2.36×10^{-2} (nPrOH)	36.6
$E = -18.36$						

Table 8.2. Continued.
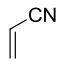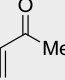
Electro-phile	Nucleo-phile	$T/$ °C	$k_2^{exp}/M^{-1}\,s^{-1}$	Ref.	k_2^{calcd} (20 °C)/$M^{-1}\,s^{-1}$	k_2^{exp}/k_2^{calcd}
1f	Acac$^-$	40	2.64×10^{-4} (H$_2$O) [b]	[6a]	3.89×10^{-4} (H$_2$O)	0.68
	4-PyO$^-$	25	8.5×10^{-3} (H$_2$O)	[6j]	8.65×10^{-3} (H$_2$O)	0.98
	2-PyO$^-$	25	5.0×10^{-3} (H$_2$O)	[6j]	3.75×10^{-4} (H$_2$O)	13.3
$E = -19.06$	DMAP	25	4.03×10^{-3} (H$_2$O)	[6j]	5.18×10^{-4} (H$_2$O)	7.79
	MorAP	25	2.34×10^{-3} (H$_2$O)	[6j]	3.97×10^{-5} (H$_2$O)	58.9
	AP	25	2.90×10^{-3} (H$_2$O)	[6j]	2.93×10^{-5} (H$_2$O)	98.9
	BrAP	25	8.1×10^{-4} (H$_2$O)	[6j]	8.21×10^{-5} (MeCN)	9.86
	Pip	25	5.08×10^{-1} (H$_2$O)	[6h]	3.91×10^{-1} (H$_2$O)	1.30
	Pyr	25	6.60×10^{-1} (H$_2$O)	[6h]	1.24×10^{-1} (H$_2$O)	5.31
	Mor	30	5.75×10^{-4} (MeOH)	[6h]	4.56×10^{-3} (MeOH/MeCN)	0.13
		25	5.02×10^{-2} (H$_2$O)	[6h]	1.39×10^{-2} (H$_2$O)	3.61
	Me$_2$NH	25	6.59×10^{-1} (H$_2$O)	[6h]	1.07×10^{-1} (H$_2$O)	6.13
	Et$_2$NH	25	9.24×10^{-2} (H$_2$O)	[6h]	4.78×10^{-3} (H$_2$O)	19.3
	nPr$_2$NH	25	8.89×10^{-2} (H$_2$O)	[6h]	2.30×10^{-4} (MeCN)	387
	MeNH$_2$	25	9.3×10^{-3} (H$_2$O)	[6h]	1.74×10^{-3} (H$_2$O)	5.35
	EtNH$_2$	25	7.7×10^{-3} (H$_2$O)	[6h]	2.58×10^{-4} (H$_2$O)	29.8
	nPrNH$_2$	25	8.9×10^{-3} (H$_2$O)	[6h]	6.20×10^{-4} (H$_2$O)	14.4
	iPrNH$_2$	25	2.80×10^{-3} (H$_2$O)	[6h]	1.12×10^{-4} (H$_2$O)	25.1
	nBuNH$_2$	25	1.01×10^{-2} (H$_2$O)	[6h]	9.83×10^{-2} (MeCN)	1.03
	AllylNH$_2$	25	4.84×10^{-3} (H$_2$O)	[6h]	6.95×10^{-3} (H$_2$O)	6.96
	HOEtNH$_2$	30	3.10×10^{-3} (H$_2$O) [b]	[6a]	1.82×10^{-4} (H$_2$O)	17.0
	Gly	30	5.00×10^{-3} (H$_2$O)	[6c]	6.06×10^{-4} (H$_2$O)	8.26
	GlyGly	30	1.37×10^{-3} (H$_2$O)	[6c]	2.72×10^{-4} (H$_2$O)	5.04
	Ala	30	3.53×10^{-3} (H$_2$O)	[6c]	3.11×10^{-4} (H$_2$O)	11.3
	β-Ala	30	8.92×10^{-3} (H$_2$O)	[6c]	4.34×10^{-4} (H$_2$O)	20.6
	Phe	30	1.76×10^{-3} (H$_2$O)	[6c]	2.42×10^{-3} (H$_2$O)	0.73
	Met	30	1.76×10^{-3} (H$_2$O)	[6c]	3.80×10^{-4} (H$_2$O)	4.64
	OH$^-$	25	2.6×10^{-4} (H$_2$O)	[7h]	5.77×10^{-6} (H$_2$O)	45.0
	MeO$^-$	20	3.84×10^{-2} (MeOH)	[7b]	1.46×10^{-2} (MeOH)	2.63
	EtO$^-$	20	5.25×10^{-2} (EtOH)	[7b]	7.40×10^{-3} (EtOH)	7.09
	nPrO$^-$	20	9.58×10^{-2} (nPrOH)	[7b]	7.59×10^{-3} (nPrOH)	12.6
	iPrO$^-$	20	2.87×10^{-1} (iPrOH)	[7b]	7.81×10^{-2} (iPrOH)	3.68
	Cys^{2-}	30	1.74 (H$_2$O)	[8b]	6.86×10^{1} (H$_2$O)	0.03
	SAc^{2-}	30	4.26 (H$_2$O)	[8b]	3.40×10^{1} (H$_2$O)	0.13
	SO$_3^{2-}$	25	1.7×10^{-1} (H$_2$O) [b]	[8a]	5.65×10^{-2} (H$_2$O)	3.01
1g	4-PyO$^-$	25	9.6×10^{-1} (H$_2$O)	[6k]	1.49×10^{-1} (H$_2$O)	6.43
	DMAP	25	5.5×10^{-1} (H$_2$O)	[6k]	1.44×10^{-2} (H$_2$O)	38.2
	MorAP	25	3.62×10^{-1} (H$_2$O)	[6k]	2.00×10^{-3} (H$_2$O)	181
	AP	25	4.2×10^{-1} (H$_2$O)	[6k]	1.47×10^{-3} (H$_2$O)	285
	BrAP	25	7.8×10^{-2} (H$_2$O)	[6k]	4.38×10^{-3} (MeCN)	17.8
	Mor	30	1.38 (MeOH)	[6g]	2.03×10^{-1} (MeOH/MeCN)	6.78
$E = -16.48$	Gly	30	4.00×10^{-1} (H$_2$O)	[6c]	1.89×10^{-2} (H$_2$O)	21.1
	MeO$^-$	19	3.88×10^{-1} (MeOH)	[7a]	4.05×10^{-1} (MeOH)	0.96
	EtO$^-$	19	1.53 (EtOH)	[7a]	3.51×10^{-1} (EtOH)	4.36
	iPrO$^-$	19	3.05 (iPrOH)	[7a]	2.22 (iPrOH)	1.38

Table 8.2. Continued.
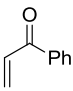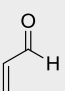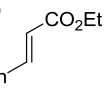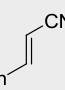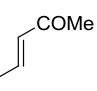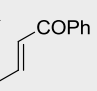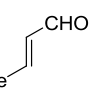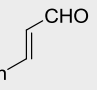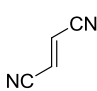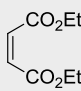
Electro-phile	Nucleo-phile	$T/$ °C	$k_2^{exp}/M^{-1}\,s^{-1}$	Ref.	k_2^{calcd} (20 °C)/$M^{-1}\,s^{-1}$	k_2^{exp}/k_2^{calcd}
1h	Mor	30	3.82 (MeOH)	[6g]	1.21 (MeOH/MeCN)	3.15
	NH_3	25	2.9×10^{-2} (H_2O)	[6d]	3.84×10^{-4} (H_2O)	75.5
	$MeNH_2$	25	5.68 (H_2O)	[6d]	1.77×10^{-1} (H_2O)	32.1
	$EtNH_2$	25	2.76 (H_2O)	[6d]	4.06×10^{-2} (H_2O)	68.0
Ph (acryloyl)	$iPrNH_2$	25	1.26 (aq. EtOH)	[6d]	8.93×10^{-2} (MeCN)	14.1
	$nBuNH_2$	25	1.98 (aq. EtOH)	[6d]	1.00 (MeCN)	1.98
$E = -15.26$	$tBuNH_2$	25	2.47×10^{-1} (aq. EtOH)	[6d]	7.91×10^{-3} (MeCN)	31.2
	$BnNH_2$	25	1.48 (aq. EtOH)	[6d]	2.21×10^{-1} (MeCN)	6.70
	$AllylNH_2$	25	1.98 (aq. EtOH)	[6d]	2.55×10^{-1} (MeCN)	7.76
	$HOEtNH_2$	25	3.78 (H_2O)	[6d]	1.50×10^{-1} (H_2O)	25.1
	OH^-	25	4×10^{-2} (H_2O)	[7c]	1.18×10^{-3} (H_2O)	33.8
1i	4-PyO^-	25	0.96 (H_2O)	[6k]	1.12 (H_2O)	0.86
	DMAP	25	2.39 (H_2O)	[6k]	1.51×10^{-1} (H_2O)	15.8
	MorAP	25	1.04 (H_2O)	[6k]	3.19×10^{-2} (H_2O)	32.6
$E = -14.65$	AP	25	1.96 (H_2O)	[6k]	2.36×10^{-2} (H_2O)	83.2
	BrAP	25	1.10×10^{-1} (H_2O)	[6k]	7.31×10^{-2} (MeCN)	1.51
	Mor	30	1.25 (MeOH)	[6g]	2.99 (MeOH/MeCN)	0.42
2b CO_2Et, Ph	Ma^-	25	2.96×10^{-4} (EtOH)	[5]	1.64×10^{-3} (DMSO)	0.18
$E = -24.51$						
2f CN, Ph	Pip	45	no reaction (H_2O)	[7h]	1.69×10^{-3} (H_2O)	-
	EtO^-	39	3.72×10^{-4} (EtOH)	[7g]	1.92×10^{-6} (EtOH)	194
$E = -24.57$						
2g COMe, Ph	OH^-	25	1×10^{-4} (aq. EtOH)[c]	[7c]	2.30×10^{-8} (H_2O)	4.36×10^3
	OH^-	25	3.16×10^{-4} (H_2O)	[7j]	2.30×10^{-8} (H_2O)	1.38×10^4
$E = -22.99$						
2h COPh, Ph	Pip	20	3.56×10^{-3} (DMSO)	[6i]	2.83×10^{-2} (DMSO)	0.13
	Pyr	25	2.31×10^{-2} (DMSO)	[6i]	3.64×10^{-1} (MeCN)	0.06
	$nPrNH_2$	25	5.5×10^{-4} (C_6H_6)	[6l]	2.07×10^{-3} (MeCN)	0.27
$E = -19.37$	$nBuNH_2$	25	7.1×10^{-4} (C_6H_6)	[6l]	2.61×10^{-3} (MeCN)	0.27
	OH^-	25	3.8×10^{-4} (aq. EtOH)	[7c]	3.72×10^{-6} (H_2O)	102
	$P(OMe)_3$	55	3.4×10^{-6} (neat)	[9]	5.96×10^{-8} (MeOH/MeCN)	57.0
2i CHO, Me	DMAP	25	8×10^{-3} (H_2O)	[6k]	4.92×10^{-4} (H_2O)	16.3
	OH^-	25	3.94×10^{-2} (H_2O) [d]	[7f]	5.46×10^{-6} (H_2O)	7.22×10^3
$E = -19.10$						
2j CHO, Ph	OH^-	25	2.20×10^{-3} (H_2O)	[7i]	2.48×10^6 (H_2O)	887
	Cys^{2-}	25	1.22×10^1 (H_2O)	[8c]	3.83×10^1 (H_2O)	0.32
$E = -19.66$						

Table 8.2. Continued.

Electrophile	Nucleophile	$T/°C$	$k_2^{exp}/M^{-1}\,s^{-1}$	Ref.	k_2^{calcd} (20 °C)/$M^{-1}\,s^{-1}$	k_2^{exp}/k_2^{calcd}
3c $E = -15.70$	MeO^-	24	9.93×10^{-2} (MeOH)	[7d]	1.10 (MeOH)	0.09
3e	Pip	34	1.79×10^{-2} (EtOH) [e]	[6e]	3.36×10^{-3} (EtOH)	5.32
	nBuNH$_2$	34	1.54×10^{-3} (EtOH) [e]	[6e]	2.18×10^{-3} (EtOH)	0.71
	nPrNH$_2$	34	5.16×10^{-4} (EtOH) [e]	[6e]	1.03×10^{-4} (EtOH)	5.02
$E = -17.79$	BnNH$_2$	34	5.00×10^{-4} (EtOH) [e]	[6e]	1.81×10^{-4} (EtOH)	2.76

[a] Calculated from E in Chart 8.1 and N, s_N in Table 8.1 by eq 8.1; [b] Average of the reported k_2 values; [c] Deviations from pseudo first-order kinetics were observed;[7c] [d] Reevaluated from the k_1-values in ref. [7f] (for details see Experimental Section); [e] Reevaluated from the k_1-values in ref. [6e] (for details see Experimental Section).

8.2.2 Reactions with C-Nucleophiles

The experimental and calculated reaction rates of the additions of the C nucleophiles, i.e., the carbanions of acetylacetone (Acac$^-$) and diethylmalonate (Ma$^-$), to acrylonitrile (**1f**) and ethyl cinnamate (**2b**) agree within a factor better than 6 (Table 8.2). The difference in temperature for the determination of the kinetics and reactivity parameters is negligible, but the deviation between experimental and calculated rate constant for the reaction of Ma$^-$ and ethyl cinnamate **2b** would probably even be smaller, if N and s_N parameters for Ma$^-$ in EtOH would be available.

8.2.3 Reactions with N-Nucleophiles

8.2.3.1 General

Rates of the additions of NH$_3$, primary amines (including amino acids), and secondary amines to the acceptor-substituted olefins **1−3** listed in Table 8.2 can in general be predicted within the limit of confidence of eq 8.1 with few exceptions (71 out of 79 rate constants). The rate constants calculated for the additions of amines in ethanol are suitable for direct comparison, because previous work has shown that N and s_N of amines differ only slightly in methanol, ethanol, and acetonitrile.[12c, d, 15] If the temperatures had been corrected to 20 °C, the agreement between calculated (20 °C) and experimental rate constants would become even better.

The good agreement between the experimental and calculated second-order rate constants ($k_2^{exp} \approx k_2^{clacd}$) for the reactions of amines with the Michael acceptors **1**,**2** in Table 8.2 indicates, that these rate constants refer to the formation of a single C−N-bond, as eq 8.1 is only valid for direct C−Nu bond formations.[20] Our interpretation of k_2^{exp} for the reactions of amines with diethyl maleate (**3e**) thus differs from the interpretation of Rappoport and co-workers[6e] in the original work, who assigned the second order rate constants k_2^{exp} to $K \cdot k_{rot}$ with K as the equilibrium constant for the amine addition and k_{rot} as the rate constants of rotation around the σ-bond of the intermediate aza-Michael adduct.

8.2.3.2 Reactions in Protic Solvents

In protic solvents like water or alcohols the reactions of the Michael acceptors **1**−**3** with amines proceed in many cases faster than calculated by eq 8.1, although the N and s_N of the amines were determined in these solvents (Table 8.2). The polarity of the amine also seems to have an influence on the predictability of the rate constant by eq 8.1, as amines with short alkylchains (e.g. Me, Et) and 4-amino-substituted pyridines tend to react faster with the activated double bond of **1**−**3** in protic solvents than calculated by eq 8.1 ($k_2^{exp}/k_2^{calcd} \geq 2$), while the corresponding reaction rates of amines with longer alkylchains (e.g. nPr, nBu) and pyridine anions in H_2O and alcohols deviate to a smaller extent.

The reason for the by a factor of 113 to 285 enhanced experimental rates of the reactions of N,N-dimethylacrylamide **1d** with DMAP and of methylvinylketone **1g** with MorAP and AP is unclear. The deviation between experimental and calculated rate constants for the reactions of acrylonitrile **1f** with nPr$_2$NH may be due to the fact that k_2^{exp} refers to water, while k_2^{calcd} refers to MeCN.

The experimental rate constants of the reactions of pyridone anions with the acrylonitrile **1f**, methylvinylketone **1g**, and acrolein **1i** can be reproduced with high accuracy by eq 8.1 as the deviation k_2^{exp}/k_2^{calcd} stays below a factor of 14.

8.2.3.3 Reactions in Aprotic Solvents

For the reactions of amines in solvents like ethers or benzene the corresponding reactivity parameters N and s_N are not available. Thus, it is not surprising that the comparison of k_2^{exp} and k_2^{calcd} becomes poorer, when N and s_N parameters of the amines in MeCN or DMSO have to be used for the calculation of k_2^{calcd} (Table 8.2). Nevertheless, the deviations between the

experimental and calculated rate constants for the additions of ethanolamine (HOEtNH$_2$; N, s_N in MeCN) and diethanolamine ((HOEt)$_2$NH; N, s_N in DMSO) to ethyl acrylate **1b** in THF are below a factor of 2, and the deviations for the additions of n-propylamine (nPrNH$_2$; N, s_N in MeCN) and n-butylamine (nBuNH$_2$; N, s_N in MeCN) to chalcone **2h** in benzene are below a factor of 4. Interestingly, the rate constants calculated from the estimated reactivity parameters for nBu$_2$NH in MeCN describe the experimental rate constants well. The rate constants of the reactions of benzylamine (BnNH$_2$; N, s_N in MeCN) and allylamine (AllylNH$_2$; N, s_N in MeCN) with ethyl acrylate **1b** in THF, however, cannot be reproduced by eq 8.1, which can be explained by the fact that charge separation is less favorable in THF than in MeCN.

No reaction was observed between aniline and ethyl acrylate **1b** or between piperidine (Pip) and cinnamonitrile **2f**, although the reactions should occur slowly according to eq 8.1. Maybe these reactions are hampered by unfavorable thermodynamics, although the reactions could proceed according to eq 8.1, i.e., in terms of kinetics.

8.2.4 Reactions with O-Nucleophiles

The deviations between the experimental and calculated rate constants of the addition of OH$^-$ to the Michael acceptors **1−2** are larger than for other investigated nucleophiles. In all investigated cases these additions were found to proceed faster than calculated by eq 8.1, so that only 2 out of 7 rate constants can be predicted within the limit of confidence of eq 8.1 (Table 8.2).

It should be noted, however, that all reactions of OH$^-$, which show so strong deviations refer to reactions with unsaturated aldehydes and ketones. Thus the additions of OH$^-$ to chalcone **2h** and cinnamaldehyde **2j** proceed 100 and 800 times faster than calculated, and the reactions of OH$^-$ and benzylideneacetone **2g** or crotonaldehyde **2i** proceed even 10^3 times faster than calculated, i.e., these reactions cannot be described by eq 8.1. As the N and s_N parameters of OH$^-$ have been determined in water and the temperature differences are negligible, these factors can be excluded as the reason for the faster reactions of OH$^-$ with the unsaturated carbonyl compounds. The big deviations of k_2^{exp} and k_2^{calcd}, as well as deviations from pseudo-first-order kinetics for the reaction of benzylideneacetone **2g** with OH$^{-[7c]}$ indicate a change of mechanism for these Michael additions.

The rate constants for the reactions of alkoxides (RO$^-$) with the activated ethylenes **1** can be calculated with high accuracy by eq 8.1, not exceeding a deviation of a factor of 13 for 14 of the 15 reactions listed in Table 8.2. Only the addition of EtO$^-$ to cinnamonitrile **2f** proceeds 194

times faster than calculated by eq 8.1. In all cases, the comparisons of experimental and calculated rate constants are unproblematic, because the nucleophilicity parameters N and s_N for alkoxides have been determined in the corresponding alcohol and the temperatures which were employed in the experiments are all close to 20 °C.

8.2.5 Reactions with S-Nucleophiles

The experimental rate constants for the additions of SO_3^{2-} to methyl acrylate **1a** and acrylonitrile **1f** can be reproduced by eq 8.1 within a factor of 4 (Table 8.2). The addition of cysteine dianion (Cys^{2-}) to cinnamaldehyde **2j** proceeds by a factor 3, and its addition to acrylonitrile **1f** by a factor 33 more slowly than calculated by eq 8.1. The rate constant for the addition of mercaptoacetic acid dianion (SAc^{2-}) to **1f** can be reproduced within a factor of 8. In all cases, the solvent is H_2O, the same in which the nucleophilicity parameters N and s_N of these nucleophiles were determined and the temperature difference is negligible.

8.2.6 Reactions with P-Nucleophiles

The addition of $P(OMe)_3$ to chalcone **2h** in neat $P(OMe)_3$ at 55 °C is 57 times faster than calculated for this reaction in methanol at 20 °C. This small difference, which is even reduced when the difference in temperature is considered indicates that the influence of the solvent on the reactivity of $P(OMe)_3$ must be small (Table 8.2).

8.2.7 Correlation Analysis

The plot of $(\log k_2)/s_N$ versus the nucleophilicity parameters N in Figure 8.1 for the reactions of acrylonitrile **1f** with the pyridinium ylides **4**[3] and the sulfonium ylide **5a**[4] was used to determine the E parameter of **1f** (black dots). The rate constants from Table 8.2 for the reactions of **1f** with other the types of nucleophiles, which were collected from the literature, also correlate fairly well (colored dots). From this correlation we conclude that eq 8.1 can generally be used for estimating rate constants, even when the reaction conditions are not exactly the same as those used to determine the reactivity parameters s_N, N, and E.

Remarkably, the deviations from the correlation line for 40 of the 41 rate constants depicted in Figure 8.1 stays below two orders of magnitude over a reactivity range of 18 orders of magnitude. Because of the small sensitivity parameters s_N for most of the nucleophiles

considered, the deviations in Figure 8.1 ($\Delta((\log k_2)/s_N)$) look larger than they actually are ($\Delta \log k_2$).
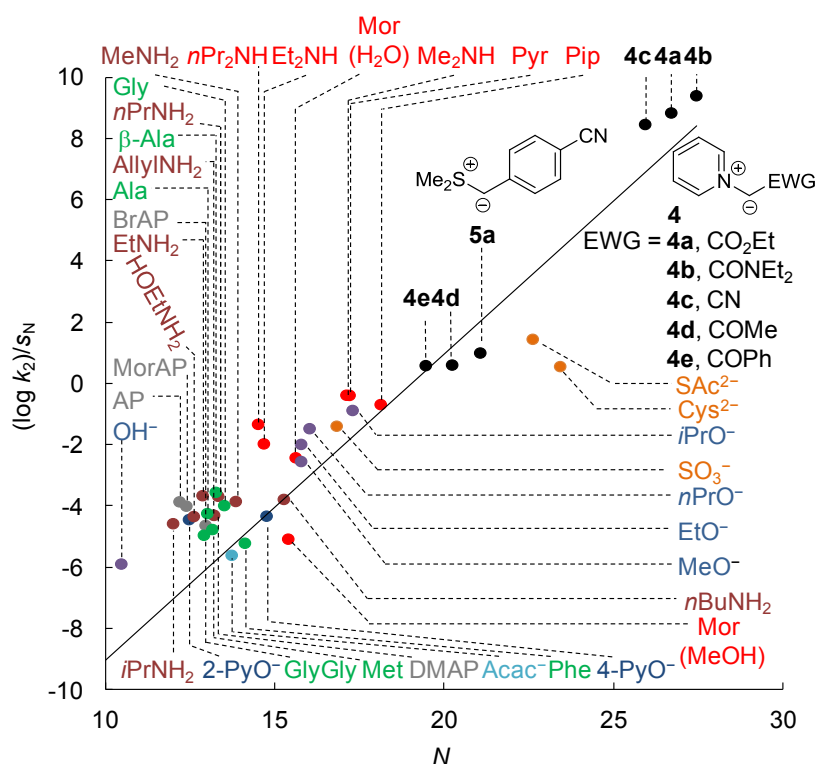

Figure 8.1. Correlation of the rate constants of the reactions of acrylonitrile 1f with pyridinium ylides 4 and sulfonium ylide 5 (black dots) and reported rate constants for its reactions with other nucleophiles (colored dots; rate constants from Table 8.2). Only the black symbols were employed to draw the correlation line.

While acetylacetone anion (Acac⁻), amines with long alkylchains (e.g. n-BuNH$_2$), pyridine anions (PyO⁻), alkoxides (RO⁻), and S nucleophiles (except Cys^{2-}) show no or relatively small deviations from the correlation line, amines with short alkylchains (e.g. Me$_2$NH, Et$_2$NH) and OH⁻ react between a factor 5 to 99 faster than calculated, which leads to a clustering of rate constants in a small reactivity range ($N = 12 - 14$) above the correlation line. All reactions of amines with acrylonitrile **1f** were carried out in H$_2$O showing the accelerating effect of this solvent on the aza-Michael addition.

8.2.8 Estimation of Reactivity Parameters

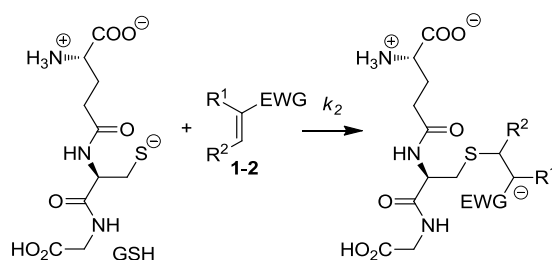### 8.2.8.1 Estimation of Nucleophilicity Parameters

Gluthathione (GSH) is an important biomolecule and a reference nucleophile for reactivity essays as its thiol group is taken as a surrogate for protein thiol groups.[22] An estimate of its nucleophilicity values would thus be highly interesting. As many rate constants for the reactions of GSH with various Michael acceptors, including **1a**,**b**,**f**,**g**,**i** and **2b**,**c**,**i**,**j** (Scheme 8.3), have been reported[8b, 22] it is an ideal candidate to test the applicability of eq 1 for the estimation of nucleophilicity parameters N and s_N from reported rate constants.

The second order rate constants for the reactions of GSH with **1a**,**b**,**f**,**g**,**i** and **2b**,**c**,**i**,**j** have previously been determined (25 °C, pH 6.8–7.4; for details see Experimental Section, Table 8.9),[8b, 22] and the temperature difference between the conditions under which the second order rate constants and the electrophilicity parameters E were determined is negligible. The rates of the reactions of glutathione with Michael acceptors are slightly dependent on the pH-value, as the rate of its reaction with acrylonitrile **1f** is increased by a factor of 3.9 when the pH is raised from 6.0 to 11.0.[8b]

The correlation of the reported rate constants $\log k_2$ for the reactions of GSH with **1a**,**b**,**f**,**g**,**i** and **2b**,**c**,**i**,**j** versus the electrophilicity parameters E is astonishingly good. According to eq 8.1 the slope of the correlation provides the nucleophile-specific slope parameter $s_N = 0.34$ and the intercept on the abscissa the nucleophilicity parameter $N = 17.01$ of GSH.

The tripeptide GSH is less reactive than the amino acid cysteine (Cys^{2-} $N = 23.43$, $s_N = 0.42$; Table 8.1) or mercaptoacetic acid (SAc^{2-} $N = 22.62$, $s_N = 0.43$; Table 8.1). The reaction of GSH with cinnamaldehyde **2j** proceeds 122 times more slowly than the corresponding reaction of Cys^{2-} (Table 8.2). The differences in reactivity between GSH and Cys^{2-} may be attributed to the bulkiness of GSH compared to Cys^{2-}, or be caused by the difference in pH (GSH: pH 6.8–7.4; Cys^{2-} pH 10.8[13]) at which the reactivity parameters were determined.

Scheme 8.3. Reaction of glutathione (GSH) with the acceptor-substituted olefins 1−2.
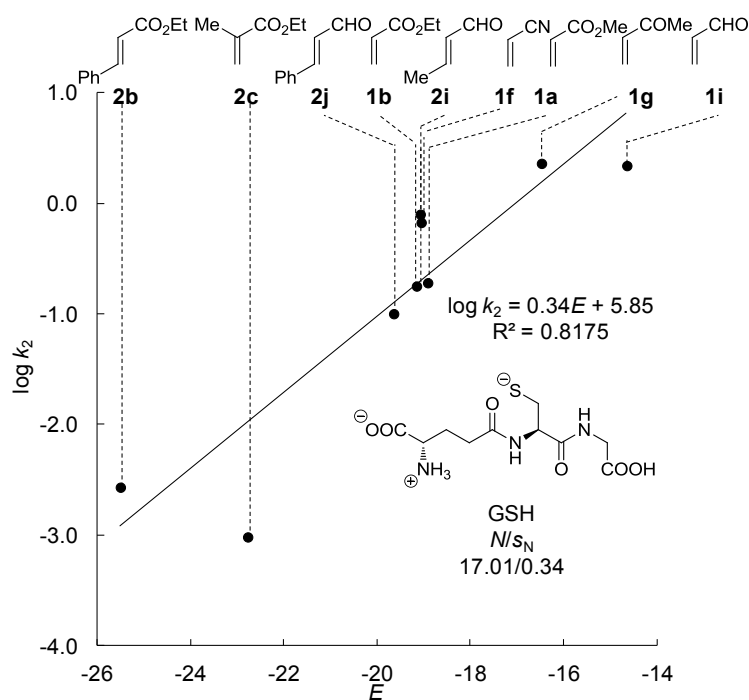
Figure 8.2. Correlation of k_2-values for the reactions of GSH with **1a,b,f,g,i** and **2b,c,i,j** at 25 °C (pH 6.8–7.4) reported in refs. [8b, 22] versus the corresponding electrophilicity parameters E.

8.2.8.2 Estimation of Electrophilicity Parameters from Literature Data on Michael Additions

The plots of $(\log k_2)/s_N$ in Figure 8.3 for the reactions of (4-methyoxy)phenylvinylketone **6a**,[6h] methylvinylsulfone **6b**,[6c, k] N-methyl-N-phenylethenesulfonamide **6c**,[7e] and acrylamide **6d**[6c, g, k] with amines, pyridines, and alkoxides in H_2O and alcohols at 25 and 30 °C versus the corresponding nucleophilicity parameters N and s_N from Table 8.1 correlate linearly (for details see Experimental Section). The nucleophilicity parameters for the employed amines and pyridines were in most cases determined in the solvents in which k_2 was determined, making their use unproblematic, and the difference in the temperature used for the determination of N and s_N and k_2^{exp} is negligible in all cases.

Eq 8.1 requires a slope of 1.0 for the correlations of $(\log k_2)/s_N$ versus the nucleophilicity parameter N. Figure 8.3 shows that this requirement is roughly met for the reactions of amines, pyridines, and alkoxides with (4-methoxy)phenylvinylketone **6a**, methylvinylsulfone **6b**, N-methyl-N-phenylethenesulfonamide **6c**, and acrylamide **6d**. Therefore, we estimated the electrophilicity parameter E of these Michael acceptors by least square-fitting, i.e., minimization of $\Delta^2 = \sum(\log k_2 - s_N(N + E)^2)$ (details see Experimental Section). Deviations from

380

the correlation lines in Figure 8.3 are surprisingly small for all four activated ethylenes and do not exceed a factor of 17, i.e., they are within the limit of confidence of eq 8.1.

The electrophilicity parameter $E = -13.16$ derived for the *p*-methoxy substituted phenylvinylketone **6a** from its reactions with amines in H_2O is 2.1 orders of magnitude lower than the electrophilicity parameter $E = -15.26$ of the parent phenylvinylketone **1h** determined from its reactions with the pyridinium (**4**) and sulfonium ylides (**5**) in DMSO (Chart 8.1).

In previous studies, we have shown that *p*-MeO-substitution of an aryl group directly attached to the CC-double bond decreases the electrophilicity of different activated ethylenes, including nitrostyrenes and bissulfonyl ethylenes,[23] by approximately 1 order of magnitude in aprotic solvents. The opposite ordering of the reactivity for (4-methoxy)phenylvinylketone **6a** and phenylvinylsulfone **1h** may be caused by the fact, that for the determination of the electrophilicity parameter E of **6a** only rate constants of its reactions with amines in water were considered. As we already showed above (Table 8.2, Figure 8.1), the rate constants of aza-Michael reactions in water are accelerated by 1−2 orders of magnitude, so that the estimated E parameter for (4-methoxyphenyl)vinylketone **6a** is only reliable within the limit of confidence of eq 8.1.

The same observation can be made for methylvinylsulfone **6b**. Although the rate constants for the reactions of methylvinylsulfone **6b** with pyridines and amines in H_2O correlate with the corresponding nucleophilicity parameters N, the estimated electrophilicity parameter of $E = -15.20$ seems to be too high: according to this electrophilicity parameter, methylvinylsulfone **6b** would be 3 orders of magnitude more reactive than its phenyl-substituted analogue phenylvinylsulfone **1e** ($E = -18.35$).

For *N*-methyl-*N*-phenylethenesulfonamide **6c** the estimated E parameter of -18.16 is in the range of the related phenylvinylsulfone **1e** ($E = -18.35$; Chart 8.1). However, the E parameter of *N*-methyl-*N*-phenylethenesulfonamide **6c** is based on only three rate constants of reactions with alkoxides in the corresponding alcohol and is not statistically confirmed.

For the estimation of the electrophilicity parameter $E = -19.00$ of acrylamide, only rate constants of its reactions with amines and pyridines in protic solvents (H_2O, MeOH) were considered, so that its reactivity might be overestimated, as it is rated 4 orders of magnitude more reactive than its alkylated analogue *N*,*N*-dimethyl acrylamide **1d** ($E = -23.54$; Chart 8.1).
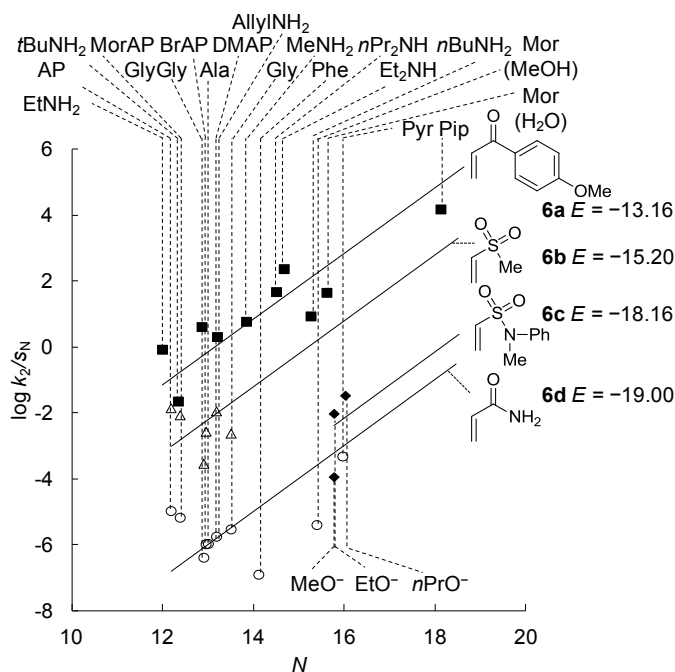
Figure 8.3. Correlation of reported k_2-values for the reactions of (4-methyoxyphenyl)vinylketone 6a (squares),[6h] methylvinylsulfone 6b (triangles),[6c, k] N-methyl-N-phenylethenesulfonamide 6c (diamonds),[7e] and acrylamide 6d (dots)[6c, g, k] with pyridines, amines, and alkoxides in H_2O and alcohols at 25 to 30 °C (the slopes are fixed to 1.0 as required by eq 8.1; for a detailed list of the k_2 values and the estimation of E see Exerimental Section).

8.3 Application of the Linear Free-Energy Relationship log $k_2 = s_N(N + E)$ to Concerted Reactions

Rates of [3+2]-cycloadditions of diazomethanes[16] and of Diels-Alder reactions of dienes[17] with different Michael acceptors like **1–3** have been reported, as well as the corresponding rate constants of their stepwise reactions with benzhydrylium ions **7**. [18, 19] The rates of these stepwise reactions were used to determine the nucleophilicity parameters N and s_N of diazomethanes[18] and dienes.[19]

Figure 8.4 plots the rate constants of the reactions of diphenyldiazomethane (left) and cyclopentadiene (right) with benzhydrylium ions **7** (filled circles) and with the different Michael acceptors **1−3** (open circles) versus the electrophilicity parameters E of the benzhydrylium ions **7**, and the acceptor-substituted ethylenes **1−3**.
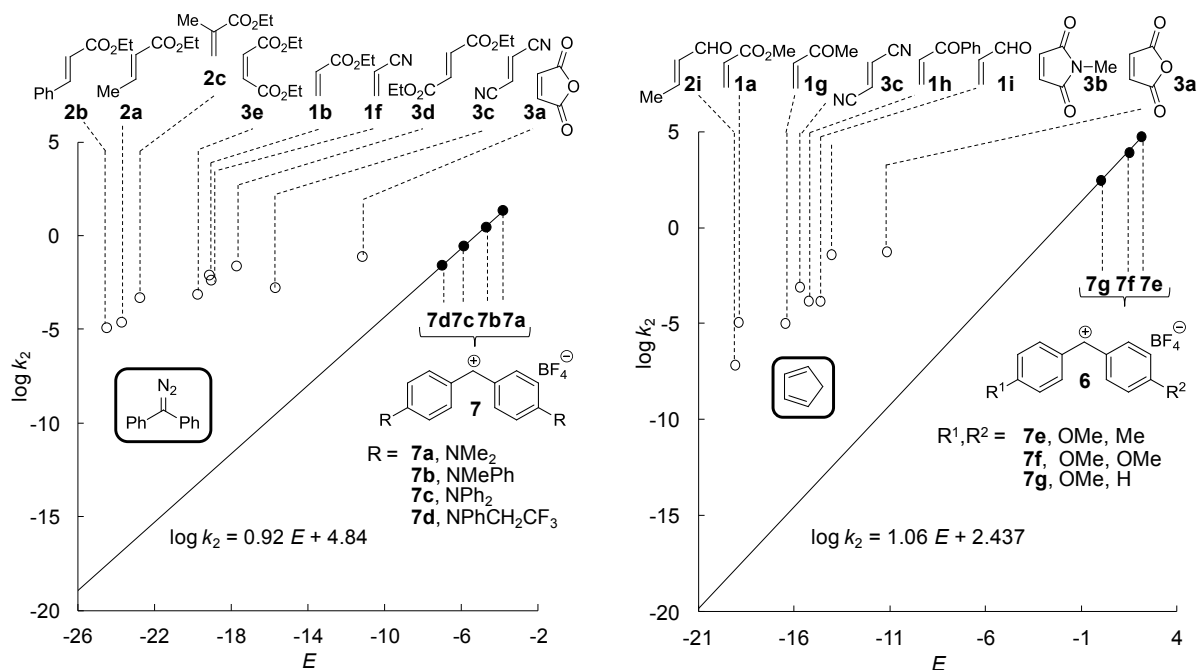
Figure 8.4. Correlation of the log k_2 values of the CC-bond forming reactions of diphenyl diazomethane (left)[18] and cyclopentadiene (right)[19a, b] with the benzhydrylium tetrafluoroborates 7 (filled circles, CH$_2$Cl$_2$, 20 °C) versus the corresponding E parameters. Open circles refer to the reactions with the acceptor-substituted olefins 1−3 (from Table 8.3).

An extrapolation of the correlation line obtained in Figure 8.4 for the rate-determining one-bond formations from reactions of diphenyldiazomethane and cyclopentadiene with the benzhydrylium ions **7** as depicted in Scheme 8.4 predict rate constants of 10^{-18} to 10^{-6} M^{-1}s^{-1} for the formation of zwitterions **8** and **10** (Scheme 8.4) from the corresponding reactions with the Michael acceptors **1**–**3**. The actually observed rate constants of 10^{-8} to 10^{-2} M^{-1}s^{-1} (open circles; Figure 8.4), however, are 5−12 orders of magnitude larger than expected for reactions involving the zwitterions **8** and **10** depicted in Scheme 8.4. This observation indicates that none of these reactions follows eq 8.1, which describes reactions with formation of *one* new σ-bond in the rate determining step.[20] The rate constants of the reactions of diphenyldiazomethane and cyclopentadiene with the Michael acceptors **1**–**3** thus do not refer to reactions in which a single σ-bond is formed in the rate-determining step, i.e., they cannot proceed via zwitterionic intermediates. In agreement with previous work,[16, 17] these reactions can be seen as concerted processes and *two* σ-bonds are simultaneously formed in the rate determining step (Scheme 8.4).

Although the rate constants of the reactions of diphenyldiazomethane and cyclopentadiene with the activated double bonds of **1**−**3** depicted in Figure 8.4 cannot be predicted by eq 8.1,

Scheme 8.4. Mechansim of the reactions of diphenyldiazomethane[18] with a benzhydrylium Salt 7 (a) and with fumaronitrile 1c (b).[a] Reactions c, d show to the mechansim of the reactions of cyclopenatdiene with reactions benzhydrylium ions (c)[19b] and fumaronitrile (d).[b]
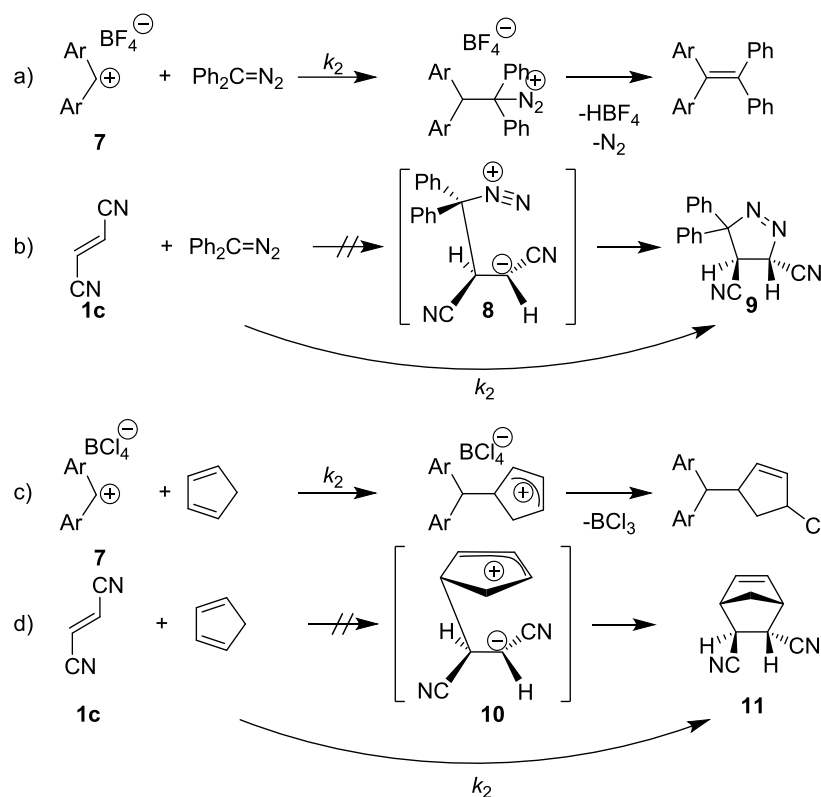
[a] Stereochemistry for the [3+2]-cycloadduct **8** in analogy to ref. [16e]; [b] Stereochemistry for the Diels-Alder adduct **10** from ref [26].

the rate constants show a dependence on the electrophilicity of the employed Michael acceptor **1−3**, as log k_2 increases linearly with increasing electrophilicity E.

A complementary analysis can be made for the reactions of methyl acrylate **1a**[1b] and of maleic anhydride **3a**[1a] with diazomethanes and dienes (Figure 8.5). The electrophilicity parameters E of these compounds have been derived from the rate constants of their stepwise reactions with pyridinium (**4**) and sulfonium ylides **5** (filled circles; Figure 8.5). The rate constants of their reactions with diazomethanes or dienes, however, lie far above the correlation lines. This observation demonstrates that the reactions of **1a** and **3a** with diazomethanes or dienes, do not proceed via zwitterionic intermediates. Instead, they follow a concerted mechanism and cannot be described by eq 8.1.

However, the rate constants for the concerted reactions of methyl acrylate **1a** and maleic anhydride **3a** with diazomethanes and dienes depend on the nucleophilicity parameters N and s_N, as (log k_2)/s_N increases with increasing nucleophilicity N.
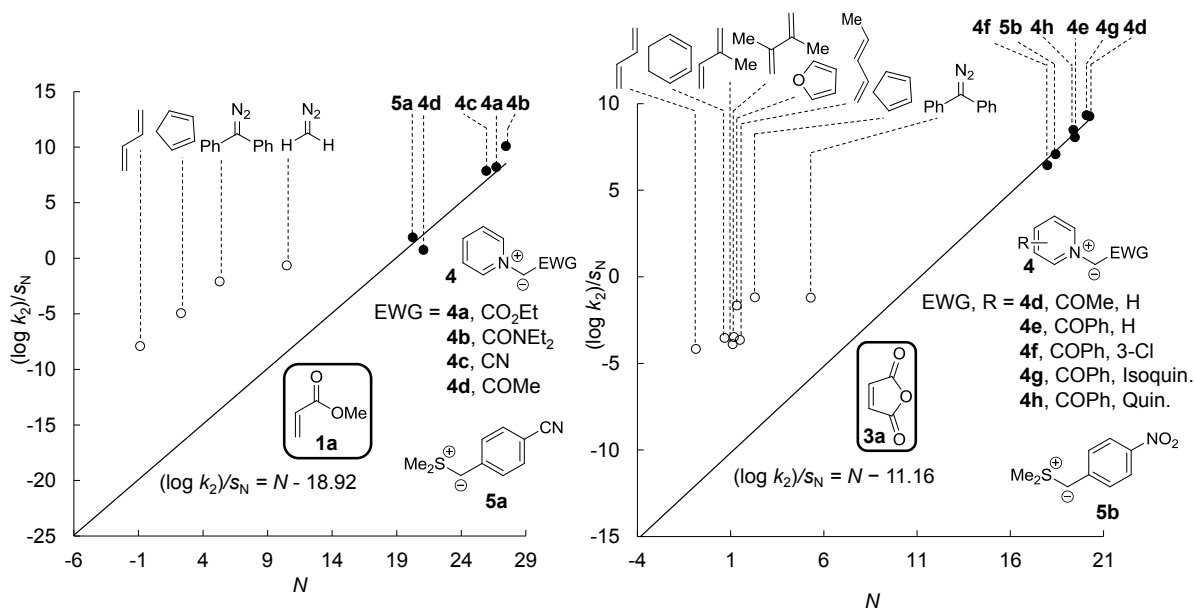
Figure 8.5. Correlation of $(\log k_2)/s_N$ of the stepwise reactions of methyl acrylate 1a (left)[1b] and maleic anhydride 3a (right)[1a] with pyridinium ylides 4 and sulfonium ylides 5 versus the corresponding N parameters (filled circles, DMSO, 20 °C). Open circles refer to the reactions of 1a and 3a with diazomethanes and dienes (from Table 8.3).

The gap between the correlation lines for the stepwise (k_2^{calcd}) and concerted (k_2^{exp}) processes in Figures 8.4 and 8.5 may be used to calculate the "free enthalpy of concert" $\Delta G_{\text{concert}}$ (eq 8.2), which is a measure for the interaction of the positively and negatively charged termini of a hypothetical zwitterionic intermediate in the transition state.[21] It should be noted that this interpretation only compares concerted mechanisms with stepwise processes via zwitterions and neglects the alternative via diradicals.[24]

Table 8.3 lists the rate constants from the literature for the reactions of diazomethanes[16] and dienes[17] with the Michael acceptors **1**−**3** including those depicted in Figures 8.4 and 8.5. The rate constants of the reactions in Table 8.3 were determined at 20–40 °C and are compared with the calculated values at 20 °C, neglecting the small differences in temperature (Table 8.3).

The solvents in which the reactivity parameters s_N, N, and E were determined differ in all cases from the solvents used to determine k_2^{exp}. Cycloadditions via zwitterionic intermediates are strongly affected by the solvent polarity,[27] while the rates of concerted (k_2^{exp}; Table 8.3) cycloadditions generally show only a small dependence on solvent polarity.[16d, 25] A variation of the solvent may, instead, result in a change of mechanism.

Table 8.3. Comparison of experimental (k_2^{exp})[16-17] and calculated (k_2^{calcd})[a] second-order rate constants and "free enthalpies of concert" $\Delta G_{concert}$[b] for the reactions of diazomethanes and dienes with the acceptor-substituted olefins 1−3.
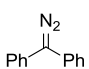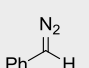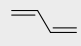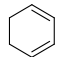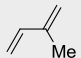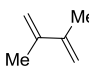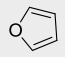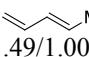
Nuc. N/s_N	Elec.	Solvent	$T/$ °C	$k_2^{exp}/M^{-1}\,s^{-1}$	Ref.	k_2^{calcd} (20 °C, CH$_2$Cl$_2$)/ M^{-1} s^{-1}	$k_2^{exp}/$ k_2^{calcd}	$\Delta G_{concert}/$ kJ mol^{-1}
Ph$_2$C=N$_2$ (Ph—C(N$_2$)—Ph) 5.29/0.92[c]	1a	DMF	40	8.31×10^{-3}	[16c]	2.87×10^{-13}	2.90×10^{10}	62.7
	1b	DMF	40	8.12×10^{-3}	[16c]	1.74×10^{-13}	4.66×10^{10}	64.0
	1f	DMF	40	4.34×10^{-3}	[16a]	2.16×10^{-13}	2.01×10^{10}	61.8
	2a	DMF	40	2.46×10^{-5}	[16a]	1.09×10^{-17}	2.26×10^{12}	74.1
	2b	DMF	40	1.25×10^{-5}	[16a]	2.09×10^{-18}	5.97×10^{12}	76.6
	2c	DMF	40	5.05×10^{-4}	[16a]	8.18×10^{-17}	6.17×10^{12}	76.7
	3a	DMF	40	7.90×10^{-2}	[16g]	2.88×10^{-6}	2.74×10^{4}	25.8
	3c	C$_6$H$_6$	30	1.72×10^{-3}	[16f]	2.60×10^{-10}	6.61×10^{6}	39.6
	3d	DMF	40	2.47×10^{-2}	[16g]	3.37×10^{-12}	7.33×10^{9}	59.1
	3e	C$_6$H$_5$Cl	25	7.60×10^{-4}	[16e]	8.55×10^{-14}	8.89×10^{9}	56.7
Ph—C(N$_2$)—H 9.35/0.83[c]	1b	DMF	40	2.73×10^{-1}	[16d]	7.23×10^{-9}	3.78×10^{7}	45.4
CH$_2$N$_2$ 10.48/0.78[c]	1a	THF	25	2.3×10^{-1}	[16b]	2.59×10^{-7}	8.86×10^{5}	33.9
	1b	DMF	25	1.12	[16c]	1.70×10^{-7}	6.58×10^{6}	38.9
	2a	THF	25	1.9×10^{-3}	[16b]	4.63×10^{-11}	4.10×10^{7}	43.5
	2c	THF	25	1.4×10^{-2}	[16b]	2.56×10^{-10}	5.46×10^{7}	44.1
	3e	THF	25	9.20×10^{-2}	[16b]	9.30×10^{-8}	9.89×10^{5}	34.2
(allyl/butadiene) −0.87/1.00[d]	1a	toluene	20	$1.28 \times 10^{-8,\,[g]}$	[17d]	1.61×10^{-20}	7.96×10^{11}	66.8
	1i	toluene	20	$4.88 \times 10^{-8,\,[g]}$	[17d]	2.98×10^{-16}	1.64×10^{8}	46.1
	2i	toluene	20	$1.01 \times 10^{-10,\,[g]}$	[17d]	1.08×10^{-20}	9.38×10^{9}	56.0
	3a	dioxane	30	6.83×10^{-5}	[17a]	6.57×10^{-13}	1.04×10^{8}	45.7
0.67/1.10[d]	3a	dioxane	30	1.32×10^{-4}	[17a]	1.96×10^{-12}	6.72×10^{7}	45.4
	3b	EtOH	25	4.02×10^{-4}	[17f]	1.82×10^{-15}	2.20×10^{11}	64.7
(isoprene) 1.10/0.98[e]	1i	toluene	20	$3.88 \times 10^{-7,\,[g]}$	[17d]	3.26×10^{-14}	1.19×10^{7}	39.7
	2i	toluene	20	$6.04 \times 10^{-8,\,[g]}$	[17d]	1.18×10^{-18}	5.11×10^{10}	60.1
	3a	dioxane	30	1.54×10^{-4}	[17a]	9.81×10^{-11}	1.57×10^{6}	36.0
(2,3-dimethylbutadiene) 1.17/1.00[d]	3a	dioxane	30	3.36×10^{-4}	[17a]	7.20×10^{-11}	4.66×10^{6}	38.1
	3b	EtOH	25	1.35×10^{-3}	[17f]	1.26×10^{-13}	1.07×10^{10}	57.2
	3c	dioxane	20	$3.49 \times 10^{-7,\,[h]}$	[17c]	2.89×10^{-15}	1.21×10^{8}	45.4
(furan) 1.33/1.29[f]	3a	MeCN	40	7.29×10^{-3}	[17e]	1.33×10^{-13}	5.50×10^{10}	62.3
(1-methylbutadiene) 1.49/1.00[d]	3a	dioxane	30	2.27×10^{-4}	[17a]	1.51×10^{-10}	1.51×10^{6}	35.9

Table 8.3. Continued.

Nuc. N/s_N	Elec.	Solvent	$T/$ °C	$k_2^{exp}/M^{-1} s^{-1}$	Ref.	k_2^{calcd} (20 °C, CH_2Cl_2)/ $M^{-1} s^{-1}$	k_2^{exp}/k_2^{calcd}	$\Delta G_{concert}/$ kJ mol^{-1}
	1a	dioxane	20	1.18×10^{-5}	[17b]	2.39×10^{-18}	4.95×10^{12}	71.2
	1f	dioxane	20	1.04×10^{-5}	[17b]	1.72×10^{-18}	6.03×10^{12}	71.7
	1g	dioxane	30	1.51×10^{-4}	[17d]	9.31×10^{-16}	1.62×10^{11}	65.0
	1i	dioxane	30	1.48×10^{-4}	[17d]	7.99×10^{-14}	1.85×10^{9}	53.8
	2i	dioxane	30	7.00×10^{-8}	[17d]	1.56×10^{-18}	4.47×10^{10}	61.8
2.30/1.06[d]	**3a**	dioxane	20	5.56×10^{-2}	[17b]	2.80×10^{-10}	1.99×10^{8}	46.6
		dioxane	30	9.21×10^{-2}	[17a]	2.80×10^{-10}	3.29×10^{8}	49.4
	3b	dioxane	20	3.95×10^{-2}	[17b]	3.35×10^{-13}	1.18×10^{11}	62.1
		EtOH	25	3.02×10^{-1}	[17f]	3.35×10^{-13}	9.02×10^{11}	68.2
	3c	dioxane	20	8.06×10^{-4}	[17b]	6.12×10^{-15}	1.32×10^{11}	62.4

[a] Calculated from E (Chart 8.1) and N, s_N (Table 8.3) by eq 8.1; [b] Calculated by eq 8.2 for the temperature at which k_2 was determined; [c] N and s_N for CH_2Cl_2 from ref. [18]; [d] N and s_N for CH_2Cl_2 from ref. [19d]; [e] N and s_N for CH_2Cl_2 from ref. [19c]; [f] N and s_N for CH_2Cl_2 at from ref. [19e]; [g] Calculated from activation parameters in ref. [17d] by using the Eyring equation; [h] Calculated from activation parameters in ref. [17c] by using the Eyring equation.

First of all, one can recognize that with exception of the reaction of diphenyldiazomethane with **3a**, all calculated rate constants k_2^{calcd} in Table 8.3 are smaller than 2×10^{-7} M^{-1} s^{-1}, i.e., none of these reactions can proceed via zwitterionic intermediates. From the ratio k_2^{exp}/k_2^{calcd}, the "free enthalpy of concert" $\Delta G_{concert}$ relative to the zwitterionic pathway was derived using eq 8.2.[21] If a diradical intermediate is feasible, $\Delta G_{concert}$ may be smaller, however, than the $\Delta G_{concert}$ values listed in Table 8.3 which measure the concertedness of the reaction relative to zwitterionic intermediates.

The "free enthalpies of concert" $\Delta G_{concert}$ for the [3+2]-cycloadditions of diphenyldiazomethane decrease with increasing electrophilicity of the olefins **1−3**, i.e., from 77 kJ mol^{-1} for the reaction with ethyl cinnamate **2b**, the least electrophilic Michael acceptor in the series, to 26 kJ mol^{-1} for the reaction with maleic anhydride **3a**, the most electrophilic activated ethylene. Similarly, $\Delta G_{concert}$ decreases for the Diels-Alder reactions of cyclopentadiene with increasing electrophilicity from 73 kJ mol^{-1} with methyl acrylate **1a**, to 47 kJ mol^{-1} with maleic anhydride **3a**.

The "free enthalpy of concert" $\Delta G_{concert}$ also decreases with increasing nucleophilicity of the diazomethane or diene: $\Delta G_{concert}$ decreases from 73 kJ mol^{-1} in the reaction of methyl acrylate **1a** with cyclopentadiene to 34 kJ mol^{-1} in the reaction of **1a** with diazomethane. For maleic anhydride **3a** the "free enthalpy of concert" $\Delta G_{concert}$ decreases from 62 kJ mol^{-1} in the reaction with furan, to 26 kJ mol^{-1} in reaction with diphenyldiazomethane.

The correlation between the reactivity parameters N and E and the "free enthalpy of concert" $\Delta G_{concert}$ may now allow us to estimate the concertedness of different types of pericyclic reactions – always with the caveat that reactions via intermediate diradicals are not considered.

8.4 Conclusion

The good agreement between reported experimental rate constants and those calculated using eq 8.1 for the reactions of the Michael acceptors **1−3** with C, N, O, S, and P nucleophiles in 96 of the investigated 110 cases demonstrates the applicability of the linear free-energy relationship log $k_2 = s_N(N + E)$ for the prediction of the rate constants of a broad variety of polar organic reactions.

Although the reactivity parameters determined in this work from reported rate constants of the reactions of gluthathione (GSH) with the Michael acceptors **1** and **2**, and the reactions of the activated ethylenes **6** with pyridines, amines, and alkoxides may not be very accurate, the fair correlations between the reported rate constants and reactivity parameters are obvious. Considering the broad validity range of eq 8.1 of over 30 orders of magnitude[20f] the observed deviations from the correlation lines, which in all cases lie within the limit of confidence of eq 8.1, are relatively small, showing that eq 8.1 can be used to estimate reactivity parameters of nucleophiles and electrophiles from reported rate constants.

For reactions in which more than one bond is formed in the rate determining step, e.g., for concerted cycloadditions, the rate constants cannot be calculated by eq 8.1 as two σ-bonds are formed simultaneously in the rate-determining step. However, we could show that eq 8.1 is a practical tool to differentiate between stepwise or highly asynchronous, and concerted reactions.

We found that rate constants of [3+2]-cycloadditions of diazomethanes and of Diels-Alder reactions of dienes with the acceptor-substituted olefins **1–3** decrease with decreasing nucleophilicity of the 1,3-dipole or 1,3-diene and decreasing electrophilicity of **1–3**. The reactivity parameters s_N, N, and E may thus be used as an orientation for the ordering of the reactivity of the reactants in pericyclic reactions.

8.5 Experimental Section

8.5.1 General

The k_1 values reported in refs. [6e, 7f] for the reactions of **2i** with OH$^-$ and of **3e** with amines were plotted against the concentrations of the nucleophiles to derive more reliable k_2 values, as the second-order rate constants given in refs. [6e, 7f] scatter. The k_1 values in ref. [6e], which deviate strongly from the other reported k_1 values, were not used for the determination of k_2.

The electrophilicity parameters E of the activated ethylenes **6** were determined by least-squares minimization, i.e., least-squares fitting of by minimizing $\Delta^2 = \sum(\log k_2 - s_N(N + E))^2$

8.5.2 Reevaluation of the Kinetics Reported in the Literature

8.5.2.1 Reaction of 2i with OH$^-$ from Ref. [7f]

Table 8.4. Kinetics of the reactions of 2i with OH$^-$ (H$_2$O; 25 °C) from ref. [7f].

[**2i**]/mol L^{-1}	[OH$^-$]/mol	k_1/s^{-1}
1.56×10^{-5}	3.73×10^{-2}	1.10×10^{-3}
1.56×10^{-5}	6.67×10^{-2}	2.38×10^{-3}
1.56×10^{-5}	1.00×10^{-1}	3.73×10^{-3}
k_2(20 °C) = 1.79×10^{-2} L mol^{-1} s^{-1}		
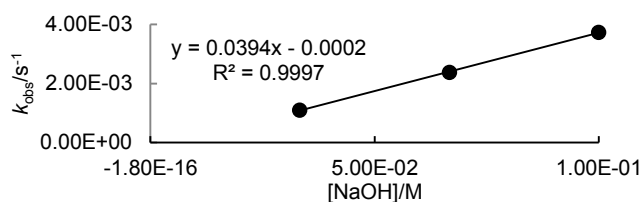
8.5.2.2 Reactions of 3e with Amines from Ref. [6e]

Table 8.5. Kinetics of the reactions of 1e with piperidine (Pip; EtOH (95%); 34 °C) from ref. [6e].

[**1e**]/mol L^{-1}	[Pip]/mol L^{-1}	k_1/s^{-1}
2×10^{-5}	4.00×10^{-3}	8.33×10^{-5}
2×10^{-5}	1.00×10^{-2}	1.64×10^{-4}
2×10^{-5}	2.00×10^{-2}	3.63×10^{-4}
2×10^{-5}	4.00×10^{-2}	7.18×10^{-3}
k_2(20 °C) = 1.79×10^{-2} L mol^{-1} s^{-1}		
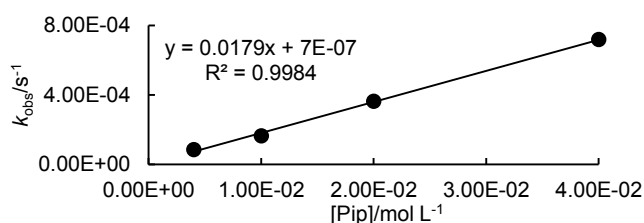
Table 8.6. Kinetics of the reactions of 1e with *n*-butylamine (EtOH (95%); 34 °C) from ref. [6e].

[**1e**]/mol L^{-1}	[nBuNH$_2$]/mol L^{-1}	k_1/s^{-1}
2×10^{-5}	1.01×10^{-2}	3.48×10^{-5}
2×10^{-5}	2.02×10^{-2}	6.25×10^{-5}
2×10^{-5}	1.01×10^{-1}	1.89×10^{-4}
2×10^{-5}	2.02×10^{-1}	3.34×10^{-4}
k_2(20 °C) = 1.54×10^{-3} L mol^{-1} s^{-1}		
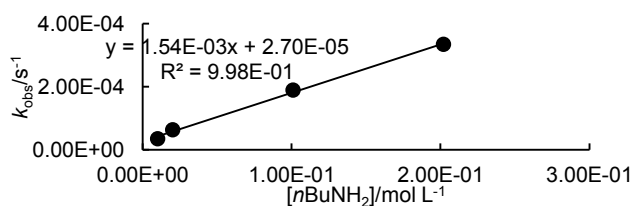
Table 8.7. Kinetics of the reactions of 1e with dipropylamine (EtOH (95%); 34 °C) from ref. [6e].

[**1e**]/mol L^{-1}	[nPr$_2$NH]/mol L^{-1}	k_1/s^{-1}
2×10^{-5}	2.19×10^{-2}	1.19×10^{-5}
2×10^{-5}	3.65×10^{-2}	1.80×10^{-5}
2×10^{-5}	5.84×10^{-2}	2.87×10^{-5}
2×10^{-5}	7.30×10^{-2}	3.39×10^{-5}
2×10^{-5}	1.46×10^{-2}	6.90×10^{-5}
k_2(20 °C) = 4.61×10^{-4} L mol^{-1} s^{-1}		

y = 4.61E-04x + 1.33E-06
R² = 9.99E-01
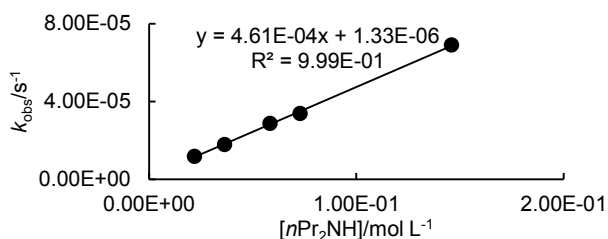
Table 8.8. Kinetics of the reactions of 1e with benzylamine (EtOH (95%); 34 °C) from ref. [6e].

[**1e**]/mol L^{-1}	[BnNH$_2$]/mol L^{-1}	k_1/s^{-1}
2×10^{-5}	9.17×10^{-2}	1.17×10^{-4}
2×10^{-5}	1.46×10^{-2}	2.18×10^{-4}
2×10^{-5}	1.84×10^{-2}	2.15×10^{-4}
2×10^{-5}	3.67×10^{-1}	2.85×10^{-4}
k_2(20 °C) = 5.16×10^{-4} L mol^{-1} s^{-1}		

y = 5.16E-04x + 1.07E-04
R² = 7.94E-01
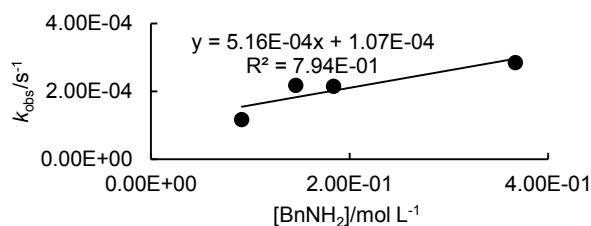
8.5.3   Determination of Reactivity Parameters from Reported Rate Constants

8.5.3.1   Reactions of GSH with 1,2 from Refs. [8b, 22]

Table 8.9. Experimental second-order rate constants (k_2^{exp}) for the reactions of the GSH with 1a,b,g,i and 2b,c,i,j in H$_2$O at 25 °C. k_2 values taken from refs. [8b, 22].

Elec.	E	k_2^{exp}/M^{-1} s^{-1}	pH	Ref.
1a	−18.92	1.91×10^{-1}	7.4	22
1b	−19.16	1.79×10^{-1}	7.4	22
1g	−16.48	2.30	7.4	22
1f	−19.06	6.72×10^{-1}	6.8	8b
1i	−14.65	2.20	7.4	22
2b	−24.51	2.70×10^{-3}	7.4	22
2c	−22.78	9.59×10^{-4}	7.4	22
2i	−19.10	9.82×10^{-2}	7.4	22
2j	−19.66	1.00×10^{-1}	7.4	22
N = 17.01	s_N = 0.34			

log k_2 = 0.3438 E + 5.8487
R² = 0.8175

390
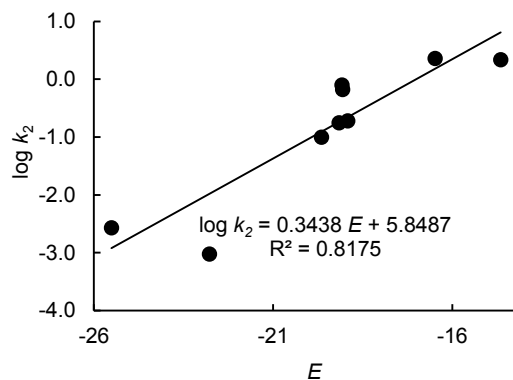
8.5.3.2   Reactions of (4-Methoxy)phenylvinylketone 6a with Amines from Ref. [6h]

Table 8.10. Experimental (k_2^{exp}) and calculated (k_2^{calcd})[a] second-order rate constants for the reactions of (4-methoxy)phenylvinylketone 6a with amines and pyridines in H_2O at 25 °C. k_2 values from ref. [6h].

Nuc.	k_2^{exp}/$M^{-1}s^{-1}$	k_2^{calcd}/$M^{-1}s^{-1}$	k_2^{exp}/k_2^{calcd}
MeNH$_2$	2.60	2.32	1.12
EtNH$_2$	2.30	6.78×10^{-1}	3.39
iPrNH$_2$	9.20×10^{-1}	2.24×10^{-1}	4.11
nBuNH$_2$	3.95	2.13×10^{1}	0.19
tBuNH$_2$	8.00×10^{-2}	2.86×10^{-1}	0.28
AllylNH$_2$	1.49	1.06	1.40
Et$_2$NH	1.83×10^{1}	6.38	2.87
Pr$_2$NH	2.23×10^{1}	1.20×10^{1}	1.86
Pip	7.00×10^{1}	1.54×10^{2}	0.46
Mor	7.90	2.13×10^{1}	0.37
	$E = -13.16$[a]		

[a] Calculated by eq 8.1 using the N and s_N parameters given in Table 8.1 and E in this Table; For the correlation for the determination of E see 8.5.3.6.

8.5.3.3   Reactions of Methylvinylsulfone 6b from Refs. [6c, k]

Table 8.11. Experimental (k_2^{exp}) and calculated (k_2^{calcd})[a] second-order rate constants for the reactions of methylvinylsulfone 6b with amines and pyridines in H_2O at 25 and 30 °C. k_2 values taken from refs. [6c, k].

Nuc.	T/°C	k_2^{exp}/$M^{-1}s^{-1}$	Ref	k_2^{calcd}/$M^{-1}s^{-1}$	k_2^{exp}/k_2^{calcd}
DMAP	25	8.25×10^{-2}	[6k]	7.47×10^{-2}	1.10
GlyGly	30	9.00×10^{-3}	[6c]	4.68×10^{-2}	0.19
Gly	30	3.06×10^{-2}	[6c]	1.04×10^{-1}	0.29
BrAP	25	1.95×10^{-2}	[6k]	3.15×10^{-2}	0.62
AP	25	6.10×10^{-2}	[6k]	1.03×10^{-2}	5.93
MorAP	25	4.40×10^{-2}	[6k]	1.39×10^{-2}	3.16
		$E = -15.20$[a]			

[a] Calculated by eq 8.1 using the N and s_N parameters given in Table 8.1 and E in this Table The correlation for the determination of E see 8.5.3.6.

8.5.3.4 Reactions of *N*-Methyl-*N*-Phenylethenesulfonamide 6c with Alkoxides from Ref. [7e]

Table 8.12. Experimental (k_2^{exp}) and calculated (k_2^{calcd})[a] second-order rate constants for the reactions of *N*-methyl-*N*-phenylethenesulfonamide 6c with alkoxides in the corresponding alcohol at 25 °C. k_2 values taken from ref. [7e].

Nuc.	Solvent	$T/°C$	$k_2^{exp}/M^{-1}s^{-1}$	$k_2^{calcd}/M^{-1}s^{-1}$	k_2^{exp}/k_2^{calcd}
MeO−	MeOH	25	6.28×10^{-3}	4.63×10^{-2}	0.14
EtO−	EtOH	25	4.93×10^{-2}	2.83×10^{-2}	1.74
*n*PrO−	*n*PrOH	25	9.48×10^{-2}	3.21×10^{-2}	2.95
			$E = -18.16$[a]		

[a] Calculated by eq 8.1 using the N and s_N parameters given in Table 8.1 and E in this Table The correlation for the determination of E see 8.5.3.6.

8.5.3.5 Reactions of Acrylamide 6d with Amines and Pyridines from Refs. [6c, g, k]

Table 8.13. Experimental (k_2^{exp}) and calculated (k_2^{calcd})[a] second-order rate constants for the reactions of acrylamide 6d with amines and pyridines in H$_2$O and MeOH at 25 and 30 °C. k_2 values taken from refs. [6c, g, k].

Nuc.	Solvent	$T/°C$	$k_2^{exp}/M^{-1}s^{-1}$	Ref	$k_2^{calcd}/M^{-1}s^{-1}$	k_2^{exp}/k_2^{calcd}
DMAP	H$_2$O	25	6.10×10^{-4}	[6k]	5.55×10^{-4}	1.10
GlyGly	H$_2$O	30	2.00×10^{-4}	[6c]	2.92×10^{-4}	0.68
Gly	H$_2$O	30	6.30×10^{-4}	[6c]	6.51×10^{-4}	0.97
Ala	H$_2$O	30	3.50×10^{-4}	[6c]	3.34×10^{-4}	1.05
Pyr	MeOH	30	8.27×10^{-3}	[6g]	1.23×10^{-2}	0.67
BrAP	H$_2$O	25	1.00×10^{-4}	[6k]	8.92×10^{-5}	1.12
Mor	MeOH	30	3.57×10^{-4}	[6g]	4.94×10^{-3}	0.07
AP	H$_2$O	25	5.30×10^{-4}	[6k]	3.18×10^{-5}	16.7
MorAP	H$_2$O	25	3.90×10^{-4}	[6k]	4.31×10^{-5}	9.04
Phe	H$_2$O	30	2.22×10^{-4}	[6c]	2.58×10^{-3}	0.09
			$E = -19.07$[a]			

[a] Calculated by eq 8.1 using the N and s_N parameters given in Table 8.1 and E in this Table The correlation for the determination of E see 8.5.3.6.
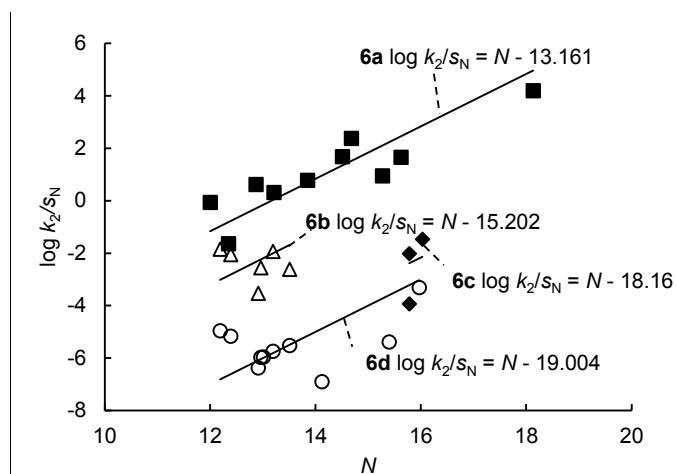
8.5.3.6 Correlations of $(\log k_2)/s_N$ of the Reactions of 6 with Nucleophiles

Figure 8.6. Correlation of (log k_2/s_N) versus N for 6a(4-methoxy)phenylvinylketone 6a (squares), methylvinylsulfone 6b (triangle), N-methyl-N-phenylethenesulfonamide 6c (diamonds), and acrylamid 6d (circles). The slopes of the correlations were set to 1.0.

8.6 References

[1]   (a) D. S. Allgäuer, H. Mayr, *Eur. J. Org. Chem.* **2013**, *submitted*; (b) D. S. Allgäuer, H. Asahara, H. Mayr, *To be published* **2013**.

[2]   D. S. Allgäuer, H. Mayr, *To be published* **2013**.

[3]   D. S. Allgäuer, P. Mayer, H. Mayr, *J. Am. Chem. Soc.* **2013**, *135*, 15216–15224.

[4]   R. Appel, N. Hartmann, H. Mayr, *J. Am. Chem. Soc.* **2010**, *132*, 17894−17900.

[5]   Reactions with C-Nucloephiles: K. T. Finley, D. R. Call, G. W. Sovocool, W. J. Hayles, *Can. J. Chem.* **1967**, *45*, 571-573.

[6]   Reactions with N-Nucleophiles: (a) Y. Ogata, M. Okano, Y. Furuya, I. Tabushi, *J. Am. Chem. Soc.* **1956**, *78*, 5426-5428; (b) N. Ogata, T. Asahara, *Bull. Chem. Soc. Jap.* **1966**, *39*, 1486-1490; (c) M. Friedman, J. S. Wall, *J. Org. Chem.* **1966**, *31*, 2888-2894; (d) I. Šestáková, V. Horák, P. Zuman, *Collect. Czech. Chem. Commun.* **1966**, *31*, 3889-3902; (e) Z. Grunbaum, S. Patai, Z. Rappoport, *J. Chem. Soc. B* **1966**, 1133−1137; (f) K. Sanui, N. Ogata, *Bull. Chem. Soc. Jap.* **1967**, *40*, 1727-1727; (g) H. Shenhav, Z. Rappoport, S. Patai, *J. Chem. Soc. B* **1970**, 469-476; (h) G. J. Dienys, L. J. J. Kunskaite, A. K. Vaitkevicius, A. V. Klimavicius, *Org. Reactiv., Engl. Ed.* **1975**, *12*, 275-282; (i) J. Szczesna, M. Kostecki, S. Kinastowski, *Rocz. Akad. Roln. Poznaniu* **1988**, *192*, 99-104; (j) J. W. Bunting, A. Toth, C. K. M. Heo, R. G. Moors, *J. Am. Chem. Soc.* **1990**, *112*, 8878-8885; (k) C. K. M. Heo, J. W. Bunting, *J. Org. Chem.* **1992**, *57*, 3570-3578;

(l) M. Kostecki, J. Szczesna, S. Kinastowski, *Rocz. Akad. Roln. Poznaniu* **1993**, *256*, 25-32; (m) K. L. Mallik, M. N. Das, *Z. Phys. Chem.* **1960**, *25*, 205-216; (n) M. Friedman, *J. Am. Chem. Soc.* **1967**, *89*, 4709-4713; (o) J. Horáleka, E. Krejcara, J. Churáček, *Collect. Czech. Chem. Commun.* **1988**, *53*, 833-838.

[7]   Reactions with O-Nucleophiles: (a) N. Ferry, F. J. McQuillin, *J. Chem. Soc.* **1962**, 103-113; (b) B.-A. Feit, A. Zilkha, *J. Org. Chem.* **1963**, *28*, 406-410; (c) P. Carsky, P. Zuman, V. Horvak, *Collect. Czech. Chem. Commun.* **1965**, *30*, 4316-4336; (d) R. N. Ring, G. C. Tesoro, D. R. Moore, *J. Org. Chem.* **1967**, *32*, 1091−1094; (e) W. G. Davies, E. W. Hardisty, T. P. Nevell, R. H. Peters, *J. Chem. Soc. B, Phys. Org.* **1970**, 998-1004; (f) J. P. Guthrie, *Can. J. Chem.* **1974**, *52*, 2037-2040; (g) B. A. Feit, R. Pazhenchevsky, B. Pazhenchevsky, *J. Org. Chem.* **1976**, *41*, 3246-3250; (h) O. Adomeniene, G. Dienys, Z. Stumbreviciute, *Org. Reactiv., Engl. Ed.* **1978**, *15*, 38-44; (i) J. P. Guthrie, K. J. Cooper, J. Cossar, B. A. Dawson, K. F. Taylor, *Can. J. Chem.* **1984**, *62*, 1441-144; (j) J. P. Guthrie, J. Cossar, K. F. Taylor, *Can. J. Chem.* **1984**, *62*, 1958-1964.

[8]   Reactions with S-Nucleophiles: (a) M. Morton, H. Landfield, *J. Am. Chem. Soc.* **1952**, *74*, 3523-3526; (b) M. Friedman, J. F. Cavins, J. S. Wall, *J. Am. Chem. Soc.* **1965**, *87*, 3672-3682; (c) T.-R. Kim, S.-J. Yun, B.-B. Park, *Bull. Kor. Chem. Soc.* **1986**, *7*, 25-29.

[9]   Reactions with P-Nucleophiles: I. Petnehazy, G. Clementis, Z. M. Jaszay, L. Toke, C. D. Hall, *J. Chem. Soc., Perkin Trans. 2* **1996**, 2279-2284.

[10]   (a) R. Lucius, R. Loos, H. Mayr, *Angew. Chem., Int. Ed.* **2002**, *41*, 91−95; (b) T. Bug, H. Mayr, *J. Am. Chem. Soc.* **2003**, *125*, 12980−12986.

[11]   (a) F. Brotzel, B. Kempf, T. Singer, H. Zipse, H. Mayr, *Chem. Eur. J.* **2007**, *13*, 336−345; (b) M. Breugst, H. Mayr, *J. Am. Chem. Soc.* **2010**, *132*, 15380−15389; (c) T. A. Nigst, J. Ammer, H. Mayr, *J. Phys. Chem. A* **2012**, *116*, 8494−8499.

[12]   (a) S. Minegishi, H. Mayr, *J. Am. Chem. Soc.* **2002**, *125*, 286−295; (b) H. Mayr, A. R. Ofial, *Angew. Chem.* **2006**, *118*, 1844−1854; (c) F. Brotzel, Y. C. Chu, H. Mayr, *J. Org. Chem.* **2007**, *72*, 3679−3688; (d) T. Kanzian, T. A. Nigst, A. Maier, S. Pichl, H. Mayr, *Eur. J. Org. Chem.* **2009**, 6379−6385.

[13]   F. Brotzel, H. Mayr, *Org. Biomol. Chem.* **2007**, *5*, 3814−3820.

[14]   T. B. Phan, H. Mayr, *Can. J. Chem.* **2005**, *83*, 1554−1560.

[15]   T. B. Phan, M. Breugst, H. Mayr, *Angew. Chem., Int. Ed.* **2006**, *45*, 3869−3874.

[16]   [3+2]-Cycloaddtions with diazomethanes: (a) R. Huisgen, H. Stangl, H. J. Sturm, H. Wagenhofer, *Angew. Chem.* **1961**, *73*, 170; (b) A. Ledwith, Y. Shih-Lin, *J. Chem. Soc. B* **1967**, 83−84; (c) L. Fisera, J. Geittner, R. Huisgen, H.-U. Reissig, *Heterocycles* **1978**,

10, 153−158; (d) J. Geittner, R. Huisgen, H.-U. Reissig, *Heterocycles* **1978**, *11*, 109−112; (e) G. Swieton, J. Von Jouanne, H. Kelm, R. Huisgen, *J. Org. Chem.* **1983**, *48*, 1035−1040; (f) T. Oshima, T. Nagai, *Tetrahedron Letters* **1985**, *26*, 4785−4788; (g) R. Huisgen, E. Langhals, *Tetrahedron Lett.* **1989**, *30*, 5369−5372.

[17]   Diels-Alder reactions with dienes: (a) J. Sauer, D. Lang, A. Mielert, *Angew. Chem., Int. Ed. Engl.* **1962**, *1*, 268−269; (b) J. Sauer, H. Wiest, A. Mielert, *Chem. Ber.* **1964**, *97*, 3183−3207; (c) J. Sauer, D. Lang, H. Wiest, *Chem. Ber.* **1964**, *97*, 3208−3218; (d) B. Blankenburg, H. Fiedler, M. Hampel, H. G. Hauthal, G. Just, K. Kahlert, J. Korn, K. H. Müller, W. Pritzkow, Y. Reinhold, M. Röllig, E. Sauer, D. Schnurpfeil, G. Zimmermann, *J. Prakt. Chem.* **1974**, *316*, 804−816; (e) M. W. Lee, W. C. Herndon, *J. Org. Chem.* **1978**, *43*, 518−518; (f) A. Meijer, S. Otto, J. B. F. N. Engberts, *J. Org. Chem.* **1998**, *63*, 8989−8994.

[18]   T. Bug, M. Hartnagel, C. Schlierf, H. Mayr, *Chem. Eur. J.* **2003**, *9*, 4068−4076.

[19]   (a) H. Mayr, R. Schneider, B. Irrgang, C. Schade, *J. Am. Chem. Soc.* **1990**, *112*, 4446–4454; (b) T. Siegmund, Ludwig-Maximilian Universität (München), **1999**; (c) H. Mayr, T. Bug, M. F. Gotta, N. Hering, B. Irrgang, B. Janker, B. Kempf, R. Loos, A. R. Ofial, G. Remennikov, H. Schimmel, *J. Am. Chem. Soc.* **2001**, *123*, 9500−9512; (d) H. Mayr, B. Kempf, A. R. Ofial, *Acc. Chem. Res.* **2003**, *36*, 66−77; (e) J. Ammer, C. Nolte, H. Mayr, *J. Am. Chem. Soc.* **2012**, *134*, 13902−13911.

[20]   (a) H. Mayr, M. Patz, *Angew. Chem., Int. Ed. Engl.* **1994**, *33*, 938−957; (b) H. Mayr, T. Bug, M. F. Gotta, N. Hering, B. Irrgang, B. Janker, B. Kempf, R. Loos, A. R. Ofial, G. Remennikov, H. Schimmel, *J. Am. Chem. Soc.* **2001**, *123*, 9500−9512; (c) H. Mayr, B. Kempf, A. R. Ofial, *Acc. Chem. Res.* **2003**, *36*, 66−77; (d) H. Mayr, A. R. Ofial, *Pure Appl. Chem.* **2005**, 1807−1821; (e) H. Mayr, A. R. Ofial, *J. Phys. Org. Chem.* **2008**, *21*, 584−595; (f) For a comprehensive database of nucleophilicity parameters N, s_N and electrophilicity parameters E, see http://www.cup.lmu.de/oc/mayr/.

[21]   (a) M. Hartnagel, K. Grimm, H. Mayr, *Liebigs Ann.* **1997**, 71−80. (b) H. Mayr, A. R. Ofial, J. Sauer, B. Schmied, *Eur. J. Org. Chem.* **2000**, 2013−2020. (c) C. Fichtner, H. Mayr, *J. Chem. Soc., Perkin Trans. 2* **2002**, 1441−1444.

[22]   J. A. H. Schwöbel, D. Wondrousch, Y. K. Koleva, J. C. Madden, M. T. D. Cronin, G. Schüürmann, *Chem. Res. Toxicol.* **2010**, *23*, 1576-1585.

[23]   (a) T. Lemek, H. Mayr, *J. Org. Chem.* **2003**, *68*, 6880−6886; (b) S. T. A. Berger, F. H. Seeliger, F. Hofbauer, H. Mayr, *Org. Biomol. Chem.* **2007**, *5*, 3020−3026; (c) O. Kaumanns, R. Lucius, H. Mayr, *Chem. Eur. J.* **2008**, *14*, 9675−9682; (d) I. Zenz, H.

Mayr, *J. Org. Chem.* **2011**, *76*, 9370−9378; (e) H. Asahara, H. Mayr, *Chem. Asian J.* **2012**, *7*, 1401−1407.

[24]   (a) R. A. Firestone, *J. Org. Chem.* **1968**, *33*, 2285−2290; (b) R. Huisgen, *J. Org. Chem.* **1968**, *33*, 2291−2297; (c) R. A. Firestone, *J. Org. Chem.* **1972**, *37*, 2181−2191.

[25]   R. Huisgen, in *1,3-Dipolar Cycloaddition Chemistry* (Ed.: A. Padwa), Wiley, New York, **1984**, p. 1−176.

[26]   I. Hunt, C. D. Johnson, *J. Chem. Soc., Perkin Trans. 2* **1991**, 1051-1056.

[27]   (a) R. Huisgen, G. Steiner, *Tetrahedron Lett.* **1973**, *14*, 3763–3768; (b) R. Brückner, R. Huisgen, *Tetrahedron Lett.* **1990**, *31*, 2557–2560.